University of Ghana http://ugspace.ug.edu.gh

DESIGN, SYNTHESIS, CHARACTERIZATION, ANTIMALARIAL AND ADME EVALUATION OF ANALOGUES OF MMV902507(SFK78) AND MMV1900279

BY: ANNOR DEBORAH

(11007599)

THIS DISSERTATION IS SUBMITTED TO THE DEPARTMENT OF CHEMISTRY

IN PARTIAL FULFILLMENT OF THE REQUIREMENTS FOR THE AWARD OF MPHIL CHEMISTRY

DEPARTMENT OF CHEMISTRY,

UNIVERSITY OF GHANA,

LEGON

OCTOBER 2024.

University of Ghana http://ugspace.ug.edu.gh

DECLARATION

This research project is submitted in partial fulfillment of the requirements for the award of the Master of Philosophy degree in Chemistry, University of Ghana, Legon. I, Deborah Annor declare that this book is of my own findings from the research under the supervision of Professor Richard Kwamla Amewu at the Department of Chemistry and has not been published for the award of any degree in the university except where acknowledgement has been made in text.

Student Miss Deborah Annor

Co-Supervisor Dr Anita Adjoa Oppong

Principal Supervisor: Prof. Richard K. Amewu

University of Ghana http://ugspace.ug.edu.gh

DEDICATION

This book is dedicated to God Almighty.

University of Ghana http://ugspace.ug.edu.gh

ACKNOWLEDGEMENT

I thank the almighty God for how far he has brought me, for his guidance, his grace and his mercies never ending. I also express my immense gratitude to my supervisor, Professor Richard Kwamla Amewu for his support, guidance, patience and supervision throughout this research, Mr. Fritz Plange and the entire DIG group for their support. I thank the Bill and Melinda Gates foundation for funding the project, MMV, H3D and Noguchi for analyzing and testing the compounds for this project. I thank my family most especially my mother Vida Annor for her advice, care, prayers, support, love, and motivation throughout the years. I thank my Pastor for his prayers, guidance and encouragement and my uncle Samuel Odei for his support. I thank Mr. Samuel Owusu-Atwah (General) for running my FTIR data. Thomas Mensah for running and generating my NMR data. I am grateful to Gary Knox, Justice Akwensi and Crystal Ade. My final gratitude goes to the Department of Chemistry for giving me the opportunity to pursue MPhil Chemistry in the University of Ghana.

INTEGRI PROCEDAMUS

University of Ghana http://ugspace.ug.edu.gh

Table of Contents

DECLARATION ii

DEDICATION iii

ACKNOWLEDGEMENT iv

ABSTRACT xxiii

Chapter 1 1

1.1 INTRODUCTION 1

1.2 Malaria 1

1.3 Malaria in Ghana 2

1.4 Epidemiology 3

1.5 Malaria Parasite 5

1.5.1 Plasmodium falciparum 6

1.5.2 Plasmodium vivax 7

1.5.3 Plasmodium malariae 8

1.5.4 Plasmodium ovale 9

1.5.5 Plasmodium knowlesi 10

1.5.6 Life Cycle of Plasmodium Parasite 11

1.6 Malaria Prevention 13

1.6.1 Vector Control 13

1.6.2 Malaria Chemoprevention 16

University of Ghana http://ugspace.ug.edu.gh

1.6.3 Malaria Vaccines 17

1.7 Antimalarials and their Mode of Action 18

1.7.1 Antifolates 19

1.7.2 Aminoquinolines 20

1.7.3 Endoperoxides 21

1.8 Malaria Chemotherapy 23

1.9 Plasmodium Resistance 24

1.10 Problem Statement 26

1.11 Hypothesis 26

1.12 Aim 26

1.13 Specific Objectives 26

Chapter 2 28

Literature Review 28

2.1 Nitrogen Heterocycles 28

2.2 Purines 30

2.2.1 Anticancer Activity of the purine moiety 33

2.2.2 Antiviral Activity of the Purine moiety 36

2.2.3 AntiMicrobial Activity of the Purine Moiety 39

2.2.4 Antimalarial Activity of the Purine Moiety 41

2.3 The Pyrrolo Pyridine Moiety. 43

University of Ghana http://ugspace.ug.edu.gh

2.3.1 Synthesis of the Pyrrolo Pyridine Moiety 45

2.3.2 Antimicrobial Activity of Pyrrolo Pyridines 46

2.3.3 Anticancer activity of the pyrrolo pyridine 48

2.4 Phosphatidylinositol 4 Kinase (PI4K) 50

2.5 Sulfonamides 51

2.6 Phenotypic Screening 52

Chapter 3 56

3.1 The Hit Compound MMV902507 (SFK78) 56

3.2 Materials 57

3.3 Chromatography for Separation and Purification 57

3.4 Nuclear Magnetic Resonance (NMR) 58

3.5 Fourier Transform Infrared Spectroscopy (FTIR) 58

3.6 LC-MS 58

3.7 Melting Point 58

3.8 Medicinal Chemistry Plan 59

3.9 General Procedure for Synthesizing Sulfonyl Chloride Intermediate. 60

3.9.1 Synthesis of 5-bromo-1H-pyrrolo[2,3-b] pyridine-3-sulfonyl chloride (ADA081, 1). 60

3.10 General Procedure for Synthesizing sulfonamide Intermediate. 61

3.10.1 Synthesis of 4-((5-bromo-1H-pyrrolo[2,3-b] pyridin-3-yl) sulfonyl) morpholine (ADA082, 2). 61

University of Ghana http://ugspace.ug.edu.gh

3.10.2 Synthesis of 5-bromo-3-((4-(pyrimidin-2-yl) piperazin-1-yl) sulfonyl) -1H-pyrrolo[2,3-b] pyridine (ADA086, 3). 62

3.10.3 Synthesis of tert-butyl 4-((5-bromo-1H-pyrrolo[2,3-b] pyridin-3-yl) sulfonyl) piperazine-1-carboxylate (ADA089, 4). 63

3.10.4 Synthesis of 1-(4-((5-bromo-1H-pyrrolo[2,3-b] pyridin-3-yl) sulfonyl) piperazin-1-yl) ethan-1-one (ADA094, 5). 64

3.10.5 Synthesis of 4-(1-((5-bromo-1H-pyrrolo[2,3-b] pyridin-3-yl) sulfonyl) piperidin-4-yl) morpholine (ADA098, 6). 64

3.11 General Procedure for Suzuki Cross-Coupling Reaction on Sulfonamide Intermediate (Final Compounds). 65

3.11.1 Synthesis of 4-((5-(4-chlorophenyl)-1H-pyrrolo[2,3-b] pyridin-3-yl) sulfonyl) Morpholine (ADA 083,6). 66

3.11.2 Synthesis of 4-((5-(3,4-dimethoxyphenyl)-1H-pyrrolo[2,3-b] pyridin-3-yl) sulfonyl) Morpholine (ADA 084, 7). 67

3.11.3 Synthesis of 4-((5-(4-(methyl sulfonyl) phenyl)-1H-pyrrolo[2,3-b] pyridin-3-yl) sulfonyl) Morpholine (ADA 085, 8). 68

3.11.4 Synthesis of 4-((5-(4-(trifluoromethyl) phenyl)-1H-pyrrolo[2,3-b] pyridin-3-yl) sulfonyl) morpholine (ADA087, 9). 69

3.11.5 Synthesis of 5-(3,4-dimethoxyphenyl)-3-((4-(pyrimidin-2-yl) piperazin-1-yl) sulfonyl)-1H-pyrrolo[2,3-b] pyridine (ADA088, 10). 70

3.11.6 Synthesis of 5-(4-(methyl sulfonyl) phenyl)-3-((4-(pyrimidin-2-yl) piperazin-1-yl) sulfonyl)-1H-pyrrolo[2,3-b] pyridine (ADA090, 11). 71

University of Ghana http://ugspace.ug.edu.gh

3.11.7 Synthesis of tert-butyl 4-((5-(4-chlorophenyl)-1H-pyrrolo[2,3-b] pyridin-3-yl) sulfonyl) piperazine-1-carboxylate (ADA091, 12). 72

3.11.8 Synthesis of tert-butyl 4-((5-(3,4-dimethoxyphenyl)-1H-pyrrolo[2,3-b] pyridin-3-yl) sulfonyl) piperazine-1-carboxylate (ADA092, 13). 73

3.11.9 Synthesis of tert-butyl 4-((5-(4-(methyl sulfonyl) phenyl)-1H-pyrrolo[2,3-b] pyridin-3-yl) sulfonyl) piperazine-1-carboxylate (ADA093, 14)..... 74

3.11.10 Synthesis of 1-(4-((5-(4-chlorophenyl)-1H-pyrrolo[2,3-b] pyridin-3-yl) sulfonyl) piperazin-1-yl) ethan-1-one (ADA095, 15)..... 75

3.11.11 Synthesis of 1-(4-((5-(4-(methyl sulfonyl) phenyl)-1H-pyrrolo[2,3-b] pyridin-3-yl) sulfonyl) piperazin-1-yl) ethan-1-one (ADA096, 16). 76

3.11.12 Synthesis of 1-(4-((5-(3,4-dimethoxyphenyl)-1H-pyrrolo[2,3-b] pyridin-3-yl) sulfonyl) piperazin-1-yl) ethan-1-one (ADA097, 17). 77

3.11.13 Synthesis of 4-(1-((5-(3,4-dimethoxyphenyl)-1H-pyrrolo[2,3-b] pyridin-3-yl) sulfonyl) piperidin-4-yl) Morpholine (ADA099, 18)..... 78

3.11.14 Synthesis of 5-(2-methoxyphenyl)-3-((4-(pyrimidin-2-yl) piperazin-1-yl) sulfonyl)-1H-pyrrolo[2,3-b] pyridine (ADA106,19)..... 79

3.11.15 Synthesis of 5-(benzo[d] [1,3] dioxol-5-yl)-3-((4-(pyrimidin-2-yl) piperazin-1-yl) sulfonyl)-1H-pyrrolo[2,3-b] pyridine (ADA107, 20)..... 80

3.11.16 Synthesis of 5-(3-methoxyphenyl)-3-((4-(pyrimidin-2-yl) piperazin-1-yl) sulfonyl)-1H-pyrrolo[2,3-b] pyridine (ADA108, 21)..... 81

3.12 General Procedure for Deprotection of Boc Products..... 82

University of Ghana http://ugspace.ug.edu.gh

3.12.1 Synthesis of 5-(4-chlorophenyl)-3-(piperazin-1-ylsulfonyl)-1H-pyrrolo[2,3-b] pyridine (ADA101, 22)..... 82

3.12.2 Synthesis of 5-(3,4-dimethoxyphenyl)-3-(piperazin-1-ylsulfonyl)-1H-pyrrolo[2,3-b] pyridine hydrochloride (ADA 102, 23). 83

3.12.3 Synthesis of 5-(4-(methyl sulfonyl) phenyl)-3-(piperazin-1-ylsulfonyl)-1H-pyrrolo[2,3-b] pyridine hydrochloride (ADA103, 24). 84

3.13 RESULTS AND DISCUSSION 85

3.14 Chemistry 85

3.15 Reaction Mechanism for Synthesized Analogues 89

3.16 Spectral Analysis. 91

3.16.1 Proton (^{1}H) NMR Analysis of ADA081 92

3.16.2 Carbon (^{13}C) NMR for ADA081 92

3.16.3 Proton (^{1}H) NMR Analysis of ADA086 93

3.16.4 Carbon (^{13}C) NMR for ADA086 94

3.16.5 Proton (^{1}H) NMR Analysis of ADA090 95

3.16.6 Carbon (^{13}C) NMR for ADA090 97

3.16.7 FT-IR Analysis of ADA090 98

3.16.8 LC-MS Analysis for ADA090 99

3.17 Antimalarial Biological Activity Results..... 100

3.18 ADME Evaluation of synthesized Analogues. 102

University of Ghana http://ugspace.ug.edu.gh

3.19 Physicochemical Parameters of Synthesized Analogues 104

Chapter 4 106

4.1 MMV1900279 106

4.2 Medicinal Chemistry Strategy for the Synthesis of the Analogues of MMV1900279 107

4.3 General Procedure for 5-amino-1H-imidazole-4-carboxamide derivatives. 108

4.3.1 Synthesis of 5-amino-1-cyclopentyl-1H-imidazole-4-carboxamide (ADA110, 1). ... 108

4.3.2 Synthesis of 5-amino-1-(tetrahydro-2H-pyran-4-yl)-1H-imidazole-4-carboxamide (ADA111, 2). 109

4.3.3 Synthesis of 5-amino-1-(oxetan-3-yl)-1H-imidazole-4-carboxamide (ADA114, 3)...110

4.3.4 Synthesis of *tert*-butyl 4-(5-amino-4-carbamoyl-1H-imidazol-1-yl) piperidine-1-carboxylate (ADA127, 4) 110

4.3.5 Synthesis of 5-amino-1-cyclobutyl-1H-imidazole-4-carboxamide (ADA134, 5)..... 111

4.4 General Procedure for Amide Coupling Synthesis 112

4.4.1 Synthesis of 5-(cyclohexanecarboxamido)-1-(tetrahydro-2*H*-pyran-4-yl)-1*H*-imidazole-4-carboxamide (ADA112, 6). 112

4.4.2 Synthesis of 5-benzamido-1-cyclopentyl-1H-imidazole-4-carboxamide (ADA115, 7). 113

4.4.3 Synthesis of 5-(cyclohexanecarboxamido)-1-(oxetan-3-yl)-1*H*-imidazole-4-carboxamide (ADA116, 8). 114

4.4.4 Synthesis of 5-benzamido-1-(oxetan-3-yl)-1H-imidazole-4-carboxamide (ADA119, 9) 115

University of Ghana http://ugspace.ug.edu.gh

4.4.5 Synthesis of 5-isobutyramido-1-(oxetan-3-yl)-1*H*-imidazole-4-carboxamide (ADA120, 10). 115

4.4.6 Synthesis of *tert*-butyl 4-(4-carbamoyl-5-(cyclohexane carboxamido)-1*H*-imidazol-1-yl) piperidine-1-carboxylate (ADA128, 11). 116

4.4.7 Synthesis of *tert*-butyl 4-(4-carbamoyl-5-(cyclopropane carboxamido)-1*H*-imidazol-1-yl) piperidine-1-carboxylate (ADA131, 12). 117

4.4.8 Synthesis of 1-cyclobutyl-5-(cyclohexanecarboxamido)-1*H*-imidazole-4-carboxamide (ADA135, 13). 118

4.4.9 Synthesis of 5-benzamido-1-cyclobutyl-1*H*-imidazole-4-carboxamide (ADA137, 14). 118

4.4.10 Synthesis of 1-cyclobutyl-5-(cyclopropanecarboxamido)-1*H*-imidazole-4-carboxamide (ADA140, 15). 119

4.4.11 Synthesis of 1-cyclobutyl-5-isobutyramido-1*H*-imidazole-4-carboxamide (ADA142, 16). 120

4.4.12 Synthesis of 1-cyclobutyl-5-(2-methoxybenzamido)-1*H*-imidazole-4-carboxamide (ADA144, 17). 121

4.4.13 Synthesis of 5-(2-(4-methoxy phenyl) acetamido)-1-(tetrahydro-2*H*-pyran-4-yl)-1*H*-imidazole-4-carboxamide (ADA147, 18)..... 122

4.5 General Procedure for Cyclization Synthesis..... 122

4.5.1 Synthesis of 2-cyclohexyl-9-(tetrahydro-2*H*-pyran-4-yl)-1,9-dihydro-6*H*-purin-6-one (ADA113, 19). 123

University of Ghana http://ugspace.ug.edu.gh

4.5.2 Synthesis of 9-cyclopentyl-2-phenyl-1,9-dihydro-6*H*-purin-6-one (ADA117, 20) ... 124

4.5.3 Synthesis of 2-cyclohexyl-9-(oxetan-3-yl)-1,9-dihydro-6*H*-purin-6-one (ADA118, 21) 125

4.5.4 Synthesis of 2-isopropyl-9-(oxetan-3-yl)-1,9-dihydro-6H-purin-6-one (ADA123, 22) 125

4.5.5 Synthesis of *tert*-butyl 4-(2-cyclohexyl-6-oxo-1,6-dihydro-9*H*-purin-9-yl) piperidine-1-carboxylate (ADA129, 23) 126

4.5.6 Synthesis of *tert*-butyl 4-(2-cyclopropyl-6-oxo-1,6-dihydro-9*H*-purin-9-yl) piperidine-1-carboxylate (ADA132, 24) 127

4.5.7 Synthesis of 9-cyclobutyl-2-cyclohexyl-1,9-dihydro-6*H*-purin-6-one (ADA136, 25) 128

4.5.8 Synthesis of 9-cyclobutyl-2-phenyl-1,9-dihydro-6*H*-purin-6-one (ADA138, 26)..... 128

4.5.9 Synthesis of 9-cyclobutyl-2-cyclopropyl-1,9-dihydro-6*H*-purin-6-one (ADA141, 27) 129

4.5.10 Synthesis of 9-cyclobutyl-2-isopropyl-1,9-dihydro-6*H*-purin-6-one (ADA143, 28)130

4.5.11 Synthesis of 9-cyclobutyl-2-(2-methoxyphenyl)-1,9-dihydro-6*H*-purin-6-one (ADA145, 29) 131

4.5.12 Synthesis of 2-(4-methoxybenzyl)-9-(tetrahydro-2*H*-pyran-4-yl)-1,9-dihydro-6H-purin-6-one (ADA148, 30) 132

4.6 RESULTS AND DISCUSSION 132

4.7 Chemistry 132

University of Ghana http://ugspace.ug.edu.gh

4.7.1 Reaction Mechanism for Synthesized Analogues 133

4.8 Spectral Analysis 139

4.8.1 Proton NMR Analysis of ADA110 139

4.8.2 Carbon (^{13}C) NMR Analysis of ADA110 140

4.8.3 FTIR Data for ADA110 141

4.8.4 Proton NMR Analysis of ADA115 142

4.8.5 Carbon NMR Analysis of ADA115 143

4.8.6 Proton NMR Analysis of ADA117 144

4.8.7 Carbon NMR Analysis of ADA117 146

4.8.8 FTIR Analysis of ADA117 147

4.8.9 LCMS Analysis of ADA117 148

4.9 Antimalarial Biological Activity of Synthesized Analogues of MMV1900279 149

4.10 Solubility of Synthesized Analogues of MMV1900279 152

Chapter 5 153

5.1 Conclusions 153

5.2 Recommendations 154

REFERENCES 155

APPENDICES 170

APPENDIX I: NMR DATA 170

APPENDIX II: FT-IR Spectrum 222

University of Ghana http://ugspace.ug.edu.gh

APPENDIX III: LCMS Data 246

University of Ghana http://ugspace.ug.edu.gh

List of Figures

Figure 1.1: Global trends in a) Malaria cases and b) Malaria deaths between the year 2000-2023[5]. 2

Figure 1.2: Malaria epidemiology[5]. 4

Figure 1.3:Malaria cases in WHO Africa region[5] 5

Figure 1.4: Trophozoites of Plasmodium falciparum[13] 7

Figure 1.5: Schizonts of P. vivax.[24] 8

Figure 1.6: sporozoites of P. malariae[28]. 9

Figure 1.7: gametocytes of p. ovale[31]. 10

Figure 1.8: Trophozoites of P. knowlesi[34]. 11

Figure 1.9: Life cycle of the plasmodium parasite[37] 12

Figure 1.10: Insecticides for IRS[51] 15

Figure 1.11: Insecticides used for ITNs[53] 16

Figure 1.12: SMC treatment in children[60] 17

Figure 1.13: Past antimalarial drugs. 18

Figure 1.14: Antimalarial antifolate[76] 19

Figure 1.15: Antimalarial Aminoquinolines[80] 20

Figure 1.16: Endoperoxides Antimalarials[89,90] 22

Figure 1.17: Mode of action of endoperoxides[94]. 23

Figure 1.18: Clinical drugs for First line malaria treatment[70] 24

Figure 2.1: Nucleotide bases and Coenzymes that contains the heterocyclic nitrogen[116,119]. 29

Figure 2.2: Pyridine and Pyrimidine fused Heterocycles[125,126] 30

Figure 2.3: The Purine Core Structure[132]. 30

University of Ghana http://ugspace.ug.edu.gh

Figure 2.4: Purine-containing biomolecules[132]. 32

Figure 2.5: Clinically used Purine-based drugs[139,145] 33

Figure 2.6: Anti-Cancer activity of purine compounds against PC-3 cell line[148]. 34

Figure 2.7: PU1-1 as KRAS G12D inhibitor[149]. 35

Figure 2.8: Reference Drugs for anticancer evaluation[150]. 35

Figure 2.9: Lamivudine as reference drug and FZJ13 as potent against HIV-1 strain[154] 37

Figure 2.10: Reference drug against HIV-1 protease[153]. 38

Figure 2.11: 2,6-diaminopurine derivative as potent antiviral agent[151]. 39

Figure 2.12: Reference drugs and selected purine derivatives as potent antimicrobial agents[157].40

Figure 2.13: 2,6-disubstituted purine analogs as potent Pf3D7 inhibitors[161] 43

Figure 2.14: The Azaindole core[183] 44

Figure 2.15: Drugs with the pyrrolo pyridine moiety[176]. 45

Figure 2.16: Derivatives of pyrrolo[2,3-b] pyridine and ketoconazole for antimicrobial and antifungal evaluation[186] 47

Figure 2.17: Derivatives of 7-azaindole benzamide for anticancer evaluation[189] 49

Figure 2.18: Plasmodium PI4K inhibitors[197–199]. 51

Figure 2.19: Clinically used drugs with the sulfonamide moiety[204]. 52

Figure 2.20: Potential Drug candidates identified through phenotypic screening[212–214] 54

Figure 3.1: Previous work done on SFK78 57

Figure 3.2: Medicinal Chemistry plan for hit compound **MMV902507** 59

Figure 3.3: Mechanism for Chloro sulfonation. 89

Figure 3.4: Mechanism for sulfonamide formation. 90

Figure 3.5: The mechanism of Suzuki cross coupling step. 91

University of Ghana http://ugspace.ug.edu.gh

Figure 3.6: ^{1}H spectrum of ADA081 92

Figure 3.7: ^{13}C spectrum of ADA081 93

Figure 3.8: ^{1}H spectrum of ADA086 94

Figure 3.9: ^{13}C spectrum for ADA086 95

Figure 3.10: ^{1}H NMR Spectra for ADA090. 96

Figure 3.11: ^{13}C Spectra for ADA090. 98

Figure 3.12: FT-IR data for ADA090 99

Figure 3.13: LC data for ADA090. 99

Figure 3.14: MS data for ADA090. 100

Figure 3.15: A plot of exp. Log D against calc. Log D. 105

Figure 4.1: Previous work done on MMV1900279. 107

Figure 4.2: Mechanism for imidazole formation. 135

Figure 4.3: Mechanism for amide coupling. 136

Figure 4.4: Mechanism of the cyclization reaction. 136

Figure 4.5: Proton NMR data of ADA110 140

Figure 4.6: Carbon NMR spectrum of ADA110. 141

Figure 4.7: FTIR spectrum of ADA110. 142

Figure 4.8: Proton NMR spectra for ADA115. 143

Figure 4.9: Carbon NMR spectra of ADA115. 144

Figure 4.10: Proton NMR spectra of ADA117. 145

Figure 4.11: Carbon NMR spectra of ADA117. 146

Figure 4.12: FTIR chromatogram for ADA117. 147

Figure 4.13: LC spectrum for ADA117 148

University of Ghana http://ugspace.ug.edu.gh

Figure 4.14: MS spectrum for compound ADA117 149

Figure 4.15: A graph of PIC50 against Log D. 151

University of Ghana http://ugspace.ug.edu.gh

List of Tables

Table 2.1: Anticancer activities of synthesized thiopurines by Kowalska et al[150]. 36

Table 2.2: In-vitro IC50 data for analogues against HIV-1 protease[153]..... 38

Table 2.3: Anti bacteria inhibition of 6-[4-(4-prpoxyphenyl) piperazin-1-yl]-9H-purine derivatives[157]. 40

Table 2.4: Anti-Fungal inhibition of 6-[4-(4-prpoxyphenyl) piperazin-1-yl]-9H-purine derivatives[157]. 41

Table 2.5: Selectivity index and IC50 values for synthesized purine analogs[160]. 42

Table 2.6: 2,6-disubstituted purine analogs and their IC50 values[161]. 43

Table 3.1: Structure of synthesized analogues. 86

Table 3.2: Antimalarial activity against 3D7 strain and physicochemical parameters of synthesized analogues. 101

Table 4.1: Structures of compounds. 137

Table 4.2: Anti-plasmodial activity results of the synthesized analogues. 150

INTEGRI PROCEDAMUS

University of Ghana http://ugspace.ug.edu.gh

List of Schemes

Scheme 2.1: Synthesis of 7-azaindole and it's derivatives by Popowycz et.al. (a) LDA, THF, -78 ºC, 2 h then R^1COMe, -78 ºC to rt (b) H_2SO_4/AcOH 1:3,130 ºC, 30 min, 84–98 %; (c) m-CPBA, CH_2Cl_2, rt. (d) R^2NH_2, n-BuOH, 110 ºC, then aq HCl, 63–95 %. 45

Scheme 2.2: Classic Bartoli reaction of nitropyridines to make the 6-azaindole. (a) THF, -78 ºC to -20 ºC, 1 - 16 h, then aq NH_4Cl, 0 ºC 46

Scheme 2.3: Modified Bartoli reaction nitropyridines by Voloshchuk et.al. (a) DMFDMA, DMF 90 ºC - 120 ºC, 0.5 2 h. (b) Pd/C, H_2, MeOH, 50 ºC, 3 days. 46

Scheme 3. 1: Synthesis of derivatives of sulphonamide. Reagents and conditions: a) r.t 1hthen 50 ºC then 1h and110 ºC 1h, b) THF, Et_3N, r.t 12 h, c) Pd(dppf)Cl_2, $NaHCO_3$(aq), 90 ºC 12h. 85

Scheme 4. 1: Reaction scheme for synthesized analogues. a) 1. $HC(OC_2H_5)_3$, reflux 90°C, 40 mins, MeCN, 2. Amine reflux, 95 °C, 40 mins, MeCN, b) Pyridine, K_3PO_4, reflux 70 °C, 8h. c) $C(CH_3)_3OK$, EtOH, 75°C, reflux 16h. 133

INTEGRI PROCEDAMUS

University of Ghana http://ugspace.ug.edu.gh

List of Abbreviations

ACTs. Artemisinin combination therapies

AQ. Amodiaquine

DARC. Duffy Antigen Receptor for Chemokine

DDT. Dichlorodiphenyltrichloroethane

DHA. Dihydro Artemisinin

DHFR. Dihydrofolate reductase

DNA. Deoxyribonucleic acid

FPIX. Ferriprotoporphyrin IX

HBsAg. Hepatitis B surface antigen

IDCs. Intraerythrocytic Developmental Cycles

IRS. Indoor Residual Spraying

ITC. Intermittent treatment for Children

LLITBNs. Long lasting Insecticide treated bed nets

LUM. Lumifantrine

MFQ. Mefloquine

PBO. Pyrethroid-Piperonal Butoxide

PfCSP. *Plamodium falciparum* circumsporozoites protein

*pf*K13. *Plasmodium falciparum* Kelch 13 gene

RBCs. Red Blood Cells

SMC. Seasonal malaria chemotherapy

WHO. World Health Organization

University of Ghana http://ugspace.ug.edu.gh

ABSTRACT

Malaria which is predominant in Sub-Saharan Africa has long existed among individuals globally. According to the WHO malaria report 2024, 263 million cases and 597,000 deaths were recorded globally in 2023, and Africa carried the highest burden. Over the years, efforts by the scientific community to eradicate the disease yielded some results, however, the emergence of resistance to antimalarial drugs has threatened these positive gains as the mortality and morbidity is on the rise in recent times. Therefore, there is the need to find new chemical matter with novel mechanism of action against the parasite. Phenotypic screening is an approach that has been used in drug discovery to find new chemical entities. **MMV902507 (SFK78)** and **MMV1900279** are chemical entities that were identified through phenotypic screening of various chemical libraries. I here in report the chemical modifications of these phenotypic hits and the antimalarial properties, as well as their ADME properties.

The hits (**MMV902507 (SFK78)** and **MMV1900279)** possessed antimalarial activity against the blood and liver stages of the Plasmodium parasite. It displayed no cross resistance against the drug resistant Dd2 strain of the parasite. Overall, 19 compounds based on the **MMV902507 (SKF78)** scaffold were synthesized and characterized using spectroscopic and spectrometric techniques. The synthesized analogues were tested *in vitro* against the sensitive 3D7 strain of the parasite coupled with their solubilities. The compound ADA090 showed similar activity (IC_{50} value of **0.15 µM)** with the hit compound (**0.17 µM**) while ADA097 gave a better solubility of **161.94 µM** compared to the hit compound **MMV902507 (27 µM).** On the other hand, 13 compounds based on **MMV1900279** were prepared. Compound ADA129 showed superior activity of **0.1 µM** against the sensitive strain of the parasite compared to the hit compound **(0.3 µM)** when tested *in vitro* while ADA138 showed better solubility at **998 µM**. ADME evaluation of some selected

University of Ghana http://ugspace.ug.edu.gh

derivatives of **MMV902507** revealed several compounds with superior stability in Human microsomes and rat hepatocytes. Compounds ADA095, ADA096 and ADA097 were metabolically more stable than the hit **MMV902507** with ADA096 as the most stable. Compound ADA096 returned clearance of (Clint Mics 3.5 µL/min/mg) in human microsomes and (Clint Heps 2.7 µL/min/10^{-6} cells) in rat hepatocytes with half-life of 394 min and 361 min respectively. The hit compound on the other hand had (Clint Mics 578 µL/min/mg) in human microsomes and (Clint Heps 85 µL/min/10^{-6} cells) in rat hepatocytes, with half-lives of 3 min and 16 min respectively.

University of Ghana http://ugspace.ug.edu.gh

Chapter 1

1.1 INTRODUCTION

1.2 Malaria

Malaria is one of the most ancient and destructive infections of humans which has over the decades claimed millions of lives annually[1]. It continues to remain a major concern to global health as it predominantly affects children under five years and pregnant women[2]. Some symptoms of uncomplicated malaria include headache, fever, vomiting and profuse sweating[3]. In contrast, for severe malaria, symptoms include fatal lung, liver and kidney damage, severe anemia, cerebral coma and in extreme cases death. In the first trimester of pregnancy, malaria is most likely to cause miscarriage, hypoglycemia, pre-eclampsia and death[4]. Efforts over the decades to eradicate malaria saw a decline in the number of cases and deaths reported annually from 2000 to 2015 when the number of malaria cases began to increase till date **(Figure 1.1)**[5]. Despite the efforts to eradicate the disease, the morbidity remains high in several highly malaria-endemic countries.[2,6] Individuals who are asymptomatic and have low density plasmodial infections tend to transmit the parasite to other individuals unnoticed[4]. These individuals carry the gametocytes of the parasite, which contributes to the transmission of malaria, especially where malaria transmission is low, contributing to the challenge of eliminating the disease[4]. Malaria tends to be more prevalent in tropical areas where mosquito survival is high. Developing countries with a lack of effective medical care, poor housing and sanitation, and areas where stagnant water is predominant, contribute to the survival of the eggs of the mosquitoes that develop into larvae[4].

University of Ghana http://ugspace.ug.edu.gh

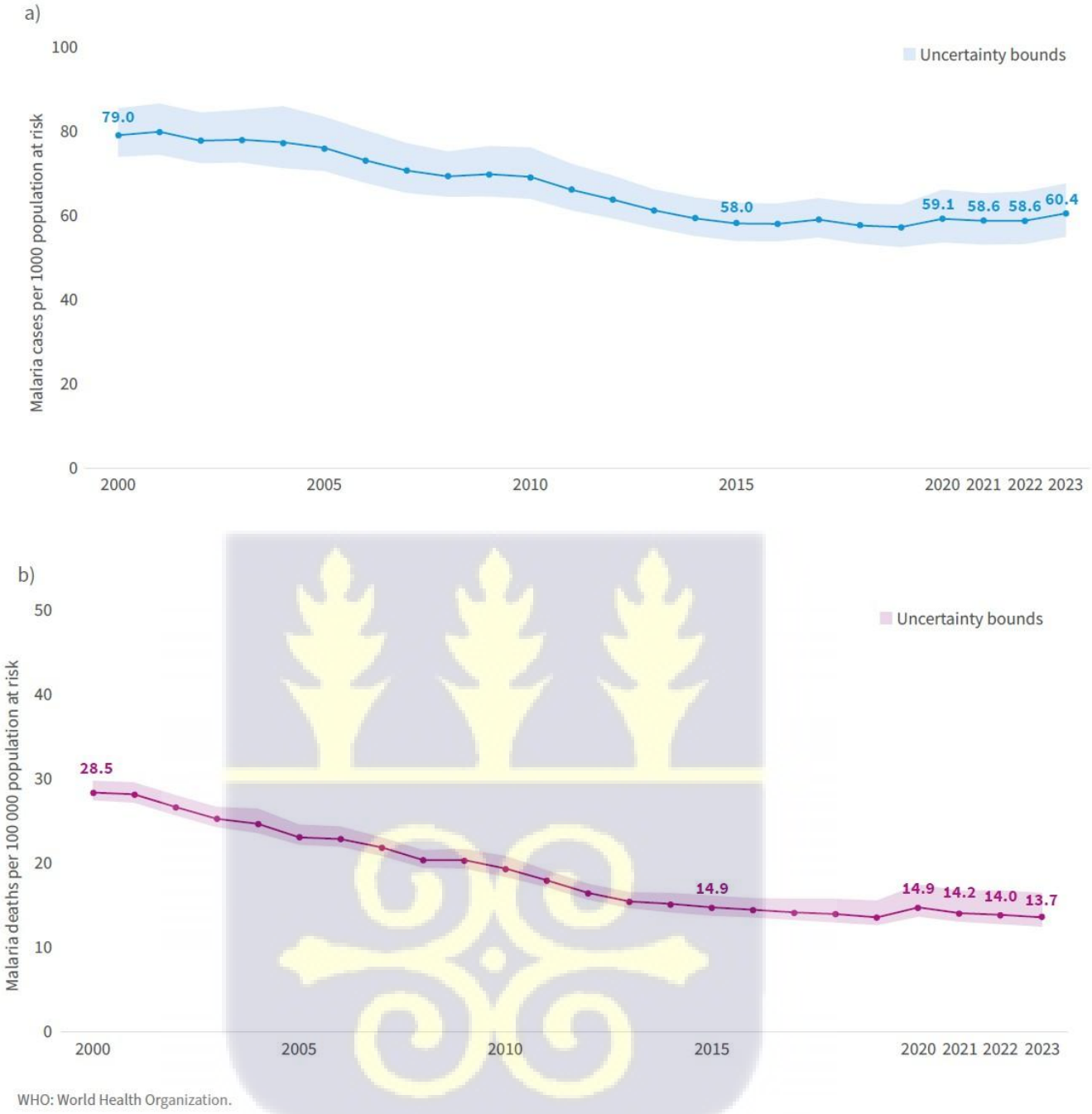


Figure 1.1: Global trends in a) Malaria cases and b) Malaria deaths between the year 2000-2023[5].

1.3 Malaria in Ghana

As a country in West Africa, Ghana is among those mostly affected by malaria. Ghana contributes to the total number of cases recorded in Sub- Saharan Africa each year with pregnant women and

University of Ghana http://ugspace.ug.edu.gh

children under 5 years being the most vulnerable to the disease[7]. In Ghana, malaria is an all-year-round infection with seasonal variations especially in areas with favorable breeding site for the growth of the vector. In 2022, findings from the Ghana Demographic and Health survey showed that malaria prevalence in rural areas was 12.8%[9], three times greater in the urban areas (4.3%)[9]. This can be attributed to the level of income of the inhabitants in the two areas. While those in the urban areas can afford to purchase the antimalarial drugs, those in the rural areas may not. Secondly, differences in knowledge of malaria prevention and treatment in these two sectors of the country could account for the difference in case numbers. For instance, in 2022, while Greater Accra recorded the lowest malaria cases in the country (2%)[9], other regions with more deprived communities such as the Upper East region of Ghana (12.2%), the Upper West of Ghana (13.4%) and Oti region of Ghana (15%)[9] had the highest malaria cases recorded. Also, Bibiani, Anhwiaso and Bekwai municipality in the Western North region of Ghana are considered high risk of the malaria infection because of limited knowledge on malaria prevention and infection[10]. There is still a wide gap in reaching the goal of eliminating the disease in the country and this remains a global health concern.

1.4 Epidemiology

According to the 2024 World Health Organization (WHO) malaria report, there were 263 million malaria cases reported globally in 83 malaria-endemic countries in 2023[5] **(Figure 1.2)**. Comparing the cases recorded in 2023 to that recorded in 2022 (252 million)[11], there was an estimated 11 million case increase in 2023[5]. Five (5) countries, Pakistan (+1.6 million), Ethiopia (+4.5 million), Nigeria (+1.4 million), Madagascar (+2.7 million) and Democratic republic of Congo (+600,000) contributed to the highest surge in Malaria cases in 2023[5].

University of Ghana http://ugspace.ug.edu.gh

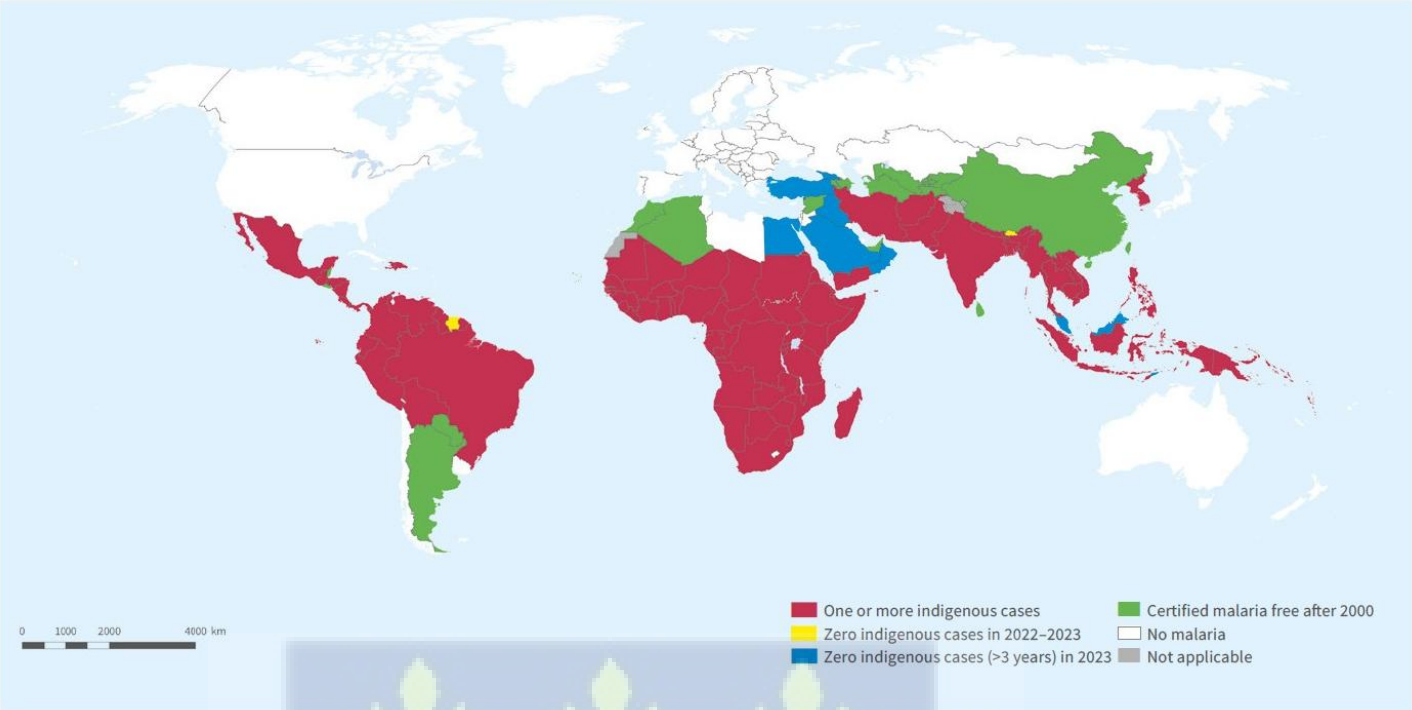


Figure 1.2: Malaria epidemiology[5].

The WHO Africa region had the highest number of malaria cases, with an estimated total of 246 million cases accounting for about 94 % of the total cases recorded globally **(Figure 1.3)**[5]. Five WHO African countries, Nigeria 26 %, Democratic Republic of the Congo 13 %, Uganda 5 %, Mozambique 4 % and Ethiopia 4 % accounted for half of the total number of malaria cases recorded globally[5].

The malaria deaths recorded globally in 2023 was 597,000 and the WHO Africa region attained the lion's share of about 569,000 deaths of the total deaths recorded globally[5]. This accounted for 95% total deaths recorded globally in 2023[5]. Since 2015, the percent deaths in children have been 76 % but declined to 73.7 % in 2023[5].

University of Ghana http://ugspace.ug.edu.gh

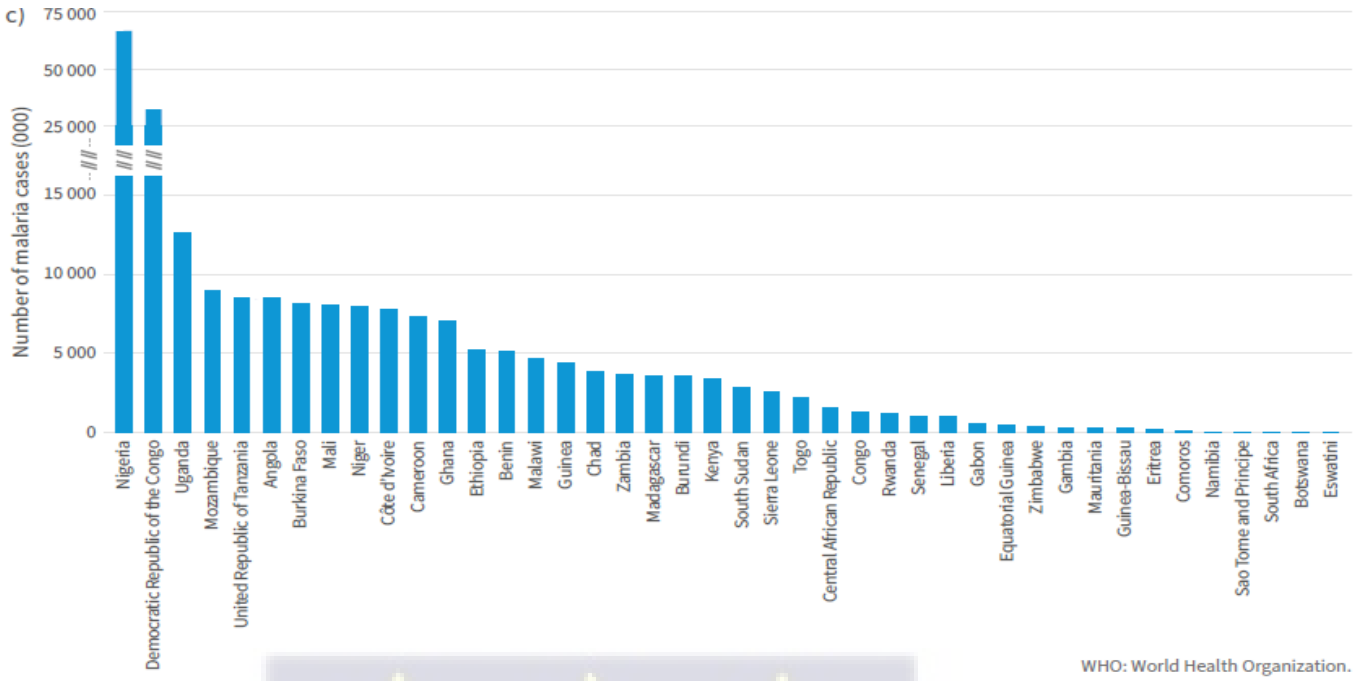


Figure 1.3:Malaria cases in WHO Africa region[5]

1.5 Malaria Parasite

Human malaria is caused by a protozoan belonging to the genus *Plasmodium*[12]. It is an amoeboid intracellular parasite that accumulate insoluble metabolite of hemoglobin[13]. The *plasmodium* genome is carried on a single set of chromosomes, in the mosquito, where meiosis and gene exchange between the homologous chromosomes occur[14]. There are 172 Plasmodium species, but only five (**5**) of them causes human malaria[13]. These include *P. falciparum*, *P. vivax*, *P. malariae*, *P. ovale* and *P. knowlesi* [15]. Among the five species of malaria, *P. falciparum* is the deadliest, however, *P. vivax* is the most predominant especially in the WHO southeast Asia region[16]. *P. falciparum* accounts for nearly 100 % malaria cases and deaths in the WHO Africa region, *P. vivax* accounts for 3.5% of malaria cases globally, while *P. knowlesi, P. malariae and P. ovale* account for >1 % malaria cases recorded globally[5].

University of Ghana http://ugspace.ug.edu.gh

1.5.1 Plasmodium falciparum

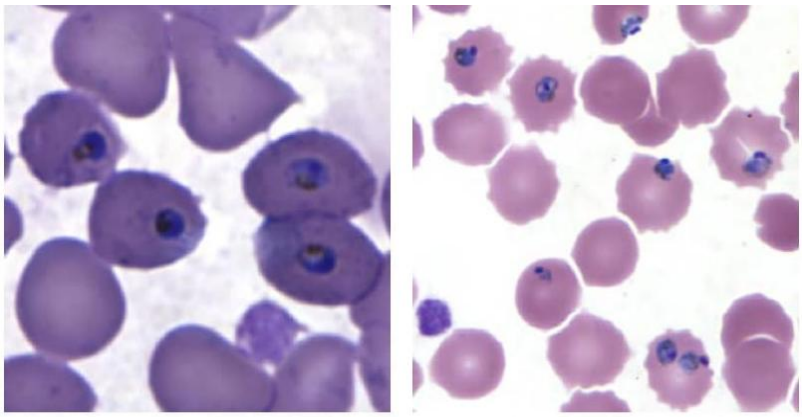
P. falciparum is the deadliest and remains high in economically poor countries, especially in Africa. It was first identified by Ronald Ross in 1880 and was responsible for an estimated 246 million malaria cases in the WHO African region according to the 2024 WHO malaria report[5,17]. It is responsible for 99% of malaria cases in the WHO Africa region and 63% in Southeast Asia[18]. A study of the genome organization of ***P. falciparum*** shows that its nucleosome consists of approximately 155 DNA base pairs around the histone octamer[19] and encodes between at least 5000 to 6000 genes[14,20] that have varying number of sub-telomeric multigene families comprising 14 chromosomes[21].

The parasite undergoes an asexual intraerythrocytic developmental cycle (IDCs) for 48 hours and a sexual stage maturity between 10-12 days to produce 8-30 new parasites[22]. It goes through the trophozoite, Schizont and gametocyte stages. The mature trophozoites **(Figure 1.4)** appear round with brown pigments in their cytoplasm[17] . They are more dense than immature trophozoites which are hardly seen in peripheral blood smears[23].

At the schizonts stage, the mitosis nuclear division and DNA synthesis leads to a multinucleate syncytium and they display 8 to 32 nuclei with dark brown pigments clumped in the middle[24].

INTEGRI PROCEDAMUS

University of Ghana http://ugspace.ug.edu.gh



Mature, compact trophozoites in a thin blood smear.

Compact trophozoites in a thin blood smear.

Figure 1.4: Trophozoites of plasmodium falciparum[17]

1.5.2 Plasmodium vivax

P. vivax* (Figure 1.5)** is the most prevalent Plasmodium species within the WHO region of the Americas, Southeast Asia and the Eastern Mediterranean regions[25]. ***P. vivax requires the Duffy antigen receptor for chemokine (DARC) to invade the red blood cells[26]. It is less prevalent in Africa due to the absence of the red blood cell surface Duffy antigen among Africans[27]. Its genome from sequencing showed 27 megabases that contains 5400 genes, comprising of 14 chromosomes[16]. The granules in the reticulocyte cytoplasm, known as Schnuffner's dots in ***P. vivax***, are small and dark, and they infect 1-2% of the red blood cells in the adult peripheral blood. Their hypnozoites can remain dormant for a period before reactivating[26].

INTEGRI PROCEDAMUS

University of Ghana http://ugspace.ug.edu.gh

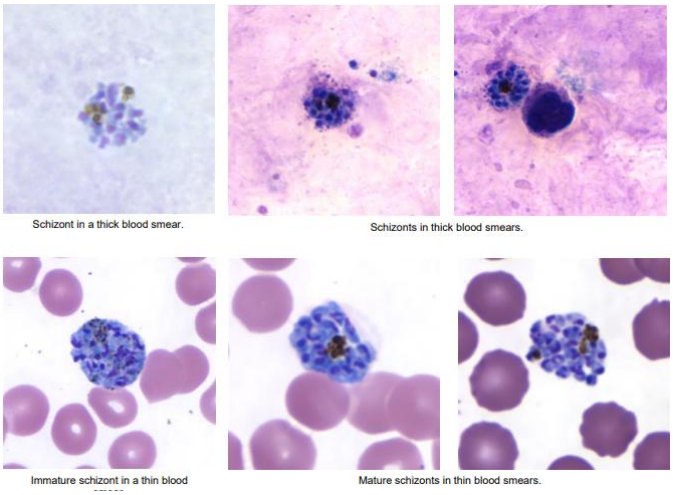


Figure 1.5: Schizonts of P. vivax.[28]

1.5.3 Plasmodium malariae

P. malariae **(Figure 1.6)** is a species of the parasitic protozoan that causes malaria and was discovered in 1880. It causes Quartan, tertian and semi tertian patterns of fever in malaria patients[29]. It is frequently endemic with ***P. falciparum*** in sub-Saharan Africa, south America, Indonesia, southeast Asia and the western pacific[30] and studies have shown that 7.4 % of ***P. malariae*** infections in these regions were mixed with ***P. falciparum*** infections. A study of the genome shows that it's trophozoite have a compact cytoplasm and a large chromatic dot and they produce 6 to 12 merozoites with a large nucleus[31].

University of Ghana http://ugspace.ug.edu.gh

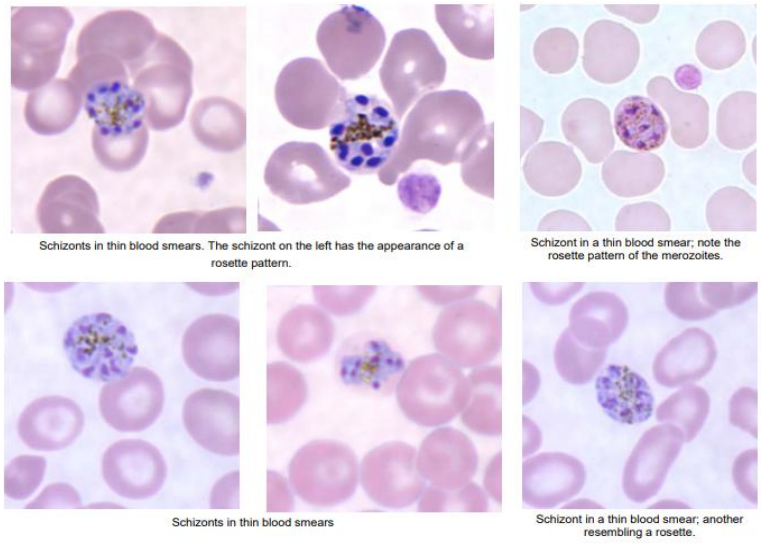


Figure 1.6: Sporozoites of P. malariae[32].

1.5.4 Plasmodium ovale

P. ovale **(Figure 1.7)** was discovered in 1922 and is endemic to WHO regions of southeast Asia and central and west Africa[33]. It is a non-falciparum malaria with disease causing sub-species which are ***P. ovale curtisi*** and ***P. ovale walkiri***. Similar to those found in ***P. vivax***, ***P. ovale*** parasites are found in enlarged stiped red blood cells and a blood film of this parasite is between 0.7 % and 10 %[34].

The trophozoites have sturdy cytoplasm and large chromatin dots with round gametocytes which fills two fluids of the red blood cells. Studies have shown that their schizonts contain 6 to14 merozoites with usually 8 in a single ring with brown pigments in the central clump[35].

INTEGRI PROCEDAMUS

University of Ghana http://ugspace.ug.edu.gh

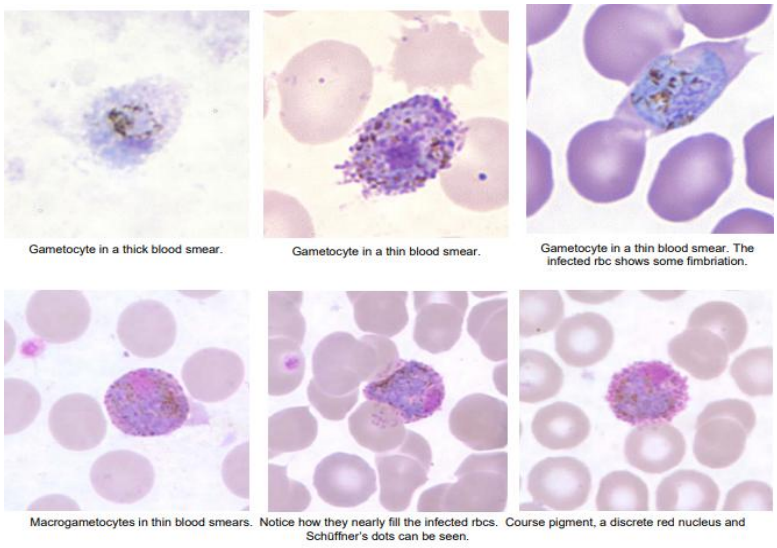


Figure 1.7: Gametocytes of p. ovale[35].

1.5.5 Plasmodium knowlesi

P. knowlesi **(Figure 1.8)** was first described by Knowles and Gupta in 1932[36]. It is endemic to Malaysia and part of southeast Asia causing severe infections and deaths especially in children below 15 years of age and like ***P. vivax***, it also requires the Duffy antigen receptor for chemokine (DARC) to invade the red blood cells. During the early trophozoite stage, it shows double chromatic dot features without the enlargement of the infected erythrocytes[37].

INTEGRI PROCEDAMUS

University of Ghana http://ugspace.ug.edu.gh

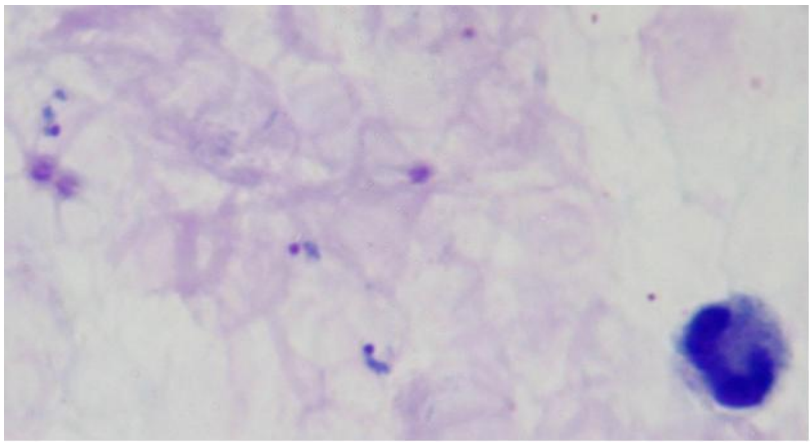


Figure 1.8: Trophozoites of P. knowlesi[38].

1.5.6 Life Cycle of Plasmodium Parasite

The plasmodium species that causes malaria alternates between the human host and mosquito with its sexual phase in the mosquito[39] **(Figure 1.9).**

During the Asexual stage transmissive forms of sporozoites is injected into the skin of a human host by the female anopheles' mosquito during a blood meal[40]. The sporozoites enter the blood stream and circulate to the liver to escape drainage by the lymphatic system[41 40]. The sporozoites cross sinusoidal barrier and invade the hepatocytes where they multiply and differentiate into schizonts with many hepatic merozoites[42]. The merozoites are released into the blood where the erythrocytic stage is initiated by invading the red blood cells (RBCs)[42].

Schizogony occurs and produces about 32 merozoites within 24 to 72 hours[40] forming a multinucleated exoerythrocytic schizont that contains thousands of daughter cells which multiplies to form more merozoites. Some of which differentiate into gametocytes to ensure parasite transmission to the mosquito vector to begin the sexual phase[42].

University of Ghana http://ugspace.ug.edu.gh

The mature gametocytes can remain in the blood of the human host for several days and this can increase the chance of being transmitted into the mosquito vector. The gametocytes enter the female anopheles' mosquito during feeding to begin the sexual phase, and both the male and the female gametocytes use protease to leave the mid gut where they differentiate into eight microgametes and one macrogamete[41,43]. They produce the zygote and the zygote transforms into a motile ookinete which crosses the epithelial layer of the midgut wall to form the oocyst[41].

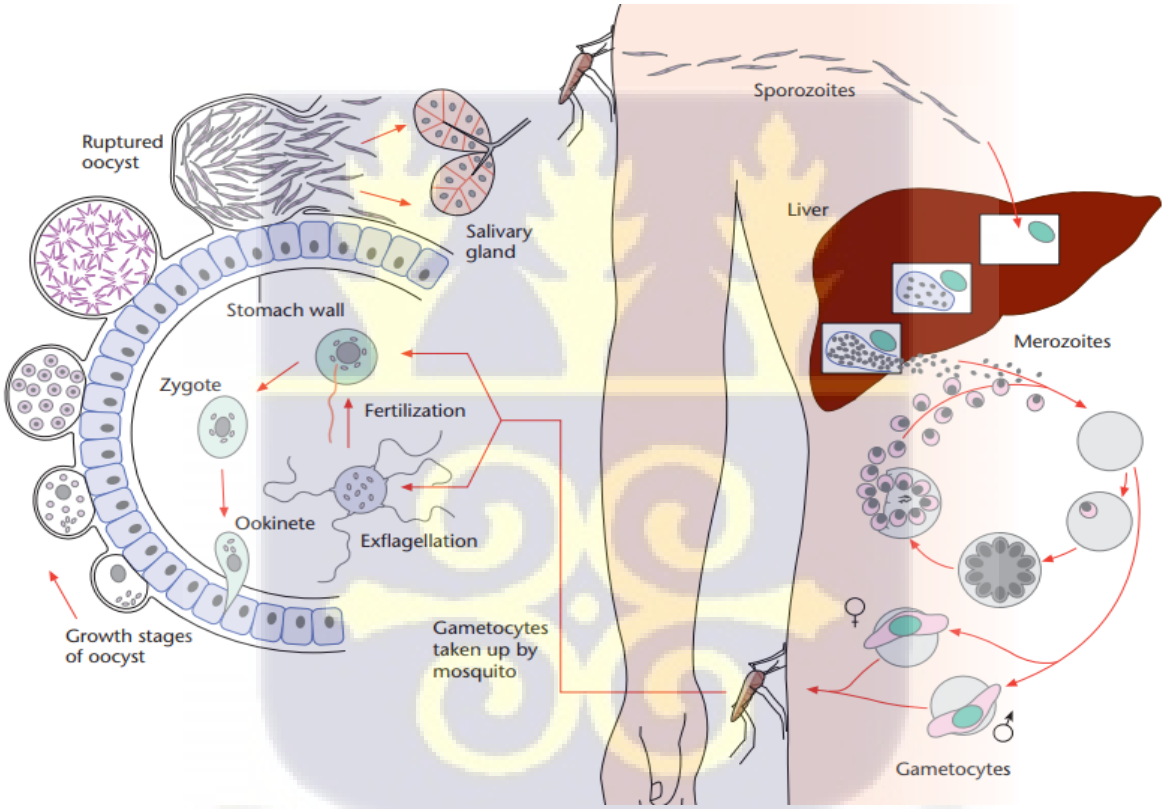


Figure 1.9: Life cycle of the Plasmodium parasite[41]

The parasite undergoes an asexual multiplication in the oocyst to form many motile sporozoites which are released into the hemolymph[41,43]. The mature sporozoites enter the salivary glands of the mosquito and remain there until transmitted into a human host then the cycle begins again[42].

University of Ghana http://ugspace.ug.edu.gh

1.6 Malaria Prevention

In the quest to eradicate malaria from endemic regions such as Africa, Asia and parts of the Americas, several strategies have been implemented to prevent its spread[44]. Organizations such as the WHO and the Medicines for malaria ventures (MMV) supports the fight against malaria by delivering medicines to treat, prevent and eliminate malaria[44]. MMV also contributes to malaria chemoprevention by supporting next generation preventive drug research and development[44]. Malaria prevention has been accomplished by means of vector control, chemoprevention and vaccines[45]. It is estimated that in 2022, 62 million malaria cases were averted due to preventive measures and vector control strategies adopted [46].

1.6.1 Vector Control

Over the decades, vector control has been the most effective and necessary strategy for combating malaria, especially in malaria-endemic regions such as sub-Saharan Africa and some of Asia[46]. Some vector control measures include the widespread use of insecticides such as DDT (Dichlorodiphenyltrichloroethane), larvicides such as *Bacillus thuringierisis serovariety israelensis* and *Bacillus sphaericus* [47] which are biological agents. Insect-killing viruses are non-toxic to humans and are highly effective in killing the anopheles mosquito. Also, genetically modified mosquitoes carry effector genes whose expression impairs the development of the malaria parasite, making the mosquitoes resistant to *Plasmodium falciparum*[48].

Indoor residual spraying, sleeping under long-acting insecticide-treated bed nets and sanitation practices such as clearing drainages and mosquito breeding sites have been utilized to reduce the spread of the infection and eliminate the disease[49]. Although these practices have led to a decrease

University of Ghana http://ugspace.ug.edu.gh

in malaria morbidity and mortality rate over the past decade, effort is still needed to eliminate the transmission of the disease.

1.6.1.1 Indoor Residual Spraying (IRS)

To be successful at eliminating malaria and other vector-borne diseases, strategies must be developed to eliminate vectors such as mosquitoes, sand flies and triatomine bugs[50]. Indoor residual spraying (IRS) which is a vector control method, is one of the strategies recommended by the WHO to eradicate the mosquito vector[5,51]. It involves the application of long-lasting insecticide to an enclosed vector resting environment such as buildings of human dwelling[51,52]. The phenomenon is that when the vector comes into contact with the insecticide, a lethal dose is absorbed, leading to its death[51]. After spraying, the insecticide can remain active for at least 1 year[53]. The IRS has significantly contributed, from the 1940s to date to the eradication of malaria[50]. For instance, Organophosphates such as malathion **1** and Temephos **2**, **Figure 1.10** were used in the 1940s for IRS[54]. However, pyrethroid-based insecticides such as Lambda-cyhalothrin **3**, Cypermethrin **4** and etofenprox **5**,[54] **Figure 1.10** have been used currently for IRS although there have been some reports of vector resistance in 55 endemic countries[5,55].

University of Ghana http://ugspace.ug.edu.gh

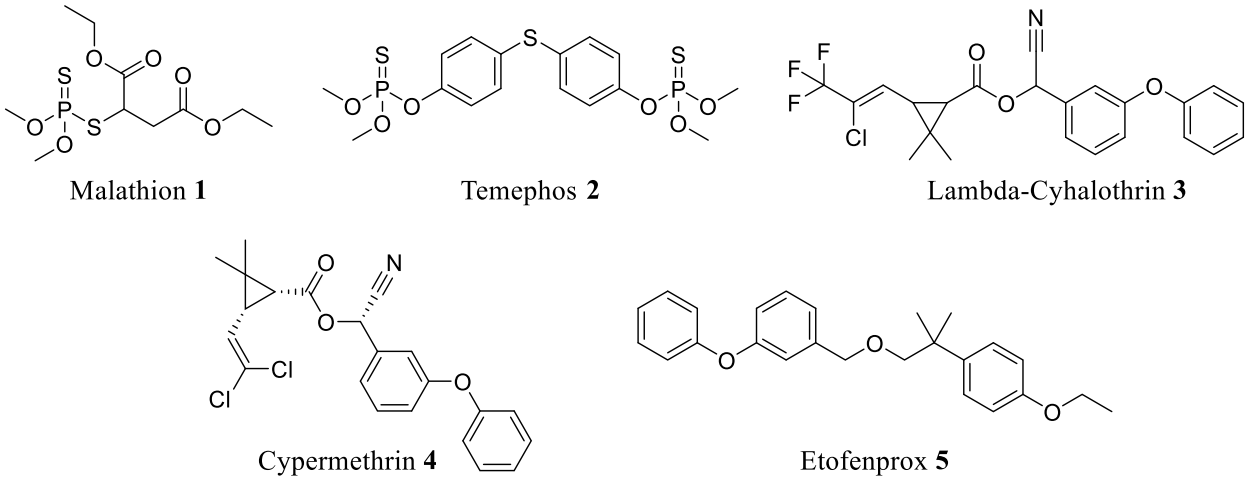
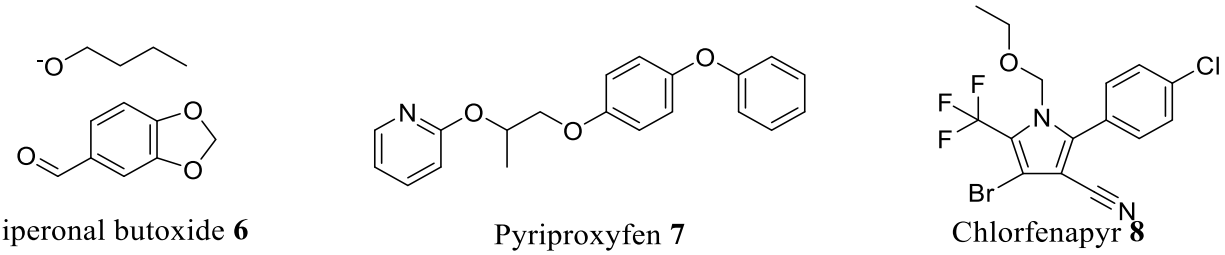


Figure 1.10: Insecticides used for Indoor Residual Spraying (IRS)[54].

1.6.1.2 Long-Lasting Insecticide Treated Bed Nets (LLITBNs)

The distribution of long-lasting insecticide-treated bed net (LLITBN) is also another vector control method that is recommended by the WHO. It is a significant vector control method because it can be used for 3 to 5 years after distribution without losing its efficacy unlike IRS which stays active for at best a year[53]. Its distribution is not an entirely complicated process as it can be distributed from vantage locations such as community health care centers[53,55]. In 2023, a total of 255 million insecticide treated nets (ITNs) were distributed to malaria endemic countries globally[5]. 58 % of ITNs were pyrethroid-piperonal butoxide (PBO) **6** nets, 22 % were standard nets while 20 % constituted dual active ingredients ITNs[5]. Dual active ITNs comes in two types, Pyrethroid-Pyriproxyfen **7** and Pyrethroid-Chlorfenapyr **8**,[56] **Figure 1.11**. They were developed to control pyrethroid resistance in the malaria vector[56].

University of Ghana http://ugspace.ug.edu.gh



Piperonal butoxide **6** Pyriproxyfen **7** Chlorfenapyr **8**

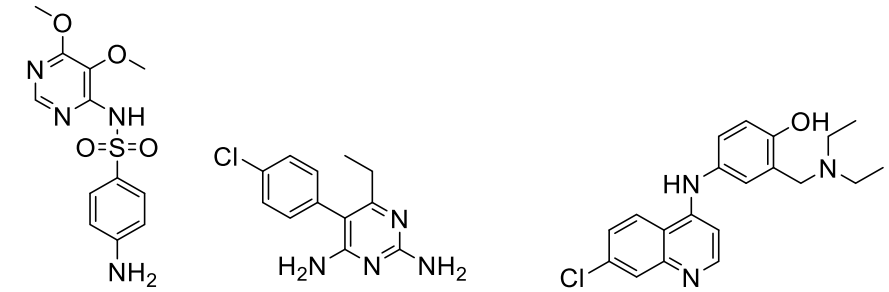
Figure 1.11: Insecticides used in Insecticide Treated Nets (ITNs)[56].

1.6.2 Malaria Chemoprevention

Malaria chemoprevention is an efficacious method that has been used to administer medicines to individuals in high-risk malaria endemic regions[57]. It is focused on the intermittent presumptive treatment in pregnant (IPTsp) women, intermittent treatment in children (ITC) and seasonal malaria chemoprevention (SMC)[45]. Sulfadoxine **9** and pyrimethamine **10** (**Figure 1.12**) are the approved drugs by WHO for administering IPTs in pregnant women. It is done monthly and has been successful in reducing the risk of infection, reducing miscarriages in pregnant women[58]. Intermittent presumptive treatment of drugs such as Sulfadoxine-Pyrimethamine[59] is administered to infants in countries where there is low to moderate malaria occurrence[60].

Seasonal malaria chemotherapy, also known as intermittent presumptive treatment in children[61] is administered to children in the WHO Sahel region, where recurrent threat of malaria is high and transmission is highly seasonal[57,60]. Sulfadoxine pyrimethamine with amodiaquine **11**, (**Figure 1.12**) is the drug administered in SMC to children between 3 and 59 months of age [45,60,62].

University of Ghana http://ugspace.ug.edu.gh



Sulfadoxine **9** Pyrimethamine **10** Amodiaquine **11**

Figure 1.12: Recommended drugs for SMC treatment in children and pregnant women[63].

1.6.3 Malaria Vaccines

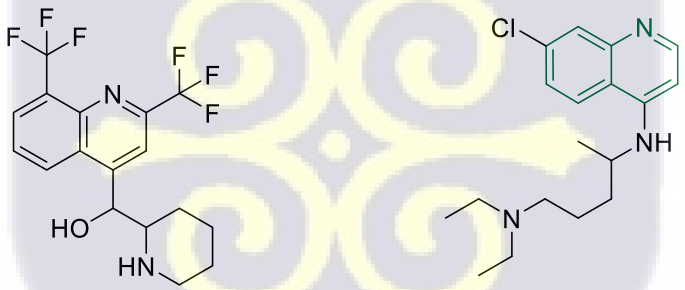
Vaccination is the most efficacious strategy for preventing malaria infection[64]. In 2021, the WHO approved the most advanced pathogen-based vaccine RTS, S[65] which is currently being used to provide partial protection of about 30 % to 50 % against severe malaria in children during clinical trials[64,65]. The RTS, S vaccine is a hepatitis B virus-like particle that contains generally fused portion of repeated domain (B-Cell epitopes) and the C- terminal (T-cell epitopes) of the circum-sporozoite protein of the 3D7 lab strain[66,67]. The Sporozoite-invasion associated protein 2 (SIAP2) in Plasmodium falciparum is located on the surface of the sporozoite that has the host cell interaction regions and hence the RTS, S vaccine targets the *Plasmodium falciparum* circum-sporozoites protein (PfCSP) and kills the parasite at the pre-erythrocytic stage[68,69]. It has been observed that the efficacy of the RTS, S vaccine reduces as the children grow older from about 78% in children between 6 and 12 weeks to 28% in children between 1-5 years[68]. This reduction in efficacy has been attributed to the decrease in the levels of the anti-CSP antibodies[68]. Also, a new vaccine, the R21/Matrix M vaccine, has recently been recommended by the WHO, for malaria prevention in children. The R21/Matrix M vaccine contains recombinant particles of the central repeat and the C-terminal circum-sporozoite protein fused to the hepatitis B surface antigen

University of Ghana http://ugspace.ug.edu.gh

(HBsAg)[70]. Its improved efficacy is due to high density of CSP antigen on the VLP surface[70]. It is safe to administer to children, cost effective, and has been shown to reduce 75 % of symptomatic malaria cases in clinical trials[71].

1.7 Antimalarials and their Mode of Action

Malaria, which has been a global burden since the 18th century is curable using antimalarials. In 1820, quinine was isolated and used to treat malaria until the parasite developed strains resistant to quinine[3]. Also, between 1940 and 1970, antimalaria drugs such as chloroquine **12**, mefloquine **13** (**Figure 1.13**), as well as other drugs with similar structural motifs were developed to combat malaria. But by the late 90s, these drugs were no longer in use or were repurposed for other uses[13,72]. In the early 2000s, Artemisinin and its derivatives were developed and approved for use as first-line treatment for uncomplicated malaria[72]. These antimalaria drugs are grouped into classes such as **Antifolates**, **Amino quinolines** and **Endoperoxides**, based on their structural similarities and their mode of action[73].



Mefloquine **13** Chloroquine **12**

Figure 1.13: Antimalarial drugs that have been repurposed.

University of Ghana http://ugspace.ug.edu.gh

1.7.1 Antifolates

This class of antimalarials is used for the treatment of uncomplicated malaria and are also used as chemoprophylaxis[74]. They inhibit the function of the dihydrofolate reductase (DHFR) enzyme in the parasite's folic acid pathway, leading to the parasite's death. Examples of antimalarial drugs which fall under this class include pyrimethamine **10** and proguanil **14**[74,75] (**Figure 1.14**). DHFR is an enzyme found in both humans and the Plasmodium parasite, but unlike the human orthologue, the DHFR in the parasite binds strongly to antifolates, leading to the disruption of folate synthesis in the Plasmodium parasite.

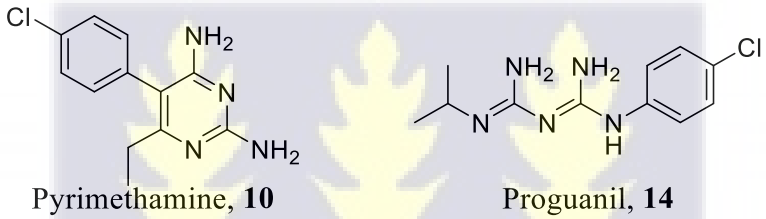


Figure 1.14: Antifolate drugs used as antimalarials[75]

1.7.1.1 Mode of Action of Antifolates

DHFR catalyzes the reactions required for the synthesis and salvaging of folate cofactors, which are important for the synthesis of thymidylate which forms d-TMP from UMP[75]. It is responsible for reducing dihydrofolate to tetrahydrofolate[76]. Antifolates inhibit the activity of the dihydrofolate reductase (DHFR) and dihydropteroate synthetase (DHFS) which deprives the parasite of these folate cofactors which are essential for producing purine and pyrimidine bases for its DNA replication and other metabolic conversions[77].

University of Ghana http://ugspace.ug.edu.gh

1.7.2 Aminoquinolines

These class of antimalarials are weak bases that were first used in the treatment of malaria in the 18th century[78]. A common aminoquinoline that was of high importance was quinine **15** which was first isolated form the bark of the cinchona tree in the 1820s[79]. In the early 1930s, other derivatives of this class of compounds such as chloroquine **12** was discovered and used to treat malaria[80]. Aminoquinolines are grouped into two; the 4-aminoquinolines which includes; Amodiaquine **11**, chloroquine **12**, quinine **15,** quinidine **16,** and Piperaquine **17**[81] and the 8-aminoquinolines which also include primaquine **18,** tafenoquine **19** and pamaquine **20**[73] (**Figure 1.15**). The 4-aminoquinolines, especially Chloroquine **12** have been of much importance, unlike the 8-aminoquinolines, because they provide high efficacy, are affordable and have few side effects[73,78]. Although the mode of action is not well explained, studies have shown that the mechanistic pathway of this class of antimalarials is to interfere in the heme detoxification pathway of the parasite which leads to its death[82].

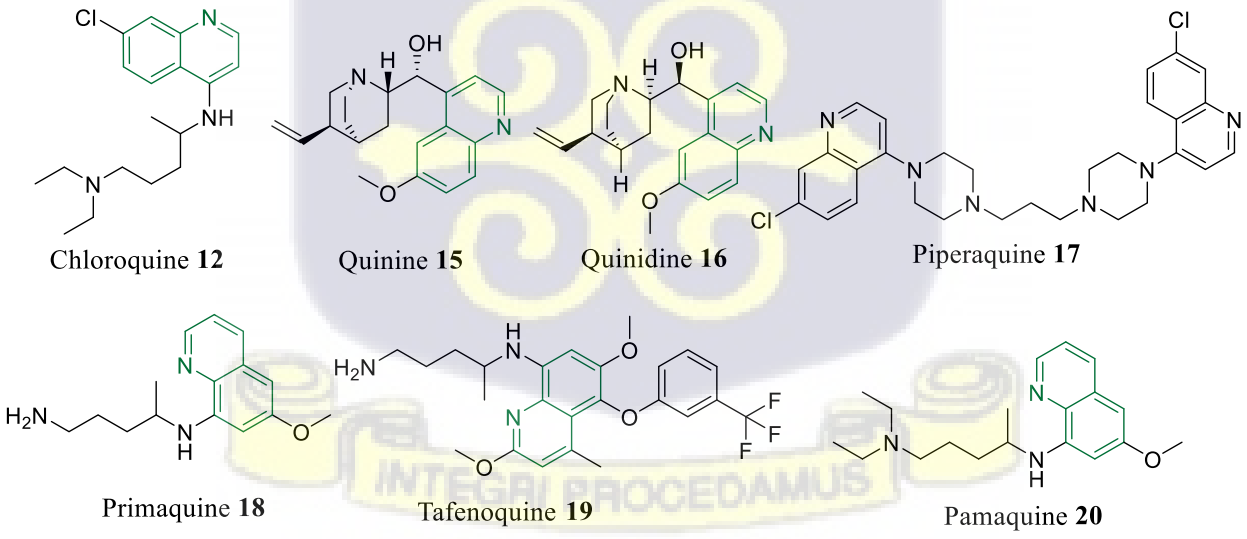


Figure 1.15: Aminoquinolines compounds used as Antimalarial drugs [79]

University of Ghana http://ugspace.ug.edu.gh

1.7.2.1 Mode of Action of Aminoquinolines

There have been several schools of thought regarding the mechanism of action of aminoquinolines. It was thought that due to the fundamental nature of aminoquinolines, they concentrate in the acidic organelles of the intraerythrocytic stages of the parasite because of the pH gradient between the acidic digestive vacuole and the extracellular medium[79]. The accumulation of the aminoquinolines in the food vacuole raises the pH the parasite's requirements, leading to its death[83]. In another consideration, Chou et al. described that the aminoquinolines inhibit the formation of hematin by complexing with ferriprotoporphyrin IX (FPIX)[82] in heme hence preventing it from polymerizing into the non-toxic insoluble polymer known as hemozoin in the heme detoxification mechanism leading to the death of the parasite[80].

1.7.3 Endoperoxides

Endoperoxide antimalarials are drugs that are known to contain a peroxide bridge within the compound[84]. Antimalarials that fall under this class include Artemisinin **21,** Artemether **22,** Artesunate **23** (**Figure 1.18**), Arteether **24**[85], Artelinate **25**[86], and Artemisone **26**[85], (**Figure 1.16**). These are also known as first-generation endoperoxides[85,86] and they combat plasmodium parasites in two steps; the first step, which is the formation of free radicals, followed by a second step, which is an alkylation of the free radicals that causes cell damage and eventually the death of the parasite[87]. While endoperoxide antimalarials such as Artemisinin **20** have short half-lives, they are known to clear peripheral blood of parasites more rapidly than other available drugs[85].

INTEGRI PROCEDAMUS

University of Ghana http://ugspace.ug.edu.gh

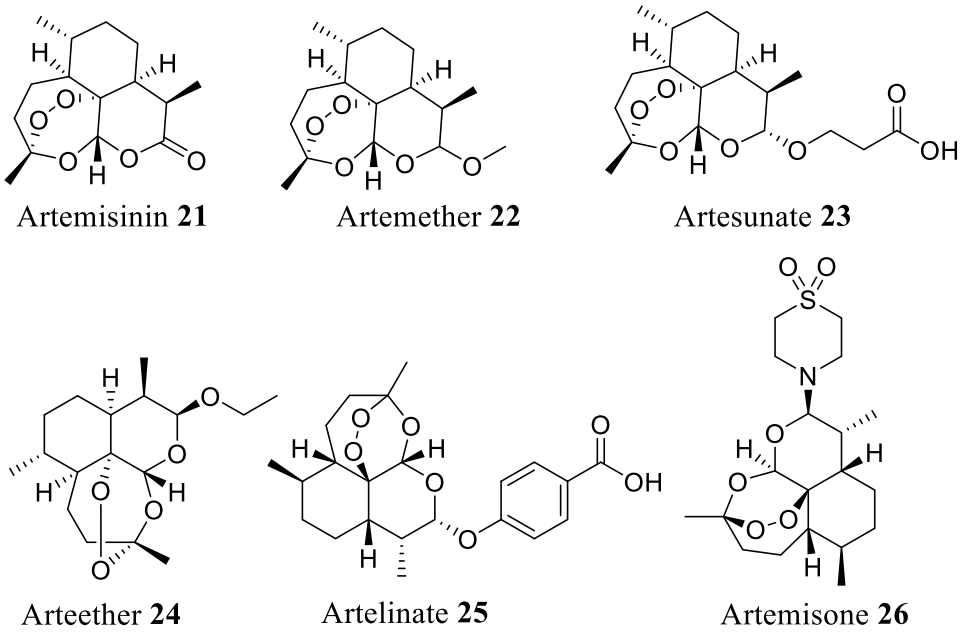


Figure 1.16: Endoperoxides as class of Antimalarials[88,89].

1.7.3.1 Mode of action of Endoperoxide

The first step of the mode of action of this class of antimalarials involves an iron- mediated cleavage of the endoperoxide bridge which is from the reaction of these endoperoxides with the iron in heme to generate a free radical[84,90]. This is analogous to the Fenton reaction where iron catalyzes the homolysis of hydrogen peroxide to produce radicals[91]. The second step is an alkylation which involves the formation of a covalent adducts[92] between the drug and target proteins in the plasmodium parasite, causing oxidative stress within the parasite and leading to its death[93] (**Figure 1.17**).

University of Ghana http://ugspace.ug.edu.gh

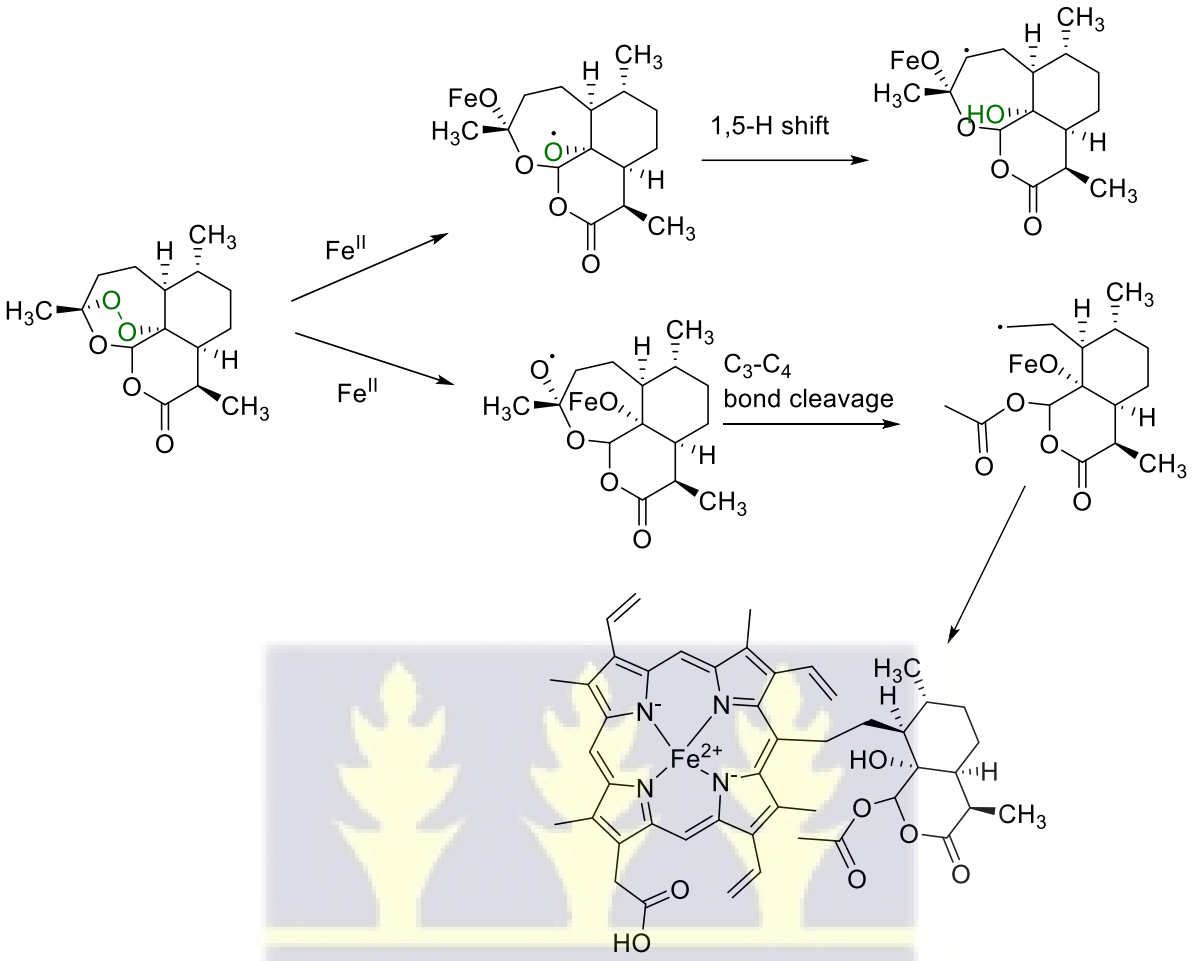


Figure 1.17: Mode of action of endoperoxides[93].

1.8 Malaria Chemotherapy

Artemisinin **21** (ART) is currently used in the treatment of malaria in malaria endemic regions as first line malaria drugs. It is used in combination with partner drugs (ACTs) that have longer half-lives than the artemisinin derivatives[94].

Artemisinin combination therapies (ACTs) that the WHO has approved are the artemether (ATM) **22**, artesunate (AS) **23** and dihydro artemisinin (DHA) **27** in combination with lumefantrine (LUM) **28,** amodiaquine (AQ) **11,** mefloquine (MFQ) **13,** pyronaridine (PYR) **29,** piperaquine (PQP) **17 (Figure 1.18)**[95,96]**.** ACTs such as artemether-lumefantrine or artesunate-amodiaquine

University of Ghana http://ugspace.ug.edu.gh

has been recommended by the WHO as first line treatment for uncomplicated *P. falciparum* malaria[97]. However, ACTs have shown some resistance to *P. falciparum* in Africa but continuous to be effective in other malaria endemic regions in which *P. falciparum* is not prevalent[95].

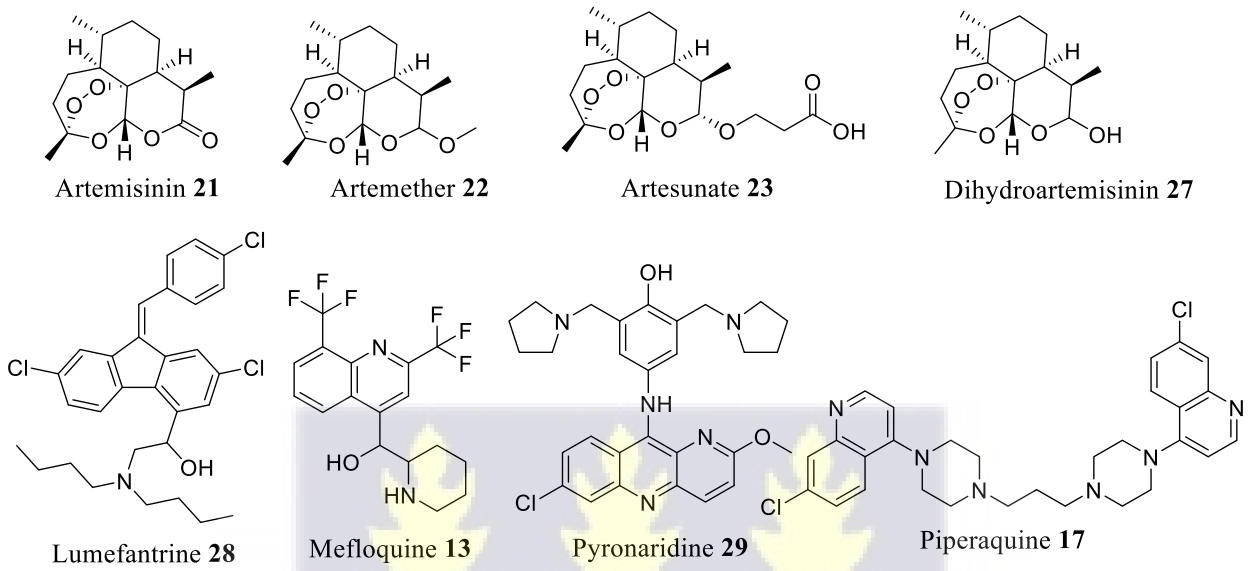


Figure 1.18: Clinical drugs for First-line malaria treatment[95]

1.9 Plasmodium Resistance

The issue of Plasmodium resistance to existing antimalarial drugs has been a major concern for over three decades[98]. It still is a major concern as *P. falciparum* has been reported to be resistant to the current treatment for uncomplicated malaria, which is the artemisinin combination therapy (ACTs) leading treatment failure[99]. Chloroquine which was used in the early 1940s to treat malaria was reported to be ineffective against *P. falciparum* malaria in sub-Saharan Africa in the 1970s which caused a drastic increase in the mortality rate in Africa[100]. This parasite resistance was due to a gene mutation that encodes the *Plasmodium falciparum* Chloroquine resistance transporter protein (*Pf*-CRT) and results in a K76T[101]. The widespread resistance to chloroquine led to its cessation of use in most part of Africa[100,102] which prompted the introduction of antifolate

University of Ghana http://ugspace.ug.edu.gh

antimalarials[103]. The introduction of antifolates antimalarials was very relieving at the time as they had a different mechanism of action and were effective antimalarials[104]. Unfortunately, shortly after the antifolates were recommended for the treatment of malaria, resistance to the drugs by the parasite was recorded[105]. The resistance was due to mutations at Ser108Asn, leading to decreased binding of antimalarial antifolates, followed by mutations at other positions leading to higher parasite resistance[103]. Currently, the ACTs, which are used as first-line treatment for malaria, have been reported to be partially ineffective due to resistance in Southeast Asia and some parts of Sub-Saharan Africa[106]. ACTs' resistance has been attributed to mutations in *P. falciparum* Kelch 13 (*pf*K13) gene which are associated with prolonged clinical parasite clearance and are involved in the endocytosis of hemoglobin required for the parasite growth in red blood cells[107,108]. The *pf*K13 gene is a 726 amino acid protein that has a similar sequence to a class of Kelch/ BTB/POZ adaptation ubiquitination and has 6 β-propeller Kelch domains and mutations and among these, C580Y has been particularly used to monitor artemisinin resistance[109]. Resistance to ACTs can be detected using the trophozoites inhibition maturation assay or the Ring Survival assay with a parasite survival rate of ≥ 1%[107,108]. Artemisinin resistance was first reported in Cambodia, which later spread to the Greater Mekong subregion and is currently detected in some parts of Africa, such as Uganda, Angola and Democratic Republic of Congo, with a 50 % failure to cure malaria after the administration of the ACTs in Southeast Asia [110–112]. Studies have shown that a 30 % increase in the resistant rate of Artemisinin, results in 20 % increase in mortality. This will be catastrophic especially for individuals in sub-Saharan Africa where the disease is most predominant[109].

University of Ghana http://ugspace.ug.edu.gh

1.10 Problem Statement

Malaria, a destructive infectious disease on humans, continues to thrive in countries with poor economic growth. Despite the efforts made in eradicating the disease and the positive gains over the years, the disease still affects over 200 million people and claims over 600,000 lives each year. Despite rolling out the RTS'S vaccine and the R21 Matrix M, there is still no 100 % effectiveness of these vaccines which therefore, possess a risk to children. The reduced efficacy of ACTs reported in Southeastern Asia and some parts of Africa has been attributed to the resistance of the *Plasmodium falciparum* Kelch 13 gene mutation. This threatens the goal of malaria elimination especially in Sub-Sahara Africa. A concerted effort is therefore required including the development of drugs with a novel mechanism of action against the parasite to eradicate the disease.

1.11 Hypothesis

Previous work on the two phenotypic hit compounds, SFK78 and MMV1900279, from the Bio focus library and the Bayer Library respectively, has shown antimalarial activity against *P. falciparum.* Further exploration of the structure-activity and structure-property relationships via chemical modifications of the two scaffolds could improve the potency and physicochemical properties, making it a suitable candidate for further development.

1.12 Aim

To design, synthesize, characterize and evaluate the antimalarial activity and ADME properties of analogues of SFK78 and MMV1900279.

1.13 Specific Objectives

1. To synthesize derivatives of SFK78 and MMV1900279.

University of Ghana http://ugspace.ug.edu.gh

2. To characterize the derivatives using spectroscopic and spectrometric techniques such as NMR and LCMS.
3. To determine their physicochemical properties such as solubility and log P.
4. To evaluate the *in vitro* antimalaria activity of the synthesized derivatives against the 3D7 and the Dd2 strains of *Plasmodium falciparum*.
5. To evaluate the *in vitro* ADME (cytotoxicity and Clearance) properties of the synthesized derivatives.
6. Investigate any emerging SAR/SPR.

University of Ghana http://ugspace.ug.edu.gh

Chapter 2

Literature Review

2.1 Nitrogen Heterocycles

Nitrogen-containing heterocycles are widely distributed in nature and continue to contribute extensively to drug discovery and development because of their broad range of applications[113,114]. In nature, they are the building blocks of life and the constituents of DNA and RNA[113], which are components of biological processes. Nucleic acid bases such as adenine **1**[115], guanine **2**[115] and cytosine **3**[115] (**Figure 2.1**) contain the pyrimidine and purine moiety[116], which are nitrogen heterocycles and are crucial to the mechanism of replication in the biological system[117]. Essential diet ingredients such as thiamin **4**[118], riboflavin **5**, Pyridoxol **6**[117] and nicotinamide **7**[119] (**Figure 2.1**) also possess nitrogen heterocycles such as pyrimidine and pyridine in their structure [114]. Some nitrogen heterocycles are important functional groups in various coenzymes such as Biotin **8**, Pyridoxal phosphate **9** and Tetrahydrofolate **10** (**Figure 2.1**) which mediate primary metabolic transformations[120].

University of Ghana http://ugspace.ug.edu.gh

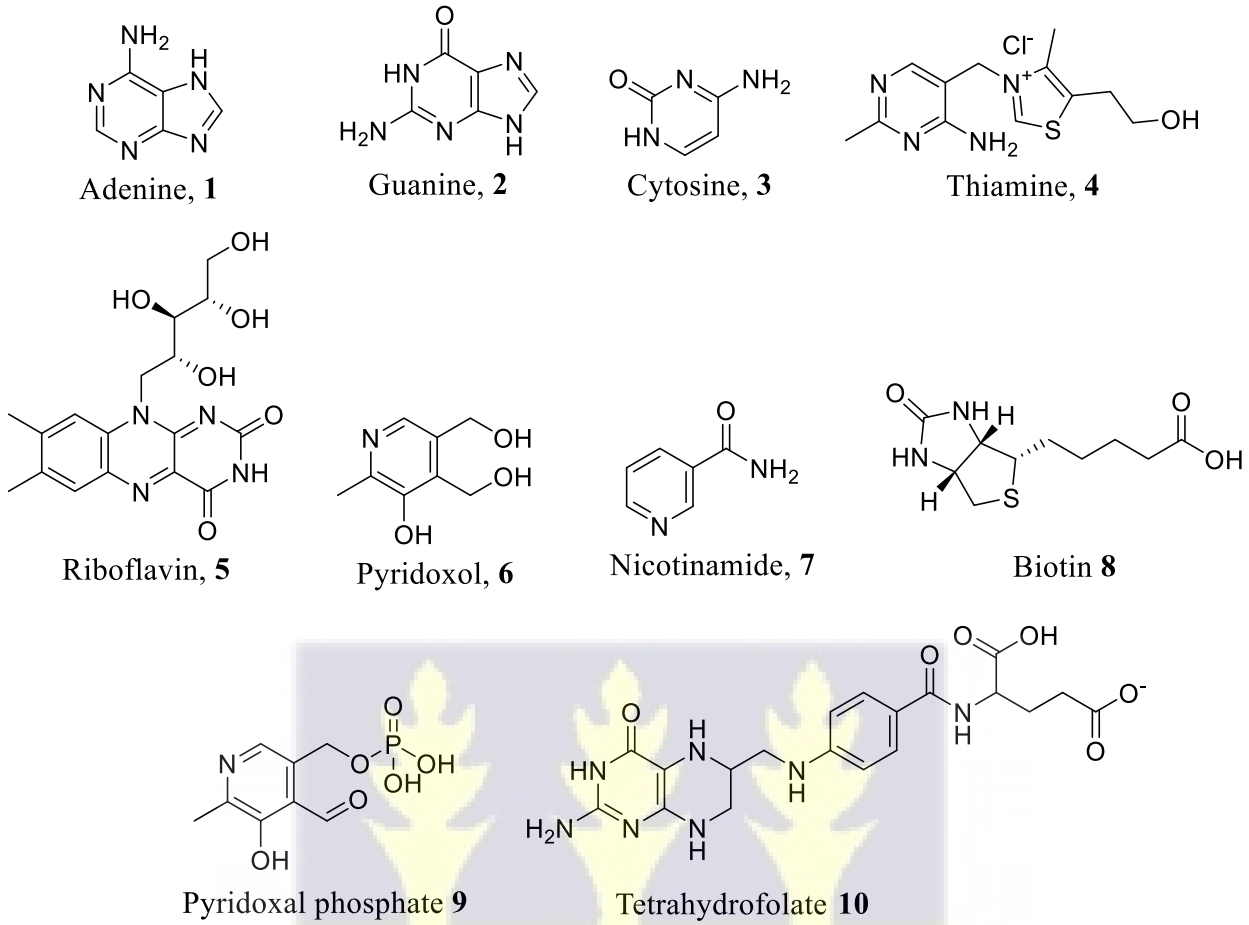


Figure 2.0.1: Nucleotide bases and Coenzymes that contains the heterocyclic nitrogen[115,118].

In drug discovery and development, nitrogen-containing heterocycles continue to contribute extensively, mainly due to their wide applications[121]. Pyridine and pyrimidine fused heterocycles are examples of nitrogen heterocycles[122] present in molecules such as vitamins, enzymes, and alkaloids[118]. They are important sources of biologically active compounds because of their distinctive structure[116,123]. Some pyridine fused heterocycles include, Pyrrolo Pyridines **11,** and Pyrido pyrimidine[124] **12 (Figure 2.2)** while some pyrimidine fused heterocycles include Purines **13**[125], Xanthine **14**[126], Pteridine **15**[126], Alloxazine **16**[125], Pyrrolo Pyrimidine **17**[127] and pyrido pyrimidine **18**[128] **(Figure 2.2),** among others, which possess diverse applications as antimicrobial, antiviral, anti-inflammatory and antimalarial medicinal properties[129].

University of Ghana http://ugspace.ug.edu.gh

The purine and pyrrolo pyridine moieties embedded in the hit compounds **MMV1900279** and **SFK78** respectively are essential classes of nitrogen heterocycles. In this project, derivatives of these two hit compounds which contain the purine and pyrrolo pyridine core will be synthesized and the antimalarial activities will be investigated.

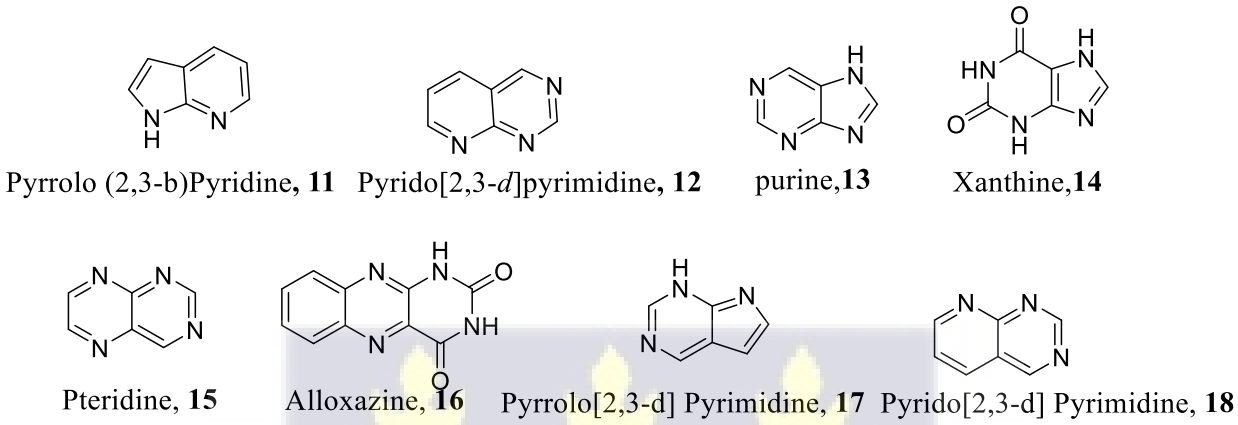


Figure 2.0.2: Pyridine and Pyrimidine fused Heterocycles[124,125].

2.2 Purines

The purine moiety which is embedded in the hit compound **MMV1900279** was first recognized by Emil Fischer in 1884 as imidazole [4,5-d] pyrimidine[130]. It contains two rings; a pyrimidine and an imidazole ring[131]. Purines possess 4 nitrogen moieties at positions 1,3,7 and 9[131,132]. The atoms in the ring are counted starting from the first nitrogen in the pyrimidine ring[131], as shown in **Figure 2.3** below.

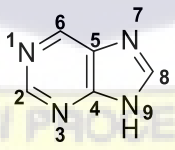


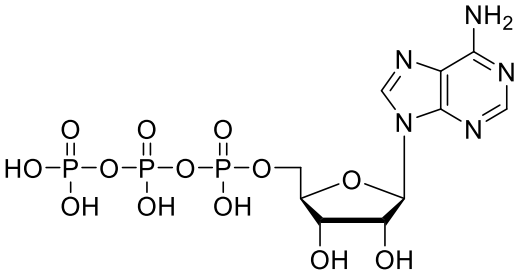
Figure 2.0.3: The Purine Core Structure[131].

University of Ghana http://ugspace.ug.edu.gh

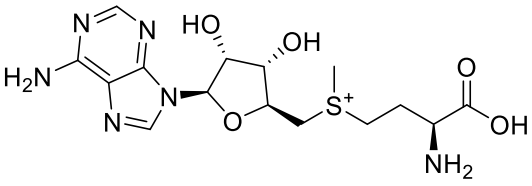
The two most abundant naturally occurring purines, also known as 6-aminopurine and 2-amino-6-oxypurine[133] are the building blocks of DNA and RNA[133], respectively. The presence of the amino and oxo groups in these purines allows them to exhibit keto-enol and amine-imine tautomerization[134]. Purines are also constituents of some essential biomolecules such as adenosine triphosphate (ATP) **19**, S-adenosyl methionine **20**, cyclic adenosine monophosphate (cAMP) **21**, nicotinamide adenosine dinucleotide (NADH) **22** and coenzyme A **23**[131,134] (**Figure 2.4**). They are essential central molecules for synthesis the of nucleic acids, energy production, cofactor reactions and intercellular and extracellular signaling[135]. Purines also play an indispensable role in drug discovery and are utilized by medicinal chemists in drug design and in the pharmaceutical industry[136]. They exhibit critical biological activities, for example, inhibition of kinases[137], sulfotransferases, phosphodiesterase and interferon inducers[130]. Some medically approved purine-based kinase inhibitors include Olomoucine **24**[138], Roscovitine **25**[138,139] and Purvalanol A **26**[140] (**Figure 2.5**). Other clinical applications of purine-based compounds include the treatment of cancer, tuberculosis and viral infections[141]. Some medically approved purine-based anticancer drugs include Mercaptopurine **27**[142], tioguanine (also known as 6-thioguanine **28)**[142] which is used for the treatment of leukemia and clofarabine **29**[123,142] used to block ribonucleotide reductase and DNA elongation. Also, Acyclovir **30**[143], Ganciclovir **31**[144] and Penciclovir **32**[144] are used clinically to treat viral infections.

INTEGRI PROCEDAMUS

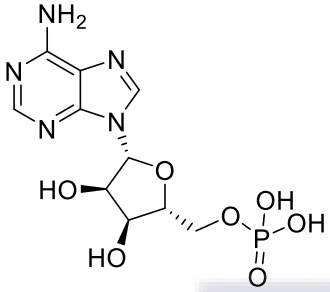
University of Ghana http://ugspace.ug.edu.gh



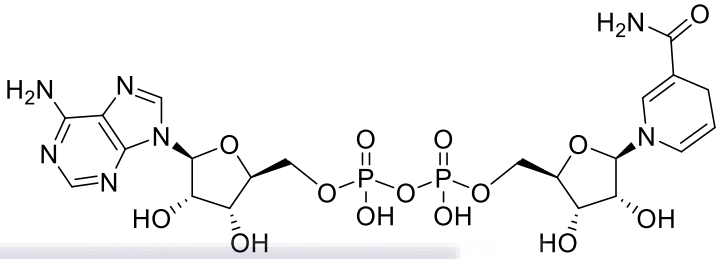
Adenosine triphosphate (ATP), **19**



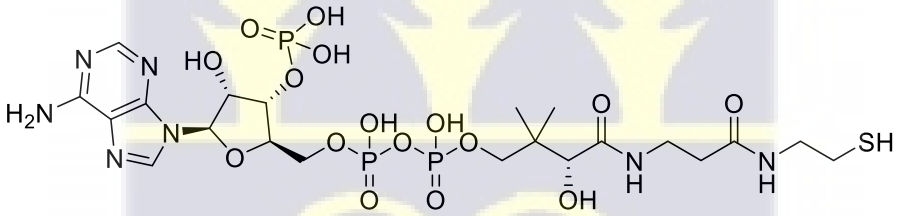
S-adenosyl methionine, **20**



Adenosine monophosphate, **21**



Nicotinamide Adenosine dinucleotide (NADH), **22**



Coenzyme A, **23**

Figure 2.0.4: Purine-containing biomolecules[131].

INTEGRI PROCEDAMUS

University of Ghana http://ugspace.ug.edu.gh

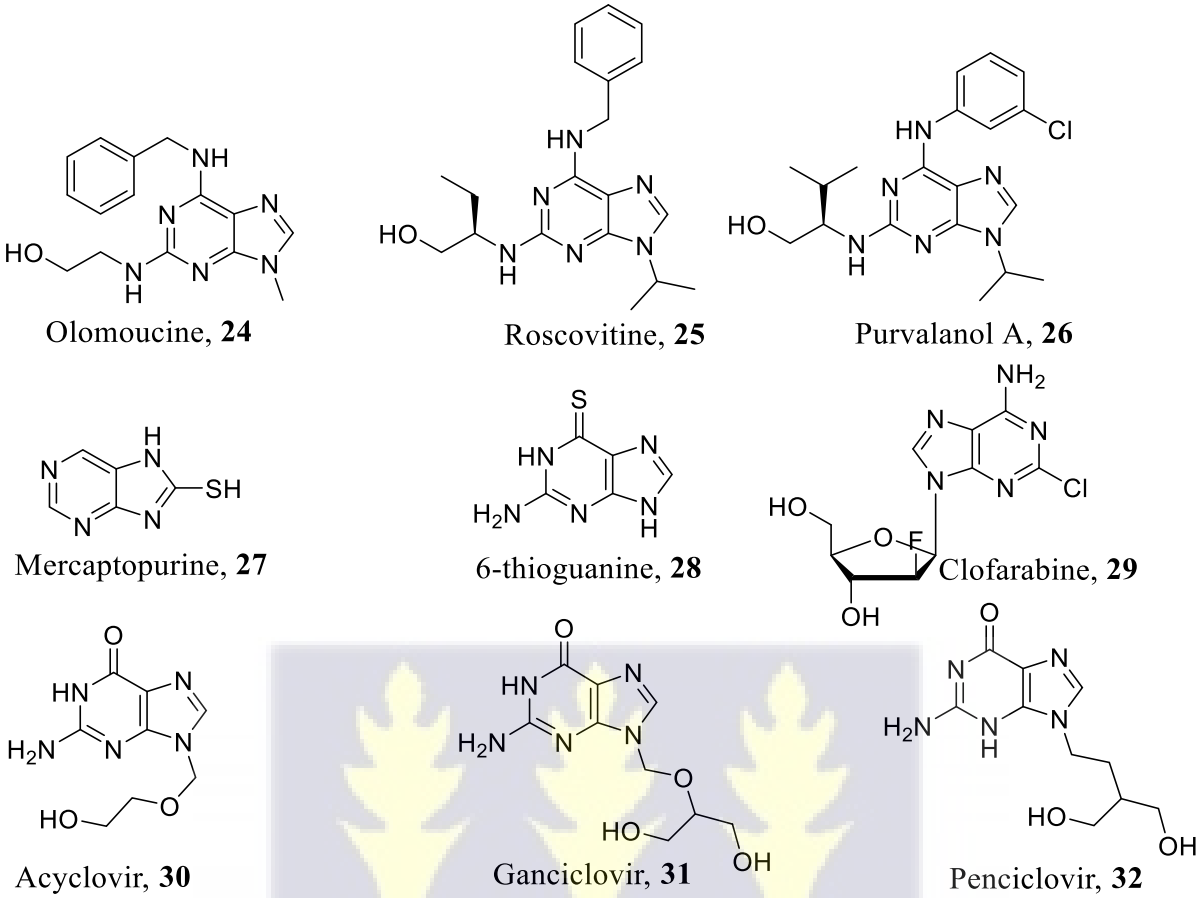


Figure 2.0.5: Clinically used Purine-based drugs[138,144].

2.2.1 Anticancer Activity of the purine moiety

Cancer is one of the indiscriminatory diseases that affects both the young and the old and is responsible for the loss of millions of lives around the globe each year[145]. Treatment regimen to combat this disease includes chemotherapy, radiation therapy and immunotherapy[146]. These treatment regimens come with numerous side effects[145].

Huang et al.[147] synthesized a series of steroidal purines that showed inhibitory activity against the human prostatic carcinoma PC-3 cell line[147]. Among the synthesized analogues, compounds **33**

University of Ghana http://ugspace.ug.edu.gh

and **34** showed promising inhibition against the human prostatic carcinoma (PC-3) cell line with IC_{50} values of **5.13 µM** and **1.8 µM**[147] respectively as shown in **Figure 2.6**.

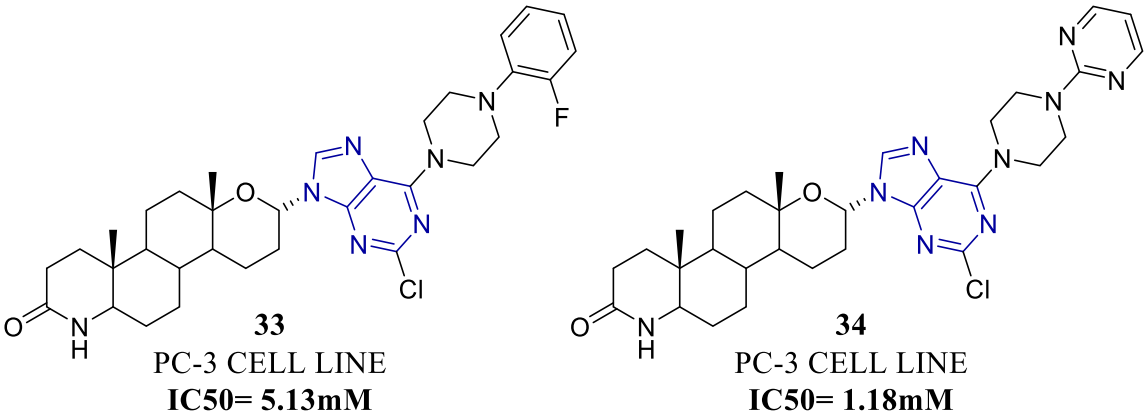
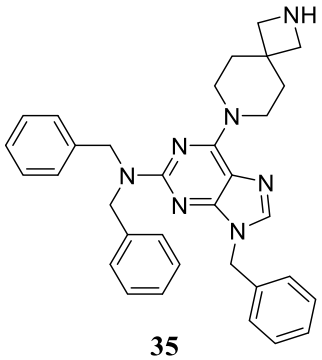


Figure 2.0.6: Anticancer activity of purine compounds against PC-3 cell line[147].

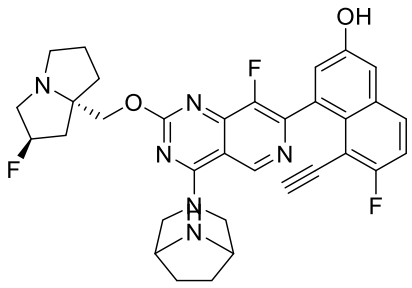
Park et al.[148] also synthesized several novel purine analogues and evaluated their inhibition activities against KRAS G12D mutations in gastric cancer (AGS), pancreatic cancer (PANC1) and colon cancer (SNU1197) cell lines[148]. These cancer cell lines were cultured and maintained in RPM1-1640 medium at 37 ºC with 5% CO_2 in a humid environment[148]. Compound **35**, shown in **Figure 2.7** below, exhibited promising inhibition against AGS, SNU11 and PANC1 cell lines with IC_{50} values of **(3.2 ± 0.4) µM**, **(3.8 ± 0.8) µM** and **(3.9 ± 0.7) µM** respectively, compared to the control, MRTX113 **36** which is a noncovalent inhibitor for KRAS G12D mutation[148].

University of Ghana http://ugspace.ug.edu.gh



35

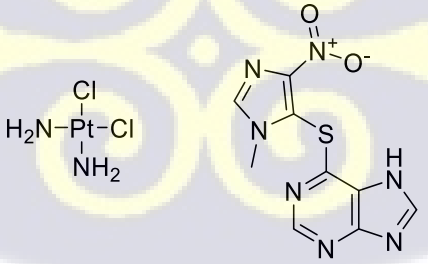
AGS cell line,**IC_{50}= (3.2 ± 0.4) mM**
SNU11 cell line, **IC_{50}=(3.8 ± 0.8)mM**
PANC1 cell line, **IC_{50}=(3.9 ± 0.7)mM**



MRTX1133, **36**
AGS cell line,**IC_{50}= 0.0065mM**
SNU11 cell line, **IC_{50}= 0.037mM**

Figure 2.0.7: PU1-1 as KRAS G12D inhibitor[148].

In another investigation, Kowalska et al.[149] synthesized some analogues of 2- and 6-substituted thiopurines. They evaluated their potencies against glioblastoma (SNB-19), melanoma (C-32) and the human ductal breast epithelial tumor (T47D) cancer cell lines, employing cisplatin (**37**) and azathioprine (**38**) (**Figure 2.8**) as reference drugs[149]. Among the synthesized analogues, compounds **39-43** exhibited promising anticancer activity against the SNB-19 and C-32 cancer cell lines with compound **35** emerging as the most potent[149] (**Table 2.1**).



CisPlatin, **37** Azathioprine, **38**

Figure 2.0.8: Reference Drugs for anticancer evaluation[149].

University of Ghana http://ugspace.ug.edu.gh

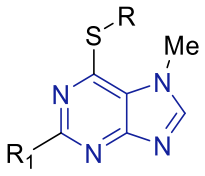


Table 2.1: Anticancer activities of synthesized thiopurines by Kowalska et al[149].

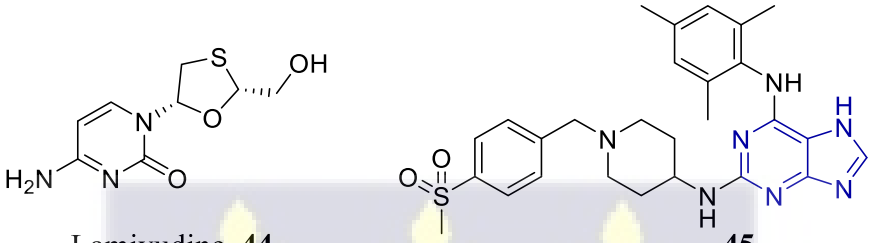
Compound	R	R_1	SNB-19 Cell line (EC_{50} µg/ml)	C-32 Cell line (EC_{50} µg/ml)
39	$(CH_2)_3N(Et)_2$	Cl	8.45	>50
40	$(CH_2)_2N(Me)_2$	$S(CH_2)_2N(Et)_2$	9.82	33.55
41	$(CH_2)_3N(Me)_2$	$S(CH_2)_2N(Me)_2$	36.28	>50
42	$(CH_2)_2N(C_4H_8)$	$S(CH_2)_2N(C_5H_{10})_2$	7.95	27.05
43	$CH_2C(C)CH_2N(C_4H_8)$	Cl	5.0	7.58
Cisplatin (**37**)	-	-	37.20	35.62
Azathioprine (**38**)	-	-	4.48	6.28

2.2.2 Antiviral Activity of the Purine moiety

Viruses account for a larger portion of newly discovered human pathogens than bacteria or Fungi[150]. Although there are several treatment options available for viral infections, many remain without effective treatments, with just a few having vaccines to prevent them[150,151]. The Human Immunodeficiency Virus (HIV) is one of the viral infections that does not have any vaccine to prevent it although there are several antiretroviral drugs for its treatment[152]. Together with influenza viruses and other viral infections, they remain a global health concern. This has created

University of Ghana http://ugspace.ug.edu.gh

a burden and has attracted much interest in the drug discovery field to find new drug candidates for their effective treatment. Based on previous work done on diaryl pyrimidine derivatives, Kang et al.[153] explored some synthetically feasible purine derivatives. They evaluated their potency against the **WT HIV-1 mutant strain** *in-vitro*, using the MTT method[153]. Compared with Lamivudine **44** (**3.12 µM**) as the reference drug, they identified the analog **45** as the most potent against the WT HIV-1 mutant strain with an EC_{50} value of **3.39 µM**[153] shown in **Figure 2.9** below.



Lamivudine, **44**
EC_{50}= **3.12 mM**

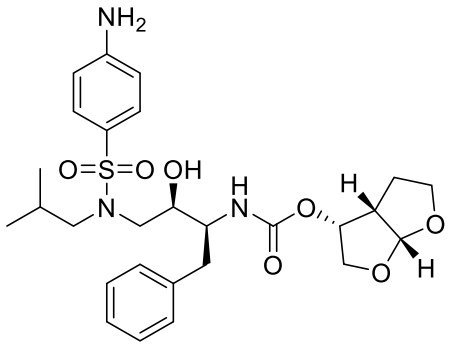
45
EC_{50}= **3.93 mM**

Figure 2.0.9: Lamivudine as reference drug and FZJ13 as potent against HIV-1 strain[153].

Zhu et al.[152] also synthesized and investigated the potency of their compounds against HIV-1 strains. They obtained micromolar activities for the synthesized analogs. However, analogues **46-48** shown in **Table 2.2** exhibited superior *in vitro* inhibitory activities against HIV-1 protease with IC_{50} values ranging from **0.043 µM-0.068 µM**[152]. They employed Darunavir (**49**) as a reference drug with an IC_{50} value of **4.01 µM** shown in **Figure 2.10** below[152]. It was proposed by Zhu and colleagues that the potency of these three analogs was a result of the hydrogen bond interaction with the amino acid residue Asp30' in the protease S2' subsite[152].

INTEGRI PROCEDAMUS

University of Ghana http://ugspace.ug.edu.gh



Darunavir, **49**

Figure 2.0.10: Darunavir as a reference drug against HIV-1 protease[152].

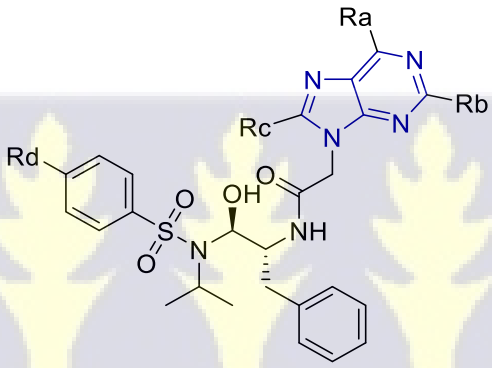


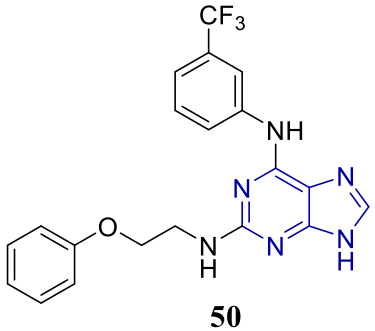
Table 2.2: In-vitro IC50 data for analogues against HIV-1 protease[152].

Compound	R_a	R_b	R_s	R_d	IC_{50} (µM)
46	Cl	H	H	OMe	0.043±0.007
47	Me	H	H	OMe	0.042±0.003
48	OH	H	H	OMe	0.068±0.003
Darunavir (49)	-	-	-	-	0.004±1

Also, Vicenti and colleagues[150] synthesized a series of 2,6-diaminopurine derivatives and evaluated their antiviral activities against the Zika virus (ZIKV) and the Dengue virus (DENV)[150]. Among the synthesized analogs, compound **50** shown in **Figure 2.11** below exhibited promising

University of Ghana http://ugspace.ug.edu.gh

antiviral activity against both viral strains with IC_{50} values of **1.1 ± 0.4 µM** and **2.6 ± 0.3 µM** respectively and good selectivity index (**SI**) of 182 and 77 respectively[150].



50

ZIKV IC_{50}= **1.1±0.4mM,**
DENV IC_{50}= **2.6±0.3mM**

Figure 2.0.11: 2,6-diaminopurine derivative as a potent antiviral agent[150].

2.2.3 Antimicrobial Activity of the Purine Moiety

The emergence of multidrug-resistant bacteria and fungi has led to a need for the development of drugs with novel mechanism of action[154]. The purine moiety which is ubiquitous in nature has been reported in the literature to possess good antimicrobial activity[155]. Hence, it has attracted interest in medicinal chemistry and drug discovery. Therefore, Nadaf et al.[156] synthesized and evaluated the antimicrobial activities of derivatives of 6-[4-(4-propoxyphenyl) piperazin-1-yl]-9H-purine with different substitutions at the C9 position[156]. The synthesized analogs were tested against Gram-positive bacteria (*Staphylococcus aureus* and *Bacillus subtilis*) and Gram-negative bacteria (*Escherichia coli* and *Pseudomonas aeruginosa*)[156]. They also tested the analogs against fungal strains (*Aspergillus flavus*, *Trichoderma harina*, *Penicillium chronogenesis* and *Candida albicans*) using the microdilution Broth method[156]. They used Tetracycline (**51**) as the reference drug during the antibacteria testing and Nystatin (**52**) and Fluconazole (**53**) as the reference drugs for antifungal testing. Among the analogs they synthesized, compounds **54 - 59** (**Figure 2.12**)

University of Ghana http://ugspace.ug.edu.gh

exhibited promising antibacterial and antifungal activity against these strains as shown in **Table 2.3** and **Table 2.4** respectively[156].

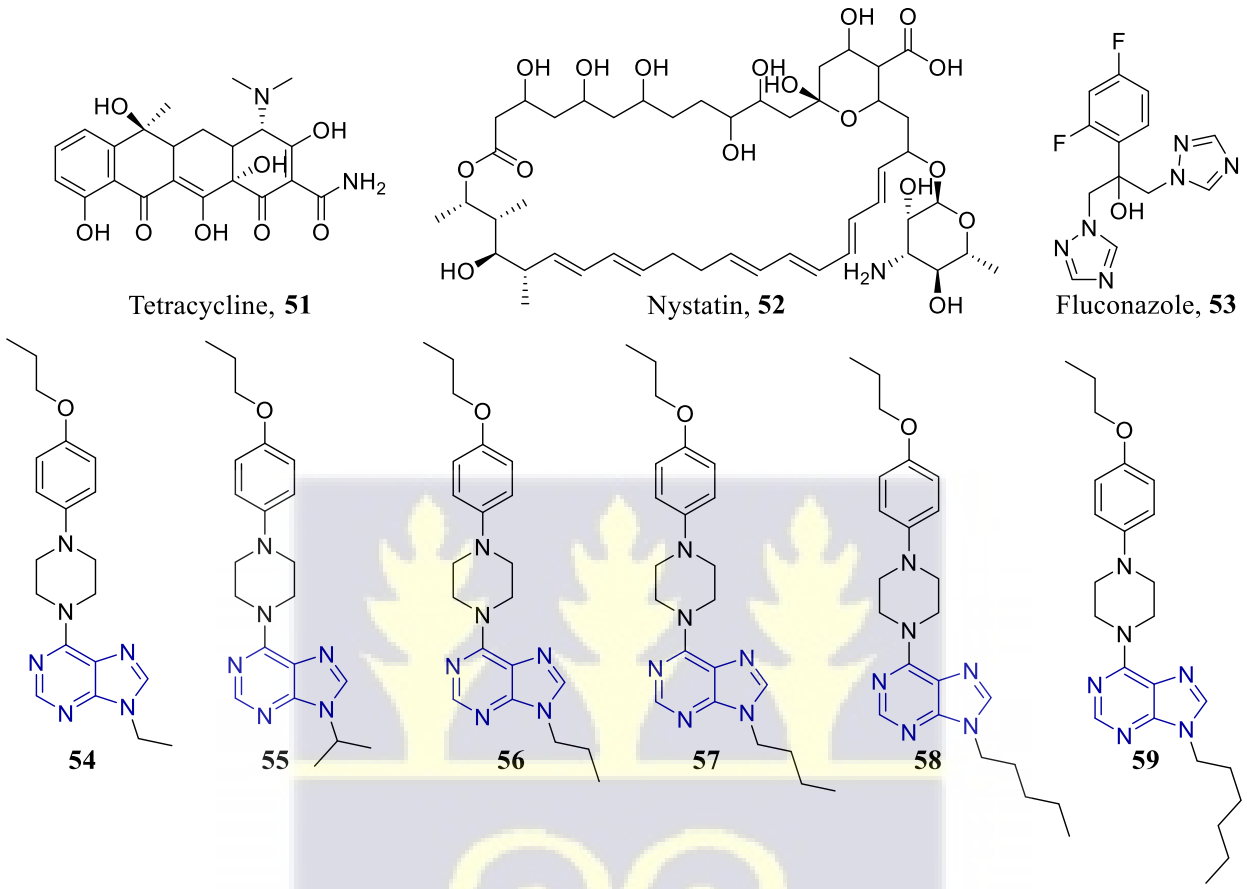


Figure 2.0.12: Reference drugs and selected purine derivatives as potent antimicrobial agents[156].

Table 2.3: Antibacterial inhibition of 6-[4-(4-propoxyphenyl) piperazin-1-yl]-9H-purine derivatives[156].

Compound	MIC (µg/mL)			
	S. aureus	*B. subtilis*	*E. coli*	*P. aeruginosa*
54	4	2	2	4
55	4	2	2	4
56	4	2	2	2

University of Ghana http://ugspace.ug.edu.gh

57	4	2	4	4
58	4	2	4	2
59	2	2	4	2
Tetracycline (**51**)	4	2	2	4

Table 2.4: AntiFungal inhibition of 6-[4-(4-propoxyphenyl) piperazin-1-yl]-9H-purine derivatives[156].

Compound	**MIC (µg/mL)**			
	A. flavus	***T. harzianum***	***P. chrysogenum***	***C. albicans***
54	4	4	2	2
55	2	2	4	2
56	2	2	4	2
57	1	2	4	4
58	8	16	8	16
59	8	16	16	8
Nystatin (**52**)	2	2	2	4
Fluconazole (**53**)	2	4	2	2

2.2.4 Antimalarial Activity of the Purine Moiety

Hypoxanthine guanine (xanthine) phosphoribosyl transferase [HG(X)PRT] is the key enzyme for the purine salvage pathway of which the plasmodium parasite relies, for replication and survival[157]. Thus, it has been recognized as a target for antimalarial development. Hence, a series of Aza acyclic nucleoside phosphonate (Aza ANPs) has been synthesized and found to inhibit the

University of Ghana http://ugspace.ug.edu.gh

chloroquine-sensitive (D6) and resistant (W2) strains of the plasmodium parasite[157]. Although most of the analogs synthesized inhibit both human HGPRT and *Pf*HGXPRT, the representative compounds **60-62** exhibited good selectivity index and promising inhibition. In contrast compounds **63** and **64** showed good inhibition but poor selectivity index[157] **Table 2.5**.

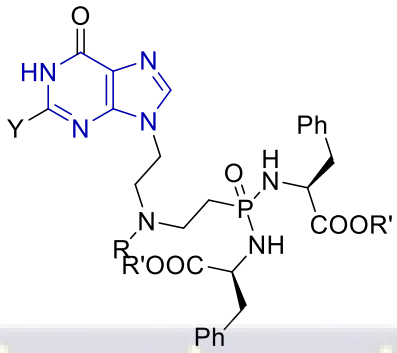


Table 2.5: Selectivity index and IC50 values for synthesized purine analogs[157].

Compound	R	R'	Y	D6 IC_{50} (µM)	W2 IC_{50} (µM)	SI
60	CH_2CH_2COOMe	Et	H	3.5±1	2.9±1	>44
61	CH_2CH_2COOMe	Et	H	11.8±2	5.6±2	>34
62	$CH_2CH_2CH_2COOMe$	Et	NH_2	8.6±2	5.7±4	>33
63	$CH_2CH_2OCH_2Ph$	iPr	NH_2	1.6±0.2	2.9±1	9
64	$CH_2CH_2OCH_2Ph$	iPr	NH_2	1.5±0.5	2.8±1	8

The synthesis of some carbocyclic methyl phosphonate nucleoside analogs bearing 2,6-disubstituted purine as nucleobase yielded the selected compounds **65-70**[158] (**Figure 2.13**). These exhibited promising *in vitro* inhibition activity against the 3D7 strain of *Plasmodium falciparum* with IC_{50} values ranging from **1-10 µM**[158] as shown in **Table 2.6** below.

University of Ghana http://ugspace.ug.edu.gh

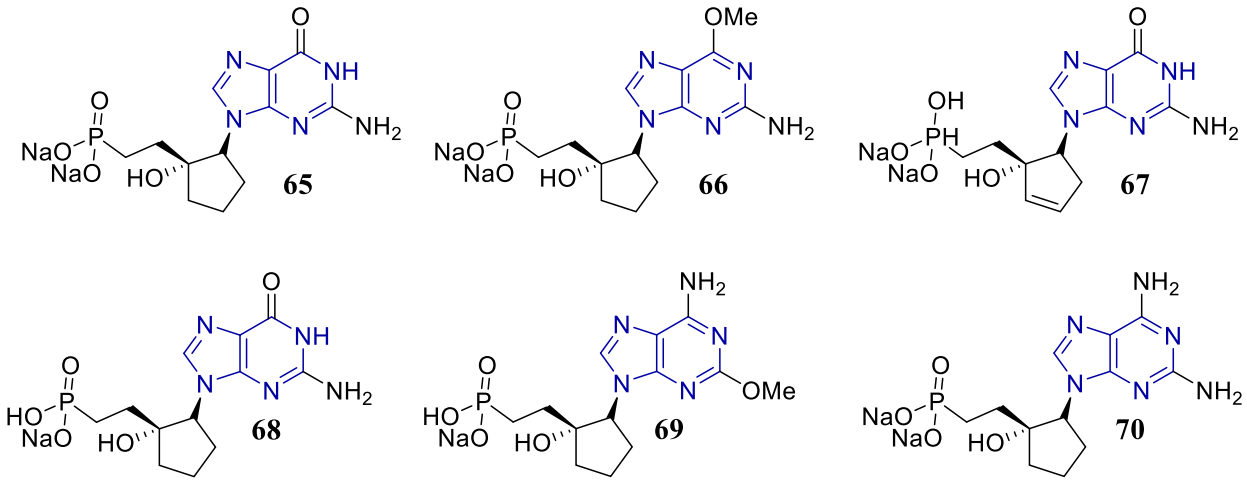


Figure 2.0.13: 2,6-disubstituted purine analogs as potent Pf3D7 inhibitors[158].

Table 2.6: 2,6-disubstituted purine analogs and their IC50 values[158].

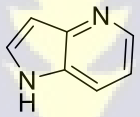
Compound	*Pf*3D7 IC_{50} (μM)
65	7.0±1
66	10.2±2
67	1.0±0.3
68	4.4±1
69	2.2±0.1
70	8.8±2

2.3 The Pyrrolo Pyridine Moiety.

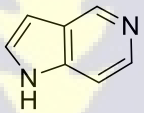
Nitrogen-containing fused heterocycles are important and unique compounds in both synthetic forms and in natural products such as vitamins, antibiotics, organic materials and agrochemicals[159]. The Pyrrolo-pyridine moiety embedded in the hit compound **SFK78** scaffold is also known as azaindole[176]. It is a nitrogen-containing planar fused heterocycle that has a π-π-lacking pyridine

University of Ghana http://ugspace.ug.edu.gh

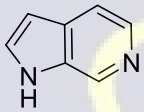
and a π-abundant pyrrole ring fused by a C-C bond[177]. It is a structural bio-isosteric chemical structure to indoles[175,178]. According to the mutual position of the nitrogen atoms fused in the pyridine and pyrrole rings in the azaindole, there are four isomers known. These are 4-azaindole(1-H-pyrrolo[3,2-b] pyridine) **71**, 5-azaindole(1H-pyrrolo[3,2-c] pyridine) **72**, -6-azaindole(1H-pyrrolo[2,3-c]pyridine) **73**, and 7-azaindole(1H-pyrrolo[2,3-b]pyridine) **74**. The most encountered is compound **74**, which has diverse biological activities including antimalarial, anti-microbial[180], anti-viral[181], anti-cancer[182] as well as kinase inhibitors[182]. Researchers have explored different ways of synthesizing the Azaindole core, from commercially available reactants such as the 2,6-dichloropyridine and nitropyridine. This azaindole core is also incorporated in the hit compound **SFK78** and its derivatives which will be synthesized and discussed in this project.



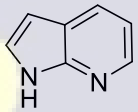
(1H-pyrrolo[3,2-b]pyridine), **71**



(1H-pyrrolo[3,2-c]pyridine), **72**



(1H-pyrrolo[2,3-c]pyridine), **73**

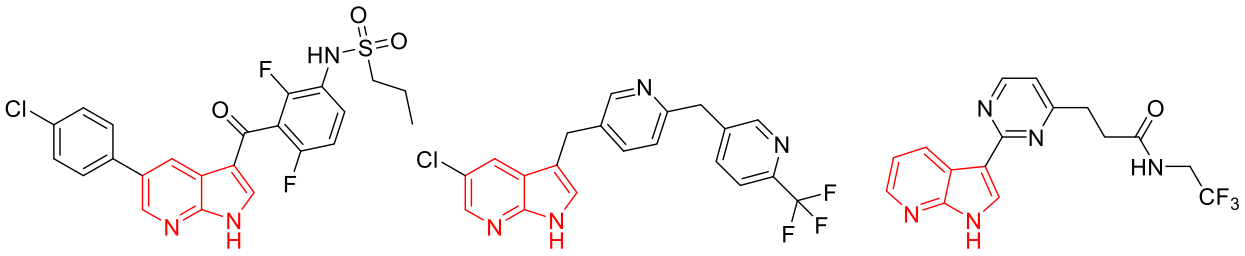


(1H-pyrrolo[2,3-b]pyridine), **74**

Figure 2.0.14: The isomers of the Azaindole core[183].

Some drugs with the Pyrrolo pyridine moiety that have been approved by the U.S. FDA and used clinically for some kinase-related diseases include Vemurafenib **75**, pexidartinib **76** and Decernotinib **77** [175,178] (**Figure 2.15**).

University of Ghana http://ugspace.ug.edu.gh



Vemurafenib, **75**
Anticancer

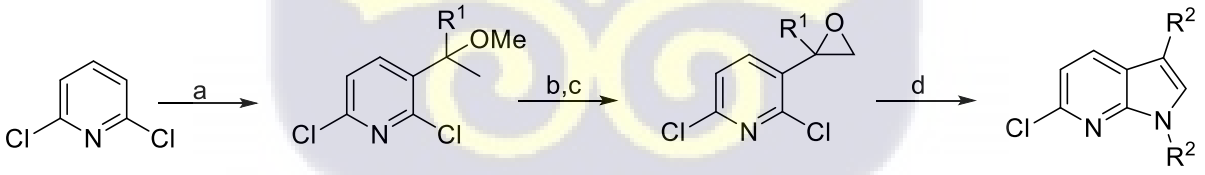
Pexidartinib, **76**
Anticancer

Decernotinib, **77**
Antiarthritis

Figure 2.0.15: Drugs with the pyrrolo pyridine moiety[176].

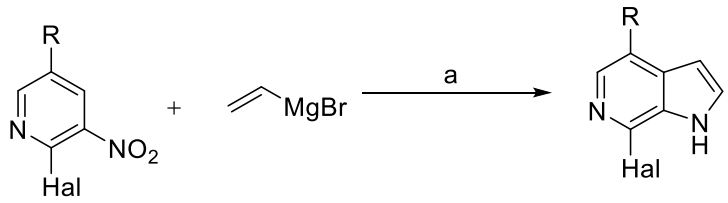
2.3.1 Synthesis of the Pyrrolo Pyridine Moiety

The Pyrrolo pyridine core incorporated in many structures has shown diverse biological activities across many disease areas therefore some researchers have come up with different synthetic methods to synthesize them. Popowyer et al.[173] reported the synthesis of 7-azaindole and its derivatives using 2,6-dichloropyridine as the starting material, which afforded yields between 63 % and 95 % as shown in **Scheme2.1** below[173]. Also, Voloshchuk et al.[174] synthesized a series of 6-azaindoles and its derivatives using a modified version of the Bartoli rection of nitropyridines as shown in **Scheme 2.2** and **Scheme 2.3** respectively, improving the yields from 27 % to 42 % in the classical Bartoli reaction, to 75 % and 100 % in the modified synthetic route[174].

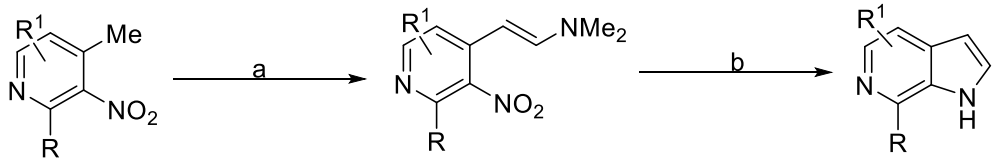


Scheme 2.1: Synthesis of 7-azaindole and it's derivatives by Popowycz et.al. (a) LDA, THF, -78 ºC, 2 h then R^1COMe, -78 ºC to rt (b) H_2SO_4/AcOH 1:3,130 ºC, 30 min, 84–98 %; (c) m-CPBA, CH_2Cl_2, rt. (d) R^2NH_2, n-BuOH, 110 ºC, then aq HCl, 63–95 %.

University of Ghana http://ugspace.ug.edu.gh



Scheme 2.2: Classic Bartoli reaction of nitropyridines to make the 6-azaindole. (a) THF, -78 °C to -20 °C, 1 - 16 h, then aq NH_4Cl, 0 °C



Scheme 2.3: Modified Bartoli reaction nitropyridines by Voloshchuk et.al. (a) DMFDMA, DMF 90 °C - 120 °C, 0.5 2 h. (b) Pd/C, H_2, MeOH, 50 °C, 3 days.

2.3.2 Antimicrobial Activity of Pyrrolo Pyridines

Bacterial resistance to existing drugs continues to be a growing problem and therefore there is a need to introduce new antibacterial drugs[180]. In light of this, Elkanzi et. al. synthesized a series of pyrrolo [2,3-b] pyridine derivatives. They evaluated their antifungal activity against strains of *Candida sp.*, *Aspergillus multiil* and *Aspergillus niger* by using the agar diffusion method with ketoconazole as a positive control.[185] The zone inhibition in millimeters (mm) of some selected synthesized compounds (**Figure 2.16**) from the group is shown in **Table 2.7** below.

University of Ghana http://ugspace.ug.edu.gh

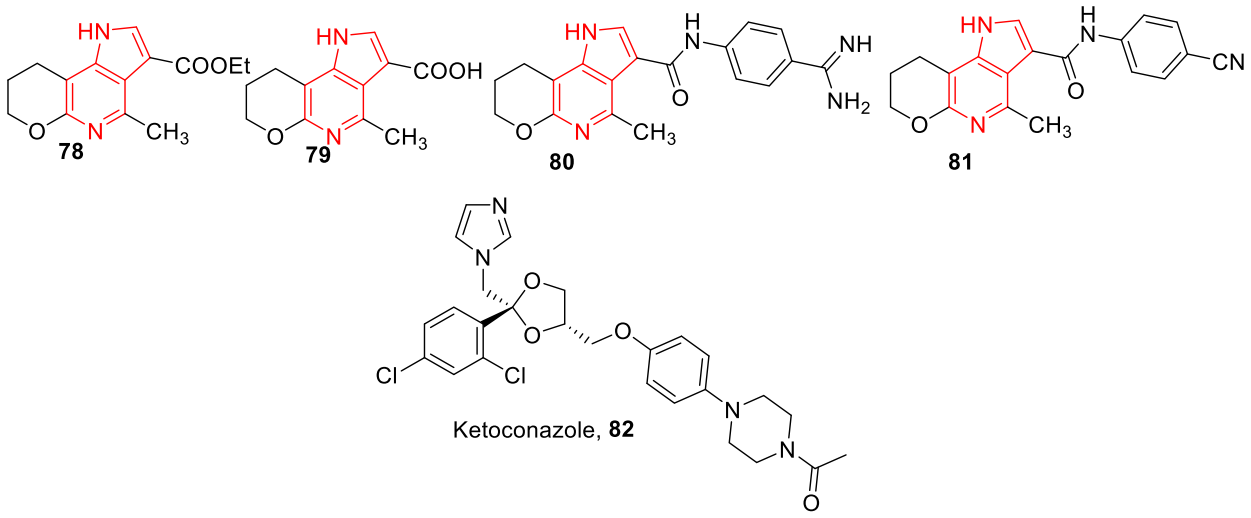


Figure 2.0.16: Derivatives of pyrrolo[2,3-b] pyridine and ketoconazole for antimicrobial and antifungal evaluation[186].

Table 2.7: Antifungal data of selected pyrrolo [2,3-b] pyridine derivatives from Elkanzi et al.[186].

Compounds	Zone of Inhibition (mm)		
	Candida sp.	*Aspergillus multi*	*Aspergillus niger*
78	12	12	13
79	10	13	8
80	13	6	9
81	11	10	15
Ketoconazole (82)	17	17	16

The compounds in **Figure 2.16** above were also evaluated for their antibacterial activity[185]. They were tested against Escherichia coli a Gram-negative bacterium and Staphylococcus aureus a

University of Ghana http://ugspace.ug.edu.gh

Gram-positive bacterium by measuring the diameter of the inhibition zone in millimeters (mm) using Ampicillin **96** as a positive control[185] **Table 2.8**.

Table 2.8: Zone inhibition of synthesized pyrrolo[2,3-b] pyridine derivatives[186].

Compounds	**Zone of inhibition (mm)** *S. aureus*	*E. coli*
91	25	21
92	10	13
93	17	19
94	22	18
Ampicillin (96)	26	26

2.3.3 Anticancer activity of the pyrrolo pyridine.

Protein tyrosine kinases (PTKs) transfer the phosphate group of ATP onto threonine, tyrosine or serine residues of proteins, initiating protein phosphorylation[187]. Receptor tyrosine kinases (RTKs) is a type of PTK that causes the occurrence and the development of malignant tumors when the c-Met membrane is over expressed by the MET (MET Proto-Oncogene, Receptor Tyrosine Kinase) gene.[187,188]

Therefore, a series of 7- azaindole benzamides was synthesized and tested for their anticancer activities[189]. The synthesized analogues were tested against lung cancer cells (A54), cervical cancer cells (HeLa) and breast cancer cells (MCF-7) using Cabozantinib as a positive control using MTT method[189]. The anticancer data obtained for some selected analogues **(Figure 2.17)** are reported in **Table 2.9** below[189].

University of Ghana http://ugspace.ug.edu.gh

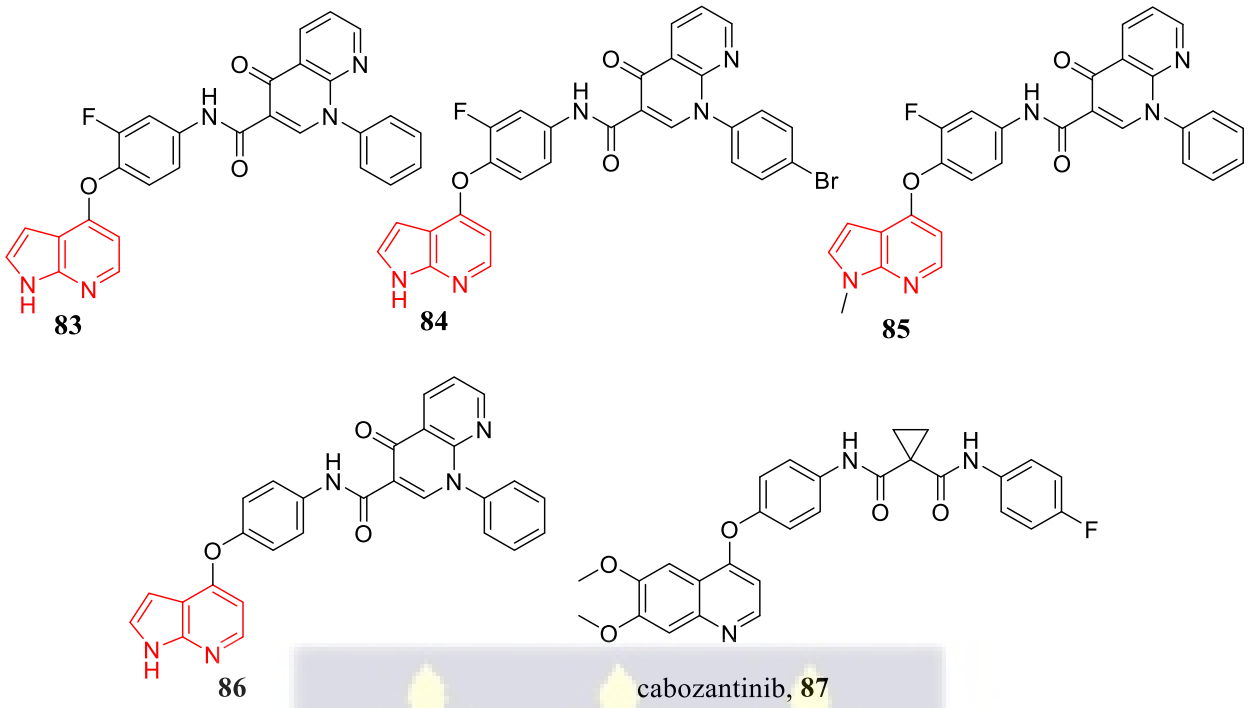


Figure 2.0.17: Derivatives of 7-azaindole benzamide for anticancer evaluation[189].

Table 2.9: Anticancer activity of derivatives of 7-azaindoles[189].

	IC_{50} (µM)		
Compounds	**A549**	**Hela**	**MCF-7**
83	6.51 ± 0.09	29 ± 3	13 ± 3
84	1.06 ± 0.04	11 ± 2	0.11 ± 0.02
85	17 ± 3	28 ± 5	15 ± 2
86	18 ± 3	80 ± 11	47 ± 6
Cabozantinib (87)	0.33 ± 0.05	79.1 ± 0.4	30.9 ± 0.2

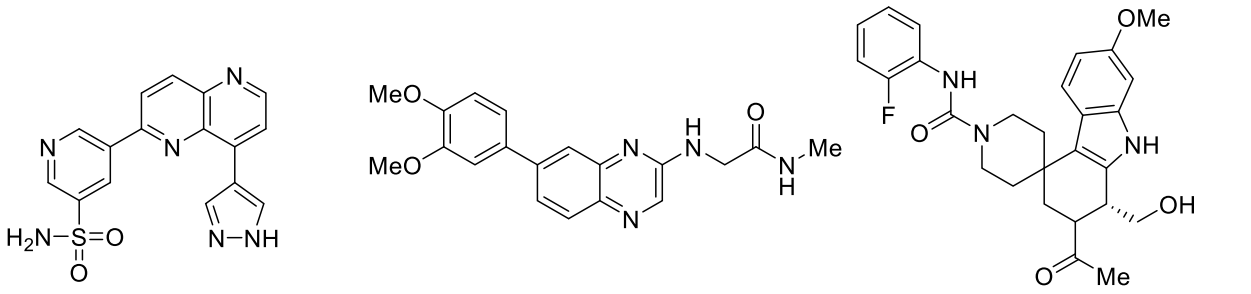
INTEGRI PROCEDAMUS

University of Ghana http://ugspace.ug.edu.gh

2.4 Phosphatidylinositol 4 Kinase (PI4K)

Phosphorylation of amino acids such as **serine, threonine and tyrosine** in protein substrates is catalyzed by protein kinases which require adenosine triphosphate (ATP), which is converted to adenosine diphosphate (ADP) during the process [190]. A kinome is a complete set of encoded protein kinases in the genome of an organism[191]. There are 518 encoded kinases in the human kinome and these kinases regulate numerous cellular processes, their disfunction can lead to many cancers[192]. Phosphatidylinositol 4 kinase (PI4K) is a kinase enzyme that regulates the phosphorylation of phosphatidylinositol (PI) to phosphatidylinositol 4 phosphate (PI4P) PI4P is vital to produce phosphatidylinositol (4,5) diphosphate and phosphatidylinositol (3,4,5) triphosphate[193,194] which are involved in the receptor-activated phospholipase C (PLC) and PI4K signaling[194]. The PI4K is a marker of the Golgi apparatus, it has two classes that can be differentiated by their sensitivity to wortmannin and adenine[195]. The human genome encodes two types of the type II and type III PI4Ks namely, the PI4KIIα, PI4KIIβ and PI4KIIIα, PI4KIIIβ respectively[195]. The plasmodium parasite also possesses about 85 protein kinases in its kinome. It also contains the PI4K enzyme that catalyzes the phosphorylation of PI to PI4P, a process that is vital for intracellular signaling and trafficking throughout the parasite's life cycle. It has attracted much attention in drug discovery as a target for new antimalarial drugs[196]. Some compounds that have exhibited inhibition against plasmodium PI4K include MMV024101 **88**[197], BOR695 **89**[198] and BRD73842 **90**[199] shown in **Figure 2.18** below.

University of Ghana http://ugspace.ug.edu.gh



MMV024101, **88**
IC_{50}(Pv PI4K) = 1. 9mM

BQR695, **89**
IC_{50}(Pv PI4K) = 3.5 nM

BRD73842, **90**
IC_{50}(Pf PI4K) = 21 nM

Figure 2.0.18: Plasmodium PI4K inhibitors[197–199].

2.5 Sulfonamides

Sulfonamides are an important class of molecules in medicinal chemistry[200]. They are known to have diverse biological activities, including antimicrobial, antitumor, antithyroid and antimalarial201. Sulfonamides are a class of compounds containing the SO_2NHR in their structure[201]**(Figure 2.19)**. They are widely used due to their low cost and high effectiveness. They are known to act by interfering with bacterial synthesis of folic acid which is needed for bacterial growth [202]. They competitively inhibit dihydropteroate synthase, a bacterial enzyme responsible for the conversion of para-aminobenzoic acid (PABA) into dihydrofolic acid which is a precursor for folic acid[202] leading to cell death. Some clinically used compounds with the sulfonamide moiety include sildenafil (**91**), a drug used to treat erectile dysfunction, probenecid (**92**) for the treatment of gouty arthritis, prontosil (**93**) to treat bacterial infection and Sulfadoxine (**94**) which is an antimalarial drug[203]. Since compounds containing the sulfonamide moiety have shown diverse biological importance in drug discovery, incorporating it in the analogues of the hit compound will have a great impact on the antimalarial activity of the synthesized analogues.

University of Ghana http://ugspace.ug.edu.gh

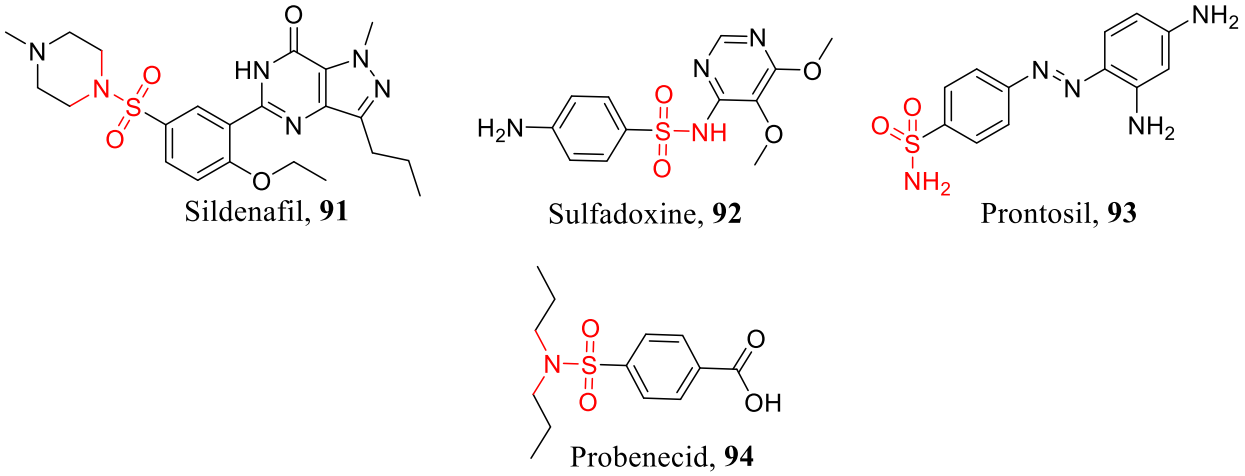


Figure 2.0.19: Clinically used drugs with the sulfonamide moiety[186].

2.6 Phenotypic Screening

As various diseases emerge and progress, there has been an increasing impetus to identify new drug entities. Consequently, scientists have used either target-based drug development (TDD) or phenotypic drug development (PDD) approaches to identify small-molecule entities[205,206]. These small-molecule entities can be developed into drugs to treat a wide range of diseases. Target-based screening examines the biological effect of a drug candidate on a purified target protein[207]. However, Phenotypic screening also known as whole-cell screening describes the methodology used to evaluate the biological effects of compounds[208]. It identifies their therapeutic impact on whole cells by observing the changes in the phenotype[208,209]. These changes occur when the cell is exposed to a compound[209]. While target based drug development employs rational mechanisms of action or hypothesis-driven approaches, phenotypic drug development, however, does not rely on mechanism of action[208]. This gives it some advantages over the former. Among the benefits of phenotypic drug discovery (PDD) are the following; the use of unbiased cellular systems to uncover novel biological pathways[210], the exclusion of drug candidates that lack membrane permeability, and the non-dependence on a specific biological target for the screening

University of Ghana http://ugspace.ug.edu.gh

methodology[210]. Phenotypic screening also enables 3compounds to have multiple target modes thus thereby enabling the emergence of a novel mechanism of action[209]. Phenotypic approaches have significantly contributed to drug discovery. About 46 of the first-in-class small molecules identified between 1999 and 2008 emerged from this methodology[210]. For example, Acoziborole **95**[208], a drug developed by Anacor pharmaceuticals was discovered through phenotypic screening using *Trypanosoma brucei* growth inhibition Assay[208]. Also, a Phenotypic screen of a compound library yielded a hit with undesirable properties. However, Lead optimization yielded GSK3186899/DDD853651 **96**[211] which proceeded to preclinical trial development for the treatment of visceral leishmaniasis. In antimalarial drug development, phenotypic screening has also contributed to the identification of some drug candidate[211]. The compound (+)-SJ000557733 **97**[212] identified through phenotypic screening, targets *pf*ATP4(*Pf*L0590c) and rapidly clears the parasite in both in vitro and in vivo assays[212]. DDD107498 **98**, another potent drug candidate, targets multiple stages of the parasite and has a novel mechanism of action[213]. The quinazolinon-2-carboxamide 19f **99** also identified through phenotypic screening also shows promising antimalarial potency[214] (**Figure 2.20**). The hit compounds MMV902507 **100** and MMV1900279 **101** (**Figure 2.20**) were also obtained through phenotypic screening of the bio-focus chemical library and the Bayer library respectively by the Medicines for Malaria Ventures (MMV). For a hit compound and its analogues to progress along the drug discovery pipeline, they need to pass the MMV criteria shown in **Table 2.10** below. This criterion guides the medicinal chemist to make rational decision when exploring the SAR of a hit compound to be able to address liabilities such as clearance, hERG and metabolic stability.

University of Ghana http://ugspace.ug.edu.gh

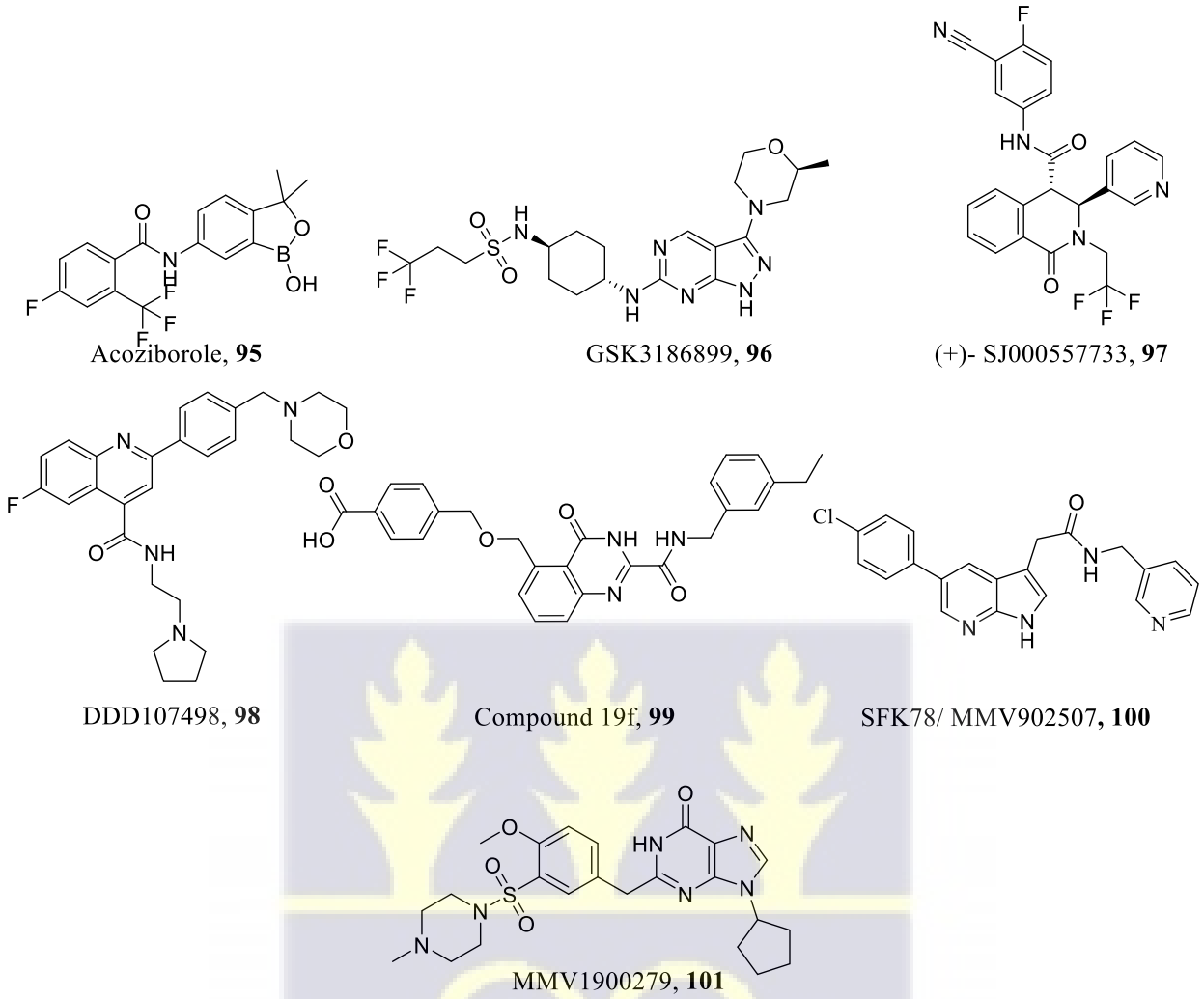


Figure 2.20: Potential Drug candidates identified through phenotypic screening[212–214].

Table 2.10: Hit Compound Compared with MMV criteria.

MMV#	Early Lead Criteria	MMV902507
Dd2 IC50 (µM)	< 0.1	0.34
Pb Liver IC50 (µM)	< 0.1	0.49
Solubility pH 7.4 (µM)	> 10	44
LogD pH 7.4	< 5	3.2

University of Ghana http://ugspace.ug.edu.gh

CLint in vitro, rat hepatocytes (µL.min-1 .10-6 cells)		85
CLint in vitro, Human microsomes (µL.min-1 .mg-1)	< 11.6	> 578
hERG % Inhibition @10µM	> 10 µM	13
CYP inhibition:		
CYP2C9/2D6/ 62 /		94
3A4 % Inhibition at 10 M	< 50 %	93
1A22 % Inhibition at 10 M	< 50 %	58
C19 % Inhibition at 10 M	< 50 %	54

INTEGRI PROCEDAMUS

University of Ghana http://ugspace.ug.edu.gh

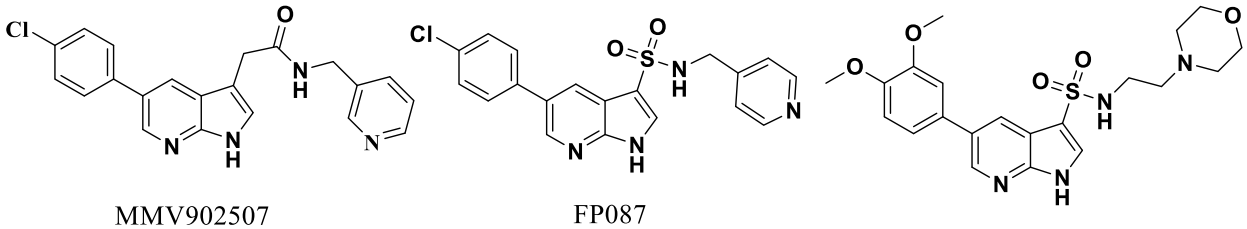
Chapter 3

3.1 The Hit Compound MMV902507 (SFK78)

To contribute to malaria eradication, researchers are exploring new potent drugs with novel mechanism of action to overcome resistance to ACTs. MMV, however, conducted a phenotypic screening of the bio-focus chemical library and SFK78 also known as MMV902507 (**Figure 3.1**) emerged as a hit compound. It was found to be active against the resistant Dd2 strain of the malaria parasite and showed Activity against the blood and liver stages of the parasite's life cycle**.** Furthermore, the hit compound showed good solubility and acceptable physicochemical properties. To establish the minimum pharmacophore, some members of the drug innovation group began structure-activity relationship (SAR) studies on the hit compound and it was observed that replacing the carboxamide functionality with a sulfonamide led to increased potency as exemplified by FP087 in **Figure 3.1**. In addition, replacement of the 4-chlorophenyl substituent with 3,4-dimethoxy substitution at position 5 gave similar potency. For example, AG050 with a 3,4-dimethoxy substitution showed an activity of **0.082 µM,** comparable to FP087 **0.062 µM**. The aim therefore is to expand the SAR and explore the importance of secondary amines on activity and also to validate that the presence of the 3,4-dimethoxy substitution at position 5 positively drives the activity.

INTEGRI PROCEDAMUS

University of Ghana http://ugspace.ug.edu.gh



MMV902507
Dd2 IC_{50}: 0.34 µM

FP087
3D7 IC_{50}: 0.062 µM
Cytotoxicity/Hep G2 cells CC50 : >25 µM

AG050
3D7 IC_{50}: 0.082 µM

Figure 3.1: Previous work done on SFK78 by some members of the Drug Innovation group.

3.2 Materials

All the reagents were obtained commercially except for those that were synthesized in the lab. Pure and sealed dichloromethane (DCM), triethylamine (Et_3N), tetrahydrofuran (THF) and 1,4-dioxane were used throughout the synthetic process.

3.3 Chromatography for Separation and Purification

Thin-layer chromatography was performed on a precoated silica gel (0.25mm layer of silica gel F254) aluminum sheet. The mobile phase is a combination of various solvents in varying ratios. UV light was also used to visualize the results on the TLC plate and flash column chromatography was performed with silica gel 60 Å particle size 35-70 micron, Davisil® grade. The flash column chromatography method was used to purify both intermediate and final compounds using silica as the stationary phase and various ratios of ethyl acetate and DCM as the mobile phase, to elute the non-polar components of the crude compound followed by the polar component of the crude compound to elute the analyte of interest. Standard 15 mL vials were used to collect the various fractions from the column.

University of Ghana http://ugspace.ug.edu.gh

3.4 Nuclear Magnetic Resonance (NMR)

^{13}C-NMR and ^{1}H-NMR spectra were obtained using a Bruker 500 MHz spectrometer at the University of Ghana. The final compounds were dissolved in suitable deuterated solvents, transferred into NMR tubes, and analyzed using the Bruker 500 MHz spectrometer. The spectra obtained were analyzed to confirm the carbon and hydrogen framework of the compound. The spectra for the compounds are reported in Appendix **I**.

3.5 Fourier Transform Infrared Spectroscopy (FTIR)

The FTIR was used to determine the presence of the functional groups in a compound. The solid samples were applied onto a sodium chloride disc. The spectra were obtained using the Perkin-Elmer FTIR spectrometer and their interpretations were made in cm^{-1}. The spectra for the compounds are reported in Appendix **II**.

3.6 LC-MS

Mass spectrometry measurements were performed using the hyphenated liquid chromatography-Mass spectrometer Agilent HPLC system. Electrospray ionization (ESI) technique was used with Agilent Jet Stream Electrospray (AJS-E) machine, and ionization was performed in positive mode. The mobile phase for the LC was 10 nM NH_4OAc in 90% methanol/water. The stationary phase was Kinetex C18, 2.6 µm 3x50 mm, 100 Å maintained at 40 ºC. The LC-MS chromatogram for the compounds can be found in Appendix **III**.

3.7 Melting Point

Melting points were measured using the SMP10 Stuart Scientific melting point apparatus. The reading was expressed in degrees Celsius (ºC). The solid samples were placed in the capillary tube and monitored until they melted to determine their melting points.

University of Ghana http://ugspace.ug.edu.gh

3.8 Medicinal Chemistry Plan for the synthesis of derivatives of MMV902507

The hit compound **MMV902507** was first resynthesized and tested against both sensitive (NF54) and resistant (Dd2) strains of the malaria parasite yielding IC_{50} values of 0.17 µM and 0.34 µM respectively, during the phenotypic screening.

The medicinal chemistry strategy for the hit compound **MMV902507** is depicted in **Figure 3.2** below.

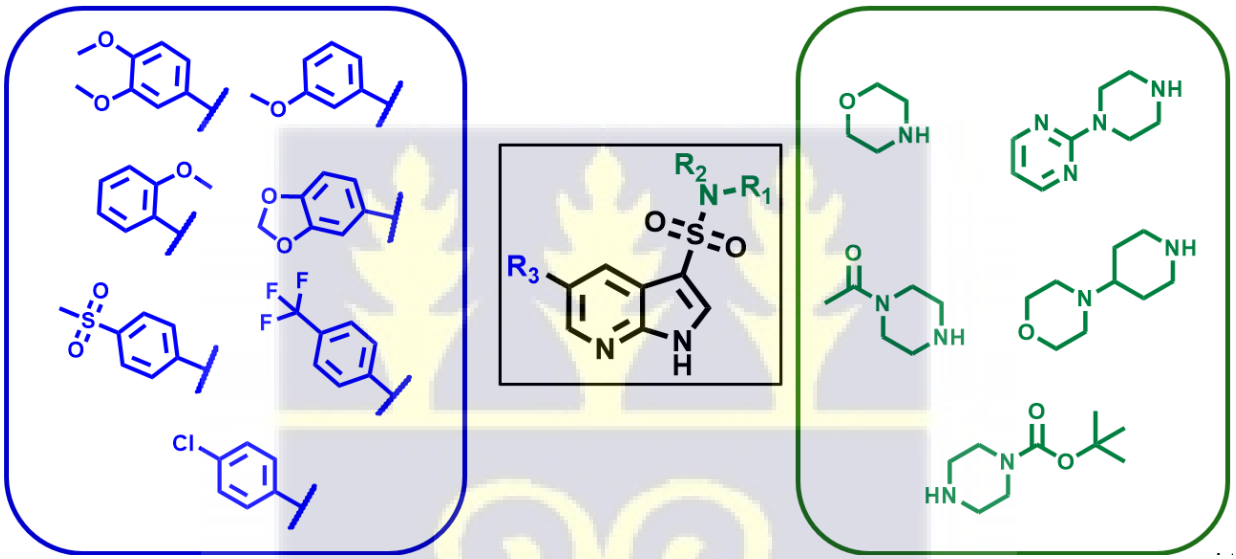
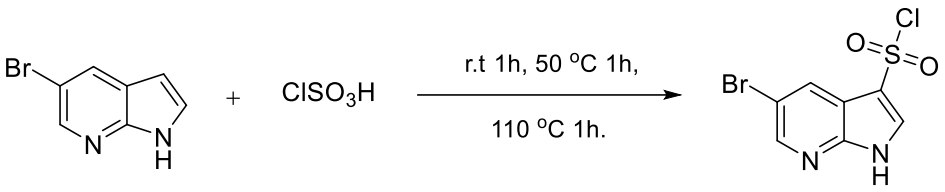


Figure 3.2: Medicinal Chemistry plan for hit compound **MMV902507**

First, changes were made on the LHS of the molecule by incorporating various substituted aromatic groups including electron-donating and withdrawing groups. Secondly, multiple sulphonamides using a variety of heterocyclic amines were incorporated on the right-hand side (RHS). The overall goal was to investigate which combination of the substitutions will retain potency compared to the phenotypic hit as well as display similar or superior pharmacokinetic properties.

University of Ghana http://ugspace.ug.edu.gh

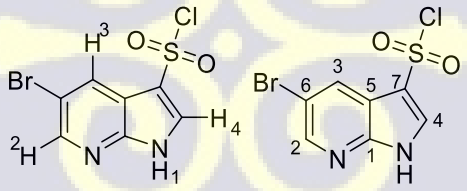
3.9 General Procedure for Synthesizing Sulfonyl Chloride Intermediate.



Scheme 2.0: General procedure for chloro sulfonation.

A flask containing chlorosulfonic acid (12 equivalent) cooled to 5 ºC was added to 5-bromo-1H-pyrrolo[2,3-b] pyridine (1 equivalent) in small portions. The mixture was allowed to warm to room temperature for 1 hour, then heated to 50 ºC for another hour after which the temperature was increased to 110 ºC for another hour. The reaction mixture was cooled to room temperature and quenched by adding dropwise to 200 mL of ice water with stirring. The resulting precipitate was stirred for about 5 minutes, and the resulting white solid was collected by filtration and dried.

3.9.1 Synthesis of 5-bromo-1H-pyrrolo[2,3-b] pyridine-3-sulfonyl chloride (ADA081, 1).

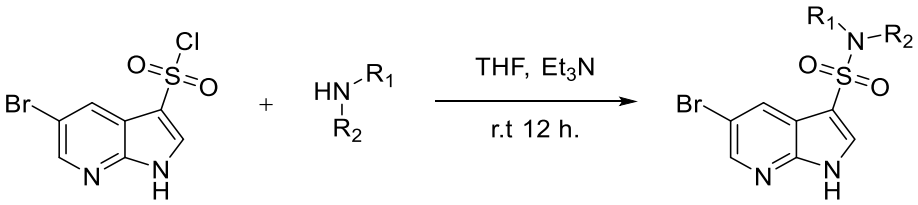


The compound above was prepared according to the general procedure for chlorosulfonation reaction described above. Chloro sulfonic acid (304.52 mmol) and 5-bromo-1H-pyrrolo[2,3-b] pyridine (25.37mmol) gave a white amorphous solid (7.3g, 98 % yield). Melting = 181-183 ºC Vmax (neat) cm^{-1} (N-H) 3110.84, (C-H) 2986.98, (C=C) 1596.91, (C=N) 1327.64, (S=O) 1156.01. ^1H NMR (500 MHz, DMSO-*d*6) δ_H 12.01 (s, $1H_1$), 8.31 (d, J = 2.3 Hz, $1H_2$), 8.20 (d, J = 2.3 Hz,

University of Ghana http://ugspace.ug.edu.gh

1H$_3$), 7.59 (d, J = 2.4 Hz, 1H$_4$). ^{13}C NMR (126 MHz, DMSO-d_6) δ_C 146.4C$_1$, 143.2 C$_2$, 130.8 C$_3$, 127.0 C$_4$, 121.9 C$_5$, 119.1 C$_6$, 111.5 C$_7$.

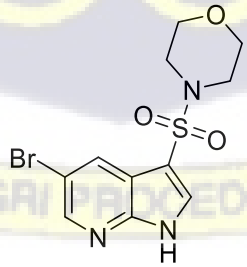
3.10 General Procedure for Synthesizing sulfonamide Intermediate.



Scheme 2.1: General synthesis for sulfonamide formation.

A solution of 5-bromo-1H-pyrrolo[2,3-b] pyridine-3-sulfonyl chloride (ADA081) (1 equivalence) was dissolved in THF (20 mL) and left to stir. The amine (1.5 equivalents) was added to Et$_3$N (2.5 equivalents), and the solution was stirred for 30 minutes. The mixture was added to ADA081 and stirred for 12 h. The crude mixture was purified by flash column chromatography to yield the intermediate.

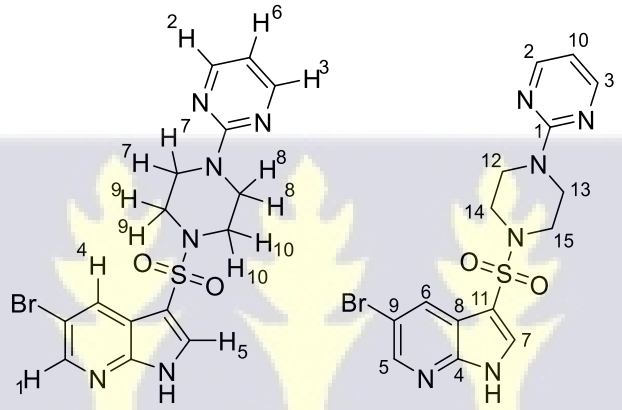
3.10.1 Synthesis of 4-((5-bromo-1H-pyrrolo[2,3-b] pyridin-3-yl) sulfonyl) morpholine (ADA082, 2).



University of Ghana http://ugspace.ug.edu.gh

The compound above was prepared according to the general procedure for sulfonamide formation using ADA081 (1.00 g, 3.38 mmol), Morpholine (0.44 mL, 5.08 mmol), Et_3N (1.18 mL, 8.46 mmol) to give a cream amorphous solid (0.47g, 40 % yield). Melting = 243 ºC-245 ºC, Vmax (neat) cm^{-1} (N-H) 3111.84, (C-H) 2996.88, (C=C) 1596.91, (C=N) 1327.64, (S=O) 1146.01.

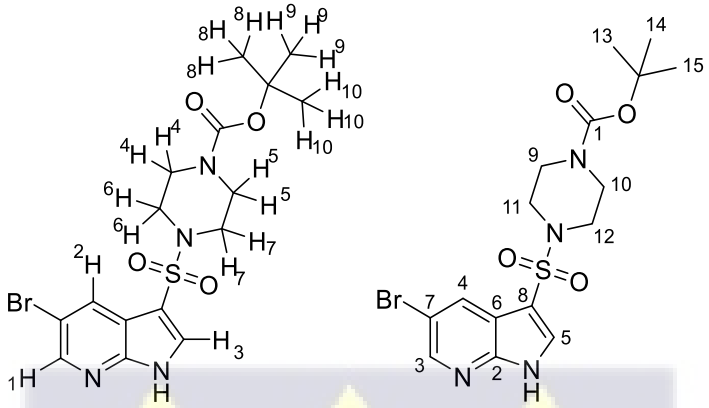
3.10.2 Synthesis of 5-bromo-3-((4-(pyrimidin-2-yl) piperazin-1-yl) sulfonyl) -1H-pyrrolo[2,3-b] pyridine (ADA086, 3).



Compound ADA086 was prepared according to the general procedure for sulfonamide formation using ADA081 (0.5 g, 1.69 mmol), 2-(Piperazin-1-yl) pyrimidine (0.36 mL, 2.53 mmol), Et_3N (0.59 mL, 4.23 mmol) to give a pale yellow amorphous solid (0.28 g, 39 % yield). Melting = 255 ºC-257 ºC, Vmax (neat) cm^{-1} (N-H) 3110.84, (C-H) 2986.98, (C=C) 1596.91, (C=N) 1327.64, (S=O) 1156.01. ^{1}H NMR (500 MHz, DMSO-d_6) δ_H 8.44 (d, J = 2.2 Hz, 1H$_1$), 8.29 (d, J = 4.7 Hz, 2H$_{2,3}$), 8.27 (d, J = 2.2 Hz, 1H$_4$), 8.20 (s, 1H$_5$), 6.59 (t, J = 4.7 Hz, 1H$_6$), 3.82 (t, J = 5.0 Hz, 4H$_{7,8}$), 2.97 (t, J = 5.0 Hz, 4H$_{9,10}$). ^{13}C NMR (126 MHz, DMSO-d6) δ_C 161.2 C$_1$, 158.4 C$_{2,3}$, 147.1 C$_4$, 145.2 C$_5$, 134.1 C$_6$, 129.9 C$_7$, 119.0 C$_8$, 113.6 C$_9$, 111.0 C$_{10}$, 107.3 C$_{11}$, 45.9 C$_{12,13}$, 42.9 C$_{14,15}$.

University of Ghana http://ugspace.ug.edu.gh

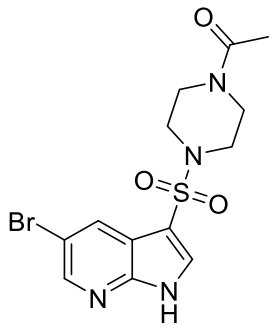
3.10.3 Synthesis of tert-butyl 4-((5-bromo-1H-pyrrolo[2,3-b] pyridin-3-yl) sulfonyl) piperazine-1-carboxylate (ADA089, 4).



Compound ADA089 was prepared according to the general procedure for sulfonamide formation using ADA081 (1.0 g, 3.38 mmol), *N*-Boc piperazine (0.95 g, 5.08 mmol), Et_3N (1.18 mL, 8.46 mmol) to give a white amorphous solid (0.28 g, 39 % yield). Melting = 239 ºC-241 ºC, Vmax (neat) cm^{-1} (N-H) 3210.84, (C-H) 2946.98, (C=C) 1546.91, (C=O) 1645.99 (C=N) 1427.64, (S=O) 1158.01. ^1H NMR (500 MHz, DMSO-d_6) δ_H 8.45 (d, J = 2.3 Hz, $1H_1$), 8.25 (d, J = 2.2 Hz, $1H_2$), 8.19 (s, $1H_3$), 3.37 (t, J = 5.2 Hz, $4H_{4,5}$), 2.87 (t, J = 5.1 Hz, $4H_{6,7}$), 1.29 (s, $9H_{8,9,10}$). ^{13}C NMR (126 MHz, DMSO-d_6) δ_C 153.5 C_1, 146.5 C_2, 145.1 C_3, 133.4 C_4, 129.7 C_5, 118.6 C_6, 113.4 C_7, 107.1 C_8, 79.4 $C_{9,10}$, 45.7 $C_{11,12}$, 28.1 $C_{13,14,15}$.

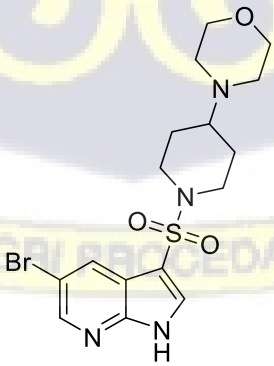
University of Ghana http://ugspace.ug.edu.gh

3.10.4 Synthesis of 1-(4-((5-bromo-1H-pyrrolo[2,3-b] pyridin-3-yl) sulfonyl) piperazin-1-yl) ethan-1-one (ADA094, 5).



Compound ADA094 was prepared according to the general procedure for sulfonamide formation using ADA081 (1.0 g, 3.38 mmol), Acetyl piperazine (0.60 mL, 5.07 mmol), Et_3N (1.18 mL, 8.46 mmol) to give a cream amorphous solid (0.28g, 21% yield). Melting = 260 ºC-262 ºC, Vmax (neat) cm^{-1} (N-H) 3178.04, (C-H) 2999.50, (C=C) 1504.91, (C=O) 1677.02, (C=N) 1397.64, (S=O) 1148.01.

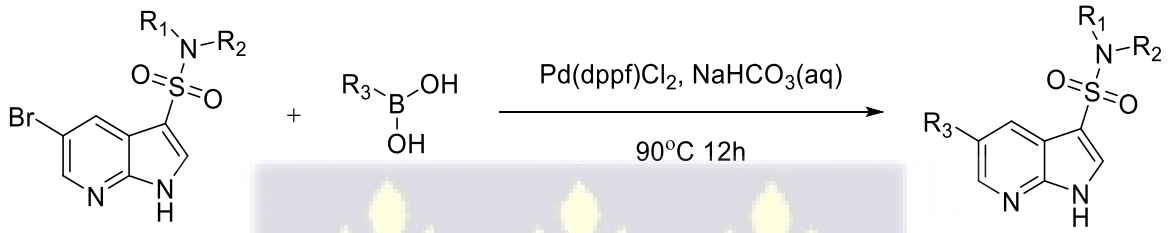
3.10.5 Synthesis of 4-(1-((5-bromo-1H-pyrrolo[2,3-b] pyridin-3-yl) sulfonyl) piperidin-4-yl) morpholine (ADA098, 6).



University of Ghana http://ugspace.ug.edu.gh

Compound ADA098 was prepared according to the general procedure for sulfonamide formation using ADA081 (0.5 g, 1.69 mmol), 4-(piperidin-4-yl) Morpholine (0.43 g, 2.54 mmol), Et_3N (0.59 mL, 4.23 mmol), to give a yellow amorphous solid (0.13 g, 14 % yield). Melting = 256 ºC-258 ºC, Vmax (neat) cm^{-1} (N-H) 3130.84, (C-H) 2986.08, (C=C) 1566.91, (C=N) 1427.64, (S=O) 1146.01.

3.11 General Procedure for Suzuki Cross-Coupling Reaction on Sulfonamide Intermediate (Final Compounds).



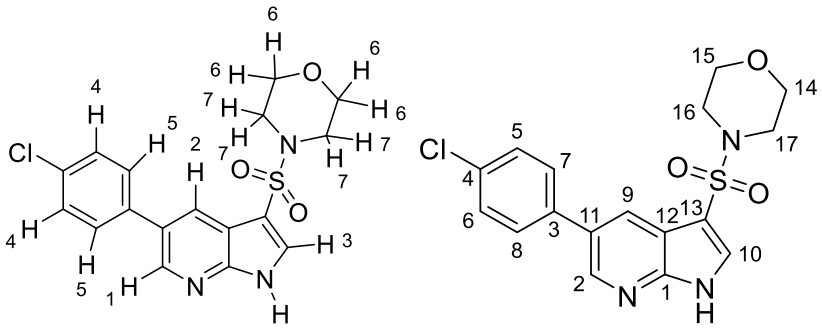
Scheme 2.2: General procedure for Suzuki cross-coupling reaction.

1,1-Bis(diphenylphosphine)ferrocene dichloropalladium (II) [Pd(dppf)] Cl_2 (0.05 equivalents) and a solution of aqueous sodium bicarbonate (2 equivalents) were added to a mixture of the sulfonamide intermediates above (1 equivalent) and various boronic acids (1.5 equivalents) in dioxane under a nitrogen atmosphere. The mixture was stirred at 95 ºC for 12 h and the crude mixture was concentrated under reduced pressure upon completion of the reaction (monitored by TLC). The crude mixture was purified by flash column chromatography to afford the desired product.

INTEGRI PROCEDAMUS

University of Ghana http://ugspace.ug.edu.gh

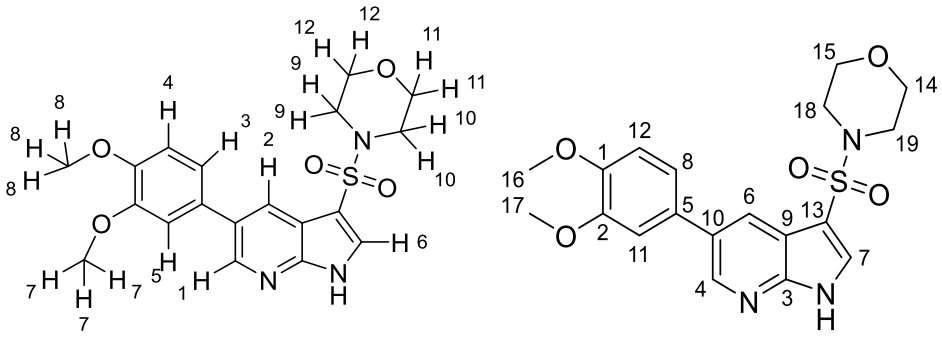
3.11.1 Synthesis of 4-((5-(4-chlorophenyl)-1H-pyrrolo[2,3-b] pyridin-3-yl) sulfonyl) Morpholine (ADA 083,6).



Compound ADA083 was prepared according to the general procedure for the cross-coupling reaction of sulfonamide intermediate using ADA082 (0.29 mmol), 4-chlorophenyl boronic acid (0.05 g, 0.43 mmol), [Pd(dppf)] Cl_2 (0.01 mmol), $NaHCO_3$ (0.58 mmol) to give a brown amorphous solid (0.04 g, 36 % yield). Melting = 215ºC-217 ºC Vmax (neat) cm^{-1}, (C-H) 2919.76, (C=C) 1453.31, (C=N) 1343.18, (S=O) 1149.74. ^{1}H NMR (500 MHz, DMSO-d_6) δ_H 8.68 (d, J = 2.2 Hz, 1H_1), 8.28 (d, J = 2.3 Hz, 1H_2), 8.20 (s, 1H_3), 7.75 (d, J = 8.4 Hz, 2H_4), 7.54 (d, J = 8.2 Hz, 2H_5), 3.62 (t, J = 4.6 Hz, 4H_6), 2.90 (t, J = 4.7 Hz, 4H_7). ^{13}C NMR (126 MHz, DMSO-d_6) δ_C 147.6 C_1, 143.7 C_2, 136.9 C_3, 132.8 C_4, 132.5 $C_{5,6}$, 129.4 $C_{7,8}$, 129.1 C_9, 125.5 C_{10}, 117.0 C_{11}, 113.6 C_{12}, 107.2 C_{13}, 65.3 $C_{14,15}$, 45.8 $C_{16,17}$. The calculated mass of the compound was 377.84. LCMS 1.021 min 75 % m/z 378.1 $[M + H]^+$.

University of Ghana http://ugspace.ug.edu.gh

3.11.2 Synthesis of 4-((5-(3,4-dimethoxyphenyl)-1H-pyrrolo[2,3-b] pyridin-3-yl) sulfonyl) Morpholine (ADA 084, 7).

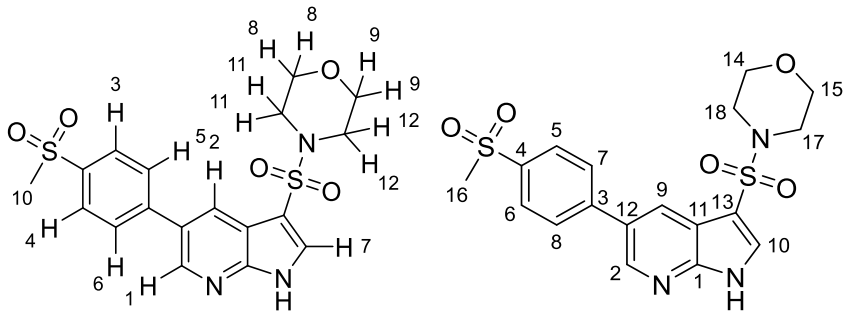


Compound ADA084 was prepared according to the general procedure for the cross-coupling reaction of sulfonamide intermediate using ADA082 (0.1 g, 0.29 mmol), 3,4-dimethoxy benzene boronic acid (0.08g, 0.43mmol), [Pd(dppf)] Cl_2 (0.01 g, 0.01 mmol), $NaHCO_3$ (0.04 g, 0.58 mmol) to give a white amorphous solid (0.01 g, 9 % yield). Melting = 227 ºC-228 ºC, Vmax (neat) cm^{-1} (N-H) 3142.49, (C-H) 2998.09, (=C-H) 3030.29, (C=C) 1586.41, (C=N) 1519.54, (S=O) 1141.90. ^1H NMR (500 MHz, DMSO-d_6) δ_H 8.70 (d, J = 2.2 Hz, $1H_1$), 8.25 (d, J = 2.2 Hz, $1H_2$), 8.19 (s, $1H_6$), 7.27 (d, J = 2.1 Hz, $1H_3$), 7.23 (d, J = 8.3, 2.2 Hz, $1H_4$), 7.10 (d, J = 8.4 Hz, $1H_5$), 3.88 (s, $3H_7$), 3.82 (s, $3H_8$), 3.65 (t, J = 4.7 Hz, $4H_{9,10}$), 2.93 (t, J = 4.7 Hz, $4H_{11,12}$). ^{13}C NMR (126 MHz, DMSO-d_6) δ_C 148.8 C_1, 148.2 C_2, 146.7 C_3, 143.3 C_4, 133.6 C_5, 130.8 C_6, 130.8 C_7, 129.1 C_8, 124.5 C_9, 119.1 C_{10}, 116.4 C_{11}, 112.0 C_{12}, 110.6 C_{13}, 68.5 $C_{14,15}$, 64.8 C_{16}, 55.2 C_{17}, 45.3 $C_{18,19}$. The calculated mass of the compound was 403.12. LCMS 2.255 min m/z 403.39 $[M]^+$.

INTEGRI PROCEDAMUS

University of Ghana http://ugspace.ug.edu.gh

3.11.3 Synthesis of 4-((5-(4-(methyl sulfonyl) phenyl)-1H-pyrrolo[2,3-b] pyridin-3-yl) sulfonyl) Morpholine (ADA 085, 8).

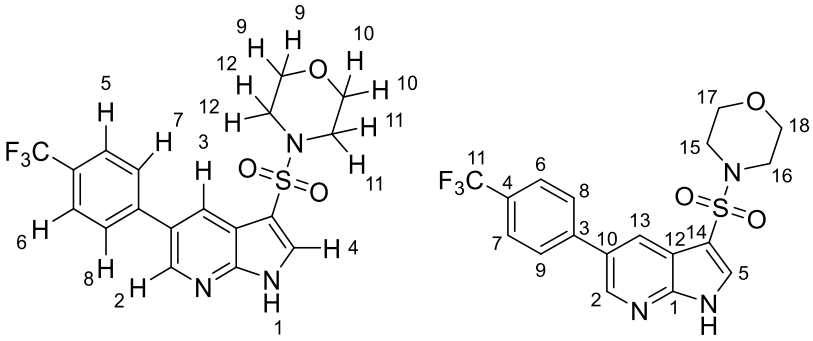


Compound ADA085 was prepared according to the general procedure for the cross-coupling reaction of sulfonamide intermediate using ADA082 (0.08 g, 0.23 mmol), 4-(methane sulfonyl) phenyl boronic acid (0.07 g, 0.35 mmol), [Pd(dppf)] Cl_2 (0.008 g, 0.01 mmol), $NaHCO_3$ (0.04 g, 0.46 mmol) to give an orange amorphous solid (0.01 g, 11 % yield). Melting = 190 ºC-191 ºC, Vmax (neat) cm^{-1}(N-H) 3341.31, (C-H) 2933.67, (=C-H) 3029.19, (C=C) 1596.31, (C=N) 1445.24, (S=O) 1148.56. ^{1}H NMR (500 MHz, DMSO-d_6) δ_H 8.78 (d, J = 2.2 Hz, 1H_1), 8.39 (d, J =2.3 Hz, 1H_2), 8.25 (s, 1H_7), 8.00 (d, J = 1.8 Hz, 2$H_{3,4}$), 7.88 (d, J = 1.9 Hz, 2$H_{5,6}$), 3.64 (t, J = 4.8 Hz, 4$H_{8,9}$), 3.20 (s, 3H_{10}), 2.93 (t, J = 4.7 Hz, 4$H_{11,12}$). ^{13}C NMR (126 MHz, DMSO-d_6) δ_C 147.4 C_1, 143.5 C_2, 141.5 C_3, 139.2 C_4, 134.2 $C_{5,6}$, 132.5 $C_{7,8}$, 127.6 C_9, 127.3 C_{10}, 125.1 C_{11}, 116.5 C_{12}, 107.0 C_{13}, 64.8 $C_{14,15}$, 45.3 C_{16}, 43.0 $C_{17,18}$. The calculated mass of the compound was 421.49. LCMS 0.809 min 100 % m/z 422.1$[M + H]^+$.

INTEGRI PROCEDAMUS

University of Ghana http://ugspace.ug.edu.gh

3.11.4 Synthesis of 4-((5-(4-(trifluoromethyl) phenyl)-1H-pyrrolo[2,3-b] pyridin-3-yl) sulfonyl) morpholine (ADA087, 9).

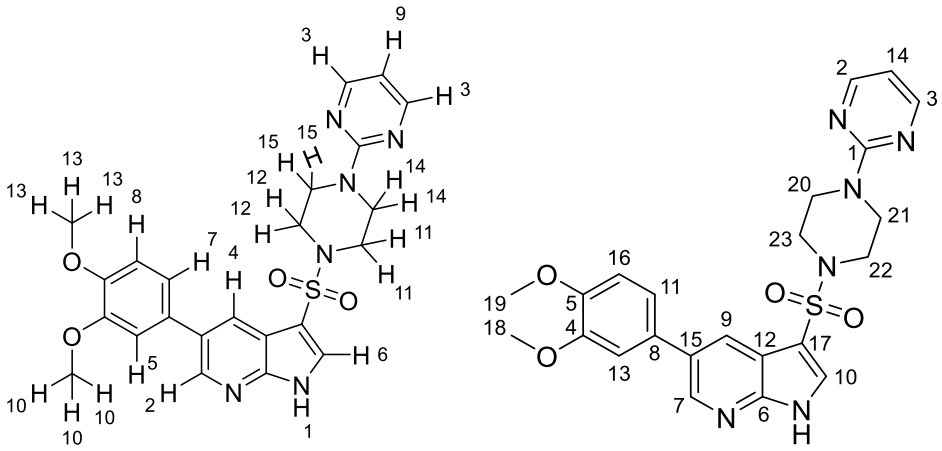


Compound ADA087 was prepared according to the general procedure for the cross-coupling reaction of sulfonamide intermediate using ADA082 (0.08 g, 0.23 mmol), 4-(trifluoro methyl) phenyl boronic acid (0.06 g, 0.35 mmol), [Pd(dppf)] Cl_2 (0.008 g, 0.01 mmol), $NaHCO_3$ (0.04 g, 0.46 mmol) to give a cream amorphous solid (0.05 g, 48 % yield). Melting = 210 ºC-211 ºC Vmax (neat) cm^{-1} (N-H) 3110.84, (C-H) 2986.98, (C=C) 1596.91, (C=N) 1327.64, (S=O) 1156.01. ^{1}H NMR (500 MHz, DMSO-d_6) δ_H 13.07 (s, $1H_1$), 8.78 (d, J = 2.3 Hz, $1H_2$), 8.39 (d, J = 2.2 Hz, $1H_3$), 8.26 (s, $1H_4$), 7.99 (d, J = 8.2 Hz, $2H_{5,6}$), 7.87 (d, J = 8.1 Hz, $2H_{7,8}$), 3.65 (t, J = 4.7 Hz, $4H_{9,10}$), 2.94 (d, J = 4.8 Hz, $4H_{11,12}$). ^{13}C NMR (126 MHz, DMSO-d_6) δ_C 147.4 C_1, 143.4 C_2, 141.7 C_3, 132.5 C_4, 128.6 C_5, 127.6 $C_{6,7}$, 127.3 $C_{8,9}$, 125.6 C_{10}, 125.3 C_{11}, 124.9 C_{12}, 116.5 C_{13}, 106.9 C_{14}, 64.7 $C_{15,16}$, 45.2 $C_{17,18}$. The calculated mass of the compound was 411.40. LCMS 1.053 min 82 % m/z 412.1 $[M + H]^+$.

INTEGRI PROCEDAMUS

University of Ghana http://ugspace.ug.edu.gh

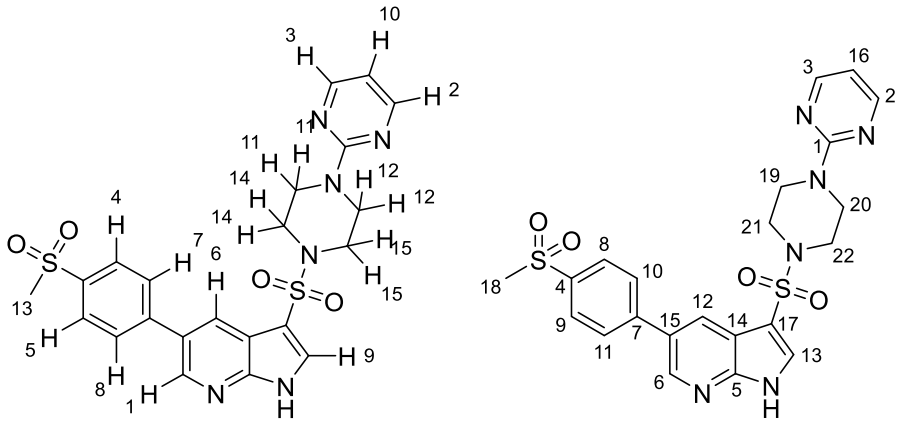
3.11.5 Synthesis of 5-(3,4-dimethoxyphenyl)-3-((4-(pyrimidin-2-yl) piperazin-1-yl) sulfonyl)-1H-pyrrolo[2,3-b] pyridine (ADA088, 10).



Compound ADA088 was prepared according to the general procedure for the cross-coupling reaction of sulfonamide intermediate using ADA086 (0.09 g, 0.21 mmol), 3,4-dimethoxy benzene boronic acid (0.07 g, 0.39 mmol), [Pd(dppf)] Cl_2 (0.009 g, 0.01 mmol), $NaHCO_3$ (0.04 g, 0.52 mmol) to give a white amorphous solid (0.021 g, 17 % yield). Melting = 268 ºC-269 ºC Vmax (neat) cm^{-1} (N-H) 3280.00, (C-H) 2834.17, (C=C) 1581.57, (C=N) 1517.92, (S=O) 1151.90. ^{1}H NMR (500 MHz, DMSO-d_6) δ_H 12.87 (s, $1H_1$), 8.66 (s, $1H_2$), 8.29 (dd, J = 4.7, 1.0 Hz, $2H_3$), 8.25 (d, J = 1.9 Hz, $1H_4$), 8.16 (s, $1H_5$), 7.25 (s, $1H_6$), 7.22 (dd, J = 8.2, 2.3 Hz, $1H_7$), 7.09 (d, J = 8.2 Hz, $1H_8$), 6.59 (t, J = 4.7 Hz, $1H_9$), 3.87 (s, $3H_{10}$), 3.83 (t, J = 4.6 Hz, $4H_{14,15}$), 3.81 (s, $3H_{11}$), 3.01 (t, J = 5.0 Hz, $4H_{12,13}$). ^{13}C NMR (126 MHz, DMSO-d_6) δ_C 160.3 C_1, 157.4 $C_{2,3}$, 148.7 C_4, 146.6 C_5, 143.2 C_6, 131.8 C_7, 130.3 C_8, 130.2 C_9, 124.5 C_{10}, 119.1 C_{11}, 116.3 C_{12}, 112.0 C_{13}, 110.6 $C_{14,15}$, 110.1 C_{16}, 106.8 C_{17}, 55.2 $C_{18,19}$, 45.0 $C_{20,21}$, 42.0 $C_{22,23}$. The calculated mass of the compound was 480.54 . LCMS 0.970 min 58 % m/z 481.1 $[M + H]^+$.

University of Ghana http://ugspace.ug.edu.gh

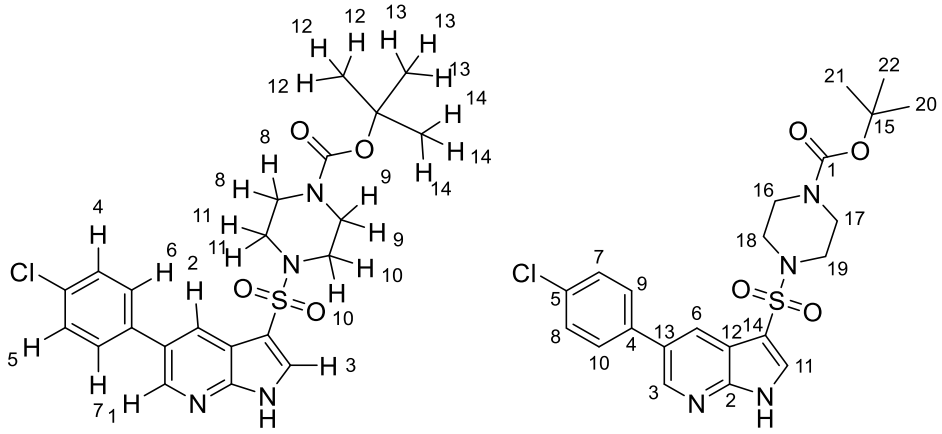
3.11.6 Synthesis of 5-(4-(methyl sulfonyl) phenyl)-3-((4-(pyrimidin-2-yl) piperazin-1-yl) sulfonyl)-1H-pyrrolo[2,3-b] pyridine (ADA090, 11).



Compound ADA090 was prepared according to the general procedure for the cross-coupling reaction of sulfonamide intermediate using ADA086 (0.09 g, 0.21 mmol), 4-(methane sulfonyl) phenyl boronic acid (0.06 g, 0.32 mmol), [Pd(dppf)] Cl_2 (0.007 g, 0.01 mmol), $NaHCO_3$ (0.04 g, 0.42 mmol) to give a light pink amorphous solid (0.045 g, 42 % yield) . Melting = 225 ºC-227 ºC, Vmax (neat) cm^{-1} (N-H) 3342.43, (C-H) 2993.65, (=C-H) 3109.17, (C=C) 1588.81, (C=N) 1548.17, (S=O) 1149.26. ^{1}H NMR (500 MHz, DMSO-d_6) δ_H 8.7 (s, 1H$_1$), 8.4 (d, J = 4.7 Hz, 2H$_{2,3}$), 8.3 (d, J = 2.3 Hz, 1H$_6$), 8.2 (d, J = 4.8 Hz, 2H$_{4,5}$), 8.1 (s, 1H$_9$), 7.9 (d, J = 4.8 Hz, 2H$_{7,8}$), 6.5 (t, J = 4.7 Hz, 1H$_{10}$), 3.7 (t, J = 5.0 Hz, 4H$_{11,12}$), 3.2 (s, 3H$_{13}$), 2.9 (t, J = 5.0 Hz, 4H$_{14,15}$). ^{13}C NMR (126 MHz, DMSO-d_6) δ_C 161.0 C$_1$, 158.4 C$_{2,3}$, 146.4 C$_4$, 144.4 C$_5$, 140.1 C$_6$, 135.2 C$_7$, 128.6 C$_{8,9}$, 128.2 C$_{10,11}$, 126.6 C$_{12}$, 126.1 C$_{13}$, 121.8 C$_{14}$, 115.2 C$_{15}$, 111.0 C$_{16}$, 108.2 C$_{17}$, 46.0 C$_{18}$, 44.1 C$_{19,20}$, 42.9 C$_{21,22}$. The calculated mass of the compound was 498.58. LCMS 0.901 min 100 % m/z 499.1 [M + H] $^+$.

University of Ghana http://ugspace.ug.edu.gh

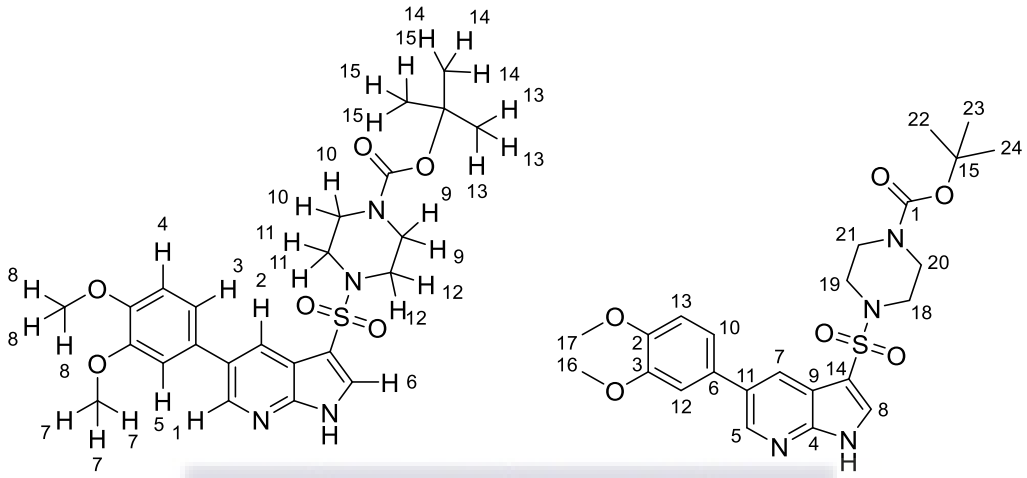
3.11.7 Synthesis of tert-butyl 4-((5-(4-chlorophenyl)-1H-pyrrolo[2,3-b] pyridin-3-yl) sulfonyl) piperazine-1-carboxylate (ADA091, 12).



Compound ADA091 was prepared according to the general procedure for the cross-coupling reaction of sulfonamide intermediate using ADA089 (0.11 g, 0.23 mmol), 4-chloro phenyl boronic acid (0.05 g, 0.35 mmol), [Pd(dppf)] Cl_2 (0.009 g, 0.01 mmol), $NaHCO_3$ (0.04 g, 0.47 mmol) to give a white amorphous solid (0.045 g, 40 % yield). Melting = 233 ºC-235 ºC Vmax (neat) cm^{-1}, (C-H) 2976.31, (C=O) 1652.81, (C=C) 1533.27, (C=N) 1424.93, (S=O) 1152.55. ^{1}H NMR (500 MHz, DMSO-d_6) δ_H 8.63 (d, J = 2.3 Hz, $1H_1$), 8.23 (d, J = 2.3 Hz, $1H_2$), 8.13 (s, $1H_3$), 7.71 (d, J = 8.6 Hz, $2H_{4,5}$), 7.50 (d, J = 8.6 Hz, $2H_{6,7}$), 3.53 (t, J = 5.0 Hz, $4H_{8,9}$), 2.84 (t, J = 5.1 Hz, $4H_{10,11}$), 1.24 (s, $9H_{12,13,14}$). ^{13}C NMR (126 MHz, DMSO-d_6) δ_C 172.5 C_1, 153.0 C_2, 143.1 C_3, 136.5 C_4, 132.4 C_5, 132.1 C_6, 128.6 $C_{7,8}$, 125.2 $C9_{,10}$, 116.5 C_{11}, 106.8 C_{12}, 100.1 C_{13}, 95.0 C_{14}, 78.8 C_{15}, 45.9 $C_{16,17}$, 41.6 $C_{18,19}$, 28.3 $C_{20,21,22}$. The calculated mass of the compound was 476.13 while its acid derivative was 420.87. LCMS 1.182 min 100 % m/z 421.1 $[M + H]^+$ corresponding to the carboxylic acid derivative of the ester.

University of Ghana http://ugspace.ug.edu.gh

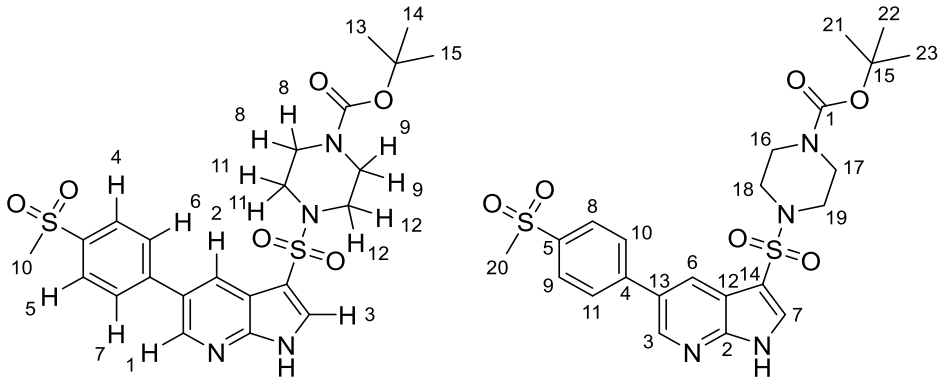
3.11.8 Synthesis of tert-butyl 4-((5-(3,4-dimethoxyphenyl)-1H-pyrrolo[2,3-b] pyridin-3-yl) sulfonyl) piperazine-1-carboxylate (ADA092, 13).



Compound ADA092 was prepared according to the general procedure for the cross-coupling reaction of sulfonamide intermediate using ADA089 (0.11 g, 0.23 mmol), 3,4-dimethoxy benzene boronic acid (0.06 g, 0.35 mmol), [Pd(dppf)] Cl_2 (0.008 g, 0.01 mmol), $NaHCO_3$ (0.039 g, 0.47 mmol) to give a pale yellow amorphous solid (0.032 g, 29 % yield). Melting = 209 ºC-211 ºC Vmax (neat) cm^{-1} (N-H) 3118.05, (C-H) 2971.33, (C=O) 1691.88, (C=C) 1598.92, (C=N) 1520.27, (S=O) 1140.88. ^{1}H NMR (500 MHz, DMSO-d_6) δ_H 8.69 (d, J = 2.2 Hz, 1H$_1$), 8.25 (d, J = 2.2 Hz, 1H$_2$), 8.17 (s, 1H$_6$), 7.27 (d, J = 2.2 Hz, 1H$_3$), 7.24 (dd, J = 8.2, 2.2 Hz, 1H$_4$), 7.10 (s, 1H$_5$), 3.88 (s, 3H$_7$), 3.82 (s, 3H$_8$), 3.41 (t, J = 5.3 Hz, 4H$_{9,10}$), 2.92 (t, J = 5.0 Hz, 4H$_{11,12}$), 1.31 (s, 9H$_{13,14,15}$). ^{13}C NMR (126 MHz, DMSO-d_6) δ_C 153.4 C$_1$, 149.2 C$_2$, 148.7 C$_3$, 147.2 C$_4$, 143.7 C$_5$, 132.4 C$_6$, 130.8 C$_7$, 130.7 C$_8$, 124.9 C$_9$, 119.6 C$_{10}$, 116.8 C$_{11}$, 112.5 C$_{12}$, 111.1 C$_{13}$, 107.2 C$_{14}$, 79.2 C$_{15}$, 55.7 C$_{16,17}$, 56.7 C$_{18,19}$, 45.6 C$_{20,21}$, 27.9 C$_{22,23,24}$. The calculated mass of the compound was 502.59. LCMS 1.054 min 86 % m/z 503.2 [M + H] $^+$.

University of Ghana http://ugspace.ug.edu.gh

3.11.9 Synthesis of tert-butyl 4-((5-(4-(methyl sulfonyl) phenyl)-1H-pyrrolo[2,3-b] pyridin-3-yl) sulfonyl) piperazine-1-carboxylate (ADA093, 14).

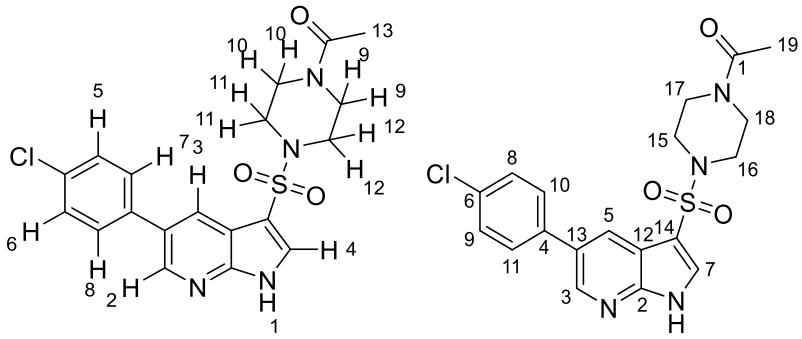


Compound ADA093 was prepared according to the general procedure for the cross-coupling reaction of sulfonamide intermediate using ADA089 (0.11 g, 0.23 mmol),4-(methane sulfonyl) phenyl boronic acid (0.07 g, 0.36 mmol), [Pd(dppf)] Cl_2 (0.008 g, 0.01 mmol), $NaHCO_3$ (0.039 g, 0.47 mmol) to give a pale yellow amorphous solid (0.042 g, 35 % yield). Melting = 228 ºC-230 ºC Vmax (neat) cm^{-1} (N-H) 3135.83, (C-H) 2984.76, (C=O) 1699.00, (C=C) 1596.31, (C=N) 1414.25, (S=O)1147.99. ^1H NMR (500 MHz, DMSO-d_6) δ_H 8.75 (d, J = 2.2 Hz, $1H_1$), 8.36 (d, J = 2.2 Hz, $1H_2$), 8.20 (s, $1H_3$), 8.02 (d, J = 8.6 Hz, $2H_{4,5}$), 8.01 (d, J = 8.5 Hz, $2H_{6,7}$), 3.37 (t, J = 4.9 Hz, $4H_{8,9}$), 3.24 (s, $3H_{10}$), 2.89 (t, J = 5.0 Hz, $4H_{11,12}$), 1.28 (s, $9H_{13,14,15}$). ^{13}C NMR (126 MHz, DMSO-d_6) δ_C 157.8 C_1, 153.8 C_2, 148.5 C_3, 144.2 C_4, 143.5 C_5, 140.0 C_6, 129.2 C_7, 128.5 $C_{8,9}$, 128.1 $C_{10,11}$, 126.4 C_{12}, 117.3 C_{13}, 96.9 C_{14}, 79.6 C_{15}, 45.9 $C_{16,17}$, 44.0 $C_{18,19}$, 28.6 C_{20}, 28.3 $C_{21,22,23}$. The calculated mass of the compound was 520.62 while its acid derivative was 464.51. LCMS 0.981 min 100 % m/z 465.1 $[M + H]^+$ corresponding to the carboxylic acid derivative of the ester.

INTEGRI PROCEDAMUS

University of Ghana http://ugspace.ug.edu.gh

3.11.10 Synthesis of 1-(4-((5-(4-chlorophenyl)-1H-pyrrolo[2,3-b] pyridin-3-yl) sulfonyl) piperazin-1-yl) ethan-1-one (ADA095, 15).

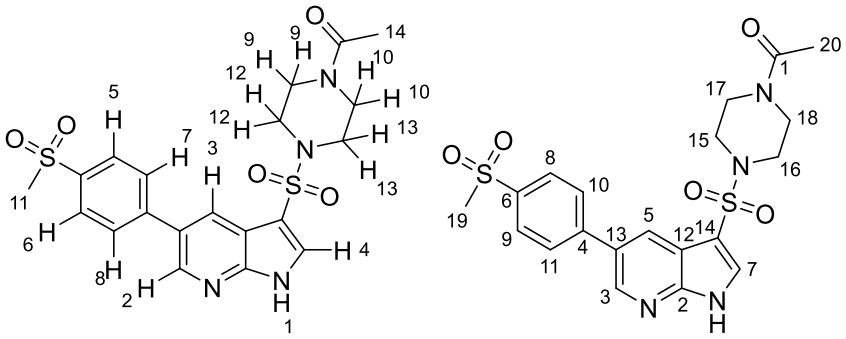


Compound ADA095 was prepared according to the general procedure for the cross-coupling reaction of sulfonamide intermediate using ADA094 (0.09 g, 0.23 mmol), 4-chloro phenyl boronic acid (0.05 g, 0.34 mmol), [Pd(dppf)] Cl_2 (0.008 g, 0.01 mmol), $NaHCO_3$ (0.039 g, 0.47 mmol) to give a white amorphous solid (0.042 g, 35 % yield). Melting = 235 ºC-237 ºC Vmax (neat) cm^{-1} (N-H) 3278.94, (C-H) 2850.06, (C=O) 1644.03, (C=C) 1440.24, (C=N) 1337.71, (S=O) 1151.83. ^{1}H NMR (500 MHz, DMSO-d_6) δ_H 12.98 (s, 1H_1), 8.71 (d, J = 2.2 Hz, 1H_2), 8.31 (d, J = 2.2 Hz, 1H_3), 8.22 (s, 1H_4), 7.82 (d, J = 8.5 Hz, 2$H_{5,6}$), 7.63 (d, J = 8.6 Hz, 2$H_{7,8}$), 3.52 (dd, J = 11.5, 5.1 Hz, 4$H_{9,10}$), 2.95 (dt, J = 22.0, 5.1 Hz, 4$H_{11,12}$), 1.91 (s, 3H_{13}). ^{13}C NMR (126 MHz, DMSO-d_6) δ_C 168.6 C_1, 147.9 C_2, 143.9 C_3, 137.2 C_4, 133.0 C_5, 132.9 C_6, 129.7 C_7, 129.4 $C_{8,9}$, 129.4 $C_{10,11}$, 125.7 C_{12}, 117.2 C_{13}, 107.8 C_{14}, 46.1 $C_{15,16}$, 45.1 $C_{17,18}$, 21.4 C_{19}. The calculated mass of the compound was 418.90. LCMS 0.961 min 100 % m/z 419.0 $[M + H]^+$.

INTEGRI PROCEDAMUS

University of Ghana http://ugspace.ug.edu.gh

3.11.11 Synthesis of 1-(4-((5-(4-(methyl sulfonyl) phenyl)-1H-pyrrolo[2,3-b] pyridin-3-yl) sulfonyl) piperazin-1-yl) ethan-1-one (ADA096, 16).

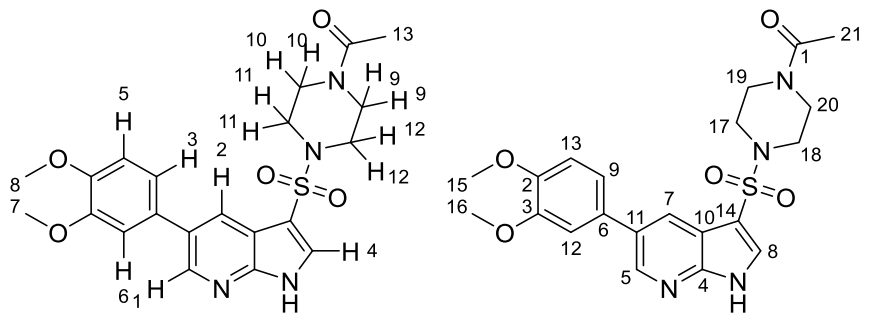


Compound ADA096 was prepared according to the general procedure for the cross-coupling reaction of sulfonamide intermediate using ADA094 (0.11 g, 0.23 mmol), 4-(methane sulfonyl) phenyl boronic acid (0.06 g, 0.35 mmol), [Pd(dppf)] Cl_2 (0.009 g, 0.01 mmol), $NaHCO_3$ (0.039 g, 0.47 mmol) to give a yellow amorphous solid (0.026 g, 24% yield). Melting = 207 ºC-209 ºC Vmax (neat) cm^{-1} (N-H) 3109.96, (C-H) 2874.17, (C=O) 1651.41, (C=C) 1469.46, (C=N) 1344.30, (S=O) 1146.81. ^{1}H NMR (500 MHz, DMSO-d_6) δ_H 13.07 (s, 1H_1), 8.80 (d, J = 2.2 Hz, 1H_2), 8.40 (d, J = 2.2 Hz, 1H_3), 8.26 (s, 1H_4), 8.07 (d, J = 8.8 Hz, 2$H_{5,6}$), 8.04 (d, J = 9.1 Hz, 2$H_{7,8}$), 3.55 (dd, J = 11.4, 5.4 Hz, 4$H_{9,10}$), 3.29 (s, 3H_{11}), 2.96 (dd, J = 21.9, 5.4 Hz, 4$H_{12,13}$), 1.91 (s, 3H_{14}). ^{13}C NMR (126 MHz, DMSO-d_6) δ_C 167.7 C_1, 147.4 C_2, 143.4 C_3, 142.6 C_4, 139.2 C_5, 132.2 C_6, 128.4 C_7, 127.6 $C_{8,9}$, 127.2 $C_{10,11}$, 125.6 C_{12}, 116.4 C_{13}, 107.2 C_{14}, 48.1 $C_{15,16}$, 44.3 $C_{17,18}$, 43.1 C_{19}, 20.5 C_{20}. The calculated mass of the compound was 462.54. LCMS 0.764 min 94 % m/z 463.1 [M + H] $^+$.

INTEGRI PROCEDAMUS

University of Ghana http://ugspace.ug.edu.gh

3.11.12 Synthesis of 1-(4-((5-(3,4-dimethoxyphenyl)-1H-pyrrolo[2,3-b] pyridin-3-yl) sulfonyl) piperazin-1-yl) ethan-1-one (ADA097, 17).

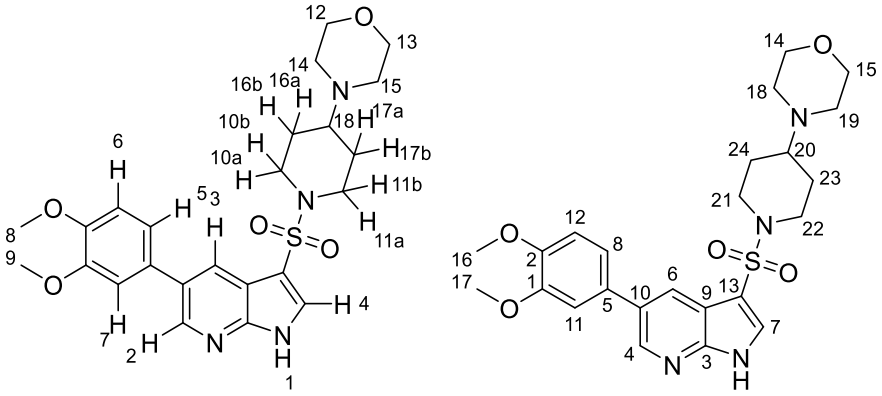


Compound ADA097 was prepared according to the general procedure for the cross-coupling reaction of sulfonamide intermediate using ADA089 (0.09 g, 0.23 mmol), 3,4-dimethoxy benzene boronic acid (0.06 g, 0.35 mmol), [Pd(dppf)] Cl_2 (0.009 g, 0.01 mmol), $NaHCO_3$ (0.039 g, 0.47 mmol) to give a cream amorphous solid (0.039 g, 37 % yield). Melting = 193 ºC-194 ºC Vmax (neat) cm^{-1} (N-H) 3122.42, (C-H) 2852.06, (C=O) 1625.85, (C=C) 1439.72, (C=N) 1344.56, (S=O) 1145.83. ^{1}H NMR (500 MHz, DMSO-d_6) δ_H 8.66 (d, J = 2.2 Hz, $1H_1$), 8.22 (d, J = 2.2 Hz, $1H_2$), 8.14 (s, $1H_4$), 7.24 (d, J = 2.2 Hz, $1H_3$), 7.20 (dd, J = 8.2, 2.1 Hz, $1H_5$), 7.07 (s, $1H_6$), 3.85 (s, $3H_7$), 3.79 (s, $3H_8$), 3.50 (t, J = 5.1 Hz, $4H_{9,10}$), 2.92 (t, J = 5.0 Hz, $4H_{11,12}$), 1.87 (s, $3H_{13}$). ^{13}C NMR (126 MHz, DMSO-d_6) δ_C 168.8 C_1, 149.8 C_2, 149.2 C_3, 145.4 C_4, 144.3 C_5, 132.9 C_6, 131.3 C_7, 130.0 C_8, 125.5 C_9, 120.1 C_{10}, 117.4 C_{11}, 113.0 C_{12}, 111.6 C_{13}, 107.8 C_{14}, 56.2 $C_{15,16}$, 46.2 $C_{17,18}$, 45.3 $C_{19,20}$, 21.5 C_{21}. The calculated mass of the compound was 444.51. LCMS 0.838 min 96 % m/z 445.1 $[M + H]^+$.

INTEGRI PROCEDAMUS

University of Ghana http://ugspace.ug.edu.gh

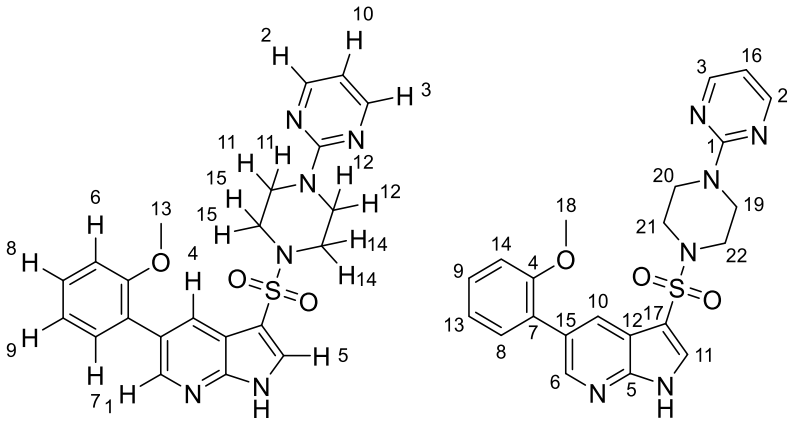
3.11.13 Synthesis of 4-(1-((5-(3,4-dimethoxyphenyl)-1H-pyrrolo[2,3-b] pyridin-3-yl) sulfonyl) piperidin-4-yl) Morpholine (ADA099, 18)



Compound ADA099 was prepared according to the general procedure for the cross-coupling reaction of sulfonamide intermediate using ADA098(0.13 g, 0.31 mmol), 3,4-dimethoxy benzene boronic acid (0.09 g, 0.47 mmol), [Pd(dppf)] Cl_2 (0.01 g, 0.02 mmol), $NaHCO_3$ (0.039 g, 0.63 mmol) to give a pale yellow amorphous solid (0.045 g, 30 % yield). Melting = 189 ºC-191 ºC Vmax (neat) cm^{-1} (N-H) 3104.21, (C-H) 2995.83, (C=C) 1515.96, (C=N) 1449.85, (S=O) 1147.17. ^1H NMR (500 MHz, DMSO-d_6) δ_H 12.85 (s, 1H_1), 8.68 (d, J = 2.2 Hz, 1H_2), 8.24 (d, J = 2.3 Hz, 1H_3), 8.15 (s, 1H_4), 7.54 (d, J = 12.2 Hz, 1H_5), 7.23 (d, J = 12.2 Hz, 1H_6), 7.09 (s, 1H_7), 3.88 (s, 3H_8), 3.82 (s, 3H_9), 3.73 (d, J = 11.5 Hz, 2$H_{10a,11a}$), 3.50 (t, J = 4.5 Hz, 4$H_{12,103}$), 2.35 (t, J = 4.5 Hz, 4$H_{14,15}$), 2.28 (td, J = 12.0, 2.4 Hz, 2$H_{10b,11b}$), 2.11 – 2.04 (m, 1H_{18}), 1.80 (d, J = 12.5 Hz, 2$H_{16a,17a}$), 1.42 (qd, J = 12.0, 3.9 Hz, 2$H_{16b,17b}$). ^{13}C NMR (126 MHz, DMSO-d_6) δ_C 149.2 C_1, 148.7 C_2, 147.1 C_3, 143.6 C_4, 132.0 C_5, 130.8 C_6, 130.6 C_7, 125.0 C_8, 119.5 C_9, 116.8 C_{10}, 112.5 C_{11}, 111.0 C_{12}, 108.0 C_{13}, 66.4 $C_{14,15}$, 60.0 $C_{16,17}$, 55.7 $C_{18,19}$, 49.2 C_{20}, 45.3 $C_{21,22}$, 26.9 $C_{23,24}$. The calculated mass of the compound was 486.59. LCMS 0.643 min 100 % m/z 487.2 $[M + H]^+$.

University of Ghana http://ugspace.ug.edu.gh

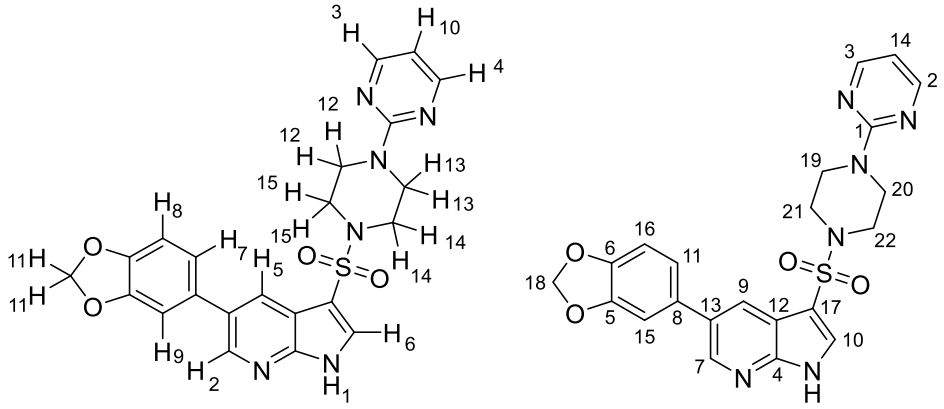
3.11.14 Synthesis of 5-(2-methoxyphenyl)-3-((4-(pyrimidin-2-yl) piperazin-1-yl) sulfonyl)-1H-pyrrolo[2,3-b] pyridine (ADA106,19)



Compound ADA106 was prepared according to the general procedure for the cross-coupling reaction of sulfonamide intermediate using ADA086 (0.10 g, 0.24 mmol), 2-methoxy benzene boronic acid (0.05 g, 0.35 mmol), [Pd(dppf)] Cl_2 (0.01 g, 0.01 mmol), $NaHCO_3$ (0.04 g, 0.47 mmol) to give a pale yellow amorphous solid (0.038 g, 36 % yield). Melting = 214 ºC-216 ºC. Vmax (neat) cm^{-1} (N-H) 3304.21, (C-H) 2995.83, (C=C) 1578.96, (C=N) 1490.85, (S=O) 1133.17. ^{1}H NMR (500 MHz, DMSO-d_6) δ_H 8.43 (s, 1H$_1$), 8.28 (d, J = 2.3 Hz, 2H$_{2,3}$), 8.20 (s, 1H$_4$), 8.14 (s, 1H$_5$), 7.39 (td, J = 7.9, 1.2 Hz, 2H$_{6,7}$), 7.15 (d, J = 8.2 Hz, 1H$_8$), 7.07 (t, J = 7.4 Hz, 1H$_9$), 6.58 (t, J = 4.7 Hz, 1H$_{10}$), 3.82 (t, J = 5.2 Hz, 4H$_{11,12}$), 3.77 (s, 3H$_{13}$), 2.99 (t, J = 5.0 Hz, 4H$_{14,15}$). ^{13}C NMR (126 MHz, DMSO-d_6) δ_C 160.3 C$_1$, 157.5 C$_{2,3}$, 155.8 C$_4$, 146.4 C$_5$, 144.$_9$ C$_6$, 131.7 C$_7$, 130.2 C$_8$, 127.6 C$_9$, 126.6 C$_{10}$, 120.5 C$_{11}$, 115.7 C$_{12,13}$, 111.3 C$_{14}$, 110.1 C$_{15,16}$, 106.8 C$_{17}$, 55.1 C$_{18}$, 45.0 C$_{19,20}$, 42.0 C$_{21,22}$. The calculated mass of the compound was 450.52. LCMS 1.067 min 87 % m/z 451.1 [M + H] $^+$.

University of Ghana http://ugspace.ug.edu.gh

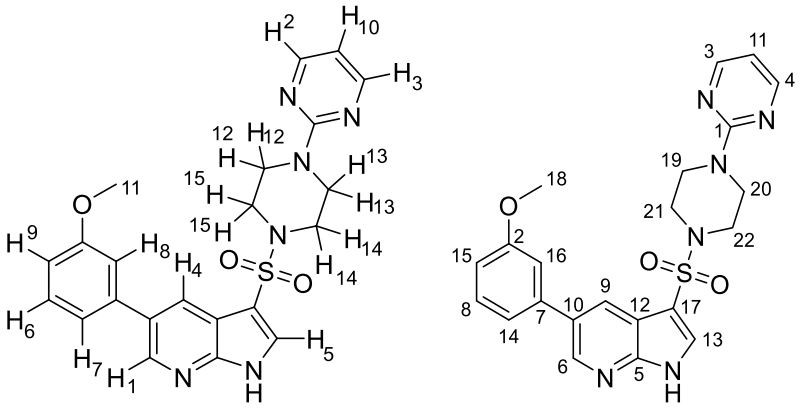
3.11.15 Synthesis of 5-(benzo[d] [1,3] dioxol-5-yl)-3-((4-(pyrimidin-2-yl) piperazin-1-yl) sulfonyl)-1H-pyrrolo[2,3-b] pyridine (ADA107, 20)



Compound ADA107 was prepared according to the general procedure for the cross-coupling reaction of sulfonamide intermediate using ADA086 (0.1 g, 0.24 mmol), 2-methoxy benzene boronic acid (0.06 g, 0.36 mmol), [Pd(dppf)] Cl_2 (0.01 g, 0.12 mmol), $NaHCO_3$ (0.039 g, 0.47 mmol) to give a pale yellow amorphous solid (0.0662 g, 60 % yield). Melting = 189 ºC-191 ºC. Vmax (neat) cm^{-1} (N-H) 3242.43, (C-H) 2983.55, (=C-H) 3109.87, (C=C) 1578.71, (C=N) 1588.27, (S=O) 1199.26. ^{1}H NMR (500 MHz, DMSO-d_6) δ_H 12.89 (s, 1H_1), 8.62 (d, J = 2.2 Hz, 1H_2), 8.31 (d, J = 4.7 Hz, 2$H_{3,4}$), 8.24 (d, J = 2.2 Hz, 1H_5), 8.18 (s, 1H_6), 7.34 (d, J = 1.9 Hz, 1H_7), 7.20 (dd, J = 8.0, 1.9 Hz, 1H_8), 7.06 (d, J = 8.1 Hz, 1H_9), 6.61 (t, J = 4.7 Hz, 1H_{10}), 6.10 (s, 2H_{11}), 3.85 (t, J = 5.0 Hz, 4$H_{12,13}$), 3.02 (t, J = 5.1 Hz, 4$H_{14,15}$). ^{13}C NMR (126 MHz, DMSO-d_6) δ_C 160.3 C_1, 157.4 $C_{2,3}$, 147.6 C_4, 146.7 C_5, 146.5 C_6, 143.1 C_7, 131.9 C_8, 131.7 C_9, 130.0 C_{10}, 124.6 C_{11}, 120.4 C_{12}, 116.3 C_{13}, 110.0 C_{14}, 108.4 C_{15}, 107.2 C_{16}, 106.8 C_{17}, 100.7 C_{18}, 45.0 $C_{19,20}$, 42.0 $C_{21,22}$. The calculated mass of the compound was 464.50. LCMS 1.045 min 100 % m/z 465.1 $[M + H]^+$.

University of Ghana http://ugspace.ug.edu.gh

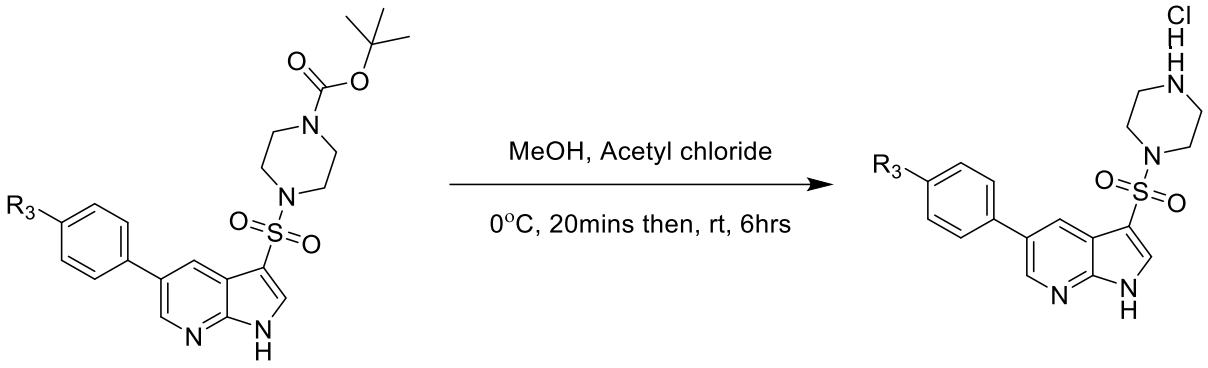
3.11.16 Synthesis of 5-(3-methoxyphenyl)-3-((4-(pyrimidin-2-yl) piperazin-1-yl) sulfonyl)-1H-pyrrolo[2,3-b] pyridine (ADA108, 21)



Compound ADA108 was prepared according to the general procedure for the cross-coupling reaction of sulfonamide intermediate using ADA086 (0.1 g, 0.24 mmol), 2-methoxy benzene boronic acid (0.05 g, 0.35 mmol), [Pd(dppf)] Cl_2 (0.01 g, 0.12 mmol), $NaHCO_3$ (0.039 g, 0.47 mmol) to give a pale yellow amorphous solid (0.064 g, 60 % yield). Melting = 213 ºC-215 ºC. Vmax (neat) cm^{-1} (N-H) 3342.43, (C-H) 2993.65, (=C-H) 3109.17, (C=C) 1588.81, (C=N) 1548.17, (S=O) 1149.26. ^{1}H NMR (500 MHz, DMSO-d_6) δ_H 8.69 (d, J = 2.1 Hz, $1H_1$), 8.31 (d, J = 4.7 Hz,, $2H_{2,3}$), 8.29 (s, $1H_4$), 8.20 (s, $1H_5$), 7.44 (t, J = 7.9 Hz, $1H_6$), 7.29 (dt, J = 7.9, 1.1 Hz, $1H_7$), 7.25 (s, $1H_8$), 7.00 (dd, J = 8.3, 2.6 Hz, $1H_9$), 6.60 (t, J = 4.7 Hz, $1H_{10}$), 3.86 (s, $3H_{11}$), 3.83 (t, J = 5.2 Hz, $4H_{12,13}$), 3.02 (t, J = 5.1 Hz, $4H_{14,15}$). ^{13}C NMR (126 MHz, DMSO-d_6) δ_C 160.3 C_1, 159.3 C_2, 157.4 $C_{3,4}$, 147.0 C_5, 143.3 C_6, 139.1 C_7, 132.0 C_8, 130.0 C_9, 129.7 C_{10}, 125.0 C_{11}, 119.1 C_{12}, 116.3 C_{13}, 112.5 C_{14}, 112.4 C_{15}, 110.0 C_{16}, 106.9 C_{17}, 54.7 C_{18}, 45.0 $C_{19,20}$, 42.0 $C_{21,22}$. The calculated mass of the compound was 450.52. LCMS 1.065 min 100 % m/z 451.1 $[M + H]^+$.

University of Ghana http://ugspace.ug.edu.gh

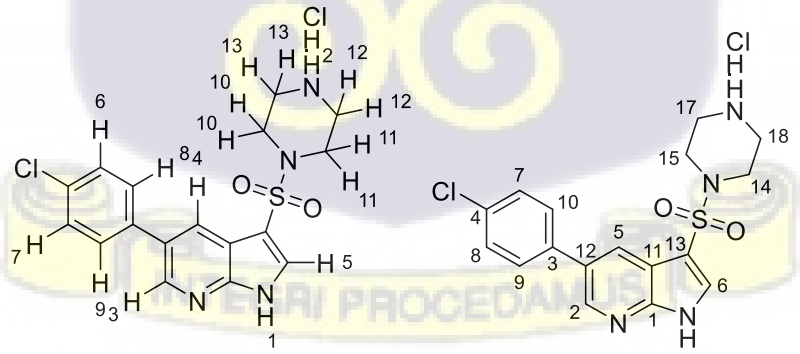
3.12 General Procedure for Deprotection of Boc Products



Scheme 2.3: General procedure for deprotection of Boc product.

To a solution of Boc-protected sulfonyl piperazine (1 equivalent) in MeOH (3 mL), acetyl chloride (10 equivalents) was added and the resulting mixture was stirred at 0 ºC for 20 minutes. The reaction mixture was warmed to room temperature and stirred for 16 h. The mixture was concentrated, and the residue was washed with diethyl ether (20 mL) to give the hydrochloride salt as an amorphous solid.

3.12.1 Synthesis of 5-(4-chlorophenyl)-3-(piperazin-1-ylsulfonyl)-1H-pyrrolo[2,3-b] pyridine (ADA101, 22).

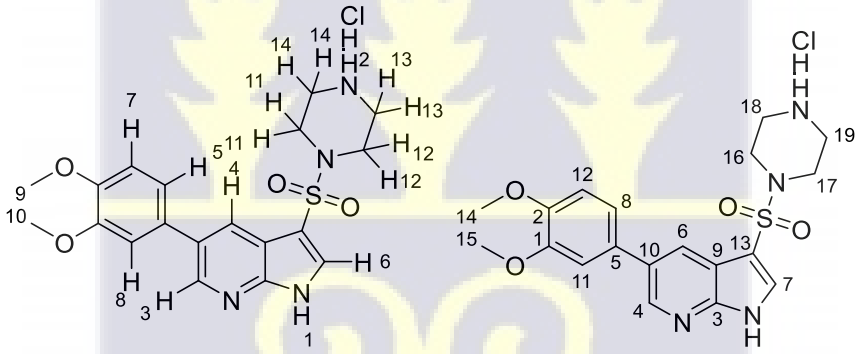


Compound ADA101 was prepared according to the general procedure for deprotection of the Boc group using ADA091 (0.035 g, 0.074 mmol), Acetyl chloride (0.05 mL, 0.74 mmol) to give a pale

University of Ghana http://ugspace.ug.edu.gh

yellow amorphous solid (0.016 g, 54% yield). Melting = 238 ºC-240 ºC Vmax (neat) cm^{-1} (N-H) 3280.23, (=C-H) 3115.48, (C-H) 2969.21, (C=C) 1573.74, (C=N) 1497.71, (S=O) 1146.92. ^{1}H NMR (500 MHz, DMSO-d_6) δ_H 12.98 (s, $1H_1$), 8.93 (s, $1H_2$), 8.54 (d, J = 2.1 Hz, $1H_3$), 8.14 (s, $1H_4$), 8.13 (s, $1H_5$), 7.61 (d, J = 8.5 Hz, $2H_{6,7}$), 7.39 (d, J = 8.5 Hz, $2H_{8,9}$), 3.01 (t, J = 5.0 Hz, $4H_{10,11}$), 2.97 (t, J = 5.1, $4H_{12,13}$). ^{13}C NMR (126 MHz, DMSO-d_6) δ_C 147.0 C_1, 143.3 C_2, 136.3 C_3, 132.7 C_4, 132.1 C_5, 129.0 C_6, 128.6 $C_{7,8}$, 124.9 $C_{9,10}$, 116.3 $C_{11,12}$, 106.3 C_{13}, 42.2 $C_{14,15}$, 41.6 $C_{16,17}$. LCMS 0.705 min 100 % m/z 377.1 $[M + H]^+$ corresponding to the mass of the free amine.

3.12.2 Synthesis of 5-(3,4-dimethoxyphenyl)-3-(piperazin-1-ylsulfonyl)-1H-pyrrolo[2,3-b] pyridine hydrochloride (ADA 102, 23).

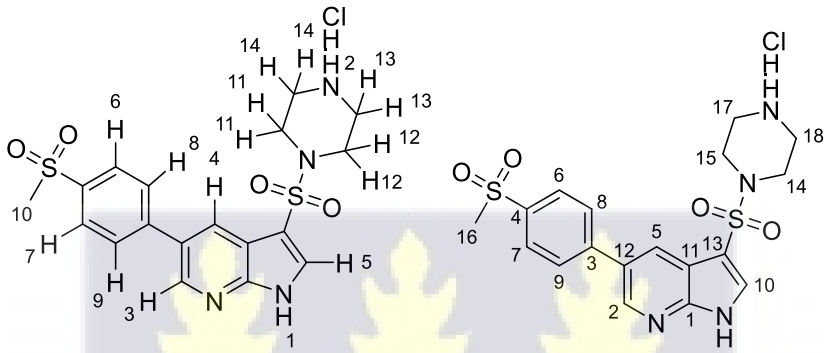


Compound ADA102 was prepared according to the general procedure for deprotection of the Boc group using ADA092 (0.030 g, 0.059 mmol), Acetyl chloride (0.04 mL, 0.59 mmol) to give a yellow amorphous solid (0.007 g, 29 % yield). Melting = 208 ºC-210 ºC Vmax (neat) cm^{-1} (N-H) 3266.90, (=C-H) 3084.22, (C-H) 2940.33, (C=C) 1594.32, (C=N) 1521.24, (S=O) 1146.23. ^{1}H NMR (500 MHz, DMSO-d_6) δ_H 12.90 (s, $1H_1$), 8.79 (s, $2H_2$), 8.54 (d, J = 2.2 Hz, $1H_3$), 8.10 (d, J = 1.9 Hz, $1H_4$), 8.08 (d, J = 2.2 Hz, $1H_5$), 7.09 (d, J = 2.1 Hz, $1H_6$), 7.06 (dd, J = 8.2, 2.1 Hz, $1H_7$), 6.92 (d, J = 8.3 Hz, $1H_8$), 3.70 (s, $3H_9$), 3.64 (s, $3H_{10}$), 3.01 (d, J = 5.0 Hz, $4H_{11,12}$) 2.79 (d, J = 8.3 Hz, $4H_{13,14}$). ^{13}C NMR (126 MHz, DMSO-d_6) δ_C 149.8 C_1, 149.3 C_2, 147.7 C_3, 144.5 C_4, 133.4

University of Ghana http://ugspace.ug.edu.gh

C_5, 131.4 C_6, 131.2 C_7, 125.4 C_8, 120.1 C_9, 117.3 C_{10}, 113.0 C_{11}, 111.6 C_{12}, 107.1 C_{13}, 56.2 $C_{14,15}$, 43.2 $C_{16,17}$, 42.6 $C_{18,19}$. LCMS 0.626 min 100 % m/z 403.1 $[M + H]^+$ corresponding to the mass of the free amine.

3.12.3 Synthesis of 5-(4-(methyl sulfonyl) phenyl)-3-(piperazin-1-ylsulfonyl)-1H-pyrrolo[2,3-b] pyridine hydrochloride (ADA103, 24).



Compound ADA103 was prepared according to the general procedure for deprotection of the Boc group using ADA093 (0.035 g, 0.067 mmol), Acetyl chloride (0.05 mL, 0.67 mmol) to give a yellow amorphous solid (0.029 g, 95 % yield). Melting = 227 ºC-230 ºC Vmax (neat) cm^{-1} (N-H) 3189.14, (=C-H) 3082.51, (C-H) 2918.12, (C=C) 1641.76, (C=N) 1435.72, (S=O) 1143.78. ^1H NMR (500 MHz, DMSO-d_6) δ_H 13.15 (d, J = 2.2 Hz, $1H_3$), 8.76 (s, $1H_1$), 8.75 (s, $2H_2$), 8.35 (d, J = 2.2 Hz, $1H_4$), 8.29 (s, $1H_5$), 8.00 (d, J = 5.5 Hz, $2H_{6,7}$), 7.96 (d, J = 5.6 Hz, $2H_{8,9}$), 3.44 (s, $3H_{10}$), 3.21 (t, J = 5.1 Hz, $4H_{11,12}$), 3.12 (t, J = 5.2 Hz, $4H_{13,14}$). ^{13}C NMR (126 MHz, DMSO-d_6) δ_C 148.1 C_1, 144.3 C_2, 143.1 C_3, 139.9 C_4, 133.6 C_5, 129.3 $C_{6,7}$, 128.3 $C_{8,9}$, 127.9 C_{10}, 126.2 C_{11}, 117.0 C_{12}, 107.2 C_{13}, 43.8 $C_{14,15}$, 42.9 C_{16}, 42.3 $C_{17,18}$. LCMS 0.572 min 98 % m/z 421.1 $[M + H]^+$ corresponding to the mass of the free amine.

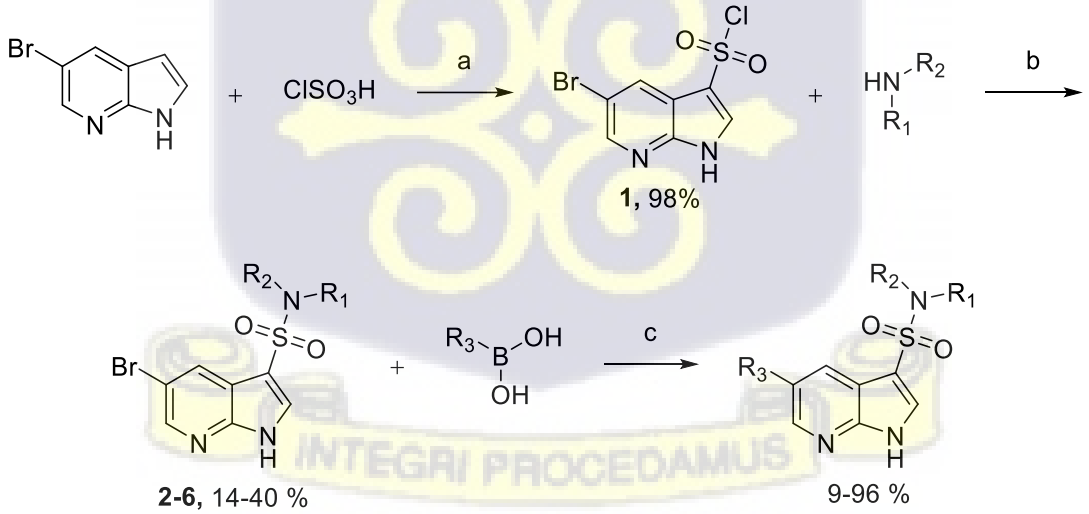
INTEGRI PROCEDAMUS

University of Ghana http://ugspace.ug.edu.gh

3.13 RESULTS AND DISCUSSION

3.14 Chemistry

The titled compounds were synthesized in three chemical steps in low to good yields ranging between 9 % and 96 %. First, commercially available 5-bromo-1H- pyrrolo[2,3-b]-pyridine was reacted with chlorosulfonic acid at 0 ºC, 50 ºC and 110 ºC temperatures at 1-hour intervals to give the compound **1**. Compound **1** was treated with different heterocyclic amines including piperidin-4-yl) morpholine, piperazin-1-yl) ethan-1-one, piperazine-1-carboxylate, 1H-pyrrolo[2,3-b] pyridine and Morpholine using Et_3N as a base and tetrahydrofuran (THF) as the solvent at room temperature to give the sulfonamide derivatives. This was followed by a Suzuki cross-coupling reaction between the 4-((5-bromo-1H-pyrrolo[2,3-b] pyridin-3-yl) sulfonyl) intermediates in dioxane and selected boronic acids using $NaHCO_3$ as a base and [Pd(dppf)] Cl_2 as a catalyst at 95 ºC **Scheme 3.1**.

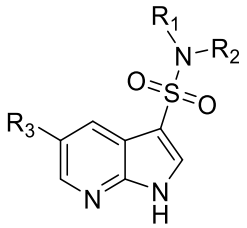


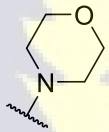
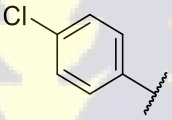
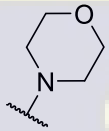
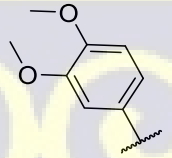
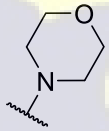
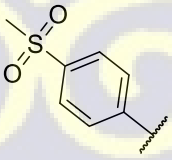
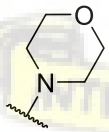
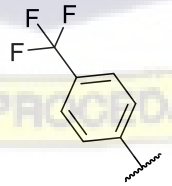
Scheme 3. 1: Synthesis of derivatives of sulphonamides. Reagents and conditions: a) r.t 1hthen 50 ºC then 1h and110 ºC 1h, b) THF, Et_3N, r.t 12 h, c) $Pd(dppf)Cl_2$, $NaHCO_3$(aq), 90 ºC 12h.

University of Ghana http://ugspace.ug.edu.gh

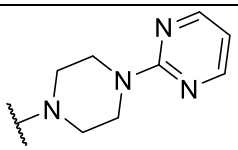
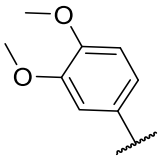
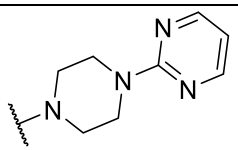
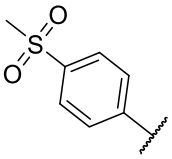
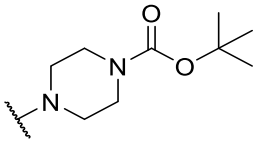
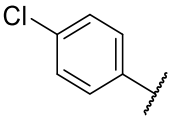
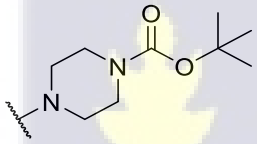
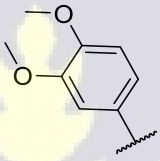
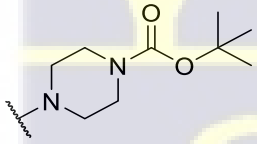
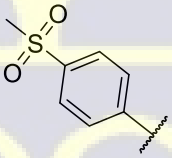
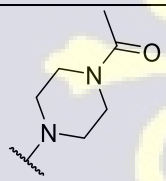
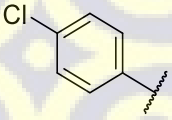
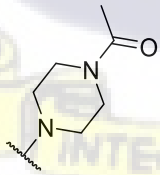
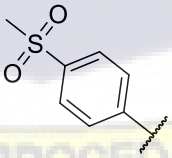
A total of 19 compounds were synthesized and the structures and yields are shown in **Table 3.1**.

Table 3.1: Structure of synthesized analogues of the hit compound SFK78.

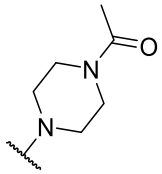
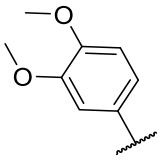
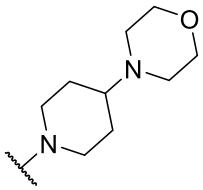
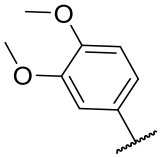
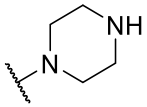
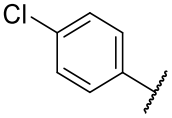
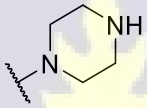
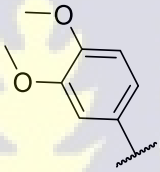
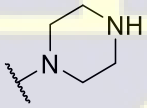
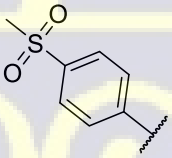
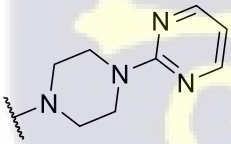
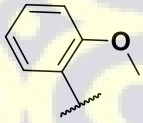
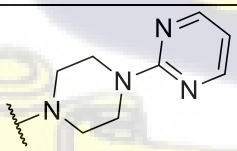
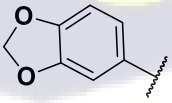
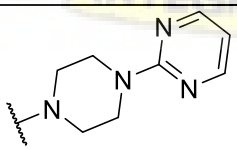
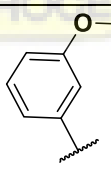


Sample Code	R^1/ R^2	R^3	% Yield	Molecular Weight(g/mol)
ADA 083			36	377.84
ADA 084			9	403.45
ADA 085			11	421.49
ADA 087			48	411.40

University of Ghana http://ugspace.ug.edu.gh

ADA 088			17	480.54
ADA 090			42	498.58
ADA 091			40	476.13
ADA 092			29	502.59
ADA 093			35	520.62
ADA 095			24	418.90
ADA 096			24	462.54

University of Ghana http://ugspace.ug.edu.gh

ADA 097			37	444.51
ADA 099			30	486.59
ADA 101			54	412.32
ADA 102			29	438.93
ADA 103			96	456.96
ADA106			36	450.52
ADA107			60	464.50
ADA108			60	450.52

University of Ghana http://ugspace.ug.edu.gh

3.15 Reaction Mechanism for Synthesized Analogues of MMV902507

The mechanism of the chlorosulfonation reaction is shown in **Figure 3.3** below. It involves an electrophilic aromatic substitution initiated by the attack of the pyrrolo pyridine on the chlorosulfonic acid leading to the cleavage of the chloro group. The chloro anion stabilizes the positive charge created on the five-membered ring. The hydroxyl group on the aryl sulfonic acid intermediate abstracts a proton from the excess acid in the mixture generating a good leaving hydroxonium ion. The chloro anion then displaces the water to form the sulfonyl chloride cation and the conjugate base generated *in situ* picks a proton from the carbon adjacent to the carbocation to regenerate aromaticity.

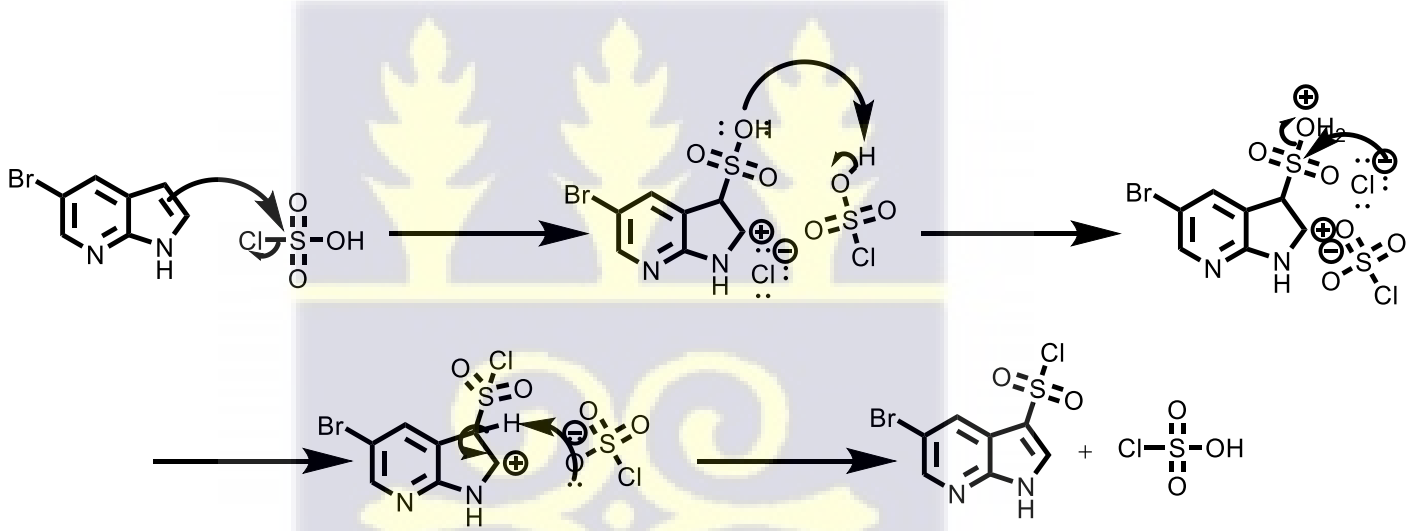


Figure 3.3: Mechanism for Chlorosulfonation reaction.

The second step of the reaction involves the reaction between the aryl sulfonyl chloride and an amine in the presence of a base to form the sulfonamide intermediate. The mechanism is shown in **Figure 3.4** below. The triethylamine (Et_3N) deprotonates the amine to make it more nucleophilic.

University of Ghana http://ugspace.ug.edu.gh

This nucleophile displaces the chloro group on the sulfonyl chloride intermediate to form the sulfonamide and HCl as the byproduct

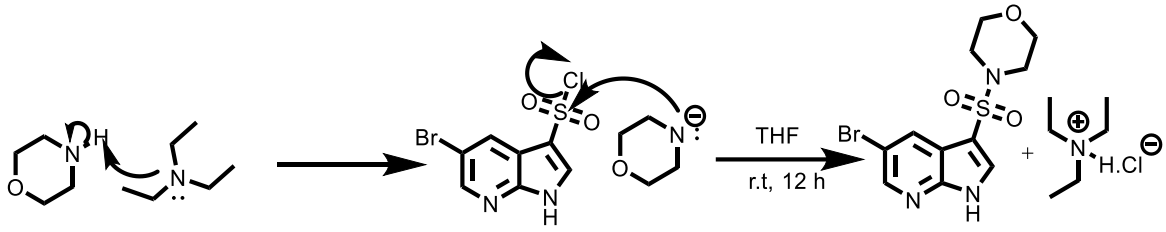


Figure 3.4: Mechanism for sulfonamide formation.

The last step of the mechanism involves a Suzuki cross-coupling reaction between the bromosulfonamide and selected aryl boronic acids using palladium as catalyst. This involves three steps: first, an oxidative addition, followed by a transmetalation and finally a reductive elimination. The mechanism starts with an oxidative addition of a Pd^0 atom to the bromosulfonamide intermediate, forming an organopalladium intermediate. The base adds to the boronic acid to form an organoborate anion, which activates the boronic acid and makes the aryl group more nucleophilic enabling it to replace the bromine via transmetalation. Finally, a reductive elimination leads to the formation of the c-c-bonded product. The mechanism is shown in **Figure 3.5** below.

INTEGRI PROCEDAMUS

University of Ghana http://ugspace.ug.edu.gh

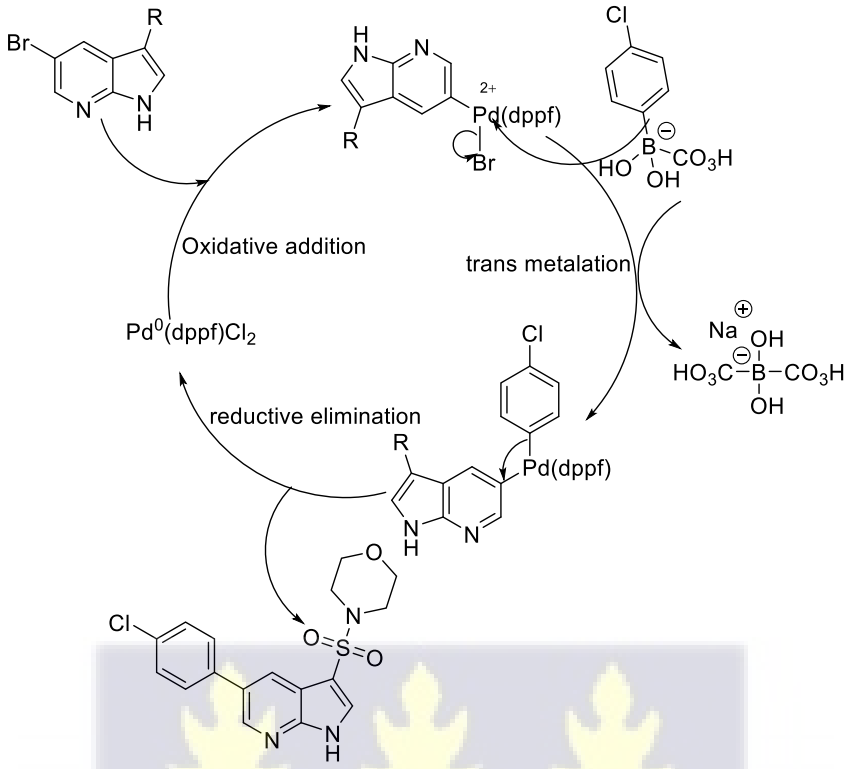


Figure 3.5: The mechanism of the Suzuki cross-coupling step.

3.16 Spectral Analysis of the synthesized analogues of MMV902507.

The synthesized analogues were characterized using 1D Nuclear Magnetic Resonance (NMR), Liquid Chromatography-Mass Spectrometry (LC-MS) and the Fourier Transform Infrared (FT-IR) spectroscopy. While NMR spectroscopy was used to determine the carbon-hydrogen connectivity of the compound, the LC-MS was used to ascertain the purity and the mass of each compound and FT-IR spectroscopy was used to confirm the functional groups present in each of the compounds. These spectroscopic and spectrometric techniques were instrumental in establishing that the titled compounds were duly synthesized.

University of Ghana http://ugspace.ug.edu.gh

3.16.1 Proton (^{1}H) NMR Analysis of ADA081

The proton spectrum of ADA081 measured in DMSO, is shown in **Figure 3.6** below. ADA081 comprises four chemically distinct protons. The singlet labeled H1 at 12.01ppm corresponds to the proton on the nitrogen, while the doublet at 8.31ppm with coupling constant (*J*= 2.3Hz) corresponds to the proton labeled H2 having a long-range coupling with H3. The doublet peak at 8.20 ppm with coupling constant (*J* = 2.3Hz) corresponds to the proton H3 which couples with H2 and the doublet at 7.59 ppm with coupling constant of (*J* = 2.4 Hz) is assigned to the proton labeled H4 also have some interactions with H1. All the peaks integrate for one proton each.

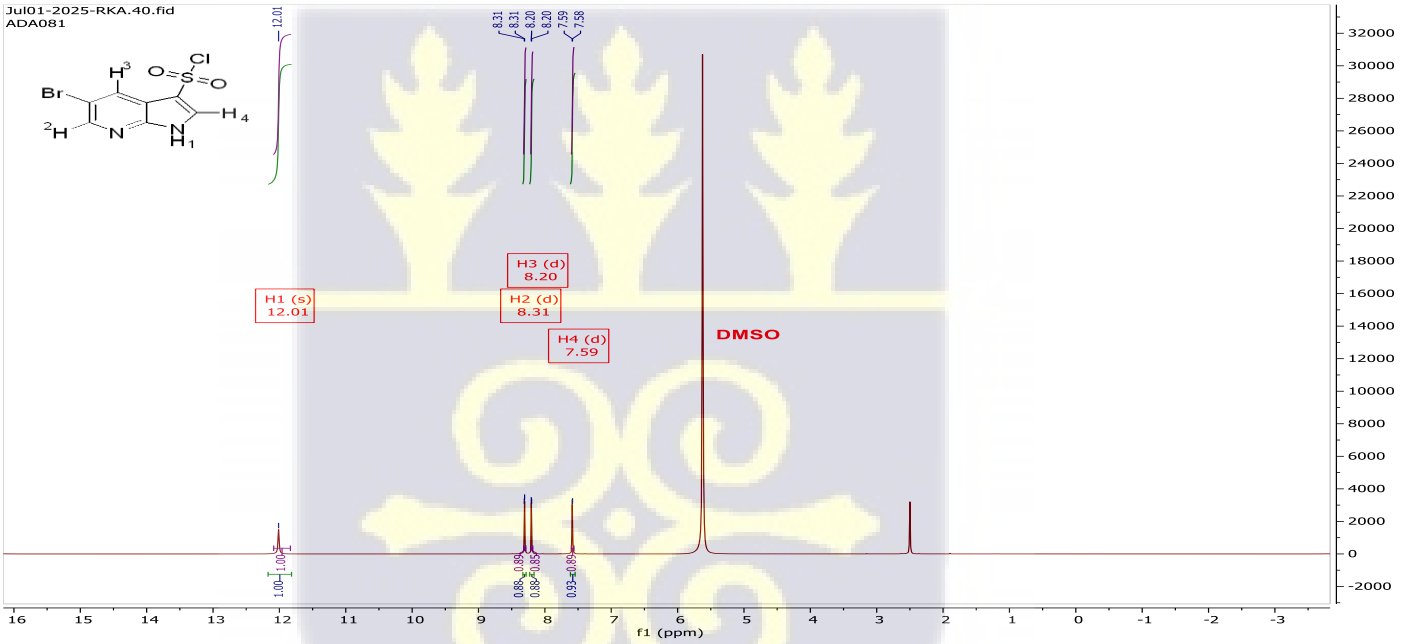


Figure 3.6: ^{1}H spectrum of ADA081

3.16.2 Carbon (^{13}C) NMR for ADA081

The carbon spectrum of compound ADA081 which was measured in DMSO is shown in **Figure 3.7** below. It comprises seven distinct peaks each corresponding to a specific carbon. The carbon labeled C1 appeared at 146.4 ppm and carbon C2 appeared at 143.2 ppm, while that of C3 appeared

University of Ghana http://ugspace.ug.edu.gh

at 130.8 ppm. The other peaks labeled C4, C5 and C6 appeared at 127.0 ppm,121.9 ppm and 119.1ppm respectively while that of C7 appeared at 111.5 ppm.

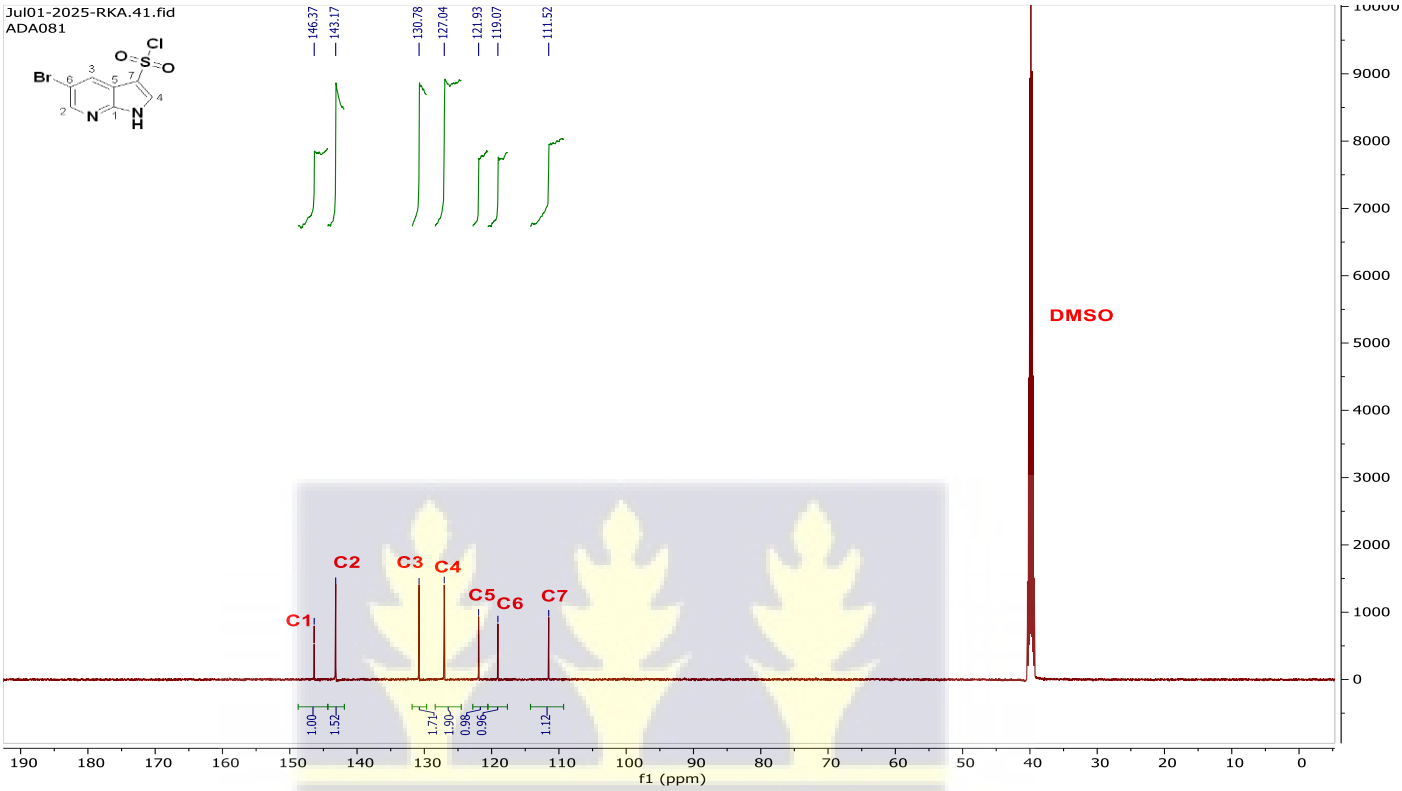


Figure 3.7: ^{13}C spectrum of ADA081

3.16.3 Proton (^{1}H) NMR Analysis of ADA086

The proton spectrum for compound ADA086 is shown in **Figure 3.8** below. The doublet at 8.44ppm with coupling constant (J = 2.2 Hz) is assigned to the proton labeled H1 which has a long-range interaction with H4. The doublet at 8.29 ppm with coupling constant (J = 4.7 Hz) is assigned to the protons labeled H2 and H3 and interacts with H6 which split them as a doublet while the doublet at 8.27ppm with coupling constant (J = 2.2Hz) is assigned to proton H4 which also interact with H1. The singlet at 8.20 ppm is assigned to the proton labeled H5 and that at 6.59 ppm is assigned to proton H6 which has two neighboring protons H2 and H3 which splits H6 as a

University of Ghana http://ugspace.ug.edu.gh

triplet. The triplet at 3.82 ppm with coupling constant (J = 5.0Hz) integrating for four protons is assigned to the protons labeled H7 and H8 which have the same chemical environment and couples with H9 and H10 likewise the triplet at 2.97ppm with a J = 5.0Hz and integrating for four protons is assigned to protons H9 and H10 interacting with protons H7and H8.

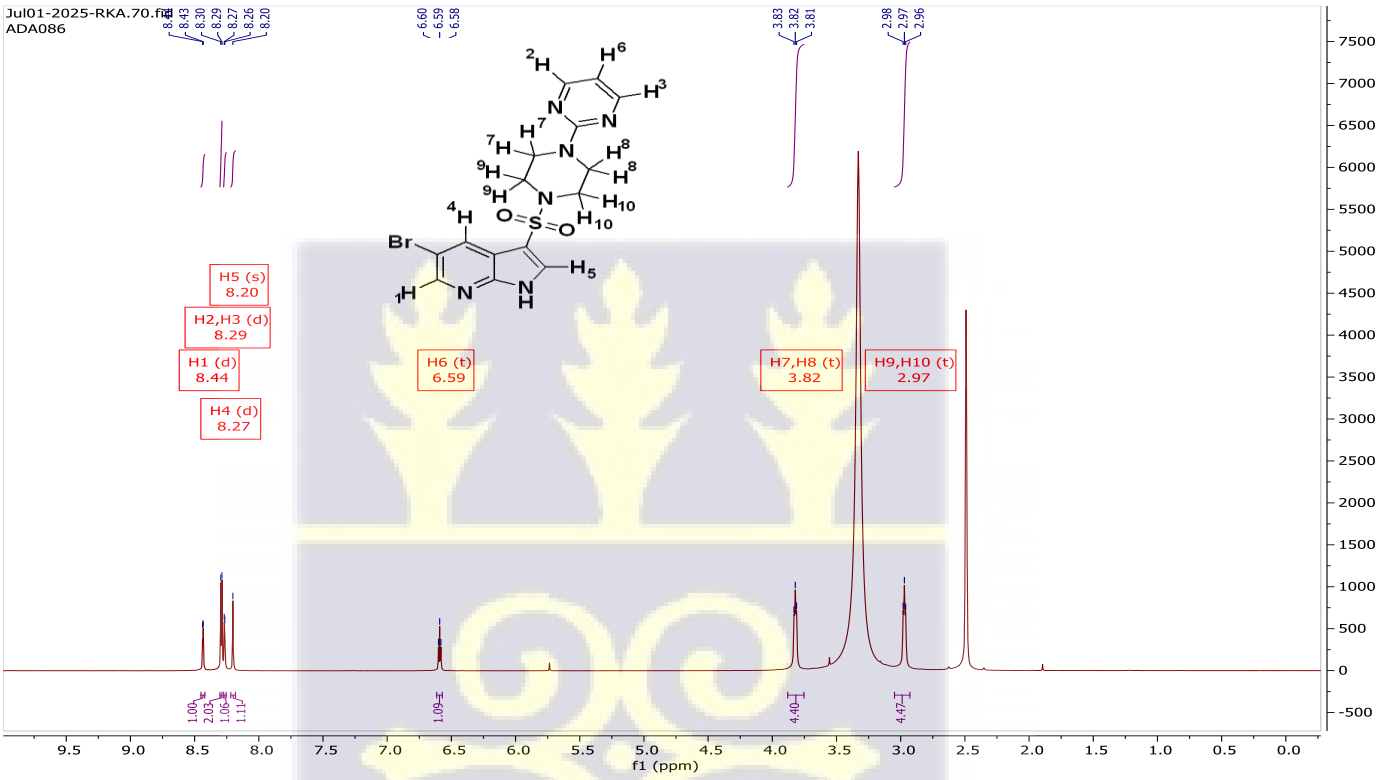


Figure 3.8: ^{1}H spectrum of ADA086

3.16.4 Carbon (^{13}C) NMR for ADA086

The carbon spectrum for compound ADA086 comprising 12 chemically distinct peaks is shown in **Figure 3.9** below. The peaks at 161.2 ppm, 158.4 ppm and 111.0 ppm are assigned to the carbons labeled C1, C2-C3 and C10 on the pyrimidine ring respectively while those at 147.1ppm,

University of Ghana http://ugspace.ug.edu.gh

145.2ppm, 134.1ppm, 129.9 ppm, 119.0 ppm, 113.6 ppm and 107.3 ppm is assigned to carbons C4, C5, C6, C7, C8, C9 and C11 respectively on the azaindole ring.

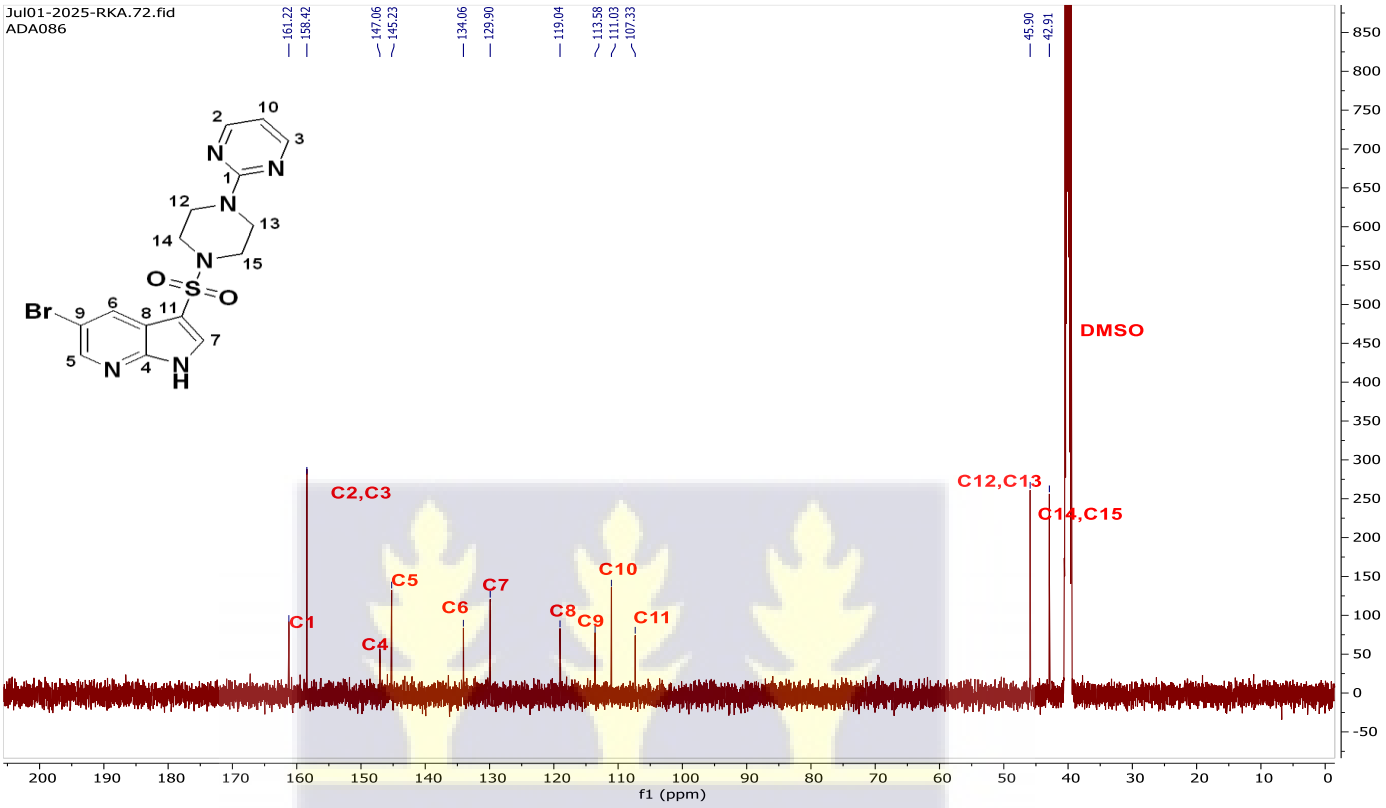


Figure 3.9: ^{13}C spectrum for ADA086

3.16.5 Proton (^{1}H) NMR Analysis of ADA090

The proton spectrum for ADA090 is shown in **Figure 3.10** below. The singlets at chemical shifts of 8.65 ppm and 8.13 ppm is assigned to protons labeled H1 and H5 respectively while the doublet at 7.78 ppm with coupling constant (J = 7.8Hz) is assigned to the proton H7 coupling long range with the hydrogen of the amine which did not appear in the spectrum due to using d-methanol used as the solvent. The doublets at 8.38 ppm and 8.30 ppm with coupling constants of 4.5 Hz and 4.7 Hz respectively are assigned to H2 and H3 interacting with H6 while the triplet at 6.49 ppm with coupling constant of 4.7 Hz is assigned to the peak labeled H8 also interacting with its neighboring

University of Ghana http://ugspace.ug.edu.gh

protons H2 and H3. The protons on the phenyl ring assigned as H4 and H6 appear as two sets of doublets (J = 4.8 Hz for both) at 8.19 ppm and 7.94 ppm coupling with each other respectively. The remaining proton labeled H10 appeared as a singlet at 3.17 ppm having no neighboring proton while the two sets of triplet peaks at 3.74 ppm and 2.92 ppm with coupling a constant of 5 Hz respectively, are assigned to the protons H9 and H11 which also couples with each other.

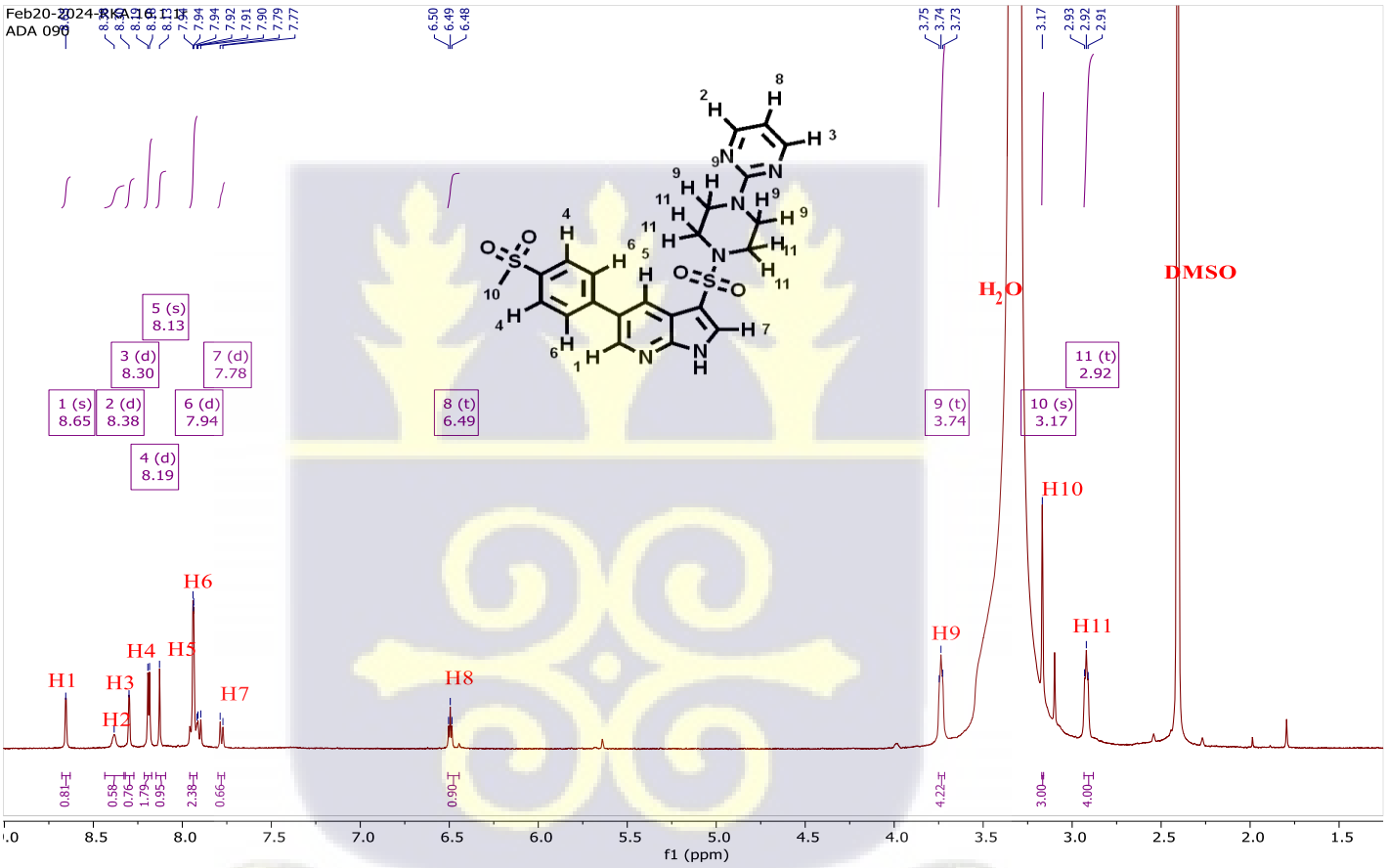


Figure 3.10: ^{1}H NMR Spectra for ADA090.

University of Ghana http://ugspace.ug.edu.gh

3.16.6 Carbon (^{13}C) NMR for ADA090

The carbon spectrum of compound ADA090 is shown in **Figure 3.11** below. From the spectra below, the carbons C1, C2-C3 and C15 on the pyrimidine ring appeared at 161.1 ppm, 158.4 ppm and 115.2 ppm respectively while carbons C5, C6, C12, C13, C14, C16 and C17 on the azaindole ring appeared at 144.4 ppm, 140.1 ppm, 126.9 ppm, 121.8 ppm, 111.1 ppm, 108.2 ppm respectively. On the phenyl ring, carbon C4 appeared at 146.4 ppm and carbon C7 at 135.2 ppm. Carbons C8 and C9 having the same chemical environment appeared at 128.6 ppm while carbons C10 and C11 appeared at 128.2 ppm. The methyl carbon labeled C18 also appeared at 46.0 ppm. The equivalent piperazine carbons C19 and C20 appeared at 44.1 ppm while C21 and C22 appeared at 42.9 ppm.

INTEGRI PROCEDAMUS

University of Ghana http://ugspace.ug.edu.gh

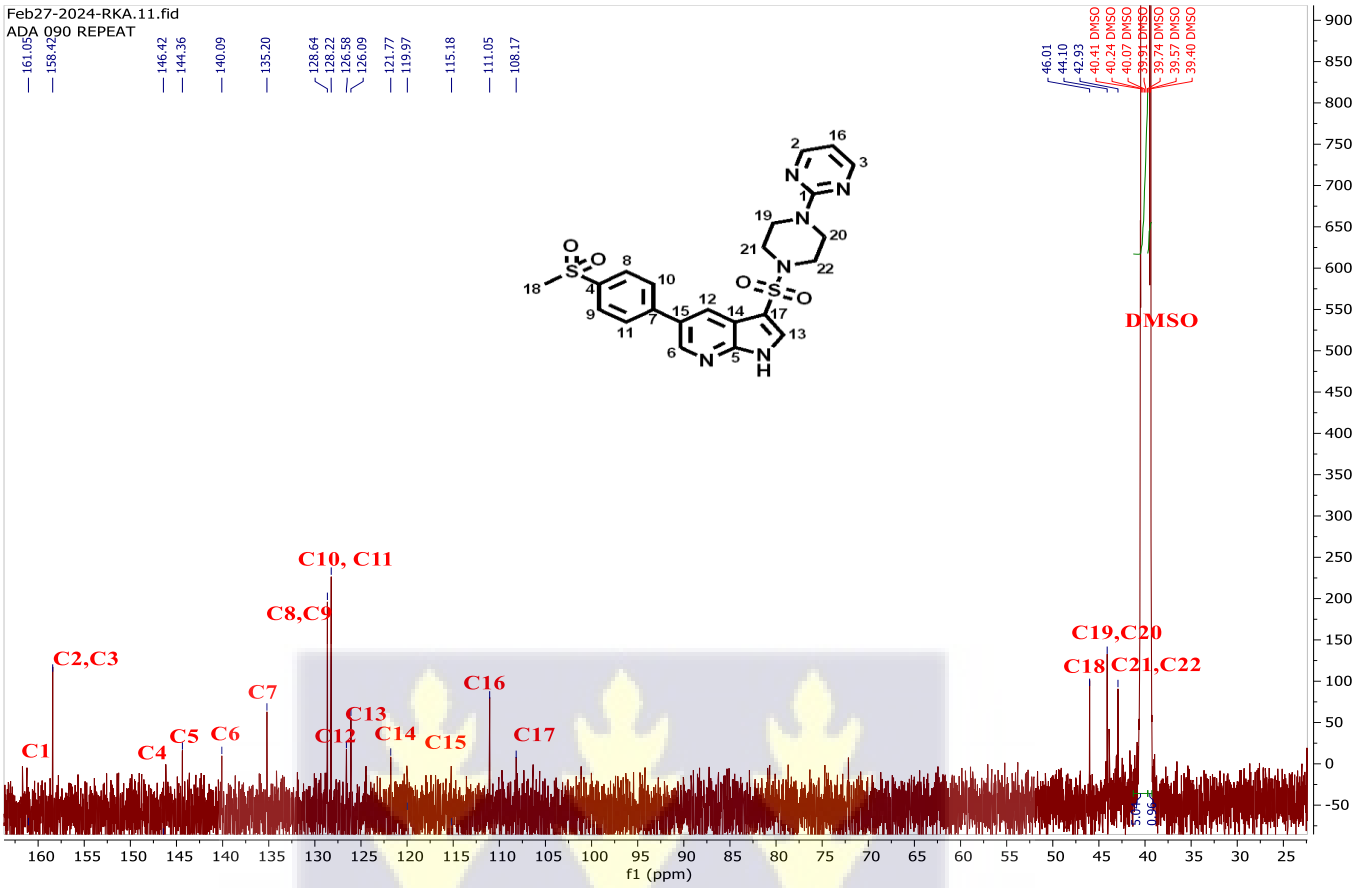


Figure 3.11: ^{13}C Spectra for ADA090.

3.16.7 FT-IR Analysis of ADA090

The FT-IR spectrum for ADA090 is presented in **Figure 3.12.** The broad peak at 3342.43 cm^{-1} is characteristic of N-H, while the peak at 3109.17 cm^{-1} is assigned to the aromatic C-H. The remaining peaks at 2993.65 cm^{-1}, 1588.81 cm^{-1} and 1548.17 cm^{-1} corresponds to sp^3 C-H, aromatic C=C and C=N respectively.

University of Ghana http://ugspace.ug.edu.gh

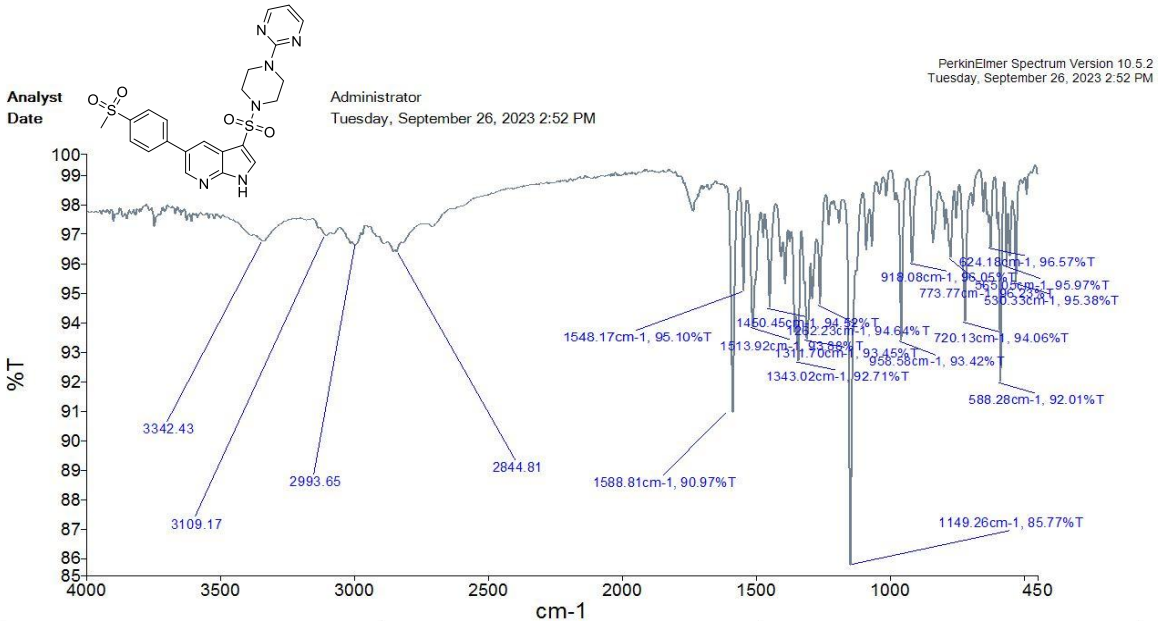


Figure 3.12: FT-IR data for ADA090

3.16.8 LC-MS Analysis for ADA090

LC-MS data was acquired for ADA090 to ascertain its purity and molecular weight. The LC **Figure 3.13)** showed that the compound was pure with 98.8 % purity at 290 nm and a retention time at 0.901 mins. On the other hand, the MS gave a peak at 100% corresponding to the molecular ion $[M + H]^+$ at 499.1 m/z (**Figure 3.14**) indicative of the calculated molecular weight of 498.58 g/mol.

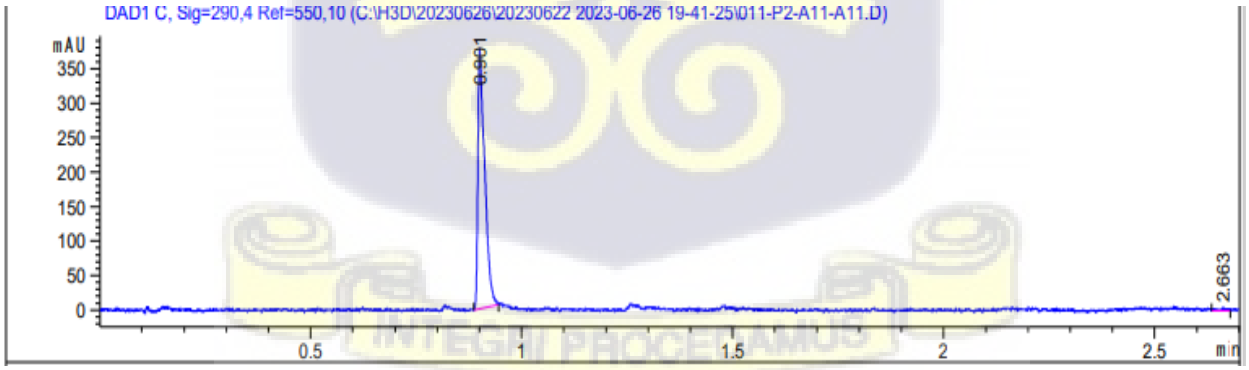


Figure 3.13: LC data for ADA090.

University of Ghana http://ugspace.ug.edu.gh

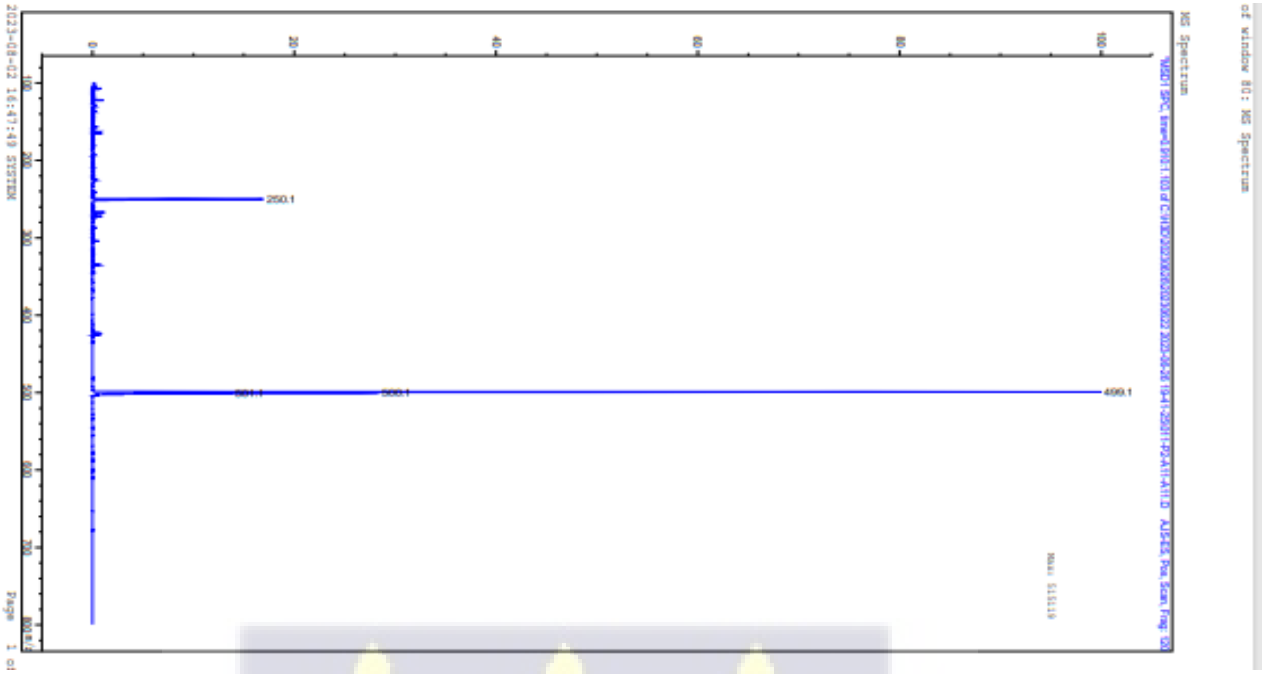


Figure 3.14: MS data for ADA090.

3.17 Antimalarial Biological Activity Results

Sixteen of the synthesized analogues were tested for antimalarial activity against the chloroquine-sensitive 3D7 strain of *Plasmodium falciparum* with Chloroquine as a control. The synthesized analogues were tested using the SYBR Green 1 Assay, according to standard procedure[215]. The compounds were prepared in DMSO, and serial dilutions was performed to obtain concentrations between 100 µM and 0.56 nM. The prepared compounds were designated into a 96 well plate and cell cultures were added and kept in a chamber, flashing with 5 % CO_2, 5 % O_2, and 90 % N_2 and incubated for 72 hours at 37 ºC. A stock of SYBR green 1 was added to lysis buffer and added to parasitized plate, incubating for 1-2 hours using the fluorescence intensity at a specific wavelength to determine the concentration. The activity obtained for the compounds ranges between 25 µM to 0.2 µM **Table 3.2**. The most active compound was **ADA090** with an IC_{50} of **0.15 µM** compared to

University of Ghana http://ugspace.ug.edu.gh

the hit compound **(0.2 µM)** while **ADA107 and ADA108** with an IC_{50} of **25 µM** were the least potent. The results showed that both electron-donating and electron-withdrawing substitutions on the LHS were tolerated. Activities of 6.4 µM (ADA083-4-Cl), 0.2 µM (ADA084-3,4-dimethoxy) and 1.21 µM (ADA087-4-CF3) were obtained. Derivatives with the 3,4-dimethoxy substitutions on the LHS were more potent than the 4-chloro substitution found in the hit compound; (**Table 3.2**). For instance, compounds ADA084, ADA092, ADA097, ADA099 and ADA102 with the 3,4-dimethoxy substitution returned activities of 0.2 µM, 0.4 µM, 0.2 µM, 0.9 µM and 0.4 µM respectively when compared to ADA107 (>25 µM) and ADA108 (>25 µM). Furthermore, monomethoxy substitution was detrimental to activity as seen in ADA108 and the benzo-dioxole substitution (ADA107) as the LHS led to a complete loss of activity. This suggests that the presence of both methoxy groups was essential for biological activity. None of the heterocyclic amines investigated on the RHS was detrimental to activity. The antimalarial data and the solubility data for the other analogues are yet to be determined.

Table 3.2: Antimalarial activity against 3D7 strain and physicochemical parameters of synthesized analogues.

Sample Code	Solubility (µM)	3D7 (µM)	Calculated Log D	exp Log D pH 7.4	tPSA
Hit	**44**				
ADA083		6.4	2.4		71
ADA084	19	0.2	1.8	3.0	89.46
ADA087		1.2	2.8		71

University of Ghana http://ugspace.ug.edu.gh

ADA099	11	0.9	2.4	2.4	92.7
ADA088		25	2.8	3.2	108.19
ADA107	3	25.0	3.0	4.6	108.19
ADA108	3	25.0	2.8	3.1	98.96
ADA90	3	0.2	2.5	3.0	123.87
ADA91		10.0	3.7		91.31
ADA92	5	0.4	2.8	3.0	109.77
ADA093		0.9	2.5		125.45
ADA101	3	1.2	2.1	2.4	73.8
ADA102	95	0.4	1.5	1.6	92.26
ADA103	3	1.3	1.2	0.2	107.94
ADA095		0.4	2.0	3.0	82.08
ADA096	15	0.4	1.2	1.0	116.22
ADA097	162	0.2	1.4	2.0	100.54
Chloroquine		0.1			

3.18 ADME Evaluation of synthesized Analogues.

In a related experiment, the ADME profiles of some selected analogues were evaluated in **Table 3.3**. First, none of the prepared analogues raised any toxicity concerns as they all returned >25 in the Hep G2 cells Luminescence assay after 72h. Secondly, the compounds retained biological

University of Ghana http://ugspace.ug.edu.gh

activity when they were tested against sensitive and resistant strains of the malaria parasite. No significant shift in IC_{50} was observed for all the tested compounds. A number of the compounds were metabolically stable in both human microsomes and rat hepatocytes when compared to the phenotypic hit. For example, ADA084, ADA095, ADA096 and ADA097 were metabolically more stable than **MMV902507.** While compounds ADA084, ADA095, ADA096 and ADA097 had low clearance of 47 µL/min/mg, 79 µL/min/mg, 4 µL/min/mg and 31 µL/min/mg respectively. The hit compound had a very high clearance of 578 µL/min/mg in human microsomes. Similarly, clearance (µL/min/10^{-6} cells) of 26, 57, 37, 14, 3, and 13 was obtained for ADA084, ADA092, ADA093, ADA095, ADA096 and ADA097 respectively while 85 µL/min/10^{-6} cells was obtained for the hit compound. Overall, compound ADA 096 emerged as the most stable. Despite the superior metabolic stability observed for most of the compounds, none of them returned superior potency than the hit compounds.

The kinetic Solubility of selected analogues was determined using the HP-LC method. The Solubility of the analogues ranged from poor to good (**3 µM- 162 µM**). Compounds ADA097 and ADA102 had good solubility values with **ADA097** being the most soluble (**162 µM**), superior to the Solubility of the hit compound (**44 µM**). Although the Solubility of most compounds was poor, it was observed that analogues with the 3,4-dimethoxy substitutions had better Solubility than other analogues. This could be due to distorted planarity in the molecule which leads to reduced pi-stacking in the molecule enhancing the solubility of these analogues.

Table 3.3: ADME evaluation of some analogues

Compound	3D7/Dd2	Log D pH 7.4	Human Microsomes	Rat Hepatocytes		Hep G2 cells	Albumax (%unbound)

University of Ghana http://ugspace.ug.edu.gh

	LDH (μM)		Clint Mics (μL/min/ mg)	T1/2 (min)	Clint Heps (μL/min/ 10^{-6} cells)	T1/2 (min)	Kinetic Solubility (μM) PBS- $pH_{7.4}$ RT	Lumine scence 72h	
MMV902507 (Hit Compound)	**0.1 / 0.1**	**3**	**578**	**3**	**85**	**16**	**27**	**>25**	**ND**
ADA084	0.2/0.4	3	47	30	26	26	19	>25	49.1
ADA090	0.2/0.2	3	462	35	92	8	3	>25	47.21
ADA092	0.4/0.5	4	230	65	57	13	5	>25	92.07
ADA093	0.9/1.6	3	298	5	38	18	23	>25	18.46
ADA095	0.4/0.5	3	79	18	14	51	3	>25	63.74
ADA096	**0.4/0.4**	**1**	**4**	**394**	**3**	**361**	**18**	**>25**	**6.05**
ADA097	0.2/0.2	2	31	45	13	51.63	162	>25	46.14

3.19 Physicochemical Parameters of Synthesized Analogues

The calculated Log D values of the synthesized analogues were obtained from StarDrop. The Log D values range from 1.2 to 3.7 and the compound with the highest calculated Log D is **ADA091**. Log D value of **ADA091** is 3.7 while **ADA096 and ADA103** gave the lowest calculated Log D value of 1.2. The Log D values of the analogues were also experimentally determined at pH 7.4. The data values ranged from 4.6 to 0.2, **ADA107** had the highest Log D value while **ADA103** had

University of Ghana http://ugspace.ug.edu.gh

the lowest Log D value experimentally. The graph below (**Figure 3.15**) shows a correlation between the experimental and calculated Log D values.

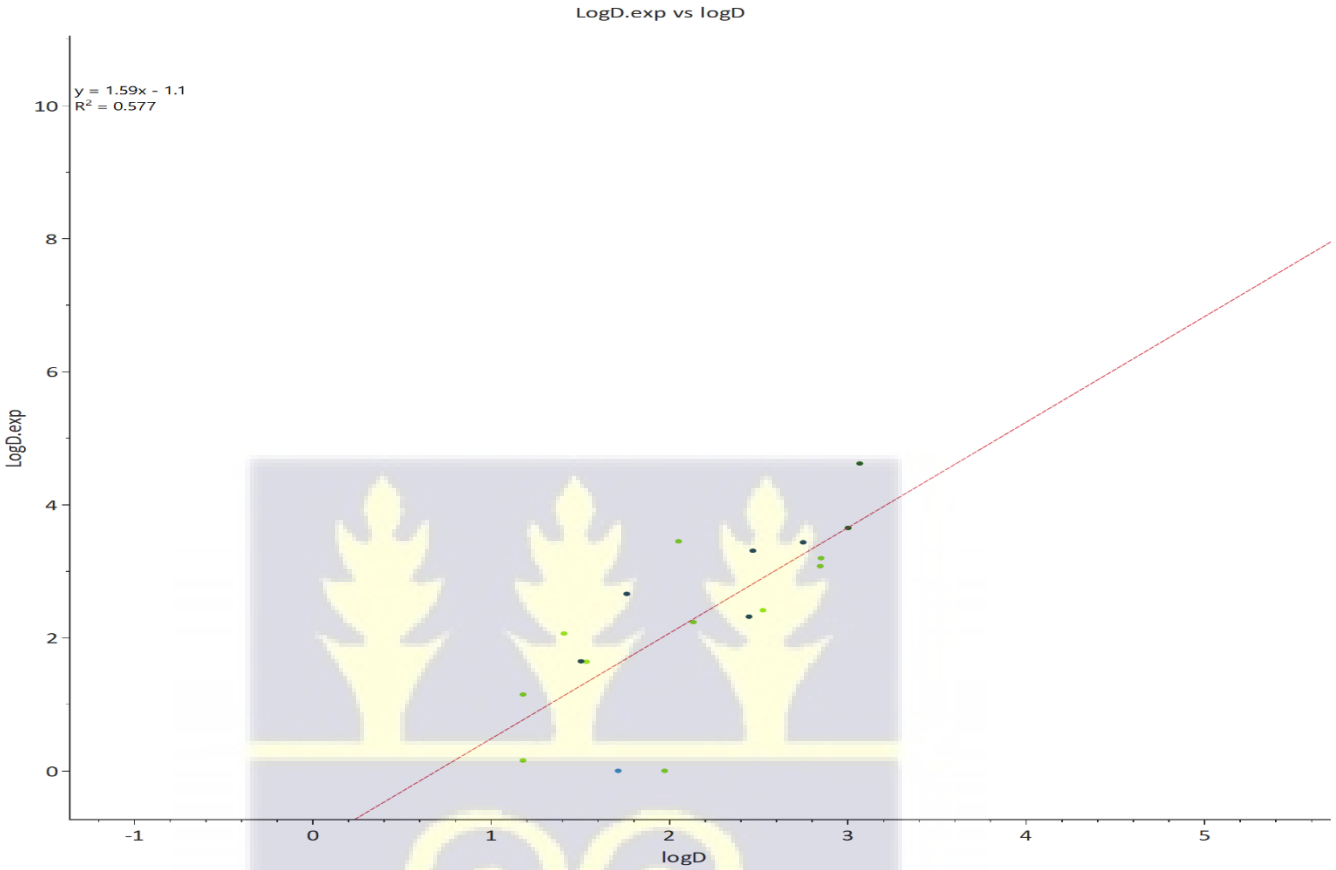


Figure 3.15: A plot of exp. Log D against calc. Log D.

INTEGRI PROCEDAMUS

University of Ghana http://ugspace.ug.edu.gh

Chapter 4

4.1 The Hit Compound MMV1900279

To identify new drug entities, Medicines for Malaria Ventures (MMV) phenotypically screened molecular entities from the Bayer Library. This phenotypic screen led to the discovery of the Hit Compound MMV1900279. It was found to be active against the sensitive NF54 strain of the parasite. The hit compound had no cross-resistance and had a good log P. value. The compound however, had a higher molecular weight value. Although the compound was found to be active against the parasite, it still does not meet the MMV criteria for progression to the next stage of the drug discovery process. Previous work in the group showed that removing the sulfonamide moiety reduced activity, as exemplified by FEP003 (**Figure 4.1**). Also, smaller groups such as cyclopropyl and methyl groups at the N9 position on the imidazole ring did not favor activity as exemplified by SD011 and FEP046 respectively. However, cyclobutyl group led to an increase in activity as seen in FEP048. By exploring and establishing the minimum pharmacophore, the groups that positively impact activity and other physicochemical parameters will be further understood. Thus, improving properties of the hit compound.

University of Ghana http://ugspace.ug.edu.gh

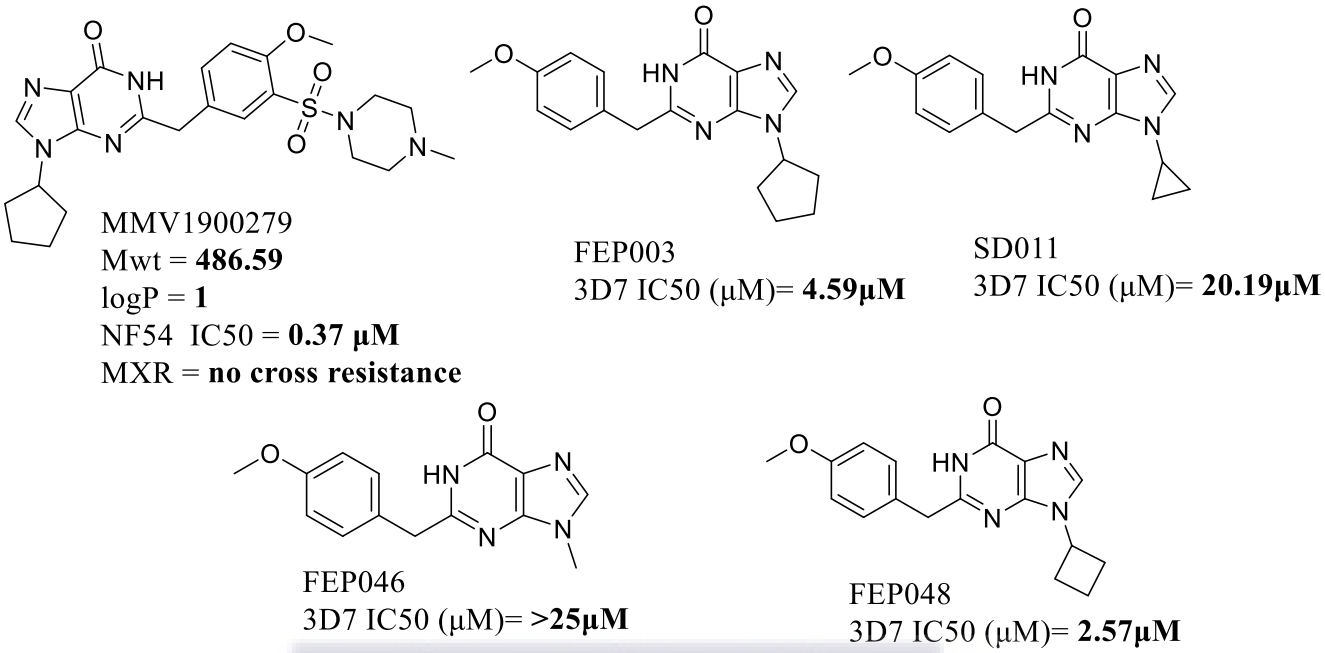


Figure 4.1: Previous work done on MMV1900279.

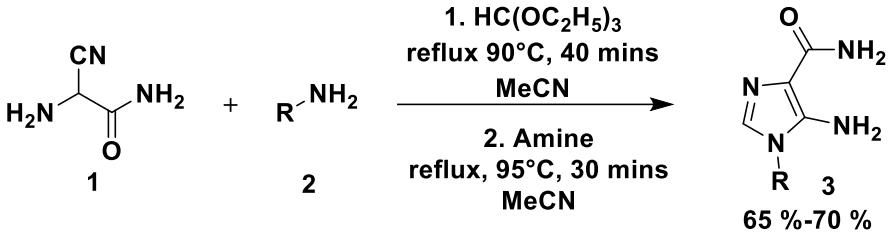
4.2 Medicinal Chemistry Strategy for the Synthesis of the Analogues of MMV1900279

The hit compound MMV1900279 was resynthesized and tested against the 3D7 strain of *P. falciparum* to validate the phenotypic data. The resynthesized hit compound FEP024 retained activity with an IC_{50} value of 0.30 µM comparable to that obtained from the phenotypic hit MMV1900279 with an IC_{50} value of 0.37 µM.

The strategy was to expand the Structure-Activity Relationship (SAR) by substituting cycloalkyl groups such as cyclohexyl, cyclopentyl and cyclobutyl and phenyl for the alkyl groups used earlier to explore the impact of hydrophobic and pi-stacking interactions on activity. Also, oxygen and nitrogen heterocyclic rings such as tetrahydropyran, oxetane and piperidine were substituted on the imidazole ring of the compounds to investigate the impact of hydrogen bond donor and acceptor on the activity as well as the solubility of the compounds.

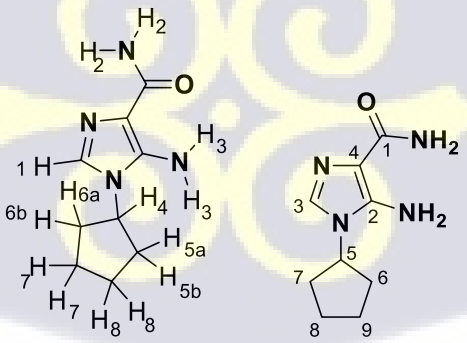
University of Ghana http://ugspace.ug.edu.gh

4.3 General Procedure for 5-amino-1H-imidazole-4-carboxamide derivatives.



In a pre-weighed round-bottom flask containing 2-amino-2-cyanocetamide (1 eqv) dissolved in MeCN (20 mL), triethyl orthoformate (1.5 eqv) was added and the reaction mixture was refluxed at 90 ºC for 40 mins then allowed to cool to room temperature. A variety of amines (1.5 eqv) was added to the mixture which was then refluxed at 90 ºC for another 30 mins. The reaction was monitored using TLC in an appropriate solvent system upon completion. The crude mixture was stirred and cooled to room temperature. A brown precipitate was formed upon cooling of the reaction mixture which was filtered and washed with MeCN to afford various intermediates.

4.3.1 Synthesis of **5-amino-1-cyclopentyl-1H-imidazole-4-carboxamide (ADA110, 1).**

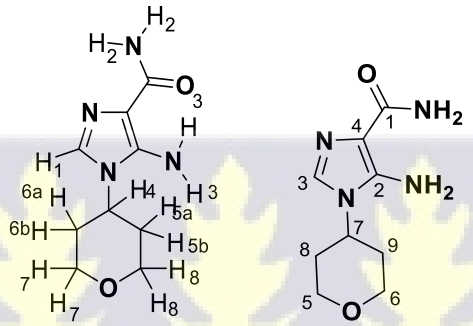


This compound was synthesized according to the general procedure for imidazole synthesis described using 2-amino-2-cyanocetamide (3.03mmol, 1 eqv), triethyl orthoformate (4.54 mmol, 1.5 eqv) and Cyclopentyl amine (4.54 mmol, 1.5 eqv) to give the intermediate above as a cream amorphous solid (0.3g, 65 %). Melting point = 171-173 ºC. Vmax (neat) cm^{-1} (N-H) 3381.88-

University of Ghana http://ugspace.ug.edu.gh

3322.43, (=C-H) 3189.12, (C-H) 2972.46, (C=O) 1657.53, (C=N) 1611.19 (C=C) 1555.55. ^{1}H NMR (500 MHz, DMSO-d_6) δ_H 7.20 (s, 1H$_1$), 6.65 (d, J = 71.2 Hz, 2H$_2$), 5.75 (s, 2H$_3$), 4.43 – 4.16 (m, 1H$_4$), 2.11 – 2.03 (m, 2H$_{5a,6a}$), 1.82 – 1.69 (m, 4H$_{5b,6b}$), 1.68 – 1.61 (m, 4H$_{7,8}$). ^{13}C NMR (126 MHz, DMSO-d_6) δ_C 166.3 C$_1$, 142.4 C$_2$, 126.5 C$_3$, 112.2 C$_4$, 53.6 C$_5$, 31.4 C$_{6,7}$, 22.7 C$_{8,9}$.

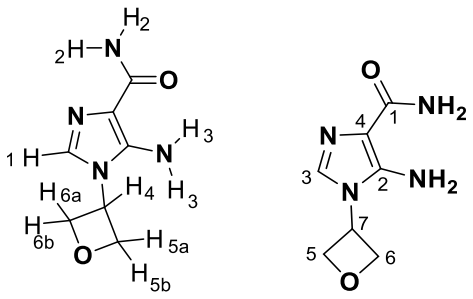
4.3.2 Synthesis of 5-amino-1-(tetrahydro-2H-pyran-4-yl)-1H-imidazole-4-carboxamide (ADA111, 2).



This compound was synthesized according to the general procedure for imidazole synthesis using 2-amino-2-cyanocetamide (1.01 mmol, 1 eqv), triethyl orthoformate (1.21 mmol, 1.2 eqv) and 4-aminotetrahydropyran (1.21 mmol, 1.2 eqv) to give the intermediate as a brown amorphous solid (0.1371g, 65 %). Melting point = 195-197 ºC. Vmax (neat) cm^{-1} (N-H) 3368.82-3306.81, (=C-H) 3185.68, (C-H) 2960.61-2858.87, (C=O) 1645.52, (C=N) 1614.32, (C=C) 1552.39. ^{1}H NMR (500 MHz, DMSO-d_6) δ_H 7.27 (s, 1H$_1$), 6.67 (d, J = 7.5 Hz, 2H$_2$), 5.83 (s, 2H$_3$), 4.11 (dddd, J = 16.0, 11.0, 7.6, 4.2 Hz, 1H$_4$), 3.97 (dd, J = 11.2, 3.4 Hz, 2H$_{5a,6a}$), 3.42 (ddt, J = 14.8, 11.5, 4.2 Hz, 2H$_{5b,6b}$), 1.85 (t, J = 12.3, 4.3, 3.8 Hz, 4H$_{7,8}$). ^{13}C NMR (126 MHz, DMSO-d_6) δ_C 166.5 C$_1$, 142.0 C$_2$, 126.7 C$_3$, 112.1 C$_4$, 66.0 C$_{5,6}$, 49.2 C$_7$, 32.2C$_{8,9}$.

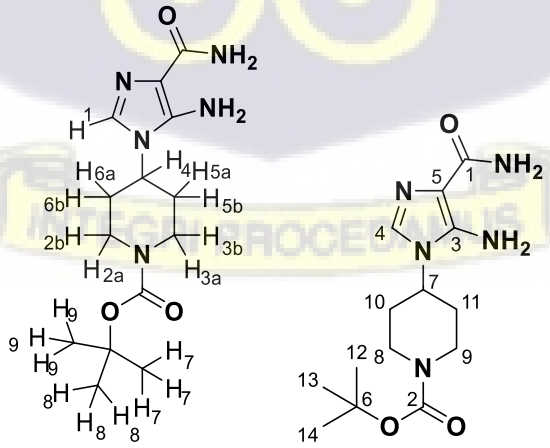
University of Ghana http://ugspace.ug.edu.gh

4.3.3 Synthesis of 5-amino-1-(oxetan-3-yl)-1H-imidazole-4-carboxamide (ADA114, 3)



This compound was synthesized according to the general procedure for imidazole synthesis described using 2-amino-2-cyanocetamide (3.03 mmol, 1 eqv), triethyl orthoformate (4.54 mmol, 1.5 eqv) and oxetane-3-amine (4.54 mmol, 1.5eqv) to give the intermediate as a light pink amorphous solid (0.39g, 71%). Melting point = 188-190 ºC. Vmax (neat) cm^{-1} (N-H) 3413.13-3269.26, (=C-H) 3114.26, (C-H) 2892.83, (C=O) 1630.35, (C=N) 1604.38, (C=C) 1556.71. ^{1}H NMR (500 MHz, DMSO-d_6) δ_H 7.58 (s, $1H_1$), 6.73 (s, $2H_2$), 5.74 (s, $2H_3$), 5.27-5.20 (m, $1H_4$), 4.90 (t, J = 7.2 Hz, $2H_{5a,6a}$), 4.78 (t, J = 6.6 Hz, $2H_{5b,6b}$). ^{13}C NMR (126 MHz, DMSO-d_6) δ_C 167.0 C_1, 143.0 C_2, 127.7 C_3, 113.2 C_4, 76.6 $C_{5,6}$, 47.5 C_7.

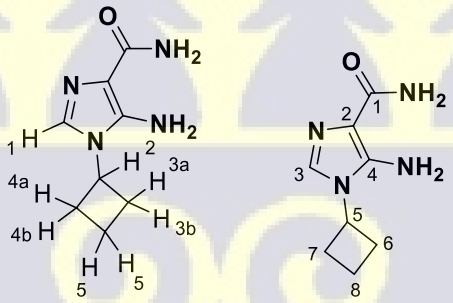
4.3.4 Synthesis of *tert*-butyl 4-(5-amino-4-carbamoyl-1H-imidazol-1-yl) piperidine-1-carboxylate (ADA127, 4)



University of Ghana http://ugspace.ug.edu.gh

The intermediate ADA127 was prepared according to the general procedure for imidazole synthesis using 2-amino-2-cyanocetamide (5.0459 mmol, 1 eqv), triethyl orthoformate (7.5688 mmol, 1.5 eqv) and 4-aminopiperidine-1-carboxylic acid t-butyl ester (7.5688 mmol, 1.5 eqv) to give a pale yellow amorphous solid (0.2669g, 58 % yield). Melting point = 208-210 ºC. Vmax (neat) cm^{-1} (N-H) 3305.88-3168, (=C-H) 3011.42, (C-H) 2974.80-2891.46, (C=O) 1671.85, (C=N) 1623.24, (C=C) 1553.02-1425.38. ^{1}H NMR (400 MHz, Methanol-d_4) δ_H 7.40 (s, $1H_1$), 4.42 – 4.26 (m, $2H_{2a,3a}$), 4.16 (t, J = 12.3 Hz, $1H_4$), 2.99 (d, J = 14.0 Hz, $2H_{2b,3b}$), 2.14 (d, J = 12.6 Hz, $2H_{5a,6a}$), 1.97 – 1.78 (m, $2H_{5b,6b}$), 1.57 (s, $9H_{7,8,9}$). ^{13}C NMR (126 MHz, MeOD) δ_C 169.4 C_1, 156.3 C_2, 144.9 C_3, 129.3 C_4, 113.1 C_5, 81.4 C_6, 52.9 $C_{7\text{-}9}$, 32.8 C_{10}, C_{11}, 28.7 $C_{12\text{-}14}$.

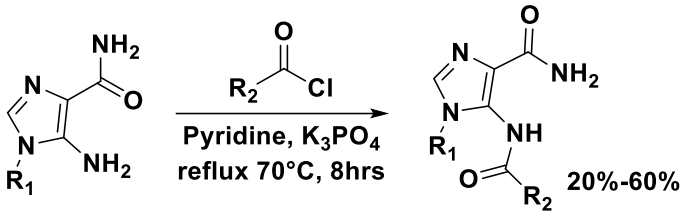
4.3.5 Synthesis of 5-amino-1-cyclobutyl-1H-imidazole-4-carboxamide (ADA134, 5)



This compound was prepared according to the general procedure for imidazole synthesis using 2-amino-2-cyanocetamide (12.11 mmol, 1 eqv), triethyl orthoformate (14.53 mmol, 1.5 eqv) and oxetane-3-amine (14.53 mmol, 1.5 eqv) to give the intermediate as a light pink amorphous solid (1.11g, 71 %). Melting point = 196-198 ºC. V_{max} (neat) cm^{-1} (N-H) 3376.87-3208.86, (=C-H) 3097.27, (C-H) 2996.74-2869.24, (C=O) 1606.05, (C=N) 1555.31, (C=C) 1456.89. ^{1}H NMR (400 MHz, Methanol-d_4) δ_H 7.45 (s, $1H_1$), 4.71 – 4.46 (m $1H_2$), 2.66 – 2.55 (ddd, J = 11.6, 9.7, 7.6 Hz, $2H_{3a,4a}$),2.54 – 2.44 (m $2H_{3b,4b}$), 2.01 (td, J = 9.8, 5.2 Hz, $2H_5$). ^{13}C NMR (126 MHz, MeOD) δ_C 169.4 C_1, 145.0 C_2, 129.7 C_3, 113.2 C_4, 49.5 C_5, 30.9 $C_{6,7}$, 16.0 C_8.

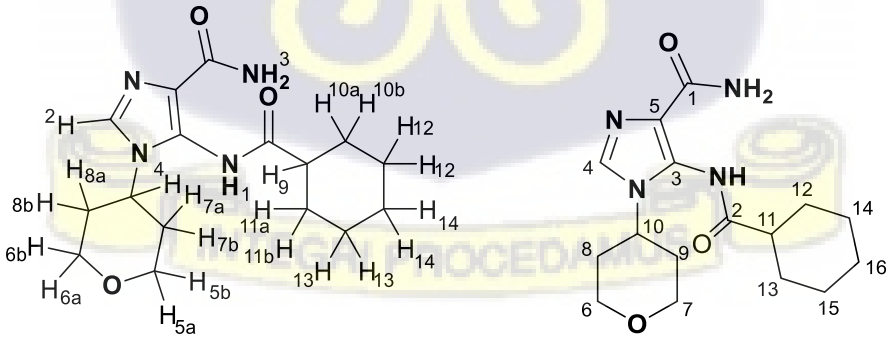
University of Ghana http://ugspace.ug.edu.gh

4.4 General Procedure for Amide Coupling Synthesis



A pre-dried, pre-weighed round-bottom flask containing molecular sieves was flashed with nitrogen to ensure an inert atmosphere. The volume of various acid chlorides (3.0 eqv) was measured into the round-bottom flask under inert conditions using DCM (5 mL). A known amount of the prepared amine intermediates (1.0 eqv) and Et_3N (3.5 eqv) were added to the acid chloride mixture and left to stir at room temperature for 4 hours under inert conditions. TLC was used to monitor the reaction until completion. The crude mixture was washed with distilled water (20 mL x 2) to remove the excess Et_3N and the organic layer was dried with $MgSO_4$ and concentrated in vacuo. The crude product was purified on a flash column with an appropriate solvent system to afford the amide intermediates.

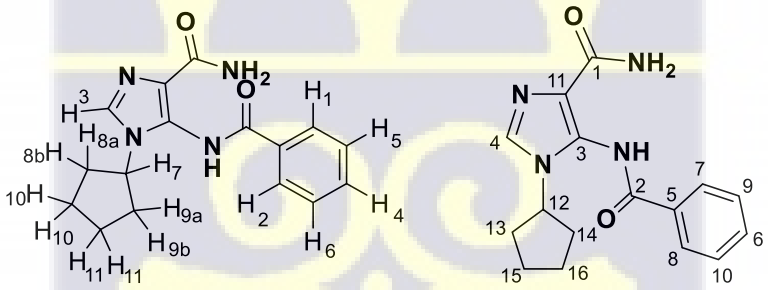
4.4.1 Synthesis of 5-(cyclohexanecarboxamido)-1-(tetrahydro-2*H*-pyran-4-yl)-1*H*-imidazole-4-carboxamide (ADA112, 6).



University of Ghana http://ugspace.ug.edu.gh

The intermediate ADA112 was synthesized according to the general synthesis of amide formation using ADA111 (1.43 mmol, 1 eqv), cyclohexane carbonyl chloride (4.28 mmol, 3 eqv) to give a white amorphous solid (0.41g, 90 %). Melting point = 160-162 ºC. V_{max} (neat) cm^{-1} (N-H) 3110.84, (C-H) 2986.98, (C=O) 1156.01 (C=C) 1596.91, (C=N) 1327.64. ^{1}H NMR (500 MHz, DMSO-d_6) δ_H 7.58 (d, J = 9.5 Hz, $1H_1$), 7.32 (s, $1H_2$), 5.90 (s, $2H_3$), 4.12 (tt, J = 10.6, 5.6 Hz, $1H_4$), 3.96 (dt, J = 11.8, 3.1 Hz, $2H_{5a,6a}$), 3.64 (td, J = 7.6, 5.3 Hz, $2H_{5b,6b}$), 3.43 (d, J = 3.0 Hz, $2H_{7a,8a}$), 3.41 (dd, J = 3.1, 5.3 Hz $2H_{7b,8b}$), 3.09 (qd, J = 7.2, 4.5 Hz, $1H_9$), 2.06 – 2.00 (m, $2H_{10a,11a}$), 1.99 – 1.91 (m, $2H_{10b,11b}$), 1.86 (q, J = 3.7 Hz, $4H_{12,13}$), 1.80 – 1.75 (m, $2H_{14}$). ^{13}C NMR (126 MHz, DMSO) δ_C 163.9 $C_{1,2}$, 142.4 C_3, 126.8 C_4, 111.5 C_5, 78.7 $C_{6,7}$, 65.9 C_{10}, 49.1 $C_{8,9}$, 45.3 C_{11}, 32.0 $C_{12,13}$, 30.1 $C_{14,15}$, 24.2 C_{16}.

4.4.2 Synthesis of 5-benzamido-1-cyclopentyl-1H-imidazole-4-carboxamide (ADA115, 7).

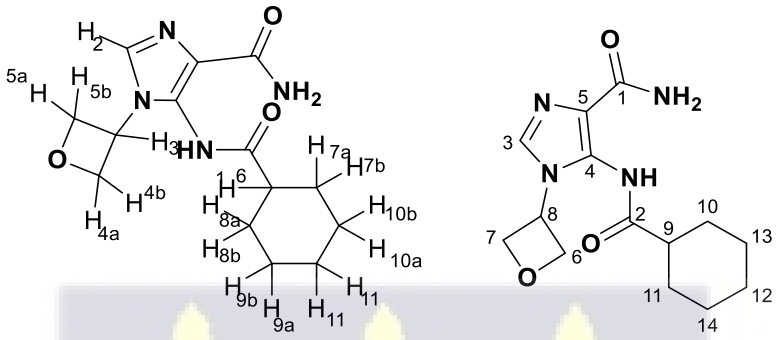


The intermediate ADA115 was synthesized according to the general amide-formation synthesis using ADA110 (1.54 mmol, 1 eqv) and benzoyl chloride (4.63 mmol, 3 eqv) yielding a light-yellow amorphous solid (0.25 g, 54 %). Melting point = 201-203 ºC, V_{max} (neat) cm^{-1} (N-H) 3310.93, (=C-H) 3113.61, (C-H) 2968.91-2873.69, (C=O) 1665.42, (C=N) 1580.35, (C=C) 1508.57-1465.78. ^{1}H NMR (400 MHz, Methanol-$d4$) δ_H 8.09 (d, J = 7.7 Hz, $2H_{1,2}$), 8.03 (s, $1H_3$), 7.75 (t, J = 7.5 Hz, $1H_4$), 7.65 (t, J = 7.7 Hz, $2H_{5,6}$), 4.57 (p, J = 7.1 Hz, $1H_7$), 2.31 (d, J = 7.9 Hz, $2H_{8a,9a}$), 1.99 – 1.98 (dd, J = 11.20, 7.90 Hz,$4H_{10,11}$), 1.86 – 1.77 (m, $2H_{8b,9b}$). ^{13}C NMR (126 MHz, MeOD)

University of Ghana http://ugspace.ug.edu.gh

δ_C 170.1 C_1, 169.8 C_2, 134.4 C_3, 134.0 C_4, 133.3 C_5, 130.7 C_6, 130.0 $C_{7,8}$, 129.5 $C_{9,10}$, 129.3 C_{11}, 59.9 C_{12}, 34.0 $C_{13,14}$, 24.8 $C_{15,16}$.

4.4.3 Synthesis of 5-(cyclohexanecarboxamido)-1-(oxetan-3-yl)-1*H*-imidazole-4-carboxamide (ADA116, 8).

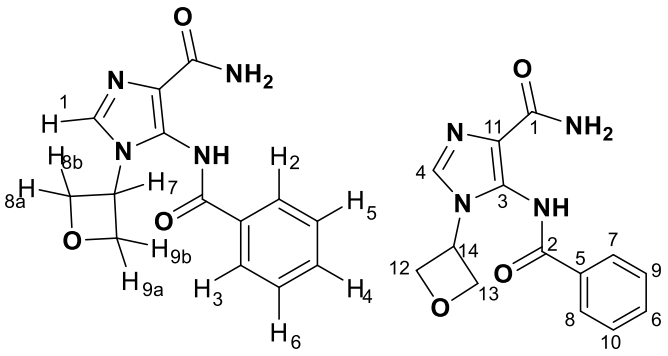


This compound was prepared according to the general procedure for amide formation using ADA114 (1.10 mmol, 1 eqv) and cyclohexane carbonyl chloride (3.29 mmol, 3 eqv) affording the intermediate as a white amorphous solid (0.15 g, 45 %). Melting point = 157-159 ºC. Vmax (neat) cm^{-1} (N-H) 3435.73-3250.14, (=C-H) 3109.17, (C-H) 2930.12-2854.74, (C=O) 1676.25, (C=N) 1592.94, (C=C) 1529.41. ^{1}H NMR (400 MHz, Methanol-d_4) δ_H 8.32 (s, 1H_1), 8.18 (s, 1H_2), 5.26 – 5.23 (m, 1H_3), 5.11 (d, J = 7.4 Hz, 2$H_{4a,5a}$), 4.95 (d, J = 7.2 Hz, 2$H_{4b,5b}$), 2.58 – 2.53 (m, 1H_6), 2.08 (d, J = 13.9 Hz, 2$H_{7a,8a}$), 1.97 – 1.92 (m, 2$H_{7b,8b}$), 1.81 (d, J = 12.0 Hz, 2$H_{9a,10a}$), 1.60 (t, J = 12.1 Hz, 2$H_{9b,10b}$), 1.49 – 1.41 (m, 2H_{11}). ^{13}C NMR (126 MHz, CDCl3) δ_C 176.41 $C_{1,2}$, 134.1 C_3, 113.8 C_4, 107.2 C_5, 77.3 $C_{6,7}$, 50.6 C_8, 44.8 C_9, 29.3 $C_{10,11}$, 25.4 C_{12}, 25.3 $C_{13,14}$.

INTEGRI PROCEDAMUS

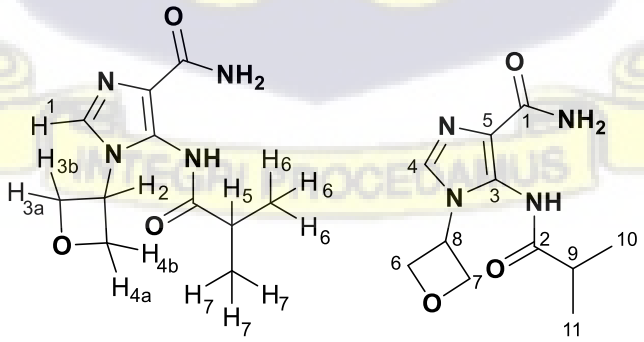
University of Ghana http://ugspace.ug.edu.gh

4.4.4 Synthesis of 5-benzamido-1-(oxetan-3-yl)-1H-imidazole-4-carboxamide (ADA119, 9)



This compound was synthesized according to the general procedure for amide formation using ADA114 (1.65 mmol, 1 eqv) and benzoyl chloride (4.94 mmol, 3 eqv) and to give the intermediate as a light yellow amorphous solid (0.13, 27 %). Melting point = 187-189 ºC. Vmax (neat) cm^{-1} (N-H) 3195.81, (=C-H) 3101.63, (C-H) 2971.13-2891.46, (C=O) 1659.47, (C=N) 1578.55, (C=C) 1510.97-1485.60. ^{1}H NMR (400 MHz, Methanol-d_4) δ_H 8.42 (s, 1H$_1$), 8.08 (d, J =7.7 Hz, 2H$_{2,3}$), 7.75 (t, J = 7.5 Hz, 1H$_4$), 7.65 (t, J = 7.6 Hz, 2H$_{5,6}$), 5.44 – 5.35 (m1H$_7$), 5.13 (t, J = 7.5 Hz, 2H$_{8a,9a}$), 5.00 (t, J = 6.8 Hz, 2H$_{8b,9b}$). ^{13}C NMR (126 MHz, DMSO) δ_C 166.4 C$_1$, 163.4 C$_2$, 132.6 C$_3$, 132.3 C$_4$, 131.8 C$_5$, 128.2 C$_6$, 128.0 C$_{7,8}$, 127.5 C$_{9,10}$, 126.9 C$_{11}$, 75.9 C$_{12,13}$, 48.3 C$_{14}$.

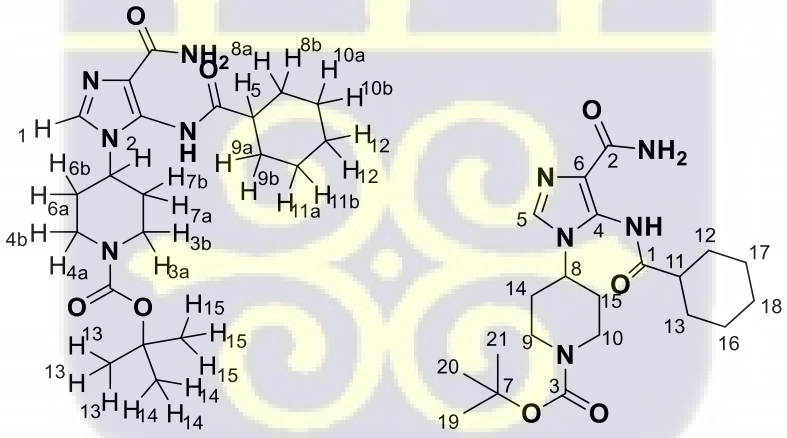
4.4.5 Synthesis of 5-isobutyramido-1-(oxetan-3-yl)-1*H*-imidazole-4-carboxamide (ADA120, 10).



University of Ghana http://ugspace.ug.edu.gh

This compound was synthesized according to the general procedure for amide formation using ADA114 (1.65 mmol, 1 eqv) and Iso-butyryl chloride (4.95 mmol, 3 eqv) yielding the intermediate as a white amorphous solid (0.08g, 19 %). Melting point = 151-153 ºC. Vmax (neat) cm^{-1} (N-H) 3459.89-3233.80, (=C-H) 3119.32, (C-H) 2971.12-2891.46, (C=O) 1735.02, (C=N) 1702.03, (C=C) 1587.08-1473.19. ^{1}H NMR (400 MHz, Methanol-d_4) δ_H 8.25 (s, $1H_1$), 5.32– 5.24 (m, $1H_2$), 5.12 (dd, J = 8.3, 6.5 Hz, $2H_{3a,4a}$), 4.97 (t, J = 6.5 Hz, $2H_{3b,4b}$), 3.23 – 3.13 (m, $1H_5$), 1.35 (d, J = 1.8 Hz, $3H_6$), 1.28 (d, J = 2.0 Hz, $3H_7$). ^{13}C NMR (126 MHz, MeOD) δ 180.9 C_1, 179.4 C_2, 161.4 C_3, 135.4 C_4, 126.8 C_5, 62.0 $C_{6,7}$, 44.4 C_8, 36.8 C_9, 19.2 $C_{10,11}$.

4.4.6 Synthesis of *tert*-butyl 4-(4-carbamoyl-5-(cyclohexane carboxamido)-1*H*-imidazol-1-yl) piperidine-1-carboxylate (ADA128, 11).

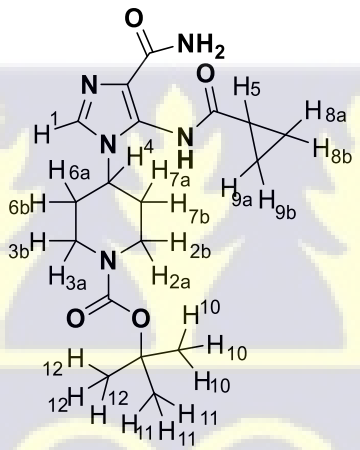


This compound was synthesized according to the general procedure for amide formation using ADA127 (1.62 mmol, 1 eqv) and cyclohexane carbonyl chloride (4.85 mmol, 3 eqv) affording the intermediate as a white amorphous solid (0.37g, 55 %). Melting point = 133-135 ºC. Vmax (neat) cm^{-1} (N-H) 3179.03, (C-H) 2926.69, (C=O) 1735.58-1689.98, (C=C) 1503.37, (C=N) 1478.46. ^{1}H NMR (500 MHz, Methanol-d_4) δ_H 8.00 (s, $1H_1$), 4.30 (t, J = 3.7 Hz, $2H_{3a,4a}$), 4.06 (t, J = 3.4 Hz,

University of Ghana http://ugspace.ug.edu.gh

$2H_{3b,4b}$), 3.87 – 3.80 (m, $1H_2$), 2.54 (tt, J = 11.6, 3.4 Hz, $1H_5$), 2.18 (tt, J = 11.7, 3.4 Hz, $2H_{6a,7a}$), 2.06 (t, J = 4.1 Hz, $2H_{6b,7b}$), 1.93 (tt, J = 11.6, 3.5 Hz, $2H_{8a,9a}$), 1.83 (t, J = 3.7 Hz, $2H_{8b,9b}$), 1.82 – 1.77 (m, $2H_{10a,11a}$), 1.51 (s, $9H_{13,14,15}$), 1.47 – 1.40 (m, $2H_{10b,11b}$), 1.33 (d, J = 2.4 Hz, $2H_{12}$). ^{13}C NMR (126 MHz, MeOD) δ_C 179.9 C_1, 178.6 C_2, 156.4 C_3, 134.3 C_4, 129.9 C_5, 127.6 C_6, 81.1 C_7, 54.8 C_8, 47.6 $C_{9,10}$, 44.3 C_{11}, 33.5 $C_{12,13}$, 30.7 $C_{14,15}$, 28.6 $C_{16,17}$, 26.9 C_{18}.

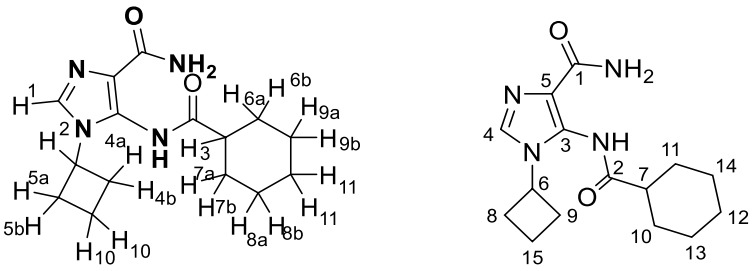
4.4.7 Synthesis of *tert*-butyl 4-(4-carbamoyl-5-(cyclopropane carboxamido)-1*H*-imidazol-1-yl) piperidine-1-carboxylate (ADA131, 12).



This compound was synthesized according to the general procedure for amide formation using ADA127 (1.62 mmol, 1 eqv) and Cyclopropane carbonyl chloride (4.85 mmol, 3 eqv) yielding the intermediate as a white amorphous solid (0.3g, 56 %). Melting point = 180-182 ºC. Vmax (neat) cm^{-1} (N-H) 3361.86, (C-H) 2969.80, (C=O) 1685.29, (C=N) 1593.85, (C=C) 1440.80. ^{1}H NMR (400 MHz, Methanol-d_4) δ_H 7.92 (s, $1H_1$), 4.33 (d, J = 12.3 Hz, $2H_{2a,3a}$), 4.15 (d, J = 12.4 Hz, $2H_{2b,3b}$), 2.97 (d, J = 12.3 Hz, $1H_4$), 2.57 (dd, J = 5.5, 2.9 Hz $1H_5$), 2.13 (d, J = 12.5 Hz, $2H_{6a,7a}$), 2.02 – 1.95 (m, $2H_{6b,7b}$), 1.56 (s, $9H_{10,11,12}$), 1.13 (dt, J = 5.3, 3.1 Hz, $2H_{8a,9a}$), 1.08 (dt, J = 5.2, 2.4 Hz, $2H_{8b,9b}$).

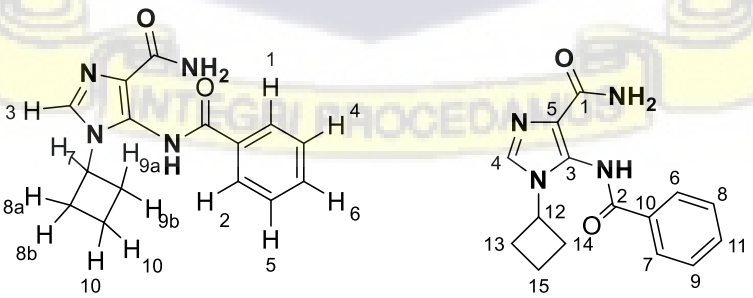
University of Ghana http://ugspace.ug.edu.gh

4.4.8 Synthesis of 1-cyclobutyl-5-(cyclohexanecarboxamido)-1*H*-imidazole-4-carboxamide (ADA135, 13).



This compound was synthesized according to the general procedure for amide formation using ADA134 (1.67 mmol, 1 eqv) and cyclohexane carbonyl chloride (4.99 mmol, 3 eqv) affording the intermediate as a white amorphous solid (0.38g, 78 %). Melting point = 155-156 ºC. Vmax (neat) cm^{-1} (N-H) 3320.21-3259.70, (=C-H) 3126.94, (C-H) 2927.08-2853.25, (C=O) 1680.97, (C=N) 1583.52, (C=C) 1449.42. ^{1}H NMR (400 MHz, Methanol-d_4) δ_H 7.93 (s, 1H$_1$), 4.69-4.55 (m, 1H$_2$), 2.89 (dt, J = 11.3, 7.0 Hz, 1H$_3$), 2.57 (t, J = 5.6 Hz, 2H$_{4a,5a}$), 2.54 – 2.46 (m, 2H$_{4b,5b}$), 2.09 (d, J = 12.7 Hz, 2H$_{6a,7a}$), 1.94 (d, J = 15.9 Hz, 2H$_{6b,7b}$), 1.83 (d, J = 12.5 Hz 2H$_{8a,9a}$), 1.61 (d, J = 12.5 Hz, 2H$_{8b,9b}$), 1.57 – 1.50 (m, 2H$_{10}$), 1.49 – 1.40 (m, 2H$_{11}$). ^{13}C NMR (126 MHz, MeOD) δ 179.4 C$_1$, 178.3 C$_2$, 161.6 C$_3$, 134.6 C$_4$, 127.0 C$_5$, 50.9 C$_6$, 46.5 C$_7$, 31.4 C$_{8,9}$, 30.1 C$_{10,11}$, 26.9 C$_{12}$, 26.6 C$_{13,14}$, 16.0 C$_{15}$.

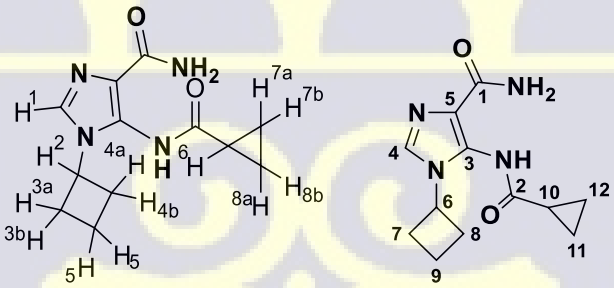
4.4.9 Synthesis of 5-benzamido-1-cyclobutyl-1*H*-imidazole-4-carboxamide (ADA137, 14).



University of Ghana http://ugspace.ug.edu.gh

This compound was prepared according to the general procedure for amide formation using ADA134 (1.67 mmol, 1 eqv) and Benzoyl chloride (4.99 mmol, 3 eqv) yielding the intermediate as a white amorphous solid (0.32g, 67 % yield). Melting point = 144-146 ºC. Vmax (neat) cm^{-1} (N-H) 3284.67, (=C-H) 3066.96, (C-H) 2952.36, (C=O) 1733.07-1673.67, (C=N) 1582.09, (C=C) 1456.24. ^{1}H NMR (400 MHz, Methanol-d_4) δ_H 8.14 (d, J = 7.8 Hz, $2H_{1,2}$), 8.06 (s, $1H_3$), 7.73 (t, J = 6.9 Hz, $1H_6$), 7.64 (t, J = 7.7 Hz, $2H_{4,5}$), 4.86 - 4.73 (m,$1H_7$), 2.61 (d, J = 9.7 Hz, $2H_{8a,9a}$), 2.56 (d, J = 10.4 Hz, $2H_{8b,9b}$), 2.00 (dt, J = 16.0, 7.2 Hz, $1H_{10}$). ^{13}C NMR (126 MHz, Methanol-d_4) δ_C 177.2 C_1, 169.1 C_2, 136.7 C_3, 133.6 C_4, 133.1 C_5, 129.4 $C_{6,7}$, 128.5 $C_{8,9}$, 114.1 C_{10}, 109.5 C_{11}, 50.7 C_{12}, 31.0 C_{13}, 18.0 C_{14}, 15.5 C_{15}.

4.4.10 Synthesis of 1-cyclobutyl-5-(cyclopropanecarboxamido)-1*H*-imidazole-4-carboxamide (ADA140, 15).

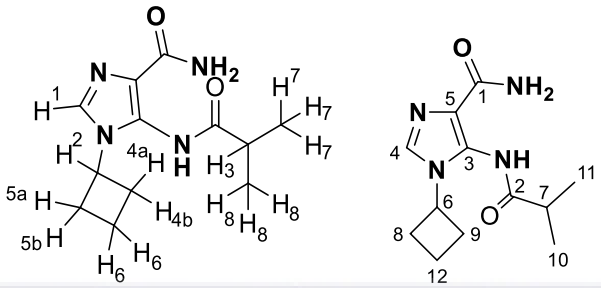


This compound was prepared according to the general procedure for amide formation using ADA134 (1.67 mmol, 1 eqv) and cyclopropane carbonyl chloride (4.99 mmol, 3 eqv) affording the intermediate as a white amorphous solid (0.15g, 36 % yield). Melting point = 149-150 ºC. Vmax (neat) cm^{-1} (N-H) 3312,55-3204.07, (=C-H) 3122.50, (C-H) 2989.21, (C=O) 1716.07, (C=N) 1669.50, (C=C) 1584.35-1545.79.^{1}H NMR (400 MHz, Methanol-d_4) δ_H 7.93 (s, $1H_1$), 4.75 - 4.54 (m, $1H_2$), 2.57 (d, J = 10.8 Hz, $2H_{3a,4a}$), 2.53 (d, J = 5.5 Hz, $2H_{3b,4b}$), 2.49 (p, J = 10.0 Hz, $1H_6$), 2.02 (dd, J = 10.8, 5.5 Hz, $2H_5$), 1.13 (td, J = 5.5, 3.1 Hz, $2H_{7a,8a}$), 1.02 (d, J = 9.1 Hz,

University of Ghana http://ugspace.ug.edu.gh

2H$_{7b,8b}$). ^{13}C NMR (126 MHz, MeOD) δ 176.7 C$_1$, 176.4 C$_2$, 143.3 C$_3$, 134.4 C$_4$, 123.5 C$_5$, 50.7 C$_6$, 31.2 C$_{7,8}$, 15.9 C$_9$, 15.4 C$_{10}$, 10.0 C$_{11}$.

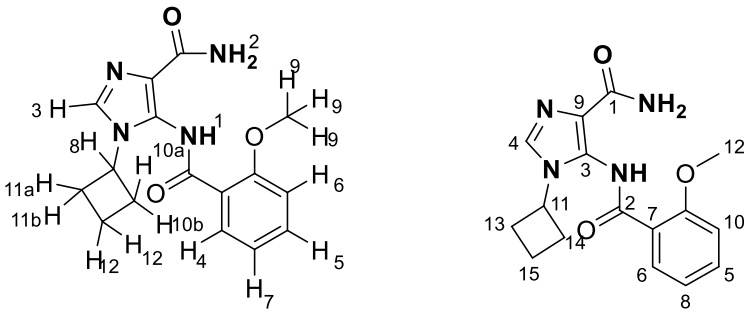
4.4.11 Synthesis of 1-cyclobutyl-5-isobutyramido-1*H*-imidazole-4-carboxamide (ADA142, 16).



This compound was synthesized according to the general procedure for amide formation using ADA134 (1.67 mmol, 1 eqv) and Iso-butyryl chloride (4.99 mmol, 3 eqv) affording the intermediate as a white amorphous solid (0.18g, 44 %). Melting point = 188-190 ºC. Vmax (neat) cm^{-1} (N-H) 3460.78-3240.24, (=C-H) 3138.05, (C-H) 2969.57-2871.46, (C=O) 1741.93-1707.11, (C=N) 1679.52, (C=C) 1586.98. ^{1}H NMR (400 MHz, Methanol-*d*$_4$) δ$_H$ 7.94 (s, 1H$_1$), 4.71 – 4.55 (m, 1H$_2$), 3.28 - 3.05 (m 1H$_3$), 2.57 (d, *J* = 9.5 Hz, 2H$_{4a,5a}$), 2.50 (d, *J* = 9.7 Hz, 2H$_{4b,5b}$), 2.00 (ddt, *J* = 12.5, 9.7, 4.0 Hz, 2H$_6$), 1.28 (d, *J* = 6.8, 2.0 Hz, 6H$_{7,8}$). ^{13}C NMR (126 MHz, MeOD) δ 179.4 C$_1$, 161.6 C$_2$, 135.4 C$_3$, 134.6 C$_4$, 132.5 C$_5$, 50.8 C$_6$, 36.2 C$_7$, 31.4 C$_{8,9}$, 19.6 C$_{10,11}$, 16.0 C$_{12}$.

University of Ghana http://ugspace.ug.edu.gh

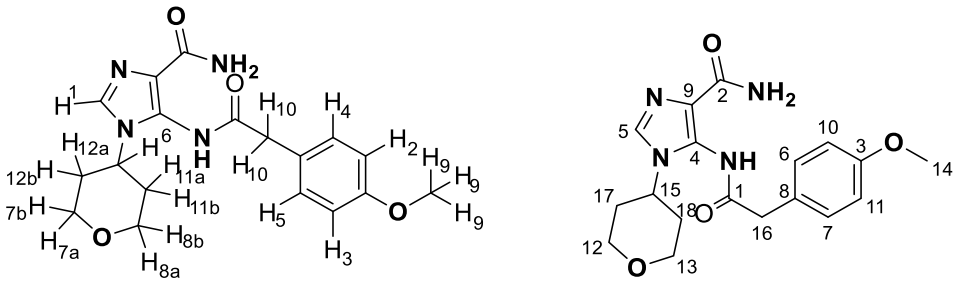
4.4.12 Synthesis of 1-cyclobutyl-5-(2-methoxybenzamido)-1*H*-imidazole-4-carboxamide (ADA144, 17).



This compound was synthesized according to the general procedure for amide formation using ADA134 (1.67 mmol, 1 eqv) and 2-methoxy benzoyl chloride (4.99 mmol, 3 eqv) yielding the intermediate as a white amorphous solid (0.2907g, 55 %). Melting point = 196-198 ºC. Vmax (neat) cm^{-1} (N-H) 3276.08, (=C-H) 3080.29, (C-H) 2948.03, (C=O) 1750.33-1674.29, (C=N) 1581.95, (C=C) 1461.17. ^{1}H NMR (500 MHz, DMSO-d_6) δ_H 11.24 (s, 1H$_1$), 9.34 (s, 2H$_2$), 7.53 (s, 1H$_3$), 7.14 (d, J = 7.0 Hz, 1H$_4$), 7.02 (dd, J = 7.8, 1.8 Hz, 1H$_5$), 6.81 (d, J = 8.1 Hz, 1H$_6$), 6.41 (d, J = 8.4 Hz, 1H$_7$), 3.81 - 3.70 (m, 1H$_8$), 3.14 (s, 3H$_9$), 1.56 (t, J = 9.8 Hz, 2H$_{10,11a}$), 1.00 (t, J = 9.2 Hz, 2H$_{10b,11b}$), 0.96 (d, J = 7.7 Hz, 2H$_{12}$). ^{13}C NMR (126 MHz, DMSO) δ_C 168.3 C$_1$, 164.6 C$_2$, 157.4 C$_3$, 133.3 C$_4$, 132.6 C$_5$, 130.5 C$_6$, 128.5 C$_7$, 123.6 C$_8$, 119.5 C$_9$, 112.6 C$_{10}$, 56.3 C$_{11}$, 55.3 C$_{12}$, 29.8 C$_{13,14}$, 14.5 C$_{15}$.

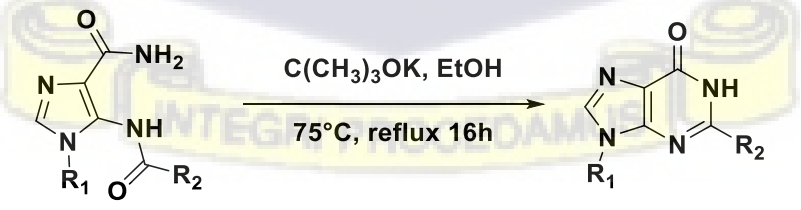
University of Ghana http://ugspace.ug.edu.gh

4.4.13 Synthesis of 5-(2-(4-methoxy phenyl) acetamido)-1-(tetrahydro-2*H*-pyran-4-yl)-1*H*-imidazole-4-carboxamide (ADA147, 18)



This compound was synthesized according to the general procedure for amide formation described above. ADA111 (1.19 mmol, 1 eqv) and (4-methoxy phenyl) acetyl chloride (3.57 mmol, 3 eqv) yielding the intermediate above. The compound was a white amorphous solid and gave (0.34g, 80 %). Melting point = 168-170 ºC. Vmax (neat) cm^{-1} (N-H) 3383.42-3230.87 (=C-H) 3108.12, (C-H) 2957.85-2864.80, (C=O) 1724.67-1662.13, (C=N) 1609.68, (C=C) 1510.59. ^{1}H NMR (400 MHz, Methanol-d_4) δ_H 7.83 (s, 1H_1), 7.44 (d, J = 8.1 Hz, 2$H_{2,3}$), 7.30 (d, J = 8.3 Hz, 2$H_{4,5}$), 4.03 – 3.97 (m, 2H_6), 3.88 (d, J = 2.0 Hz, 2$H_{7a,8a}$), 3.76 (s, 3H_9), 3.60 (d, J = 2.0 Hz, 2$H_{7b,8b}$), 3.26 (d, J = 11.8 Hz, 2H_{10}), 2.04 – 1.96 (m, 2$H_{11a,12a}$), 1.89 (d, J = 14.1 Hz, 2$H_{11b,12b}$). ^{13}C NMR (126 MHz, MeOD) δ_C 159.1 C_1, 158.7 $C_{2,3}$, 132.8 C_4, 130.0 C_5, 129.9 $C_{6,7}$, 127.2 C_8, 113.9 C_9, 113.5 $C_{10,11}$, 66.6 $C_{12,13}$, 54.4 C_{14}, 51.8 C_{15}, 39.8 C_{16}, 33.0 $C_{17,18}$.

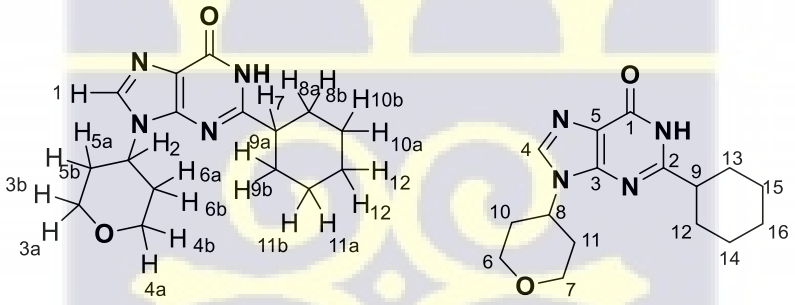
4.5 General Procedure for Cyclization Synthesis.



University of Ghana http://ugspace.ug.edu.gh

A pre-dried, pre-weighed round-bottom flask containing molecular sieves was flashed with nitrogen to ensure an inert atmosphere. The synthesized amide intermediates (1eqv) described above were weighed into the round-bottom flask. A measured volume of ethanol was used to dissolve the intermediate, which was then stirred at room temperature. The base potassium tert-butoxide (4 eqv) was weighed and added to the solution at 75 ºC and the reaction was refluxed for 16 hours to afford the desired product. TLC was used to monitor the reaction until completion. The crude mixture was washed with distilled water and extracted with ethyl acetate (30 mL). The ethyl acetate layer was dried over magnesium sulfate, then evaporated on a rotary evaporator and purified by flash column chromatography to afford the product.

4.5.1 Synthesis of 2-cyclohexyl-9-(tetrahydro-2*H*-pyran-4-yl)-1,9-dihydro-6*H*-purin-6-one (ADA113, 19).

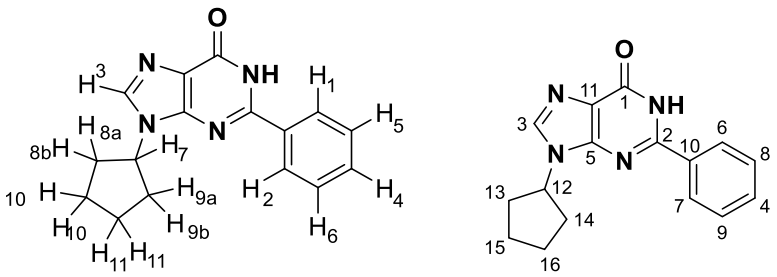


Compound ADA113 above was prepared according to the general procedure for the cyclization reaction using ADA112 (1.25 mmol, 1 eqv) and potassium tert-butoxide (4.99 mmol, 4 eqv) affording the final product as a white amorphous solid (0.16g, 43 %). Melting point = 266-268 ºC. Vmax (neat) cm^{-1} (N-H) 3115.76, (C-H) 2921.47, (C=O) 1674.33 (C=C) 1587.80, (C=N) 1374.12. ^{1}H NMR (400 MHz, Methanol-d_4) δ_H 8.15 (s, 1H$_1$), 4.82 – 4.69 (m, 1H$_2$), 4.19 (dd, J = 12.1, 4.4 Hz, 2H$_{3a,4a}$), 3.71 (t, J = 11.9 Hz, 2H$_{3b,4b}$), 2.75 (td, J = 11.7, 2.9 Hz, 2H$_{5a,6a}$), 2.46 – 2.36 (m, 2H$_{5b,6b}$), 2.16 – 2.10 (m, 1H$_7$), 2.05 (td, J = 12.9 Hz, 2H$_{8a,9a}$), 1.97 (dd, J = 13.2, 3.0 Hz, 2H$_{8b,9b}$),

University of Ghana http://ugspace.ug.edu.gh

1.76 (d, J = 12.5 Hz, 2H$_{10a,11a}$), 1.59 (d, J = 12.7 Hz, 2H$_{10b,11b}$), 1.40 (d, J = 19.2 Hz, 2H$_{12}$). ^{13}C NMR (126 MHz, MeOD) δ_C 163.5 C$_1$, 159.7 C$_2$, 150.5 C$_3$, 139.9 C$_4$, 123.5 C$_5$, 68.1 C$_{6,7}$, 53.8 C$_8$, 44.6 C$_9$, 33.8 C$_{10,11}$, 32.2 C$_{12,13,16}$, 26.8 C$_{14,15}$.

4.5.2 Synthesis of 9-cyclopentyl-2-phenyl-1,9-dihydro-6*H*-purin-6-one (ADA117, 20)

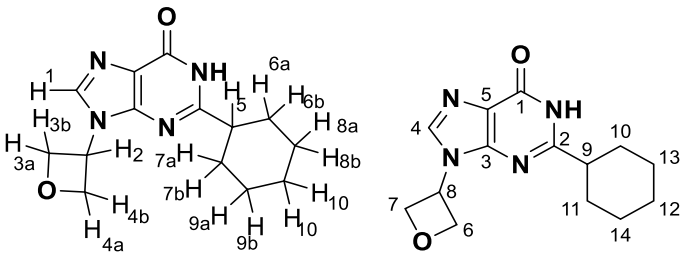


Compound ADA117 above was synthesized according to the general procedure for the cyclization reaction using ADA115 (0.13 mmol, 1 eqv) and potassium tert-butoxide (0.51 mmol, 4 eqv) affording the final product as a white amorphous solid (0.01g, 28 %). Melting point = 205-207 ºC. Vmax (neat) cm^{-1} (N-H) 3310.74, (=C-H) 3115.65, (C-H) 2965.37-2872.43, (C=O) 1665.64, (C=N) 1580.36, (C=C) 1508.58-1465.29. ^{1}H NMR (400 MHz, Methanol-d_4) δ_H 8.09 (d, J = 7.8 Hz, 2H$_{1,2}$), 8.03 (s, 1H$_3$), 7.75 (d, J = 7.8 Hz, 1H$_4$), 7.65 (t, J = 7.7 Hz, 2H$_{5,6}$), 4.66 – 4.40 (m, 1H$_7$), 2.29 (dd, J = 12.5, 4.8 Hz, 2H$_{8a,9a}$), 2.04 - 1.88 (m, 4H$_{10.11}$), 1.83 (d, J = 11.4 Hz, 2H$_{8b,9b}$). ^{13}C NMR (126 MHz, MeOD) δ_C 169.8 C$_1$, 137.0 C$_2$, 136.1 C$_3$, 134.1 C$_4$, 133.6 C$_5$, 130.0 C$_{6,7}$, 129.0 C$_{8,9}$, 114.7 C$_{10}$, 110.4 C$_{11}$, 58.6 C$_{12}$, 34.1 C$_{13,14}$, 24.8 C$_{15,16}$.

INTEGRI PROCEDAMUS

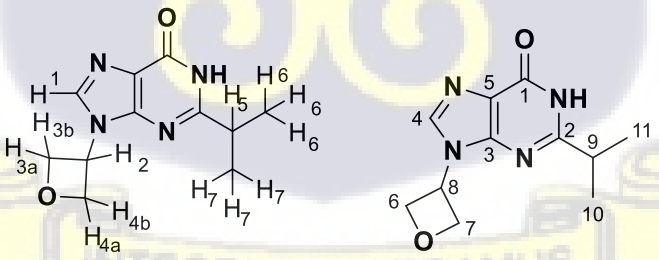
University of Ghana http://ugspace.ug.edu.gh

4.5.3 Synthesis of 2-cyclohexyl-9-(oxetan-3-yl)-1,9-dihydro-6*H*-purin-6-one (ADA118, 21)



Compound ADA118 above was prepared according to the general procedure for the cyclization reaction described using ADA116 (0.15 mmol, 1 eqv) and potassium tert-butoxide (0.60 mmol, 4 eqv) affording the final product as a white amorphous solid (0.02g, 43 %). Melting point = 243-245 ºC. Vmax (neat) cm^{-1} (N-H) 3310.74, (=C-H) 3110.66, (C-H) 2929.17-2854.12, (C=O) 1703.30, (C=N) 1578.94, (C=C) 1557.29. ^{1}H NMR (400 MHz, Methanol-d_4) δ_H 8.30 (s, 1H$_1$), 5.93 – 5.77 (m, 1H$_2$), 5.30 (t, J = 7.2 Hz, 2H$_{3a,4a}$), 5.18 (t, J = 7.1 Hz, 2H$_{3b,4b}$), 2.88 – 2.63 (m, 1H$_5$), 2.05 (d, J = 13.2 Hz, 2H$_{6a,7a}$), 1.97 (d, J = 12.2 Hz, 2H$_{6b,7b}$), 1.80 – 1.71 (m, 2H$_{8a,9a}$), 1.61 – 1.46 (m, 2H$_{8b,9b}$), 1.41 (dd, J = 21.3, 9.4 Hz, 2H$_{10}$). ^{13}C NMR (126 MHz, MeOD) δ_C 166.8 C$_1$, 163.1 C$_2$, 154.4 C$_3$, 134.1 C$_4$, 115.1 C$_5$, 78.5 C$_{6,7}$, 51.1 C$_8$, 46.0 C$_9$, 30.4 C$_{10,11}$, 26.9 C$_{12}$, 26.7 C$_{13,14}$.

4.5.4 Synthesis of 2-isopropyl-9-(oxetan-3-yl)-1,9-dihydro-6H-purin-6-one (ADA123, 22)

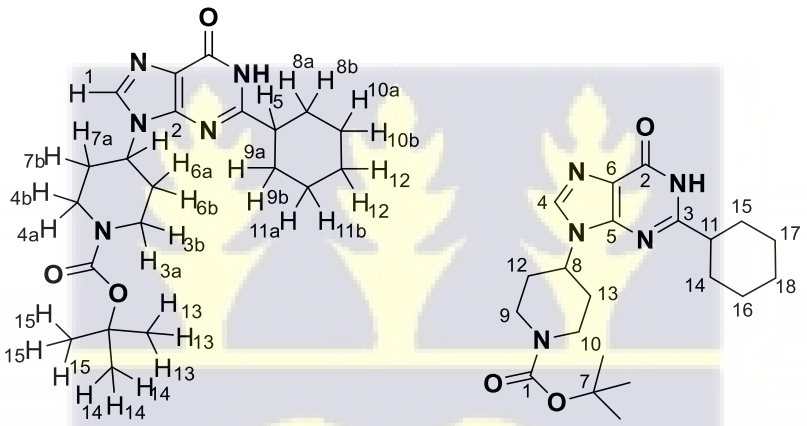


Compound ADA123 above was synthesized according to the general procedure for the cyclization reaction using ADA120 (0.28 mmol, 1 eqv) and potassium tert-butoxide (1.12 mmol, 4 eqv) affording the final product as a white amorphous solid (0.02g, 30 %). Melting point = 254-256 ºC.

University of Ghana http://ugspace.ug.edu.gh

Vmax (neat) cm^{-1} (N-H) 3110.84, (C-H) 2986.98, (C=O) 1656.01 (C=C) 1596.91, (C=N) 1327.64. ^{1}H NMR (400 MHz, Methanol-d_4) δ_H 8.31 (s, $1H_1$), 5.95 – 5.74 (m, $1H_2$), 5.29 (t, J = 6.7 Hz, $2H_{3a,4a}$), 5.18 (t, J = 7.4 Hz, $2H_{3b,4b}$), 3.13 – 3.02 (m, $1H_5$), 1.43 (d, J = 6.9, 1.9 Hz, $6H_{6,7}$). ^{13}C NMR (101 MHz, MeOD) δ_C 165.1 C_1, 160.0 C_2, 151.3 C_3, 140.6 C_4, 114.2 C_5, 78.6 $C_{6,7}$, 51.0 C_8, 35.3 C_9, 21.4 $C_{10,11}$.

4.5.5 Synthesis of *tert*-butyl 4-(2-cyclohexyl-6-oxo-1,6-dihydro-9*H*-purin-9-yl) piperidine-1-carboxylate (ADA129, 23)

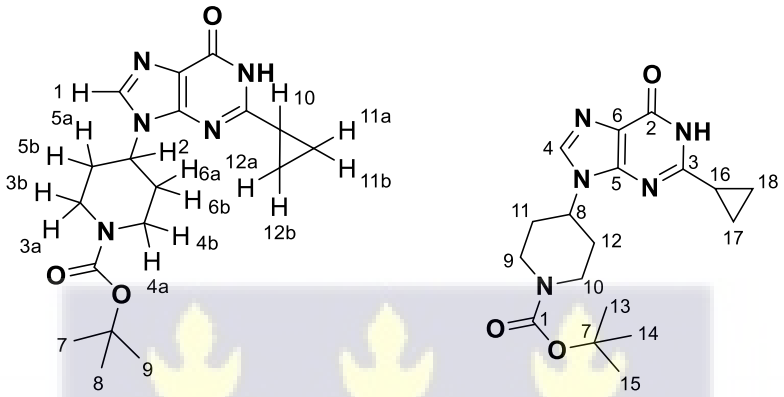


The titled compound above was synthesized according to the general procedure for the cyclization reaction described above. ADA128 (0.92 mmol, 1 eqv) and potassium tert-butoxide (3.67 mmol, 4 eqv) affording the final product above. The compound was a white amorphous solid and gave (0.10g, 27 %) Melting point = 212-218 ºC. Vmax (neat) cm^{-1} (N-H) 3562.06-3506.82, (=C-H) 3080.29, (C-H) 2931.26-2856.22, (C=O) 1660.69-1637.04, (C=N) 1595.71, (C=C) 1467.02. ^{1}H NMR (400 MHz, Methanol-d_4) δ_H 8.12 (s, $1H_1$), 4.70 (t, J = 12.3 Hz, $1H_2$), 4.36 (d, J = 13.7 Hz, $2H_{3a,4a}$), 3.06 (t, J = 13.7 Hz, $2H_{3b,4b}$), 2.82 – 2.69 (m, $1H_5$), 2.29 (tt, J = 12.9, 7.2 Hz, $2H_{6a,7a}$), 2.14 (d, J = 12.5 Hz, $2H_{6b,7b}$), 2.05 (d, J = 13.1 Hz, $2H_{8a,9a}$), 1.99 – 1.92 (m, $2H_{8b,9b}$), 1.80 – 1.68 (m, $2H_{10a,11a}$), 1.59 (d, J = 2.0 Hz, $9H_{13,14,15}$), 1.56 – 1.48 (m, $2H_{10b,11b}$), 1.48 – 1.35 (m, $2H_{12}$). ^{13}C

University of Ghana http://ugspace.ug.edu.gh

NMR (126 MHz, MeOD) δ_C 162.9 C_1, 155.9 C_2, 150.0 C_3, 139.7 C_4, 127.5 C_5, 123.0 C_6, 81.0 C_7, 54.6 C_8, 44.0 $C_{9,10}$, 32.1 C_{11}, 31.7 $C_{12,13}$, 28.2 $C_{14,15}$, 26.4 $C_{16,17}$, 26.3 C_{18}.

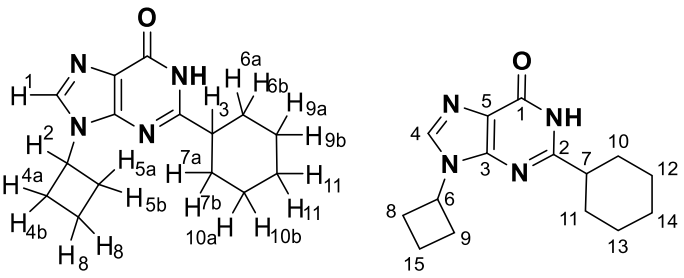
4.5.6 Synthesis of *tert*-butyl 4-(2-cyclopropyl-6-oxo-1,6-dihydro-9*H*-purin-9-yl) piperidine-1-carboxylate (ADA132, 24)



The titled compound above was synthesized according to the general procedure for the cyclization reaction described above. ADA131 (0.66 mmol, 1 eqv) and potassium tert-butoxide (2.65 mmol, 4 eqv) affording the final product above. The compound was a white amorphous solid and gave (0.17g, 70 %) Melting point = 140-142 ºC. Vmax (neat) cm^{-1} (N-H) 3464.61-3227.85, (C-H) 2970.57-2862.58, (C=O) 1676.17, (C=N) 1593.98, (C=C) 1421.25. ^{1}H NMR (400 MHz, Methanol-d_4) δ_H 7.9 (s, 1H_1), 4.6 (td, J = 12.5, 6.0 Hz, 1H_2), 4.3 (d, J = 14.1 Hz, 2$H_{3a,4a}$), 3.0 (d, J = 14.0 Hz, 2$H_{3b,4b}$), 2.1 (d, J = 12.5, 2$H_{5a,6a}$), 1.9 (dd, J = 12.5, 4.3 Hz, 2$H_{5b,6b}$), 1.6 (s, 9$H_{7,8,9}$), 1.28 – 1.23 (m, 1H_{10}), 1.1 (dd, J = 5.3, 2.8 Hz, 2$H_{11a,12a}$), 1.0 (t, J = 1.1 Hz, 2$H_{11b,12b}$). ^{13}C NMR (126 MHz, Methanol-d_4) δ_C 166.3 C_1, 161.2 C_2, 155.8 C_3, 139.2 C_4, 133.7 C_5, 129.5 C_6, 80.9 C_7, 54.1 C_8, 33.1 $C_{9,10}$, 28.1 $C_{11,12}$, 23.2 $C_{13\text{-}15}$, 15.5 C_{16}, 10.0 $C_{17,18}$.

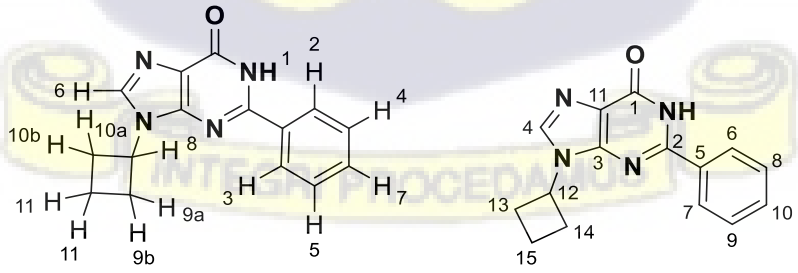
University of Ghana http://ugspace.ug.edu.gh

4.5.7 Synthesis of 9-cyclobutyl-2-cyclohexyl-1,9-dihydro-6*H*-purin-6-one (ADA136, 25)



The titled compound above was synthesized according to the general procedure for the cyclization reaction using ADA135 (1.03 mmol, 1 eqv) and potassium tert-butoxide (4.13 mmol, 4 eqv) affording the final product as a white amorphous solid (0.18g, 65 %). Melting point = 253-255 ºC. Vmax (neat) cm^{-1} (=C-H) 3082.74, (C-H) 2998.25-2851.77, (C=O) 1697.02, (C=N) 1589.89, (C=C) 1547.25-1518.27. ^{1}H NMR (400 MHz, Methanol-*d*$_4$) δ_H 8.18 (s, 1H$_1$), 5.20-5.05 (m, 1H$_2$), 2.81 (t, *J* = 10.2 Hz, 1H$_3$), 2.76 (d, *J* = 11.2 Hz, 2H$_{4a,5a}$), 2.66 (d, *J* = 9.1 Hz, 2H$_8$), 2.09 (d, *J* = 11.5 Hz, 2H$_{4b,5b}$), 1.97 (d, *J* = 12.3 Hz, 2H$_{6a,7a}$), 1.85 (d, *J* = 12.0 Hz, 2H$_{6b,7b}$), 1.81 – 1.70 (m, 2H$_{9a,10a}$), 1.59 – 1.49 (m, 2H$_{9b,10b}$), 1.44 (dd, *J* = 21.7, 9.0 Hz, 2H$_{11}$). ^{13}C NMR (126 MHz, MeOD) δ_H 163.4 C$_1$, 159.8 C$_2$, 150.8 C$_3$, 140.3 C$_4$, 123.3 C$_5$, 50.5 C$_6$, 49.5 C$_7$, 44.5 C$_{8,9}$, 32.2 C$_{10,11}$, 31.3 C$_{12,13}$, 27.0 C$_{14}$, 16.0 C$_{15}$.

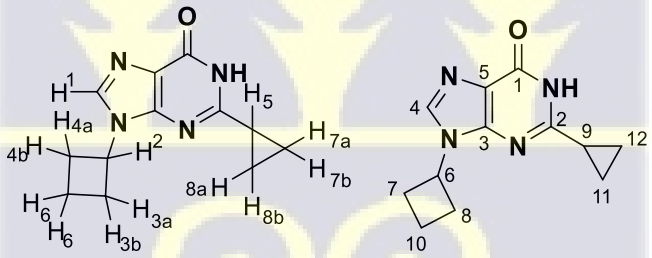
4.5.8 Synthesis of 9-cyclobutyl-2-phenyl-1,9-dihydro-6*H*-purin-6-one (ADA138, 26)



University of Ghana http://ugspace.ug.edu.gh

Compound ADA138 above was synthesized according to the general procedure for the cyclization reaction using ADA137 (1.02 mmol, 1 eqv) and potassium tert-butoxide (4.06 mmol, 4 eqv) affording the final product as a white amorphous solid (0.15g, 54 %). Melting point = 205-207 ºC. Vmax (neat) cm^{-1} (N-H) 3495.71-3379.61, (=C-H) 3124.12, (C-H) 2985.84-2871.46, (C=O) 1680.21, (C=N) 1594.20, (C=C) 1551.33-1518.61. ^{1}H NMR (400 MHz, Methanol-d_4) δ_H 8.27 (s, $1H_1$), 8.17 (d, J = 7.6, 2.0 Hz, $2H_{2,3}$), 8.09 (t, J = 7.7 Hz, $3H_{4,5}$), 7.94 (s, $1H_6$), 7.74 (s, $1H_7$), 4.77 – 4.66 (m, $1H_8$), 2.91 – 2.79 (m, $2H_{9a,10a}$), 2.77 – 2.65 (m, $2H_{9b,10b}$), 2.10 (td, J = 10.7, 4.8 Hz, $2H_{11}$). ^{13}C NMR (126 MHz, MeOD) δ_C 159.7 C_1, 155.1 C_2, 150.6 C_3, 140.9 C_4, 134.5 C_5, 133.6 $C_{6,7}$, 132.6 $C_{8,9}$, 130.0 C_{10}, 129.8 C_{11}, 50.9 C_{12}, 31.5 $C_{13,14}$, 16.1 C_{14}.

4.5.9 Synthesis of 9-cyclobutyl-2-cyclopropyl-1,9-dihydro-6*H*-purin-6-one (ADA141, 27)

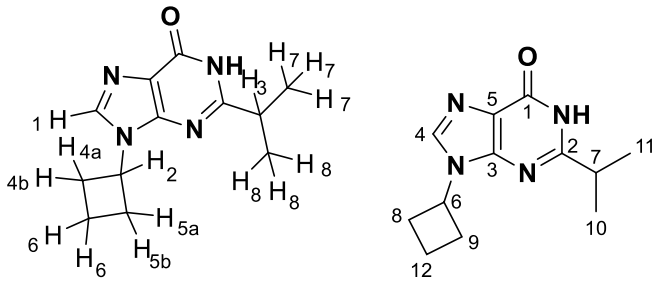


The titled compound above was synthesized according to the general procedure for the cyclization reaction using ADA140 (0.52 mmol, 1 eqv) and potassium tert-butoxide (2.09 mmol, 4 eqv) affording the final product as a white amorphous solid and gave (0.01g, 8 % yield). Melting point = 183-185 ºC. Vmax (neat) cm^{-1} (N-H) 3118.84, (C-H) 2985.07, (C=O) 1736.20 (C=C) 1660.83, (C=N) 1408.96. ^{1}H NMR (500 MHz, Methanol-d_4) δ_H 8.08 (s, $1H_1$), 5.02 - 4.93 (m, $1H_2$), 2.68 (dd, J = 9.8, 3.1 Hz, $2H_{3a,4a}$), 2.56 (d, J = 3.1 Hz, $2H_{3b,4b}$), 2.48 – 2.38 (m, $1H_5$), 2.01 (dd, J = 18.3, 8.7 Hz, $2H_6$), 1.21 (t, J = 3.9 Hz, $2H_{7a,8a}$), 1.13 (dd, J = 7.7, 4.0 Hz, $2H_{7b,8b}$). ^{13}C NMR (126 MHz,

University of Ghana http://ugspace.ug.edu.gh

MeOD) δ_C 160.3 C_1, 158.2 C_2, 149.6 C_3, 138.5 C_4, 132.9 C_5, 49.0 C_6, 29.8 $C_{7,8}$, 14.6 C_9, 13.0 C_{10}, 9.1 $C_{11,12}$.

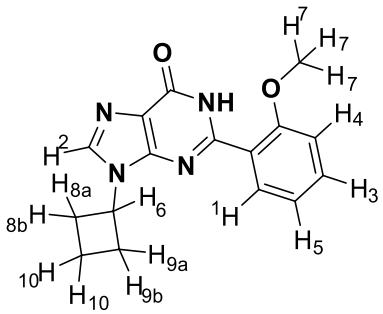
4.5.10 Synthesis of 9-cyclobutyl-2-isopropyl-1,9-dihydro-6*H*-purin-6-one (ADA143, 28)

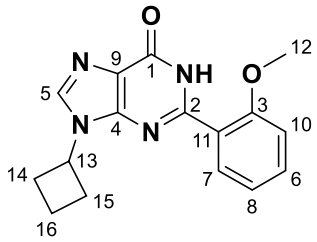


The titled compound above was synthesized according to the general procedure for the cyclization reaction using ADA142 (0.74 mmol, 1 eqv) and potassium tert-butoxide (2.94 mmol, 4 eqv) affording the final product as a white amorphous solid (0.06 g, 35 %). Melting point = 159.161 ºC. Vmax (neat) cm^{-1} (=C-H) 3090.47, (C-H) 2974.58-2869.24, (C=O) 1660.34, (C=N) 1586.86, (C=C) 1522.35. ^{1}H NMR (400 MHz, Methanol-d_4) δ_H 8.18 (d, J = 1.6 Hz, 1H_1), 5.12 (p, J = 8.6 Hz, 1H_2), 3.06 (h, J = 7.8 Hz, 1H_3), 2.80 (dddd, J = 19.5, 11.8, 7.0, 2.2 Hz, 2$H_{4a,5a}$), 2.64 (ddd, J = 19.0, 11.8, 5.0 Hz, 2$H_{4b,5b}$), 2.05 (td, J = 5.0, 2.2 Hz, 2H_6), 1.43 (s, 3H_7), 1.41 (s, 3H_8). ^{13}C NMR (126 MHz, MeOD) δ_C 164.24 C_1, 159.76 C_2, 150.74 C_3, 140.28 C_4, 123.33 C_5, 50.46 C_6, 34.89 C_7, 31.27 $C_{8,9}$, 21.15 $C_{10,11}$, 15.95 C_{12}.

University of Ghana http://ugspace.ug.edu.gh

4.5.11 Synthesis of 9-cyclobutyl-2-(2-methoxyphenyl)-1,9-dihydro-6*H*-purin-6-one (ADA145, 29)



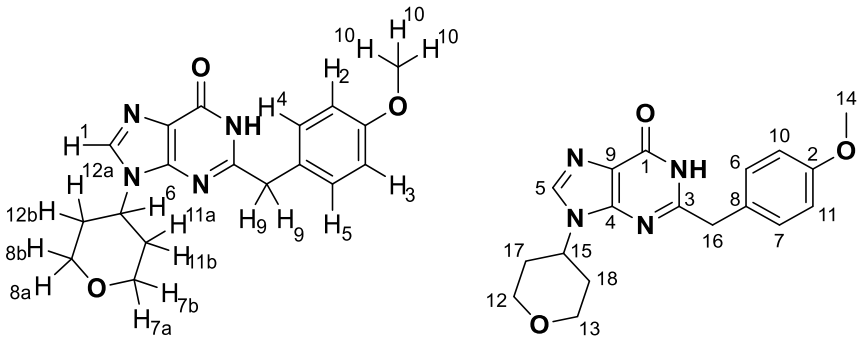


The titled compound above was synthesized according to the general procedure for the cyclization reaction using ADA144 (0.89 mmol, 1 eqv) and potassium tert-butoxide (3.58 mmol, 4 eqv) affording the final product as a white amorphous solid and gave (0.12g, 44 %). Melting point = 143-145 ºC. Vmax (neat) cm^{-1} (N-H) 3406.67-3186.74(=C-H) 3119.17, (C-H) 2924.38-2853.73, (C=O) 1667.93, (C=N) 1592.73, (C=C) 1479.27. ^{1}H NMR (400 MHz, Methanol-d_4) δ_H 8.13 (d, J = 7.8 Hz, 1H$_1$), 7.91 (s, 1H$_2$), 7.68 (t, J = 7.8 Hz, 1H$_3$), 7.31 (d, J = 8.4 Hz, 1H$_4$), 7.20 (t, J = 7.6 Hz, 1H$_5$), 4.82 - 4.71 (m, 1H$_6$), 4.19 – 4.08 (m, 3H$_7$), 2.57 (d, J = 8.7 Hz, 2H$_{8a,9a}$), 2.54 – 2.48 (m, 2H$_{8b,9b}$), 2.01 – 1.95 (m, 2H$_{10}$). ^{13}C NMR (126 MHz, MeOD) δ_C 166.1 C$_1$, 158.3 C$_{2,3}$, 134.0 C$_4$, 133.0 C$_5$, 131.3 C$_6$, 129.7 C$_7$, 124.9 C$_8$, 120.7 C$_9$, 120.3 C$_{10}$, 111.9 C$_{11}$, 55.4 C$_{12}$, 50.1 C$_{13}$, 30.1 C$_{14,15}$, 14.7 C$_{16}$.

INTEGRI PROCEDAMUS

University of Ghana http://ugspace.ug.edu.gh

4.5.12 Synthesis of 2-(4-methoxybenzyl)-9-(tetrahydro-2*H*-pyran-4-yl)-1,9-dihydro-6H-purin-6-one (ADA148, 30)



The titled compound above was synthesized according to the general procedure for the cyclization reaction described above. ADA147 (0.95 mmol, 1 eqv) and potassium tert-butoxide (3.79 mmol, 4 eqv) affording the final product above. The compound was a white amorphous solid and gave (0.13g, 41 %). Melting point = 277-279 ºC. Vmax (neat) cm^{-1} (=C-H) 3107.98, (C-H) 2956.01-2836.07, (C=O) 1671.63, (C=N) 1609.40, (C=C) 1509.35. ^{1}H NMR (400 MHz, Methanol-d_4) δ_H 8.16 (s, $1H_1$), 7.35 (d, J = 8.1 Hz, $2H_{2,3}$), 6.96 (d, J = 8.2 Hz, $2H4,_5$), 4.81 – 4.71 (m, $1H_6$), 4.22 – 4.14 (m, $2H_{7a,8a}$), 4.06 (s, $2H_9$), 3.85 (s, $3H_{10}$), 3.69 (t, J = 11.9 Hz, $2H_{7b,8b}$), 2.47 – 2.26 (m, $2H_{11a,12a}$), 2.24 – 2.01 (m, $2H_{11b,12b}$). ^{13}C NMR (126 MHz, DMSO) δ 157.9 C_1, 157.0 C_2, 156.4 C_3, 148.0 C_4, 138.0 C_5, 129.4 $C_{6,7}$, 128.2 C_8, 122.0 C_9, 113.6 $C_{10,12}$, 65.8 $C_{12,13}$, 54.7 C_{14}, 50.9 $C_{15,16}$, 32.0 $C_{17,18}$.

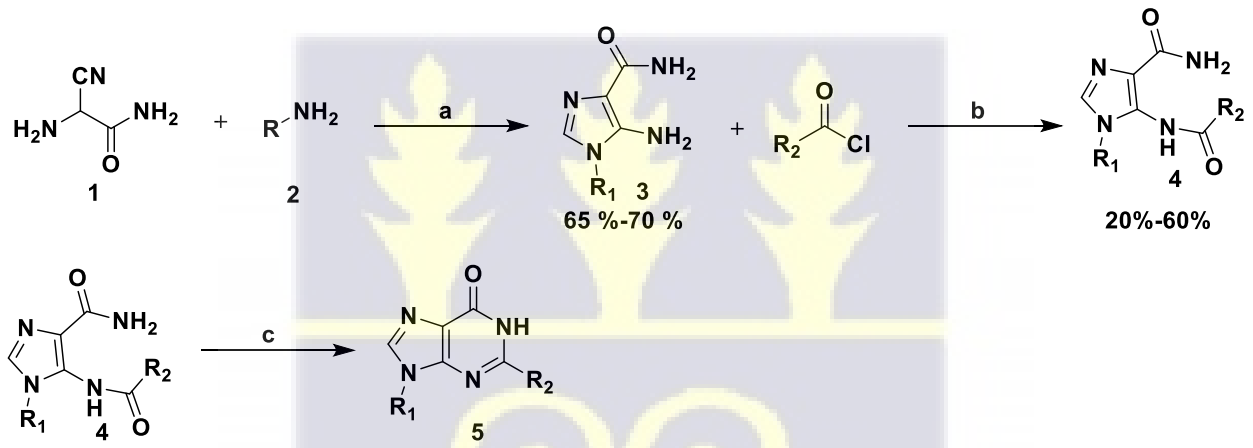
4.6 RESULTS AND DISCUSSION

4.7 Chemistry

The titled compounds were synthesized in three or four chemical steps in low-high yields (15%-80%). The first step involved the reaction of commercially available 2-amino-2-cyanoacetamide, with 1.5 equivalents of triethyl orthoformate using acetonitrile (MeCN) as the solvent. The mixture

University of Ghana http://ugspace.ug.edu.gh

was refluxed at 90 °C for 40 minutes then allowed to cooled to room temperature. In the same reaction vessel, different amines were added to the reaction mixture which was also refluxed at 95 °C for 40 minutes to afford the imidazole intermediates. In the second step, the imidazole intermediate was reacted with selected acid chlorides in a pre-dried round-bottom flask with molecular sieves. Using pyridine as the solvent, the reaction was refluxed at 70 °C for 8 hours in an inert atmosphere to afford the amide intermediate. In the third step, the amide intermediates were dissolved in ethanol and potassium *tert*-butoxide as the base. The mixture was refluxed at 75 °C for 16 hours to afford the desired oxo-purine products215 as shown in **Scheme 4.1**.



Scheme 4. 1: Reaction scheme for synthesized analogues. a) 1. $HC(OC_2H_5)_3$, reflux 90°C, 40 mins, MeCN, 2. Amine reflux, 95 °C, 40 mins, MeCN, b) Pyridine, K_3PO_4, reflux 70 °C, 8h. c) $C(CH_3)_3OK$, EtOH, 75°C, reflux 16h.

4.7.1 Reaction Mechanism for Synthesized Analogues of MMV1900279

The mechanism for the imidazole formation in the first step is shown in **Figure 4.2** below. It involves the reaction between the triethyl orthoformate and the 2-amino-2-cyanoacetamide. One of the ethoxy groups of the triethyl orthoformate is protonated by abstracting the acidic proton from the carbon that bears both the amino and cyano groups. This creates a carbanion on the 2-

University of Ghana http://ugspace.ug.edu.gh

amino-2-cyanoacetamide. On the other hand, a diethoxy methane cation intermediate is formed by eliminating one ethoxy groups as ethanol. Resonance delocalization of electrons leads to the formation of a more nucleophilic intermediate by generating the negative charge on the amino groups, which then attacks the electron-deficient center of the diethoxy methane cation intermediate to introduce a carbon to the acetamide intermediate. Subsequent intramolecular deprotonation leads to the elimination of another ethoxy group as ethanol to form the ethyl (*Z*)-*N*-(2-amino-1-cyano-2-oxoethyl) formimidate intermediate. When the selected primary amine is added to the reaction, it is deprotonated to generate a strong nucleophile which then attacks the formimidate intermediate, and the cyano group further deprotonates the amino group to facilitate the cyclisation. To aromatize the ring, the imine picks a proton from the carbon bearing the amide group to form the imidazole intermediate.

University of Ghana http://ugspace.ug.edu.gh

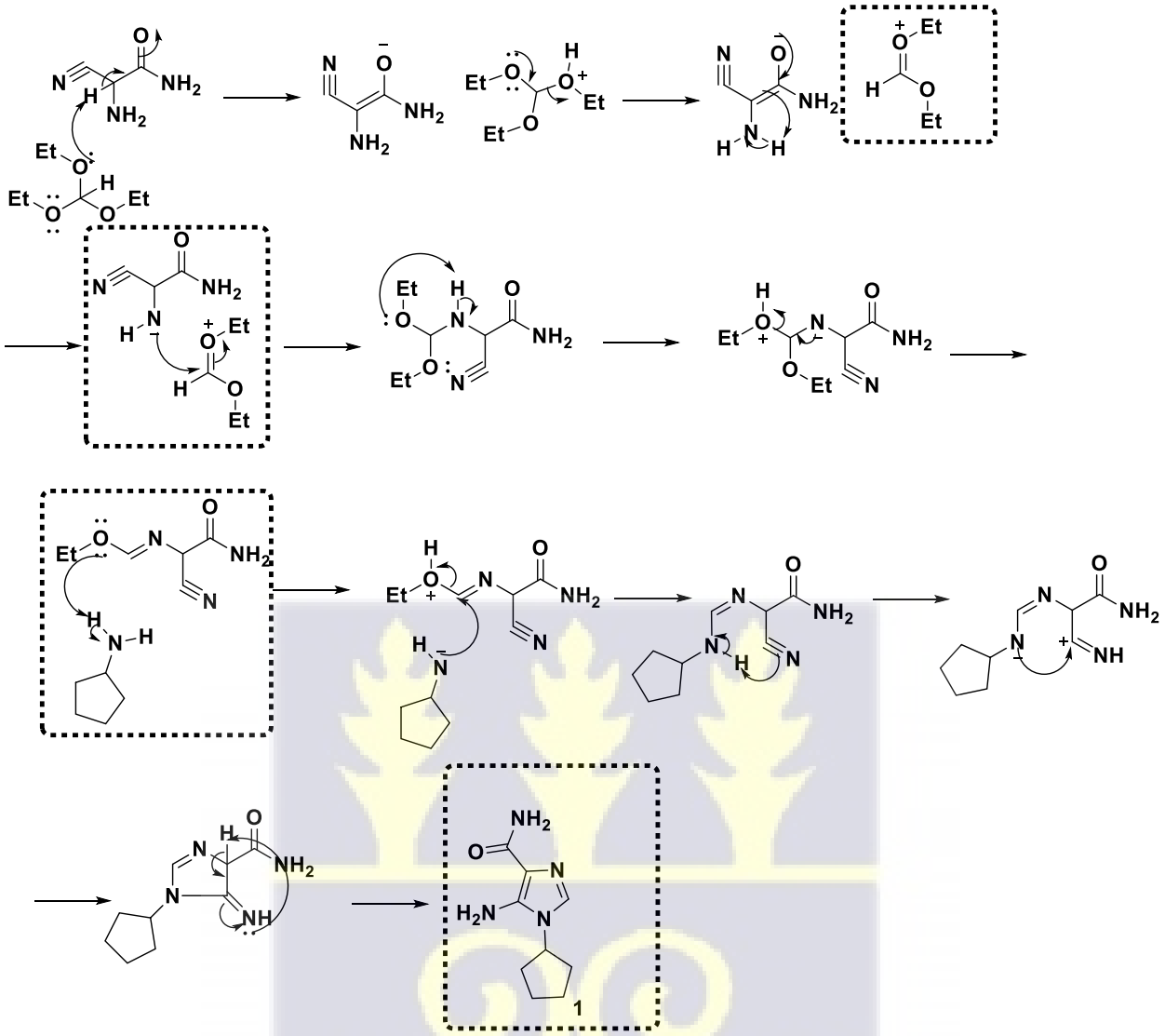


Figure 4.2: Mechanism for imidazole formation.

The mechanism for the second step is shown in **Figure 4.3** below. The second step is an amide coupling reaction, involving the reaction between the amino group on the imidazole intermediate and an acid chloride. In this reaction, the lone pair on the amino group attacks the electron-deficient carbon of the acid chloride leading to the elimination of the chloride group and the formation of a cation on the amino group. The chloride anion then deprotonates the ammonium ion forming HCl *in situ*. The base introduced in the reaction neutralizes the HCl formed in the response.

University of Ghana http://ugspace.ug.edu.gh

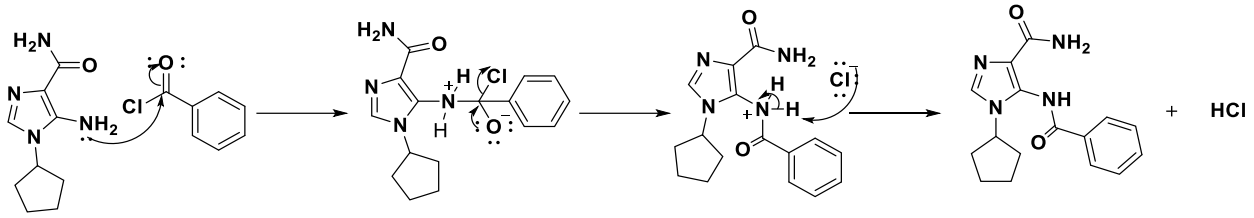


Figure 4.3: Mechanism for amide coupling.

The mechanism for the final step to obtain the desired analogues is also shown in **Figure 4.4** below. This involves the reaction of the amide intermediate with a base, heated to facilitate the formation of a pyrimidine ring. Potassium tert-butoxide, a strong base, deprotonates the primary amide to generate a strong nucleophile. The nucleophile attacks the carbonyl carbon of the second amide, leading to a ring closure. The oxygen is then protonated to form water, a good leaving group, and the formation of the cyclic imine results in the loss of water leading to the formation of the oxo-purine product.

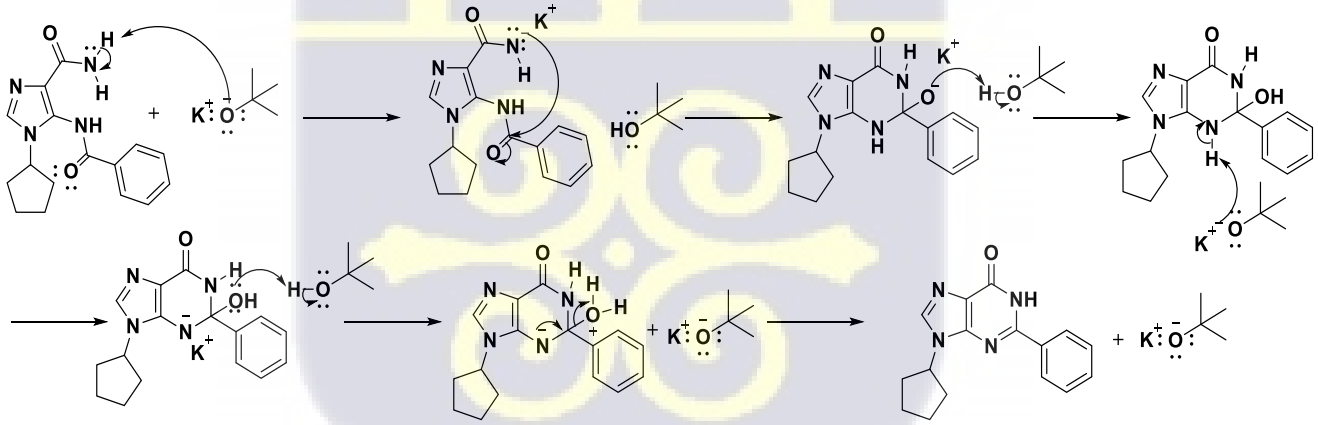


Figure 4.4: Mechanism of the cyclization reaction.

A total of 13 compounds were successfully synthesized as shown in **Table 4.1** below and characterized using spectroscopic and spectrometric methods, including ^{1}H and ^{13}C NMR, FT-IR and LC-MS. The NMR data was used to determine the carbon-hydrogen connectivity of the

University of Ghana http://ugspace.ug.edu.gh

compound to ensure the correct compounds were synthesized, the FT-IR was used to confirm the presence of functional groups in the synthesized analogues, and the LC-MS data was used to verify the purity and determine the mass of the synthesized analogues.

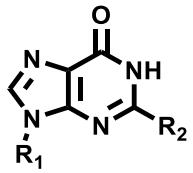
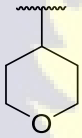
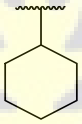
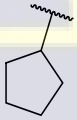
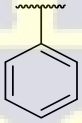
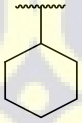
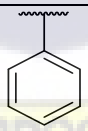
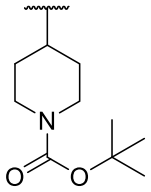
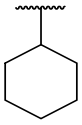
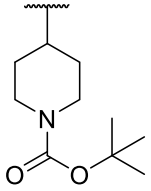
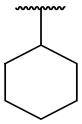
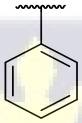
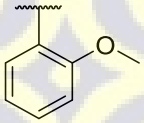
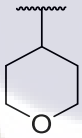
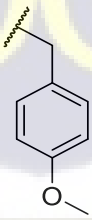


Table 4.1: Structures of synthesized Analogues of MMV1900279.

Sample Code	R1	R2	% Yield	Molecular weight
ADA113			43	302.38
ADA117			28	280.33
ADA118			43	274.32
ADA123			30	234.26
ADA125			22	268.28

University of Ghana http://ugspace.ug.edu.gh

ADA129			95	401.51
ADA132			70	359.43
ADA136			65	272.35
ADA138			54	266.30
ADA141			8	230.12
ADA143			35	232.29
ADA145			44	296.33
ADA148			41	340.38

INTEGRI PROCEDAMUS

University of Ghana http://ugspace.ug.edu.gh

4.8 Spectral Analysis of Synthesized Analogues of MMV1900279

The synthesized analogues were characterized using spectroscopic and spectrometric analysis. 1D NMR analysis was used to determine the carbon-hydrogen connectivity of the synthesized analogues, FTIR spectroscopy was used to confirm the functional groups present and LC-MS-MS was used to verify the mass of the synthesized analogues. These spectroscopic and spectrometric analyses were instrumental in establishing the synthesized analogues.

4.8.1 Proton NMR Analysis of ADA110

The proton NMR for the imidazole intermediate ADA110 comprising 7 chemically distinct proton peaks was measured in DMSO and is shown in **Figure 4.5 below**. The singlet proton labeled H1 at 7.20 ppm corresponds to the proton on the imidazole ring while the singlets labeled H2a and H2b at 6.72 and 6.58 ppm respectively correspond to the protons of the amide. The singlet labeled H3 at 5.75 ppm corresponds to the protons of the amine on the imidazole ring. The multiplet peak at 4.34 ppm corresponds to the proton H4 coupling with H5a,b and H6a,b. while the multiplet between 2.11-2.03 ppm corresponds to protons H5a and H6a which couples with protons H4, H5b and H6b, the multiplet between 1.82-1.69 ppm corresponds to protons labeled H5b and H6b which also couples with H4, H5a andH6a. Finally, the multiplet between 1.68 and 1.61 ppm corresponds to the protons H7 and H8 coupling with protons H5a,b and H6a,b.

INTEGRI PROCEDAMUS

University of Ghana http://ugspace.ug.edu.gh

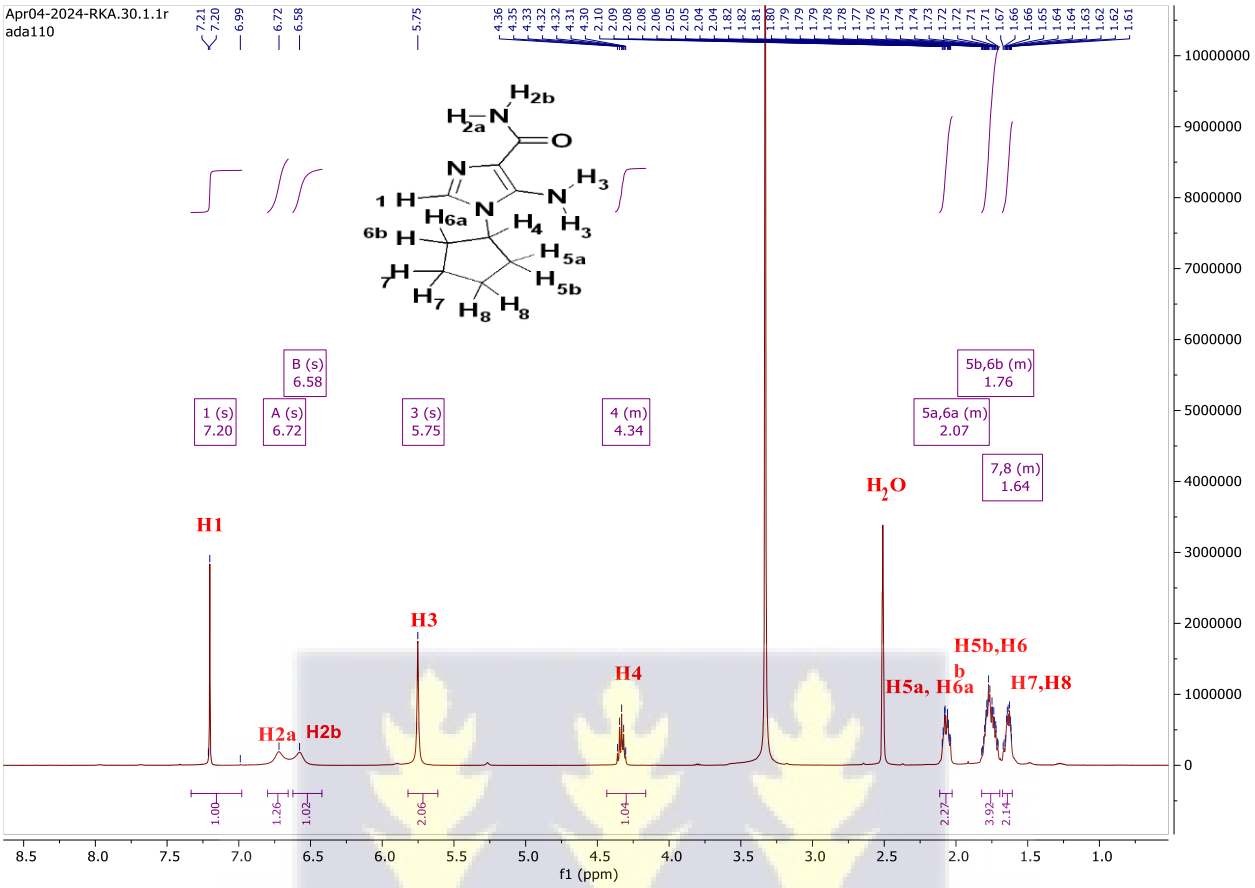


Figure 4.5: Proton NMR data of ADA110

4.8.2 Carbon (^{13}C) NMR Analysis of ADA110

The ^{13}C NMR spectrum for imidazole intermediate ADA110 comprising 7 chemically distinct carbon peaks is shown in **Figure 4.6** below. The peak at 166.3 ppm corresponds to the carbonyl carbon C1. The peaks at 142.4 ppm, 126.5 ppm and 112.2 ppm correspond to the carbons labeled C2, C3 and C4 respectively on the imidazole ring. In comparison, the peaks at 53.6 ppm,31.4 ppm and 22.7 ppm correspond to the carbons labeled C5, C6 and C7 and C8 and C9 respectively on the cyclopentyl ring.

University of Ghana http://ugspace.ug.edu.gh

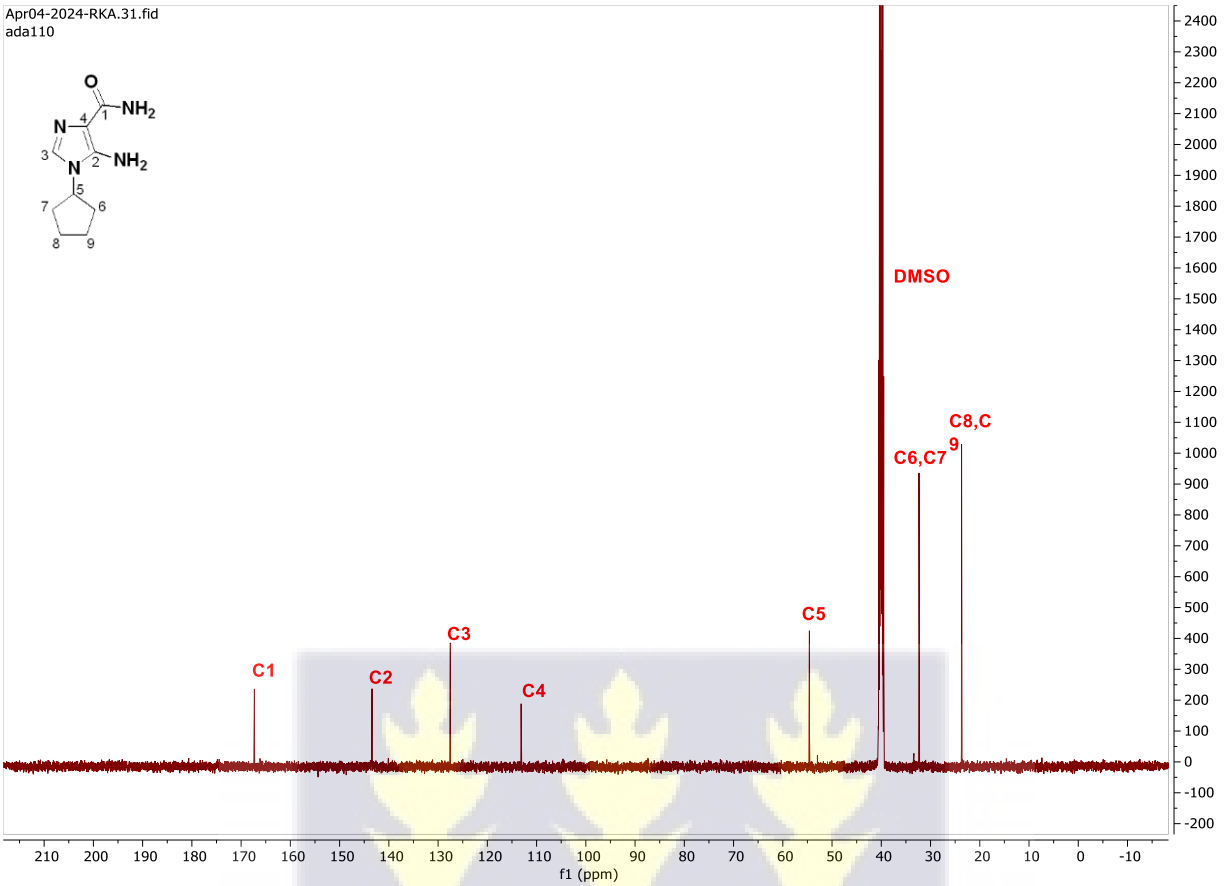
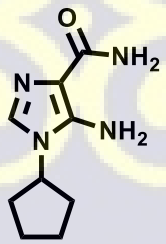


Figure 4.6: Carbon NMR spectrum of ADA110.

4.8.3 FTIR Data for ADA110



The FTIR chromatogram for ADA110 is shown in **Figure 4.6**. The broad and sharp peak between 3381.88-3322.43 cm^{-1} is characteristic of an N-H stretch. In contrast the peak at 3189.12 cm^{-1} is characteristic of an aromatic C-H stretching vibration, the remaining peaks at 2972 cm^{-1}, 1657.53

University of Ghana http://ugspace.ug.edu.gh

cm^{-1}, 1611.19 cm^{-1} and 1555.55 cm^{-1} correspond to sp^3 C-H stretch, C=O stretch at, C=N stretch and aromatic C=C stretch respectively.

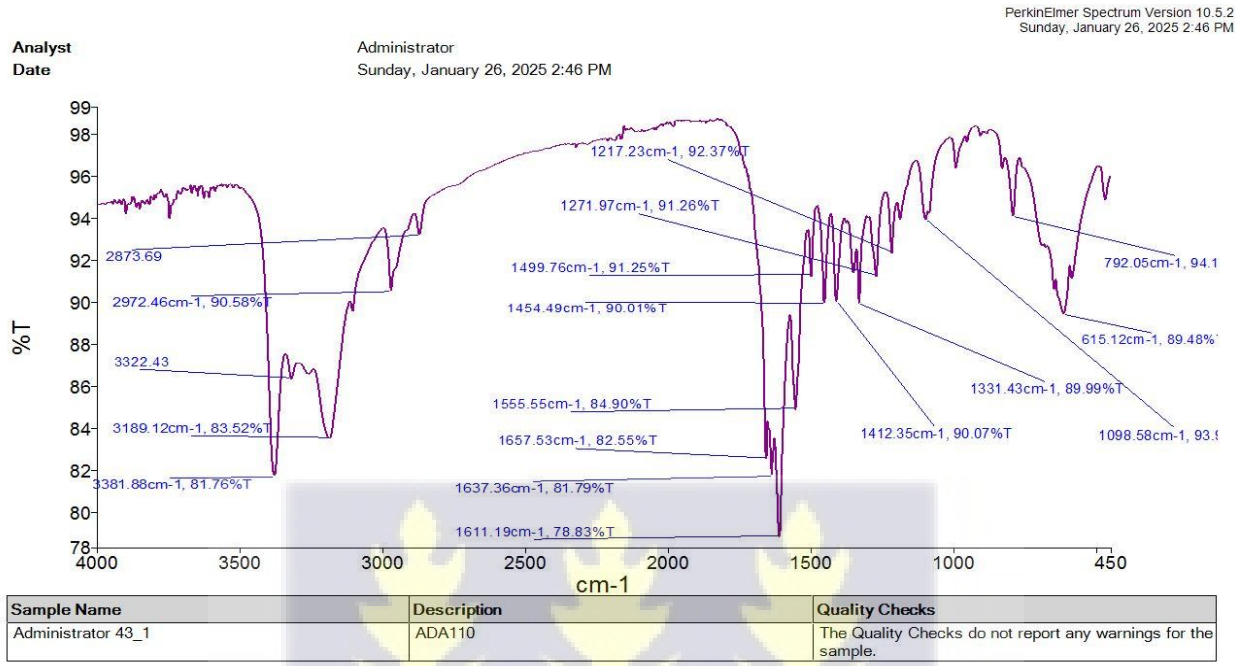


Figure 4.7: FTIR spectrum of ADA110.

4.8.4 Proton NMR Analysis of ADA115

The proton NMR for the intermediate ADA115 comprising 8 chemically distinct proton peaks was measured in MeOD and is shown in **Figure 4.8** below. The doublet at 8.09 ppm with coupling constant (J = 7.7Hz) corresponds to the protons labeled H1 and H2 which couples with H5 and H6 respectively. In comparison the singlet at 8.03 ppm corresponds to the proton labeled H3 on the imidazole ring, and the triplet at 7.75 ppm with a coupling constant (J = 7.5Hz) corresponds to the proton labeled H4 coupling with both H5 and H6. The triplet at 7.65 ppm with (J=7.7 Hz) corresponds to the protons H5 and H6 on the phenyl ring coupling with its neighboring protons H1, H2 and H4. The pentet at 4.57 ppm with (J = 7.1 Hz) corresponds to the proton H7 which couples with H8a,b and H9a,b, while the doublet at 2.31 ppm with (J = 7.9 Hz) corresponds to

University of Ghana http://ugspace.ug.edu.gh

protons H8a and H9a also coupling with H7, H8b,9b. The multiplet between 1.86-1.77 ppm corresponds to the protons H8b and H9b with its neighboring proton H7, H8a,9a, H10 and H1,whiles the doublet of doublet at 1.99-1.98 ppm with coupling constants (J = 11.20, 7.90 Hz) also corresponds to protons H10 and H11 of the cyclopentyl ring which couples with H8b and H9b.

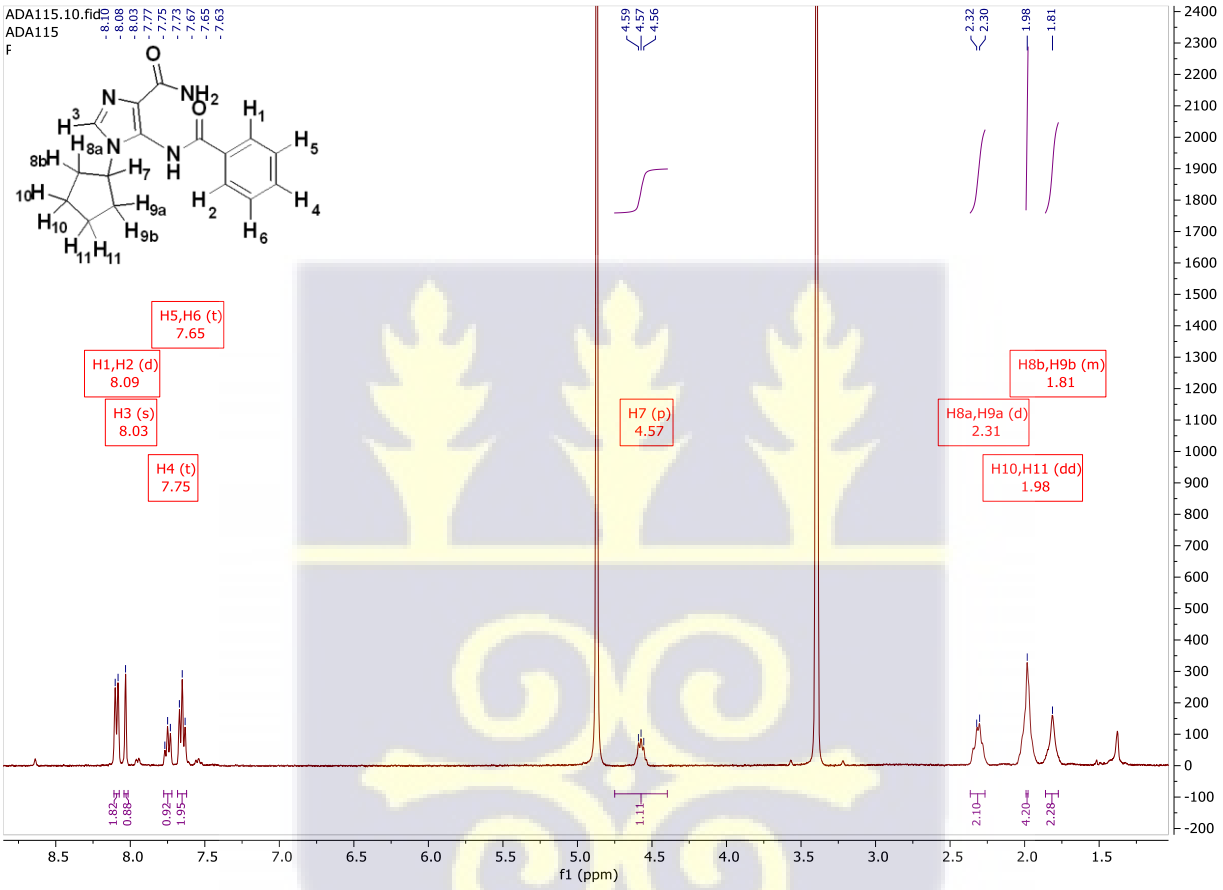


Figure 4.8: Proton NMR spectra for ADA115.

4.8.5 Carbon NMR Analysis of ADA115

The ^{13}C NMR spectrum for intermediate ADA115 comprising 12 chemically distinct carbon peaks is shown in **Figure 4.9** below. The peaks at 168.7 ppm and 168.5 ppm correspond to the carbonyl carbon C1 and C2. The peaks at 133.1.4 ppm, 133.0 ppm and 123.8 ppm correspond to the carbons

University of Ghana http://ugspace.ug.edu.gh

labeled C3, C4 and C11 respectively on the imidazole ring while the peaks at 132.6 ppm, 129.3 ppm, 128.1ppm and 127.9 ppm correspond to the carbons labeled C5, C6, C7 and C8, C9 and C10 respectively on the phenyl ring. The peaks at 58.5 ppm, 32.6 ppm and 23.4 ppm corresponds to the carbons labeled C12, C13 and C14 and C15 and C16 respectively on the cyclopentyl ring.

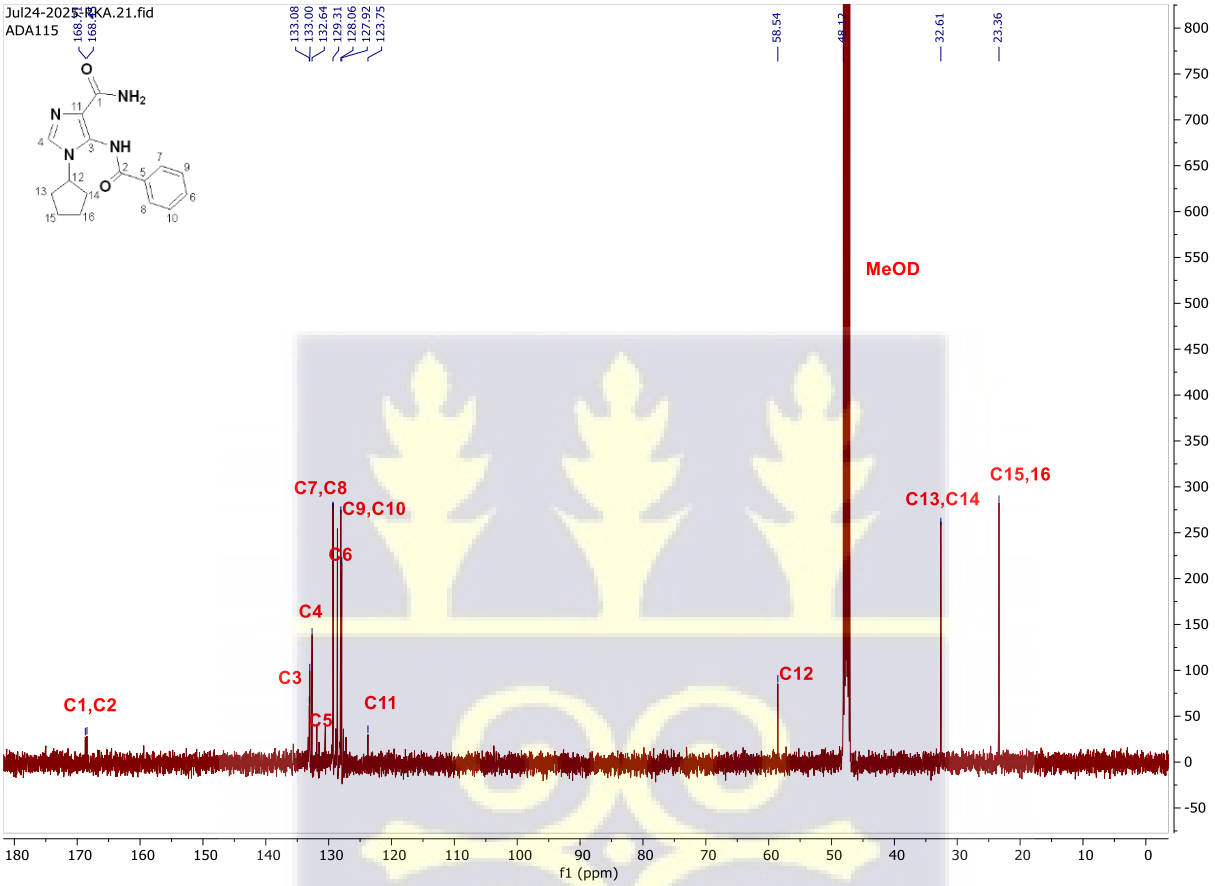


Figure 4.9: Carbon NMR spectra of ADA115.

4.8.6 Proton NMR Analysis of ADA117

The proton NMR for the intermediate ADA117 comprising 8 chemically distinct proton peaks was measured in MeOD and is shown in **Figure 4.10** below. The doublet at 8.09 ppm with coupling constant (J = 7.8Hz) corresponds to the protons labeled H1 and H2 which couples with H5 and H6 respectively. In comparison the singlet at 8.03 ppm corresponds to the proton labeled H3 on the

University of Ghana http://ugspace.ug.edu.gh

imidazole ring, and the triplet at 7.75 ppm with coupling constant (J = 7.8Hz) corresponds to the proton labeled H4 which also couples with both H5 and H6. The triplet at 7.65 ppm with (J = 7.7 Hz) corresponds to the protons H5 and H6 on the phenyl ring which couples with H4, H1 and H2. The multiplet at 4.66 – 4.40 ppm corresponds to the proton H7 which couples with H8a,b and H9a,9b, while the doublet of doublet at 2.29 ppm with (J = 12.5, 4.8 Hz) corresponds to protons H8a and H9a coupling with H7, H8b and H9b. The doublet at 1.83 ppm with (J = 11.4 Hz) corresponds to the protons H8b and H9b coupling with H7, while the doublet of doublet at 1.98 ppm with coupling constants (J = 8.7, 7.6 Hz) also corresponds to protons H10 and H11 of the cyclopentyl ring coupling with protons H8a,b and H9a,b.

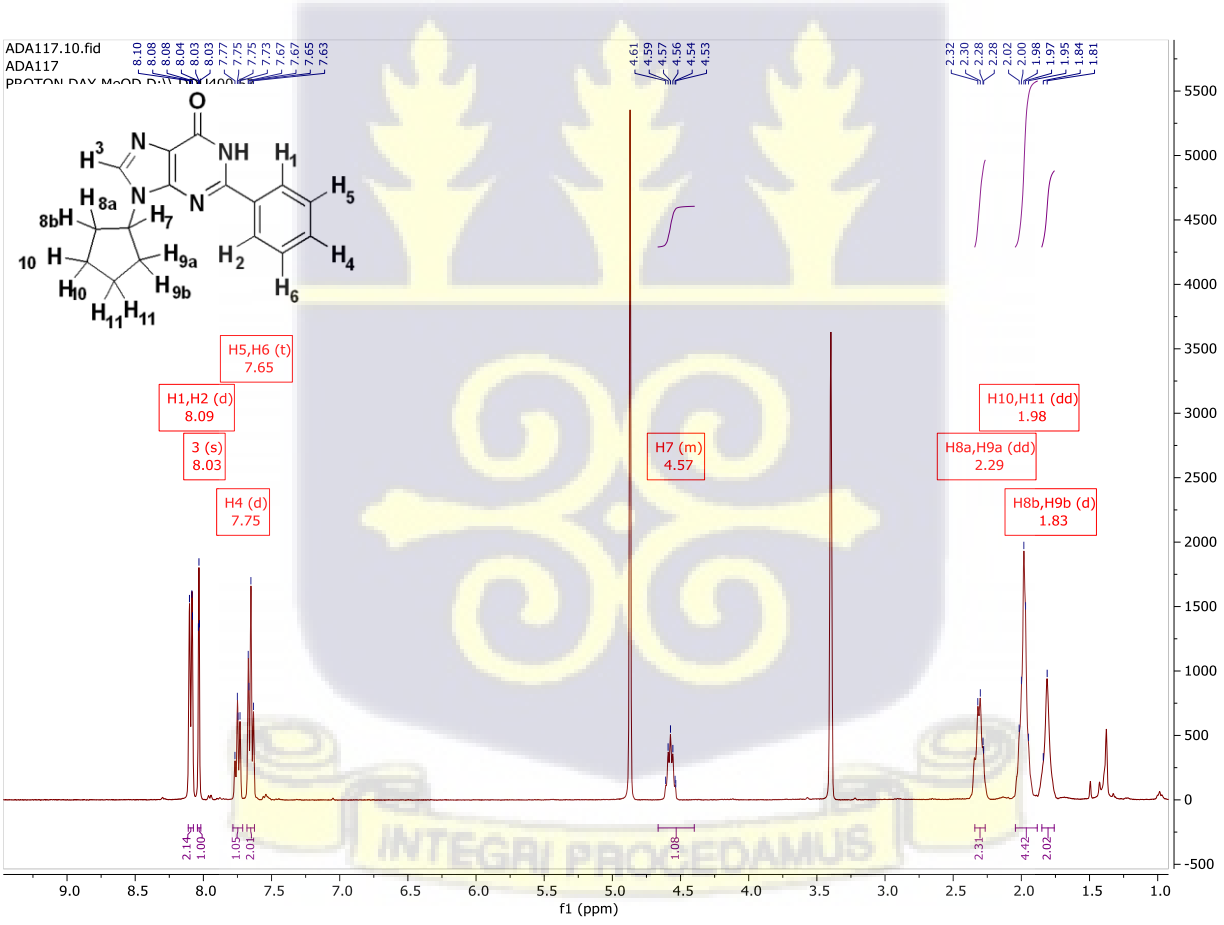


Figure 4.10: Proton NMR spectra of ADA117.

University of Ghana http://ugspace.ug.edu.gh

4.8.7 Carbon NMR Analysis of ADA117

The ^{13}C NMR spectrum for ADA117 comprising 12 chemically distinct carbon peaks is shown in **Figure 4.11** below. The peak at 169.8 ppm corresponds to the carbonyl carbon C1. The peaks at 137.1 ppm, 136.1ppm, 133.6 ppm and 110.4 ppm correspond to the carbons labeled C2, C3, C5 and C11 respectively while the peaks at 134.1 ppm, 130.0 ppm, 129.0 ppm and 114.7 ppm corresponds to the carbons labeled C4, C6 and C7 and C8, C9 and C10 respectively on the phenyl ring. The peaks at 58.6 ppm, 34.1 ppm and 24.8 ppm correspond to the carbons labeled C12, C13, C14 and C15,16 respectively on the cyclopentyl ring.

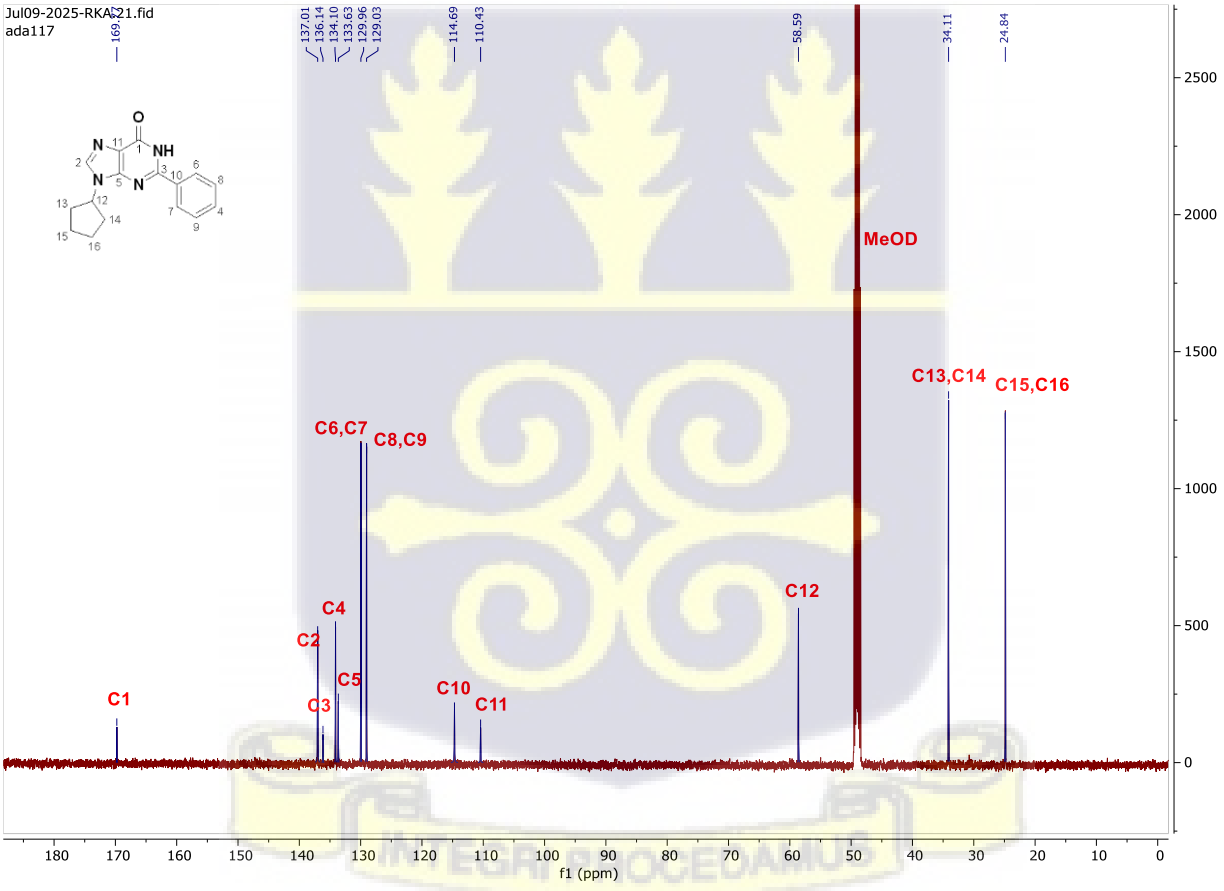
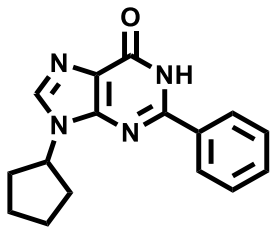


Figure 4.11: Carbon NMR spectra of ADA117.

University of Ghana http://ugspace.ug.edu.gh

4.8.8 FTIR Analysis of ADA117



The FTIR chromatogram for ADA117 is shown in **Figure 4.12** below. The broad peak at 3310.74 cm^{-1} is characteristic of (N-H) stretch vibrations. In contrast the peak at 3115.65 cm^{-1} is characteristic of an aromatic C-H stretch, the peak at 2965.37 cm^{-1} corresponds to an sp^3 C-H stretch, the remaining peaks at 1665.64 cm^{-1}, 1580.36 cm^{-1} and 1508.58 cm^{-1} correspond to carbonyl (C=O) stretch, a C=N stretching vibration and the aromatic C=C stretch respectively.

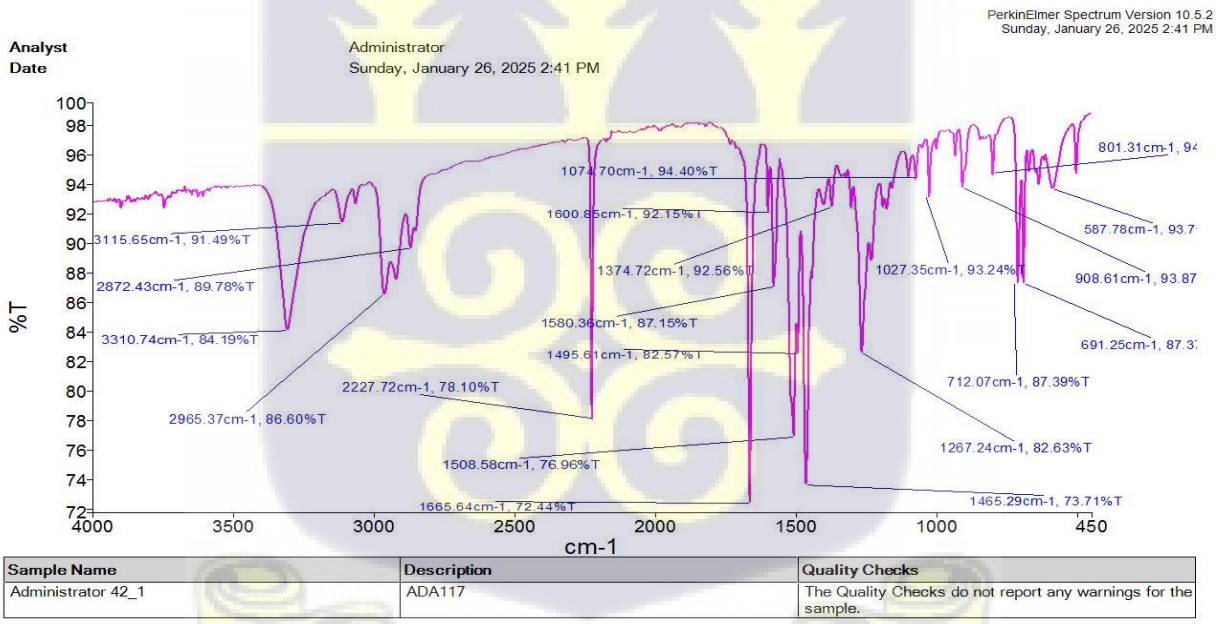
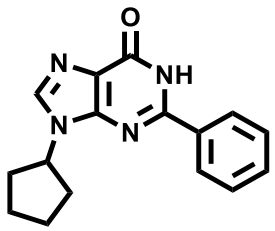


Figure 4.12: FTIR chromatogram for ADA117.

University of Ghana http://ugspace.ug.edu.gh

4.8.9 LCMS Analysis of ADA117



LC-MS data was acquired for ADA117 to ascertain its purity and molecular weight. The LC chromatogram, **Figure 4.13,** showed that the compound was pure with 100 % purity at 290 nm at a retention time of 0.865 min. The MS chromatogram on the other hand, showed a peak at 100% abundance corresponding to the $[M + H]^+$ molecular ion at 281.2 m/z (**Figure 4.14**) indicating that the calculated molecular weight of 280.33 g/mol was accurate. There is also $[2M + H]^+$peak at 561.2.

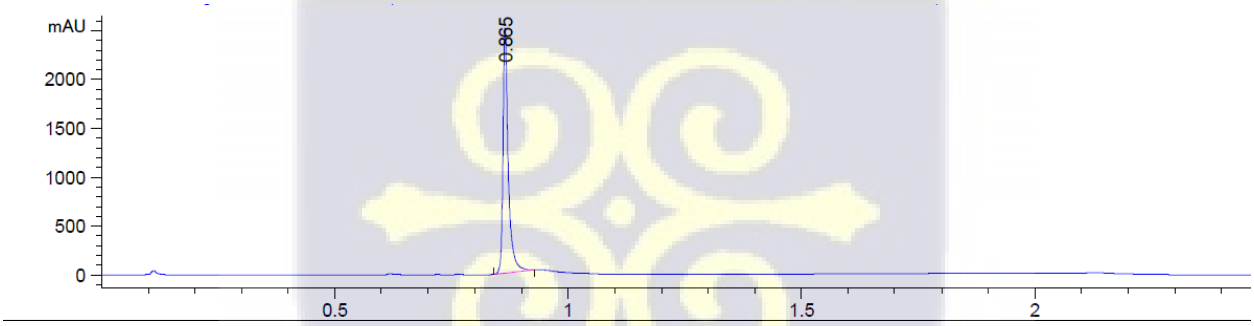


Figure 4.13: LC spectrum for ADA117

INTEGRI PROCEDAMUS

University of Ghana http://ugspace.ug.edu.gh

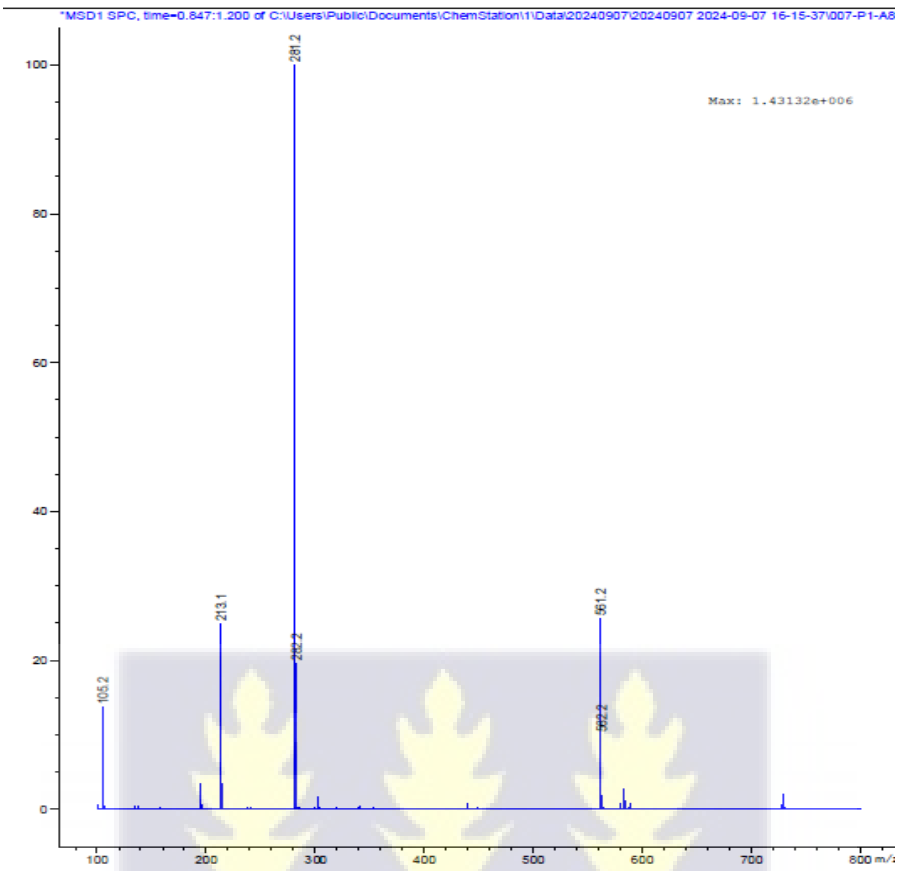


Figure 4.14: MS spectrum for compound ADA117

4.9 Antimalarial Biological Activity of Synthesized Analogues of MMV1900279

Nine of the synthesized analogues were tested for their anti-plasmodial activity against the chloroquine-sensitive 3D7 strain of *Plasmodium falciparum* using chloroquine as a control **Table 4.3**. The activity obtained for the analogues ranged between 25 µM to 0.09 µM and the most active compound was ADA 129, with an IC_{50} of 86 nM superior to the hit compound with an IC_{50} of 0.37 µM. The activity results showed that analogues with aliphatic substitutions on the pyrimidine ring had a better anti-plasmodial activity compared to analogues with aromatic substitutions on the pyrimidine ring. For instance, ADA136, with a cyclohexyl substitution on the pyrimidine, had an IC_{50} of 0.17 µM whereas ADA138 with a phenyl substitution had an IC_{50} of 6.30 µM. Furthermore, it was observed that reducing the size from a cyclohexyl group as seen in ADA136 (IC_{50}=0.17

University of Ghana http://ugspace.ug.edu.gh

μM) to a cyclopropyl group on the pyrimidine ring exemplified by ADA141 led to a loss of activity with an IC_{50} value of 2.49 μM. In addition, it was observed that substituting the cyclopentyl group on the imidazole ring as seen in FEP017 with a cyclo-butyl ring in ADA136 led to an increase in activity from an IC_{50} of 1 μM (FEP017) to 0.17 μM (ADA136). It was also observed that potency decreased when an oxetane group was introduced onto the imidazole ring. For example, ADA118, with the oxetane group on the imidazole, had an IC_{50} value of 1.55 μM, compared with ADA136 (IC_{50}=0.17 μM) with a cyclobutyl substitution. However, introducing the Boc piperidine and the tetrahydropyran substitutions increased activity. For instance, ADA129 with a Boc piperidine substituent on the imidazole ring and a cyclohexyl substituent on the pyrimidine ring had the best activity with IC50 of 0.086 μM. This analogue, ADA129, was more activity than the hit compound MMV19000279 with an IC_{50} of 0.37 μM. The activity of the synthesized analogues was plotted against calculated Log D, and the graph below (**Figure 4.15**) shows a slight correlation between the activity and Log D. The anti-malarial data and solubility data for other synthesized analogues are yet to be synthesized.

Table 4.2: Anti-plasmodial activity results of the synthesized analogues.

Sample Code	Solubility (μM)	3D7(μM)	Log D	tPSA
ADA113	-	0.11	0.90	66.29
ADA117	-	25	2.22	57.07
ADA118	77.00	1.55	1.55	66.29
ADA123	-	20.13	-0.55	66.29
ADA125	-	25	0.11	66.29
ADA129	-	0.086	2.82	86.6

University of Ghana http://ugspace.ug.edu.gh

ADA132	-	-	1.14	86.6
ADA136	350.00	0.17	2.18	57.06
ADA138	997.70	6.30	1.66	57.06
ADA141	350	2.49	0.51	57.06
ADA143	350	-	0.99	57.06
ADA145	350	-	1.13	66.29
ADA148	5.28	-	0.63	75.52
Chloroquine		0.1		
Trazodone	259.0			
Diethylstilbesterol	9.0			

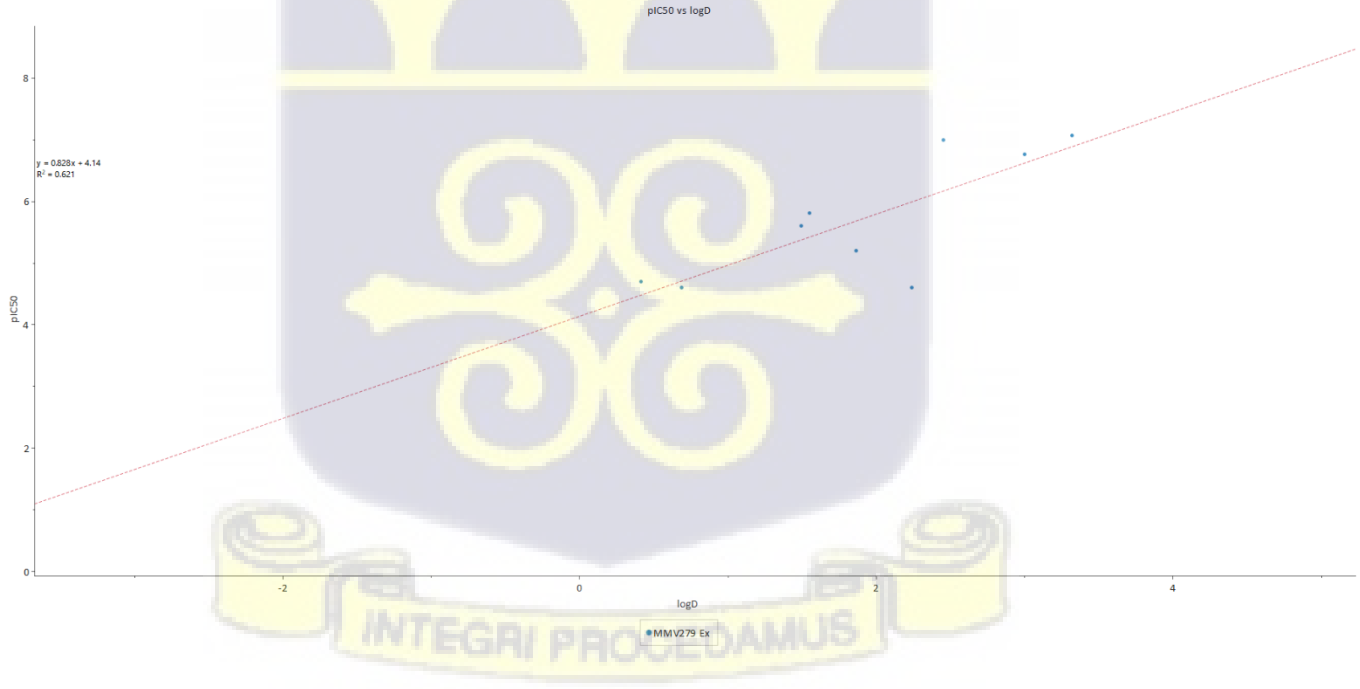


Figure 4.15: A graph of PIC50 against Log D.

University of Ghana http://ugspace.ug.edu.gh

4.10 Solubility of Synthesized Analogues of MMV1900279

The solubility of 7 synthesized analogues was determined using Trazodone (259.0 µM) and Diethylstilbesterol (9.0 µM) as controls. The compounds showed good solubility values within the range of 997.7 µM to 77.00 µM. Compound ADA148, however, returned a poor solubility of 5.28 µM while ADA138 emerged as the most soluble compound with a solubility value of 997.7 µM.

University of Ghana http://ugspace.ug.edu.gh

Chapter 5

5.1 Conclusions

In this project, analogues of two series, SFK78 and MMV1900279 were synthesized and evaluated for antimalarial activity and ADME properties. At the end of this project, 19 analogues of SFK78 were synthesized in three chemical steps in low to moderate yields (9 % to 48 %), while 13 analogues of MMV1900279 were also synthesized in three chemical steps in low to high yields (8 % to 70 %). The synthesis of analogues of SFK78 began with a chlorosulfonation reaction, followed by a sulfonamide reaction and finally a Suzuki cross-coupling reaction. Compounds which had the Boc group were also successfully deprotected in moderate to high yields (24 % to 96 %). The synthesis of analogues of MMV1900279 was initiated by imidazole formation, followed by an amide coupling, and finally a cyclization. Analogues of both series were characterized using FT-IR spectroscopy, proton and carbon-13 NMR, and LC-MS.

seventeen of the synthesized analogues of SFK78 were evaluated for their antimalarial activity and all of the compounds returned low micromolar activities in a range between (0.2 µM and 25 µM). Among the tested analogues, compounds **ADA084**,**ADA090** and **ADA097** were the most potent, with an **IC_{50}** of **0.2 µM**, while compound **ADA088** was the least potent, with an **IC_{50}** of **25 µM**. Compound ADA090 showed activity similar to the hit compound **MMV907502** which had an **IC_{50}** of **0.17µM**. All the synthesized compounds had a molecular weight less than 500 g/mol except for **ADA092** and **ADA093,** with molecular weights of **502.59** g/mol and **520.62** g/mol respectively. The ADME data obtained for some SFK78 analogues suggested that the compounds retained potency against both sensitive and resistant strains of the parasite, and none of the compounds were cytotoxic, (>25 in the Hep G2 cells Luminescence assay after 72h). Also, the compounds

University of Ghana http://ugspace.ug.edu.gh

had good clearance in both rat hepatocytes and human liver microsomes. **ADA096** was the most stable among the tested analogues.

Also, nine analogues of MMV1900279 were tested for their antimalarial activity, they all returned low micromolar activities ranging between 0.086 µM and 25 µM. Compound **ADA129** was the most potent with an **IC_{50}** of **0.086 µM** while **ADA117** was the least potent with an **IC_{50}** of **25 µM**. The solubility of 7 analogues was also determined and Compound **ADA138** (**997.78 µM**) was the most soluble while **ADA148** (**5.28 µM**) was the least soluble.

5.2 Recommendations

The SAR of the two series has been extensively explored in this project. However, I recommend that the remaining antimalarial activity data for some synthesized analogues of both SFK78 and MMV1900279 against the 3D7 sensitive strain and Dd2 resistant strain of the parasite is obtained. Also, the solubility of all the analogues should be determined along with the ADME data for MMV1900279 analogues, to assess the clearance, metabolic stability and toxicity of the synthesized analogues.

INTEGRI PROCEDAMUS

University of Ghana http://ugspace.ug.edu.gh

REFERENCES

1. WHO, *Strategic Advisory Group on Malaria Eradication. Malaria Eradication: Benefits, Future Scenarios and Feasibility. Geneva:* (2020).
2. Jagannathan, P. & Kakuru, A. Malaria in 2022: Increasing challenges, cautious optimism. *Nat Commun* **13**, 12–14 (2022).
3. Dagen, M., *Chapter 1 - History of Malaria and Its Treatment*. *Antimalarial Agents* (Elsevier Ltd, 2020).
4. Unger, H. W. *et al.* Review The effect and control of malaria in pregnancy and lactating women in the Asia-Pacific region. *Lancet Glob Health* **11**, e1805–e1818 (2023).
5. *World Malaria Report 2024*. (World Health Organization, 2024).
6. Hussein, M. I. H., Albashir, A. A. D., Elawad, O. A. M. A. & Homeida, A. Malaria and COVID-19: unmasking their ties. *Malar J* **19**, 1–10 (2020).
7. Organization, W. H. *World Malaria World Malaria Report*. (2023).
8. Sato, S. Correction to: Plasmodium—a brief introduction to the parasites causing human malaria and their basic biology (Journal of Physiological Anthropology, (2021), 40, 1, (1), 10.1186/s40101-020-00251-9). *J Physiol Anthropol* **40**, 1–13 (2021).
9. Talapko, J., Škrlec, I., Alebić, T., Jukić, M. & Včev, A. Malaria: The past and the present. *Microorganisms* **7**, (2019).
10. Bannister, L. H. & Sherman, I. W. Plasmodium In: Encyclopedia of Life Sciences (ELS). John Wiley & Sons, Ltd: Chichester, (2009).
11. White, N. J. *et al.* Malaria. *The Lancet* **383**, 723–735 (2014).
12. Luo, Z., Sullivan, S. A. & Carlton, J. M. The biology of Plasmodium vivax explored through genomics. 53–61 (2015).
13. Poostchi, M., Silamut, K., Maude, R. J., Jaeger, S. & Thoma, G. Image analysis and machine learning for detecting malaria. *Translational Research* **194**, 36–55 (2018).
14. Rathod, G. K., Jain, M., Sharma, K. K., Das, S. & Basak, A. European Journal of Medicinal Chemistry New structural classes of antimalarials. *Eur J Med Chem* **242**, (2022).
15. Ouologuem, D. T., Dara, A., Kone, A., Ouattara, A. & Djimde, A. A. Plasmodium falciparum Development from Gametocyte to Oocyst: Insight from Functional Studies. *Microorganisms* **11**, 1–27 (2023).
16. Okombo, J., Kanai, M., Deni, I. & Fidock, D. A. Genomic and Genetic Approaches to Studying Antimalarial Drug Resistance and Plasmodium Biology. *Trends Parasitol* **37**, 476–492 (2021).

University of Ghana http://ugspace.ug.edu.gh

17. Okombo, J., Kanai, M., Deni, I. & Fidock, D. A. Genomic and Genetic Approaches to Studying Antimalarial Drug Resistance and Plasmodium Biology. *Trends Parasitol* **37**, 476–492 (2021).

18. Maier, A. G., Matuschewski, K., Zhang, M. & Rug, M. Plasmodium falciparum. *Trends Parasitol* **35**, 481–482 (2019).

19. Poostchi, M., Silamut, K., Maude, R. J., Jaeger, S. & Thoma, G. Image analysis and machine learning for detecting malaria. *Translational Research* **194**, 36–55 (2018).

20. Thomson-Luque, R. *et al.* Plasmodium falciparum transcription in different clinical presentations of malaria associates with circulation time of infected erythrocytes. *Nat Commun* **12**, 4711, (2021).

21. Livingstone, M. C. *et al.* In vitro and in vivo inhibition of malaria parasite infection by monoclonal antibodies against Plasmodium falciparum circumsporozoite protein (CSP). *Sci Rep* **11**, 1–15 (2021).

22. Liu, W. *et al.* African origin of the malaria parasite Plasmodium vivax. *Nat Commun* **5**, 3346, (2014).

23. Persson, K. E. M. Malaria, Immunity, and Immunopathology. In *Encyclopedia of Immunobiology,* Elsevier Inc 4, 94–100, (2016).

24. Giemsa, W., CDC (Centers of Disease Control). Laboratory Diagnosis of malaria, Plasmodium vivax, *DPDx Laboratory Identification of Parasites of Public Health Concern* 1–4 (2014).

25. Collins, W. E. & Jeffery, G. M. Plasmodium malariae: Parasite and Disease. **20**, 579–592 (2007).

26. Kotepui, M., Kotepui, K. U., Milanez, G. D. & Masangkay, F. R. Global prevalence and mortality of severe Plasmodium malariae infection: a systematic review and meta-analysis. *Malar J* 1–13 (2020)

27. Collins, W. E. & Jeffery, G. M. Plasmodium malariae: Parasite and Disease. *Clin Microbiol Rev* **20**, 579–592 (2007).

28. Service, D. of H. and H. Laboratory diagnosis of malaria P. malariae. *Center for Disease Control and Prevention* (2022).

29. Guerra, R. I. *et al.* CASE REPORT A cluster of the first reported Plasmodium ovale spp. Infections in Peru among returning UN peacekeepers: a review of epidemiology, prevention, and diagnostic challenges in nonendemic regions. *Malar J* 1–8 (2019).

30. Tordrup, D., Virenfeldt, J., Andersen, F. F. & Petersen, E. Variant Plasmodium ovale isolated from a patient infected in Ghana. *Malar J* **10**, 1–5 (2011).

31. CDC (Centers of Disease Control). Laboratory Diagnosis of malaria 'Plasmodium ovale'. *DPDx Laboratory Identification of Parasites of Public Health Concern* 1–4 (2014).

University of Ghana http://ugspace.ug.edu.gh

32. Amir, A., Cheong, F. W., Ryan De Silva, J., Wee, J. K. & Lau, Y. L. Infection and Drug Resistance Dovepress Plasmodium knowlesi malaria: current research perspectives. *Infection Drug Resistance* 1145–1155 (2018).

33. Naserrudin, N. A., Hod, R., Jeffree, M. S., Ahmed, K. & Hassan, M. R. The Emerging Threat of Plasmodium knowlesi Malaria Infection: A Concept Paper on the Vulnerable Factors in Human. *Int J Environ Res Public Health* **19**, (2022).

34. Lee, K. S., Cox-Singh, J. & Singh, B. Morphological features and differential counts of Plasmodium knowlesi parasites in naturally acquired human infections. *Malar J* **8**, 1–10 (2009).

35. Greenwood, B. M., Bojang, K., Whitty, C. J. M. & Targett, G. A. T. Malaria. 1487–1498 (2005).

36. Venugopal, K., Hentzschel, F., Valki, G. & Marti, M. Plasmodium asexual growth and sexual development in the haematopoietic niche of the host. **18**, 177–189 (2020).

37. Bannister, L. H. & Sherman, I. W. Plasmodium In: Encyclopedia of Life Sciences (ELS). John Wiley & Sons, Ltd: Chichester, (2010).

38. Soulard, V. *et al.* Plasmodium falciparum full life cycle and Plasmodium ovale liver stages in humanized mice. *Nat Commun* **6**, (2015).

39. Venugopal, K., Hentzschel, F., Valkiūnas, G. & Marti, M. Plasmodium asexual growth and sexual development in the haematopoietic niche of the host. *Nat Rev Microbiol* **18**, 177–189 (2020).

40. Sherrard-Smith, E. *et al.* Inferring the epidemiological benefit of indoor vector control interventions against malaria from mosquito data. *Nat Commun* **13**, 36-62, (2022).

41. Phillips, M. A. *et al.* Malaria. *Nat Rev Dis Primers* **3**, 17050, (2017).

42. Organization, W. H. *World Malaria World Malaria Report Report*. (2023).

43. Benelli, G. & Beier, J. C. Current vector control challenges in the fight against malaria. *Acta Tropica* vol. 174 91–96, (2017).

44. Kamareddine, L. The biological control of the malaria vector. *Toxins* vol. 4 748–767, (2012).

45. Takken, W. & Knols, B. G. J. Malaria vector control: current and future strategies. *Trends Parasitol* **25**, 101–104 (2009).

46. Ahadzie-Soglie, A., Addai-Mensah, O., Abaka-Yawson, A., Setroame, A. M. & Kwadzokpui, P. K. Prevalence and risk factors of malaria and anaemia and the impact of preventive methods among pregnant women: A case study at the Akatsi South District in Ghana. *PLoS One* **17**, 1–12 (2022).

University of Ghana http://ugspace.ug.edu.gh

47. Operational manual on indoor residual spraying: control of vectors ofmalaria, Aedes-borne diseases, Chagas disease, leishmaniases and lymphatic filariasis. Geneva:World Health Organization; 2023.

48. Zhou, Y. *et al.* Effectiveness of indoor residual spraying on malaria control: a systematic review and meta-analysis. *Infect Dis Poverty* **11**, (2022).

49. Choi, L., Pryce, J. & Garner, P. Indoor residual spraying for preventing malaria in communities using insecticide-treated nets. *Cochrane Database of Systematic Reviews* **5**. (2019).

50. Pryce, J., Medley, N. & Choi, L. Indoor residual spraying for preventing malaria in communities using insecticide-treated nets. *Cochrane Database of Systematic Reviews* **1**, (2022).

51. Che-Mendoza, A. *et al.* Efficacy of targeted indoor residual spraying with the pyrrole insecticide chlorfenapyr against pyrethroid-resistant Aedes aegypti. *PLoS Negl Trop Dis* **15**, (2021).

52. Yakob, L., Dunning, R. & Yan, G. Indoor residual spray and insecticide-treated bednets for malaria control: Theoretical synergisms and antagonisms. *J R Soc Interface* **8**, 799–806 (2011).

53. Oxborough, R. M. *et al. Personal View Malaria Vector Control in Sub-Saharan Africa: Complex Trade-Offs to Combat the Growing Threat of Insecticide Resistance*, **8**, 806, (2024).

54. Siqueira-Neto, J. L. *et al.* Antimalarial drug discovery: progress and approaches. *Nat Rev Drug Discov* (2023)

55. White, N. J. *et al.* Malaria. *The Lancet* **383**, 723–735 (2014).

56. Plowe, C. V. Malaria chemoprevention and drug resistance: a review of the literature and policy implications. *Malaria Journal*, **21**, (2022).

57. Winstanley, P. & Ward, S. Malaria Chemotherapy. *Adv Parasitol* **61**, 47–76 (2006).

58. Yaro, J. B. *et al.* Risk of Plasmodium falciparum infection in south-west Burkina Faso: potential impact of expanding eligibility for seasonal malaria chemoprevention. *Sci Rep* **12**, 1–11 (2022).

59. Yaro, J. B. *et al.* Risk of Plasmodium vivax infection in south-west Burkina Faso: potential impact of expanding eligibility for seasonal malaria chemoprevention. *Sci Rep* **13**, 3–11 (2023).

60. Okell, L. C. *et al.* Projected health impact of post-discharge malaria chemoprevention among children with severe malarial anaemia in Africa. *Nat Commun* **14**, (2023).

61. Chuang, Y. M. *et al.* A mosquito AgTRIO mRNA vaccine contributes to immunity against malaria. *NPJ Vaccines* **8**, 1–6 (2023).

University of Ghana http://ugspace.ug.edu.gh

62. Grant, J. *et al.* Challenges and lessons learned during the planning and early implementation of the RTS,S/AS01E malaria vaccine in three regions of Ghana: a qualitative study. *Malar J* **21**, 1–12 (2022).

63. Dieng, C. C. *et al.* Genetic variations of Plasmodium falciparum circumsporozoite protein and the impact on interactions with human immunoproteins and malaria vaccine efficacy. *Infection, Genetics and Evolution* **110**, (2023).

64. Zavala, F. RTS, S: the first malaria vaccine. *Journal of Clinical Investigation* **132**, (2022).

65. Pholcharee, T. *et al.*, Structural and biophysical correlation of anti-NANP antibodies with in vivo protection against P. falciparum. *Nature Communications*, ***1***,12, (2021).

66. Plata-Pineda, S. E., Cárdenas-Munévar, L. X., Castro-Cavadía, C. J., Buitrago, S. P. & Garzón-Ospina, D. Evaluating the genetic diversity of the Plasmodium vivax siap2 locus: A promising candidate for an effective malaria vaccine? *Acta Trop* **251**, (2024).

67. Palacpac, N. M. Q., Ishii, K. J., Arisue, N., Tougan, T. & Horii, T. Immune tolerance caused by repeated P. falciparum infection against SE36 malaria vaccine candidate antigen and the resulting limited polymorphism. *Parasitol Int* **99**, (2024).

68. Datoo, M. S. *et al.* Articles Safety and efficacy of malaria vaccine candidate R21 / Matrix-M in African children: a multicenter, double- blind, randomised , phase 3 trial. *Lancet* 533–544.

69. Flannery, E. L., Chatterjee, A. K. & Winzeler, E. A. Antimalarial drug discovery — approaches and progress towards new medicines (2013).

70. Ansbro, M. R. *et al.* Modulation of Triple Artemisinin-Based Combination Therapy Pharmacodynamics by Plasmodium falciparum Genotype. *ACS Pharmacol Transl Sci* **3**, 1144–1157 (2020).

71. Nguyen, T. D. *et al.* Preventing antimalarial drug resistance with triple artemisinin-based combination therapies. (2023).

72. Fola, A. A. *et al.* Plasmodium falciparum resistant to artemisinin and diagnostics have emerged in. (2023).

73. Tse, E. G., Korsik, M. & Todd, M. H. The past, present and future of anti-malarial medicines. *Malar J* **18**, 1–21 (2019).

74. Madhav, H. & Hoda, N. An insight into the recent development of the clinical candidates for the treatment of malaria and their target proteins. *Eur J Med Chem* **210**, (2021).

75. Pethrak, C. *et al.* New Insights into Antimalarial Chemopreventive Activity of Antifolates. *Antimicrob Agents Chemother* **66**, (2022).

76. Yuthavong, Y. Basis for antifolate action and resistance in malaria. *Microbes and Infection* vol. 4 175–182 (2002).

University of Ghana http://ugspace.ug.edu.gh

77. Daskum, A. M., Chessed, G., Qadeer, M. A. & Mustapha, T. Antimalarial chemotherapy, mechanisms of action and resistance to major antimalarial drugs in clinical use: A review. *Microbes and Infectious Diseases* **2**, 130–142 (2021).

78. Tropica, A., All, E. S. B. V & Walter, T. The mode of action and the mechanism of resistance to antimalarial drugs. **56**, 157–171 (1994).

79. Winstanley, P. & Ward, S. Malaria Chemotherapy. *Adv Parasitol* **61**, 47–76 (2006).

80. Pussard, E. & Verdier, F. Antimalarial 4-aminoquinolines: mode of action and pharmacokinetics. 1–17 (1994).

81. Deshpande, S. & Kay, B. 4-aminoquinolines: An Overview of Antimalarial Chemotherapy 4-aminoquinolines: An Overview of Antimalarial Chemotherapy. (2016).

82. Ravindar, L., Aishah, S., Rakesh, K. P. & Izzaty, N. European Journal of Medicinal Chemistry Recent developments in antimalarial activities of 4-aminoquinoline derivatives. *Eur J Med Chem* **256**, 115458 (2023).

83. Deshpande, S. & Kay, B. 4-aminoquinolines: An Overview of Antimalarial Chemotherapy. *J Med Chem* **6:1**, 1-12Identifying antimalarial compounds targeting d (2016).

84. Roche, F. H., Division, P. & Basel, C.-. Haemoglobin Degradation and Haem Polymerization as Antimalarial Drug Targets. **49**, 43–48 (1997).

85. Kamchonwongpaisan, S. & Meshnick, S. R. The Mode of Action of the Antimalarial Artemisinin and its Derivatives. **27**, 587–592 (1996).

86. Meshnick, S. R., Taylor, T. E. & Kamchonwongpaisan, S. Artemisinin and the antimalarial endoperoxides: from herbal remedy to targeted chemotherapy. *Microbiol Rev* **60**, 301–315 (1996).

87. Pandey, A. V, Tekwani, B. L., Singh, R. L. & Chauhan, V. S. Artemisinin, an Endoperoxide Antimalarial, Disrupts the Hemoglobin Catabolism and Heme Detoxification Systems in Malarial Parasite. **274**, 19383–19388 (1999).

88. Koutsoupakis, C., Gialou, I., Pavlidou, E., Kapetanaki, S. & Varotsis, C. Antimalarial endoperoxides: Synthesis and implications of the mode of action. *Arkivoc* **2002**, 62–69 (2002).

89. Kamchonwongpaisan, S. & Meshnick, S. R. The Mode of Action of the Antimalarial Artemisinin and its Derivatives. **27**, 587–592 (1996).

90. Pandey, A. V, Tekwani, B. L., Singh, R. L. & Chauhan, V. S. Artemisinin, an Endoperoxide Antimalarial, Disrupts the Hemoglobin Catabolism and Heme Detoxification Systems in Malarial Parasite. **274**, 19383–19388 (1999).

91. Li, J. & Zhou, B. Biological Actions of Artemisinin: Insights from Medicinal Chemistry Studies. 1378–1397 (2010).

University of Ghana http://ugspace.ug.edu.gh

92. Kamchonwongpaisan, S. & Meshnick, S. R. The mode of action of the antimalarial artemisinin and its derivatives. *General Pharmacology* vol. 27 587–592 (1996).

93. Meshnick, S. R. & Arbor, A. The mode of action of antimalarial. 31–32 (1989).

94. Neill, P. M. O., Barton, V. E. & Ward, S. A. The Molecular Mechanism of Action of Artemisinin—The Debate Continues. 1705–1721 (2010).

95. Tetteh, J., Yorke, E., Boima, V. & Yawson, A. E. Prevalence of malaria infection and the impact of mosquito bed net distribution among children aged 6–59 months in Ghana: Evidence from the Ghana demographic health and malarial indicator surveys. *Parasite Epidemiol Control* **21**, (2023).

96. Tetteh, J. A., Djissem, P. E. & Manyeh, A. K. Prevalence, trends and associated factors of malaria in the Shai-Osudoku District Hospital, Ghana. *Malar J* **22**, 1–7 (2023).

97. GSS. World-Malaria-Day-Press-Release-from-GSS-1. *Ghana Statistical Service* **04**, 1–2 (2023).

98. Boadu, I., Nsemani, W., Ubachukwu, P. & Okafor, F. C. Knowledge and Prevalence of Malaria among Rural Households in Ghana. *J Community Med Health Educ* **10**, 1–8 (2020).

99. Hanboonkunupakarn, B., Tarning, J., Pukrittayakamee, S. & Chotivanich, K. Artemisinin resistance and malaria elimination: Where are we now? *Front Pharmacol* **13**, 1–10 (2022).

100. LU, F., HE, X. L., Richard, C. & CAO, J. A brief history of artemisinin: Modes of action and mechanisms of resistance. *Chin J Nat Med* **17**, 331–336 (2019).

101. Njiro, B. J. *et al.* treatment of uncomplicated malaria: A systematic review. **15**, 550–557 (2022).

102. Sawyer, B. J., Khan, I. H. & Le, H. V. *Antimalarial Drugs*. (2023).

103. Cunha-Rodrigues, M., Prudêncio, M., Mota, M.M. and Haas, W. Antimalarial drugs – host targets (re)visited. Biotechnology Journal, **1**, 321-332, (2006).

104. Yuthavong, Y. Basis for antifolate action and resistance in malaria. *Microbes Infect* **4**, 175–182 (2002).

105. Roper, C. *et al.* Antifolate antimalarial resistance in southeast Africa: A population-based analysis. *Lancet* **361**, 1174–1181 (2003).

106. Yuthavong, Y. Basis for antifolate action and resistance in malaria. *Microbes Infect* **4**, 175–182 (2002).

107. Meshnick, S. R., Taylor, T. E. & Kamchonwongpaisan, S. Artemisinin and the antimalarial endoperoxides: from herbal remedy to targeted chemotherapy. *Microbiol Rev* **60**, 301–315 (1996).

University of Ghana http://ugspace.ug.edu.gh

108. Wotodjo, A. N. *et al.* Genomic and Genetic Approaches to Studying Antimalarial Drug Resistance and Plasmodium Biology. *Trends Parasitol* **4**, 1–8 (2023).

109. Hanboonkunupakarn, B., Tarning, J., Pukrittayakamee, S. & Chotivanich, K. Artemisinin resistance and malaria elimination: Where are we now? *Front Pharmacol* **13**, 1–10 (2022).

110. Xie, S. C., Ralph, S. A. & Tilley, L. Artemisinin Resistance. *Trends Parasitol* **36**, 533–544 (2020).

111. Hyde, J. E. Mechanisms of resistance of Plasmodium falciparum to antimalarial drugs. **4**, 165–174 (2002).

112. Xie, S. C., Ralph, S. A. & Tilley, L. Artemisinin Resistance. *Trends Parasitol* **36**, 533–544 (2020).

113. WHO. *World Malaria Report 2022 - World | ReliefWeb*. *World Health Organization* (2022).

114. Walsh, C. T. Nature loves nitrogen heterocycles. *Tetrahedron Lett* **56**, 3075–3081 (2015).

115. Arora, P., Arora, V., Lamba, H. S. & Wadhwa, D. importance of heterocyclic chemistry: a review. *IJPSR* **3**, 2947–2954 (2012).

116. Omar, A. M., Saleh, N. M., Abdel-Rahman, A. A.-H. & El-Adl, K. *review article; anticancer activities of some fused heterocyclic moieties containing nitrogen and/or sulfur heteroatoms*. *J. Pharm Sci*, **62**, (2020).

117. Kerru, N., Gummidi, L., Maddila, S., Gangu, K. K. & Jonnalagadda, S. B. A review on recent advances in nitrogen-containing molecules and their biological applications. *Molecules*,25 (2020).

118. Joule, J. A. Natural Products Containing Nitrogen Heterocycles-Some Highlights 1990-2015. in *Advances in Heterocyclic Chemistry* vol. 119 81–106 (Academic Press Inc., 2016).

119. Kumar, A. *et al.* Nitrogen Containing Heterocycles as Anticancer Agents: A Medicinal Chemistry Perspective. *Pharmaceuticals* vol. 16 (2022).

120. Islam, M. B. *et al.* Recent Advances in Pyridine Scaffold: Focus on Chemistry, Synthesis, and Antibacterial Activities. *BioMed Research International* vol.2023, 15 (2023).

121. Arella, S., Thanyasri, P., Bhavana, P. & Reddy, S. EPRA International Journal of Research and Development (IJRD). (2023).

122. Qadir, T., Amin, A., Sharma, P. K., Jeelani, I. & Abe, H. A Review on Medicinally Important Heterocyclic Compounds. *Open Med Chem J* **16**, (2022).

123. Othman M.M. Ismail *et al.* Novel fused pyridine derivatives containing pyrimidine moiety as prospective tyrosyl-tRNA synthase inhibitors: Design, synthesis, pharmacokinetics and molecular docking studies. *J Mol Struct* **1219**, 128651 (2020).

University of Ghana http://ugspace.ug.edu.gh

124. Wang Shuai *et al.* FDA-approved pyrimidine-fused bicyclic heterocycles for cancer therapy: synthesis and clinical application. *Eur J Med Chem* **214**, 113218 (2021).

125. Tahir, T. *et al.* Pyridine scaffolds, phenols and derivatives of azo moiety: Current therapeutic perspectives. *Molecules* **26**, (2021).

126. Pathania, S. & Rawal, R. K. Pyrrolopyrimidines: An update on recent advancements in their medicinal attributes. *European Journal of Medicinal Chemistry* vol. 157 503–526 (2018).

127. Rossiter, S. & Ostovar, M. Bicyclic 6-6 Systems: Pteridines. in *Comprehensive Heterocyclic Chemistry IV* 796–855 (Elsevier, 2021).

128. Perlíková, P. & Hocek, M. Pyrrolo[2,3-d]pyrimidine (7-deazapurine) as a privileged scaffold in design of antitumor and antiviral nucleosides. *Medicinal Research Reviews* vol. 37 1429–1460 (2017).

129. Mareedu, R. S. & M, P. Synthesis of 2-(morpholin-4-yl)-5-(piperazin-1-yl)pyrido[4,3-d]pyrimidine derivatives, crsystal structure, molecular docking studies, and antioxidant activities. *J Mol Struct* **1322**, (2025).

130. Walsh, C. T. Nature loves nitrogen heterocycles. *Tetrahedron Lett* **56**, 3075–3081 (2015).

131. Manvar, A. & Shah, A. Microwave-assisted chemistry of purines and xanthines. An overview Dedicated to the late Professor V.M. Thakor on his 94th birthday. *Tetrahedron* vol. 69 8105–8127, (2013).

132. Kumari, A. Purine structure. in *Sweet Biochemistry* 117–120 (Elsevier, 2023).

133. Décout, J. L. Bicyclic 5-6 Systems: Purines. in *Comprehensive Heterocyclic Chemistry IV* 419–499 (Elsevier, 2021).

134. Somerville, R. L. Purine. in *Brenner's Encyclopedia of Genetics: Second Edition* 536–536 (Elsevier Inc., 2013).

135. Kumari, A. Purine Structures. in *Sweet Biochemistry* 89–91 (Elsevier, 2018).

136. Dračínský, M. & Pohl, R. NMR Studies of Purines. in *Annual Reports on NMR Spectroscopy* vol. 82 59–113 (Academic Press Inc., 2014).

137. Aaron, J. J. & Aaron, S. E. Purines, pyrimidines, and nucleotides. in *Encyclopedia of Analytical Science* 432–444 (Elsevier, 2019).

138. Sharma, S. *et al.* Design strategies, structure activity relationship and mechanistic insights for purines as kinase inhibitors. *European Journal of Medicinal Chemistry* vol. 112 298–346, (2016).

139. Dolečková, I. *et al.* Synthesis and biological evaluation of guanidino analogues of roscovitine. *Eur J Med Chem* **62**, 443–452 (2013).

University of Ghana http://ugspace.ug.edu.gh

140. Vlková, K., Gucký, T., Peřina, M., Řezníčková, E. & Kryštof, V. Synthesis and biological activity evaluation of novel 2,6,9-trisubstituted purine conjugates as potential protein kinases inhibitors. *Bioorg Med Chem Lett* **60**, (2022).

141. Wang, Y. *et al.* Bone-targeted 2,6,9-trisubstituted purines: Novel inhibitors of Src tyrosine kinase for the treatment of bone diseases. *Bioorg Med Chem Lett* **13**, 3067–3070 (2003).

142. Finger, V. *et al.* 2,6-Disubstituted 7-(naphthalen-2-ylmethyl)-7H-purines as a new class of potent antitubercular agents inhibiting DprE1. *Eur J Med Chem* **258**, (2023).

143. Chaurasiya, A., Wahan, S. K., Sahu, C. & Chawla, P. A. An insight into the rational design of recent purine-based scaffolds in targeting various cancer pathways. *Journal of Molecular Structure* vol. 1274, (2023).

144. Paintsil, E. & Cheng, Y.-C. *Antiviral Agents*. Elsevier Inc., (2009).

145. Thakur, S., Ansari, A. J. & Joshi, G. FDA approved fused pyrimidine-based drugs. in *Fused Pyrimidine-Based Drug Discovery* 13–38 (Elsevier, 2022).

146. Das, A. P. & Agarwal, S. M. Recent advances in the area of plant-based anticancer drug discovery using computational approaches. *Molecular Diversity* vol. 28, 901, (2024).

147. Dagar, G. *et al.* The future of cancer treatment: combining radiotherapy with immunotherapy. *Frontiers in Molecular Biosciences* vol. 11, (2024).

148. Huang, L. H., Xu, H. De, Yang, Z. Y., Zheng, Y. F. & Liu, H. M. Synthesis and anticancer activity of novel C6-piperazine substituted purine steroid-nucleosides analogues. *Steroids* **82**, 1–6 (2014).

149. Park, S. Y. *et al.* Design, synthesis, and evaluation of purine and pyrimidine-based KRAS G12D inhibitors: Towards potential anticancer therapy. *Heliyon* **10**, (2024).

150. Kowalska, A., Latocha, M. & Pluta, K. Synthesis and anticancer activity of thiosubstituted purines. *Medicinal Chemistry Research* **24**, 3107–3116 (2015).

151. Vicenti, I. *et al.* System-oriented optimization of multi-target 2,6-diaminopurine derivatives: Easily accessible broad-spectrum antivirals active against flaviviruses, influenza virus and SARS-CoV-2. *Eur J Med Chem* **224**, (2021).

152. Martina, M. G. *et al.* Nucleoside Derivatives of 2,6-Diaminopurine Antivirals Base-Modified Nucleosides with Broad-Spectrum Antimicrobial Properties. *ChemMedChem* **18**, (2023).

153. Zhu, M. *et al.* Synthesis and biological evaluation of new HIV-1 protease inhibitors with purine bases as P2-ligands. *Bioorg Med Chem Lett* **29**, 1541–1545 (2019).

154. Kang, D. *et al.* Synthesis and Preliminary Antiviral Activities of Piperidine-substituted Purines against HIV and Influenza A/H1N1 Infections. *Chem Biol Drug Des* **86**, 568–577 (2015).

University of Ghana http://ugspace.ug.edu.gh

155. Zenchenko, A. A., Drenichev, M. S., Il'icheva, I. A. & Mikhailov, S. N. Antiviral and Antimicrobial Nucleoside Derivatives: Structural Features and Mechanisms of Action. *Molecular Biology* vol. 55 786–812, (2021).

156. Wang, Y. N., Bheemanaboina, R. R. Y., Cai, G. X. & Zhou, C. H. Novel purine benzimidazoles as antimicrobial agents by regulating ROS generation and targeting clinically resistant Staphylococcus aureus DNA groove. *Bioorg Med Chem Lett* **28**, 1621–1628 (2018).

157. Nadaf, A. Q. A. *et al.* Synthesis of 6-[4-(4-Propoxyphenyl)piperazin-1-yl]-9H-purine Derivatives as Antimycobacterial and Antifungal Agents: In Vitro Evaluation and In Silico Study. *Chem Biodivers* **17**, (2020).

158. Konduri, S. *et al.* Design and synthesis of purine connected piperazine derivatives as novel inhibitors of Mycobacterium tuberculosis. *Bioorg Med Chem Lett* **30**, (2020).

159. Pathak, A. K., Pathak, V., Seitz, L. E., Suling, W. J. & Reynolds, R. C. 6-Oxo and 6-thio purine analogs as antimycobacterial agents. *Bioorg Med Chem* **21**, 1685–1695 (2013).

160. Hocková, D. *et al.* Antimalarial activity of prodrugs of N-branched acyclic nucleoside phosphonate inhibitors of 6-oxopurine phosphoribosyltransferases. *Bioorg Med Chem* **23**, 5502–5510 (2015).

161. Mohamed, S. B. *et al.* Purine containing carbonucleoside phosphonate analogues as novel chemotype for plasmodium falciparum inhibition. *Eur J Med Chem* **258**, 115581 (2023).

162. Gaffo, A. L. Crystal Diseases. in *Pathobiology of Human Disease: A Dynamic Encyclopedia of Disease Mechanisms* 1935–1949 (Elsevier Inc., 2014).

163. Torres Jiménez, R. & Puig, J. G. *Purine Metabolism in the Pathogenesis of Hyperuricemia and Inborn Errors of Purine Metabolism Associated with Disease*.

164. Dewulf, J. P., Marie, S. & Nassogne, M. C. Disorders of purine biosynthesis metabolism. *Molecular Genetics and Metabolism* vol. 136 190–198, (2022).

165. Wu, D. *et al.* Targeting purine metabolism-related enzymes for therapeutic intervention: A review from molecular mechanism to therapeutic breakthrough. *International Journal of Biological Macromolecules* vol. 282, (2024).

166. Yin, J. *et al.* Potential Mechanisms Connecting Purine Metabolism and Cancer Therapy. *Frontiers in Immunology* vol. 9, (2018).

167. Dewulf, J. P., Marie, S. & Nassogne, M. C. Disorders of purine biosynthesis metabolism. *Molecular Genetics and Metabolism* vol. 136 190–198, (2022).

168. Liu, J. *et al.* Targeting purine metabolism in ovarian cancer. *Journal of Ovarian Research* vol. 15, (2022).

169. Blanco, A. & Blanco, G. Purine and pyrimidine metabolism. in *Medical Biochemistry* 449–460 (Elsevier, 2022).

University of Ghana http://ugspace.ug.edu.gh

170. Pedley, A. M. & Benkovic, S. J. A New View into the Regulation of Purine Metabolism: The Purinosome. *Trends in Biochemical Sciences* vol. 42 141–154, (2017).

171. Yin, J. *et al.* Potential Mechanisms Connecting Purine Metabolism and Cancer Therapy. *Frontiers in Immunology* vol. 9, (2018).

172. Yang, K., Li, J. & Tao, L. Purine metabolism in the development of osteoporosis. *Biomedicine and Pharmacotherapy* vol. 155, (2022).

173. Popowycz, F., Routier, S., Joseph, B., & Mérour, J. Y., Synthesis and reactivity of 7-azaindole (1H-pyrrolo[2,3-b]pyridine). *Tetrahedron*, **63** (5), 1031–1064, (2007).

174. Voloshchuk, V. v., & Ivonin, S. P., Recent Advances in the Synthesis and Biological Activity of Pyrrolo[2,3-c]pyridines. *Journal of Organic and Pharmaceutical Chemistry*, *22*(1), 33–56, (2024).

175. Fang, G., Chen, H., Cheng, Z., Tang, Z. & Wan, Y. Azaindole derivatives as potential kinase inhibitors and their SARs elucidation. *Eur J Med Chem* **258**, 115621 (2023).

176. Motati, D. R., Amaradhi, R. & Ganesh, T. Azaindole therapeutic agents. *Bioorg Med Chem* **28**, 115830 (2020).

177. Fang, G., Chen, H., Cheng, Z., Tang, Z. & Wan, Y. Azaindole derivatives as potential kinase inhibitors and their SARs elucidation. *Eur J Med Chem* **258**, 115621 (2023).

178. Motati, D. R., Amaradhi, R. & Ganesh, T. Azaindole therapeutic agents. *Bioorg Med Chem* **28**, 115830 (2020).

179. Štarha, P. & Trávníček, Z. Azaindoles: Suitable ligands of cytotoxic transition metal complexes. *J Inorg Biochem* **197**, (2019).

180. Jose, G. *et al.* European Journal of Medicinal Chemistry Synthesis, molecular docking, antimycobacterial and antimicrobial evaluation of new pyrrolo [3 , 2- c] pyridine Mannich bases. **131**, (2017).

181. Verdonck, S. *et al.* Synthesis and Structure-Activity Relationships of 3,5-Disubstituted-pyrrolo[2,3- b]pyridines as Inhibitors of Adaptor-Associated Kinase 1 with Antiviral Activity. *J Med Chem* **62**, 5810–5831 (2019).

182. Ullah, S. *et al.* Synthesis, biological evaluation, and docking studies of novel pyrrolo[2,3-b]pyridine derivatives as both ectonucleotide pyrophosphatase/phosphodiesterase inhibitors and antiproliferative agents. *Eur J Med Chem* **217**, (2021).

183. Štarha, P. & Trávníček, Z. Azaindoles: Suitable ligands of cytotoxic transition metal complexes. *J Inorg Biochem* **197**, (2019).

184. Jose, G. *et al.* European Journal of Medicinal Chemistry Synthesis, molecular docking, antimycobacterial and antimicrobial evaluation of new pyrrolo [3 , 2- c] pyridine Mannich bases. **131**, (2017).

University of Ghana http://ugspace.ug.edu.gh

185. Elkanzi, N. A. A. Design, Synthesis, Molecular Modeling Study, and Antimicrobial Activity of Some Novel Pyrano [2 , 3- b] pyridine and Pyrrolo [2 , 3- b] pyrano [2, 3- d] pyridine Derivatives. (2018).

186. Elkanzi, N. A. A. Design, Synthesis, Molecular Modeling Study, and Antimicrobial Activity of Some Novel Pyrano [2 , 3- b] pyridine and Pyrrolo [2 , 3- b] pyrano [2 . 3- d] pyridine Derivatives. (2018).

187. Hu, H., Chen, F., Dong, Y., Liu, Y. & Gong, P. Bioorganic Chemistry Discovery of novel dual c-Met / HDAC inhibitors as a promising strategy for cancer therapy. **101**, (2020).

188. Kulagowski, J. J. *et al.* Identification of imidazo-pyrrolopyridines as novel and potent JAK1 inhibitors. *J Med Chem* **55**, 5901–5921 (2012).

189. Zhang, J. *et al.* European Journal of Medicinal Chemistry Synthesis, bioevaluation and molecular dynamics of pyrrolo-pyridine benzamide derivatives as potential antitumor agents in vitro and in vivo. **233**, (2022).

190. Patrick, G. L. & Turner, H. *Kinases and Kinase Inhibitors*. *Antimalarial Agents: Design and Mechanism of Action* (2020).

191. Vanelle, P. & Primas, N. Plasmodial Kinase Inhibitors Targeting Malaria: (2020).

192. Boura, E. & Nencka, R. Phosphatidylinositol 4-kinases: Function, structure, and inhibition. **337**, 136–145 (2015).

193. Li, Y. ping *et al.* Research progress of phosphatidylinositol 4-kinase and its inhibitors in inflammatory diseases. *Eur J Pharmacol* **907**, (2021).

194. Misehe, M. *et al.* Structure-based design and modular synthesis of novel PI4K class II inhibitors bearing a 4-aminoquinazoline scaffold. *Bioorg Med Chem Lett* **76**, (2022).

195. Graham, T. R. & Burd, C. G. Coordination of Golgi functions by phosphatidylinositol 4-kinases. *Trends Cell Biol* **21**, 113–121 (2011).

196. Liang, X. *et al.* Discovery of 6′-chloro-N-methyl-5’-(phenylsulfonamido)-[3,3′-bipyridine]-5-carboxamide (CHMFL-PI4K-127) as a novel Plasmodium falciparum PI(4)K inhibitor with potent antimalarial activity against both blood and liver stages of Plasmodium. *Eur J Med Chem* **188**, (2020).

197. Patrick, G. L. & Turner, H. Kinases and kinase inhibitors. in *Antimalarial Agents: Design and Mechanism of Action* 459–494 (Elsevier, 2020).

198. Fienberg, S. *et al.* Structural Basis for Inhibitor Potency and Selectivity of Plasmodium falciparum Phosphatidylinositol 4-Kinase Inhibitors. *ACS Infect Dis* **6**, 3048–3063 (2020).

199. Kato, N. *et al.* Diversity-oriented synthesis yields novel multistage antimalarial inhibitors. *Nature* **538**, 344–349 (2016).

University of Ghana http://ugspace.ug.edu.gh

200. Parai, M. K., Panda, G., Srivastava, K. & Kumar, S. Design, synthesis and antimalarial activity of benzene and isoquinoline sulfonamide derivatives q. **18**, 776–781 (2008).

201. Andrews, K. T. *et al.* Bioorganic & Medicinal Chemistry Letters Antimalarial activity of compounds comprising a primary benzene sulfonamide fragment. **23**, 6114–6117 (2013).

202. Hassanein, M. M. Sulfonamides: far from obsolete. **6**, 2740–2745 (2019).

203. Mondal, S. & Malakar, S. Synthesis of sulfonamide and their synthetic and therapeutic applications: Recent advances. **76**, (2020).

204. Mondal, S. & Malakar, S. Synthesis of sulfonamide and their synthetic and therapeutic applications: Recent advances. **76**, (2020).

205. Lin, M. *et al.* MalariaFlow: A comprehensive deep learning platform for multistage phenotypic antimalarial drug discovery. *Eur J Med Chem* **277**, (2024).

206. Berg L. Ellen. phenotypic screening advancing the science from discovery to regulatory science. in *Drug Discovery World* (2017).

207. Hovlid, M. L. & Winzeler, E. A. Phenotypic Screens in Antimalarial Drug Discovery. *Trends in Parasitology* vol. 32 697–707, (2016).

208. Aulner, N., Danckaert, A., Ihm, J. E., Shum, D. & Shorte, S. L. Next-Generation Phenotypic Screening in Early Drug Discovery for Infectious Diseases. *Trends in Parasitology* vol. 35 559–570, (2019).

209. Hovlid, M. L. & Winzeler, E. A. Phenotypic screens in antimalarial drug discovery. *Trends Parasitol* **32**, 697 (2016).

210. Ege, N., Bouguenina, H., Tatari, M. & Chopra, R. Phenotypic screening with target identification and validation in the discovery and development of E3 ligase modulators. *Cell Chemical Biology* vol. 28 283–299, (2021).

211. Cho, N. *et al.* new antimalarials identified by a cell-based phenotypic approach: Structure–activity relationships of 2,3,4,9-tetrahydro-1H-β-carboline derivatives possessing a 2-((coumarin-5-yl)oxy)alkanoyl moiety. *Bioorg Med Chem* **66**, (2022).

212. Jiménez-Díaz, M. B. *et al.* (+)-SJ733, a clinical candidate for malaria that acts through ATP4 to induce rapid host-mediated clearance of Plasmodium. *Proc Natl Acad Sci U S A* **111**, E5455–E5462 (2014).

213. Baragaña, B. *et al.* A novel multiple-stage antimalarial agent that inhibits protein synthesis. *Nature* **522**, 315–320 (2015).

214. Laleu, B. *et al.* Discovery and Structure-Activity Relationships of Quinazolinone-2-carboxamide Derivatives as Novel Orally Efficacious Antimalarials. *J Med Chem* **64**, 12582–12602 (2021).

University of Ghana http://ugspace.ug.edu.gh

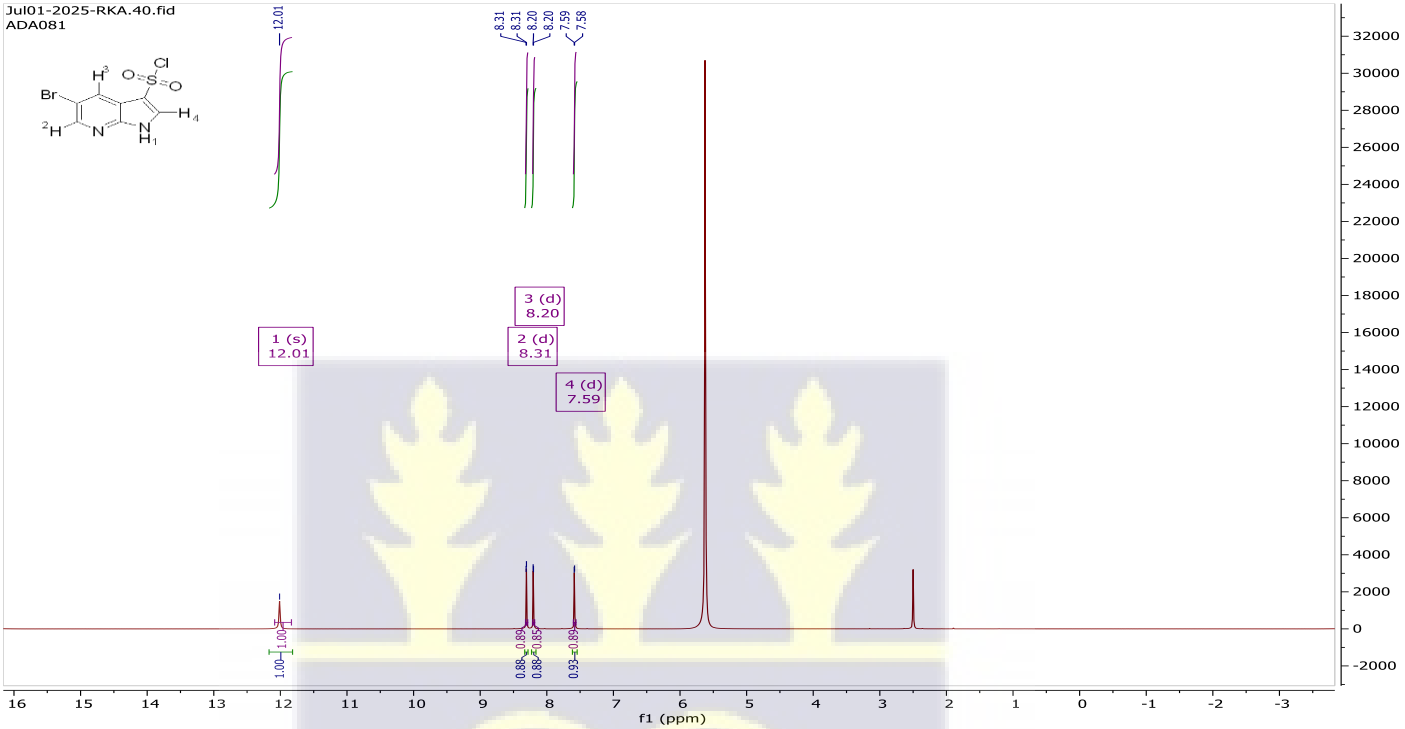
215. Hawadak, J., Chaudhry, S., Pande, V., & Singh, V., Comparison of SYBR green I and lactate dehydrogenase antimalarial in vitro assay in Plasmodium falciparum field isolates. *Journal of Pharmacological and Toxicological Methods*, *124*, (2023).

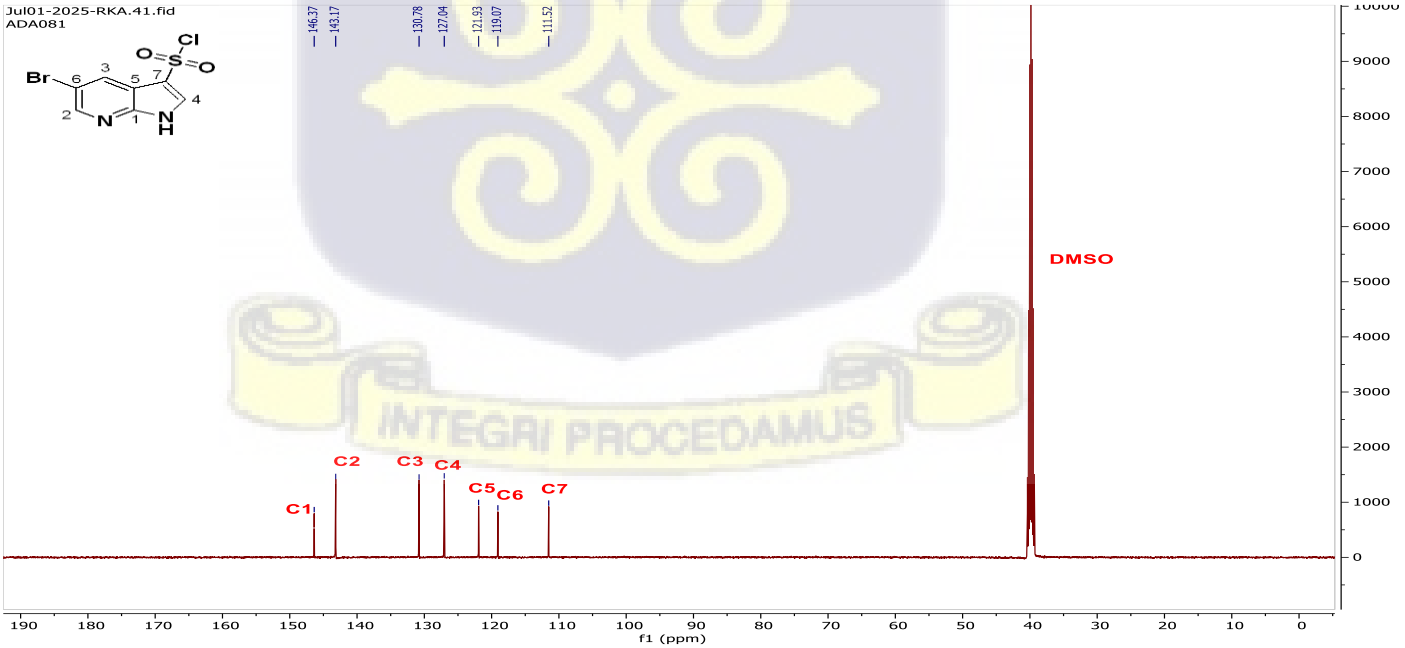
University of Ghana http://ugspace.ug.edu.gh

APPENDICES

APPENDIX I: NMR DATA

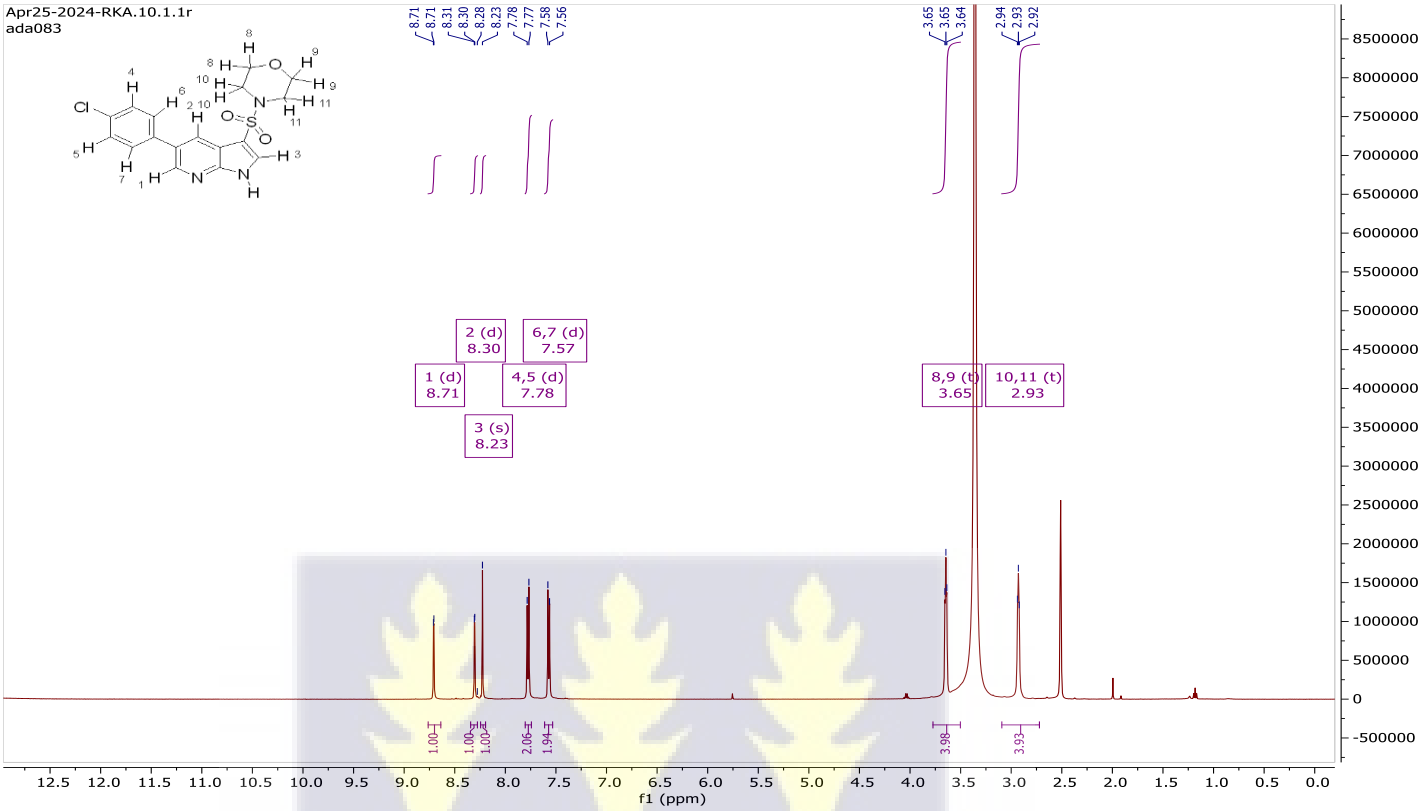
ADA081

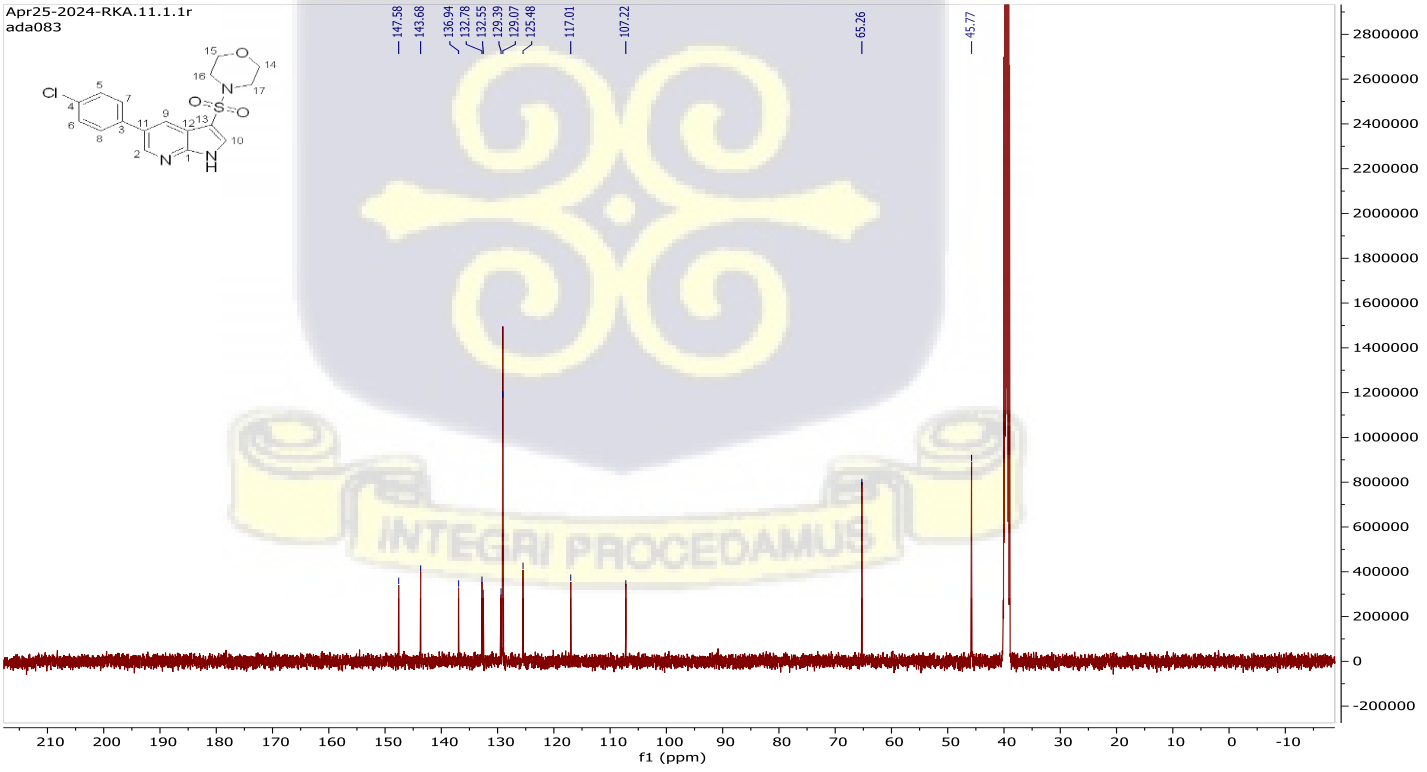




University of Ghana http://ugspace.ug.edu.gh

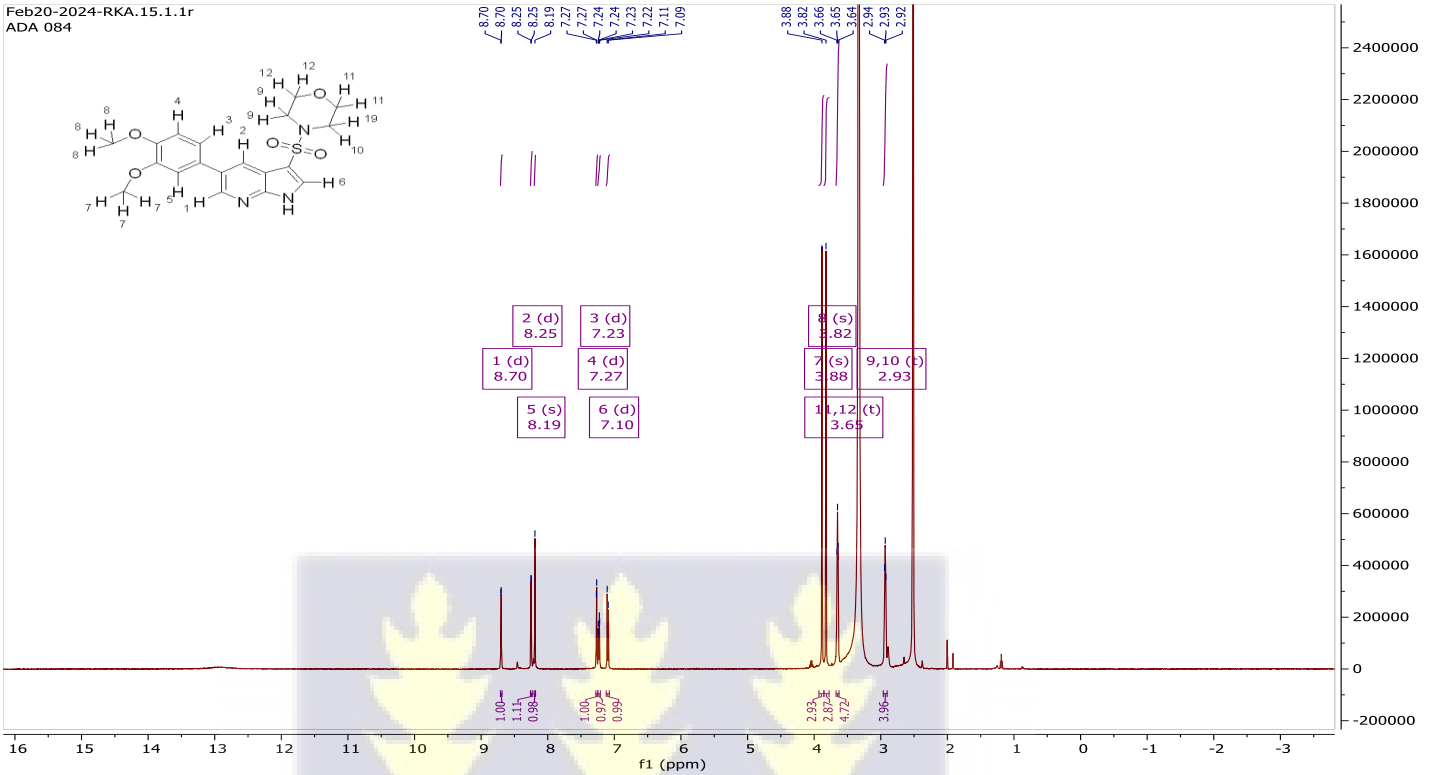
ADA083

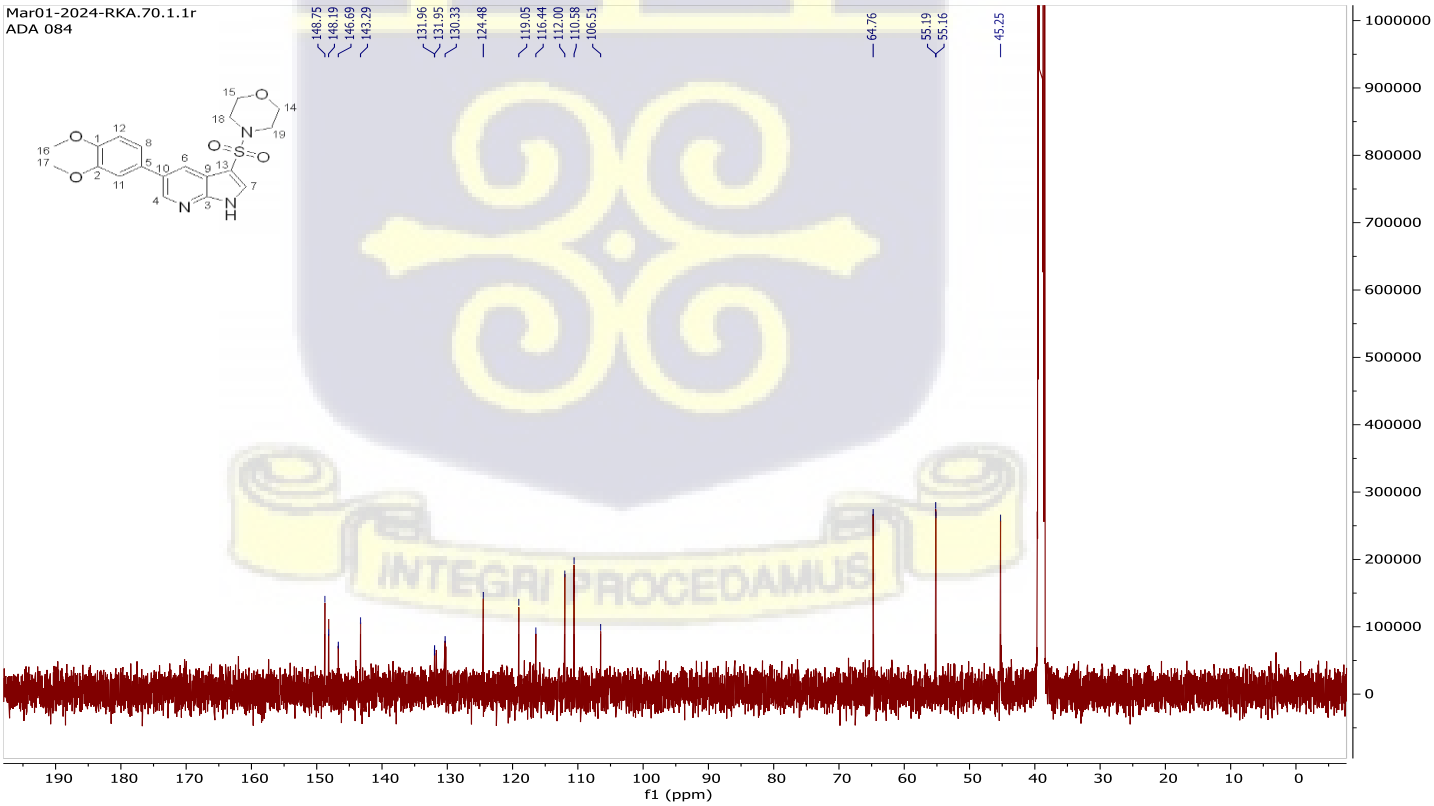




University of Ghana http://ugspace.ug.edu.gh

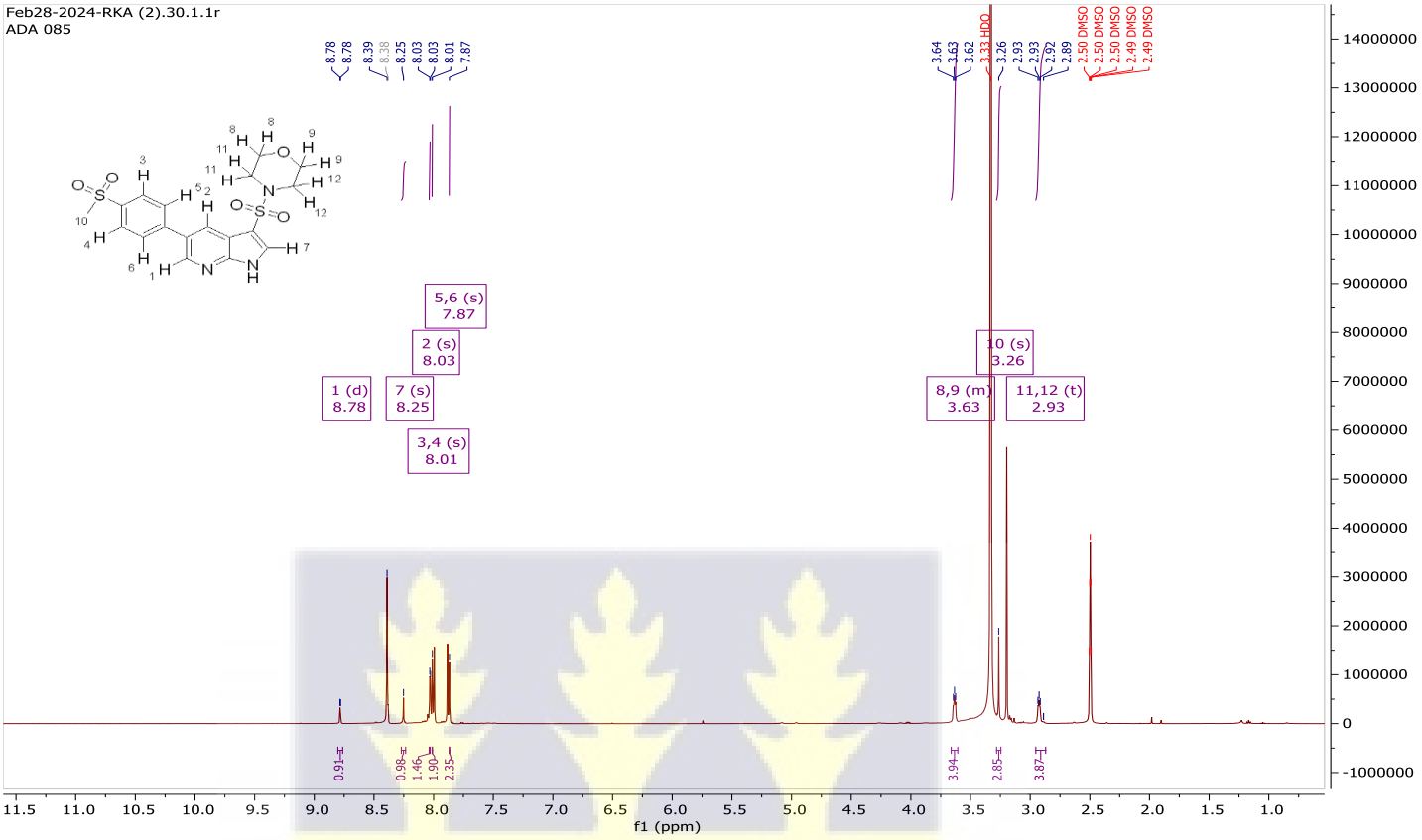
ADA084

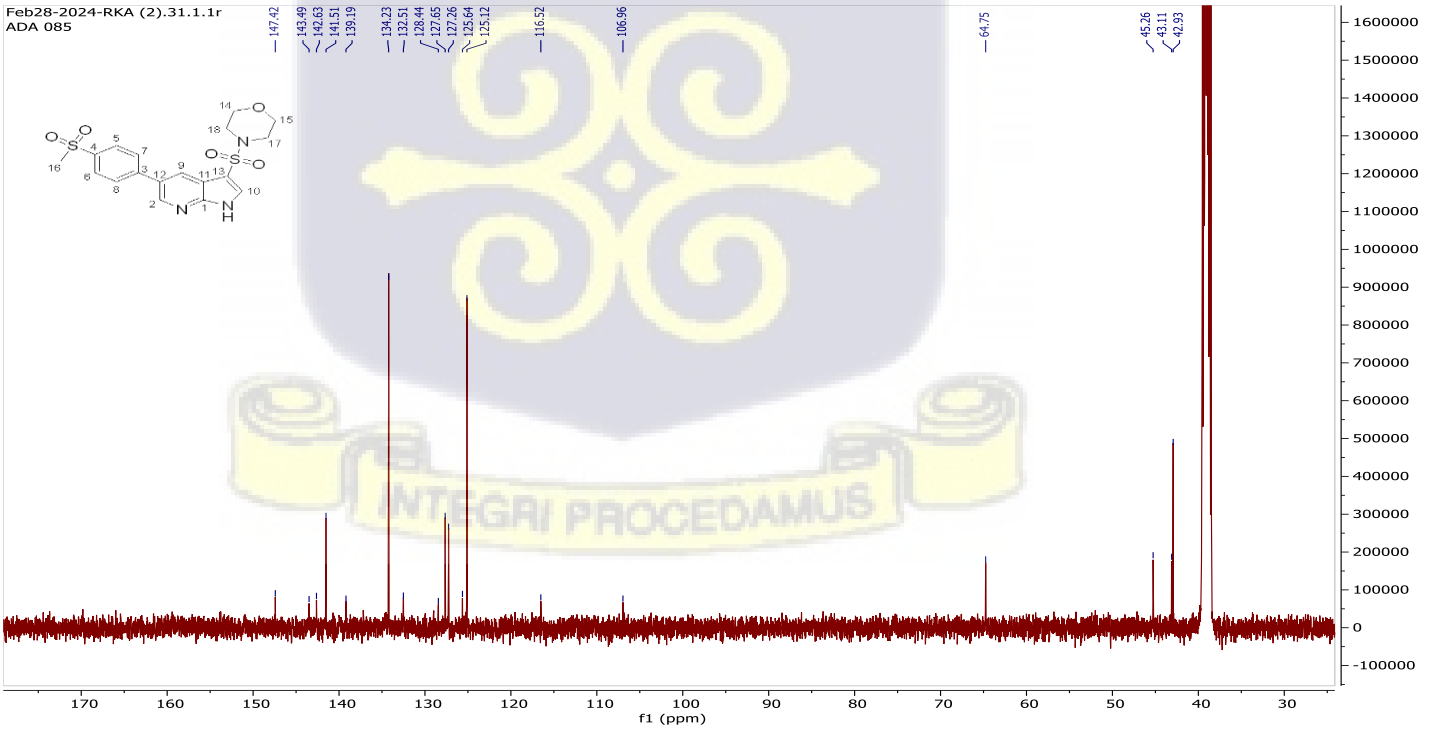




University of Ghana http://ugspace.ug.edu.gh

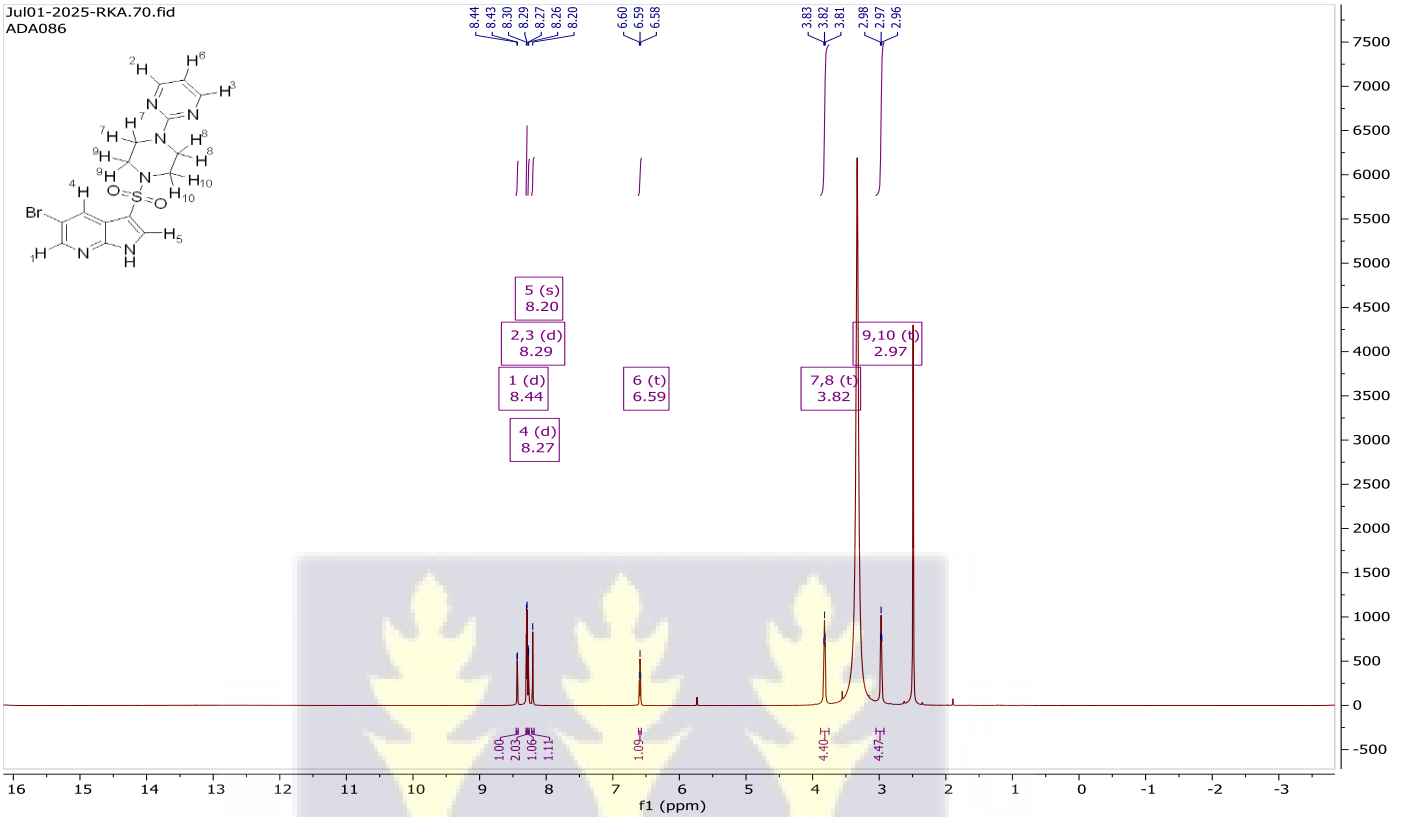
ADA085

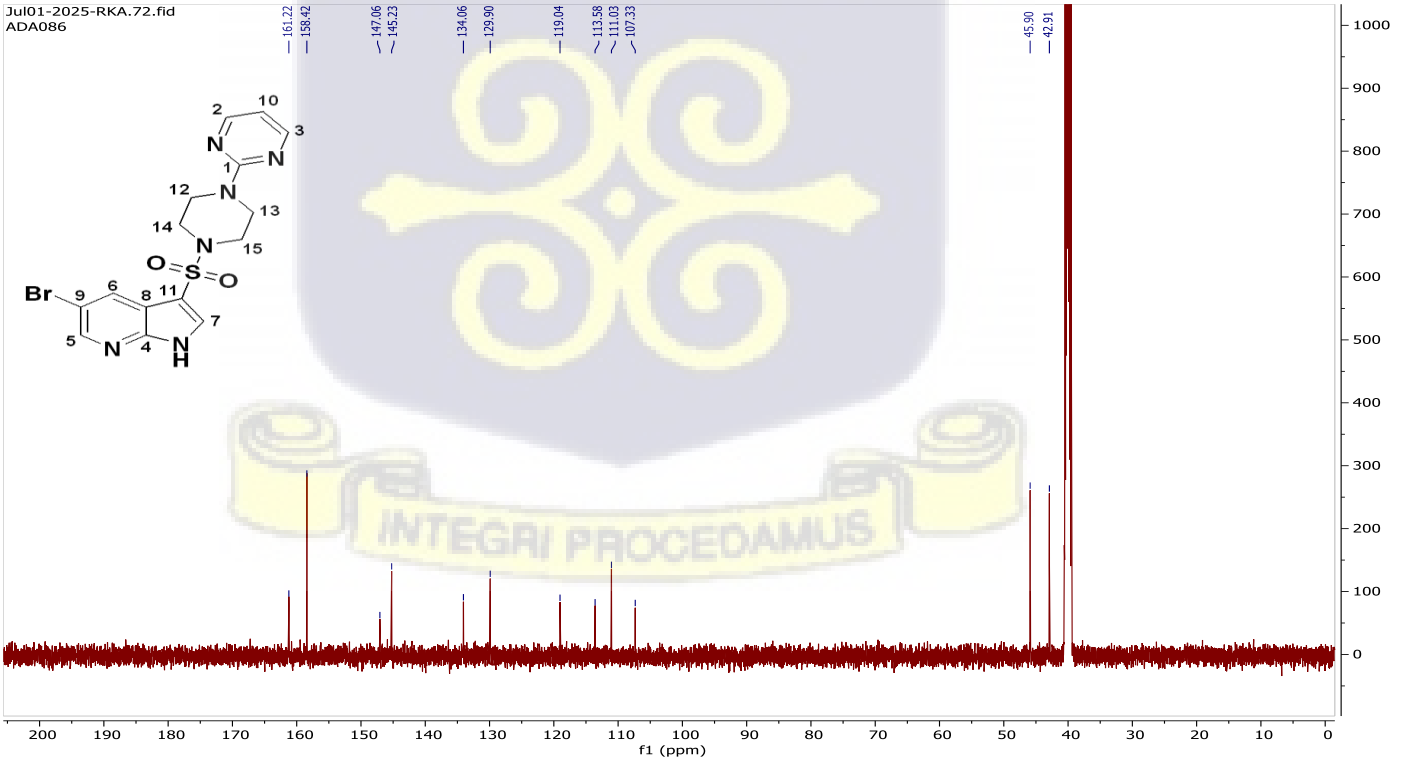




University of Ghana http://ugspace.ug.edu.gh

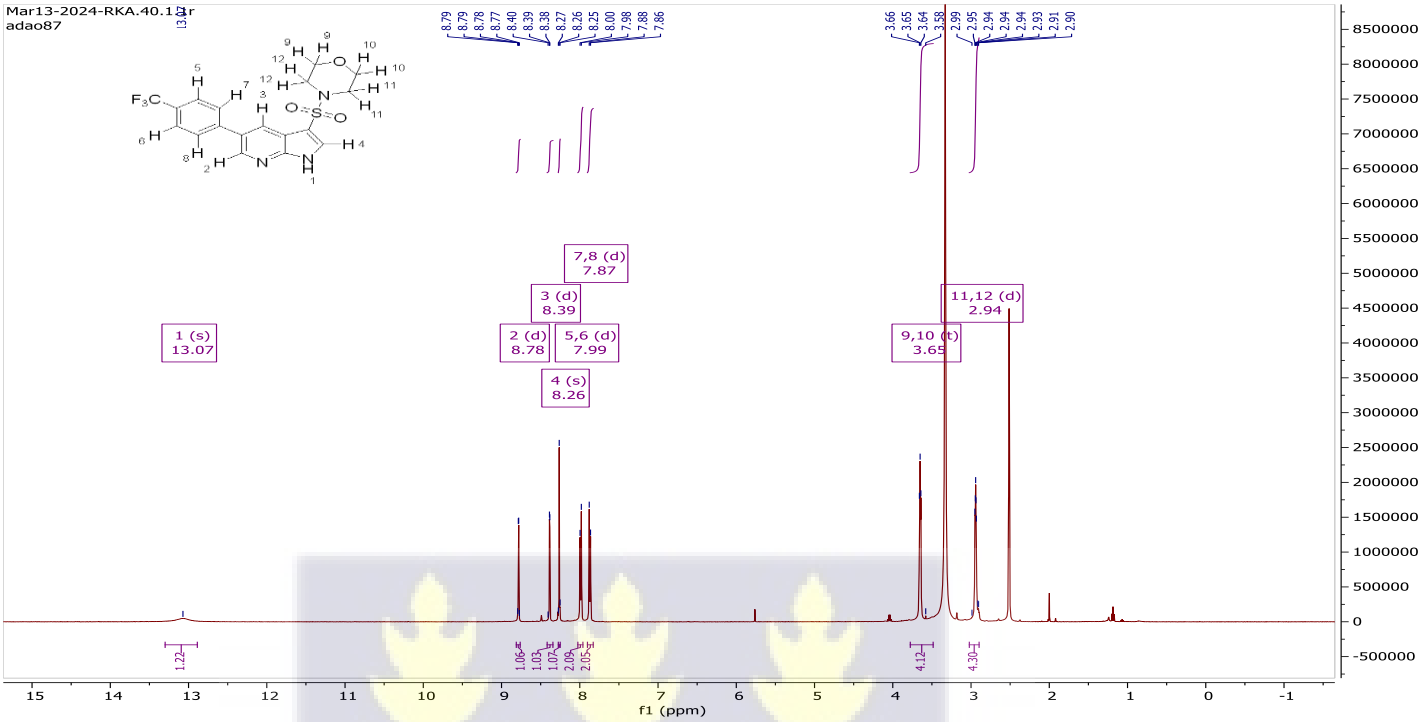
ADA086

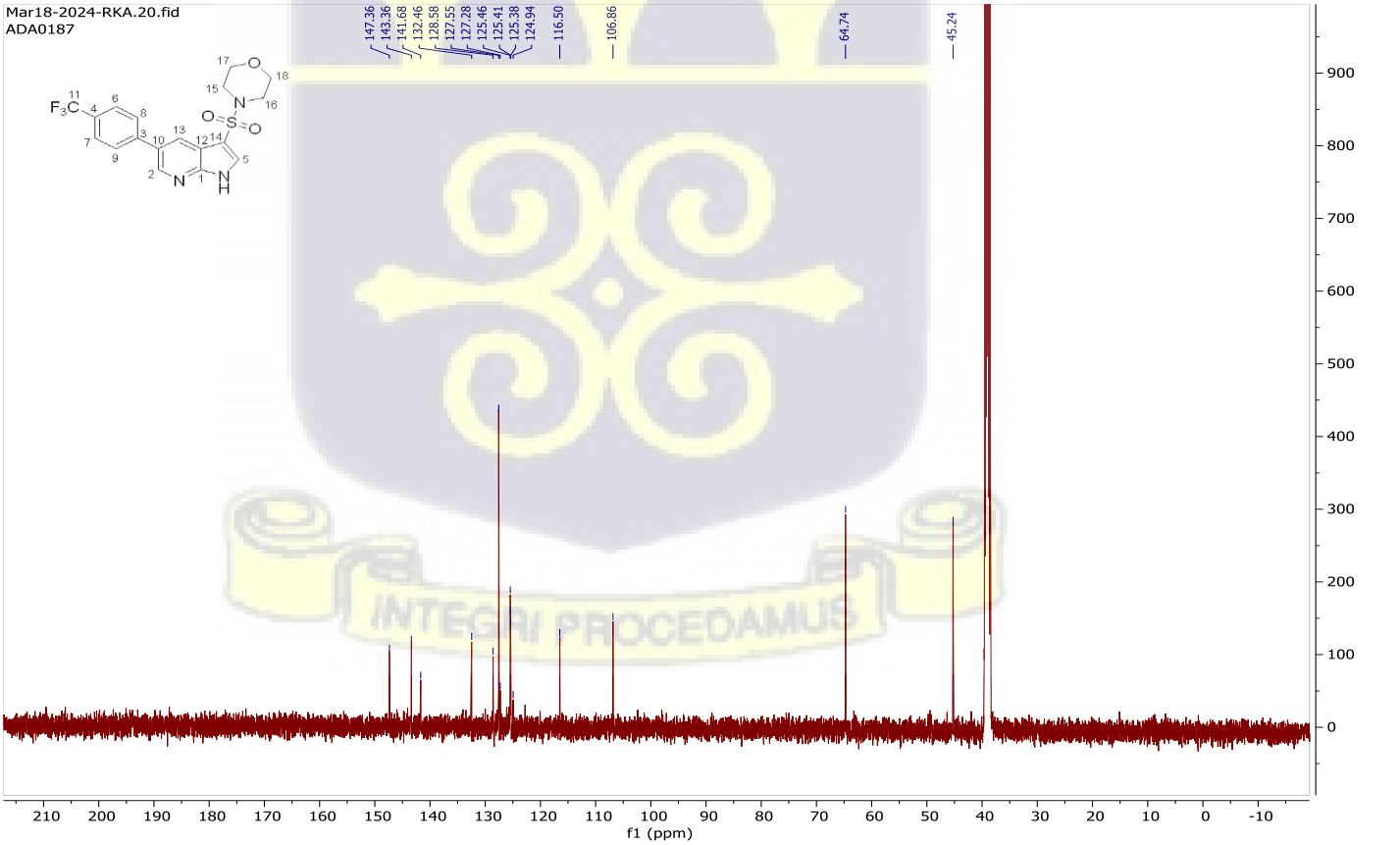




University of Ghana http://ugspace.ug.edu.gh

ADA087

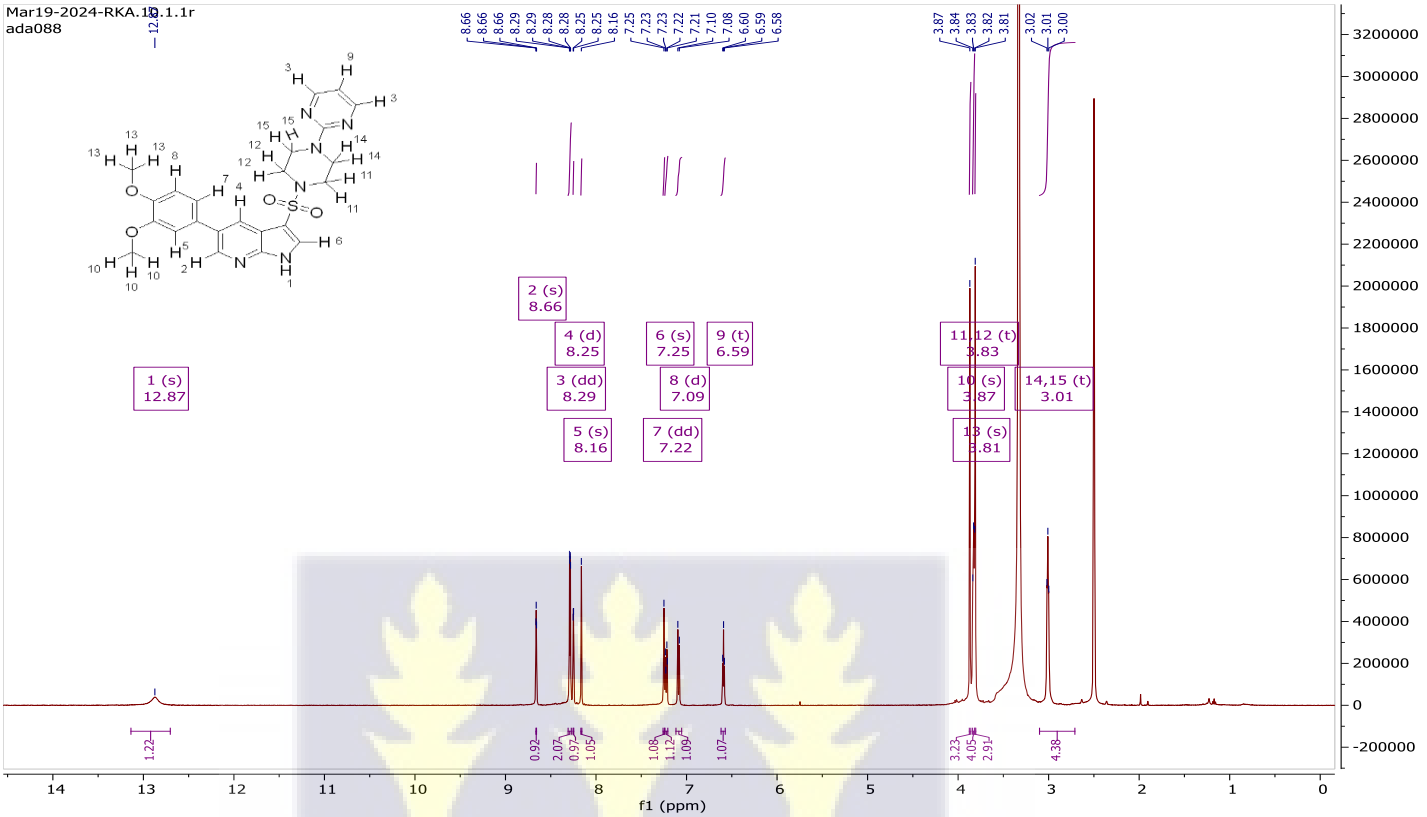


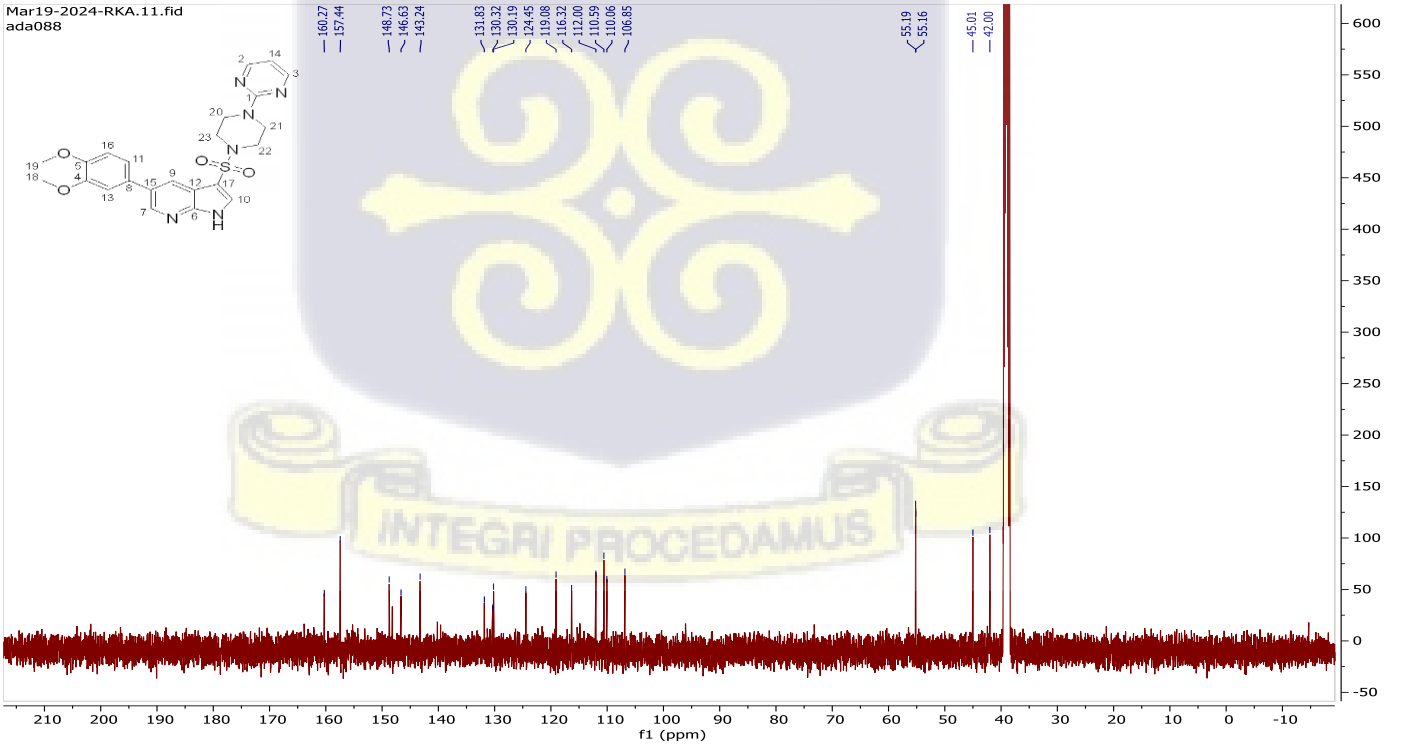


INTEGRI PROCEDAMUS

University of Ghana http://ugspace.ug.edu.gh

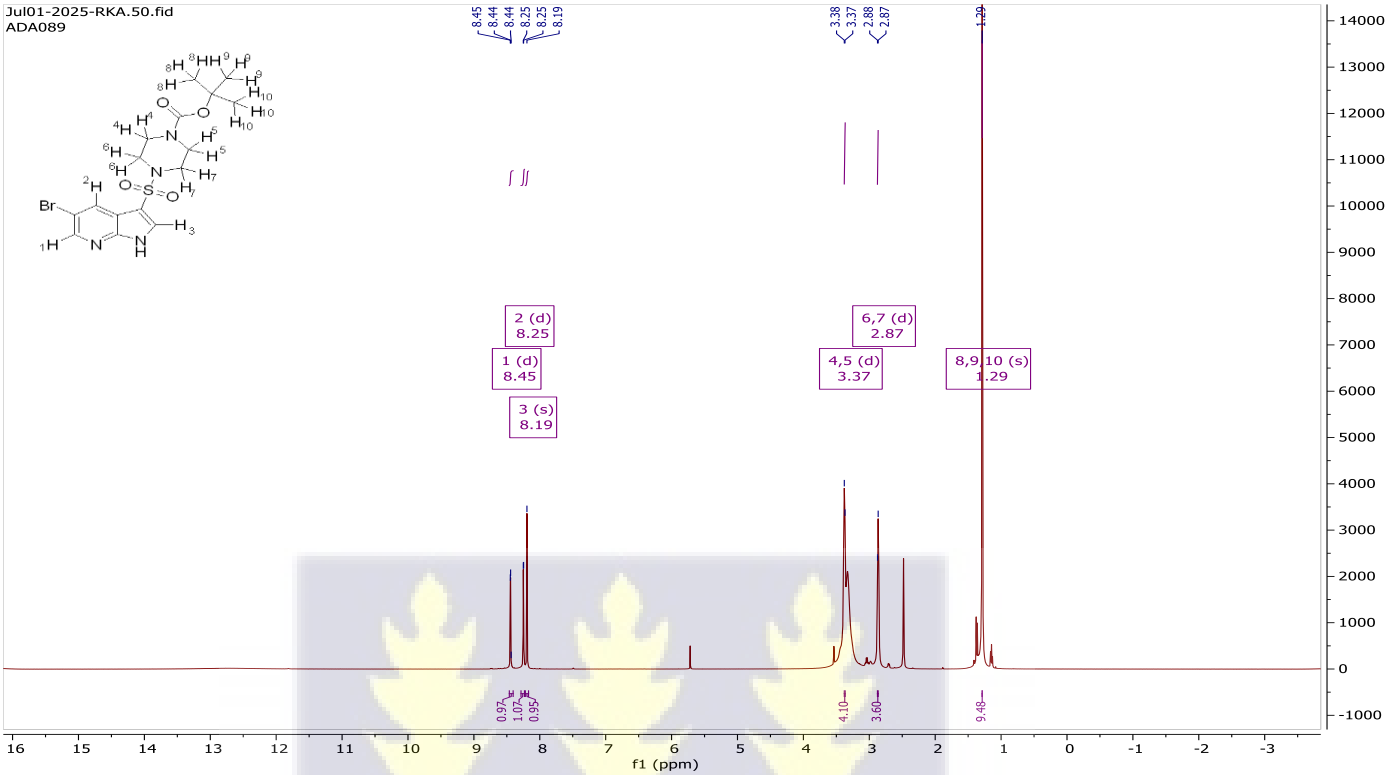
ADA088

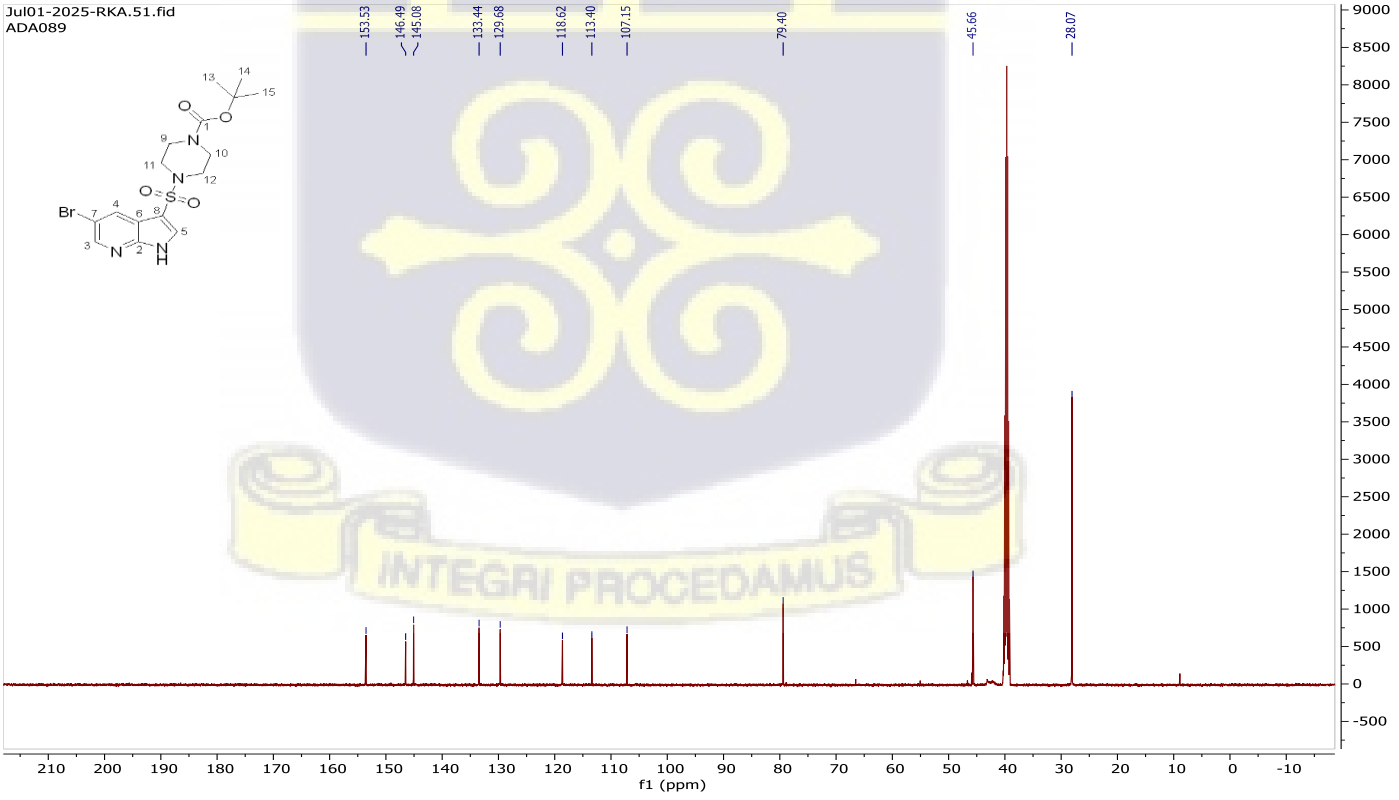




University of Ghana http://ugspace.ug.edu.gh

ADA089

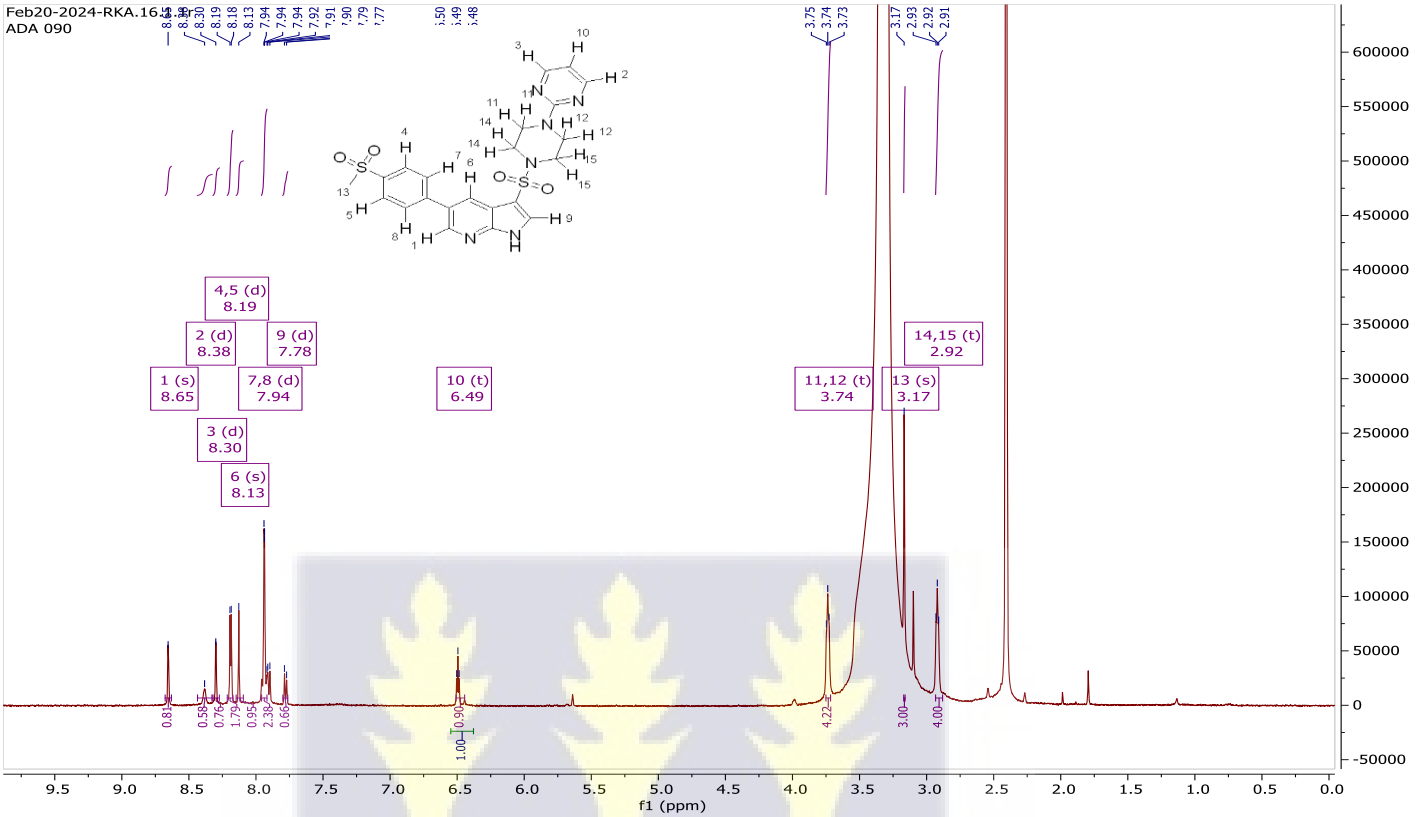


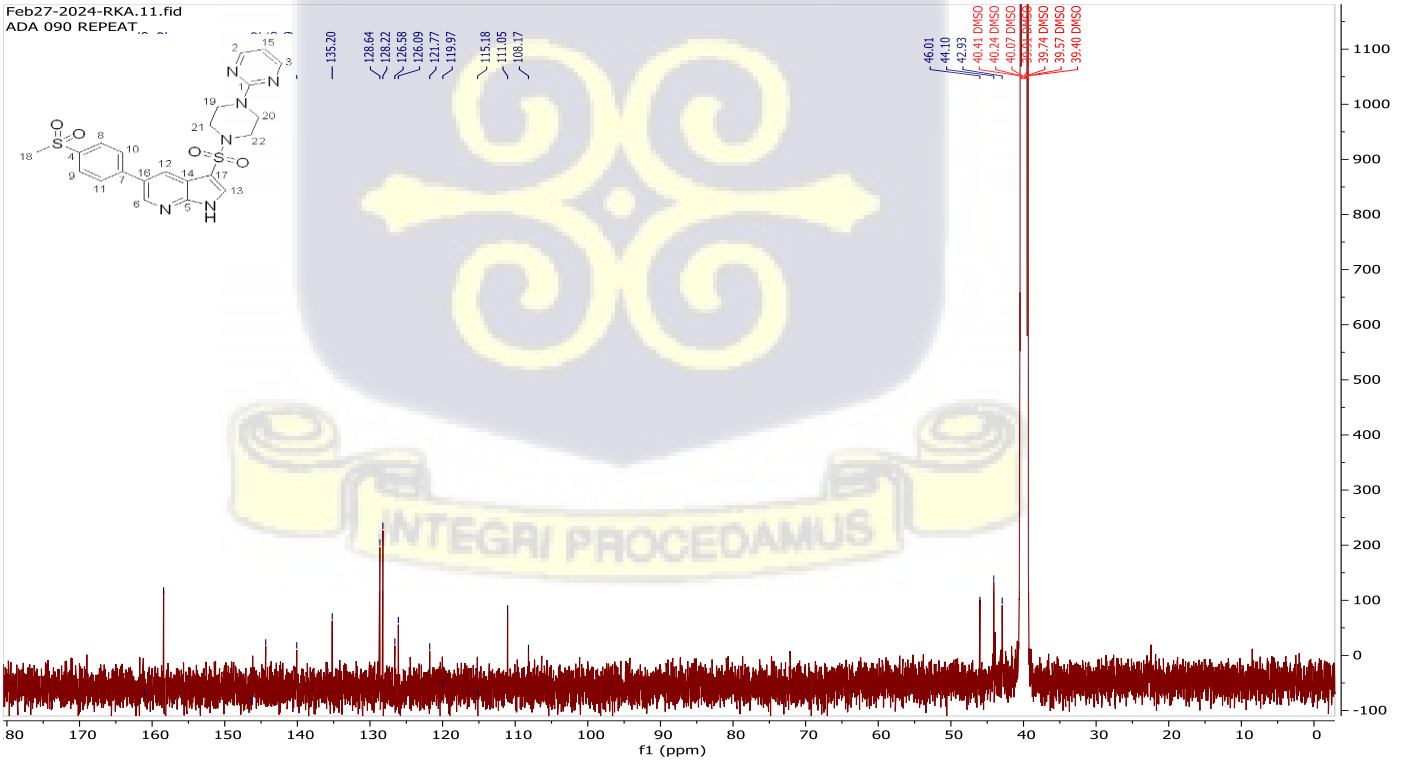


INTEGRI PROCEDAMUS

University of Ghana http://ugspace.ug.edu.gh

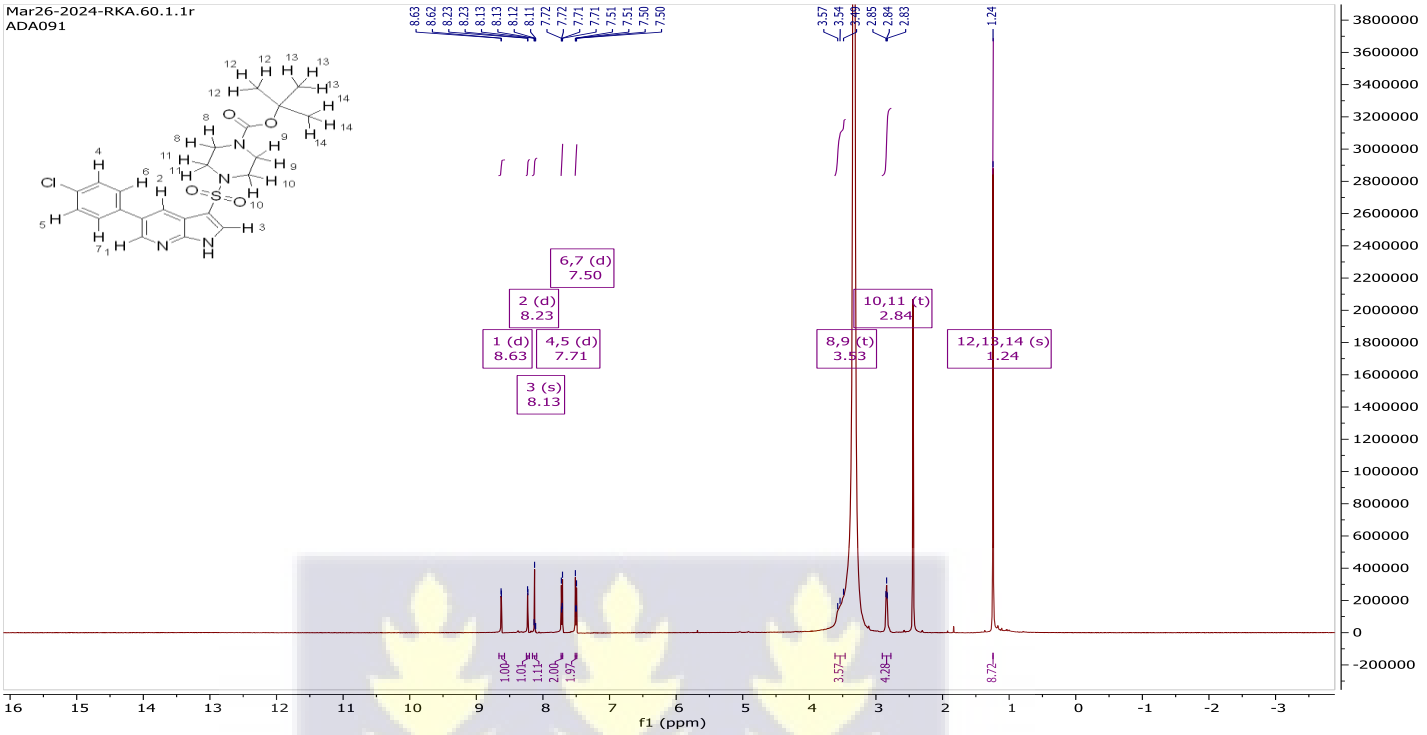
ADA090

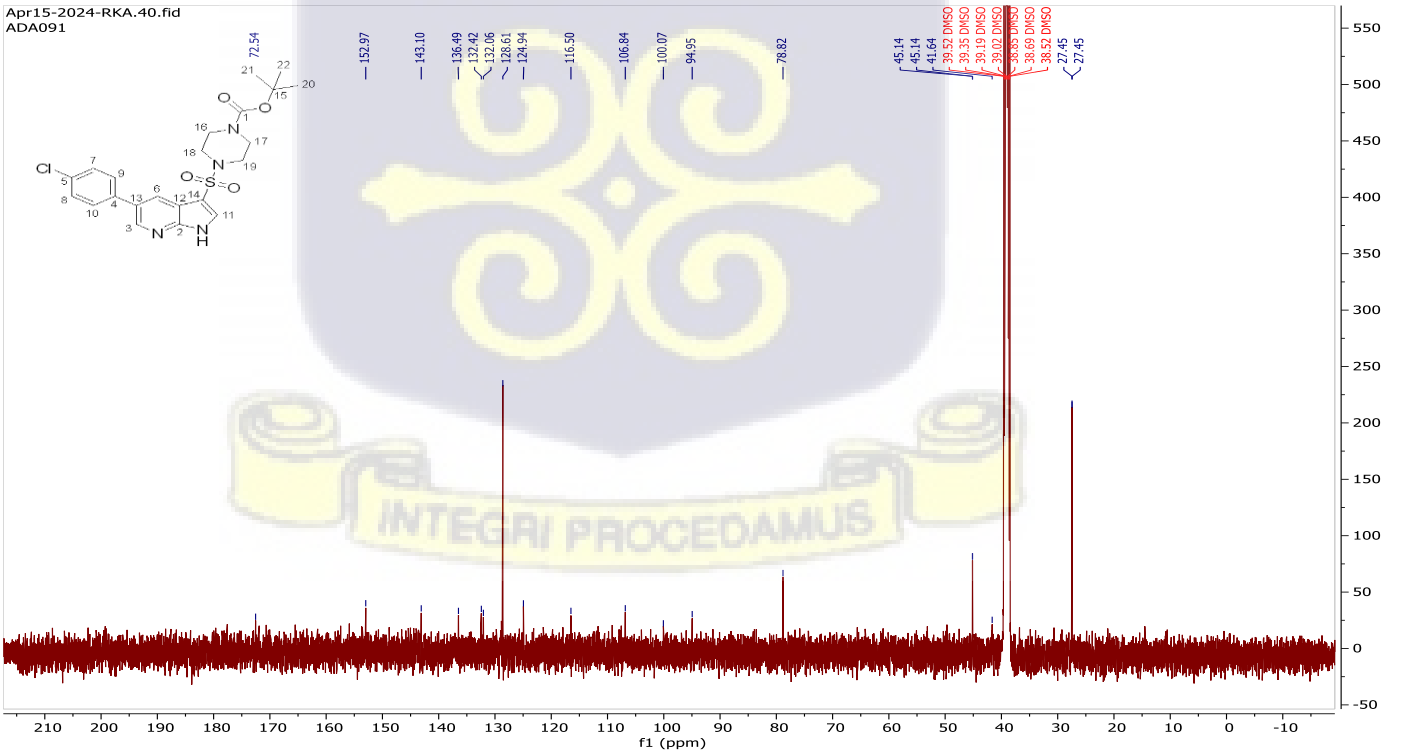




University of Ghana http://ugspace.ug.edu.gh

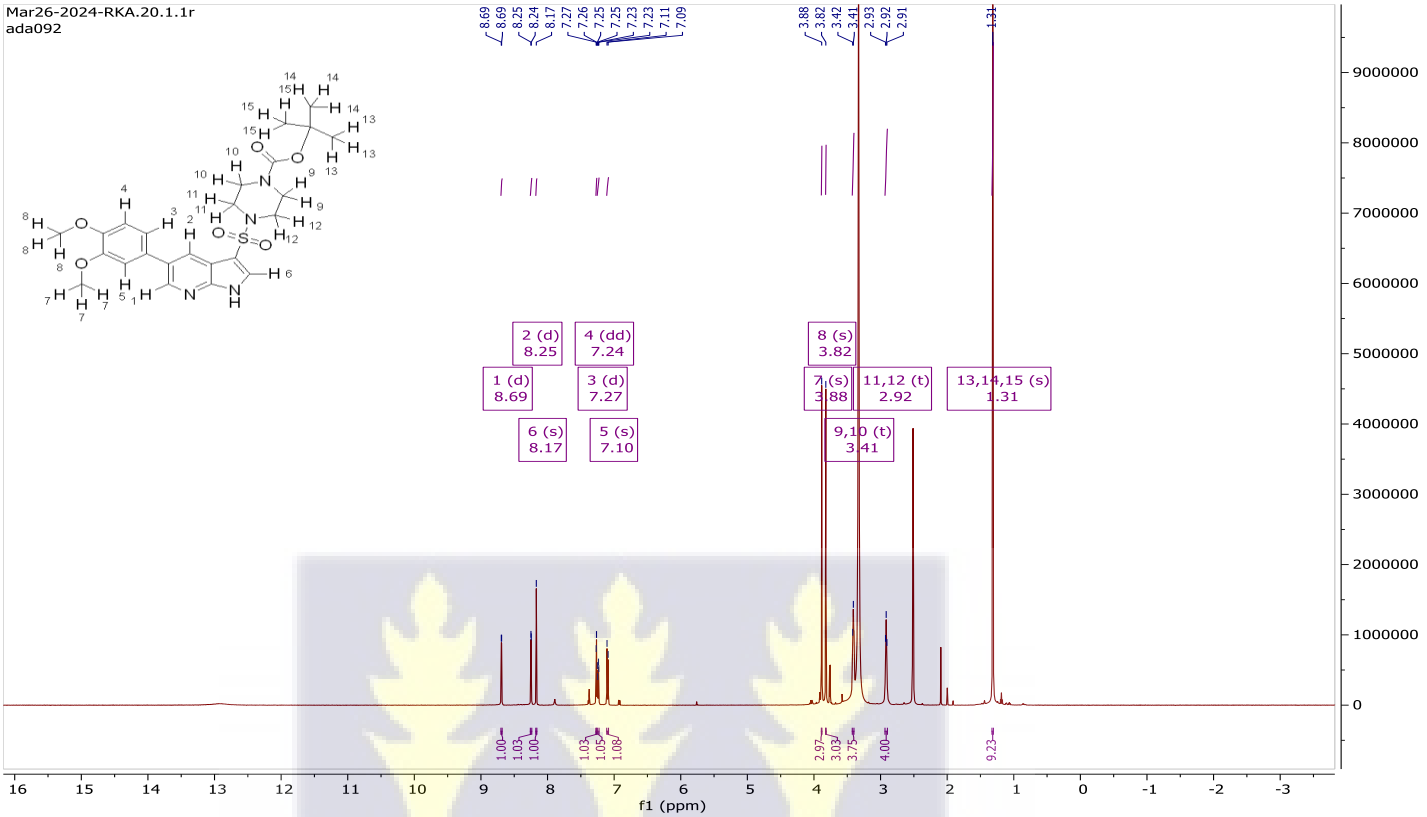
ADA091

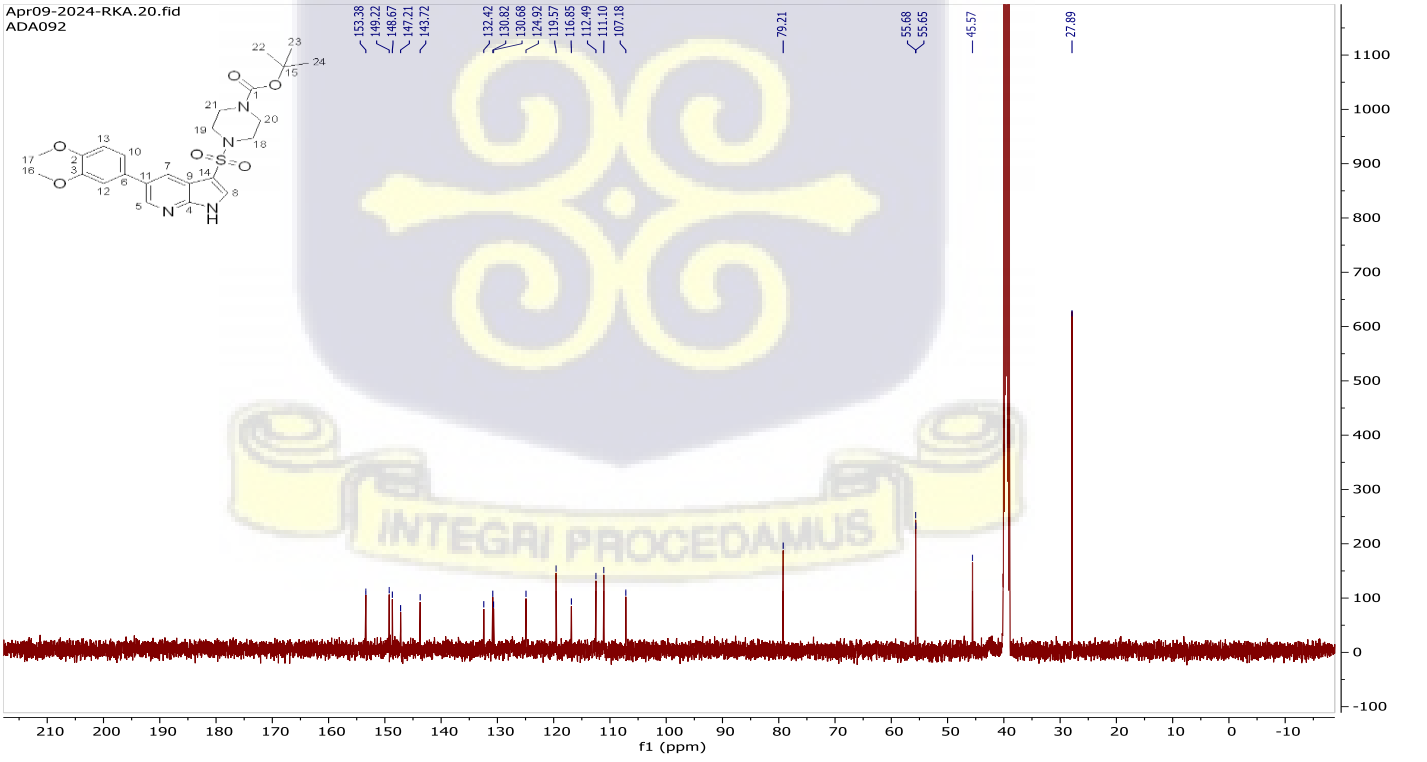




University of Ghana http://ugspace.ug.edu.gh

ADA092

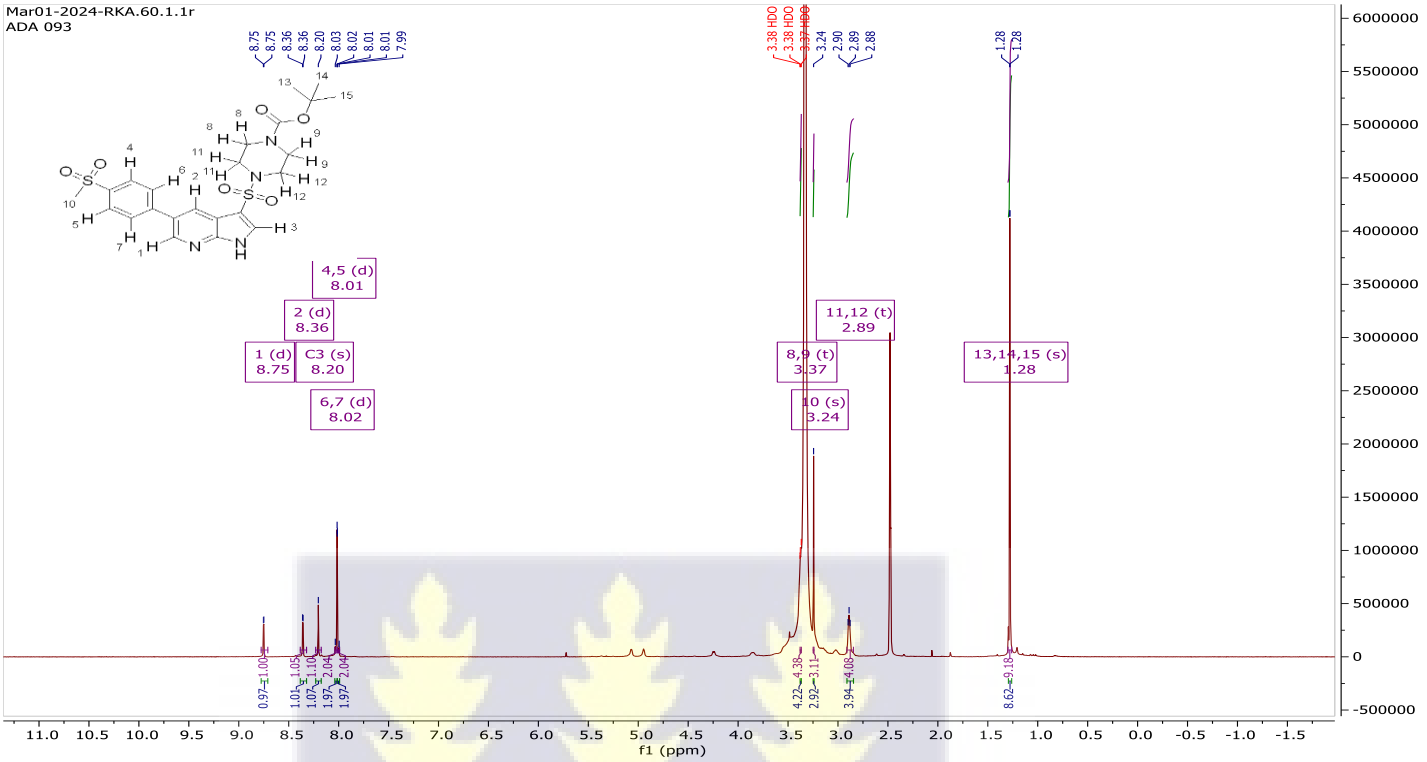


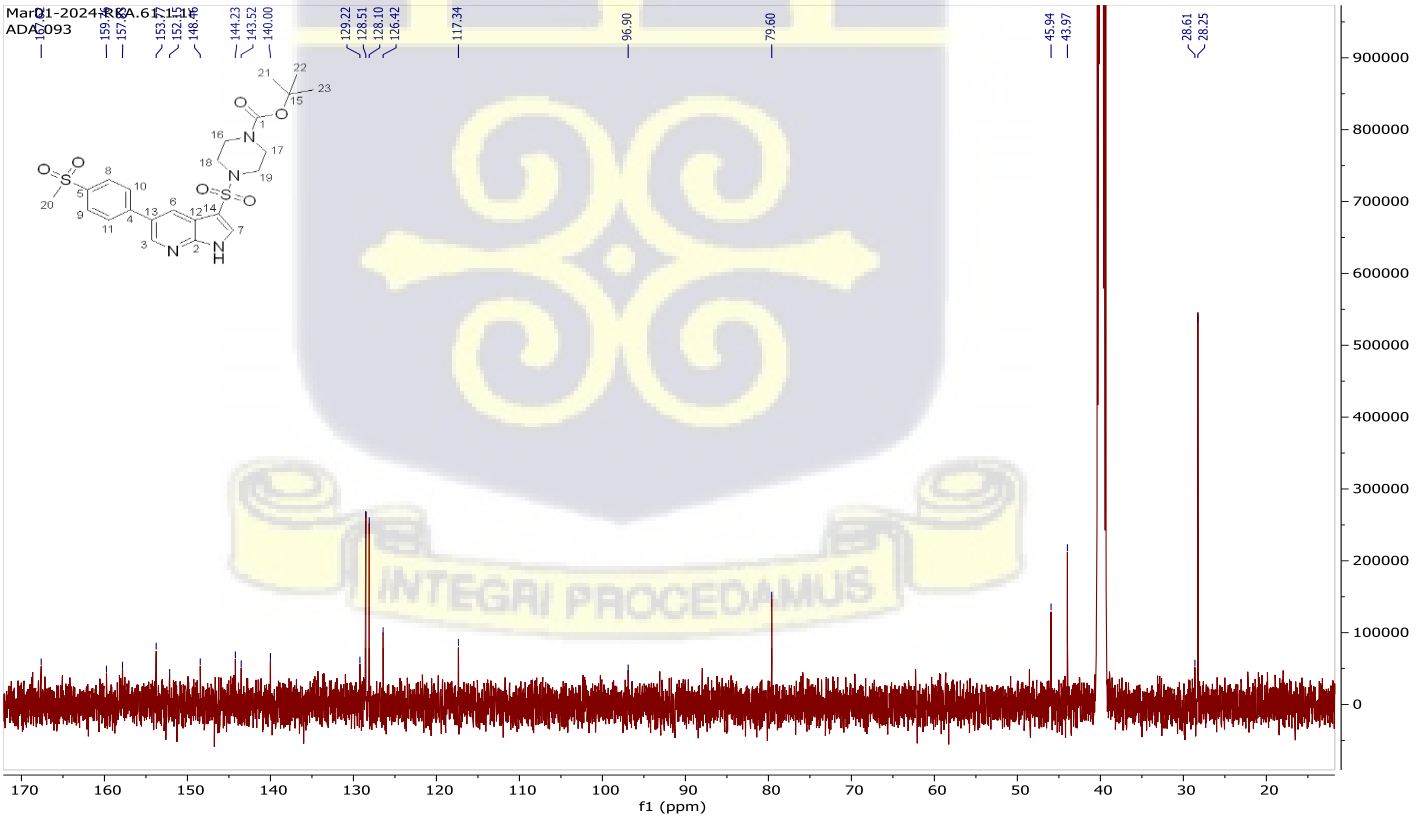


INTEGRI PROCEDAMUS

University of Ghana http://ugspace.ug.edu.gh

ADA093

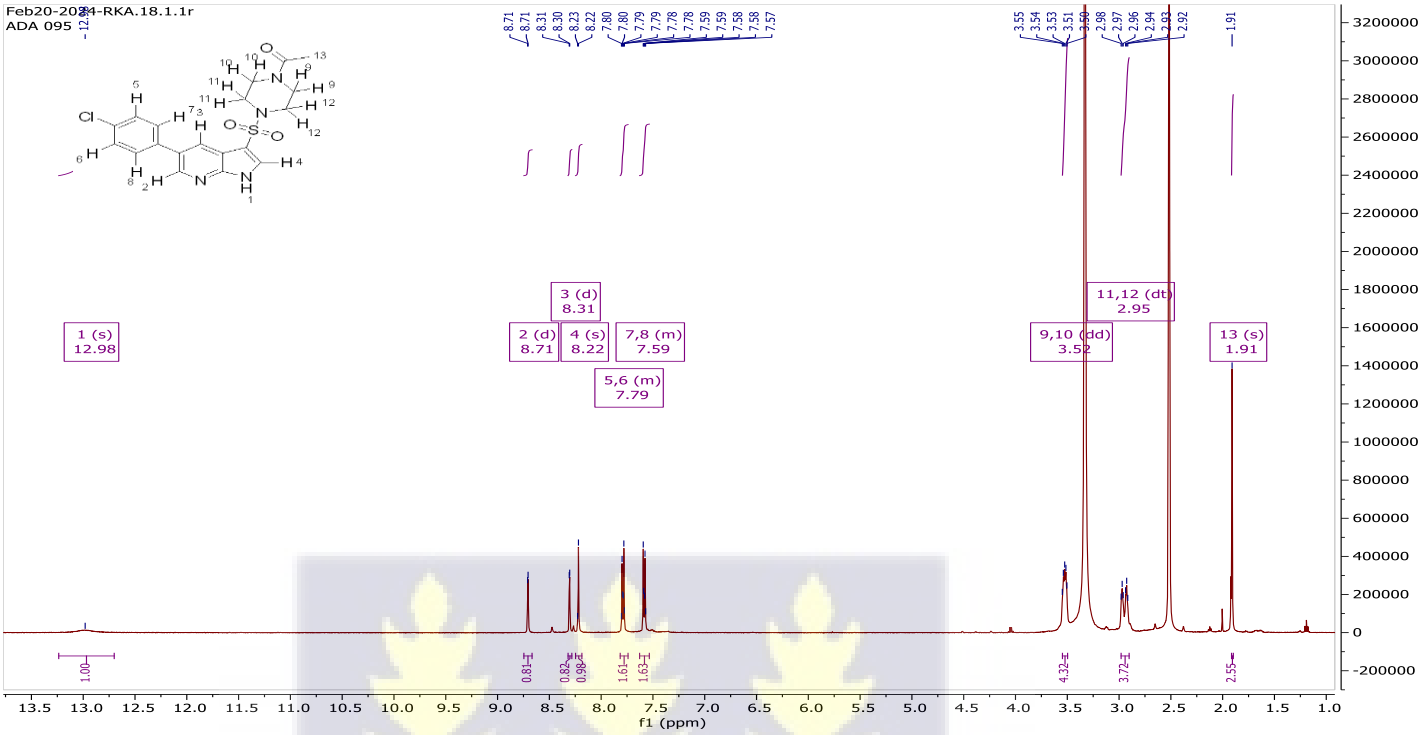


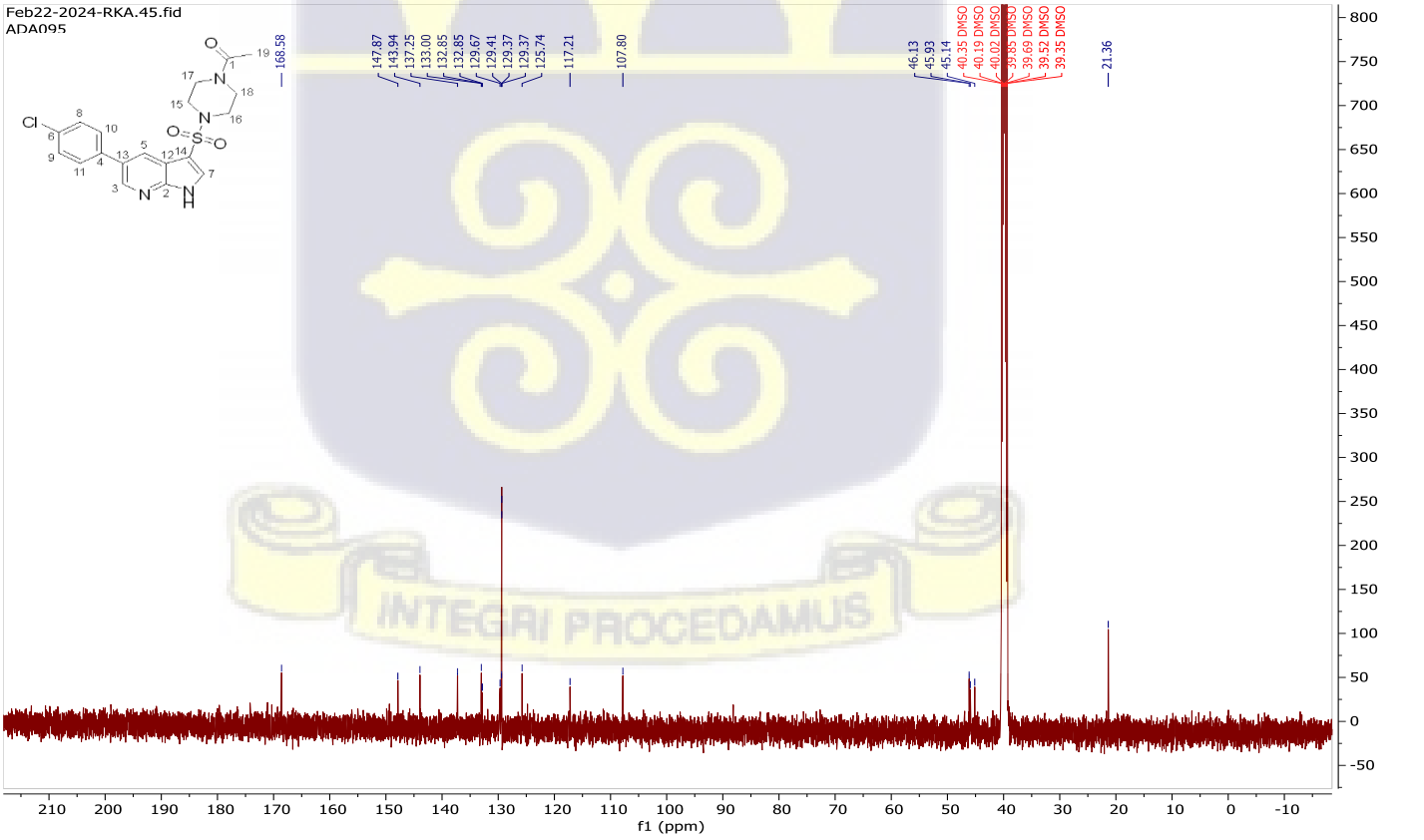


INTEGRI PROCEDAMUS

University of Ghana http://ugspace.ug.edu.gh

ADA095

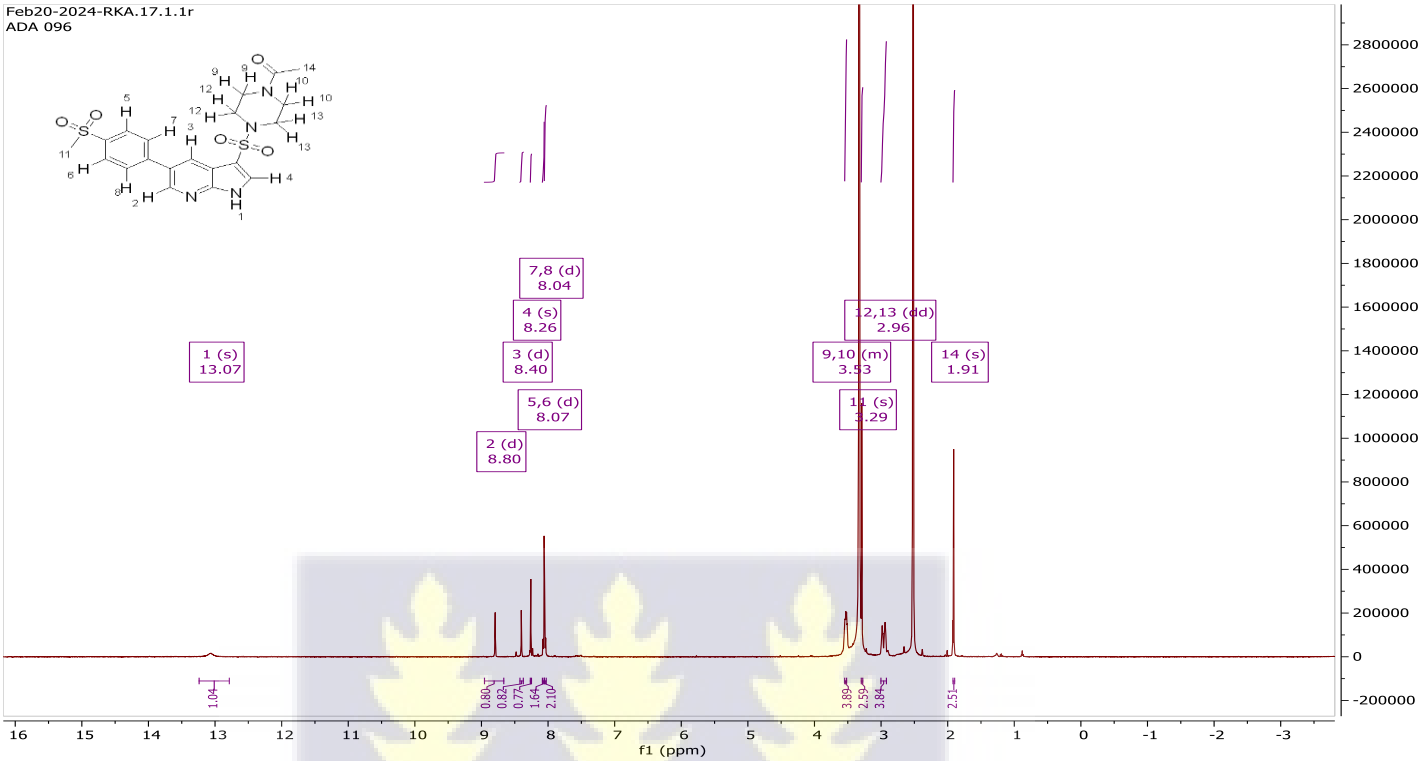


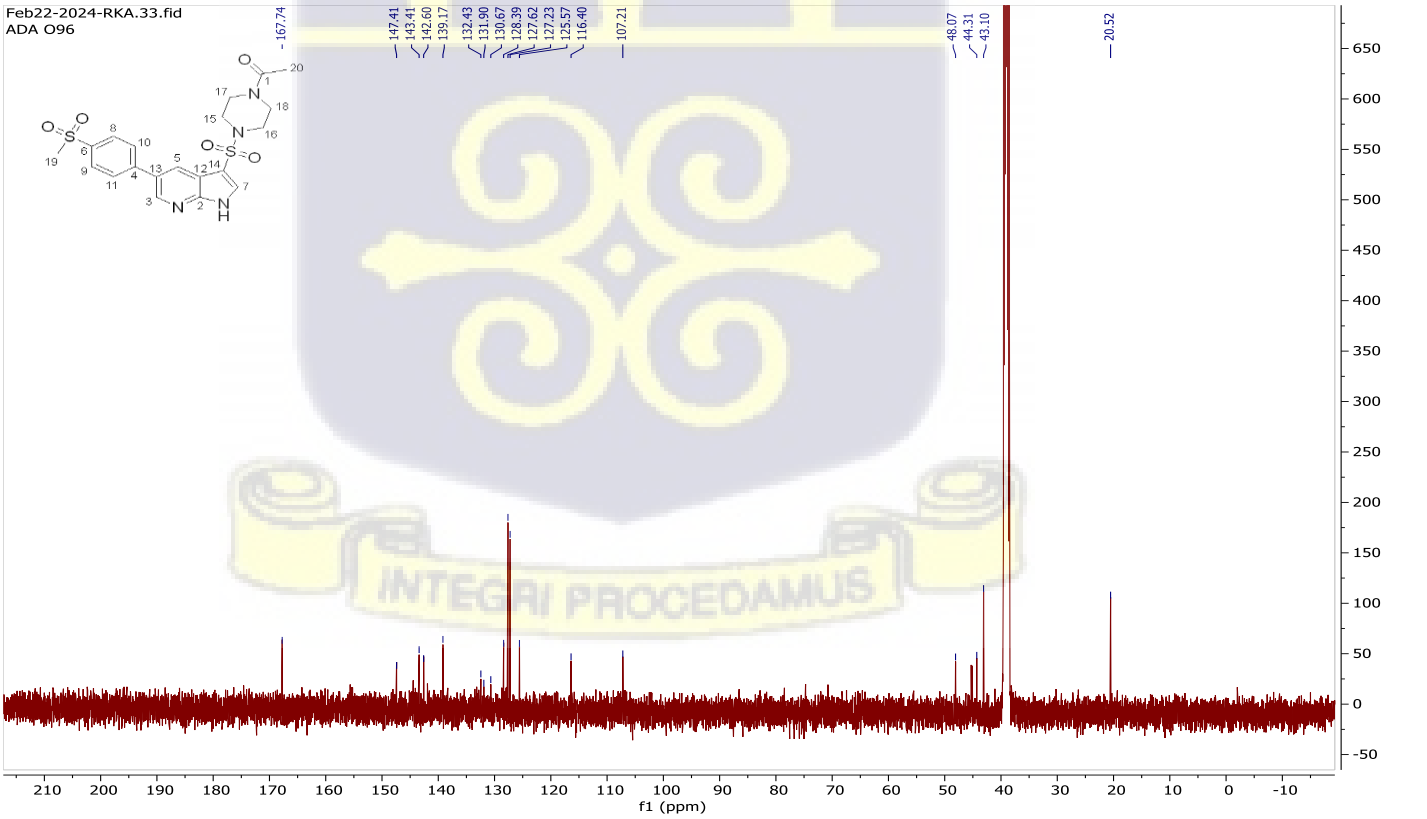


INTEGRI PROCEDAMUS

University of Ghana http://ugspace.ug.edu.gh

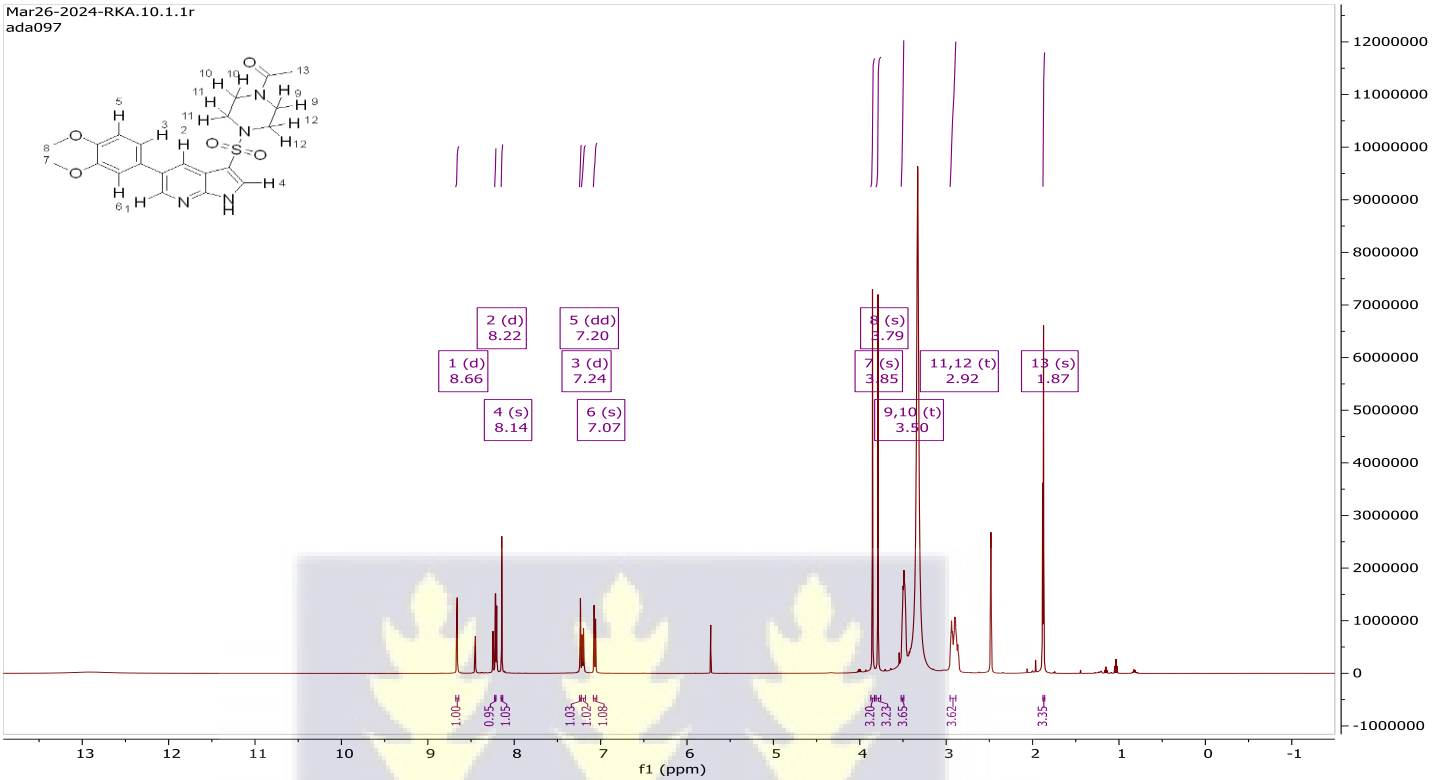
ADA096

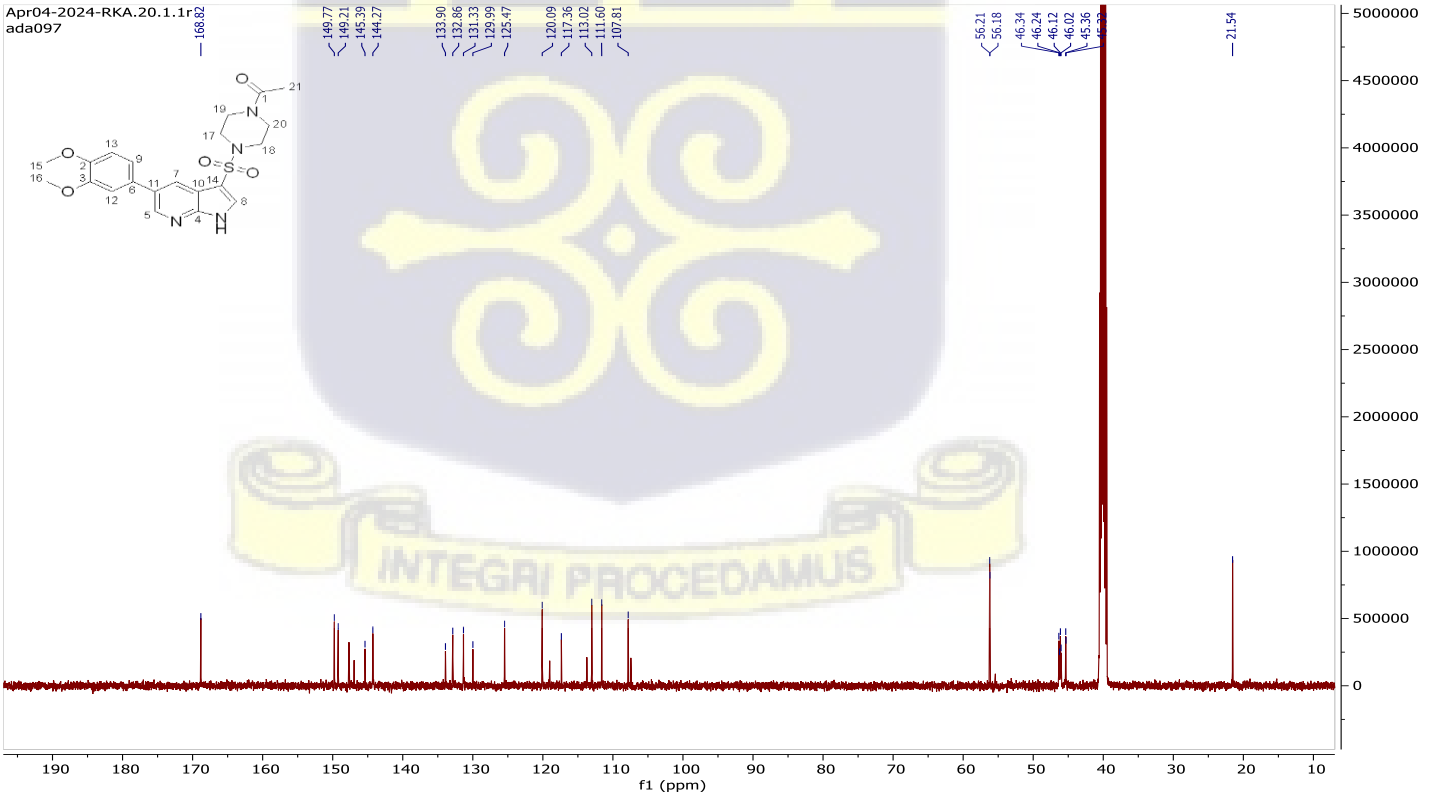




University of Ghana http://ugspace.ug.edu.gh

ADA097

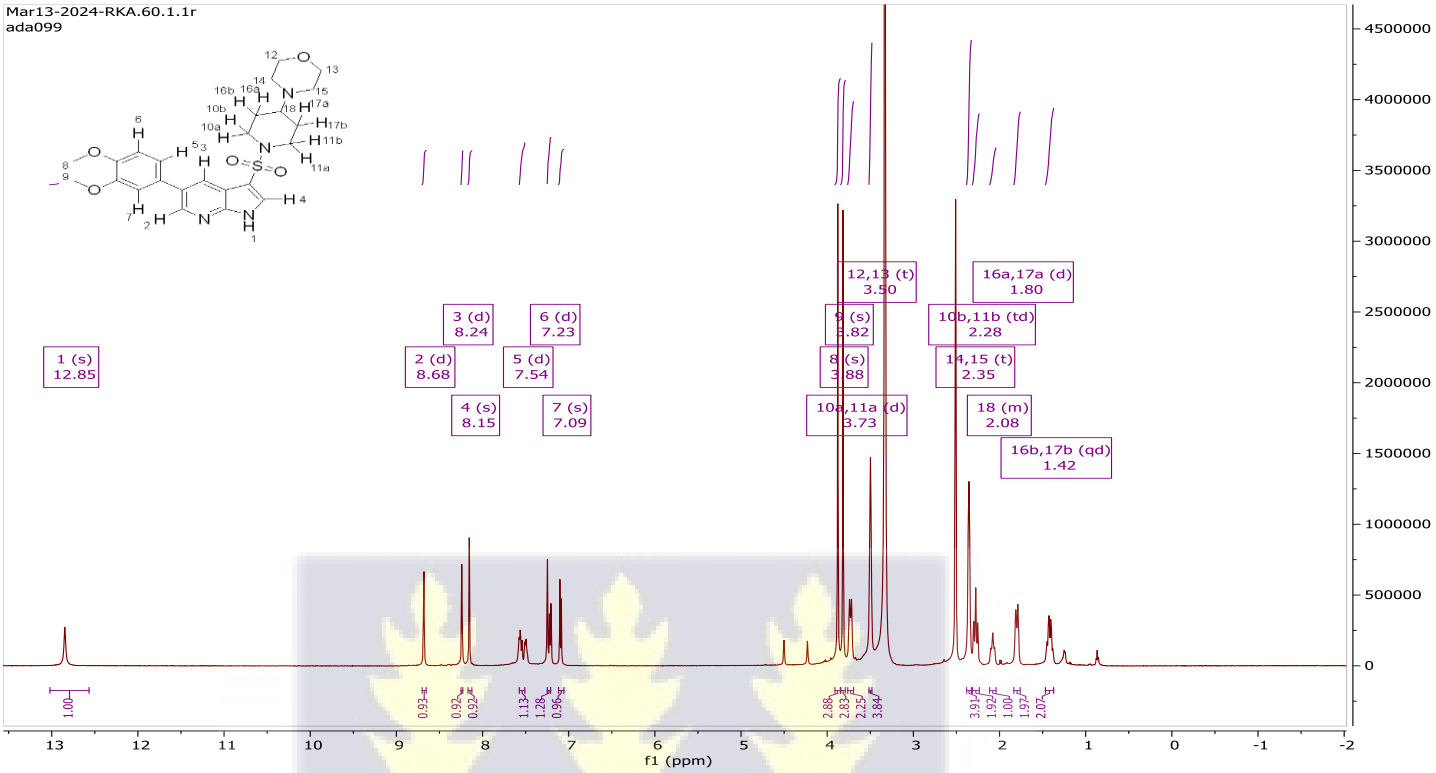


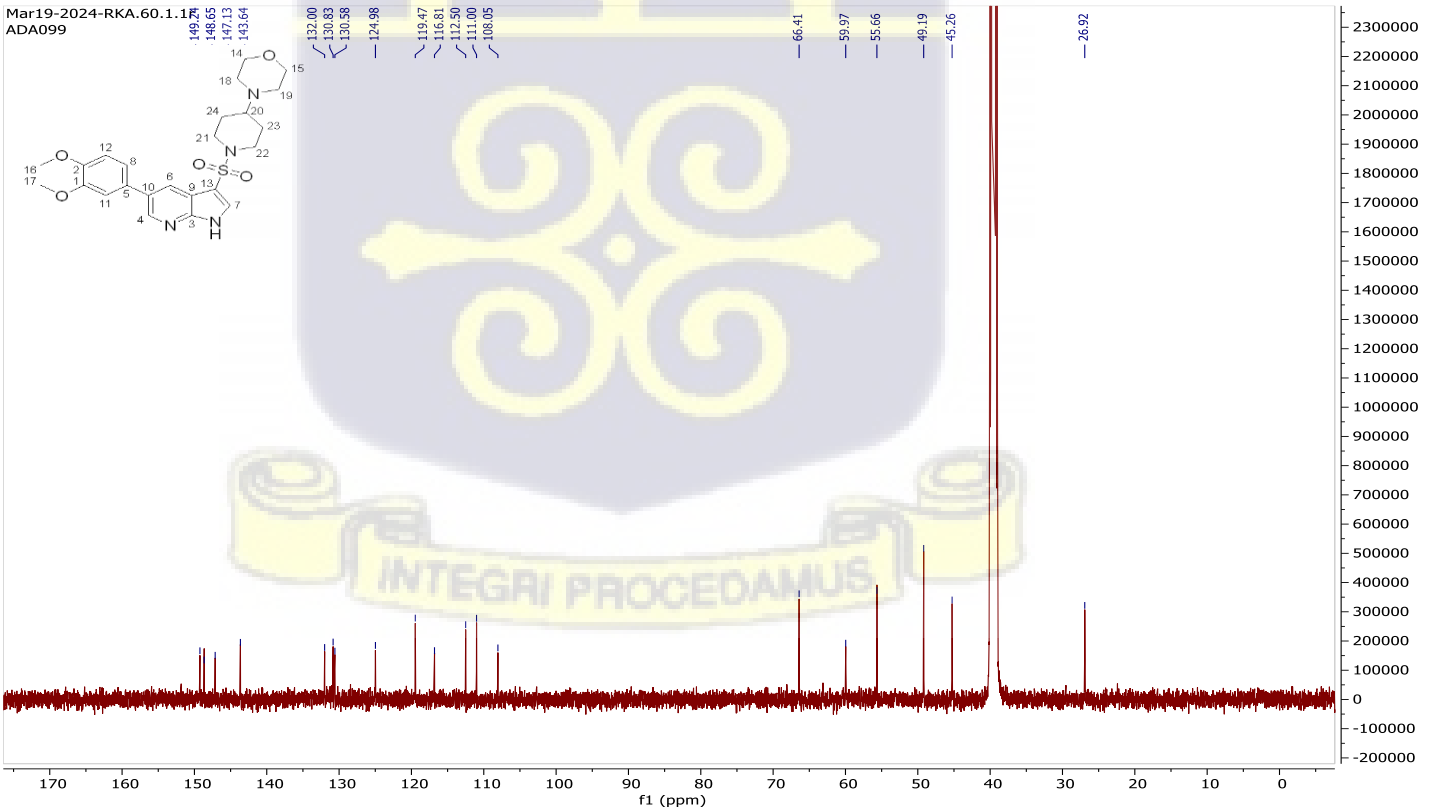


INTEGRI PROCEDAMUS

University of Ghana http://ugspace.ug.edu.gh

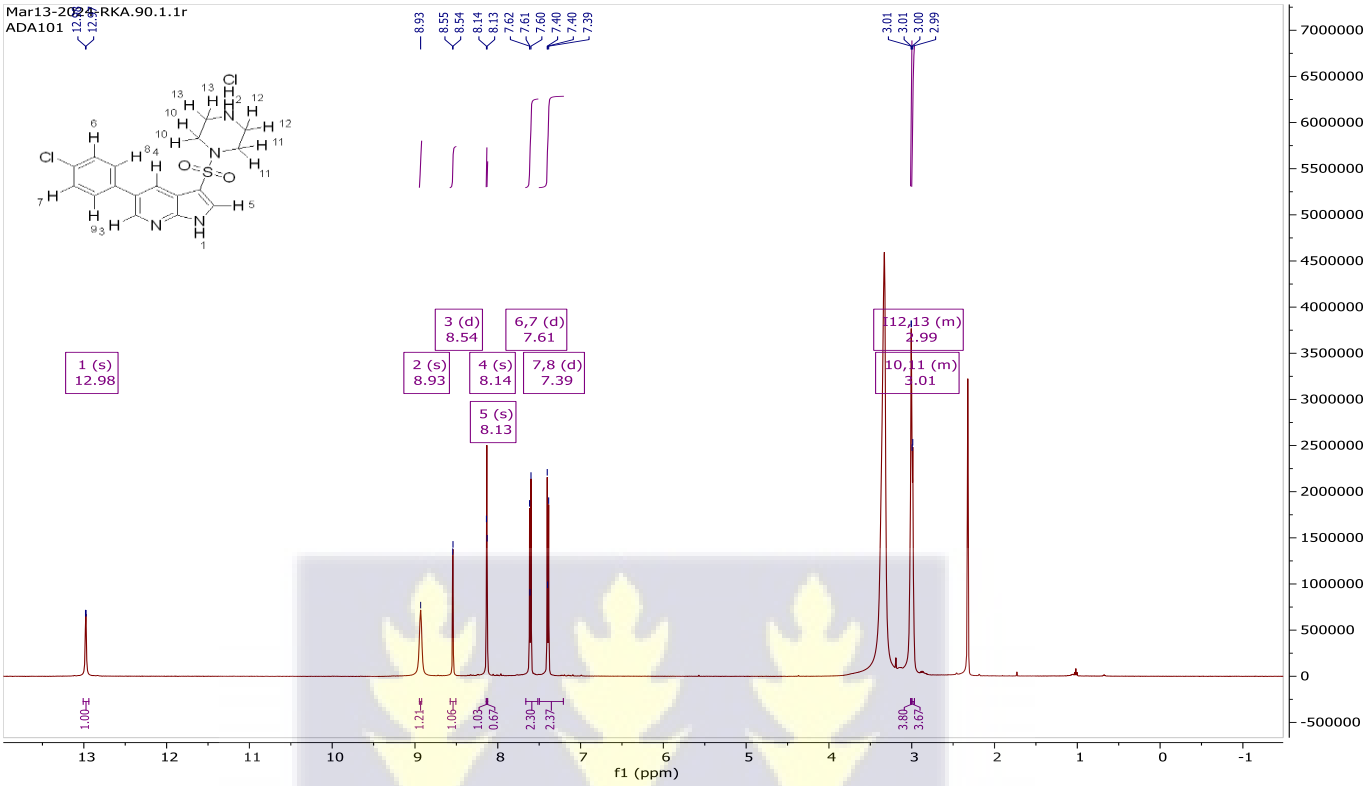
ADA099

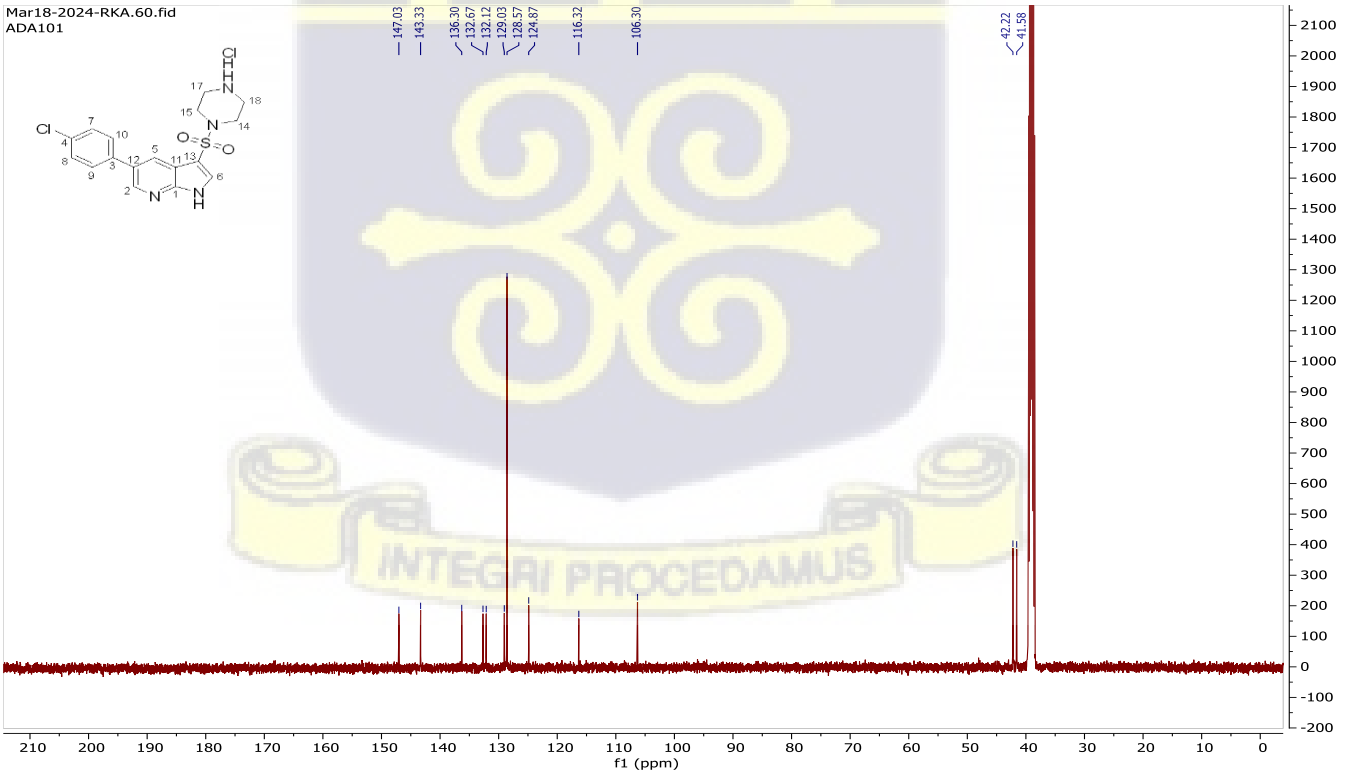




University of Ghana http://ugspace.ug.edu.gh

ADA101

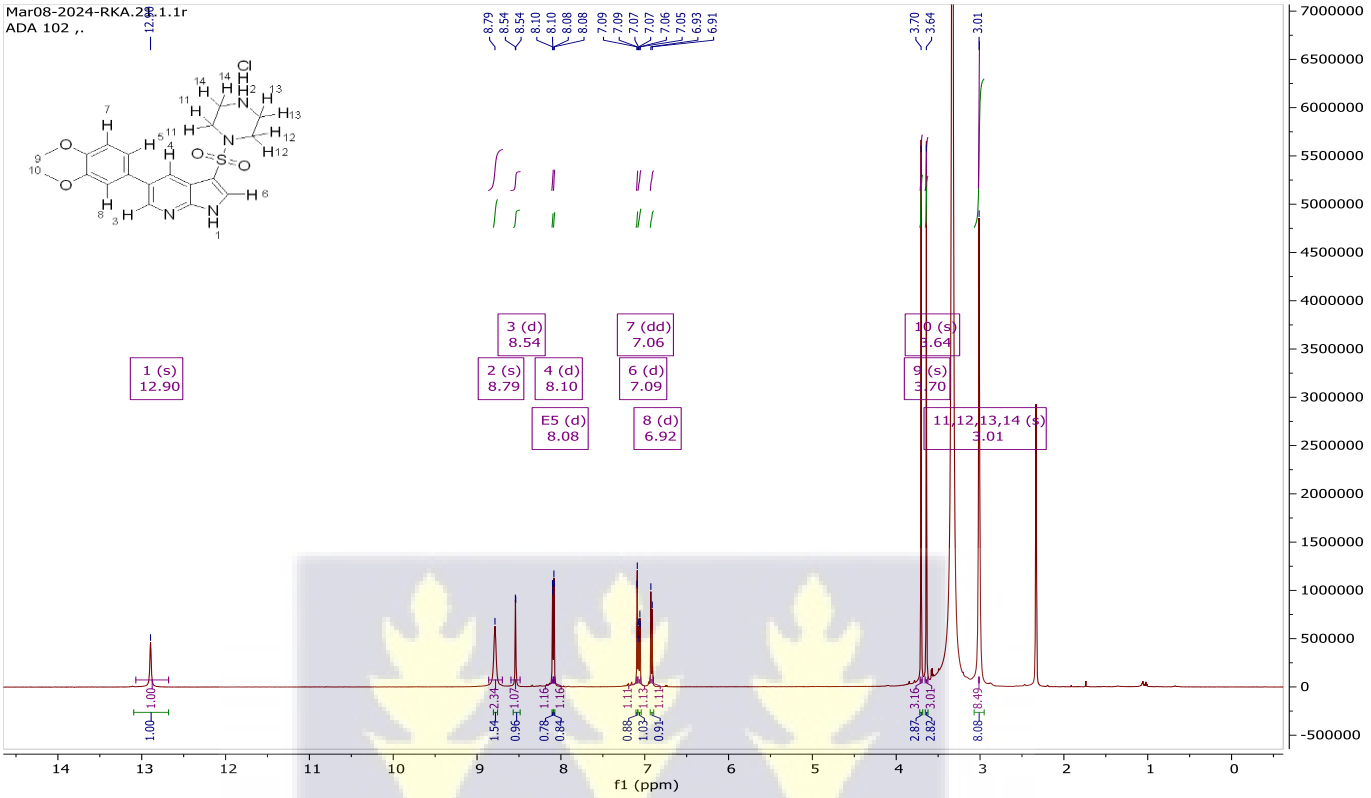


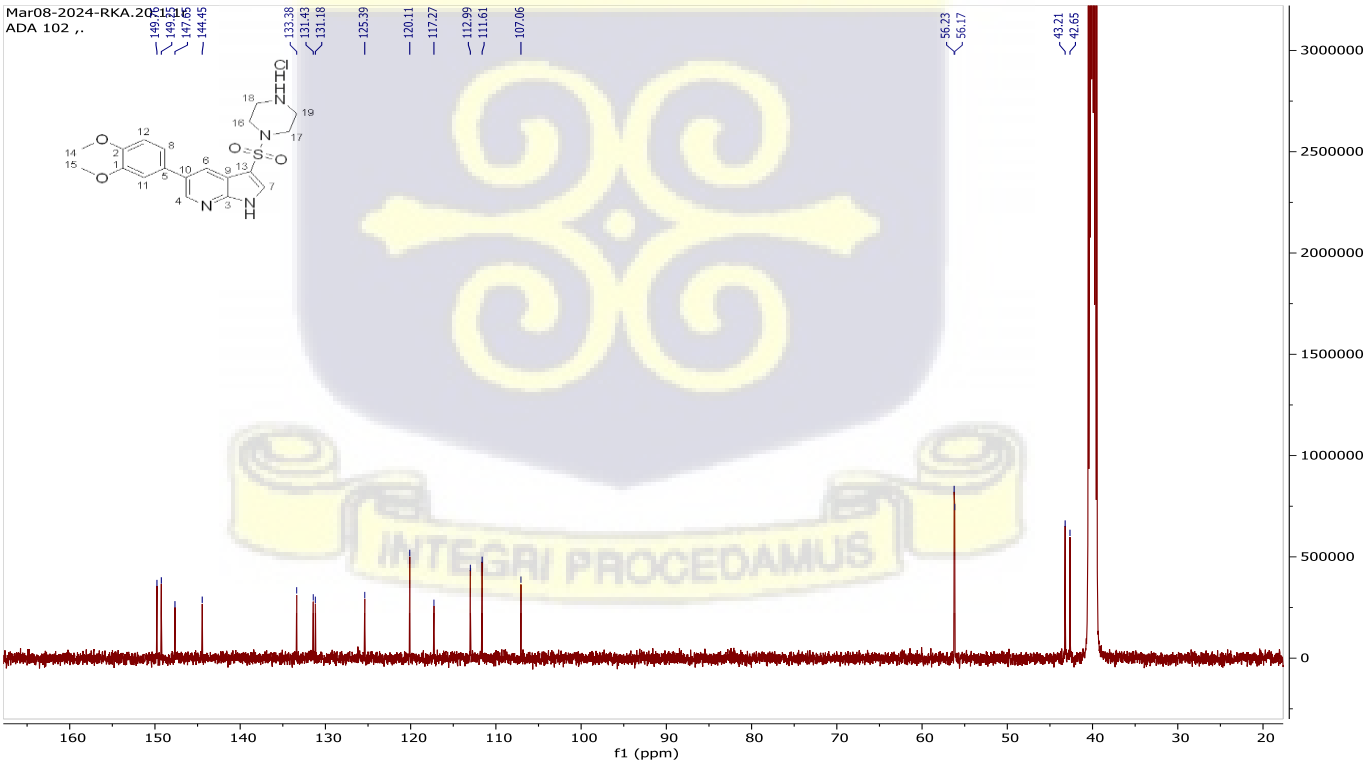


INTEGRI PROCEDAMUS

University of Ghana http://ugspace.ug.edu.gh

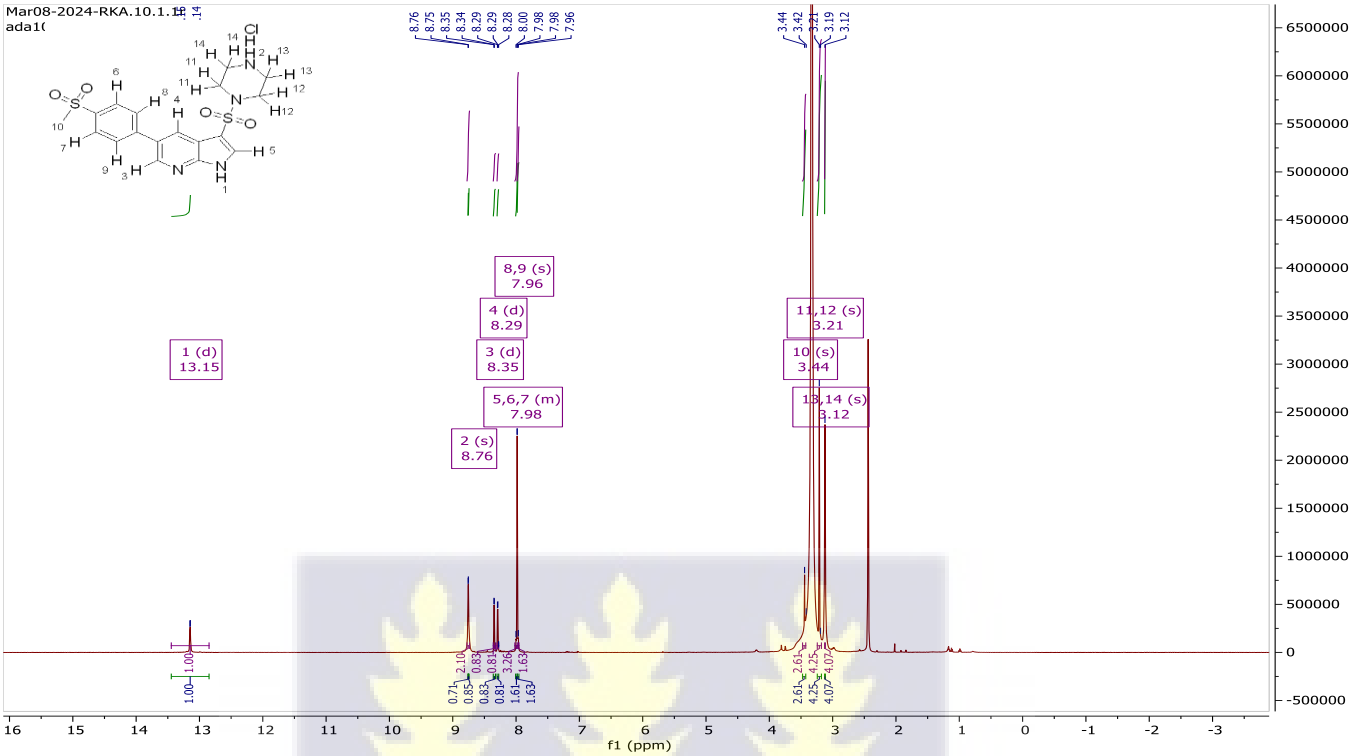
ADA102

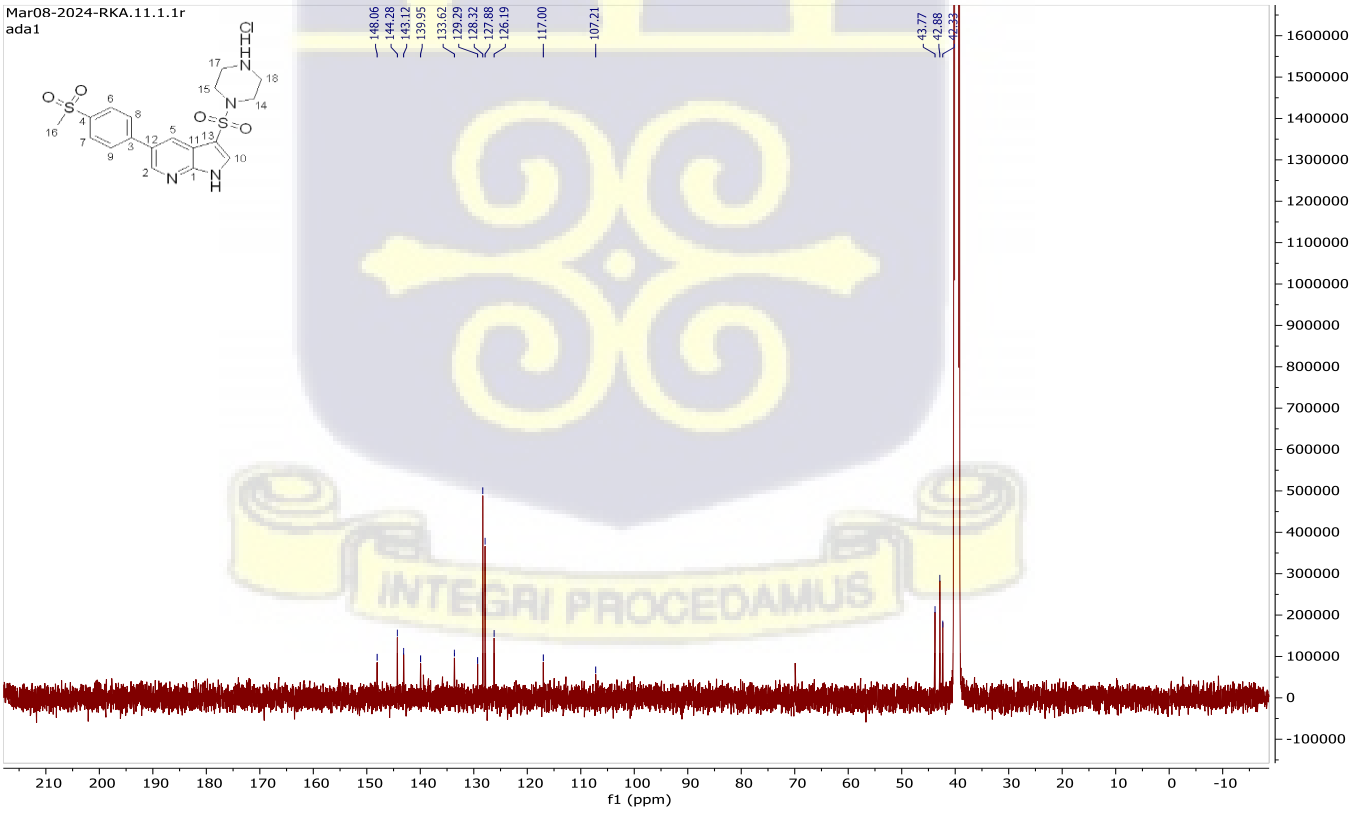




University of Ghana http://ugspace.ug.edu.gh

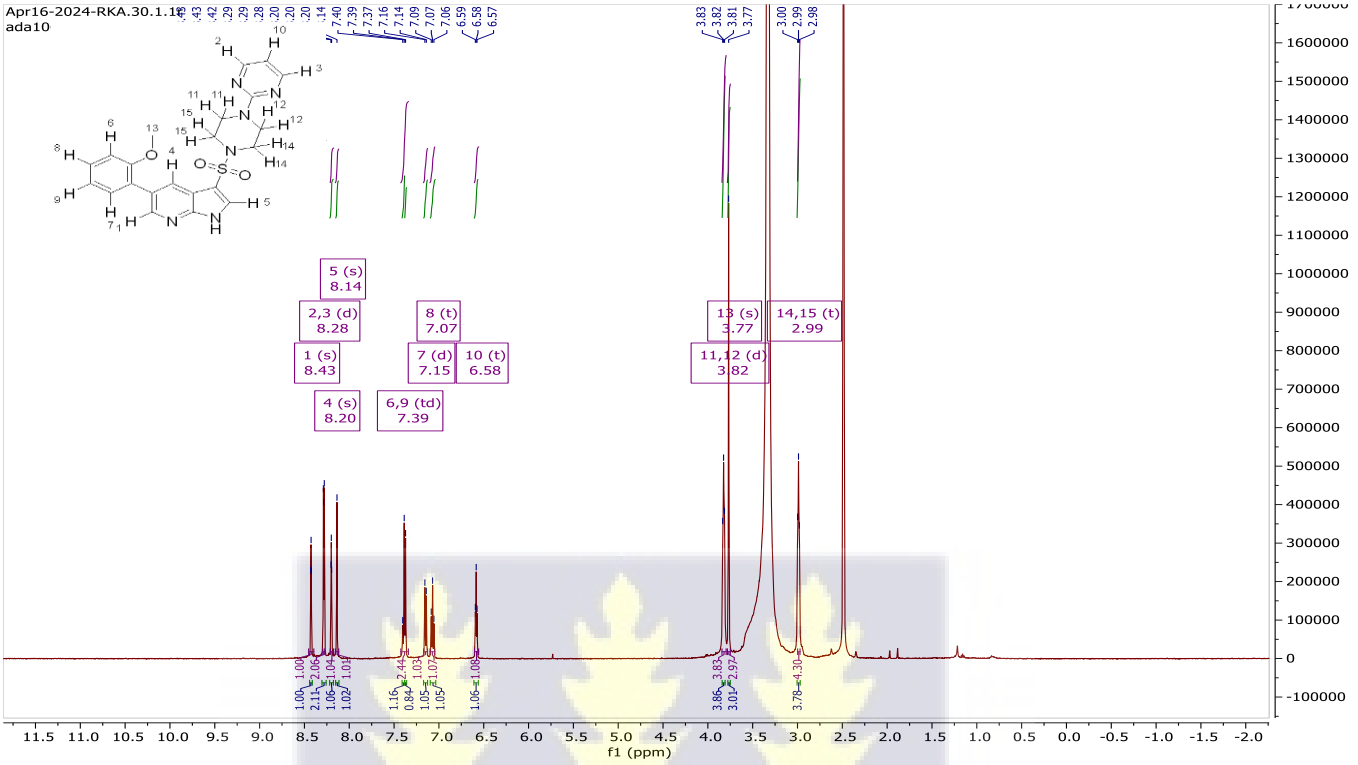
ADA103

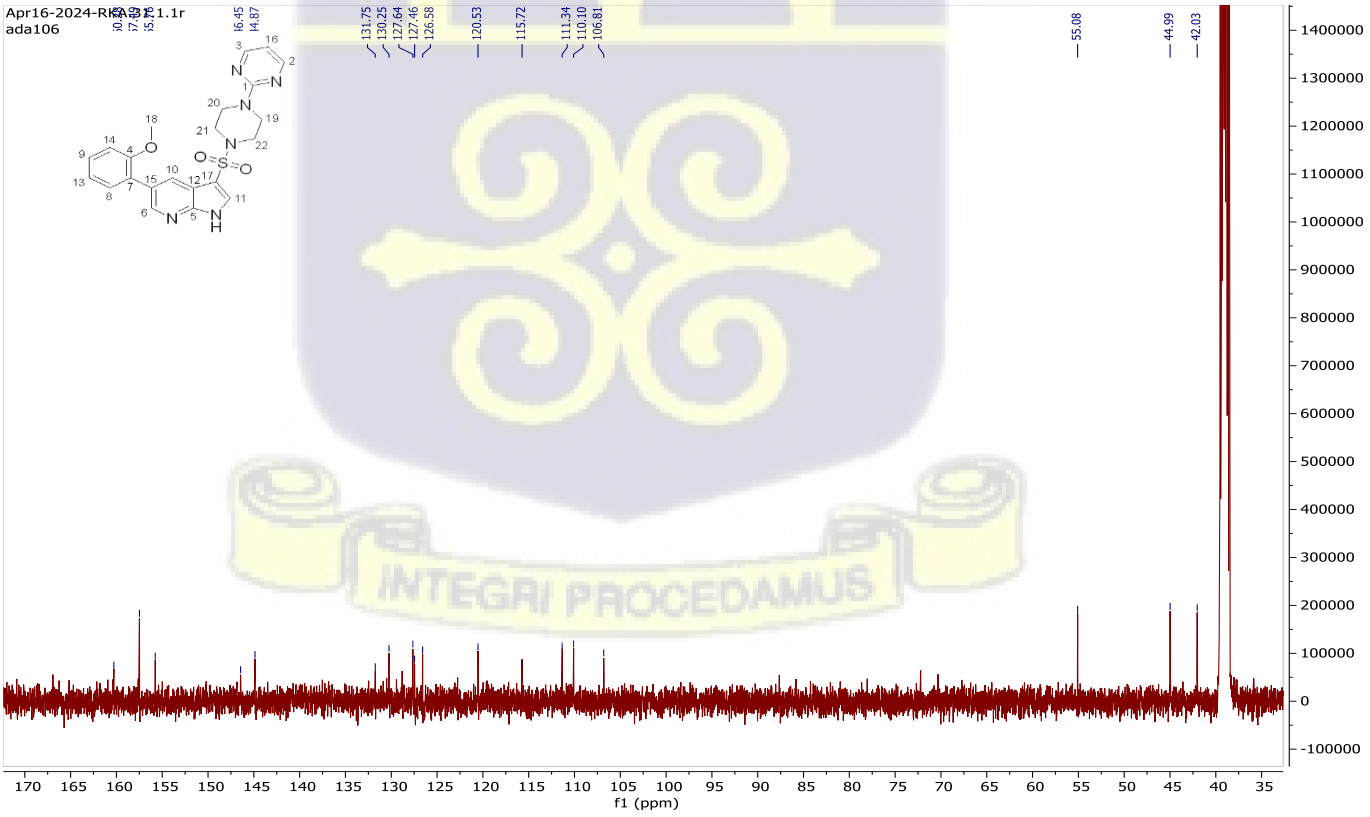




University of Ghana http://ugspace.ug.edu.gh

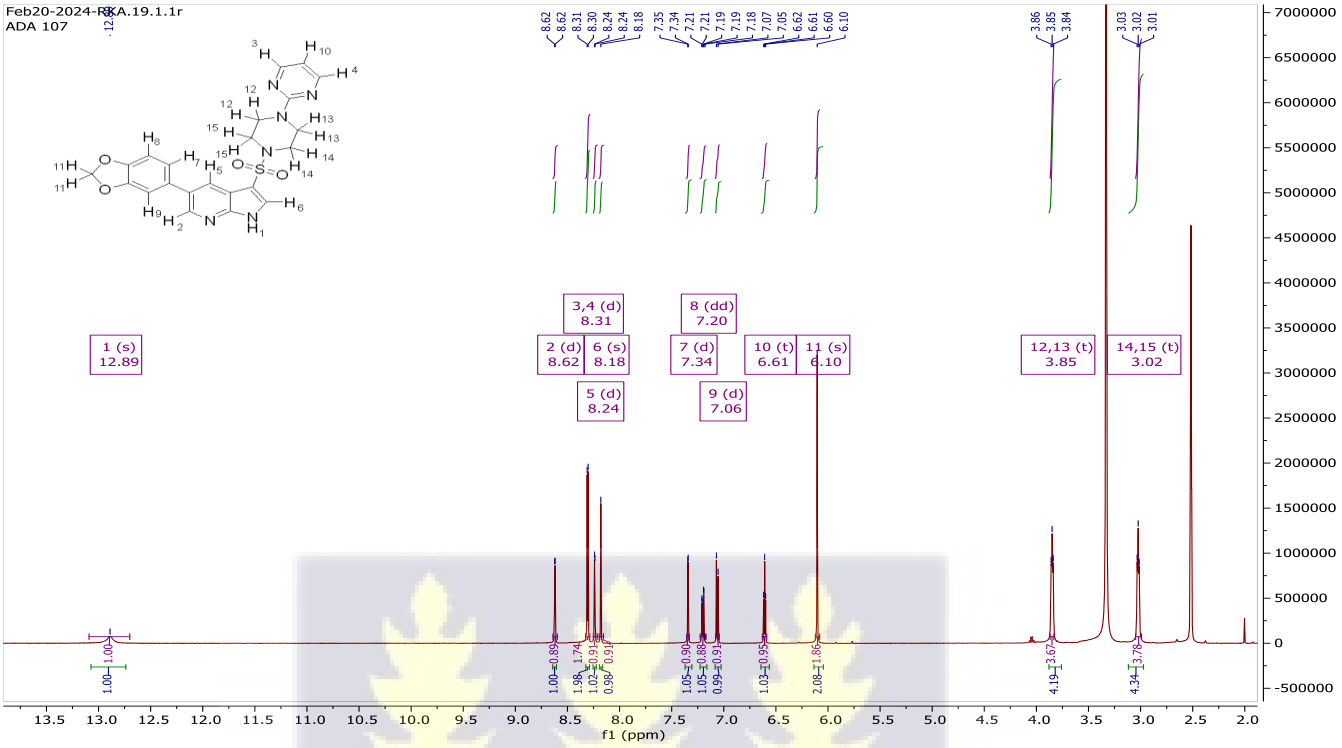
ADA106

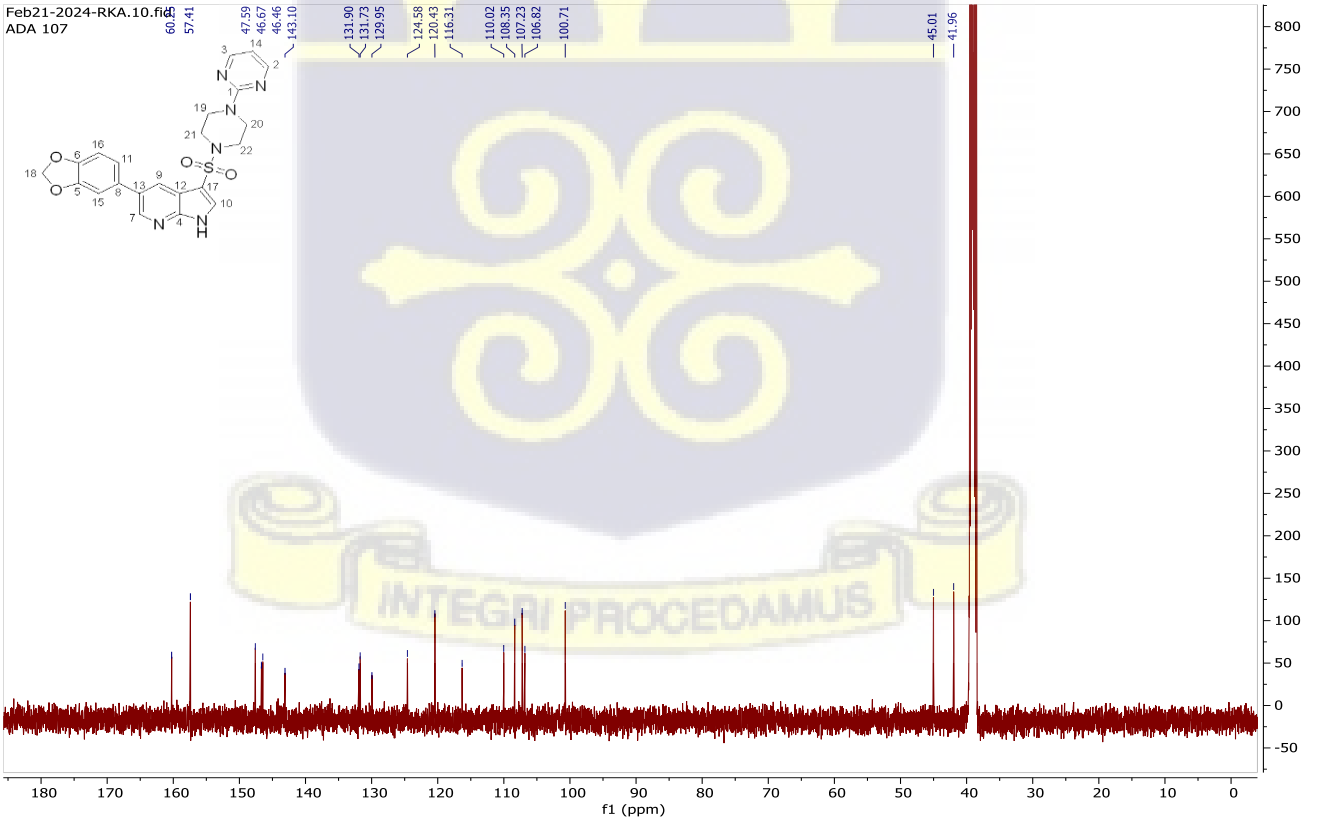




University of Ghana http://ugspace.ug.edu.gh

ADA107

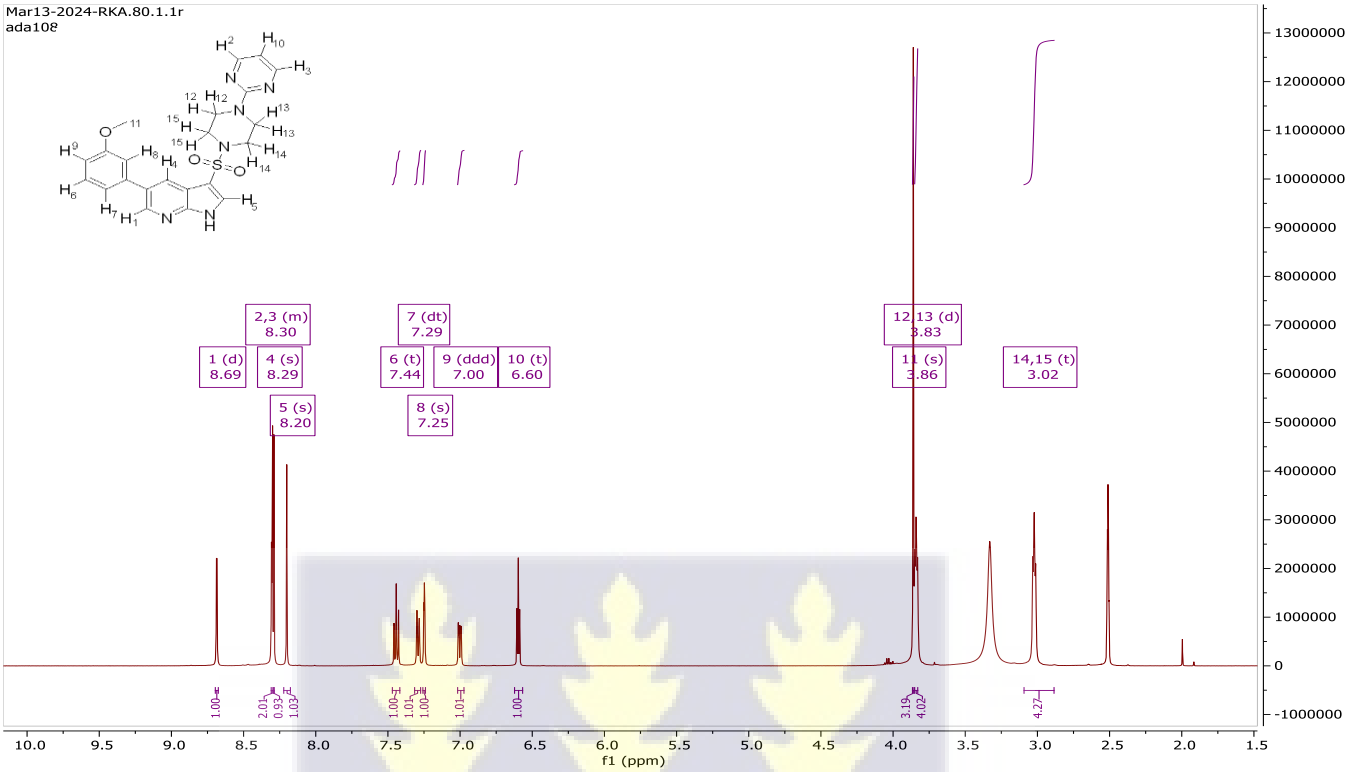


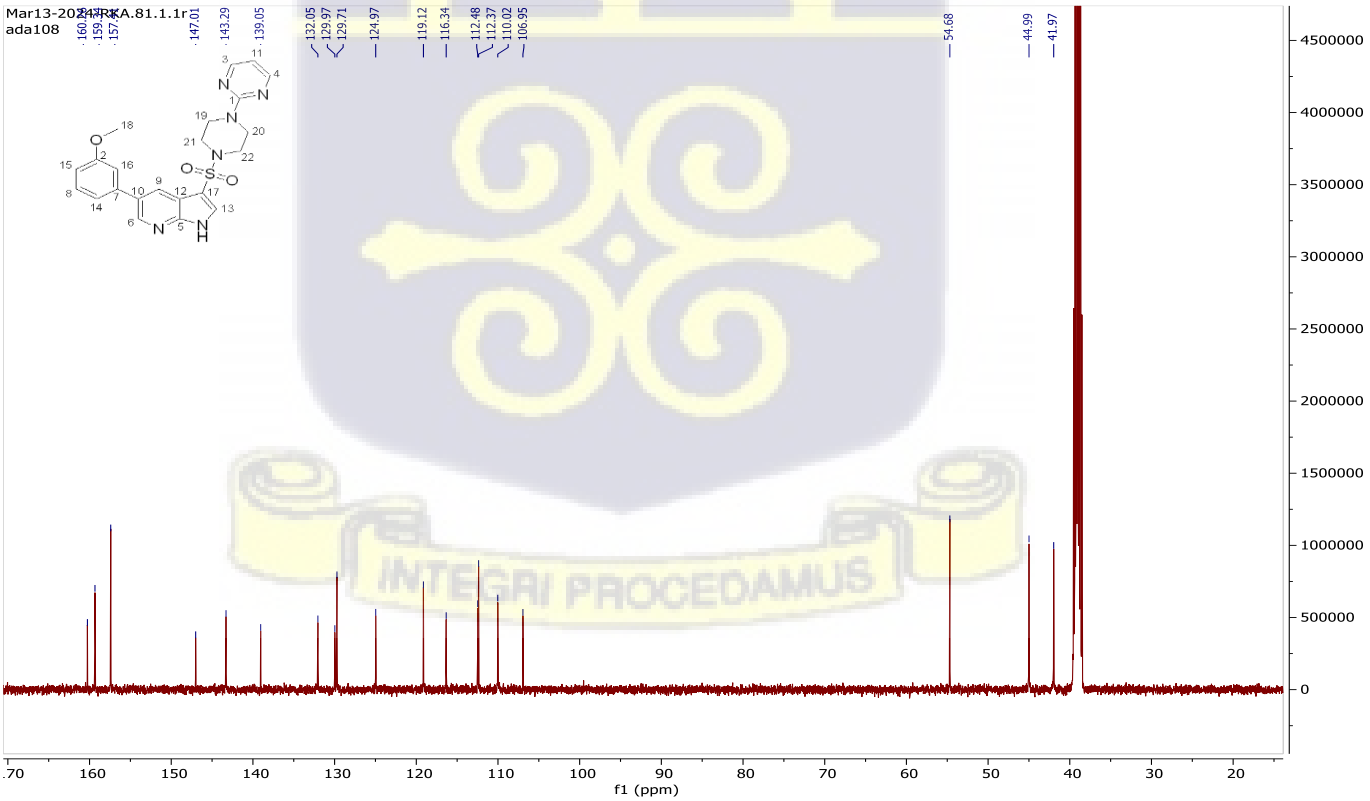


INTEGRI PROCEDAMUS

University of Ghana http://ugspace.ug.edu.gh

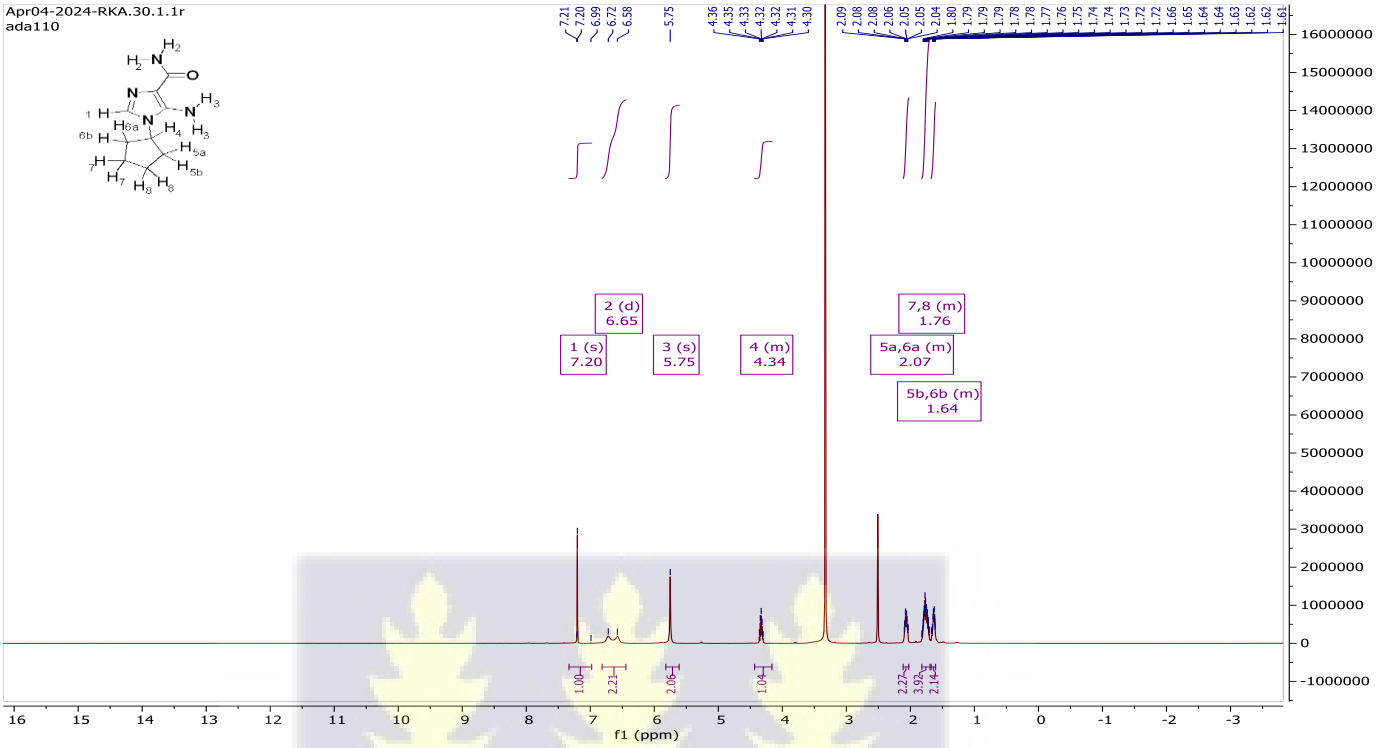
ADA108

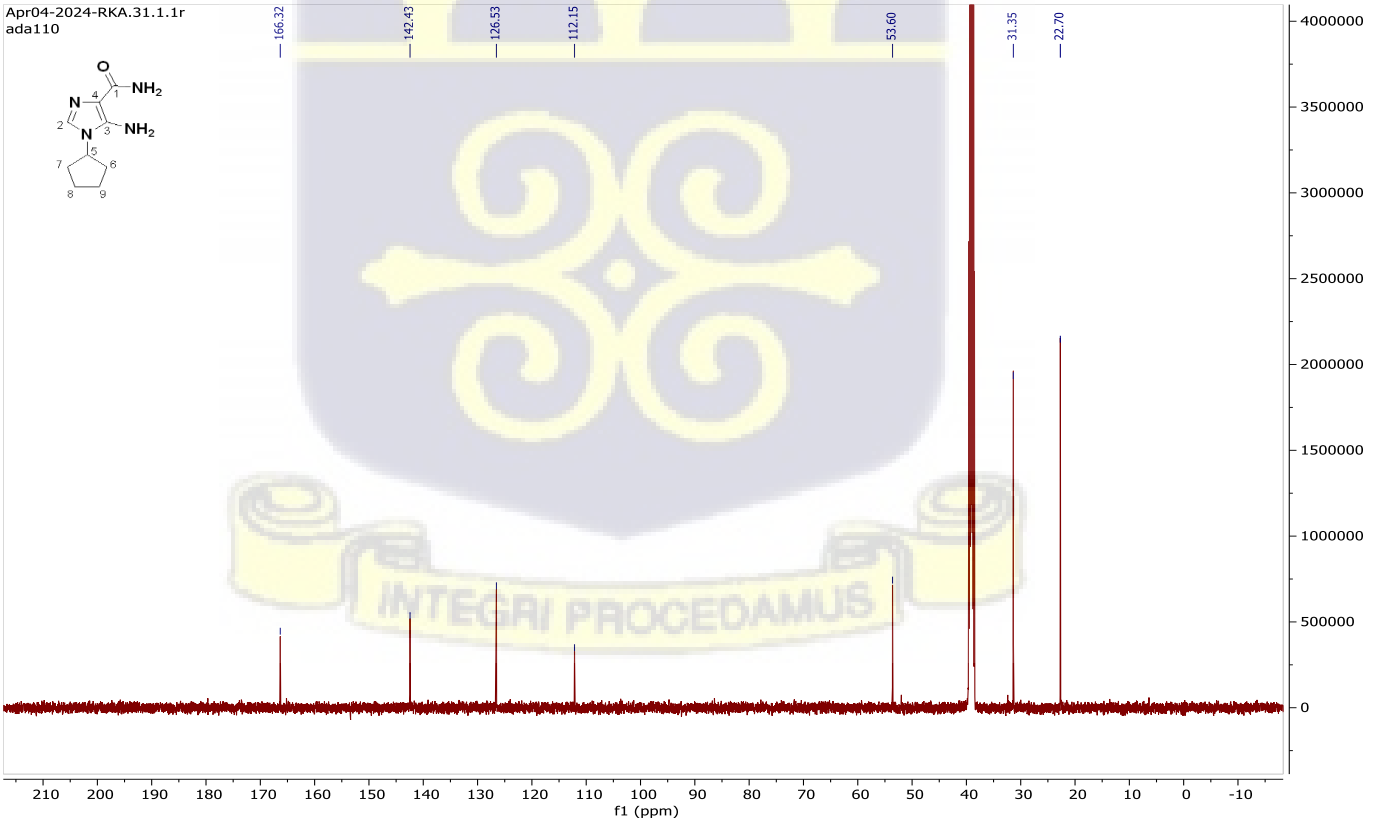




University of Ghana http://ugspace.ug.edu.gh

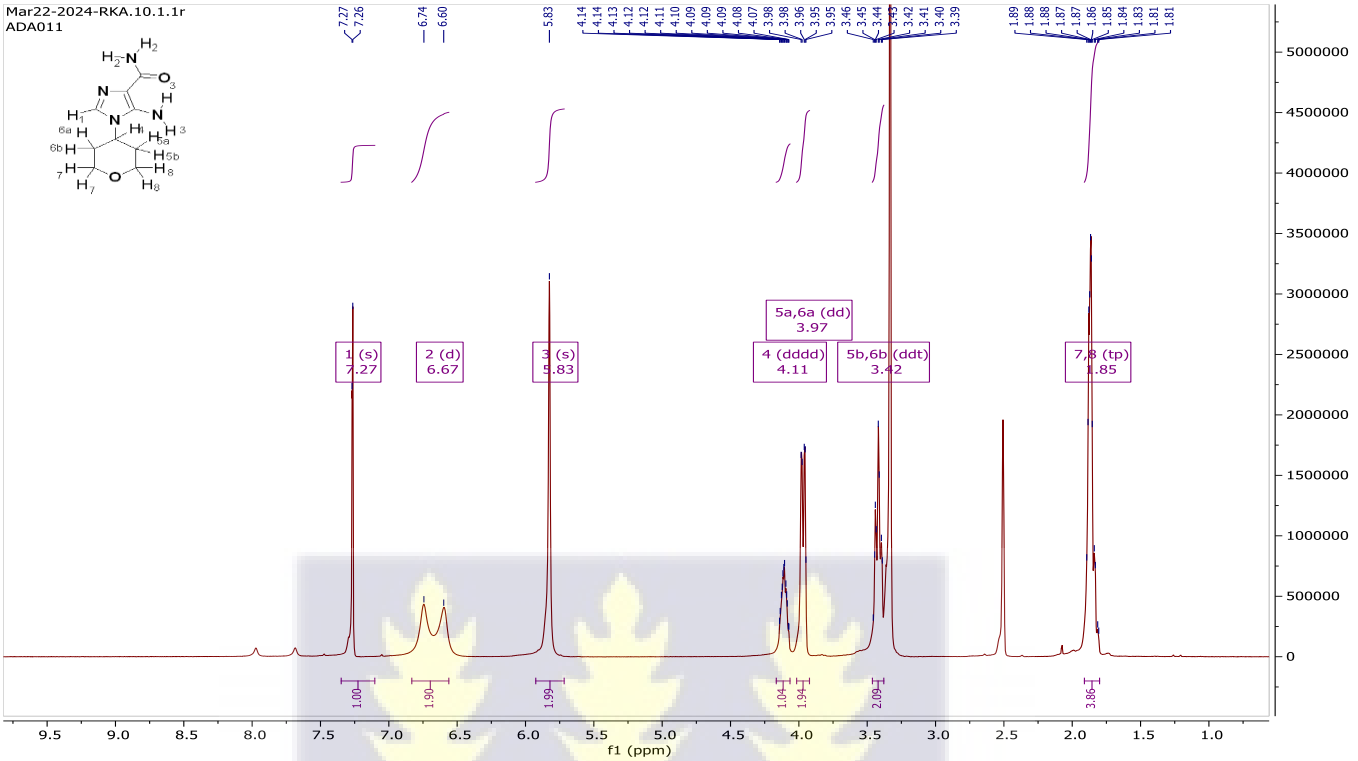
ADA110

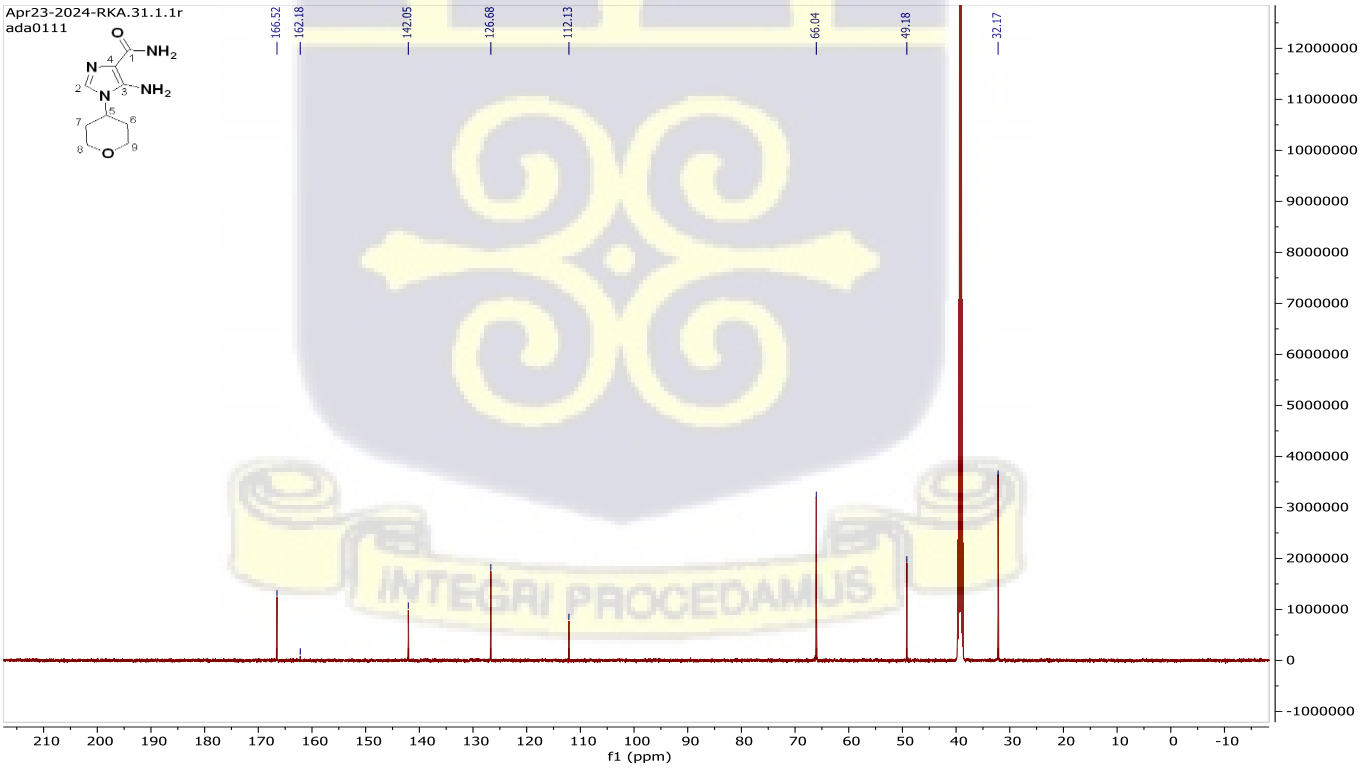




University of Ghana http://ugspace.ug.edu.gh

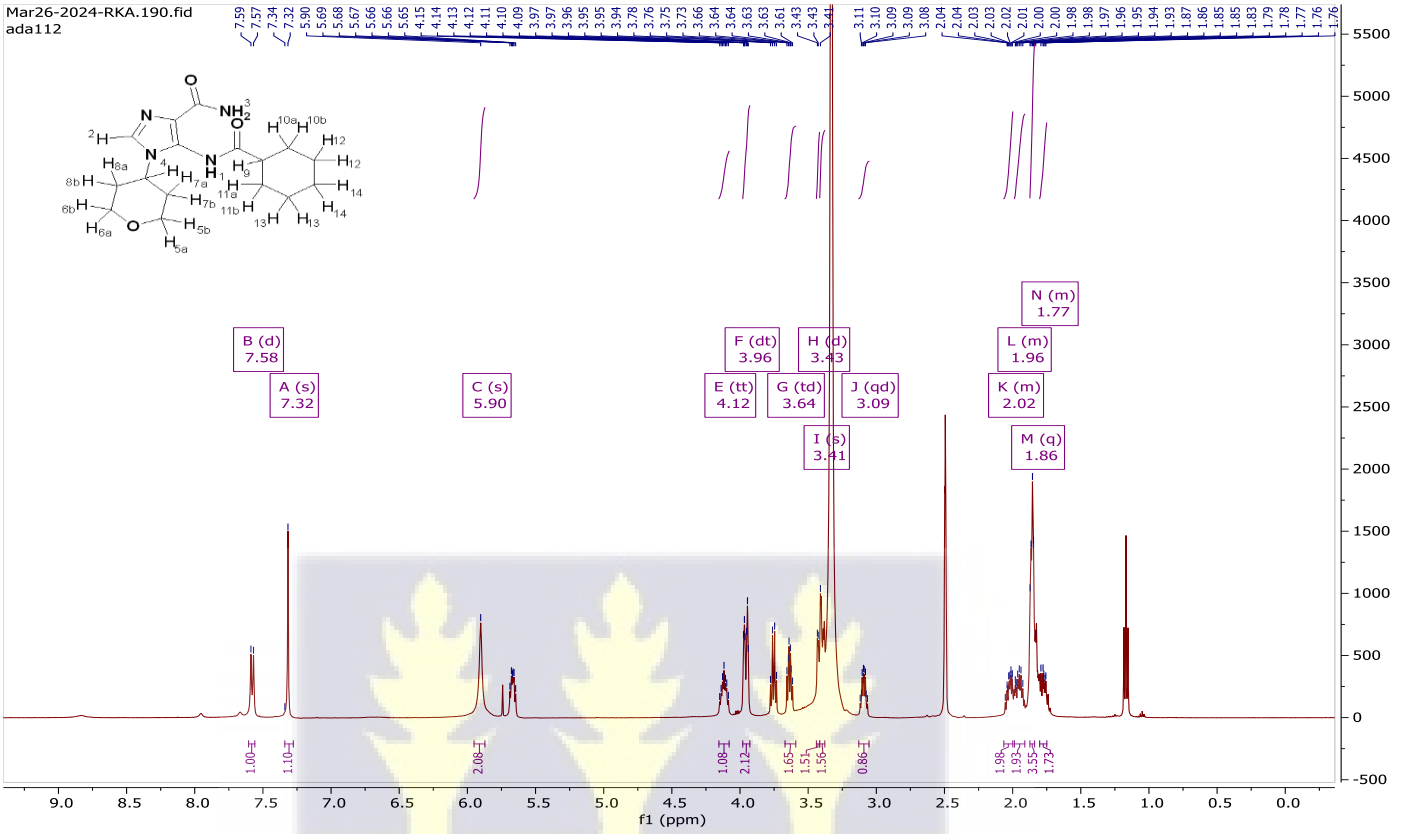
ADA111

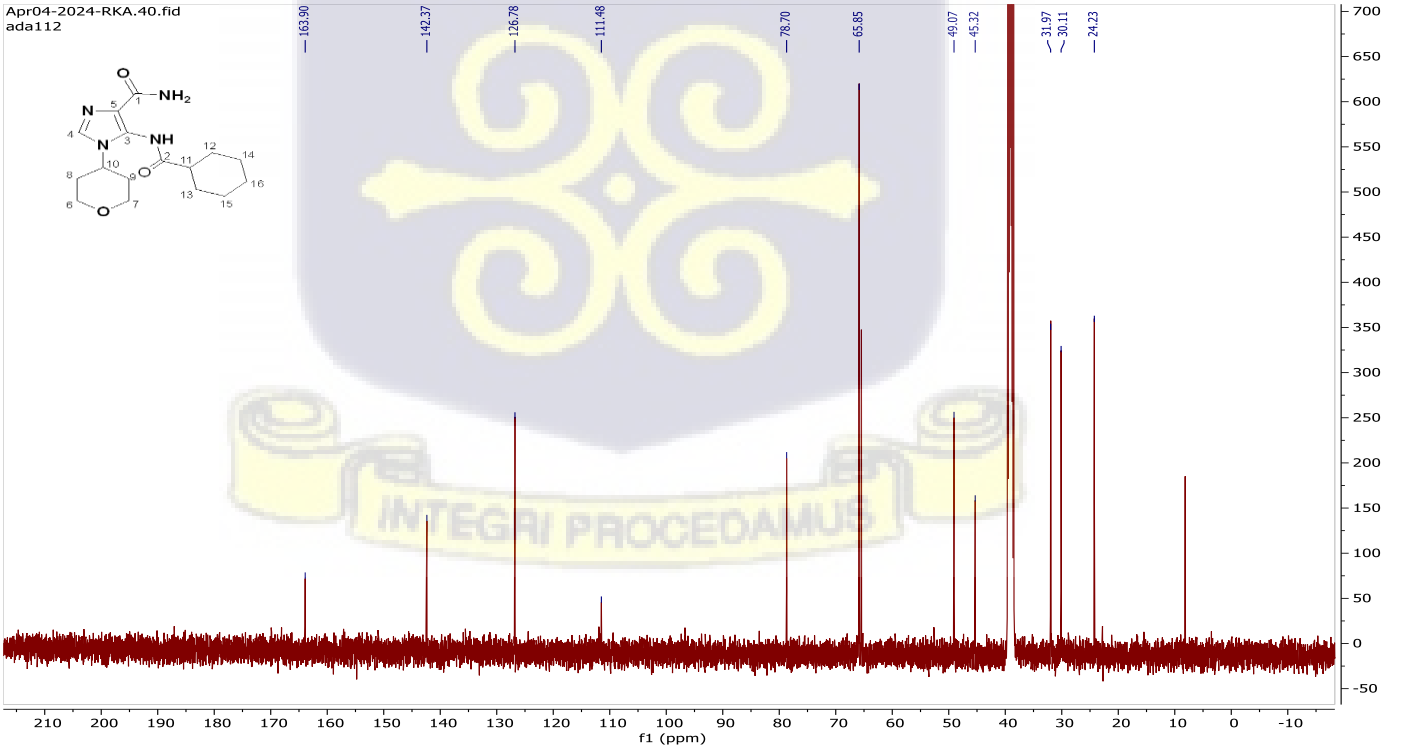




University of Ghana http://ugspace.ug.edu.gh

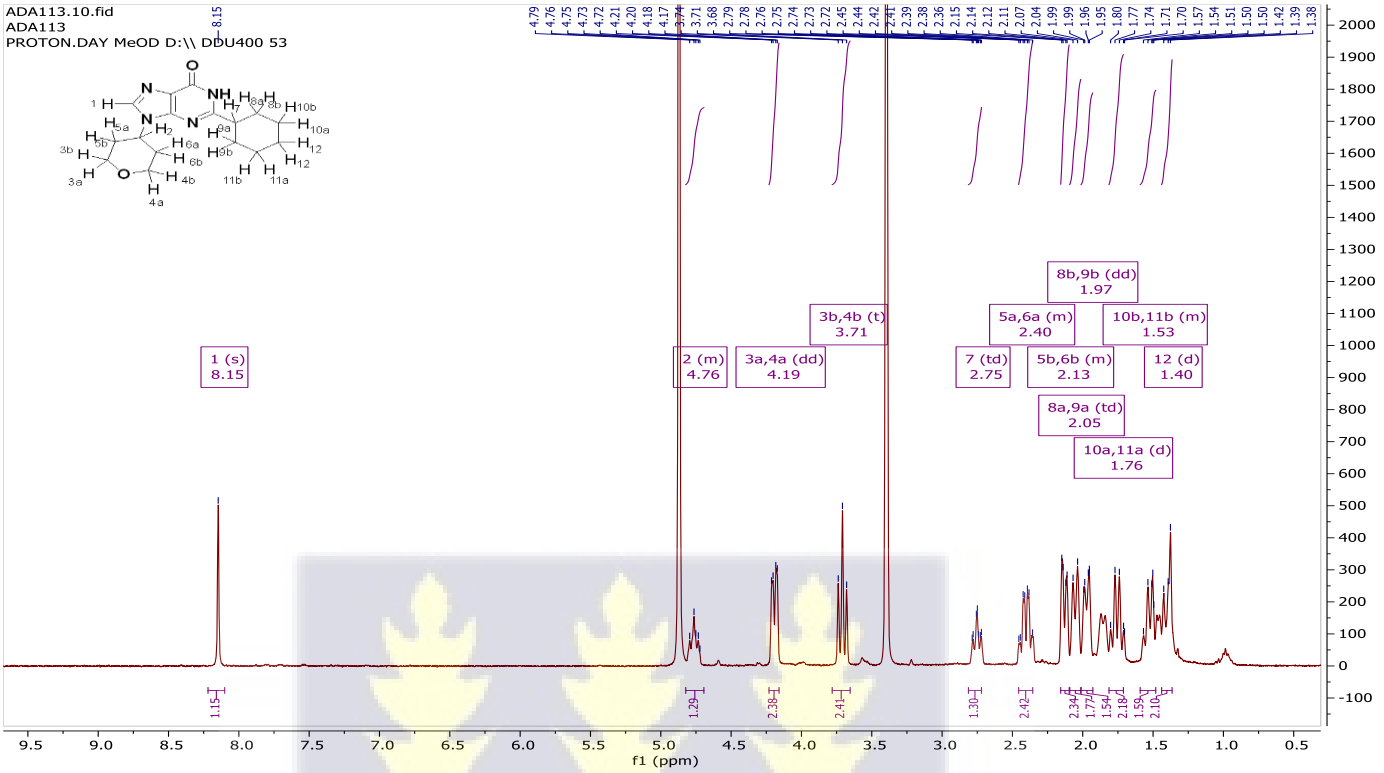
ADA112

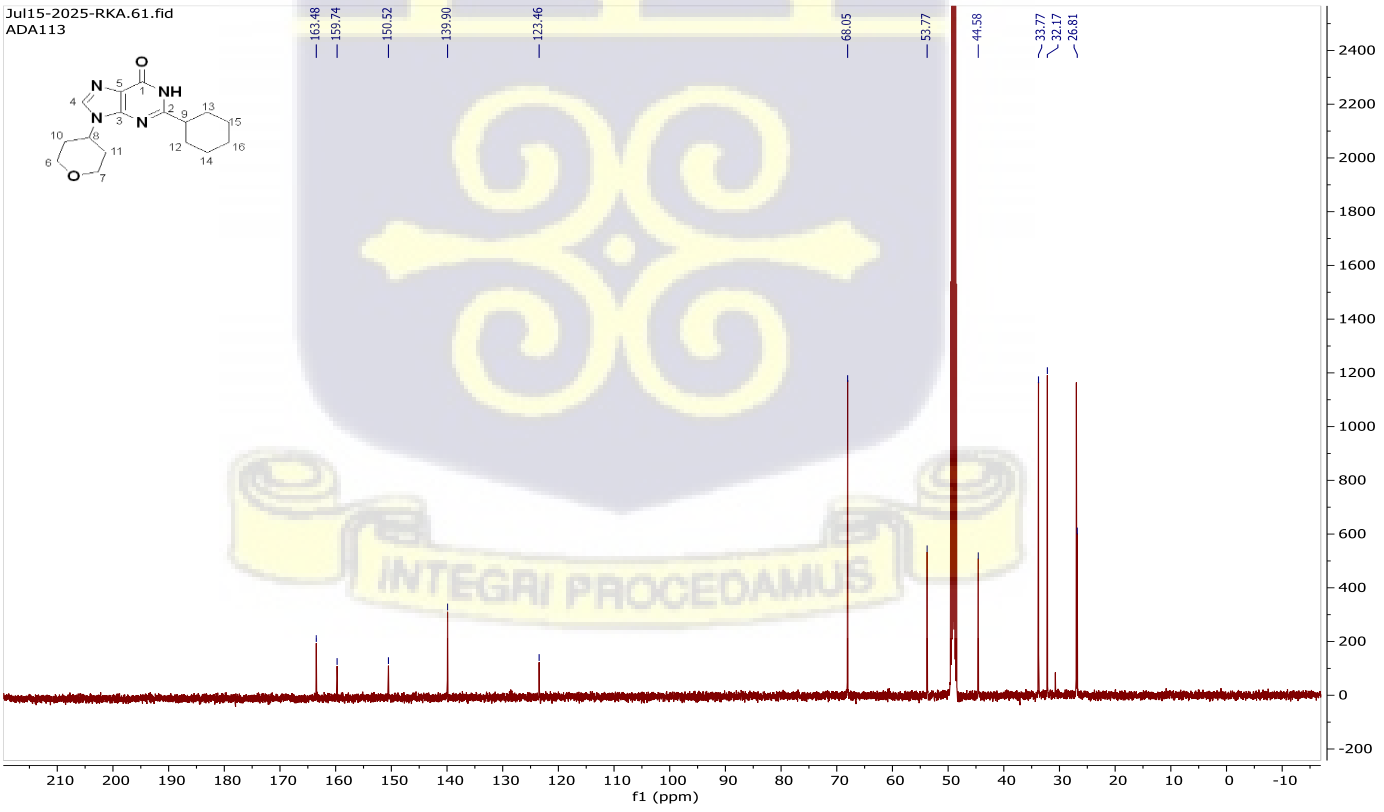




University of Ghana http://ugspace.ug.edu.gh

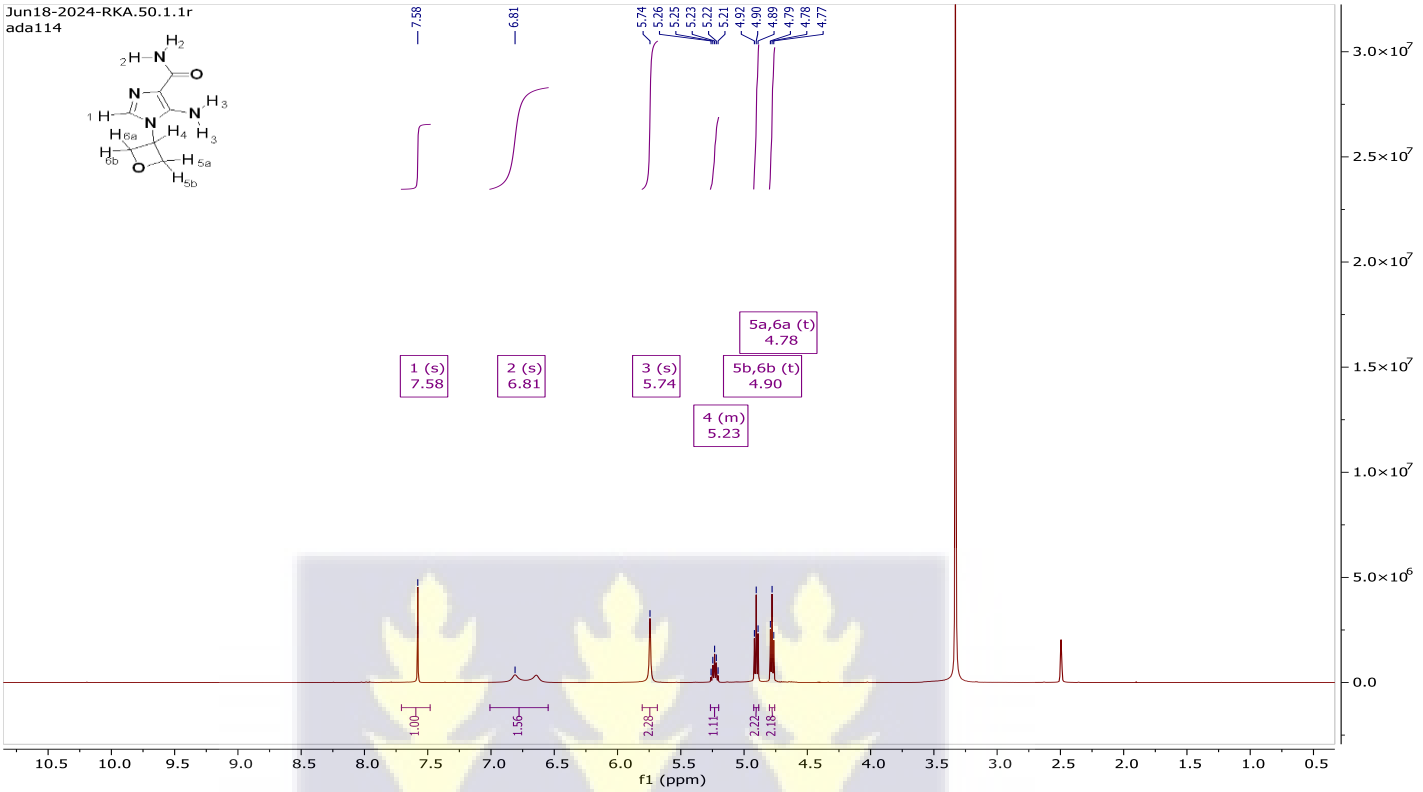
ADA113

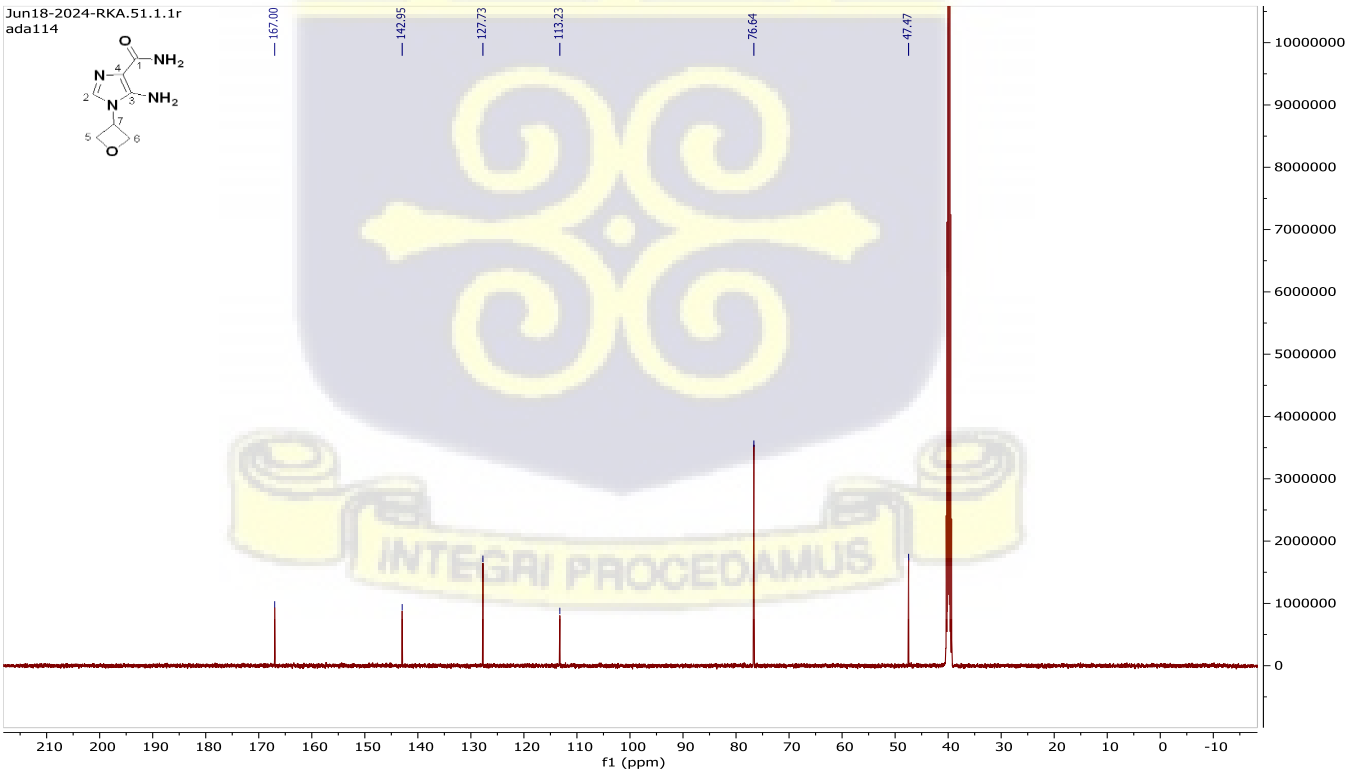




University of Ghana http://ugspace.ug.edu.gh

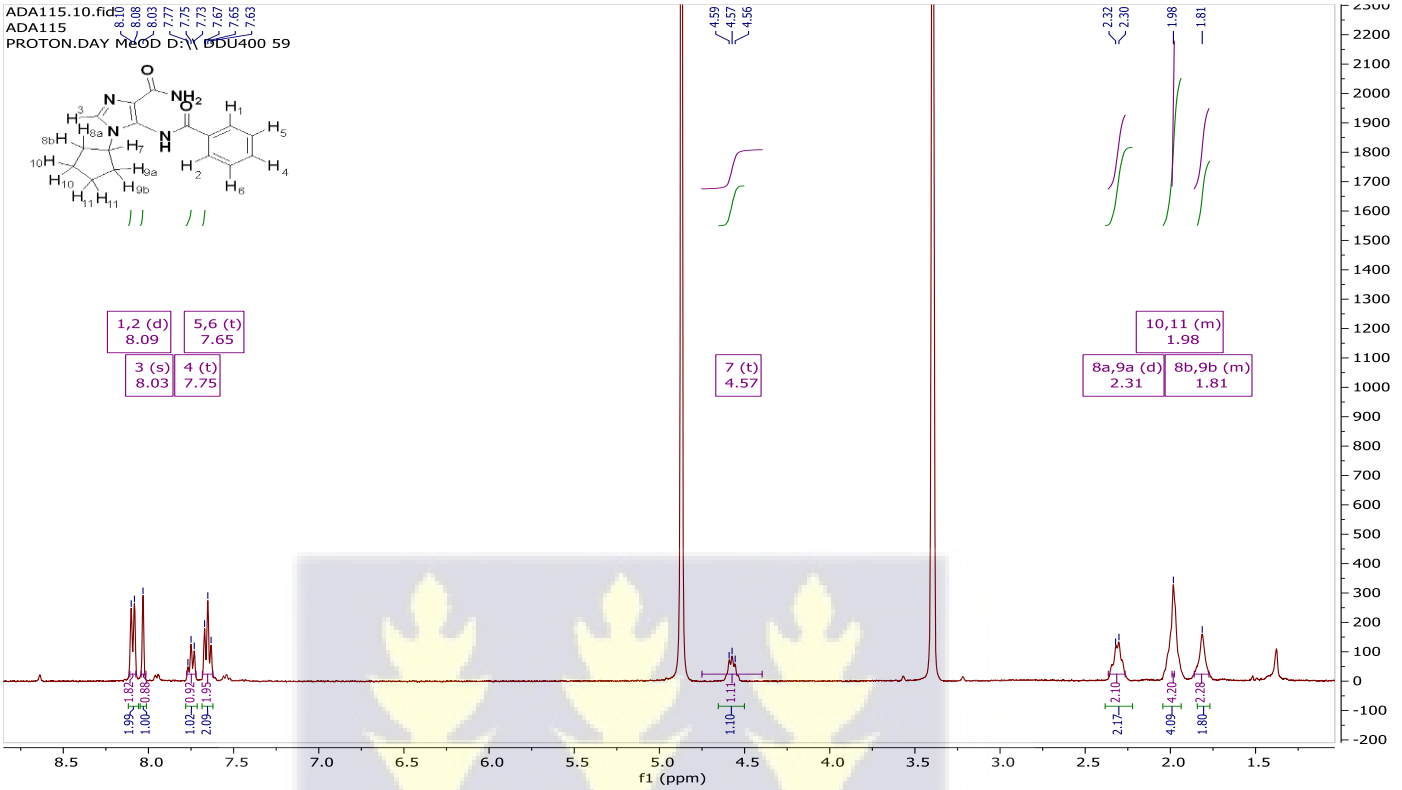
ADA114

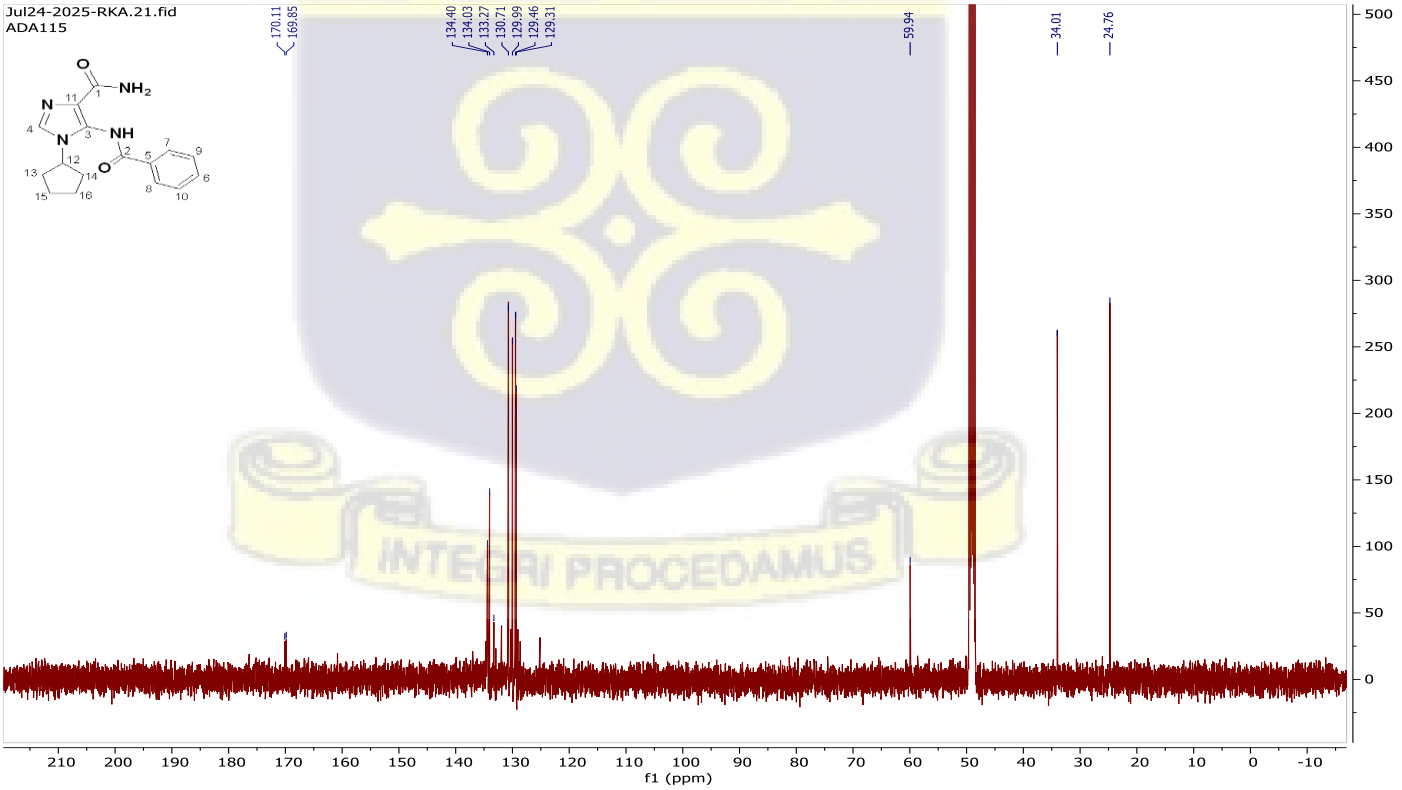




University of Ghana http://ugspace.ug.edu.gh

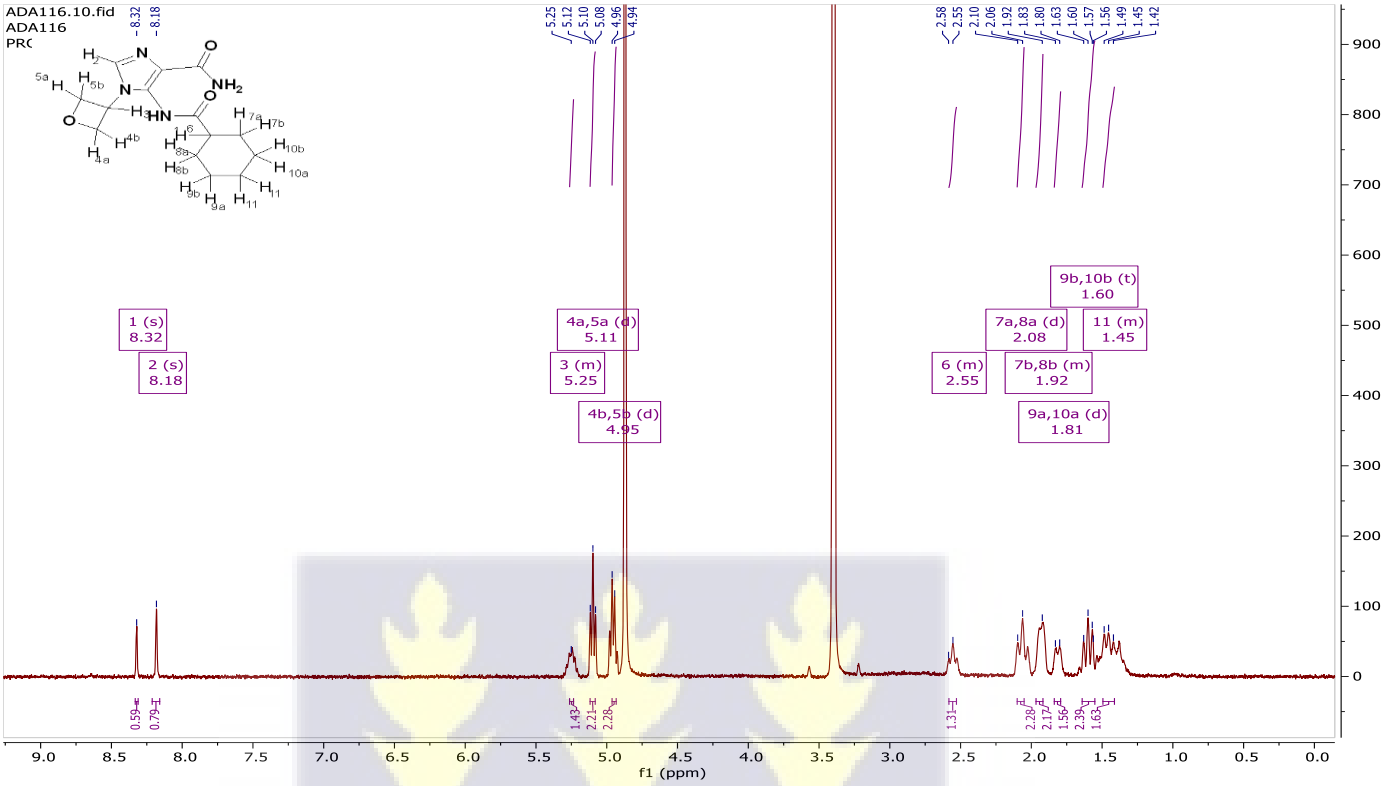
ADA115

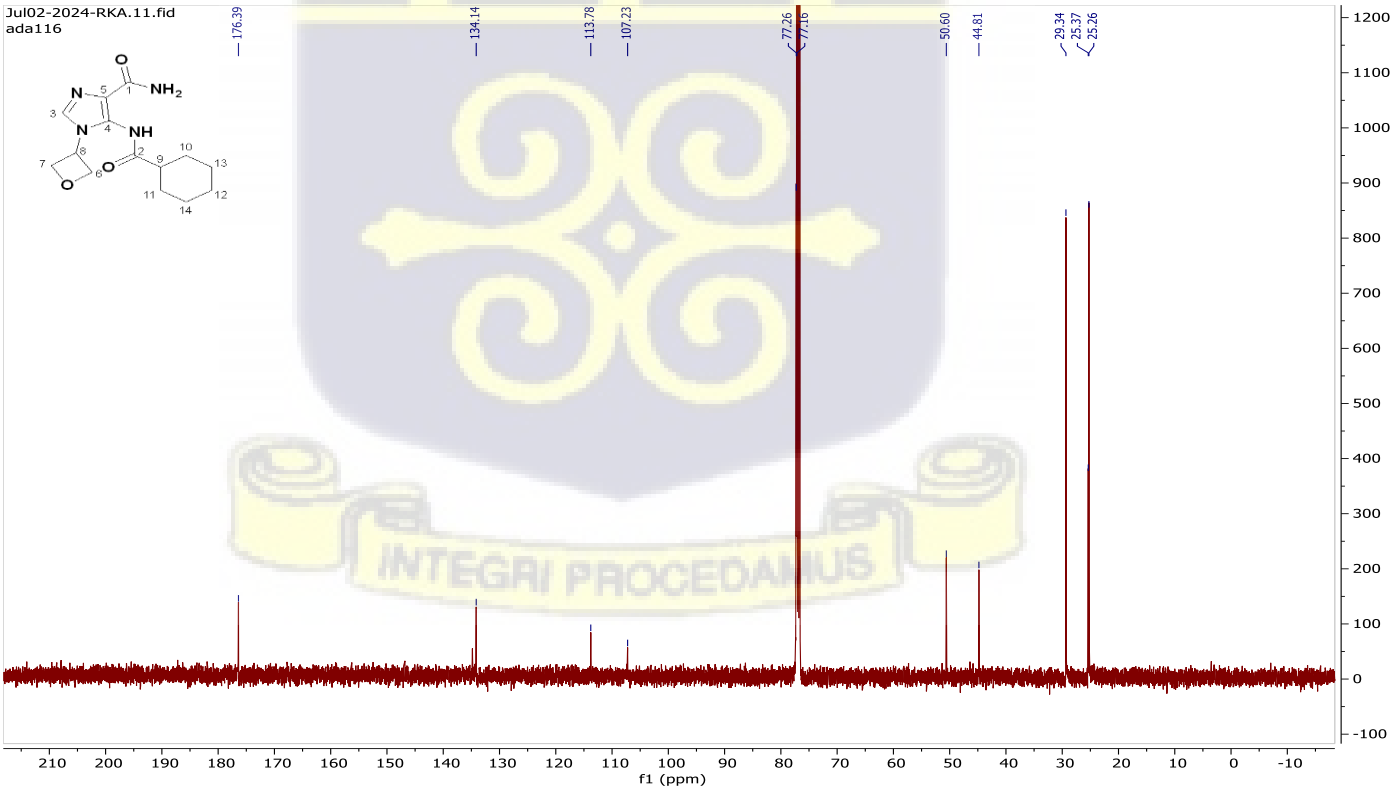




University of Ghana http://ugspace.ug.edu.gh

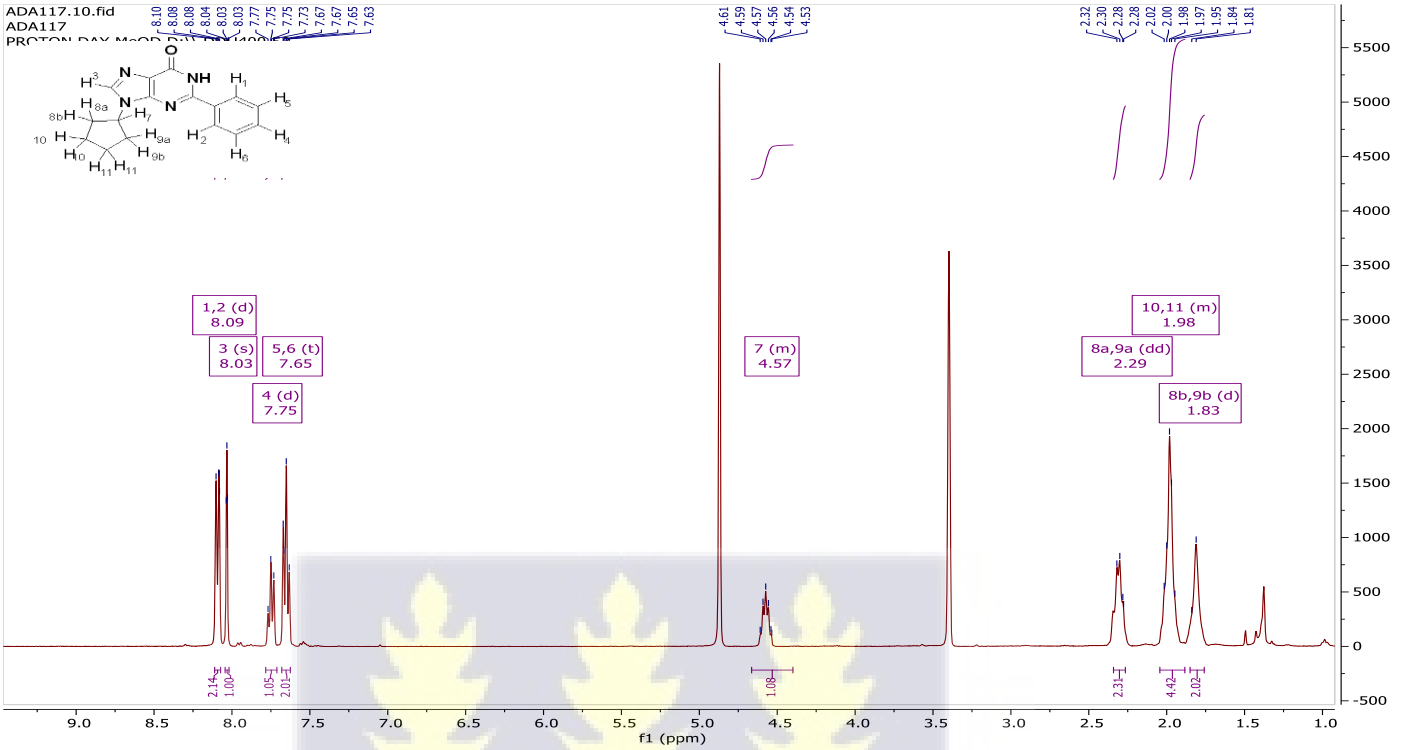
ADA116

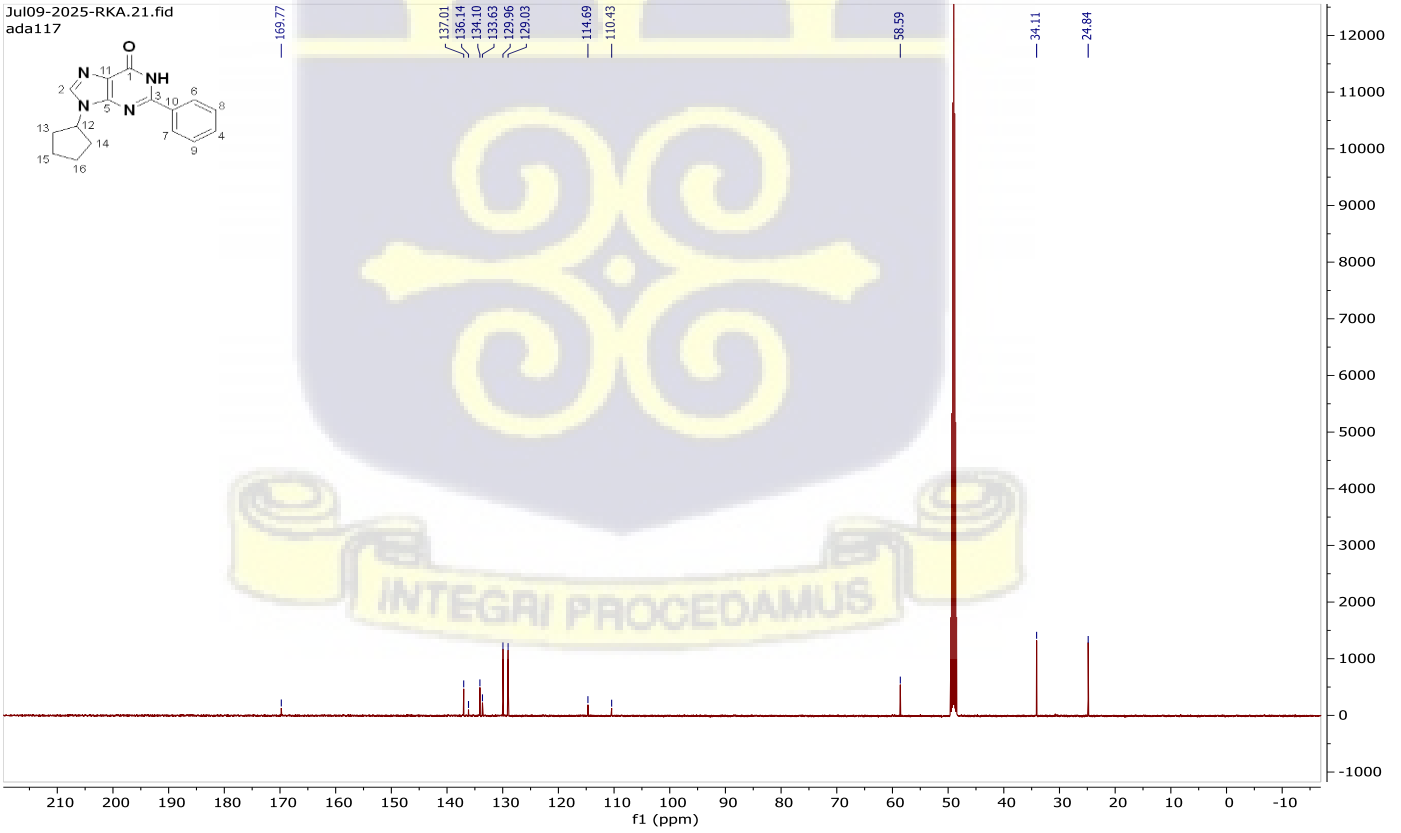




University of Ghana http://ugspace.ug.edu.gh

ADA117

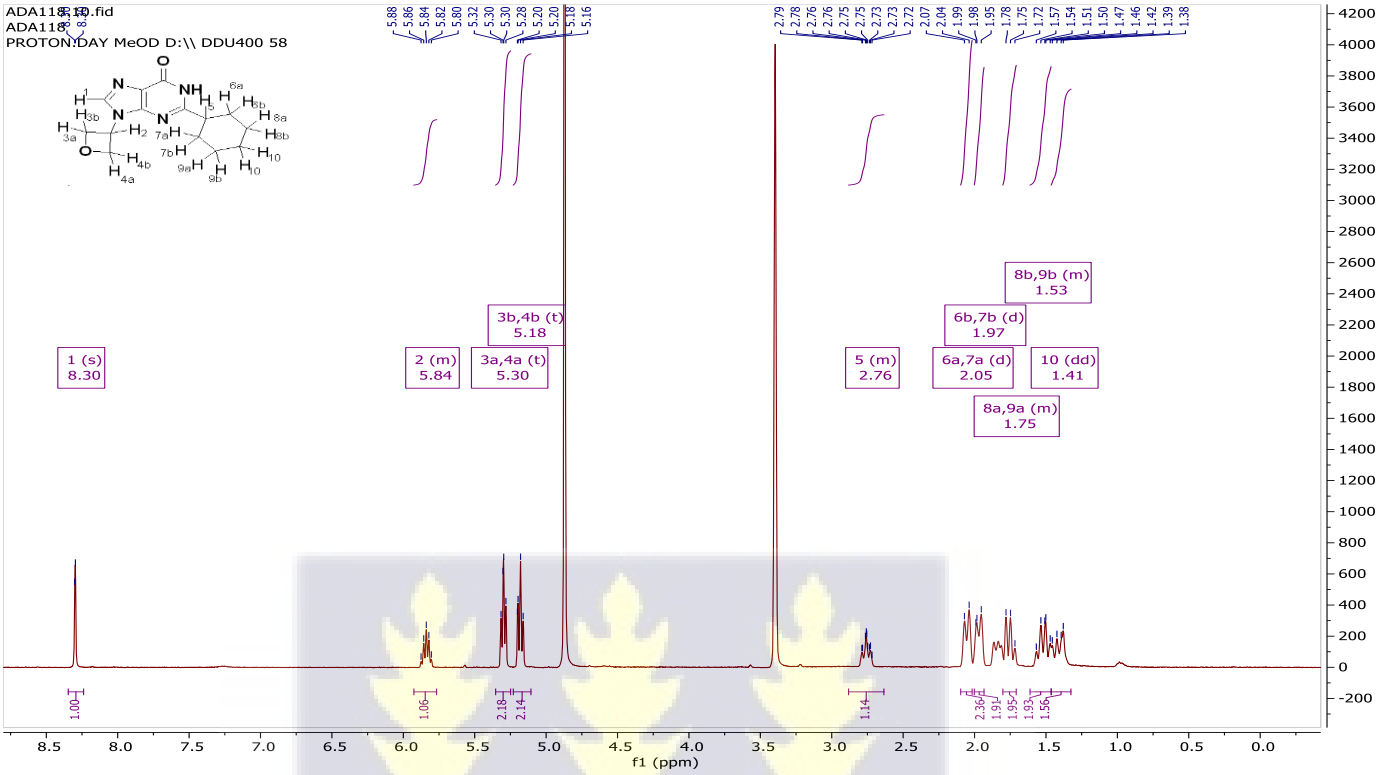




INTEGRI PROCEDAMUS

University of Ghana http://ugspace.ug.edu.gh

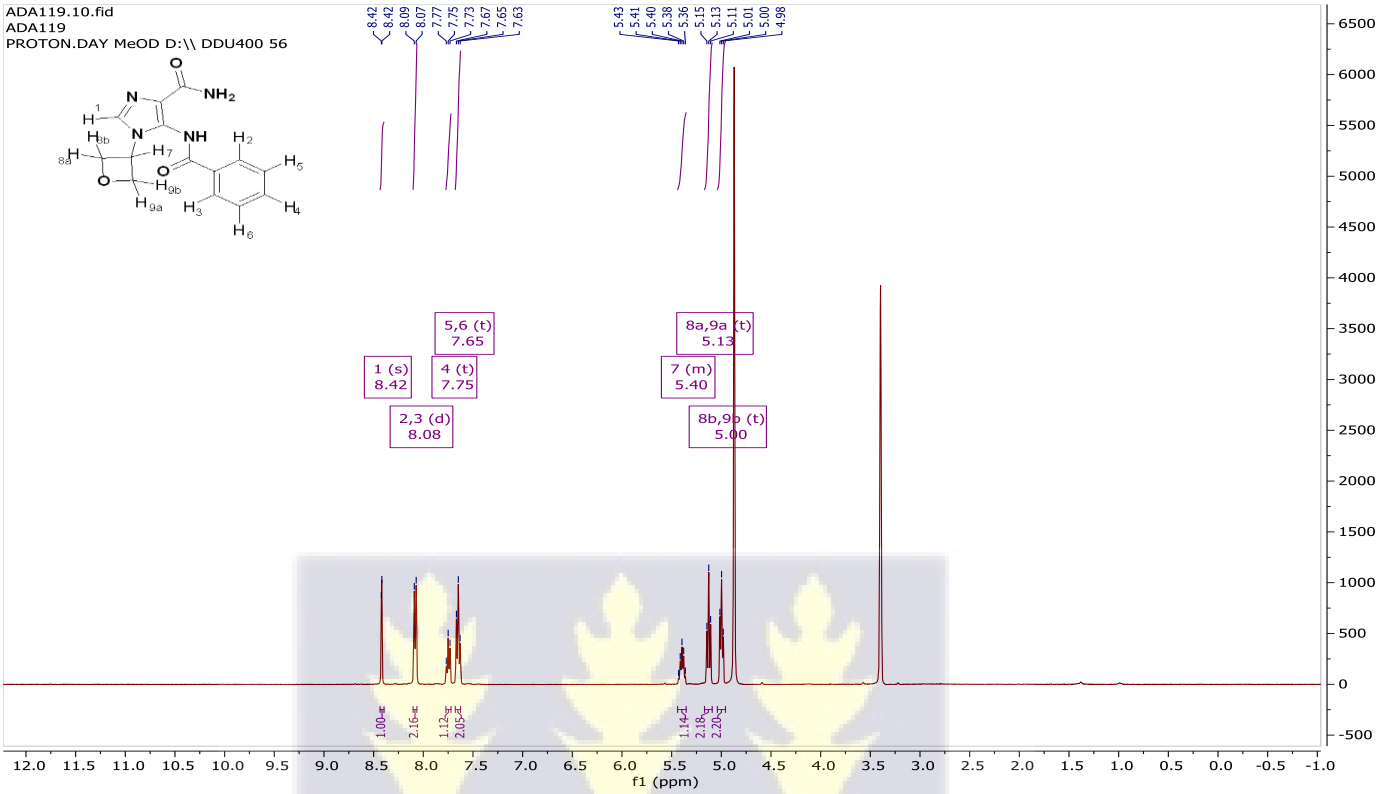
ADA118

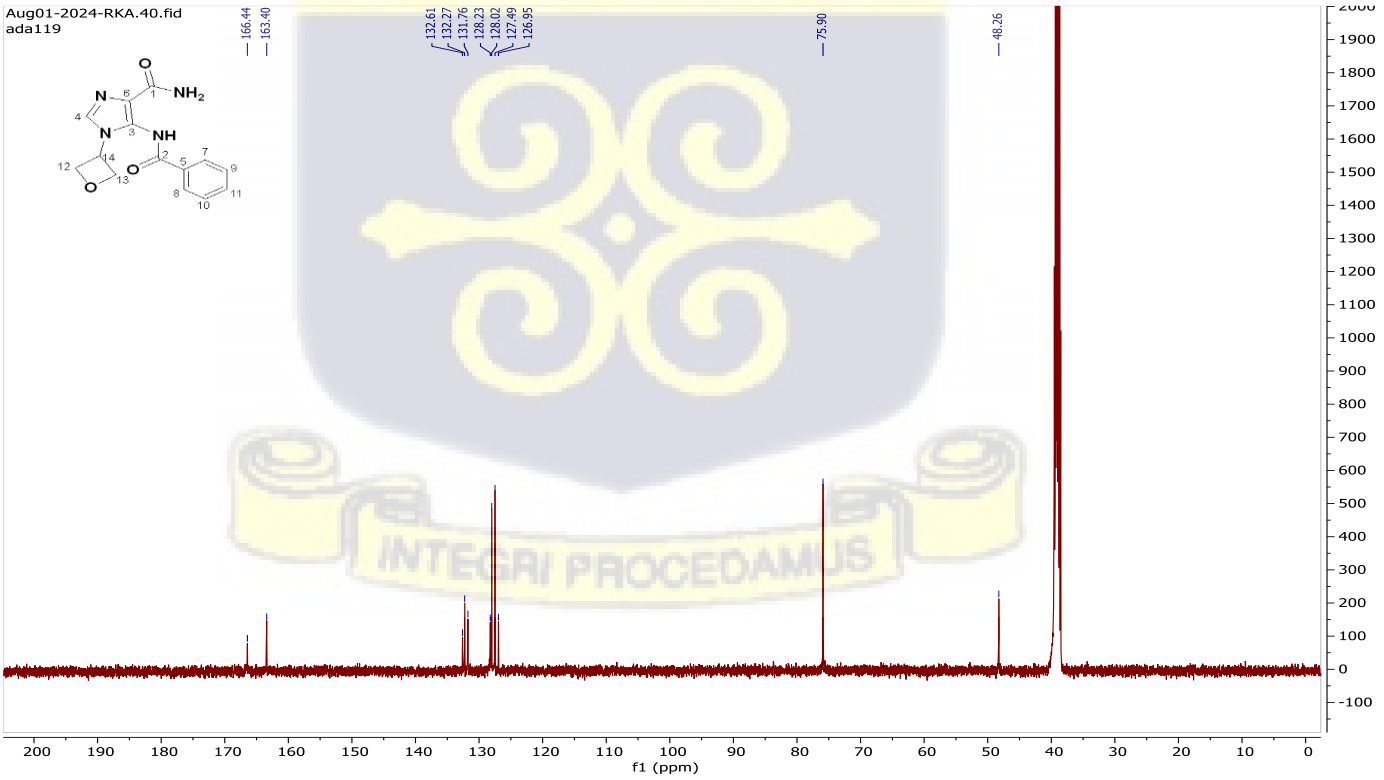


INTEGRI PROCEDAMUS

University of Ghana http://ugspace.ug.edu.gh

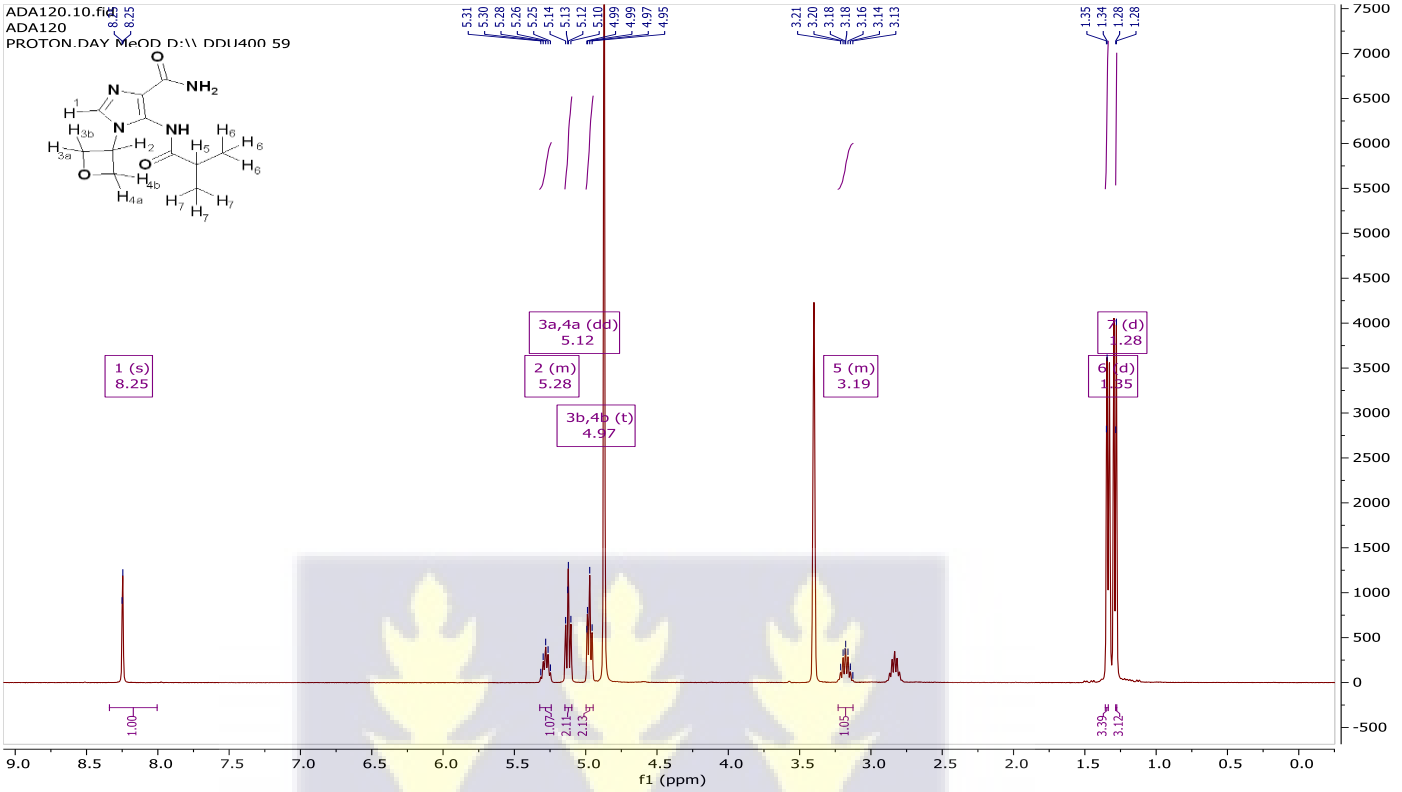
ADA119

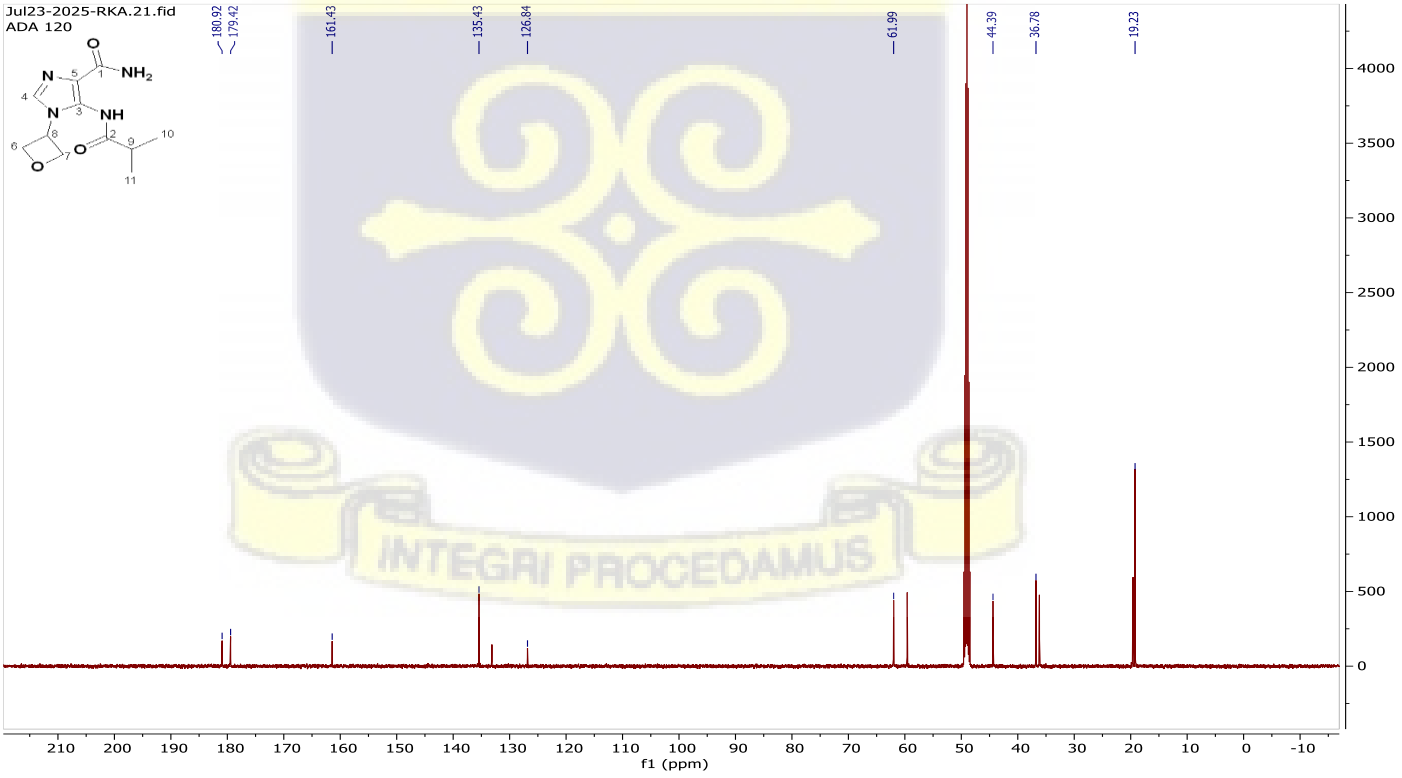




University of Ghana http://ugspace.ug.edu.gh

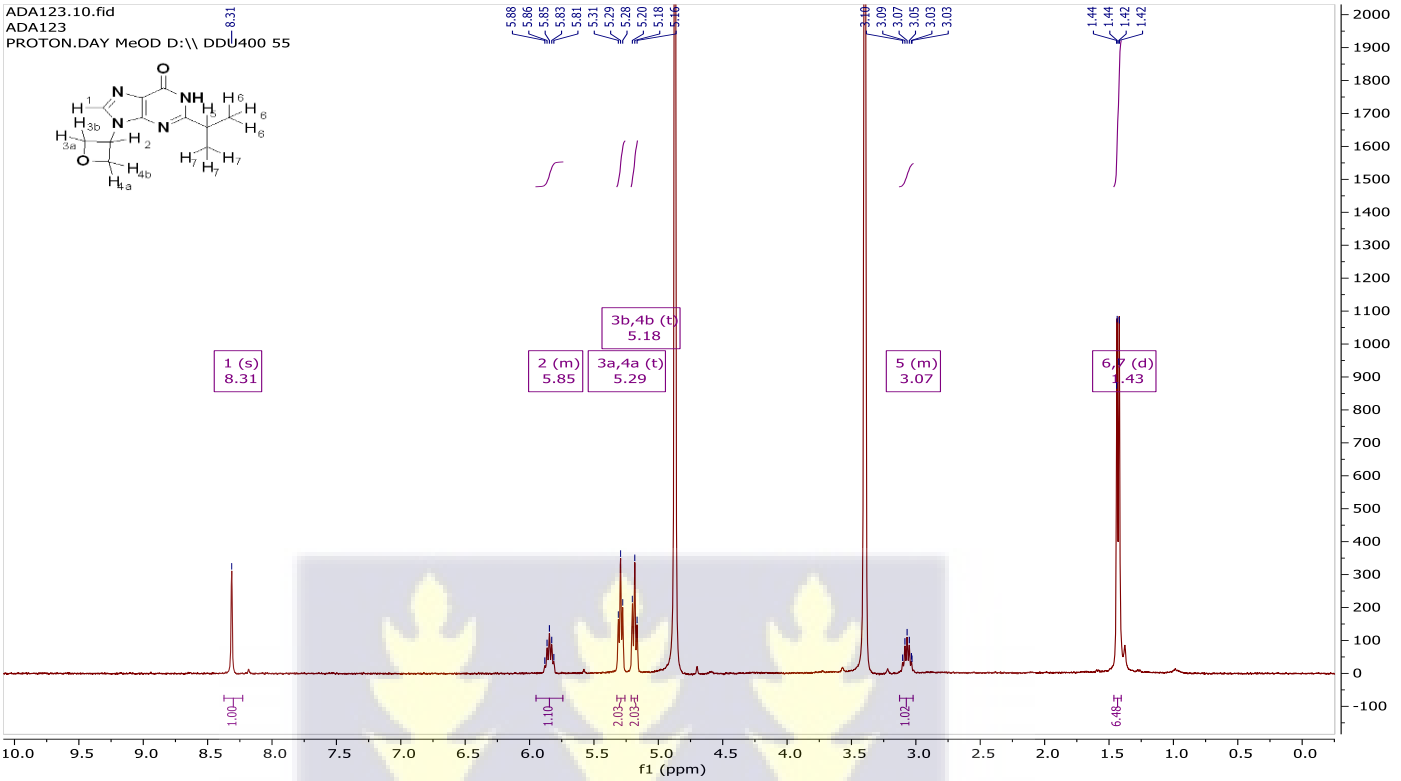
ADA120

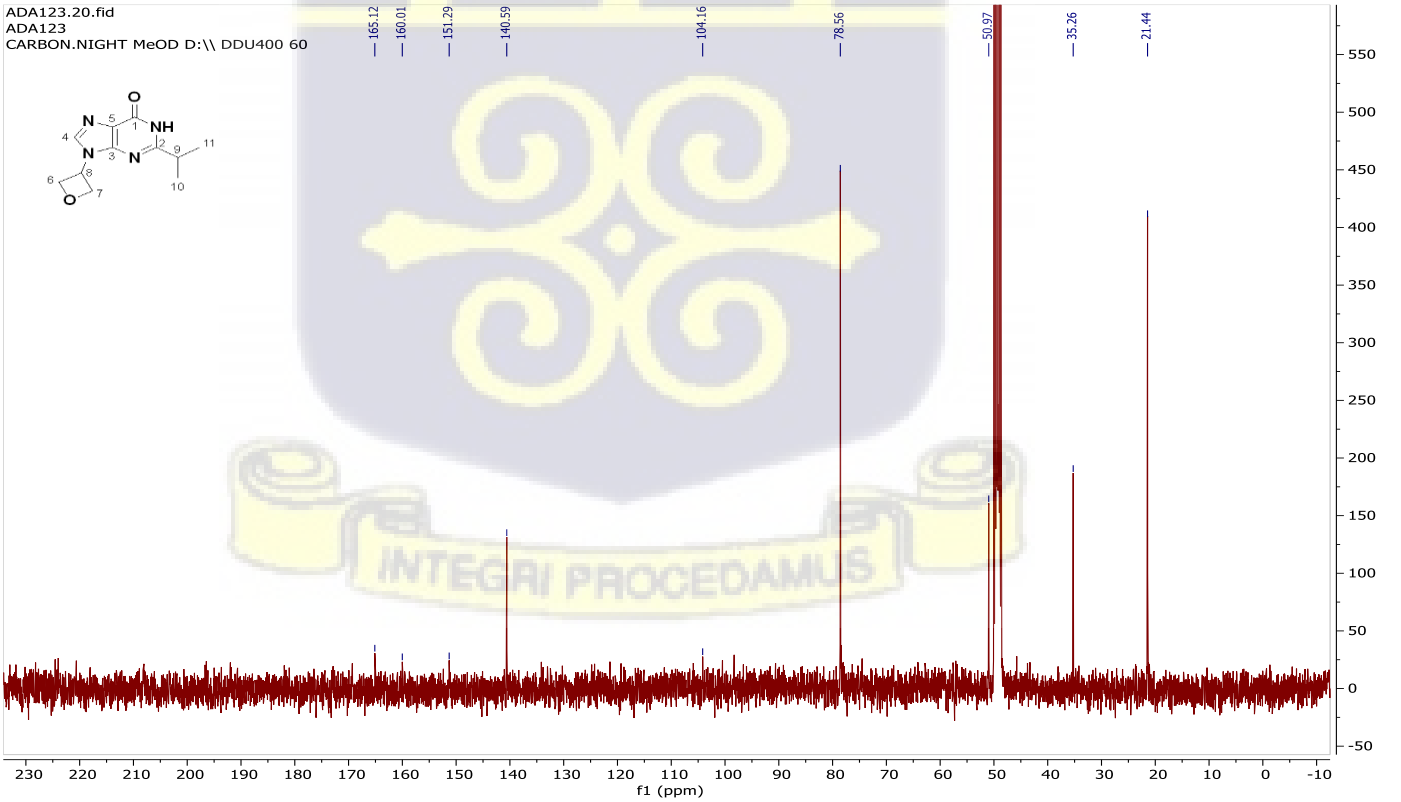




University of Ghana http://ugspace.ug.edu.gh

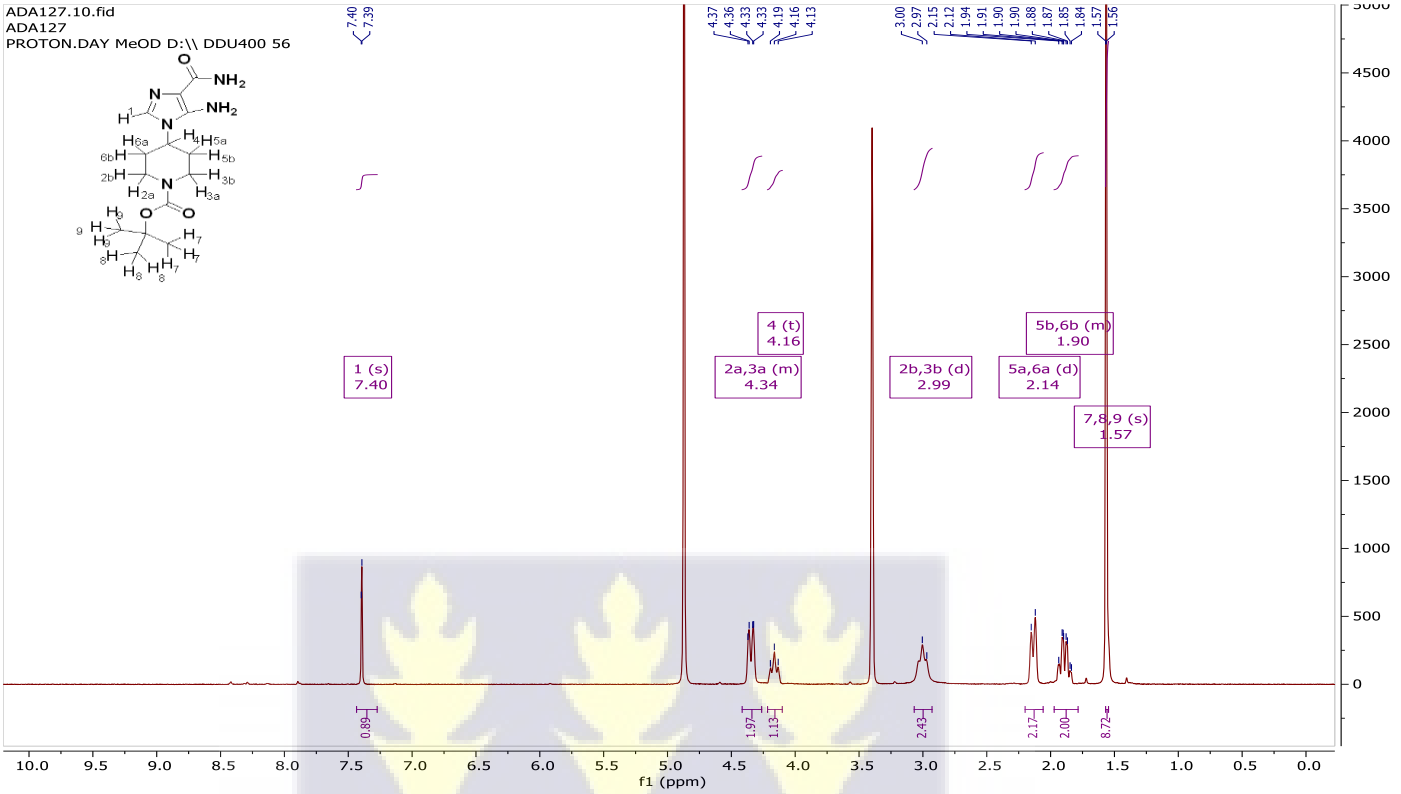
ADA123

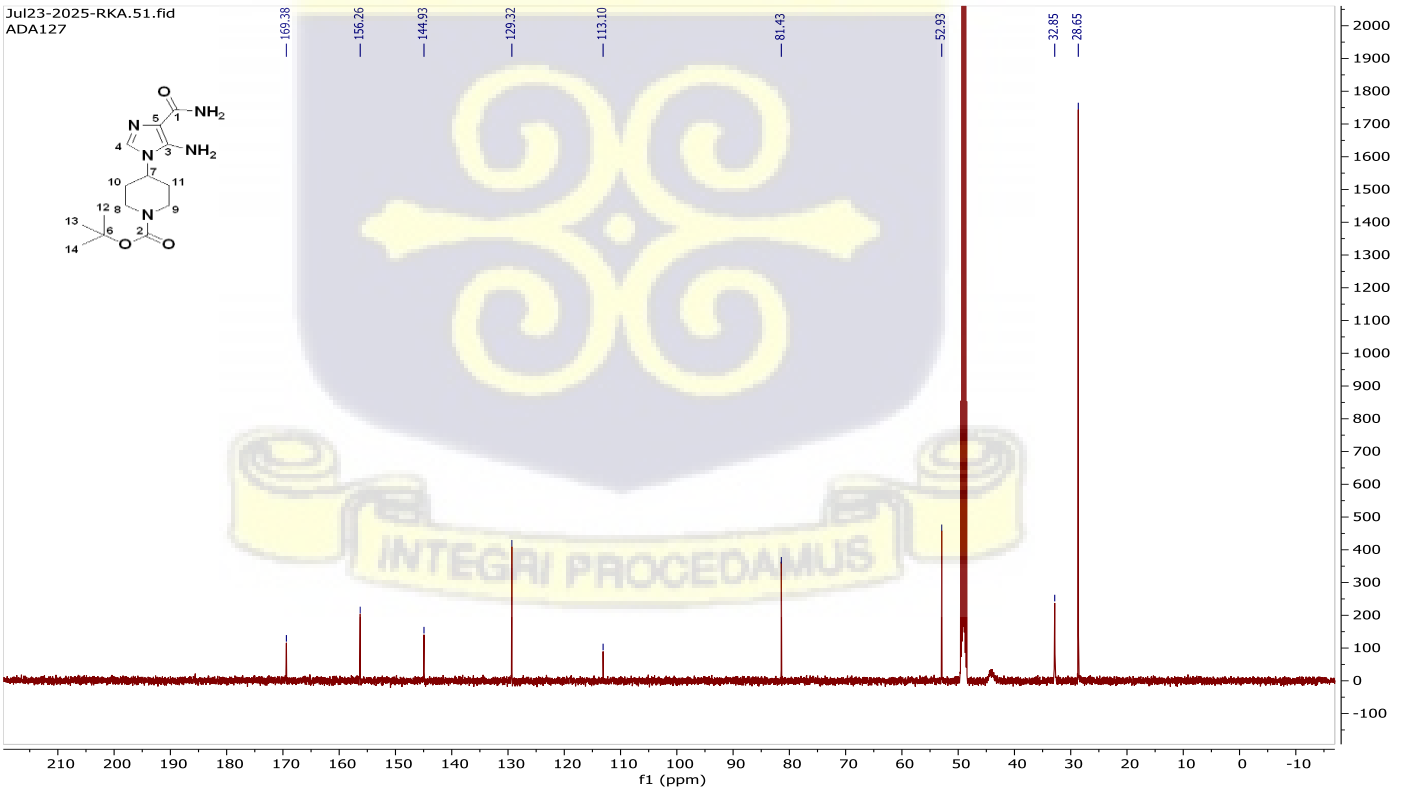




University of Ghana http://ugspace.ug.edu.gh

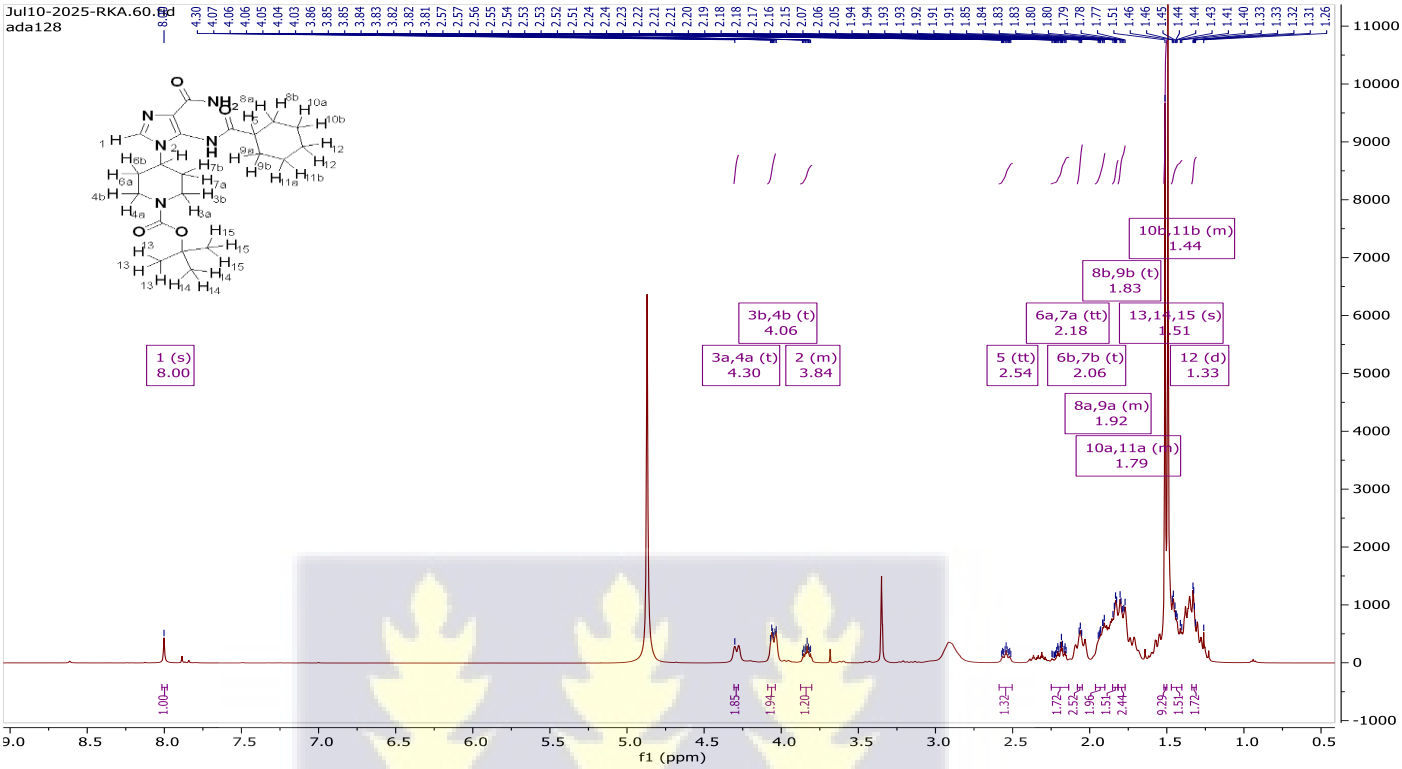
ADA127

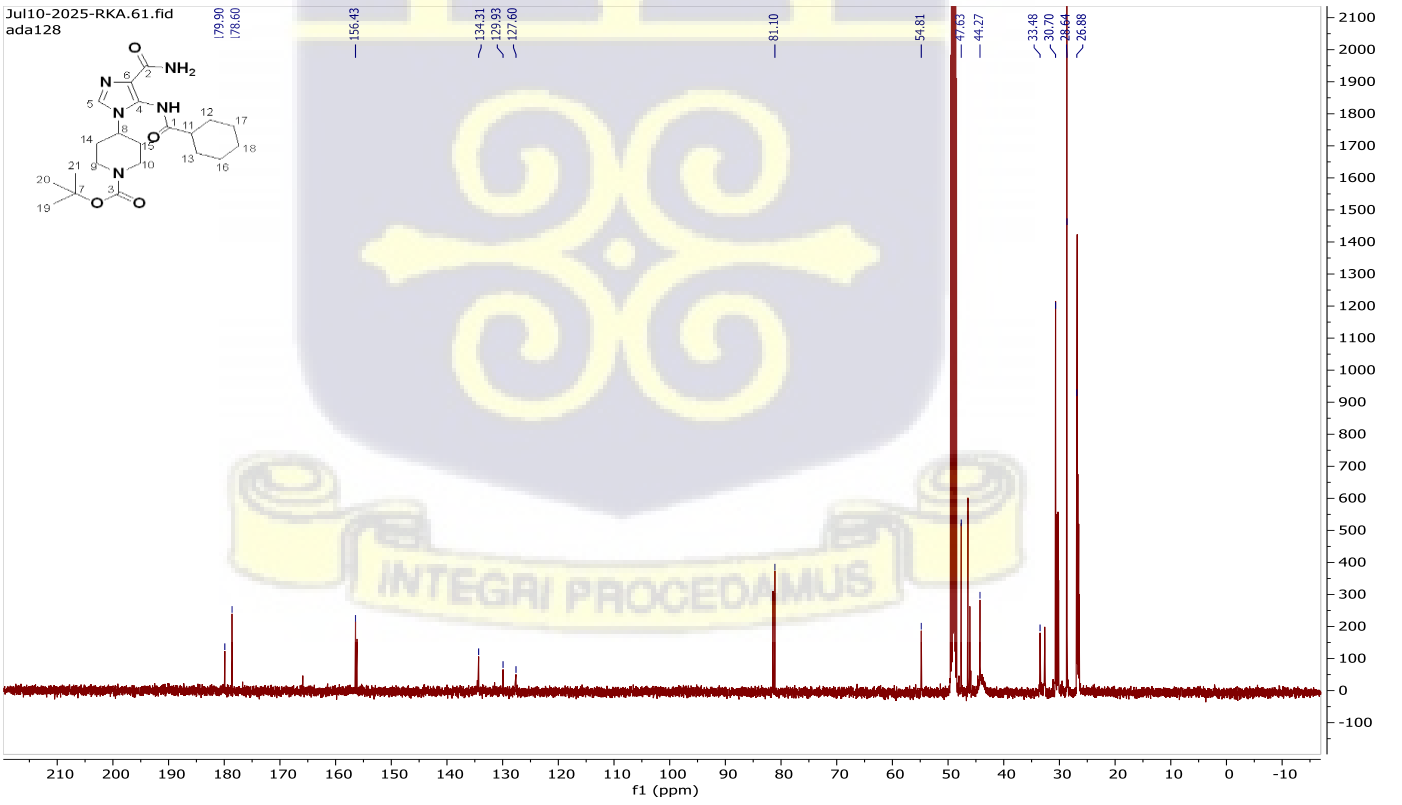




University of Ghana http://ugspace.ug.edu.gh

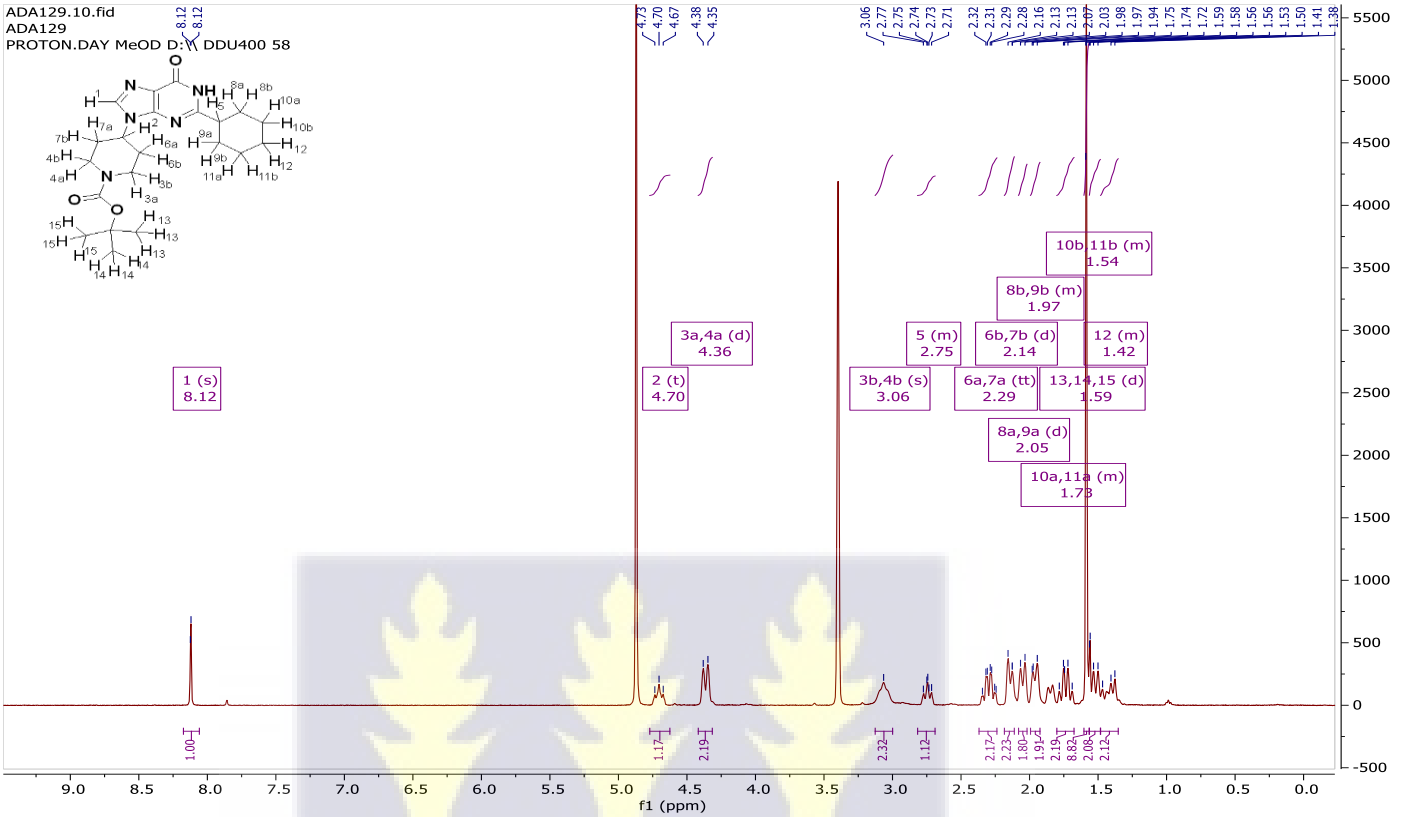
ADA128

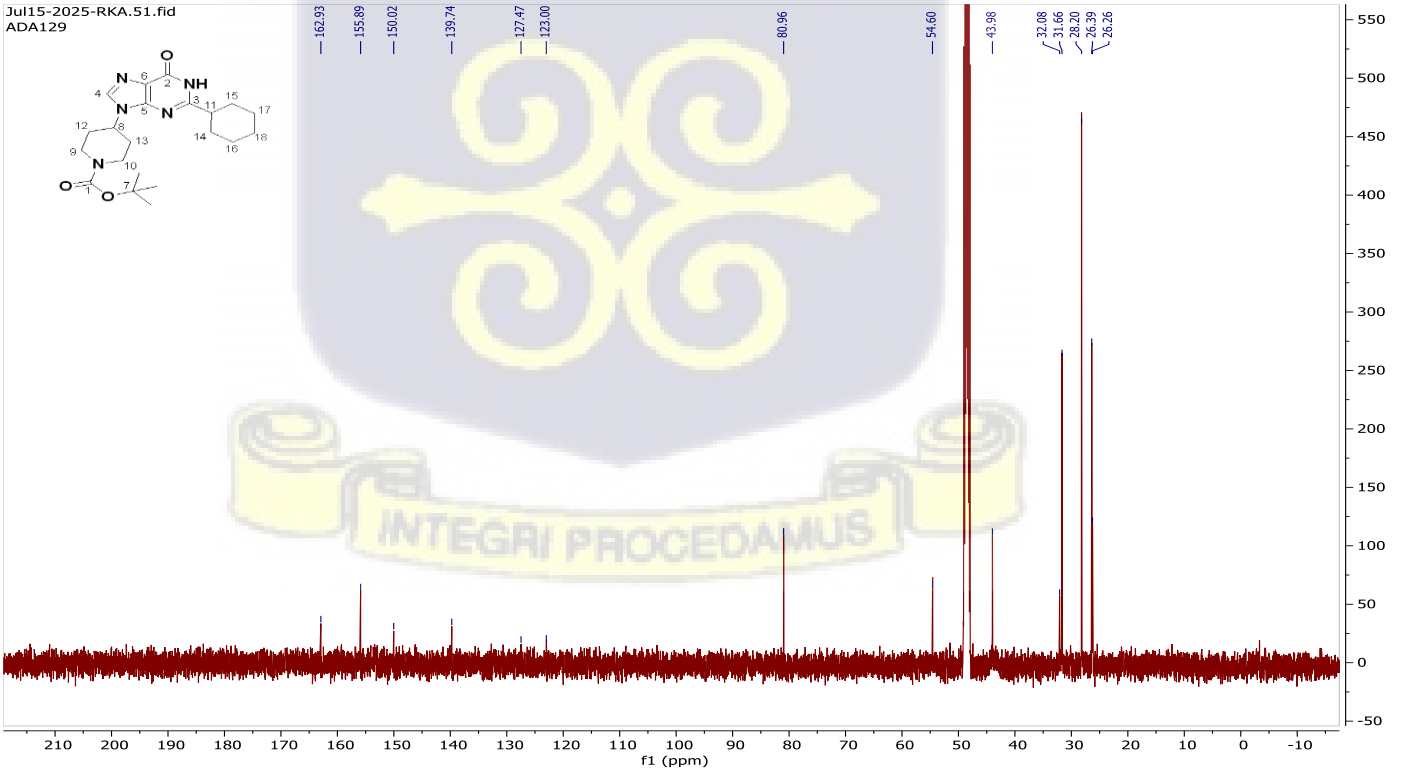




University of Ghana http://ugspace.ug.edu.gh

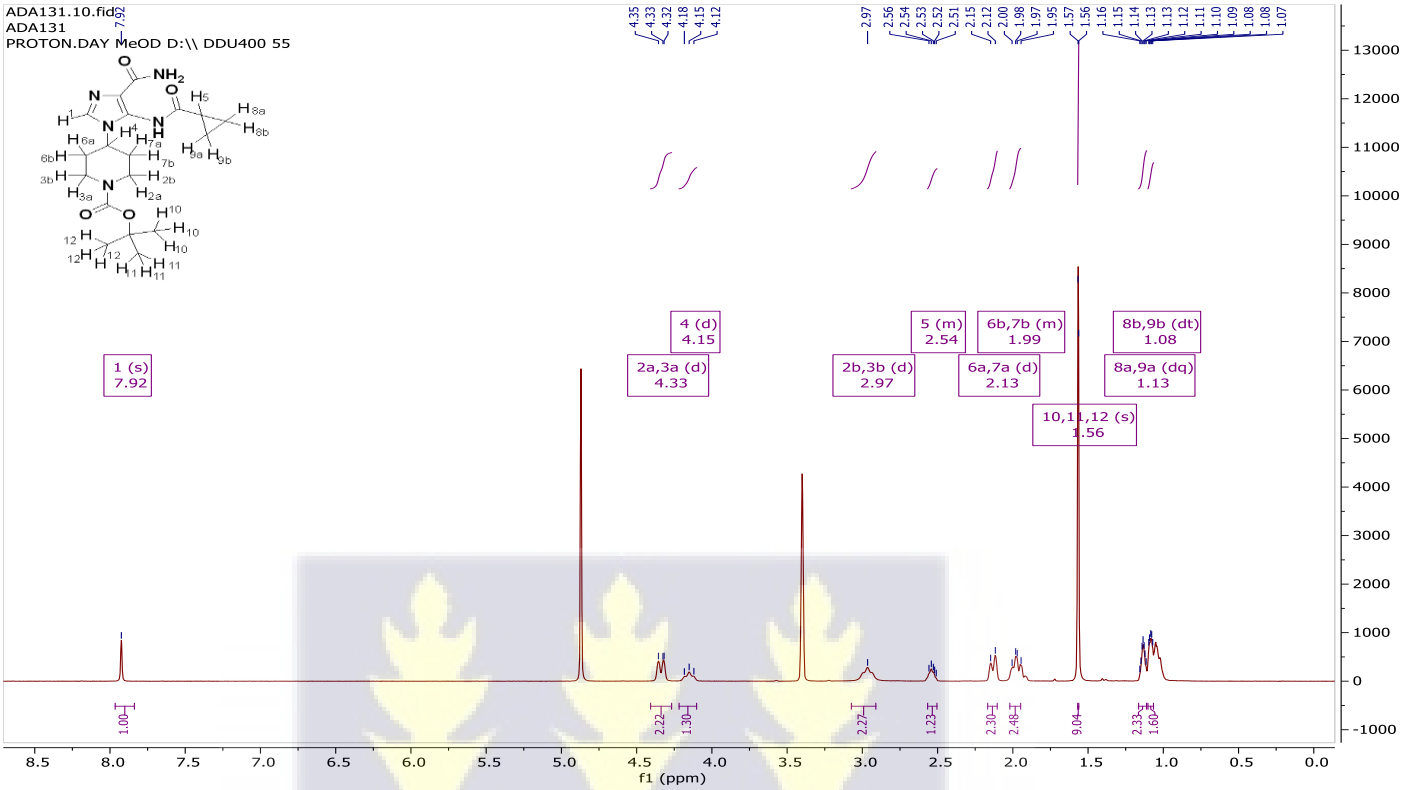
ADA129





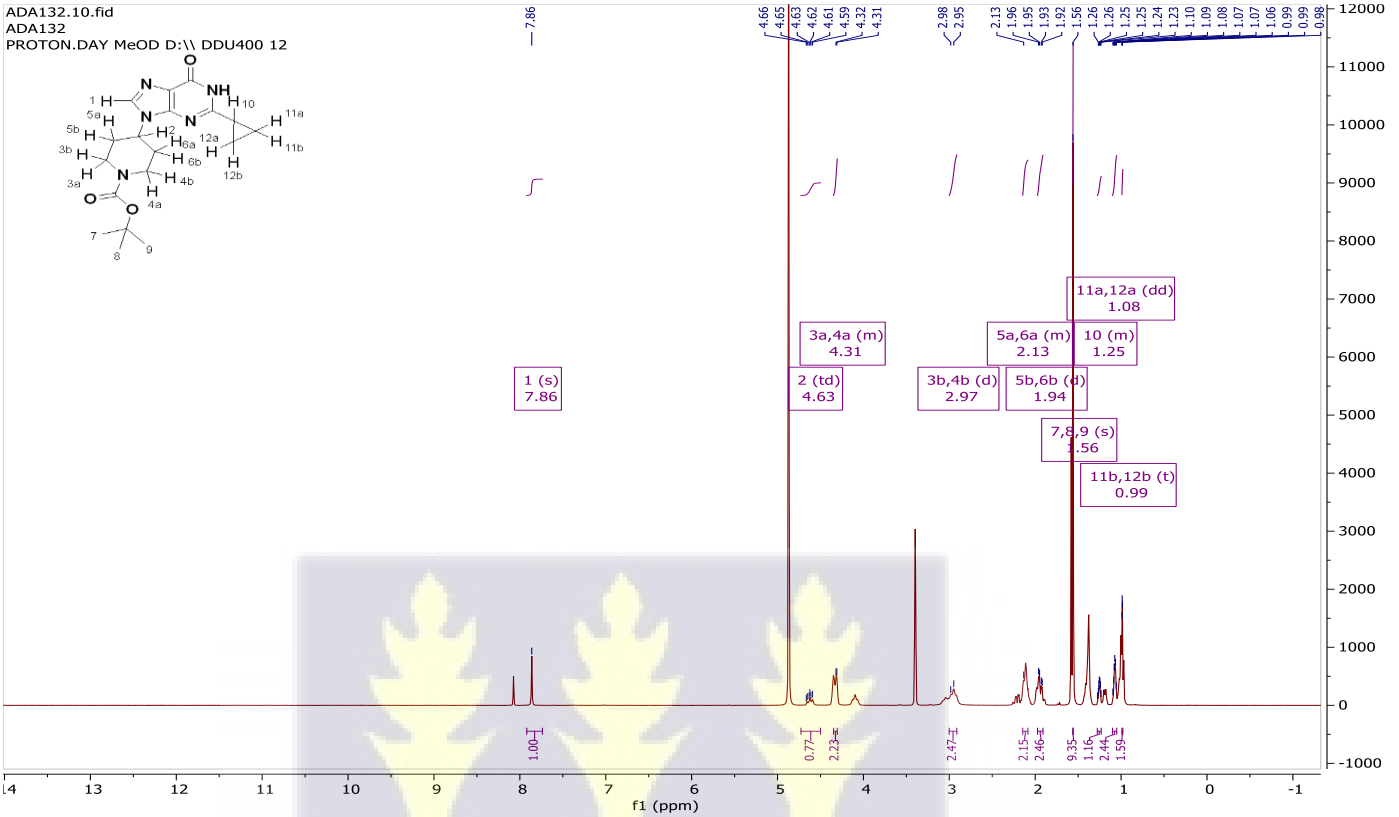
University of Ghana http://ugspace.ug.edu.gh

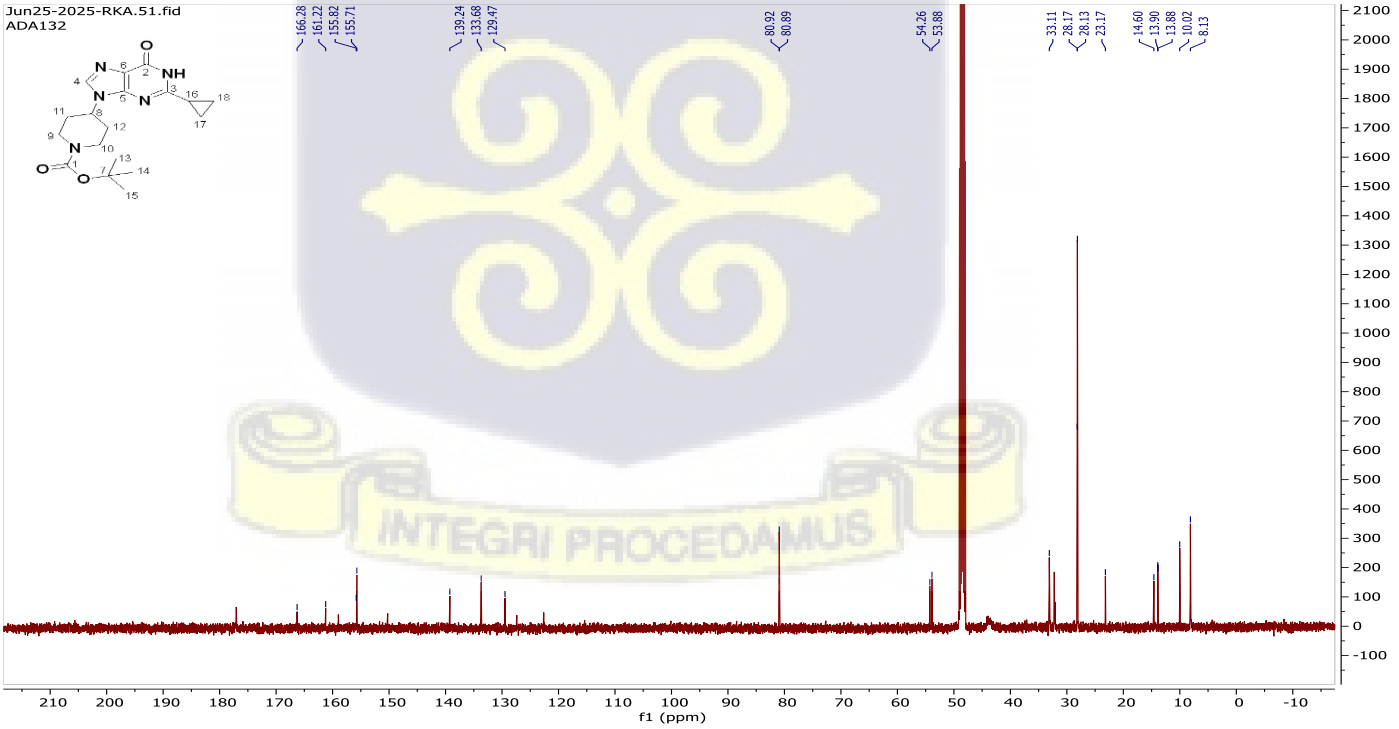
ADA131



University of Ghana http://ugspace.ug.edu.gh

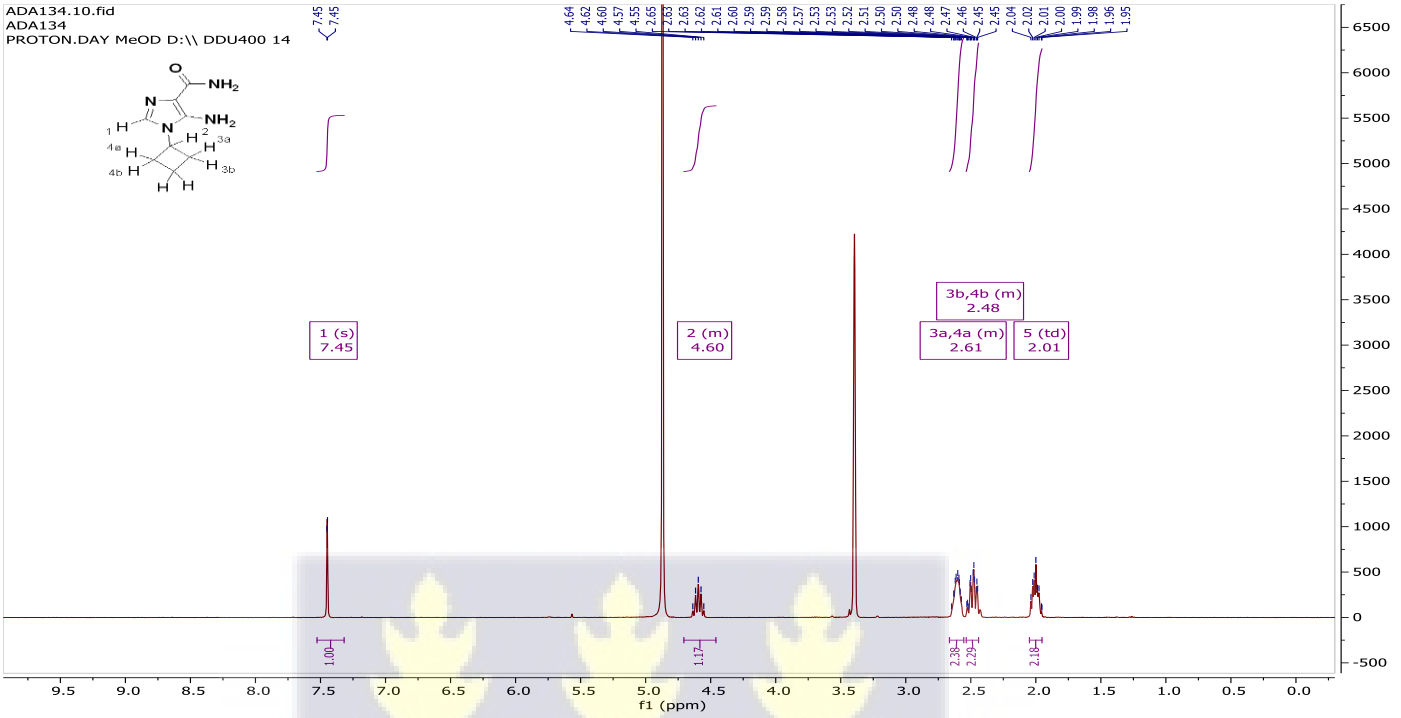
ADA132

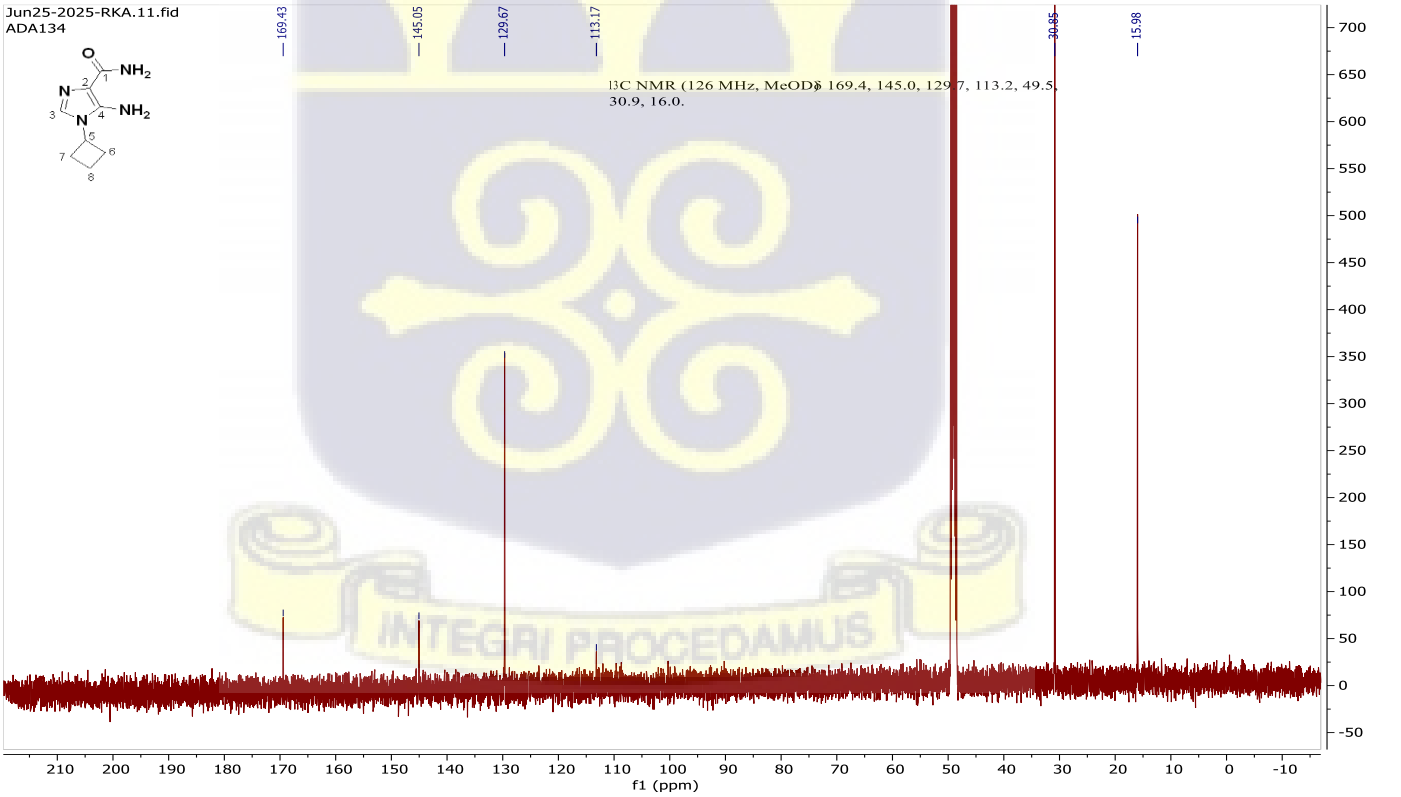




University of Ghana http://ugspace.ug.edu.gh

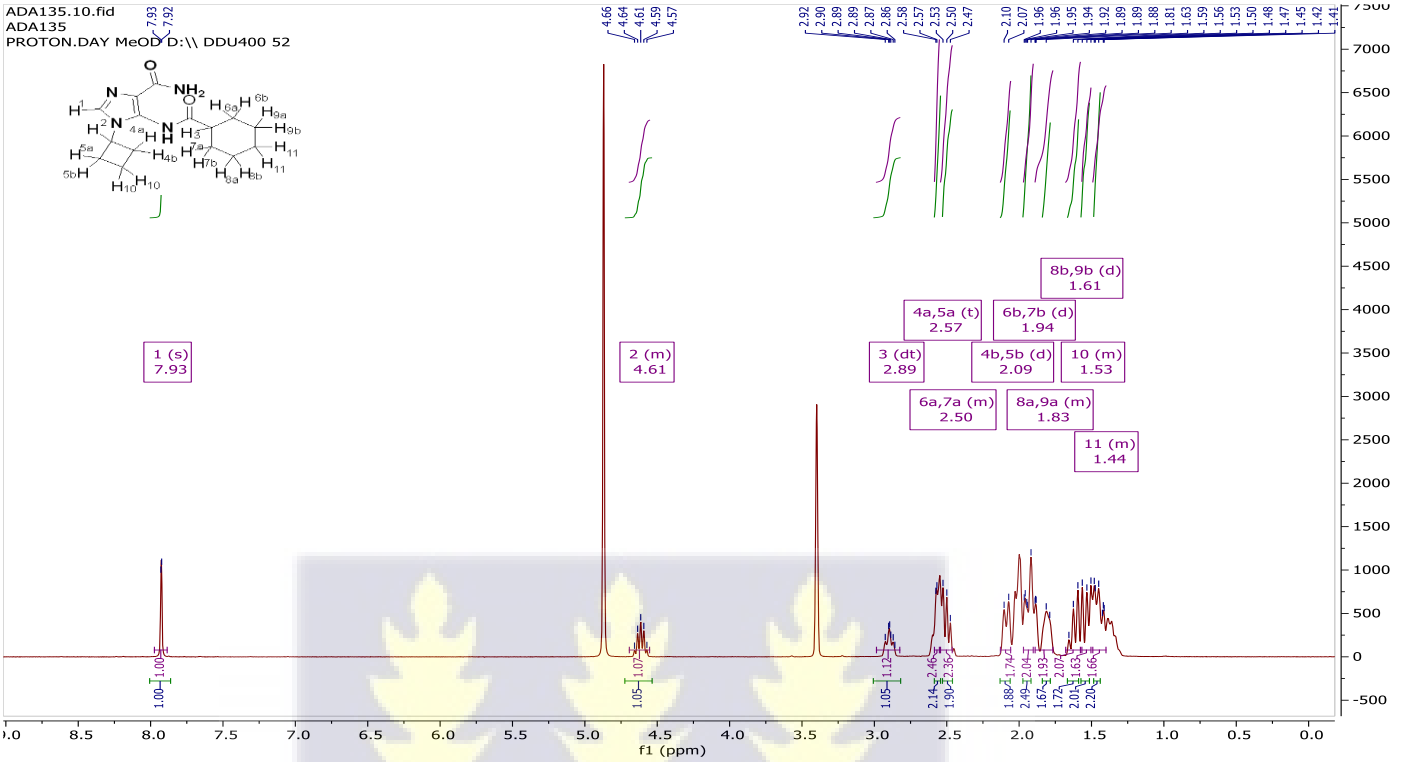
ADA134

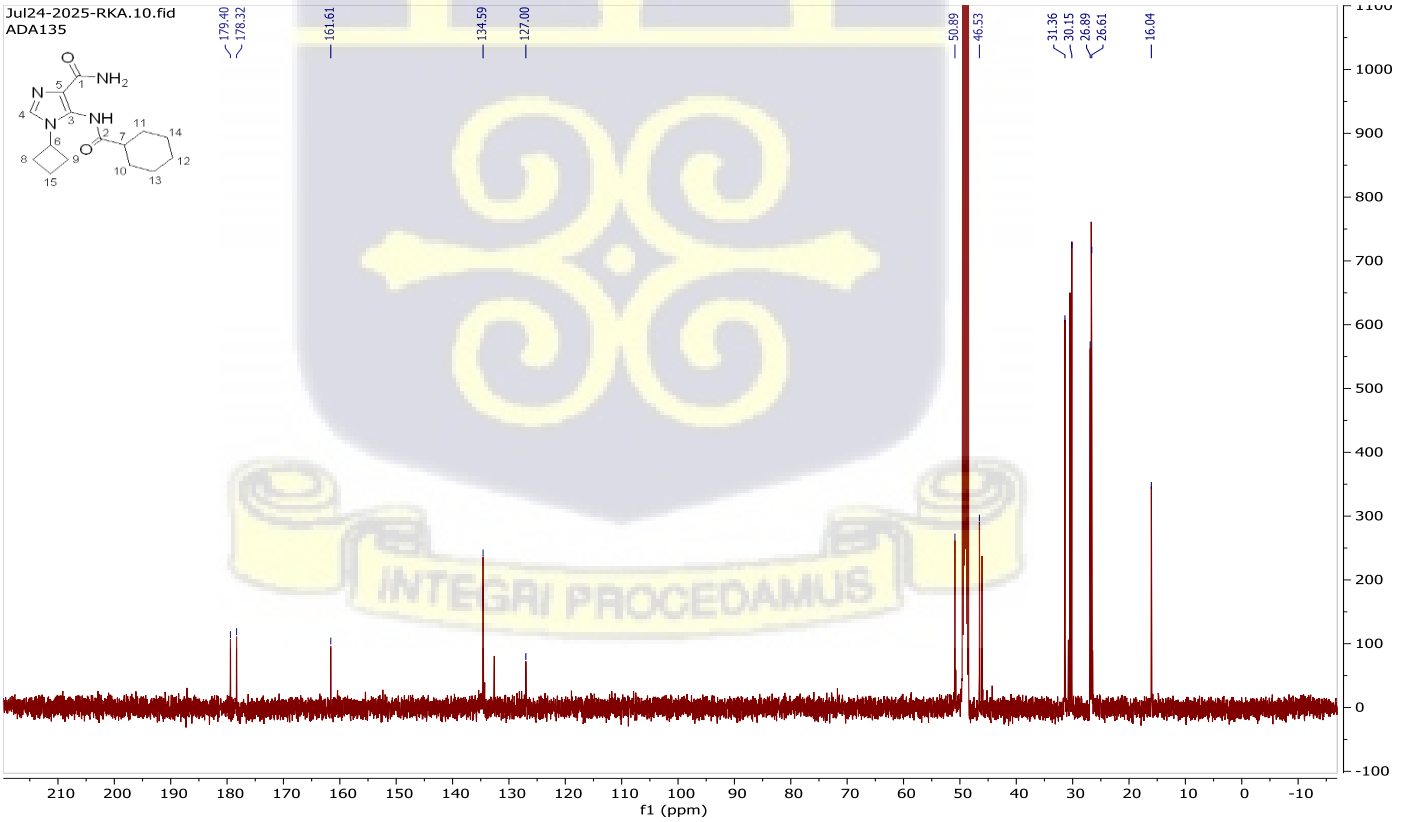




University of Ghana http://ugspace.ug.edu.gh

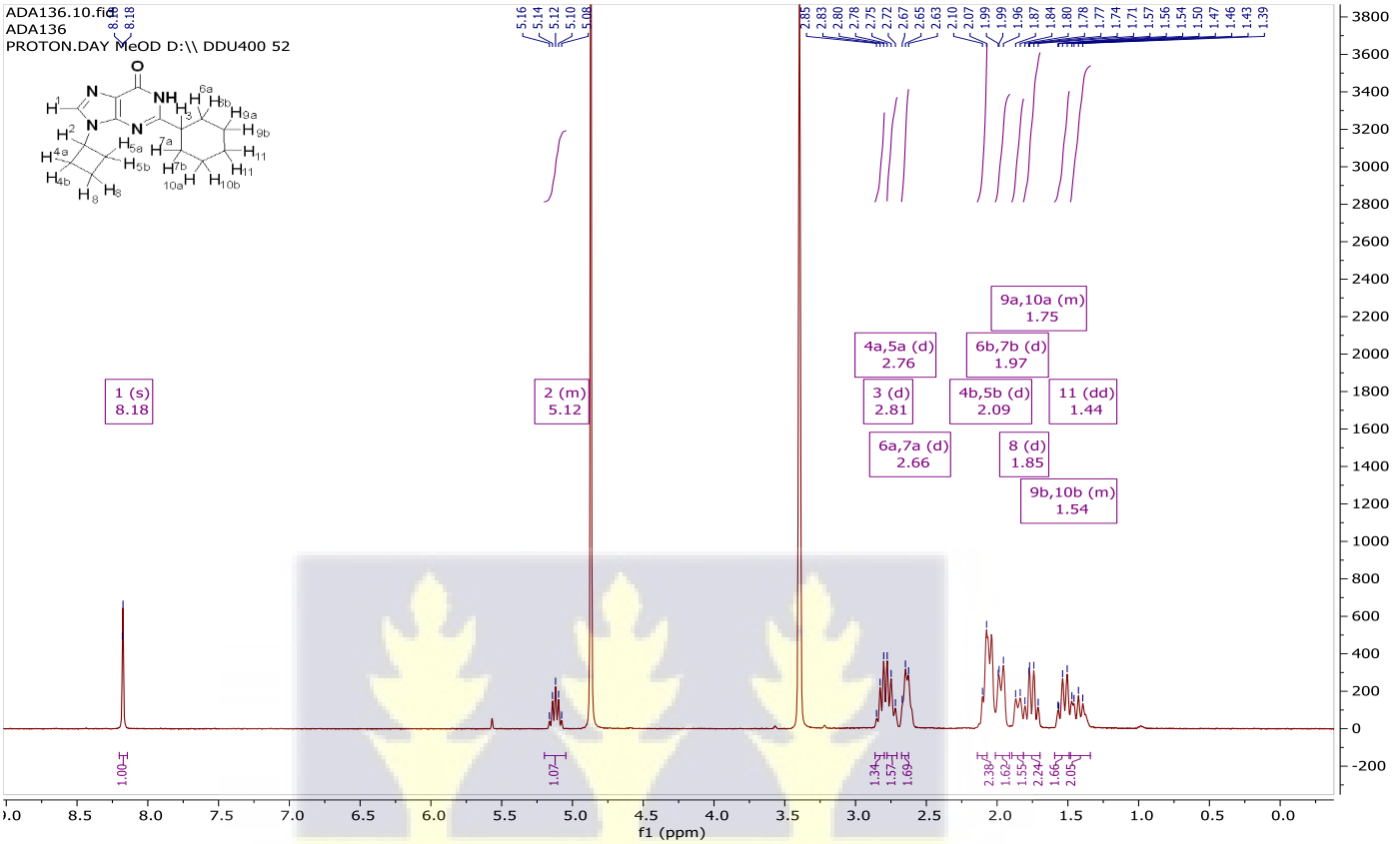
ADA135

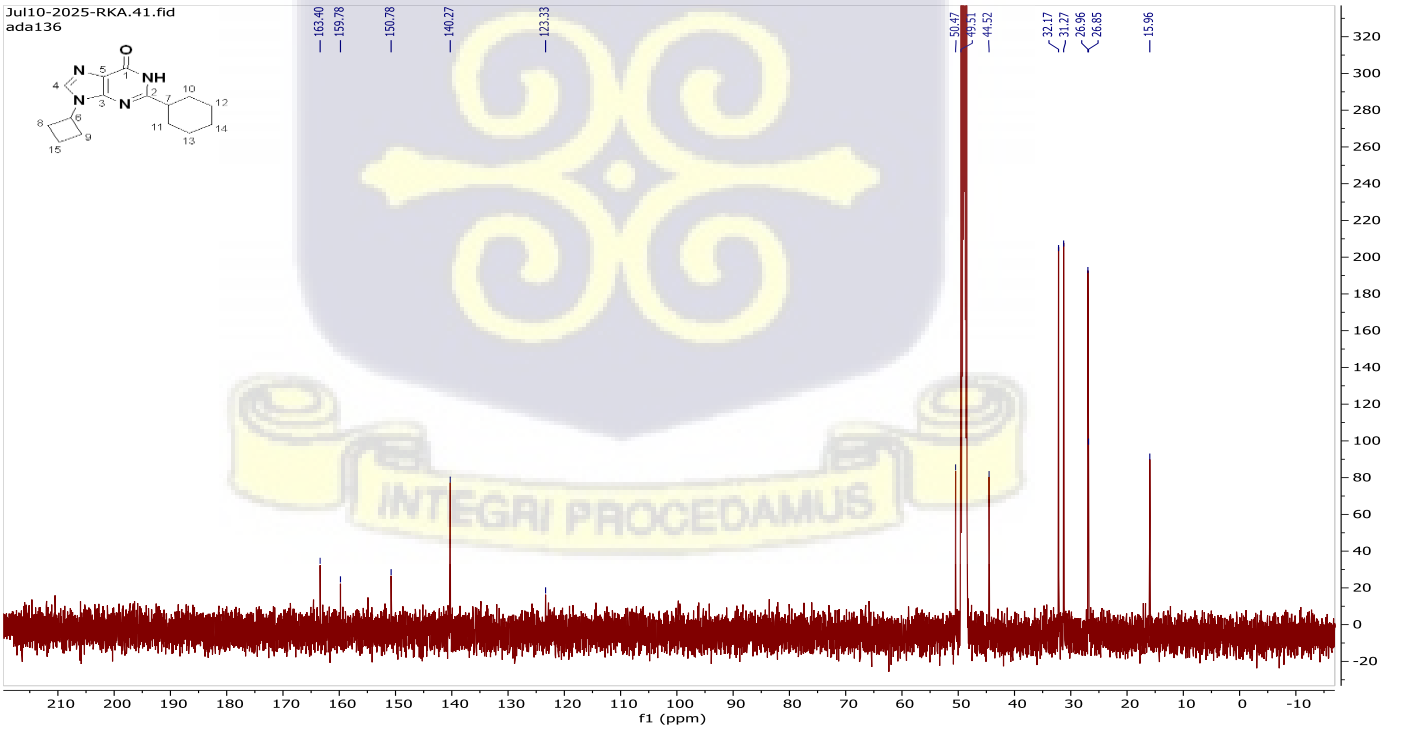




University of Ghana http://ugspace.ug.edu.gh

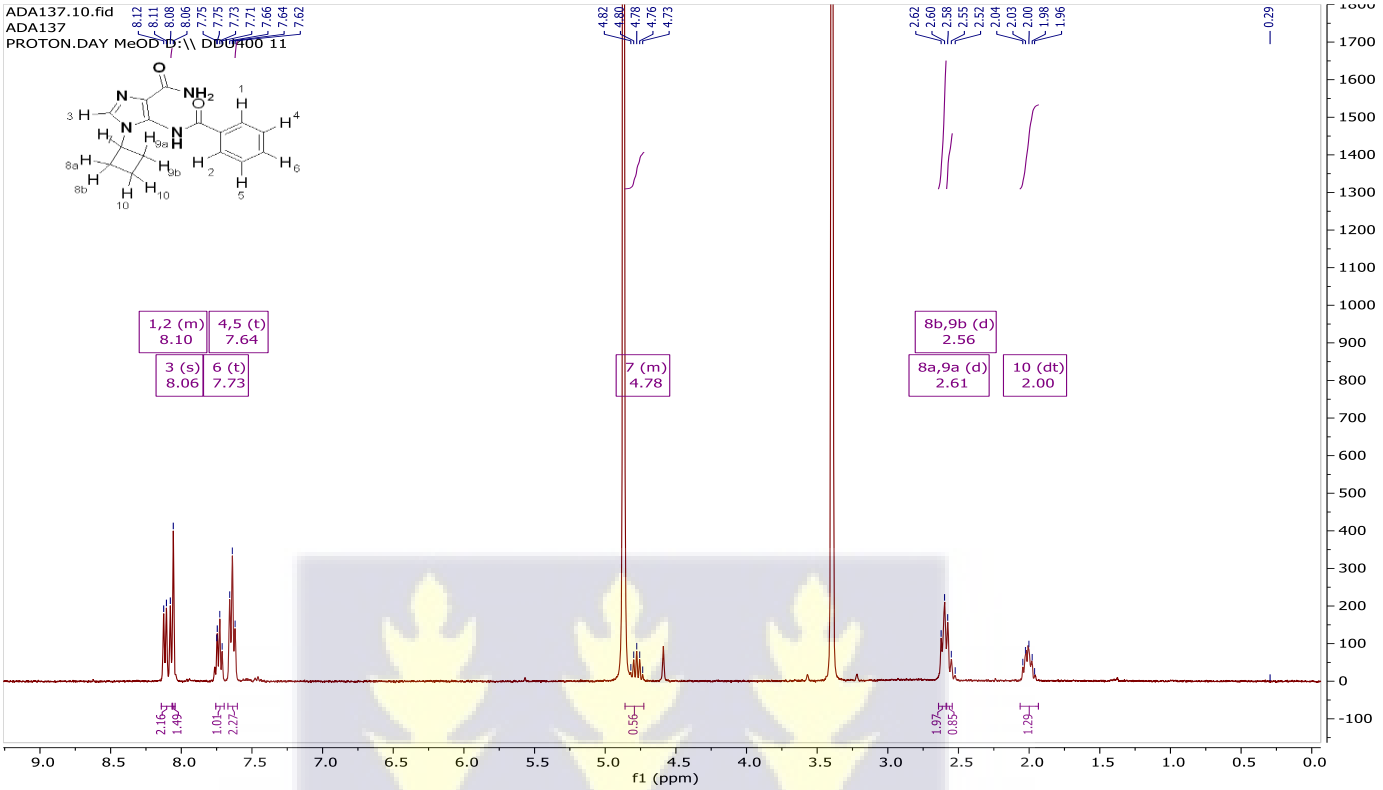
ADA136

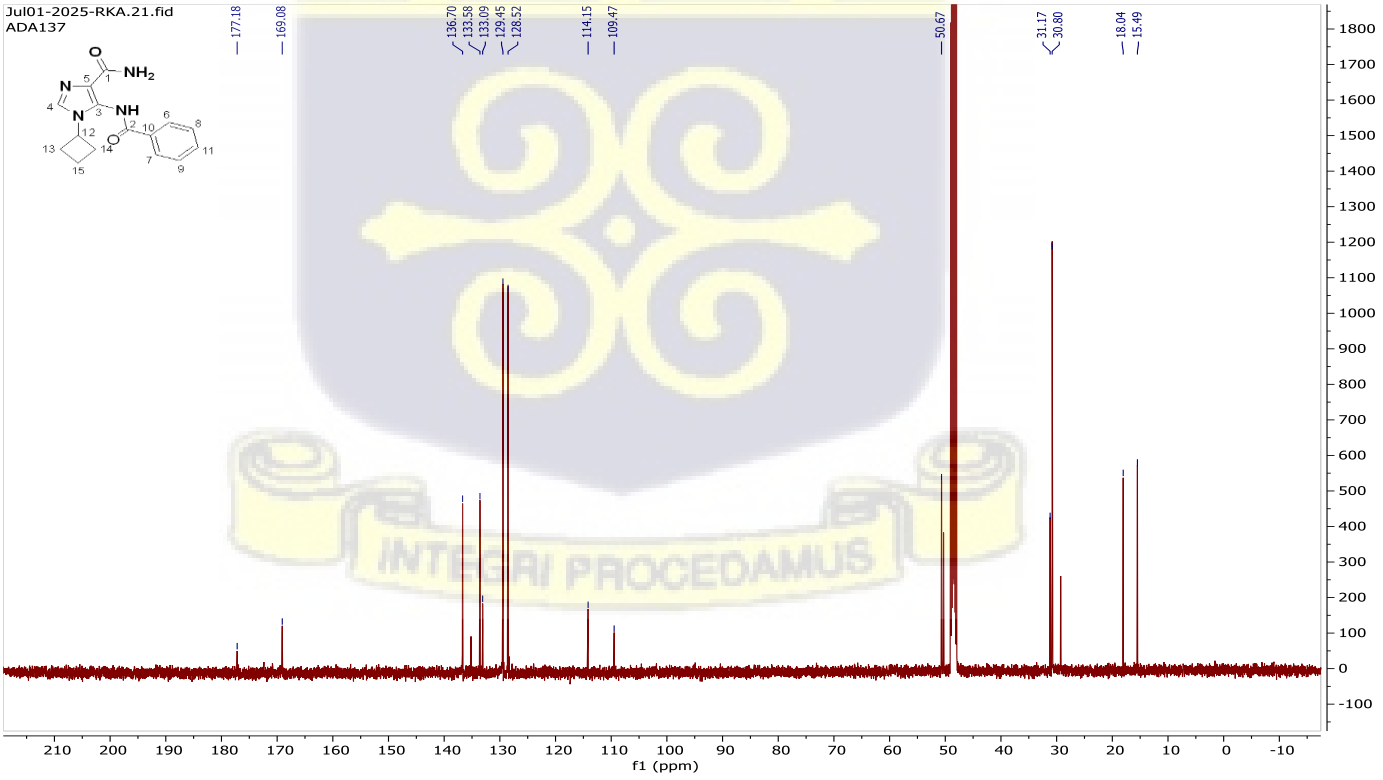




University of Ghana http://ugspace.ug.edu.gh

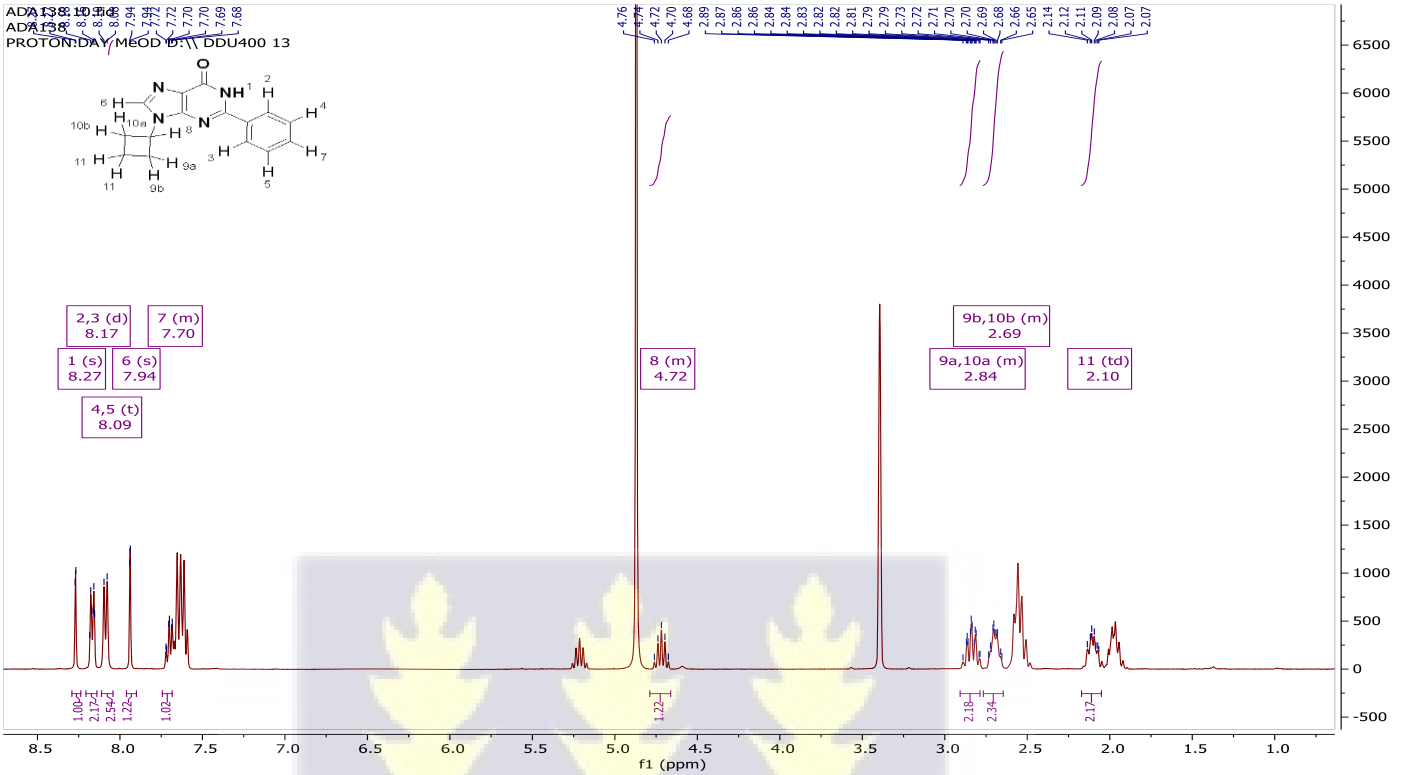
ADA137

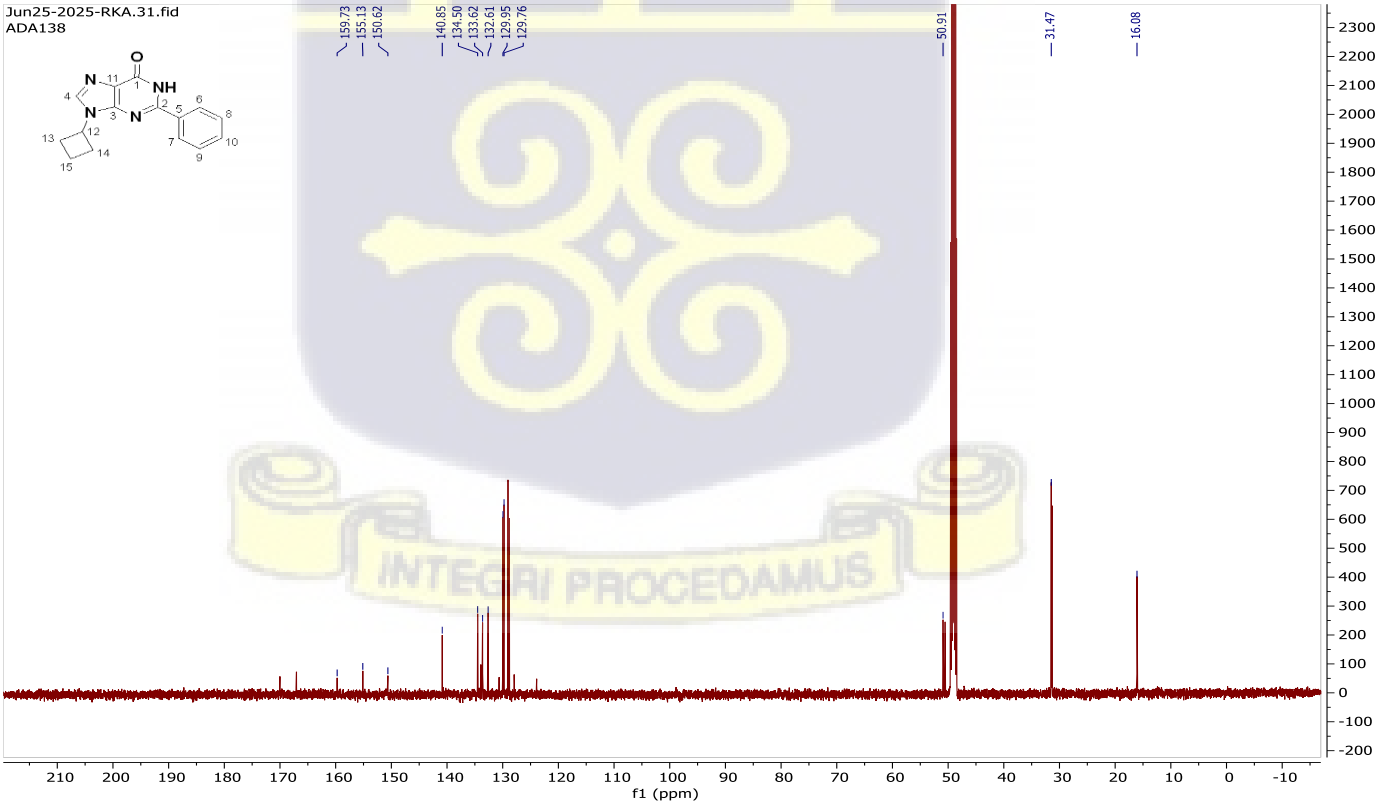




University of Ghana http://ugspace.ug.edu.gh

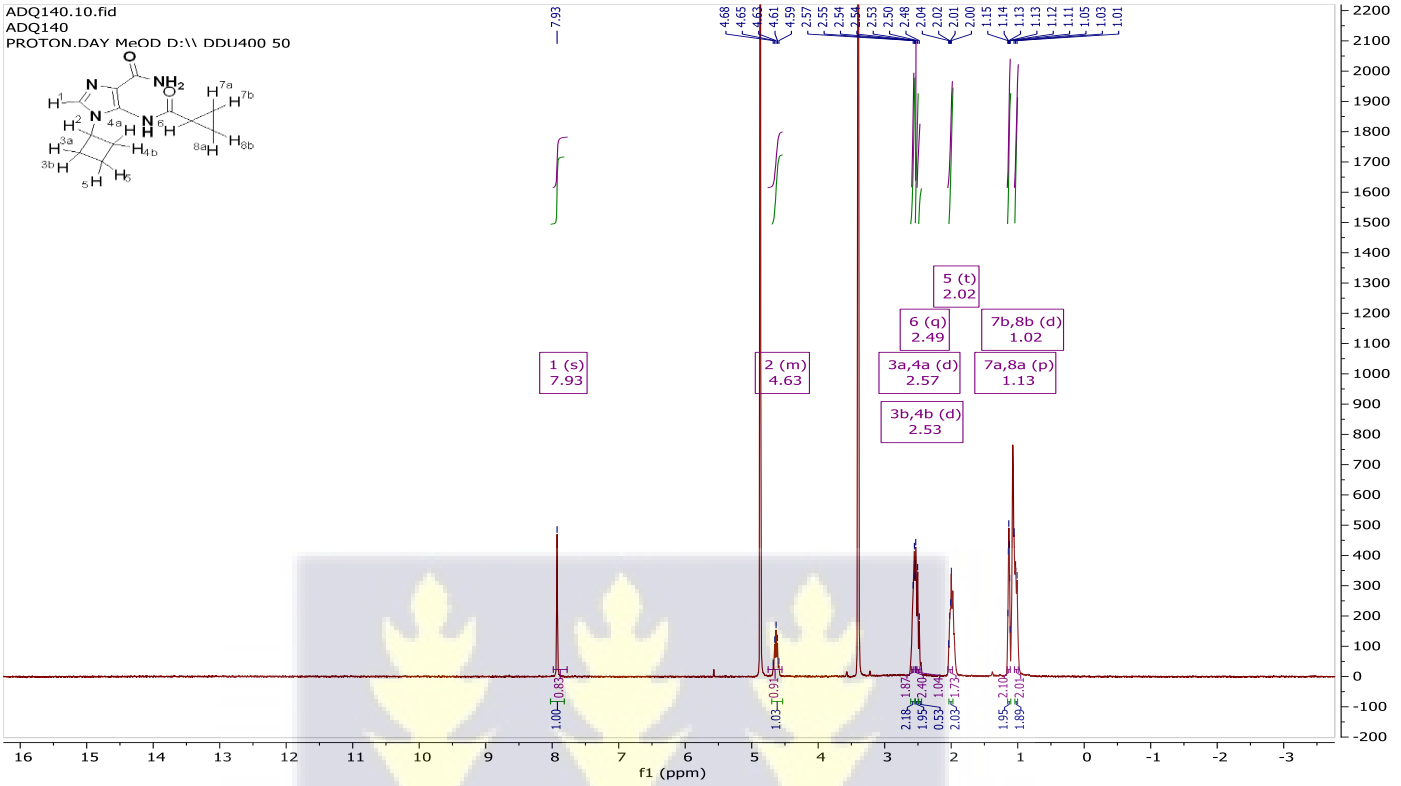
ADA138

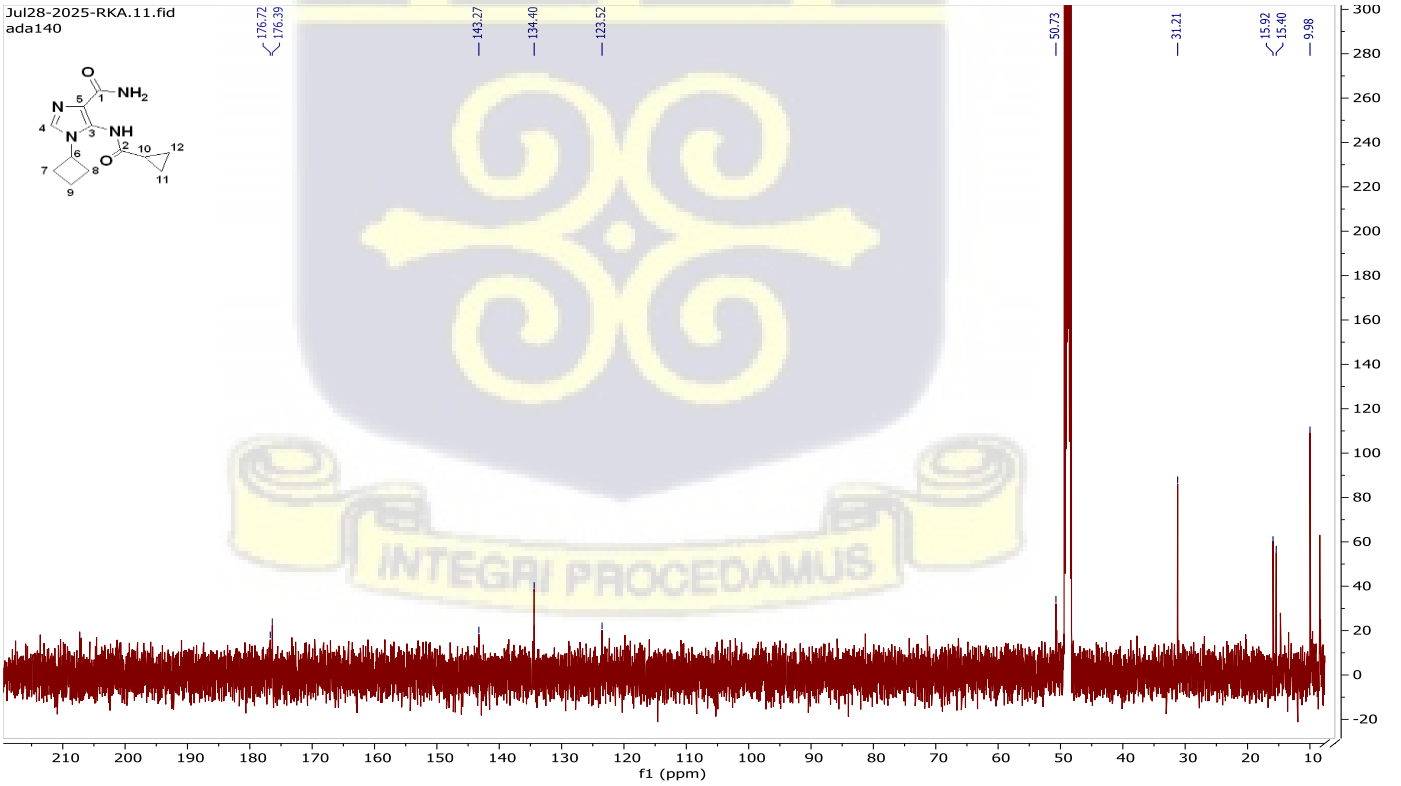




University of Ghana http://ugspace.ug.edu.gh

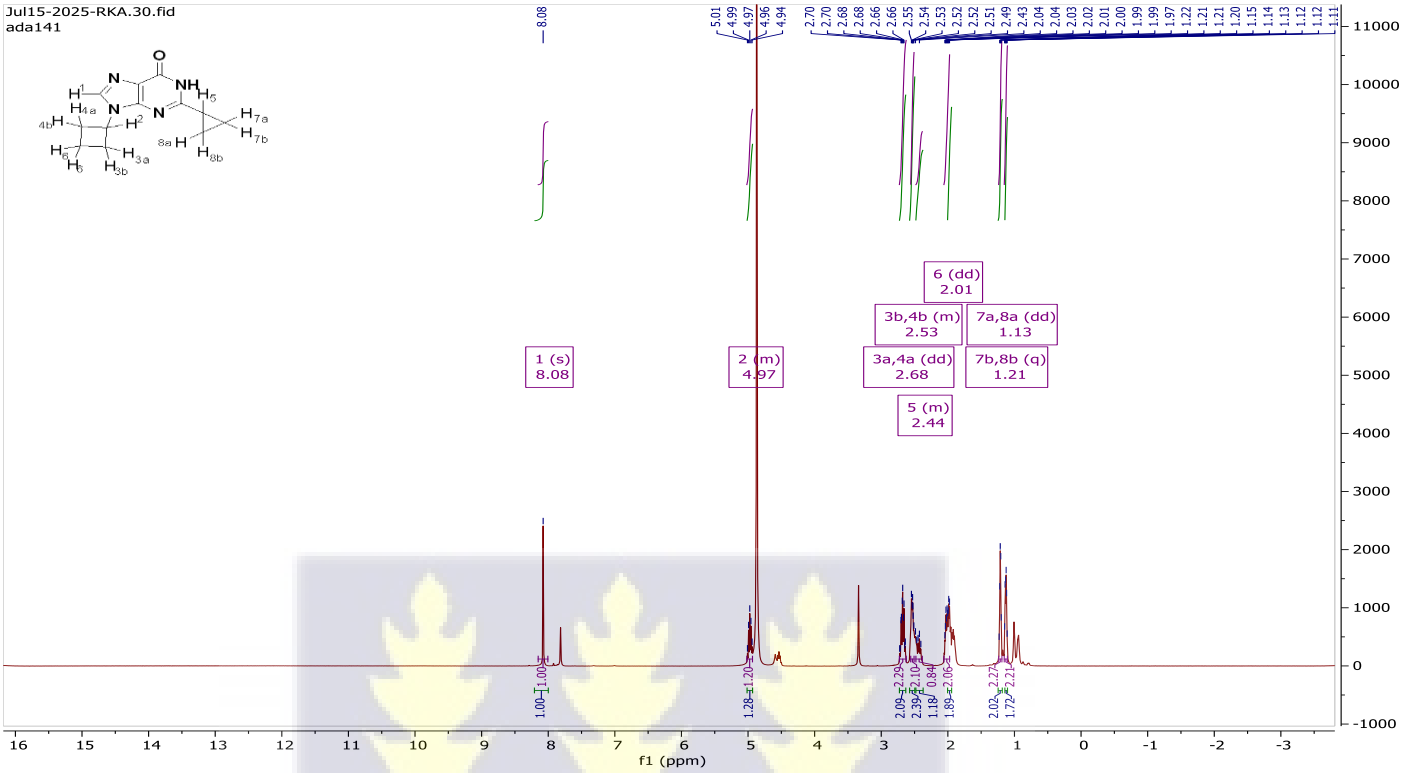
ADA140

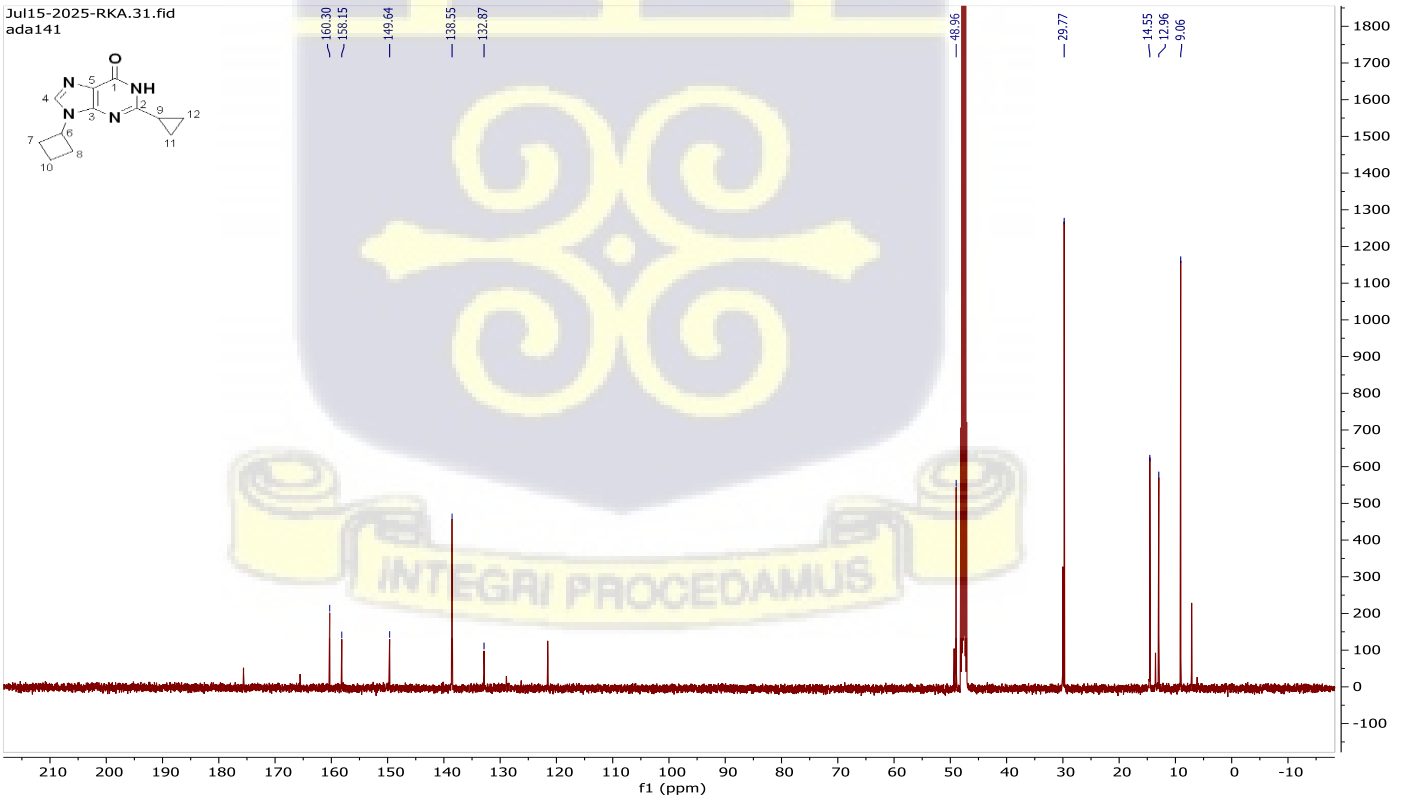




University of Ghana http://ugspace.ug.edu.gh

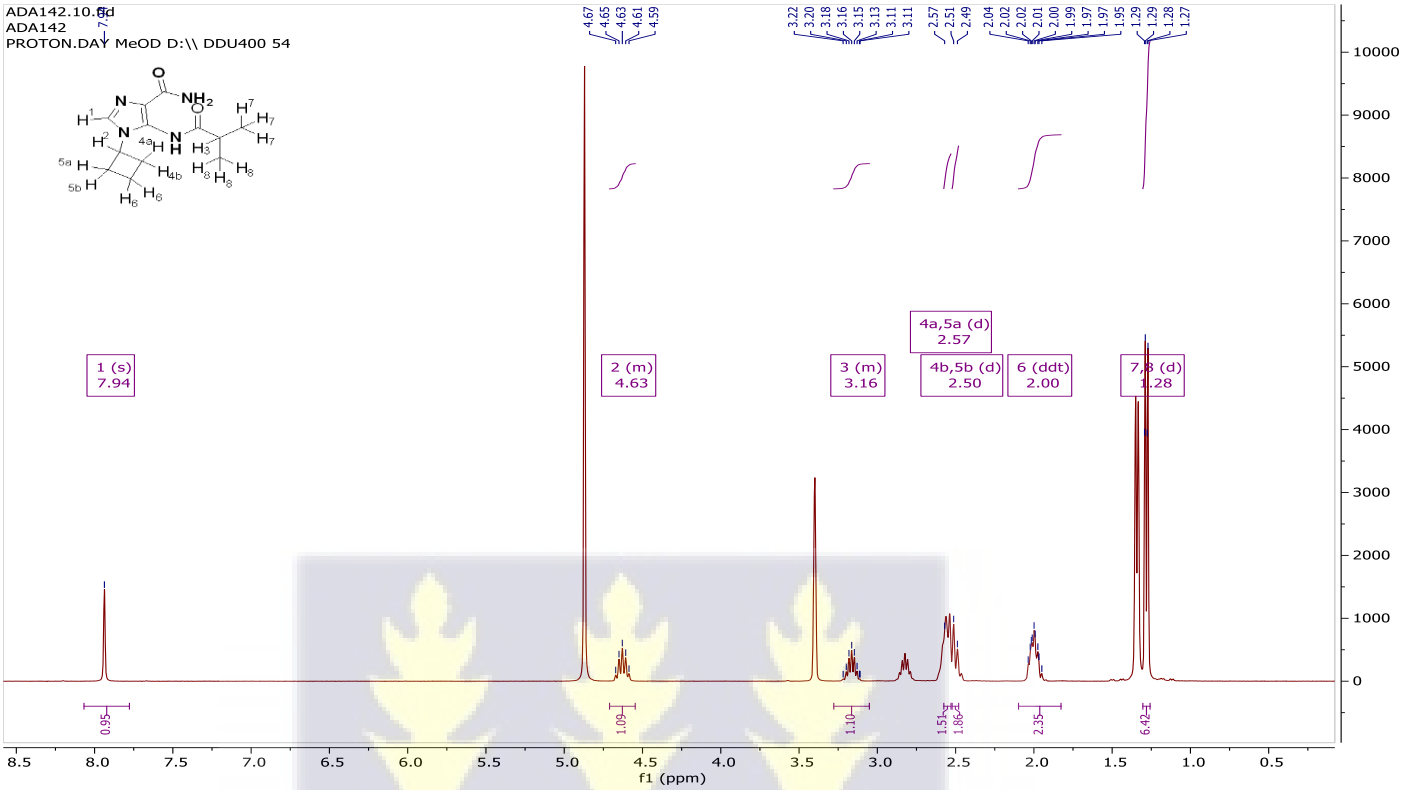
ADA141

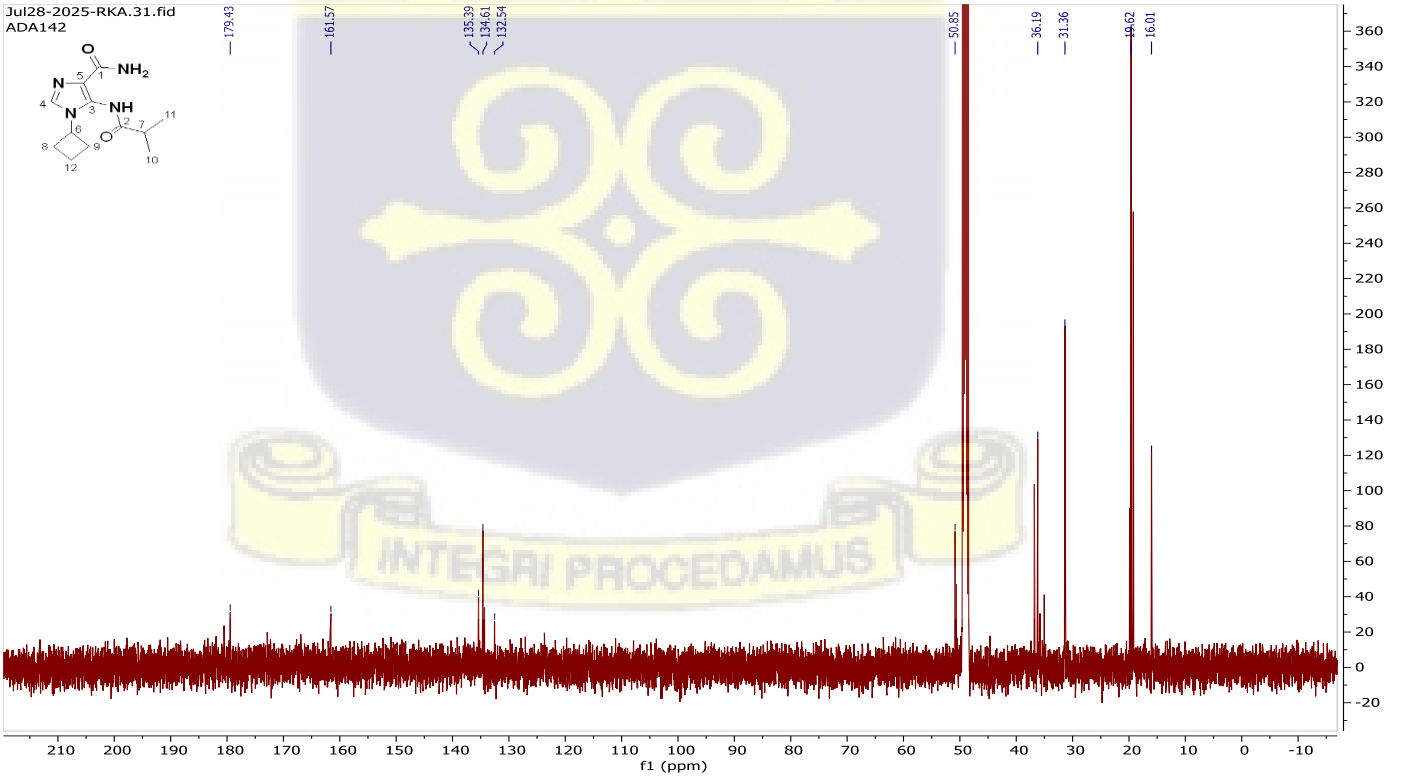




University of Ghana http://ugspace.ug.edu.gh

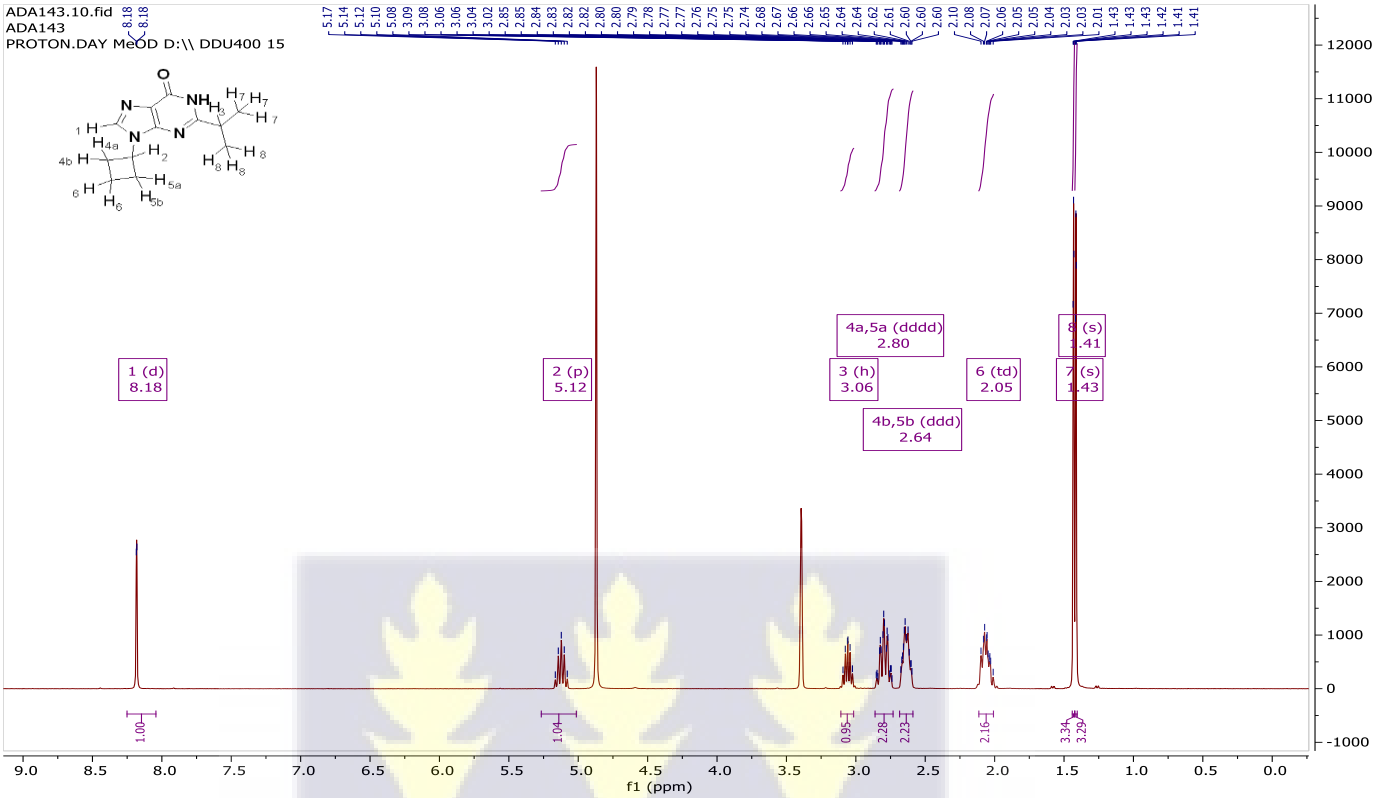
ADA142

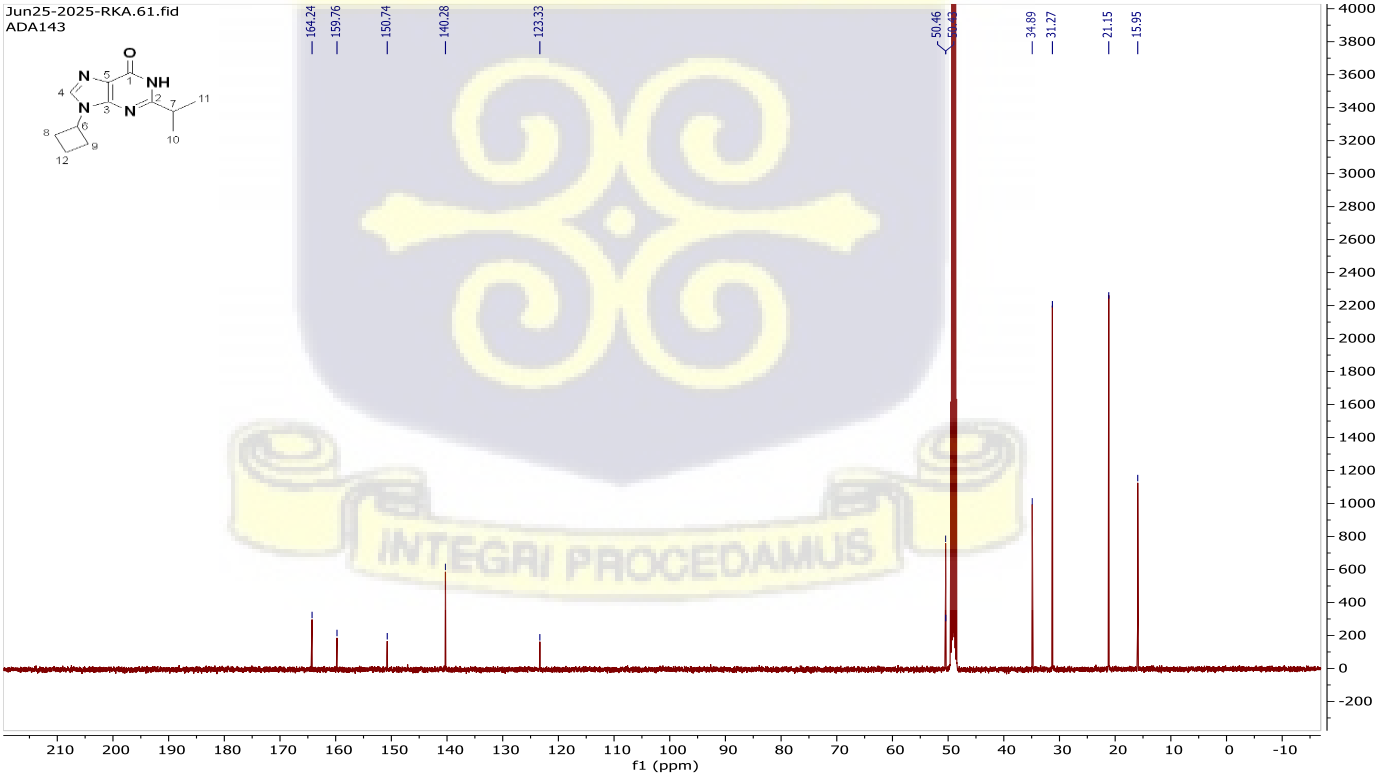




University of Ghana http://ugspace.ug.edu.gh

ADA143

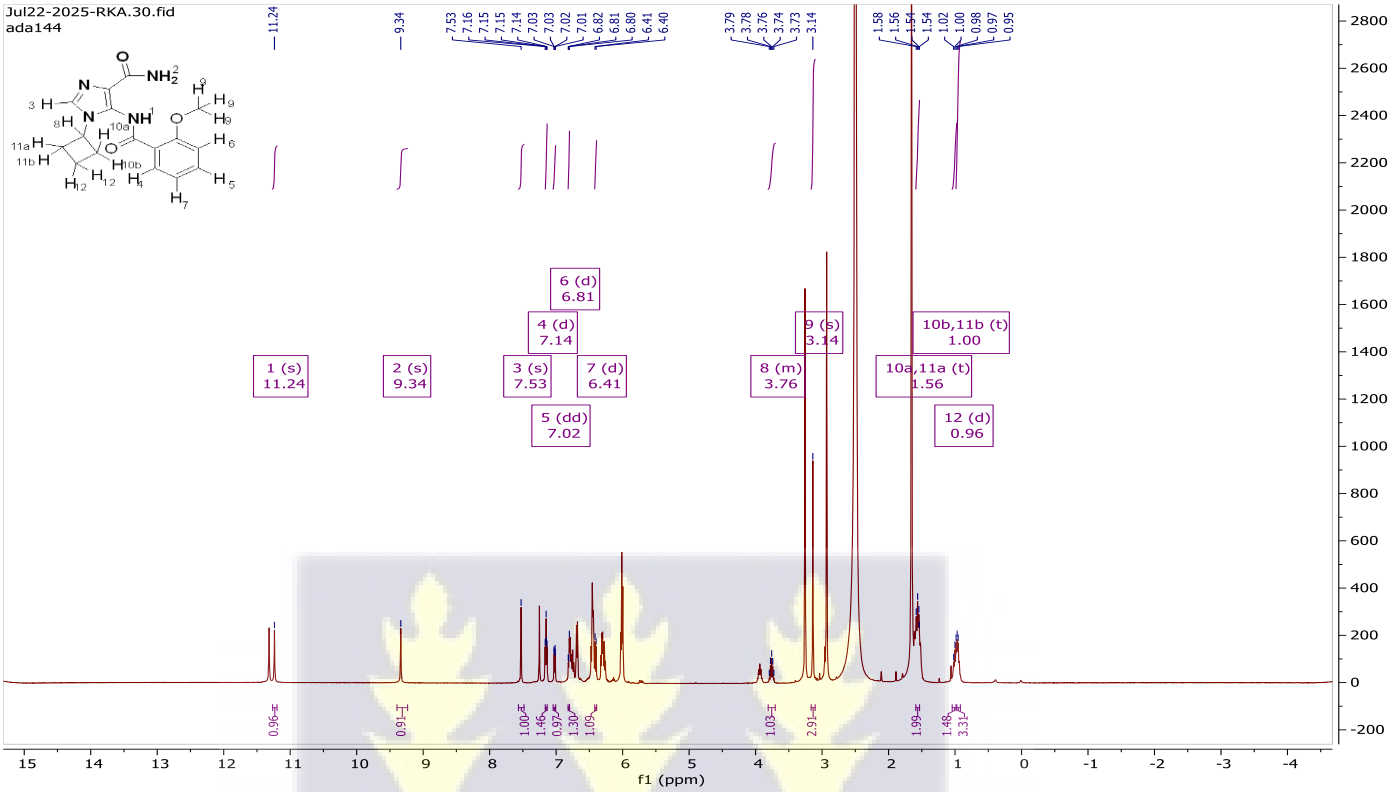


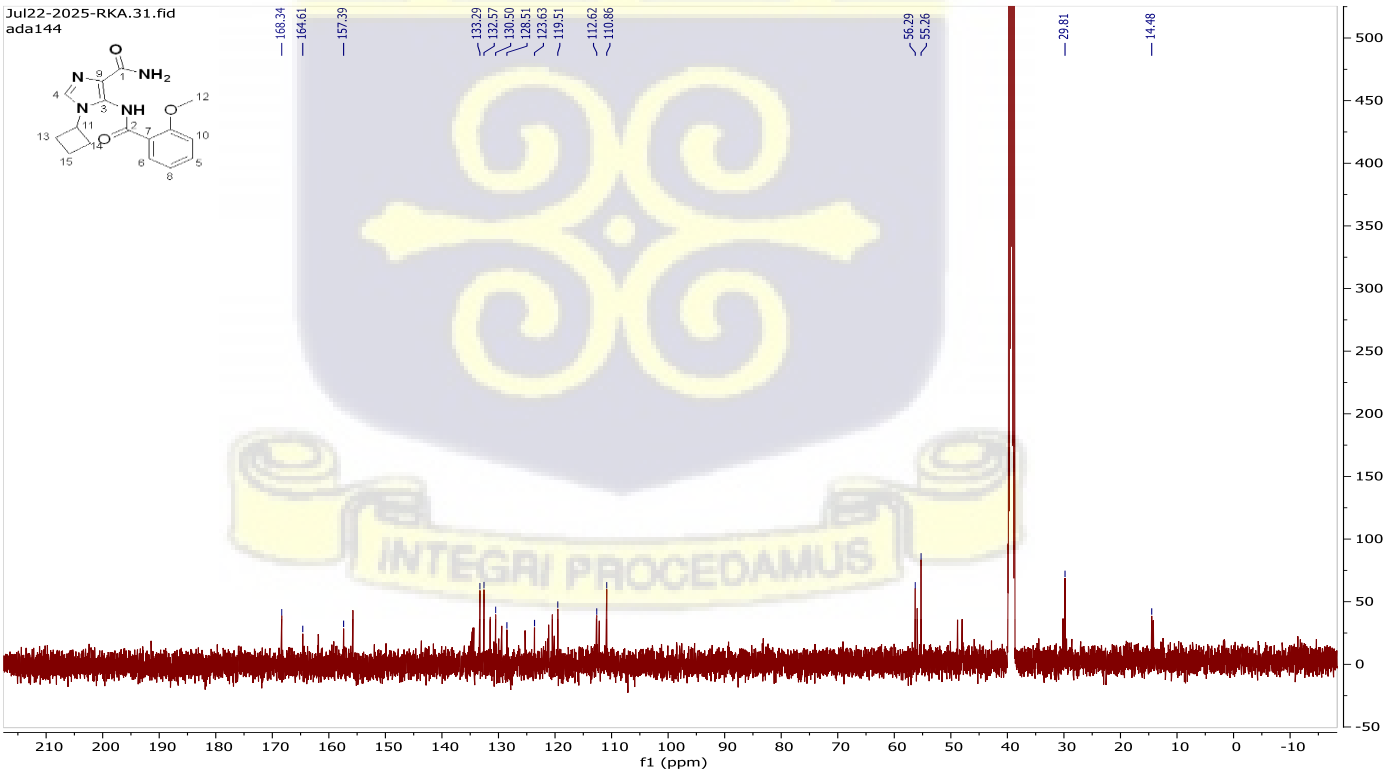


INTEGRI PROCEDAMUS

University of Ghana http://ugspace.ug.edu.gh

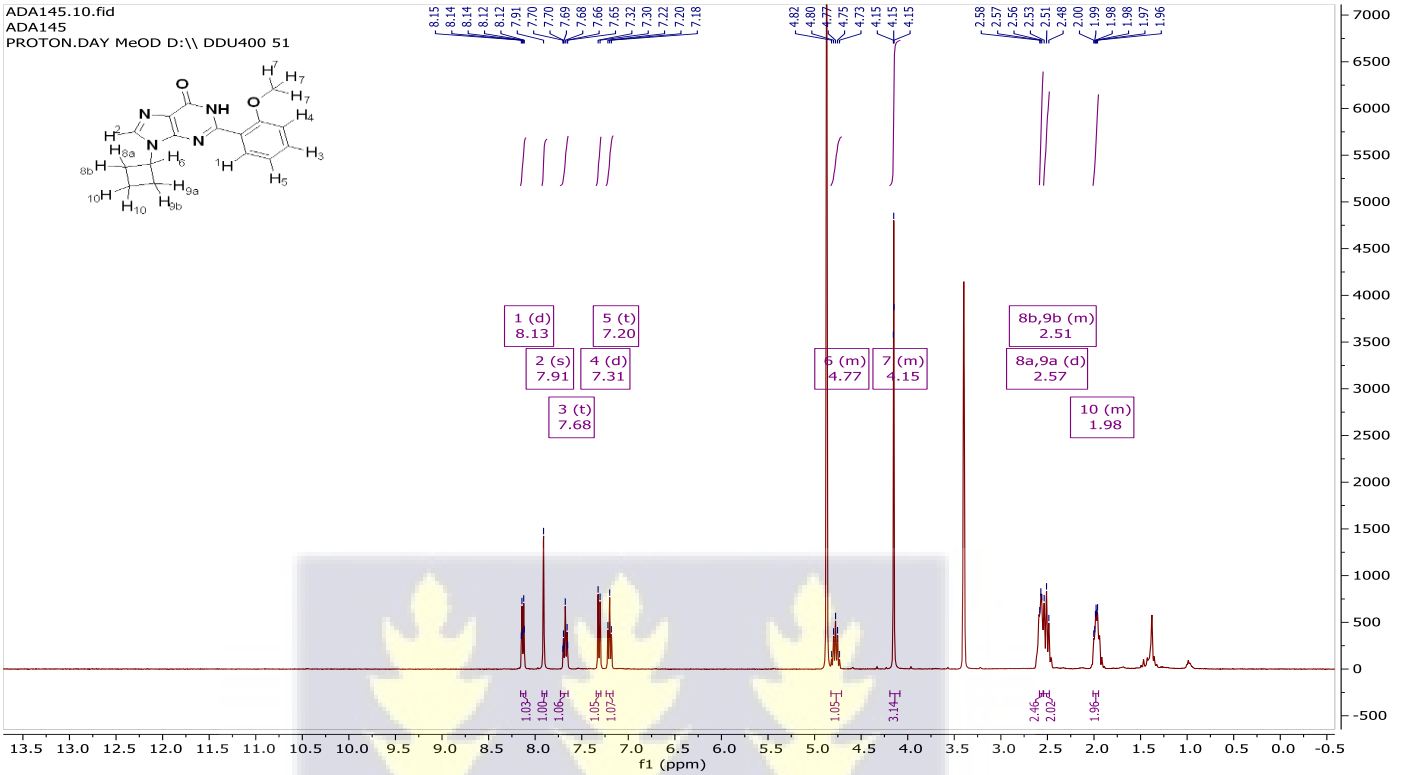
ADA144

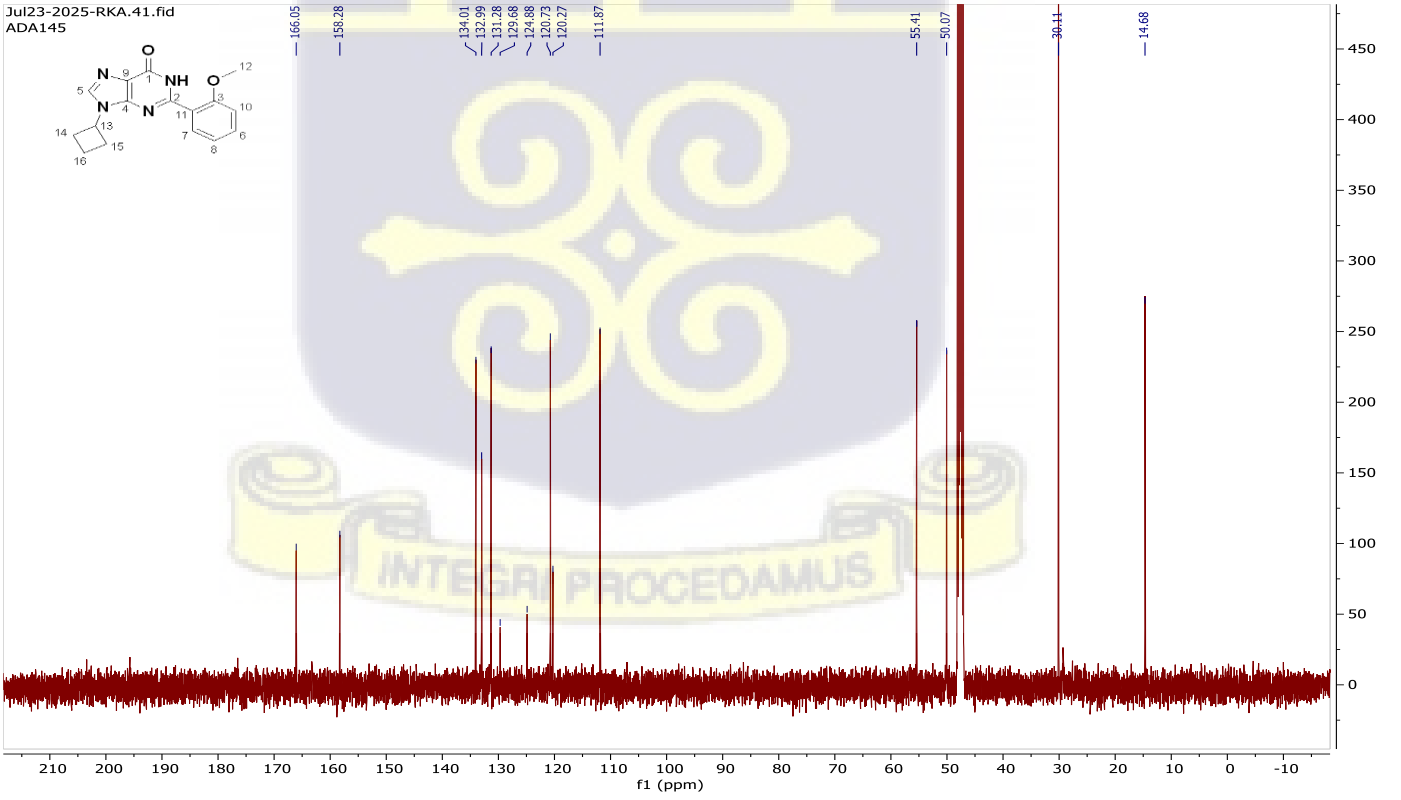




University of Ghana http://ugspace.ug.edu.gh

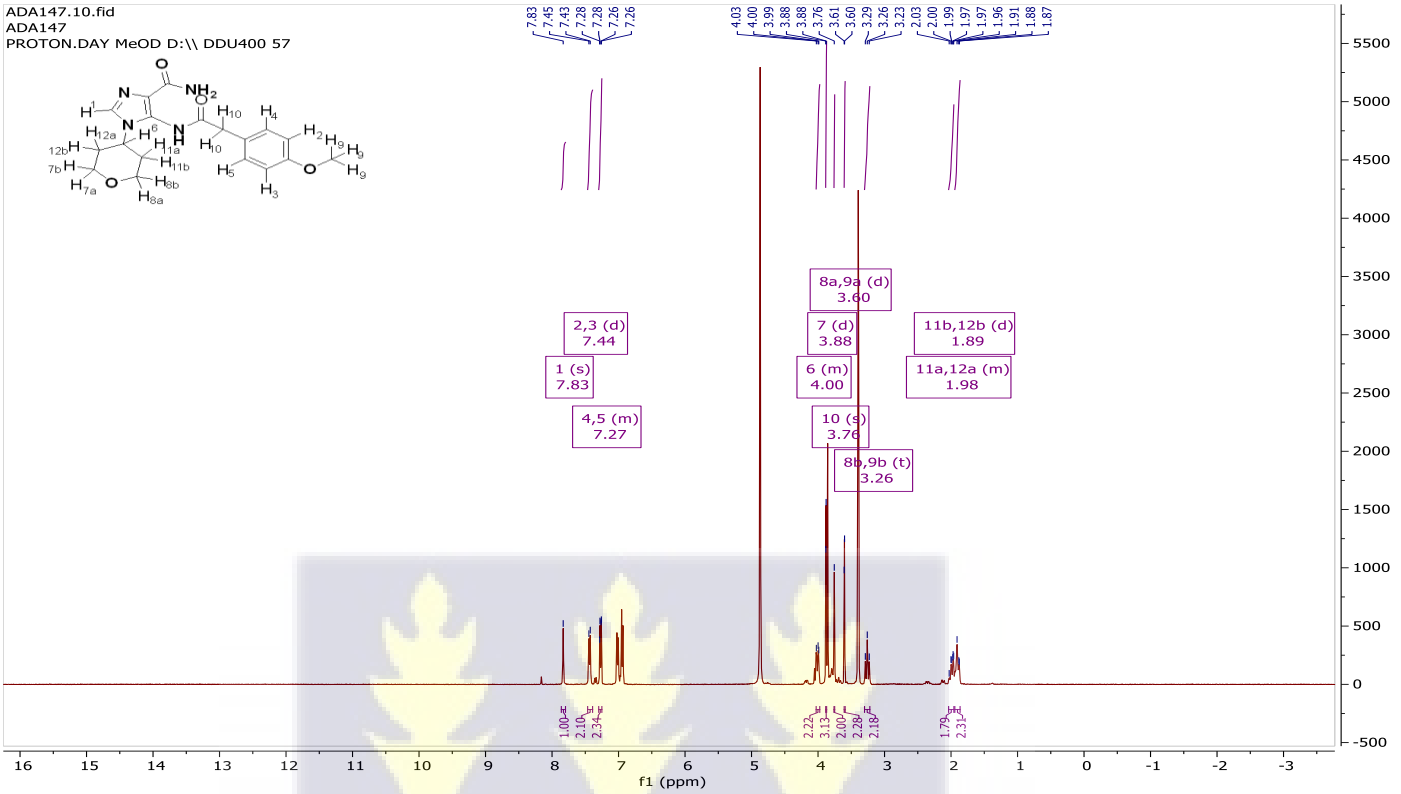
ADA145

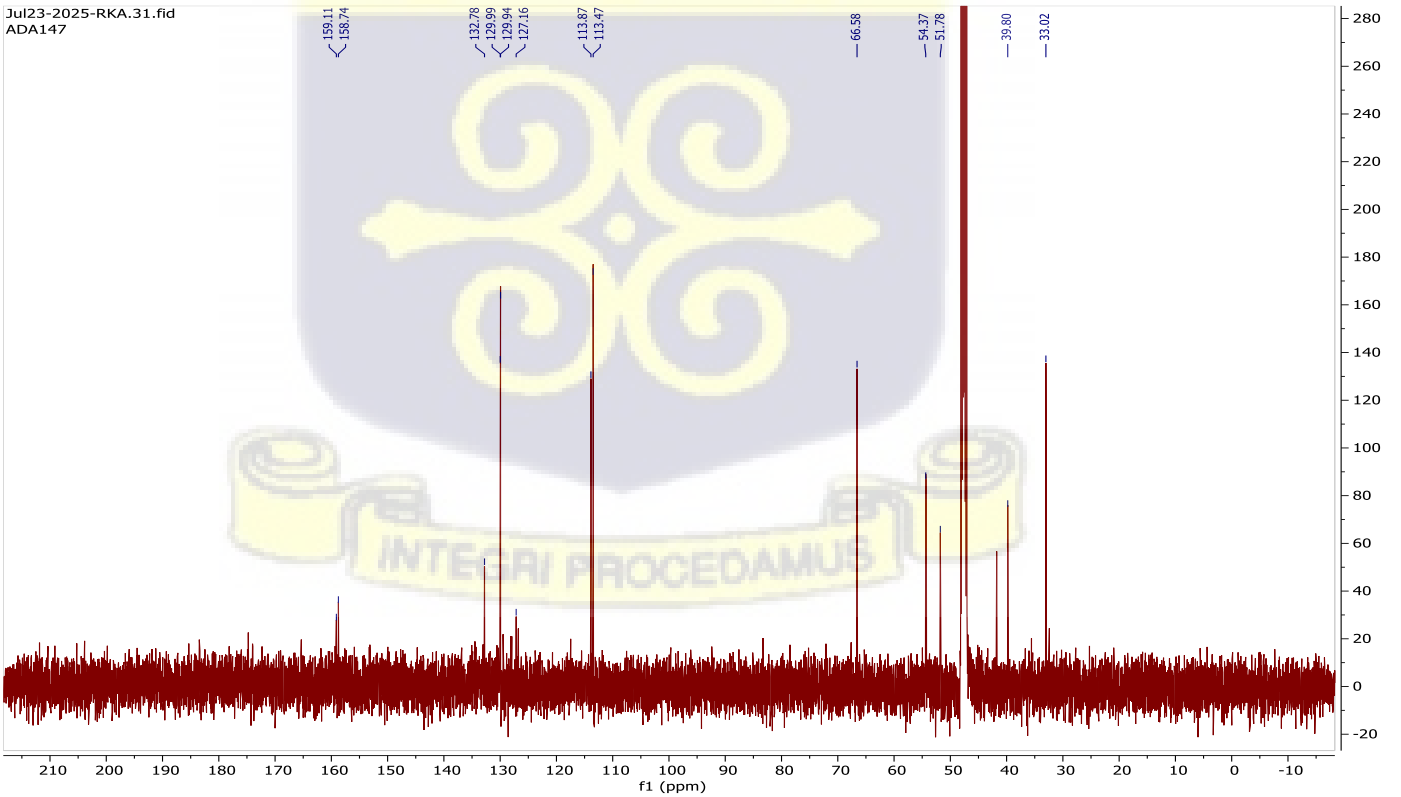




University of Ghana http://ugspace.ug.edu.gh

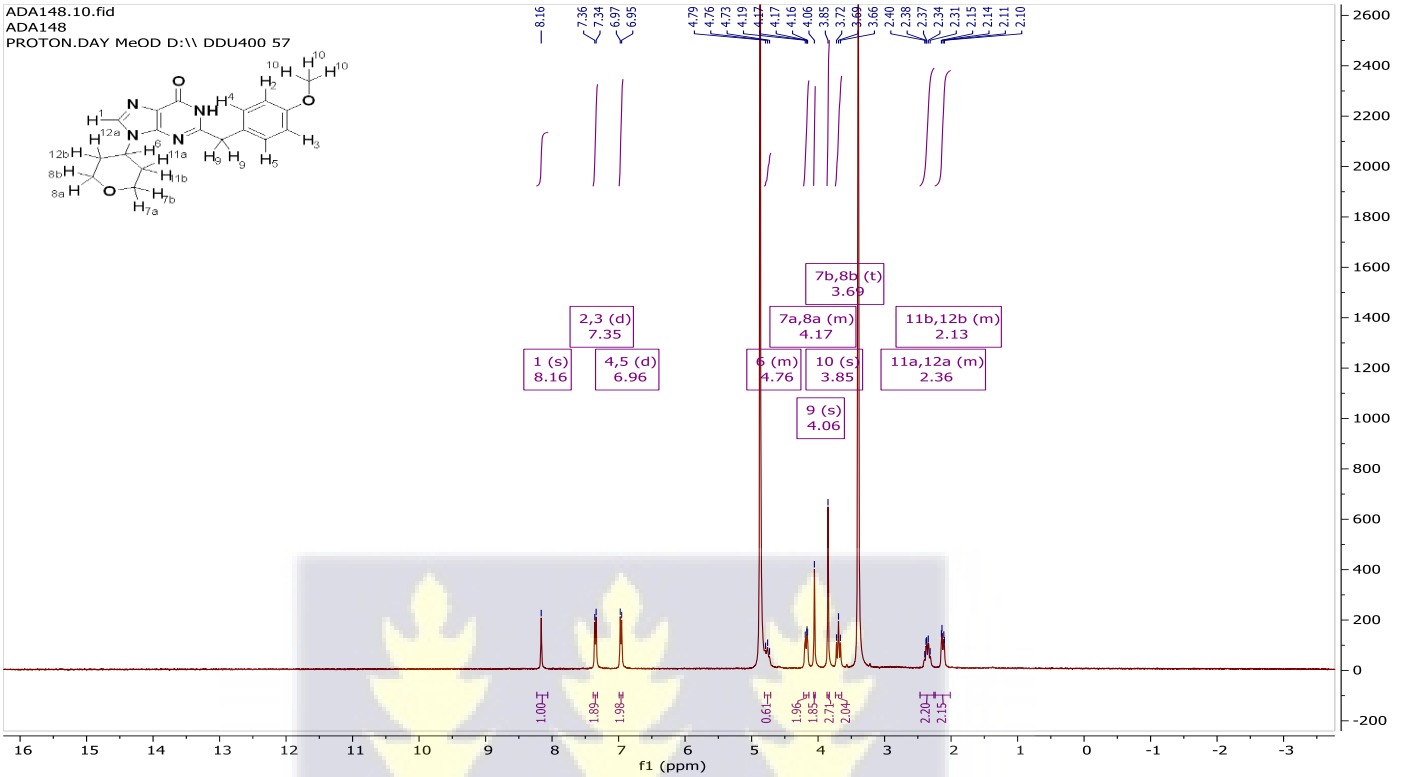
ADA147

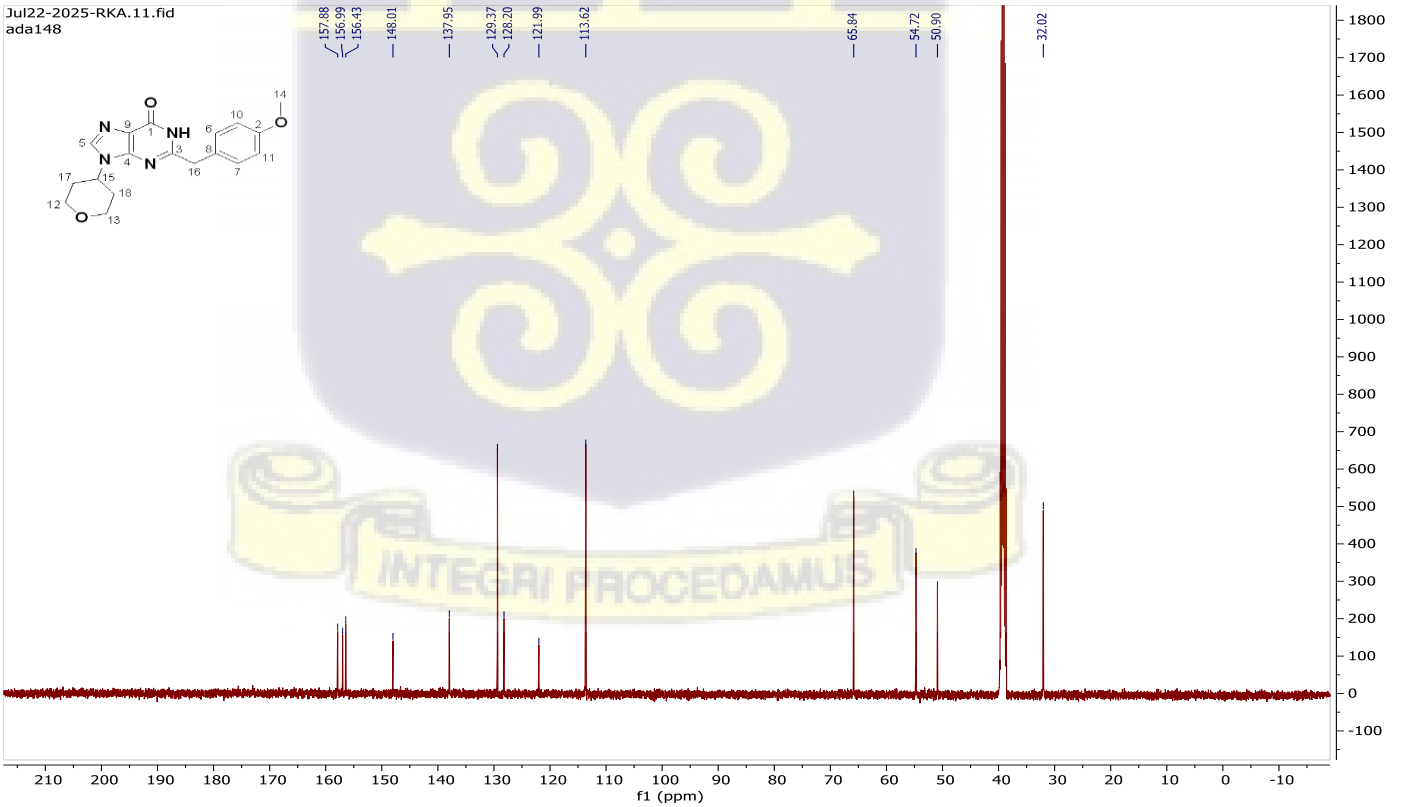




University of Ghana http://ugspace.ug.edu.gh

ADA148

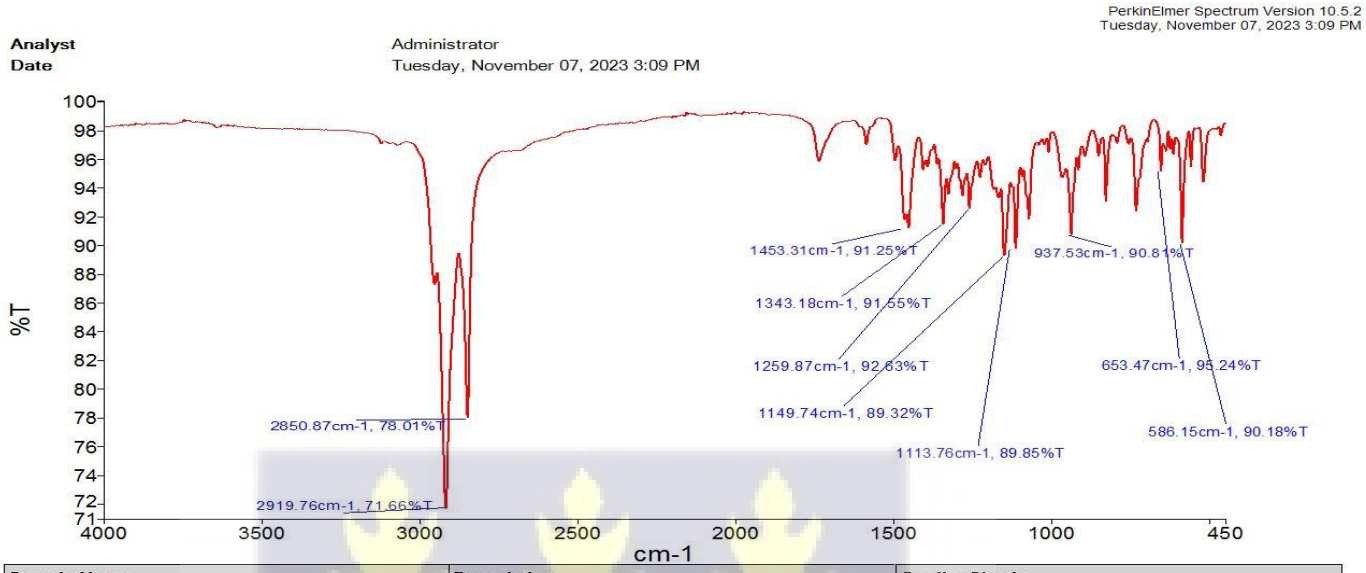




University of Ghana http://ugspace.ug.edu.gh

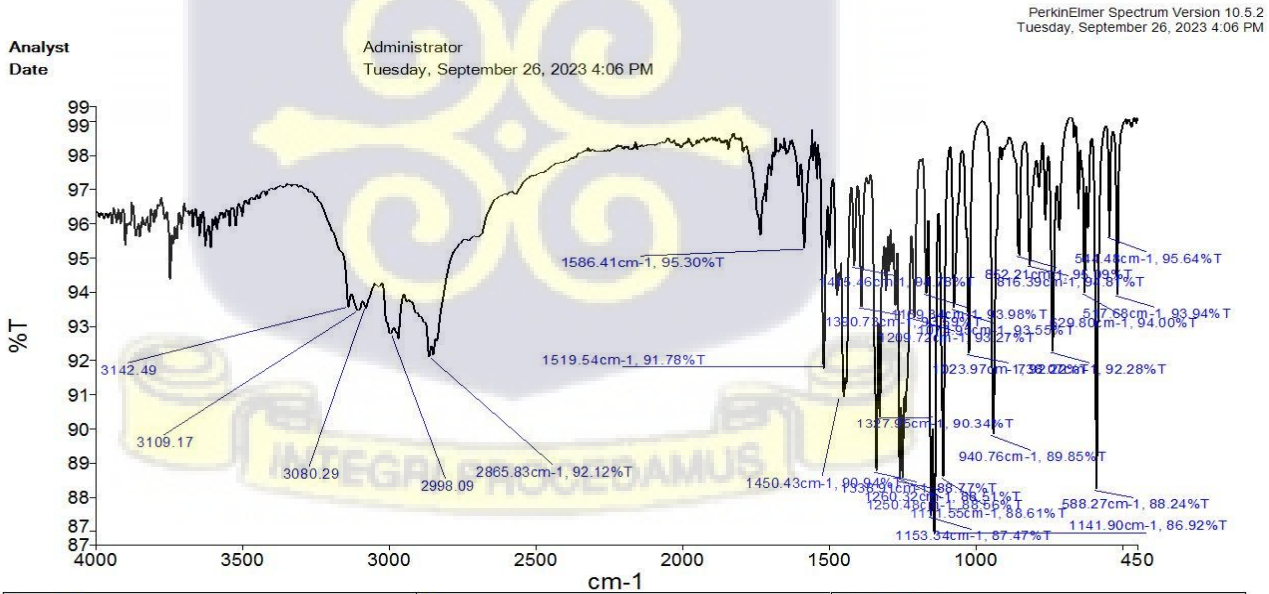
APPENDIX II: FT-IR Spectrum

ADA083



Sample Name	Description	Quality Checks
ADA-083_1	Sample 265 By Administrator Date Tuesday, November 07 2023	The Quality Checks do not report any warnings for the sample.

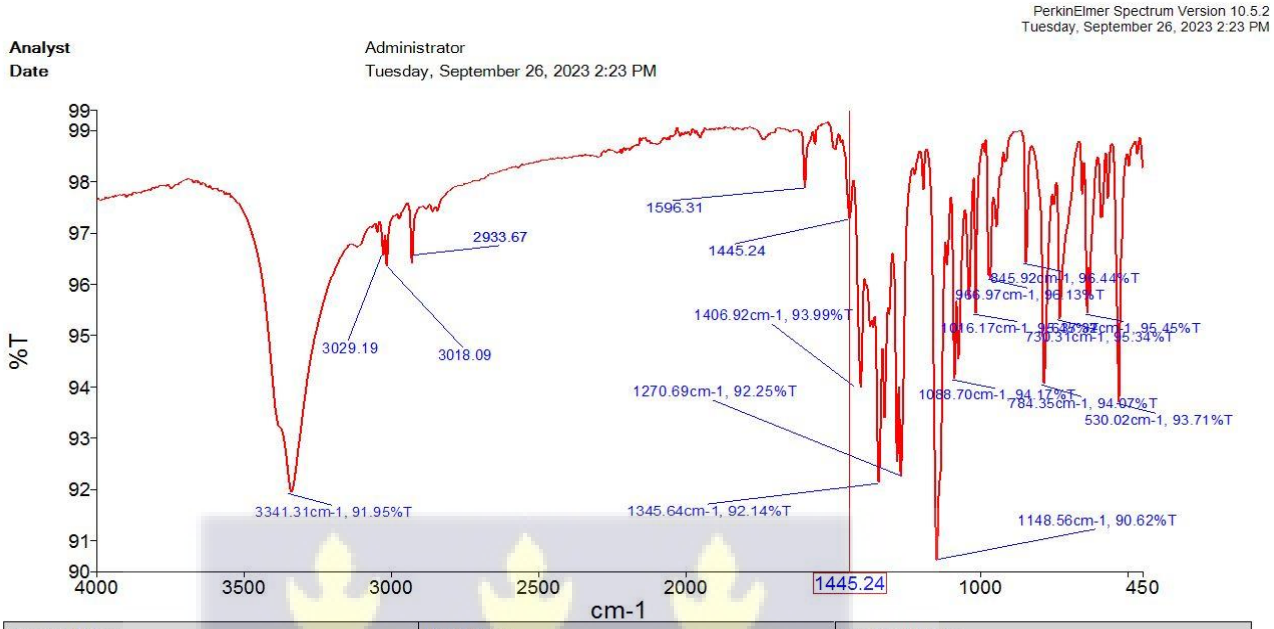
ADA084



Sample Name	Description	Quality Checks
Administrator 249_1	ADA084	The Quality Checks do not report any warnings for the sample.

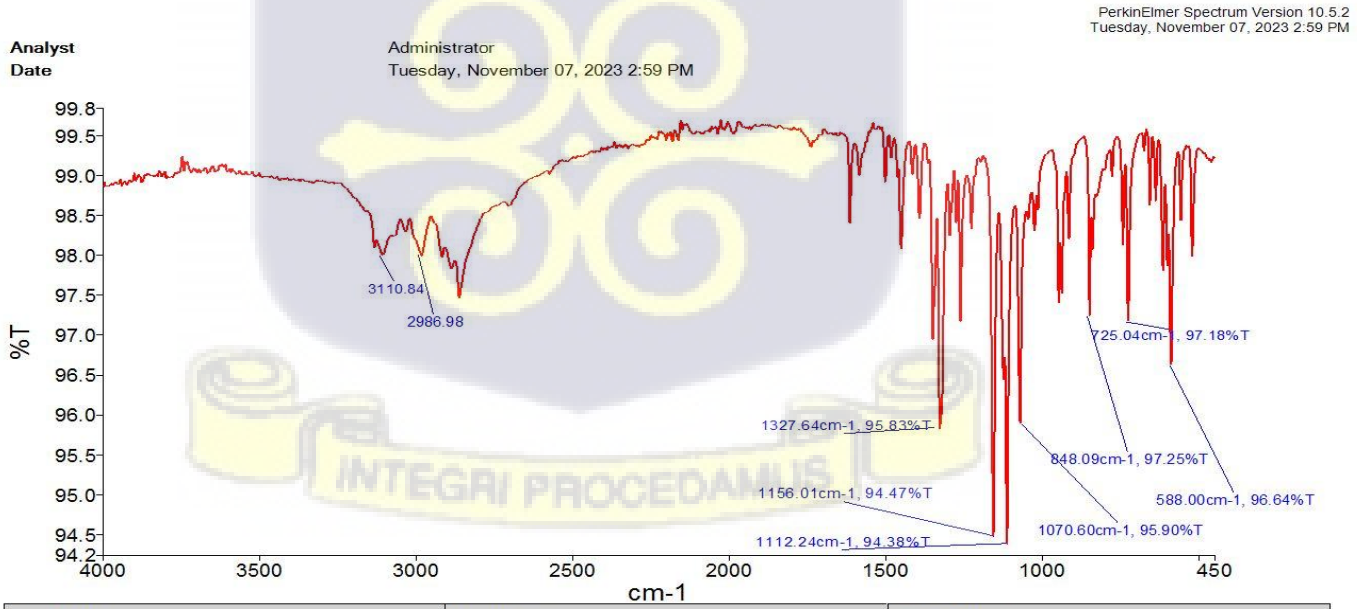
University of Ghana http://ugspace.ug.edu.gh

ADA085



Sample Name	Description	Quality Checks
Administrator 239_1	ADA085	The Quality Checks give rise to a Weak Bands warning for the sample.

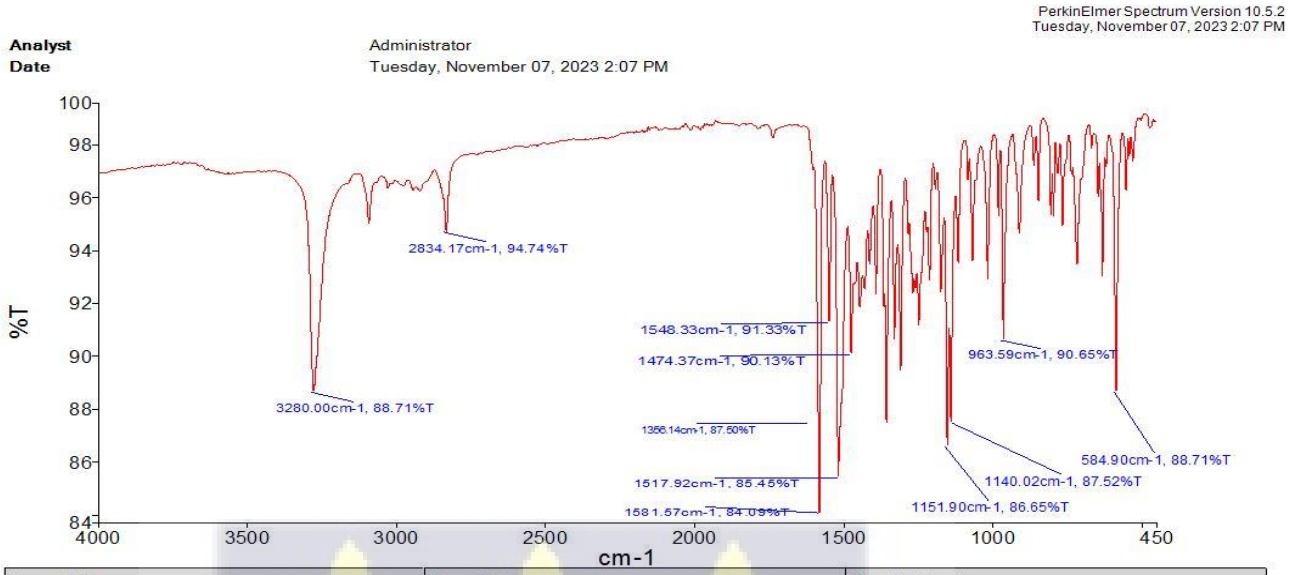
ADA087



Sample Name	Description	Quality Checks
ADA-087_1	Sample 264 By Administrator Date Tuesday, November 07 2023	The Quality Checks give rise to a Weak Bands warning for the sample.

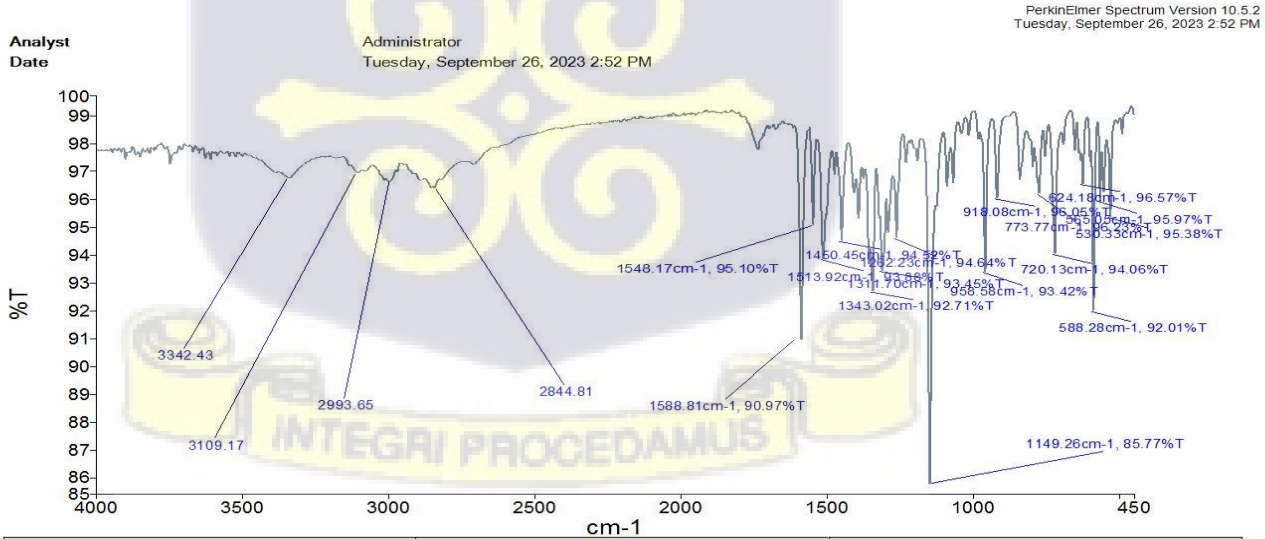
University of Ghana http://ugspace.ug.edu.gh

ADA088



Sample Name	Description	Quality Checks
ADA-088_1	Sample 259 By Administrator Date Tuesday, November 07 2023	The Quality Checks do not report any warnings for the sample.

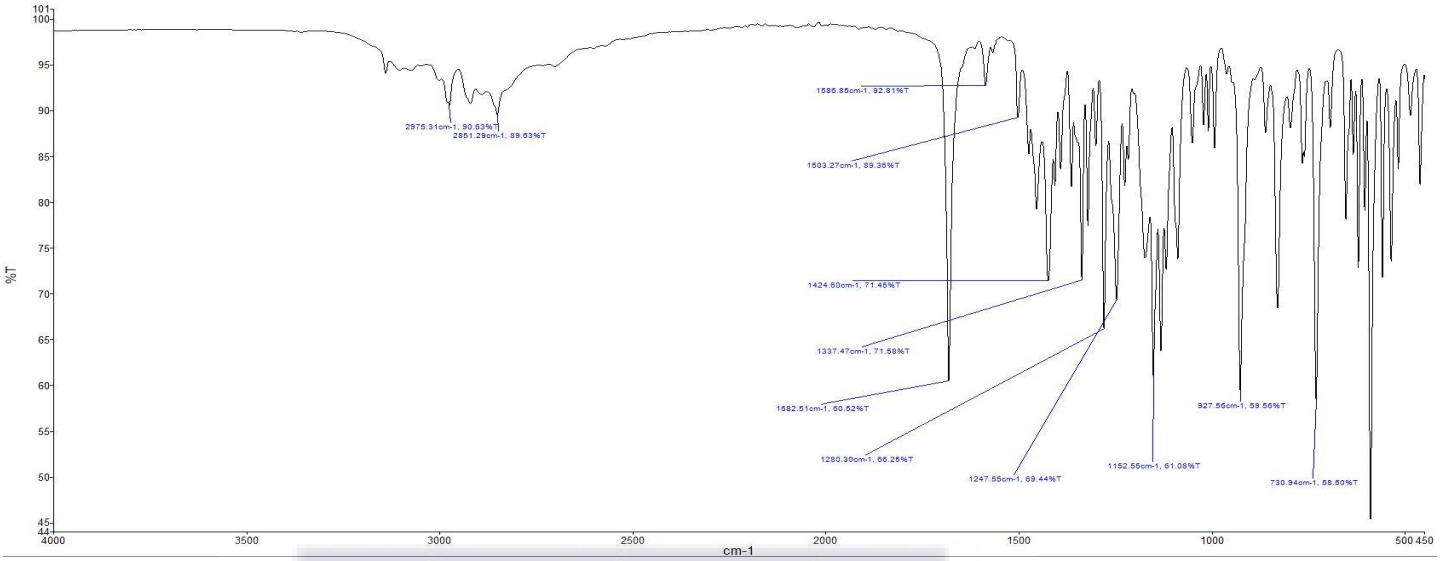
ADA090



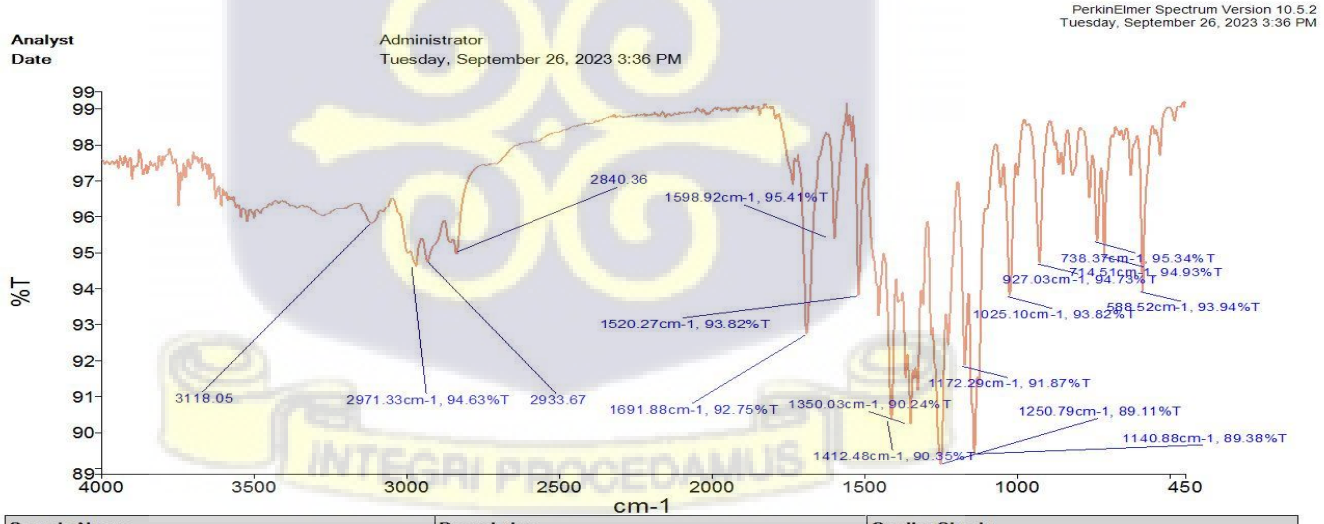
Sample Name	Description	Quality Checks
Administrator 241_1	ADA090	The Quality Checks do not report any warnings for the sample.

University of Ghana http://ugspace.ug.edu.gh

ADA091



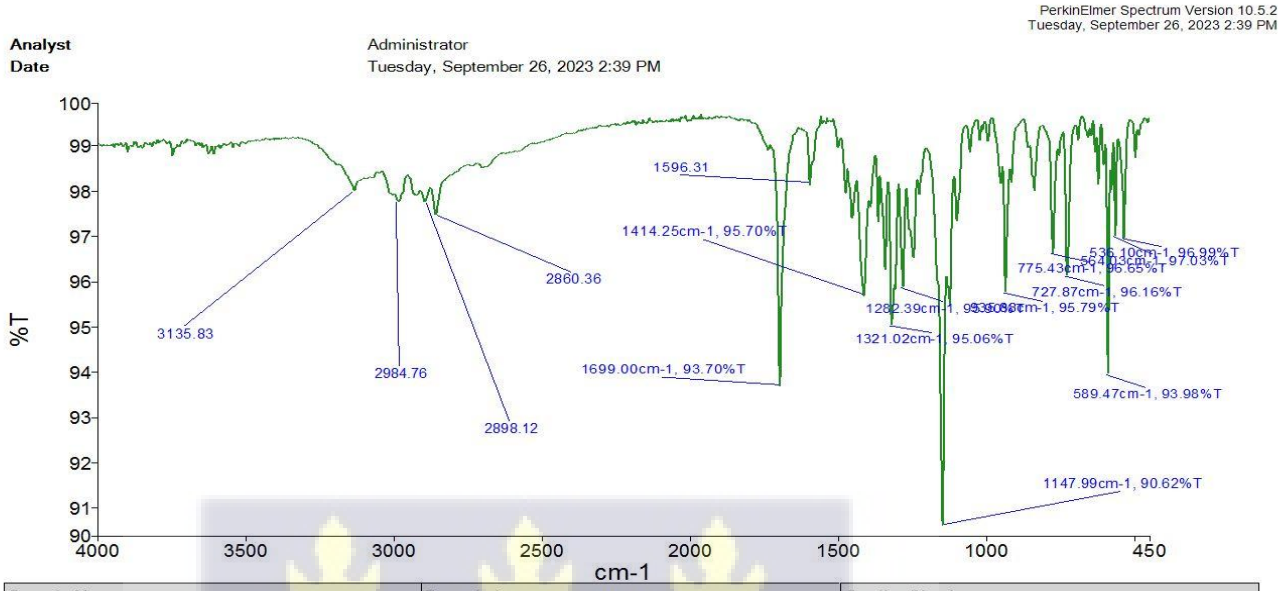
ADA092



Sample Name	Description	Quality Checks
Administrator 245_1	Sample 245 By Administrator Date Tuesday, September 26 2023	The Quality Checks give rise to a Weak Bands warning for the sample.

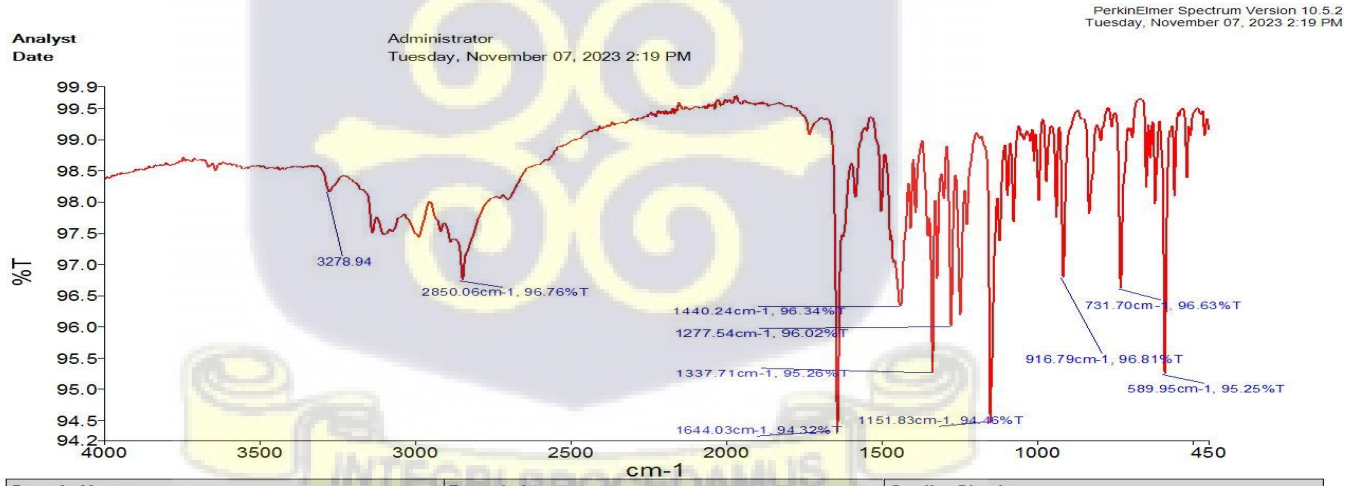
University of Ghana http://ugspace.ug.edu.gh

ADA093



Sample Name	Description	Quality Checks
Administrator 240_1	ADA093B	The Quality Checks give rise to a Weak Bands warning for the sample.

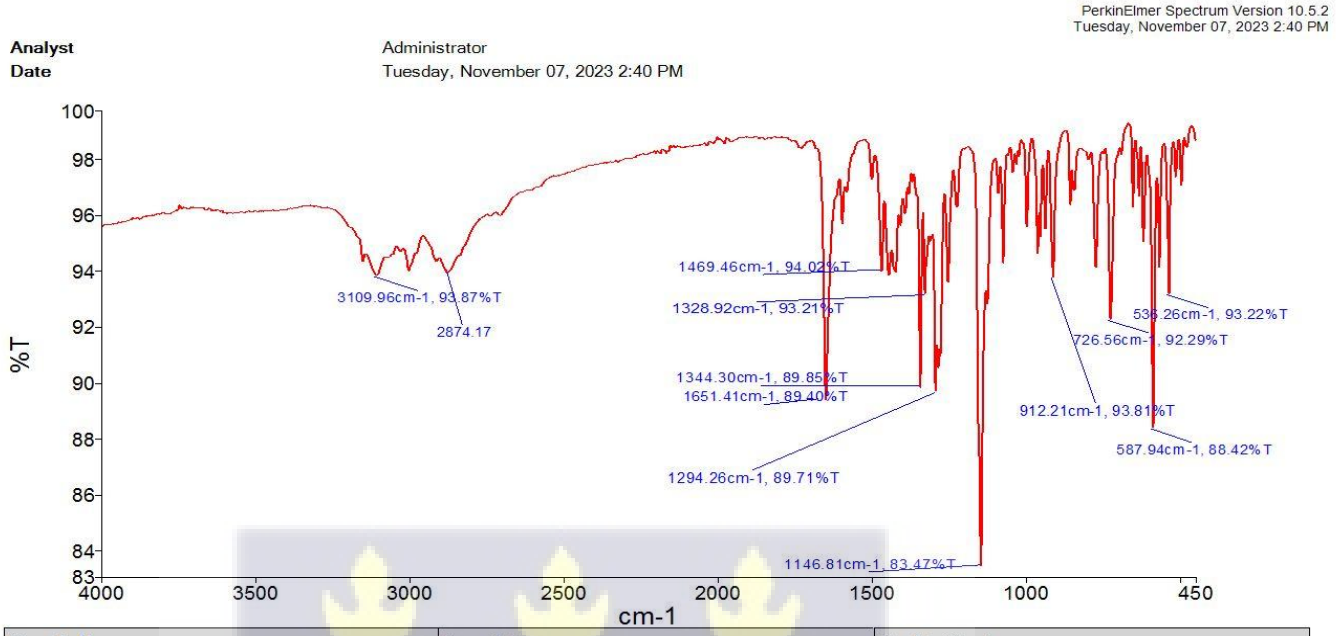
ADA095



Sample Name	Description	Quality Checks
ADA-095_1	Sample 260 By Administrator Date Tuesday, November 07 2023	The Quality Checks give rise to a Weak Bands warning for the sample.

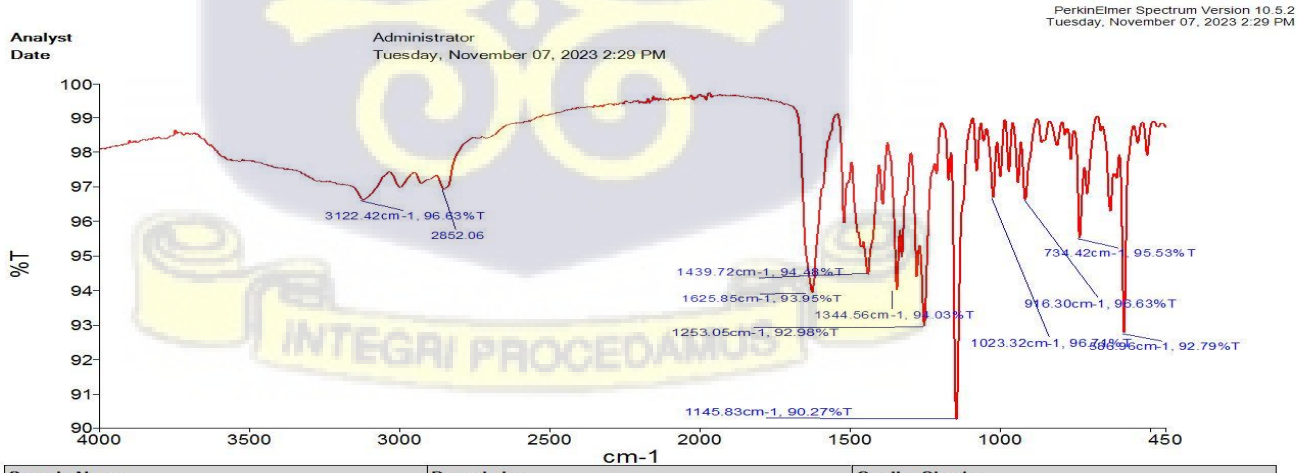
University of Ghana http://ugspace.ug.edu.gh

ADA096



Sample Name	Description	Quality Checks
ADA-096_1	Sample 262 By Administrator Date Tuesday, November 07 2023	The Quality Checks do not report any warnings for the sample.

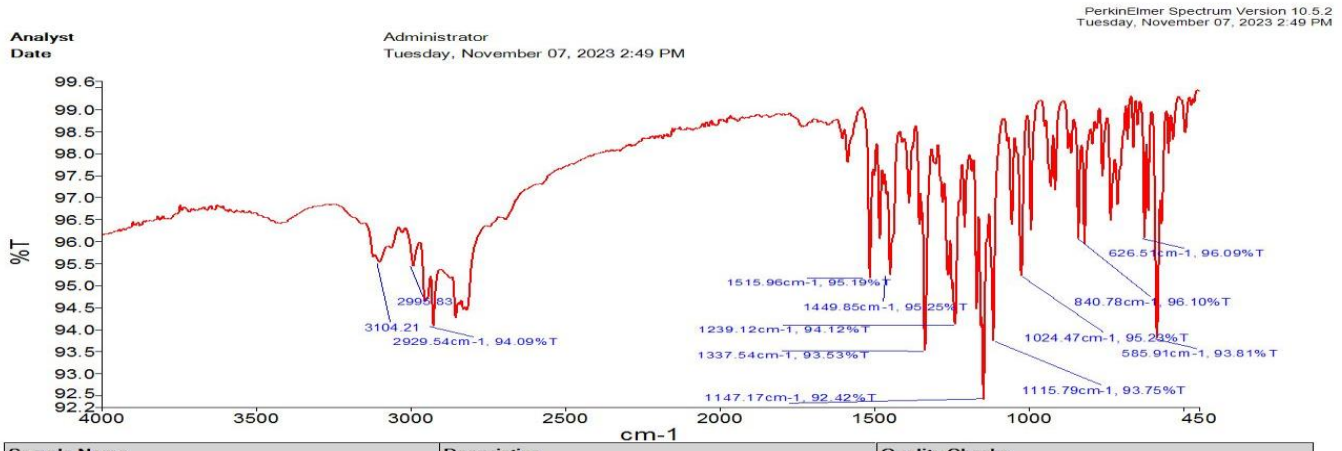
ADA097



Sample Name	Description	Quality Checks
ADA-097_1	Sample 261 By Administrator Date Tuesday, November 07 2023	The Quality Checks do not report any warnings for the sample.

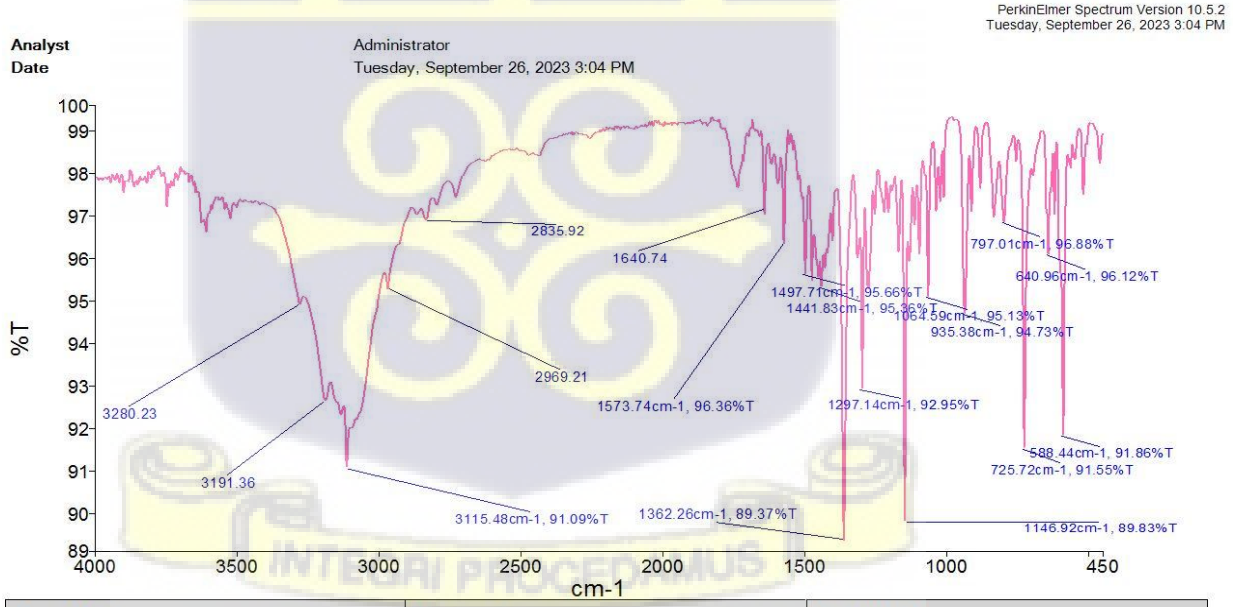
University of Ghana http://ugspace.ug.edu.gh

ADA099



Sample Name	Description	Quality Checks
ADA-099_1	Sample 263 By Administrator Date Tuesday, November 07 2023	The Quality Checks give rise to a Weak Bands warning for the sample.

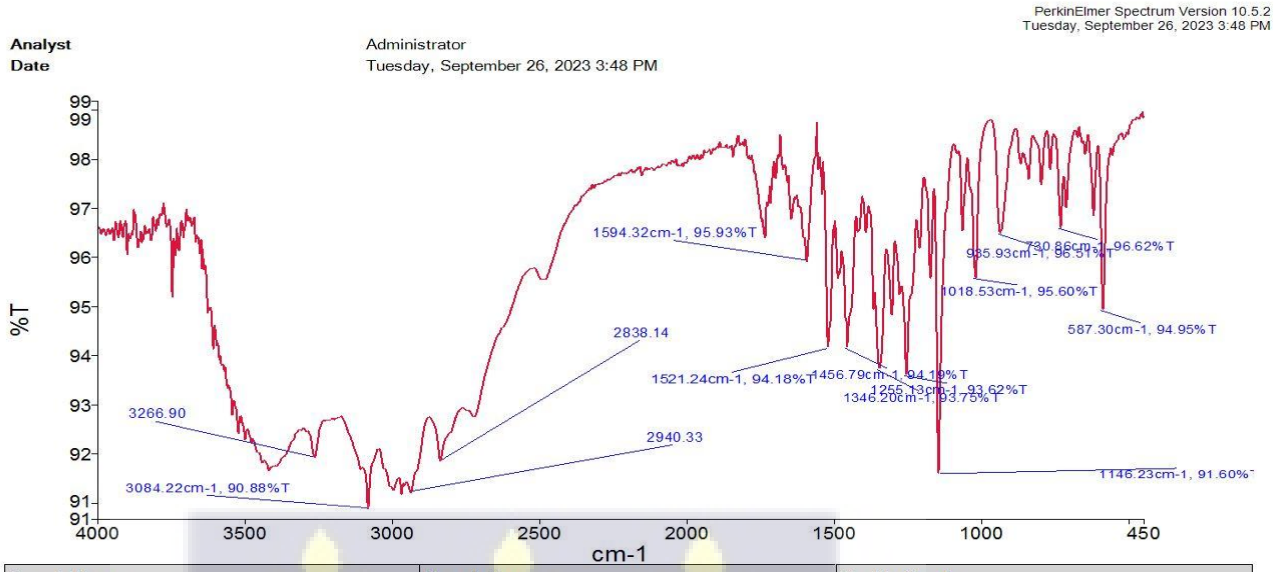
ADA101



Sample Name	Description	Quality Checks
Administrator 242_1	ADA101A	The Quality Checks do not report any warnings for the sample.

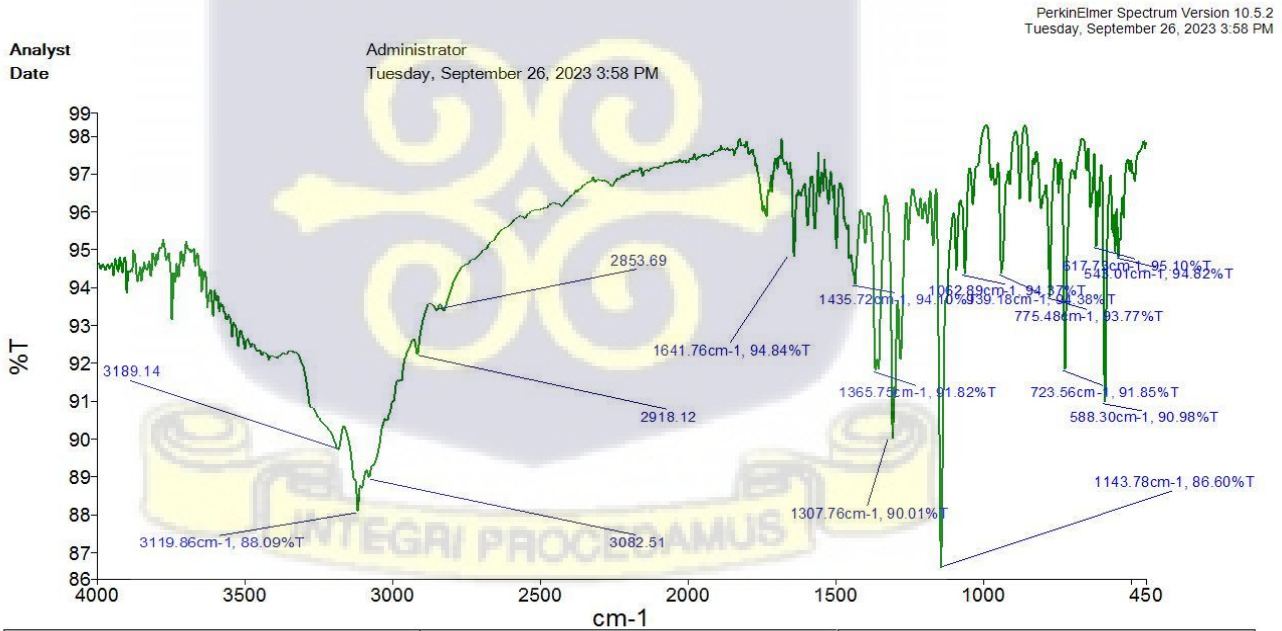
University of Ghana http://ugspace.ug.edu.gh

ADA102



Sample Name	Description	Quality Checks
Administrator 246_1	ADA102A	The Quality Checks give rise to a Weak Bands warning for the sample.

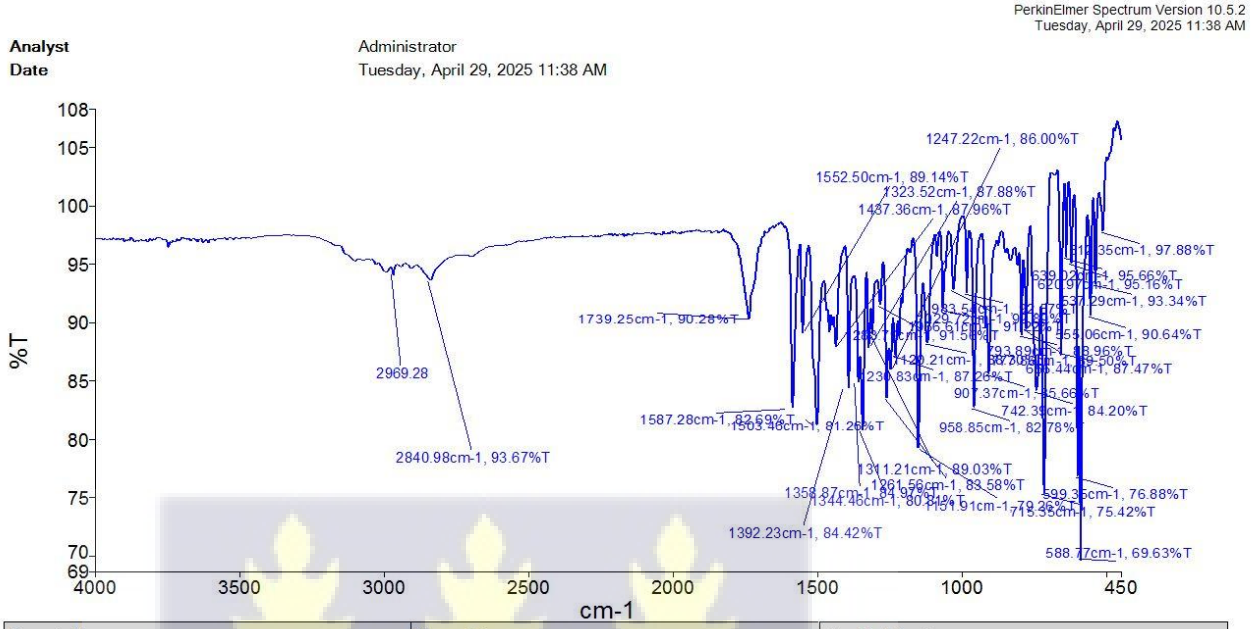
ADA103



Sample Name	Description	Quality Checks
Administrator 248_1	ADA103A	The Quality Checks do not report any warnings for the sample.

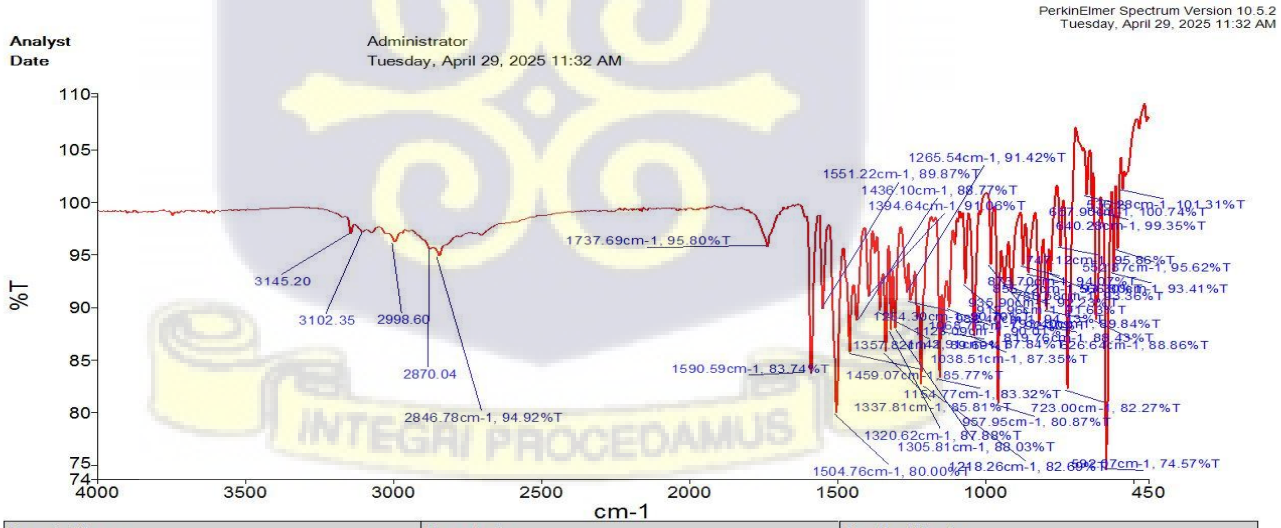
University of Ghana http://ugspace.ug.edu.gh

ADA106



Sample Name	Description	Quality Checks
Administrator 99	ADA106	The Quality Checks do not report any warnings for the sample.

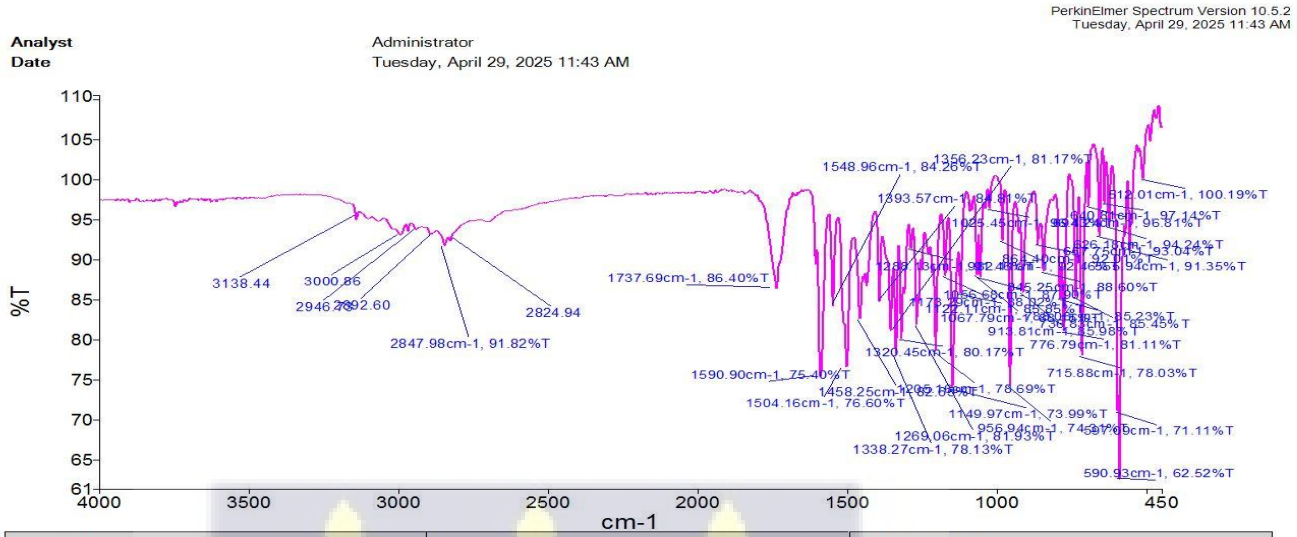
ADA107



Sample Name	Description	Quality Checks
Administrator 98	ADA107	The Quality Checks give rise to a Weak Bands warning for the sample.

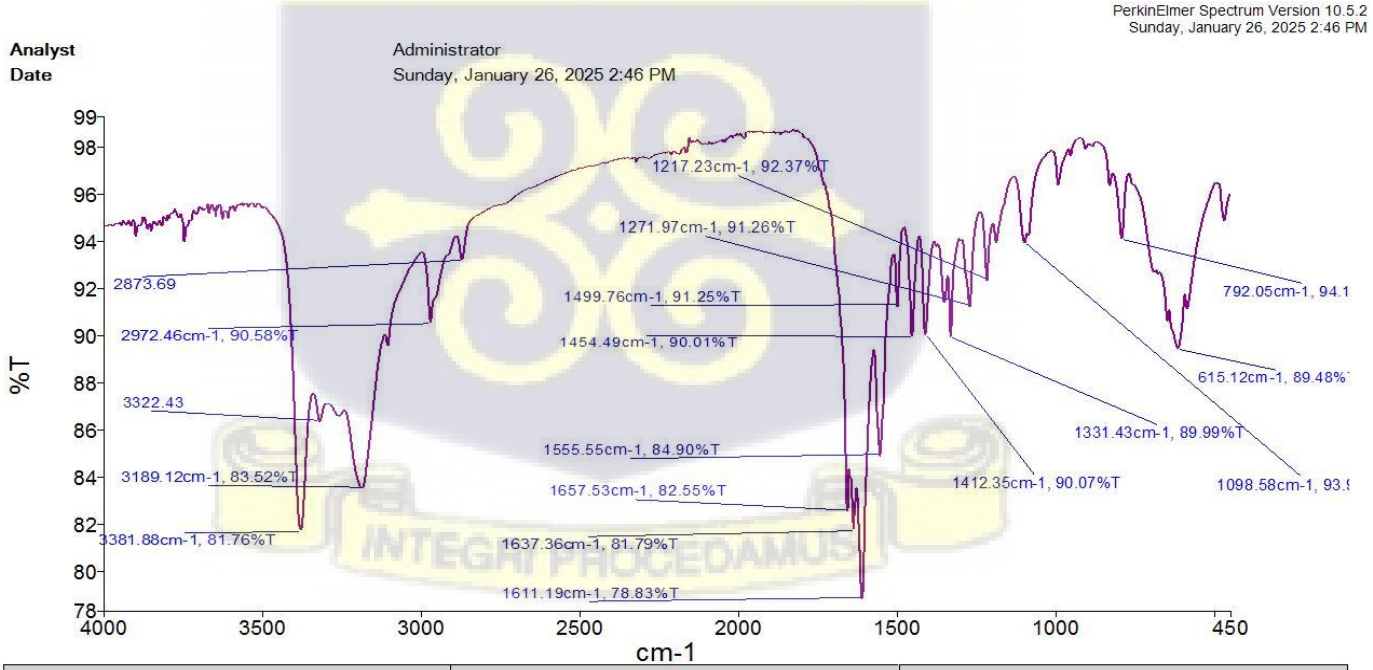
University of Ghana http://ugspace.ug.edu.gh

ADA108



Sample Name	Description	Quality Checks
Administrator 100	ADA108	The Quality Checks do not report any warnings for the sample.

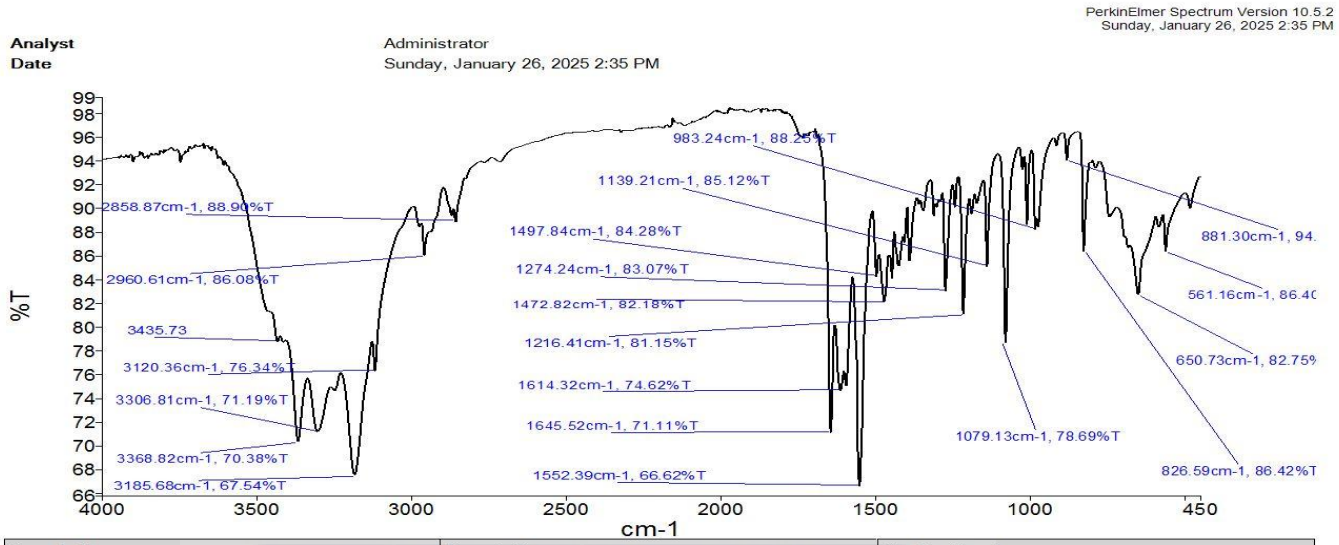
ADA110



Sample Name	Description	Quality Checks
Administrator 43_1	ADA110	The Quality Checks do not report any warnings for the sample.

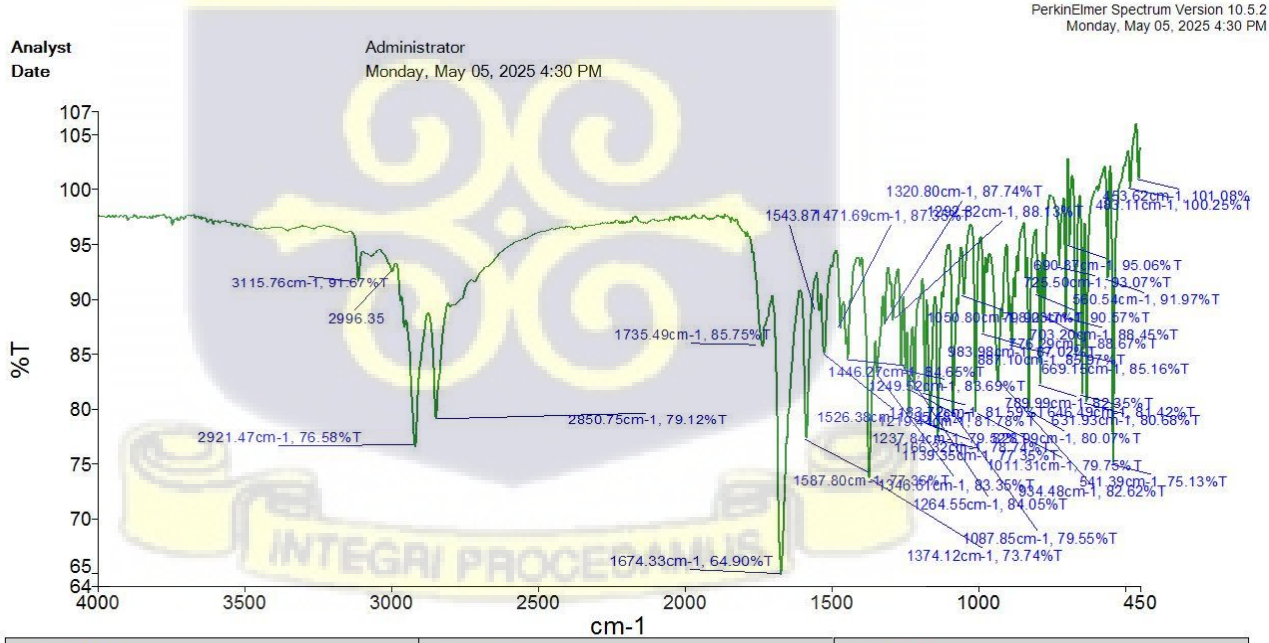
University of Ghana http://ugspace.ug.edu.gh

ADA111



Sample Name	Description	Quality Checks
Administrator 41_1	ADA111	The Quality Checks do not report any warnings for the sample.

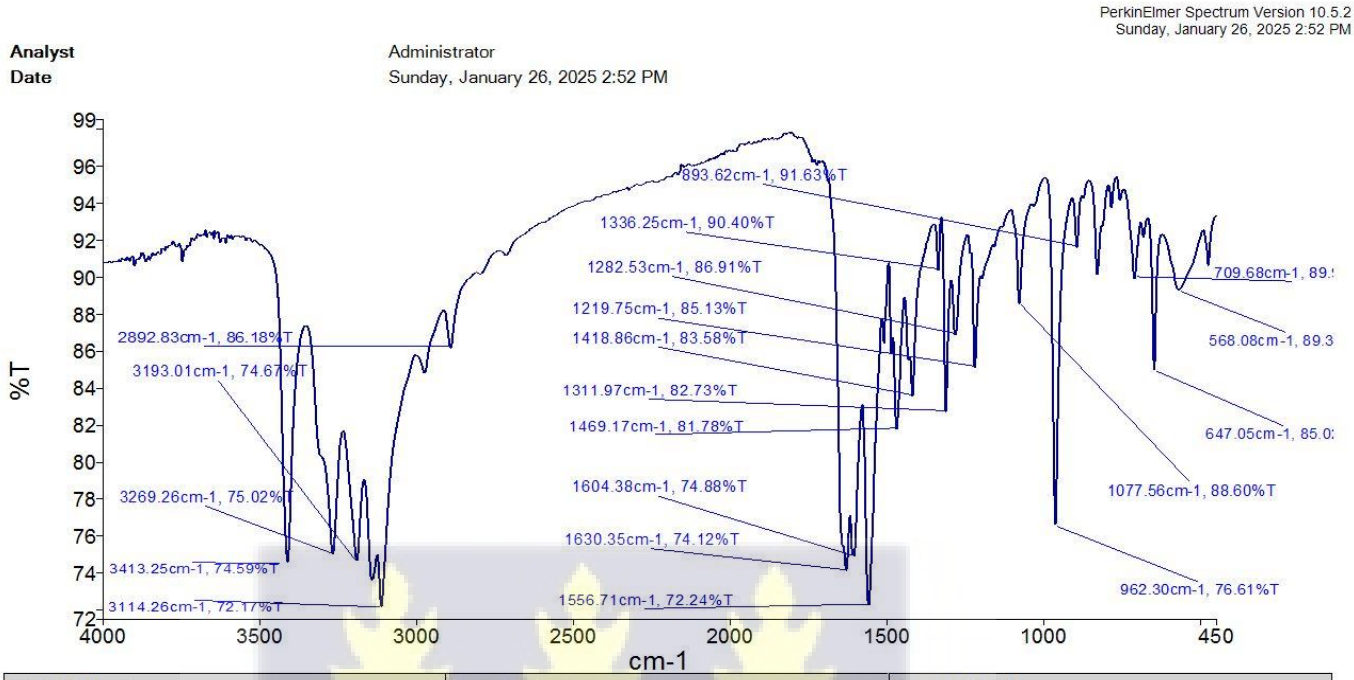
ADA113



Sample Name	Description	Quality Checks
Administrator 107	ADA113	The Quality Checks do not report any warnings for the sample.

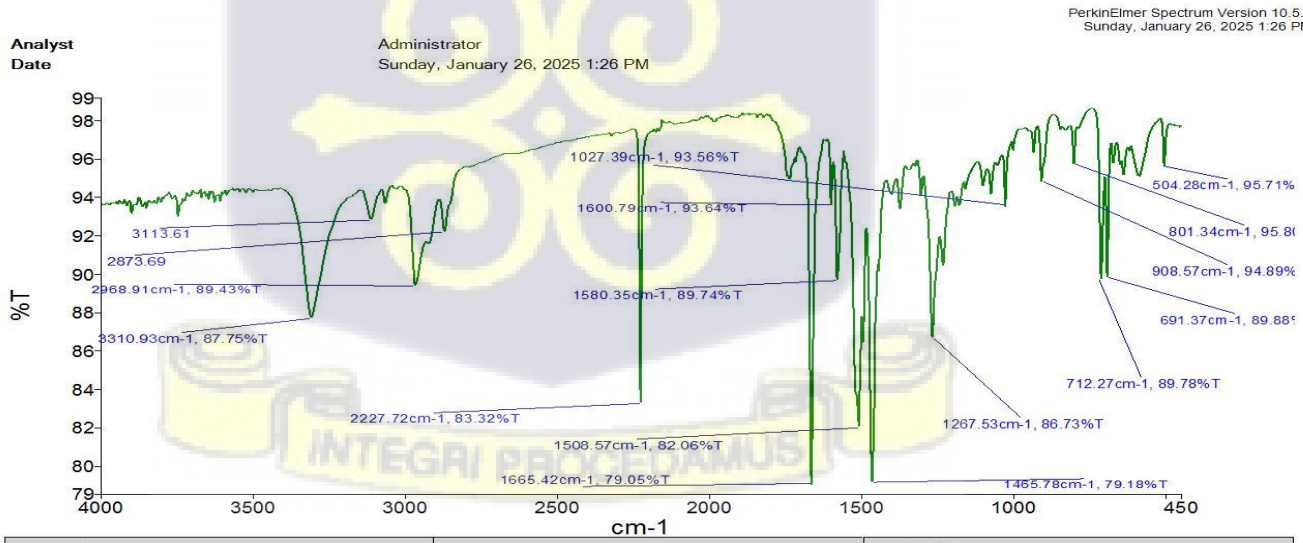
University of Ghana http://ugspace.ug.edu.gh

ADA114



Sample Name	Description	Quality Checks
Administrator 44_1	ADA114	The Quality Checks do not report any warnings for the sample.

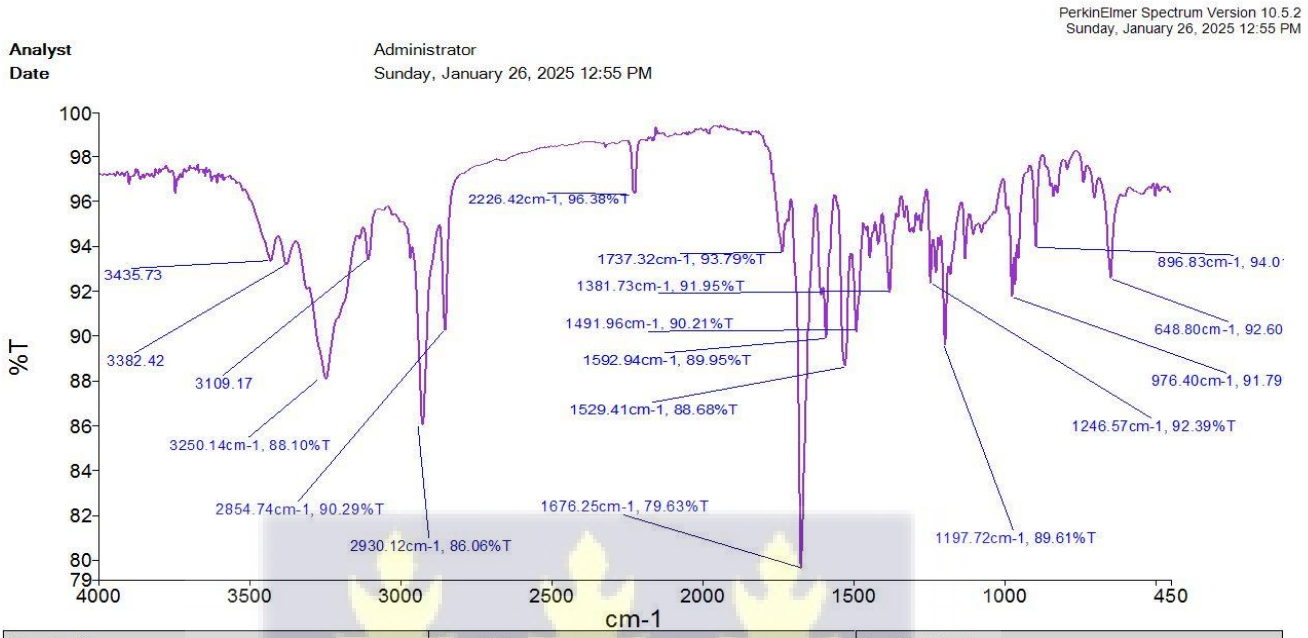
ADA115



Sample Name	Description	Quality Checks
Administrator 40_1	ADA115	The Quality Checks do not report any warnings for the sample.

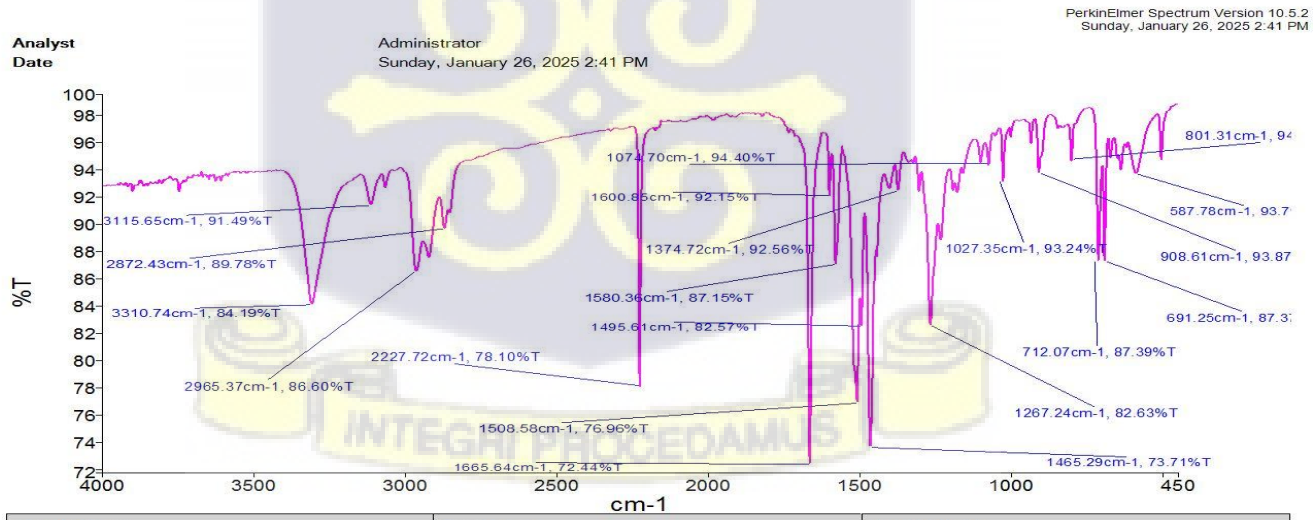
University of Ghana http://ugspace.ug.edu.gh

ADA116



Sample Name	Description	Quality Checks
Administrator 36_1	ADA116	The Quality Checks do not report any warnings for the sample.

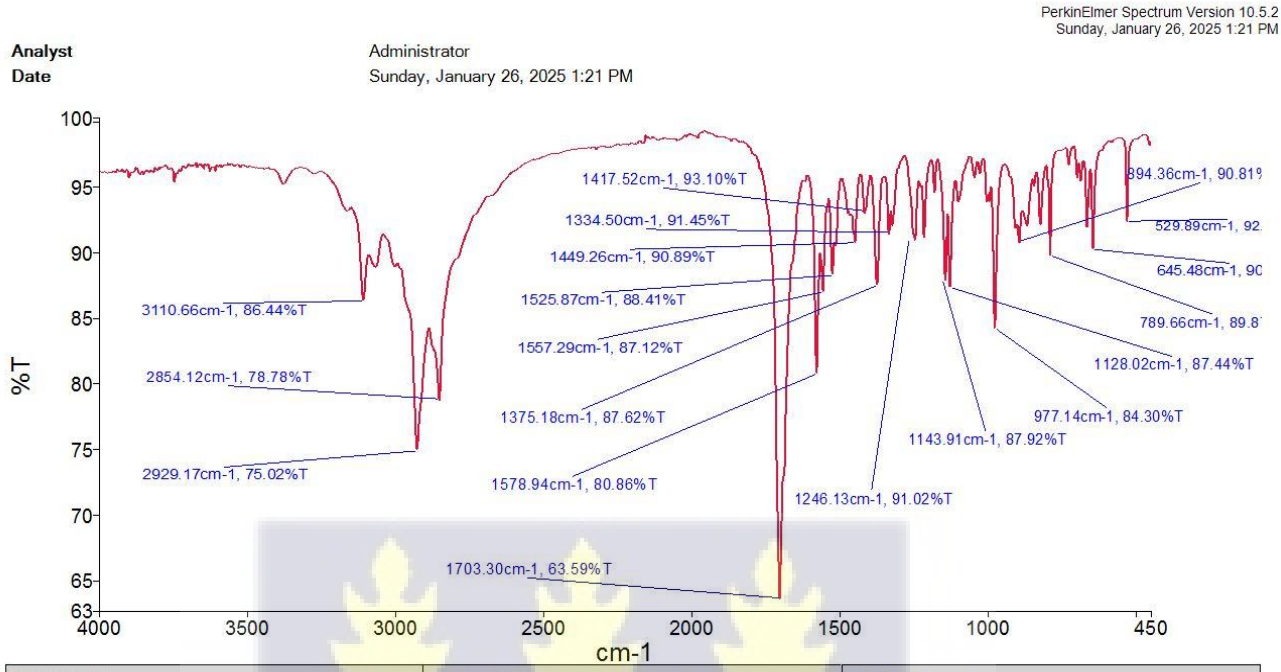
ADA117



Sample Name	Description	Quality Checks
Administrator 42_1	ADA117	The Quality Checks do not report any warnings for the sample.

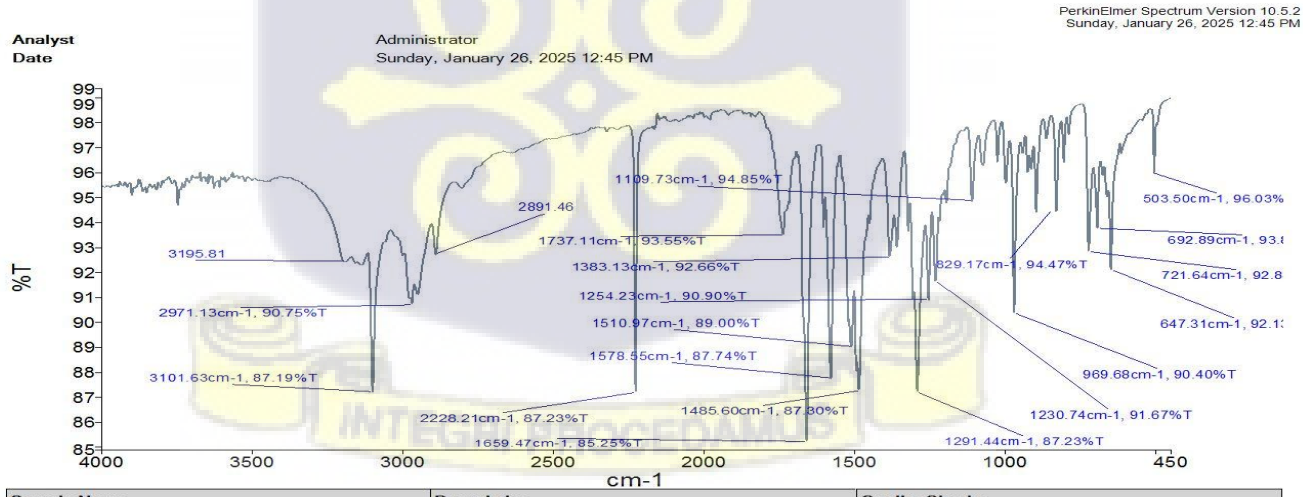
University of Ghana http://ugspace.ug.edu.gh

ADA118



Sample Name	Description	Quality Checks
Administrator 39_1	ADA118	The Quality Checks do not report any warnings for the sample.

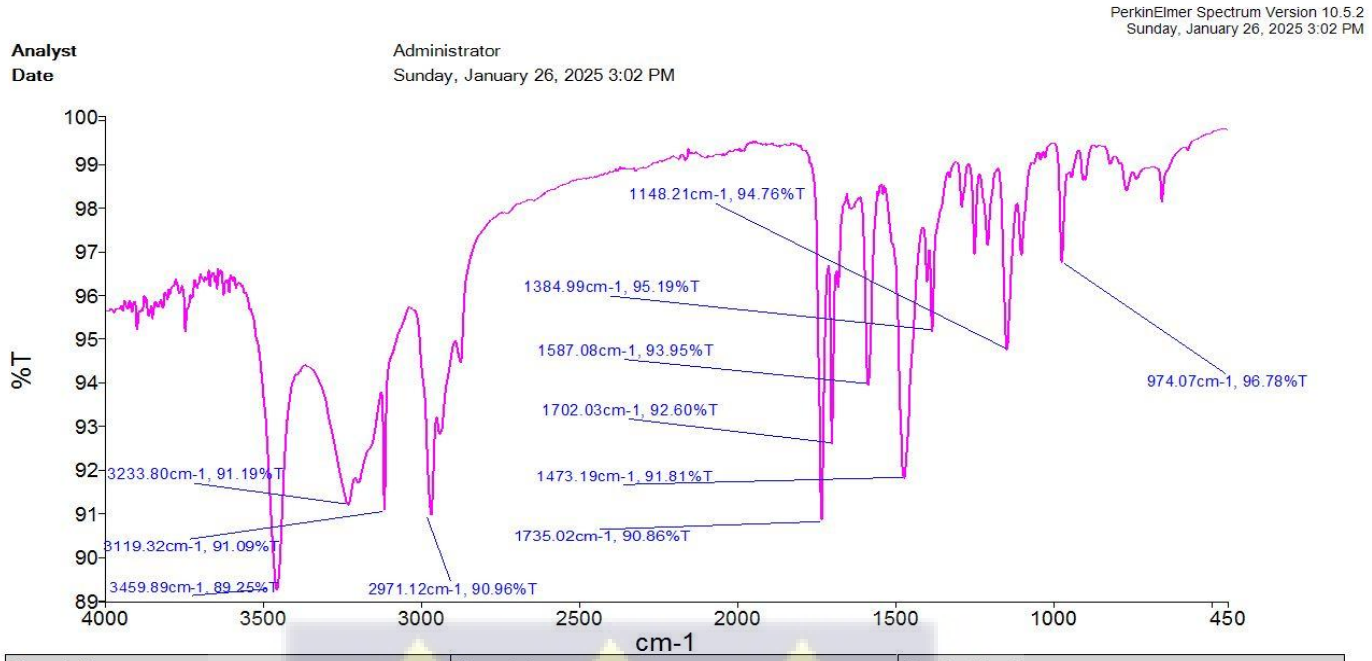
ADA119



Sample Name	Description	Quality Checks
Administrator 34_1	ADA119	The Quality Checks do not report any warnings for the sample.

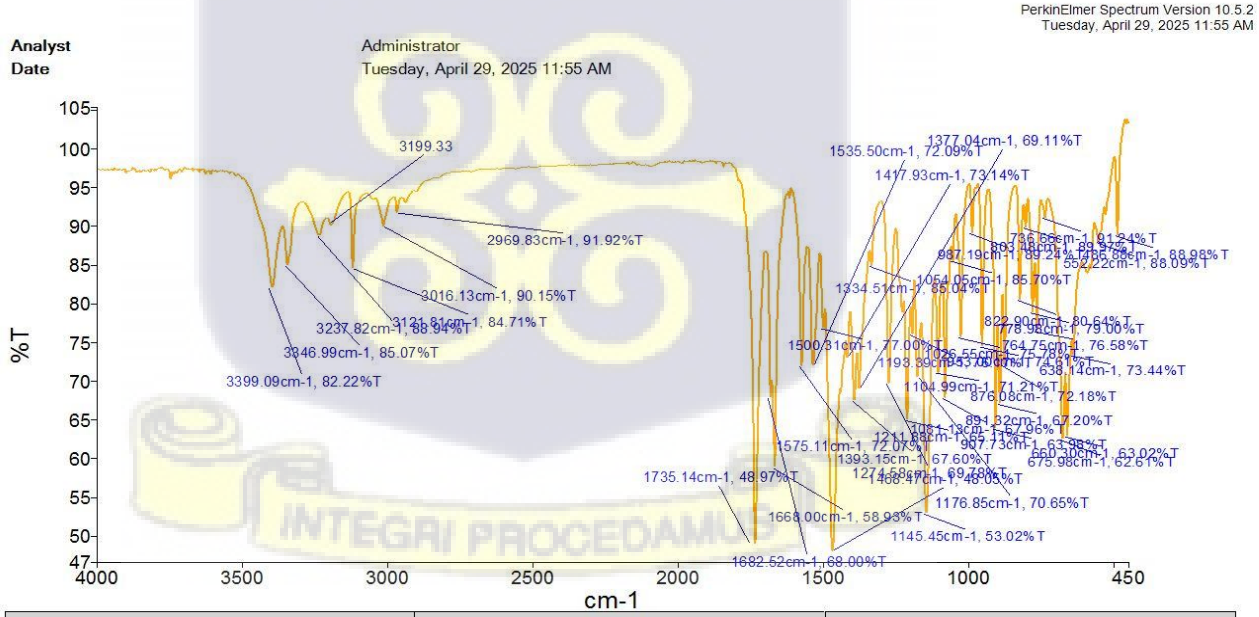
ADA120

University of Ghana http://ugspace.ug.edu.gh



Sample Name	Description	Quality Checks
Administrator 46_1_1	ADA120	The Quality Checks do not report any warnings for the sample.

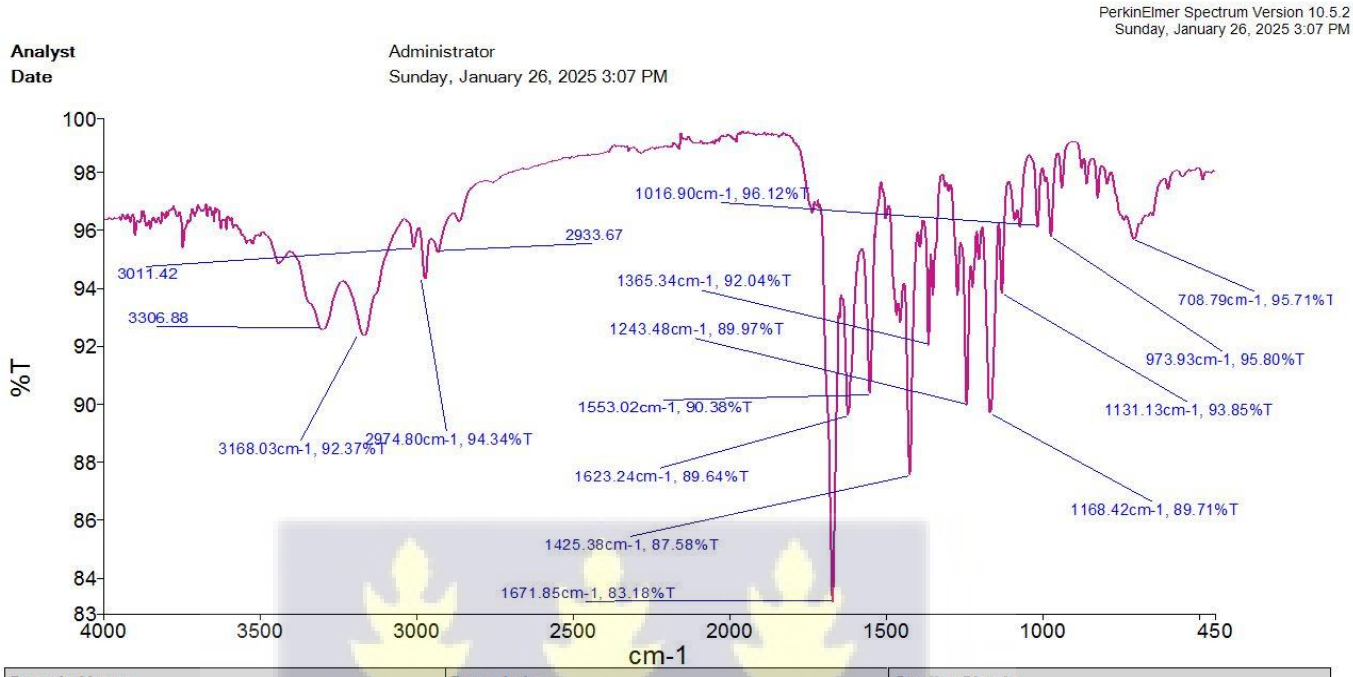
ADA123



Sample Name	Description	Quality Checks
Administrator 102	ADA123	The Quality Checks do not report any warnings for the sample.

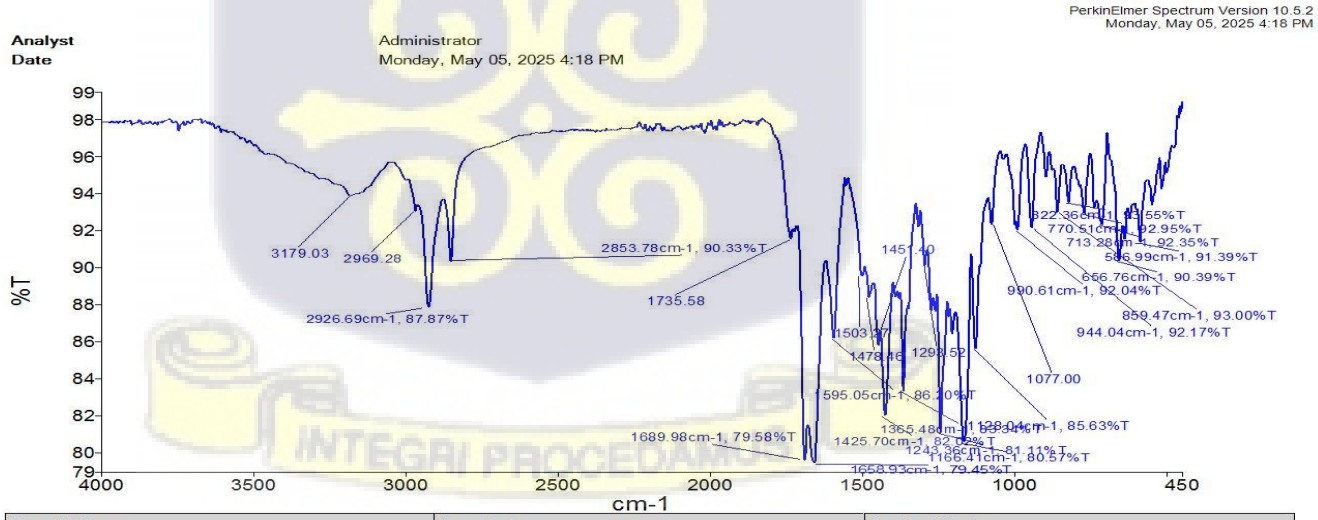
University of Ghana http://ugspace.ug.edu.gh

ADA127



Sample Name	Description	Quality Checks
Administrator 47_1	ADA127	The Quality Checks give rise to a Weak Bands warning for the sample.

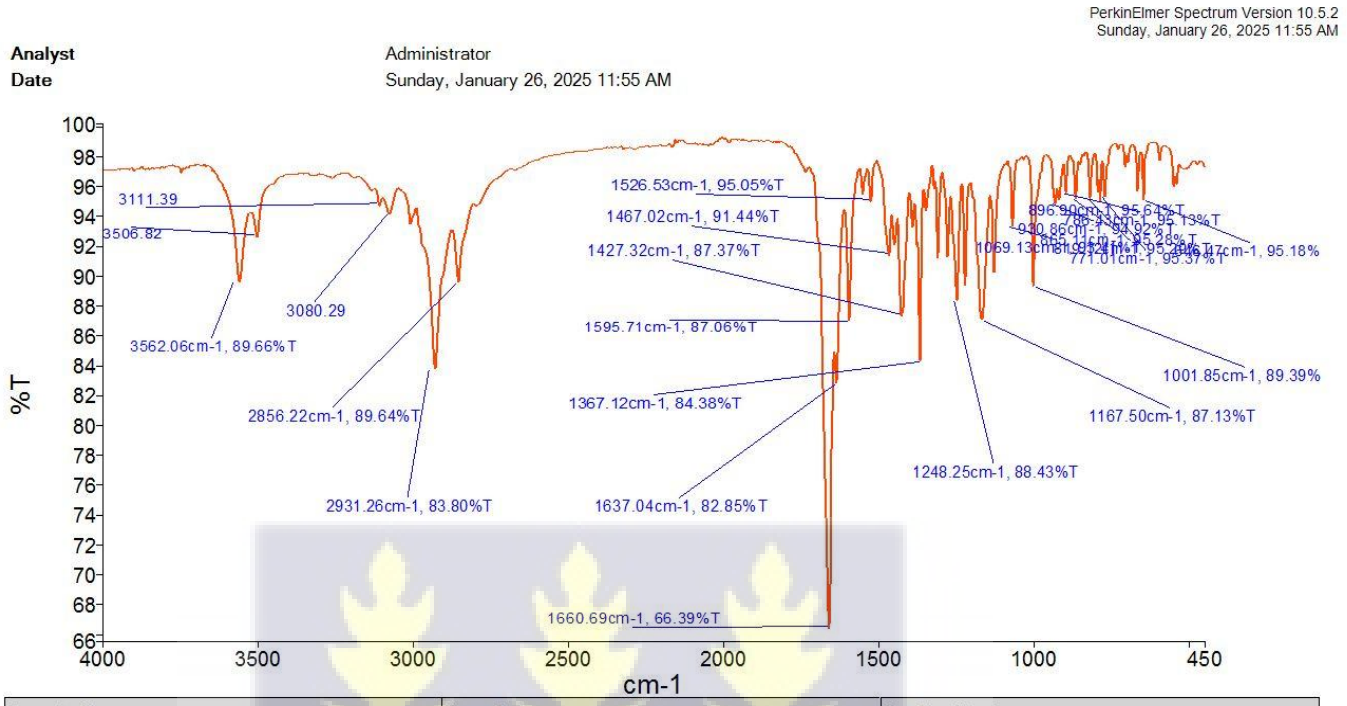
ADA128



Sample Name	Description	Quality Checks
Administrator 105	ADA128	The Quality Checks give rise to a Weak Bands warning for the sample.

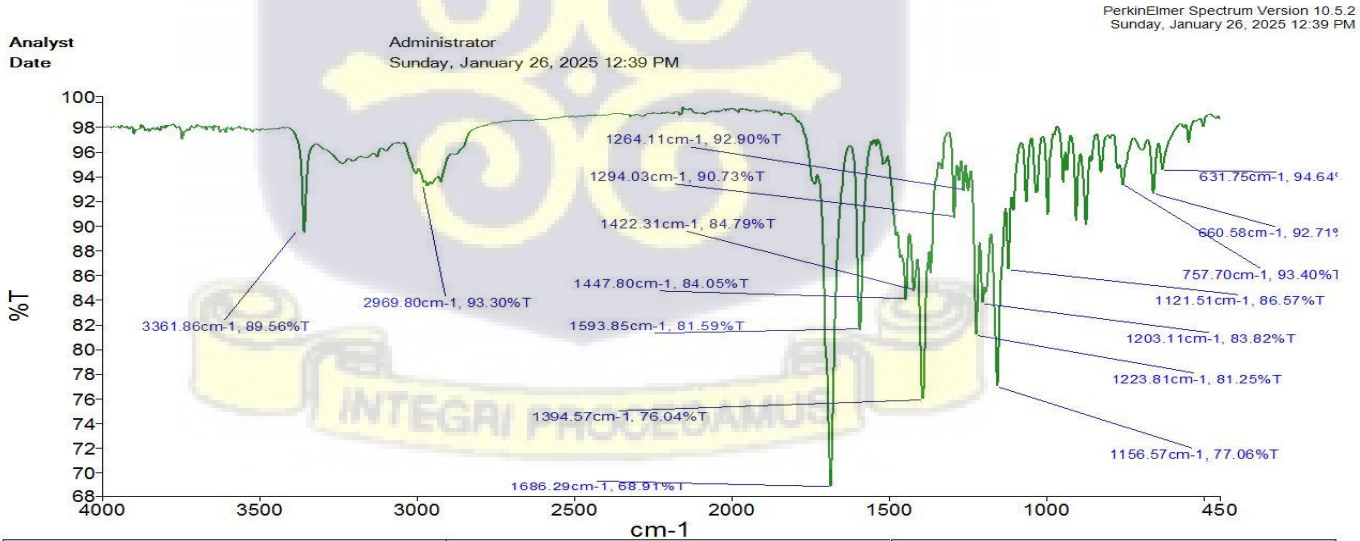
University of Ghana http://ugspace.ug.edu.gh

ADA129



Sample Name	Description	Quality Checks
Administrator 25_1	ADA129	The Quality Checks do not report any warnings for the sample.

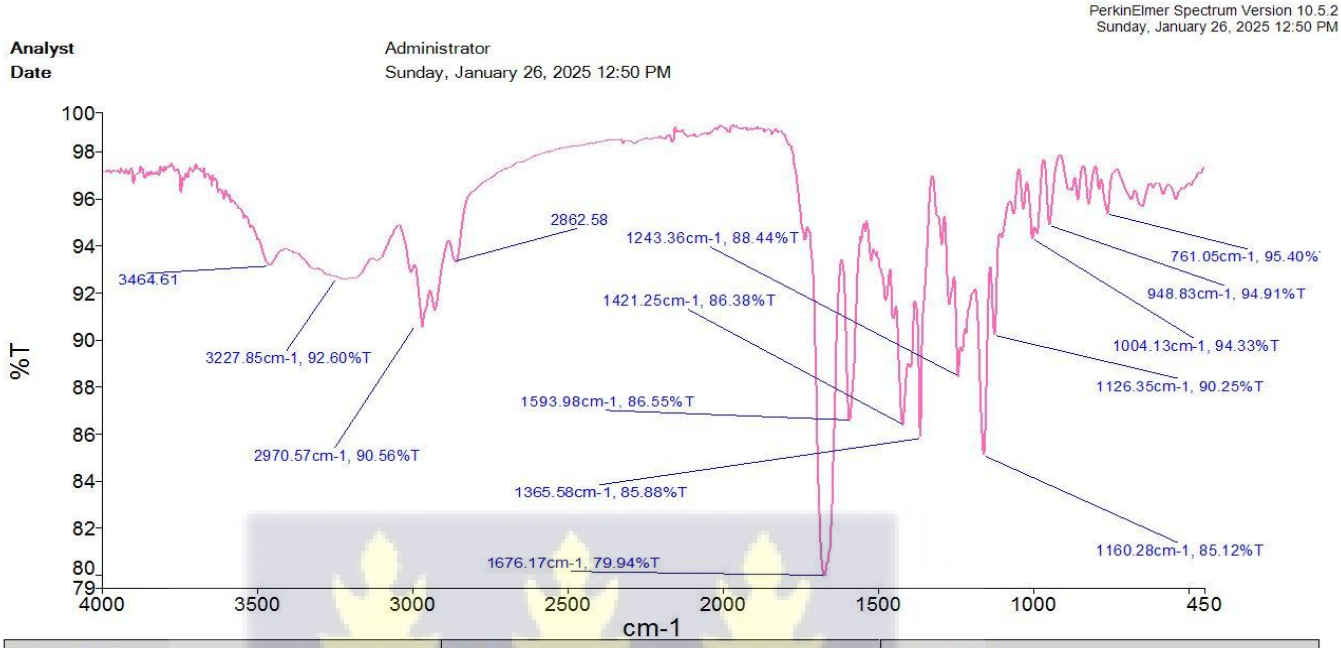
ADA131



Sample Name	Description	Quality Checks
Administrator 33_1	ADA131	The Quality Checks do not report any warnings for the sample.

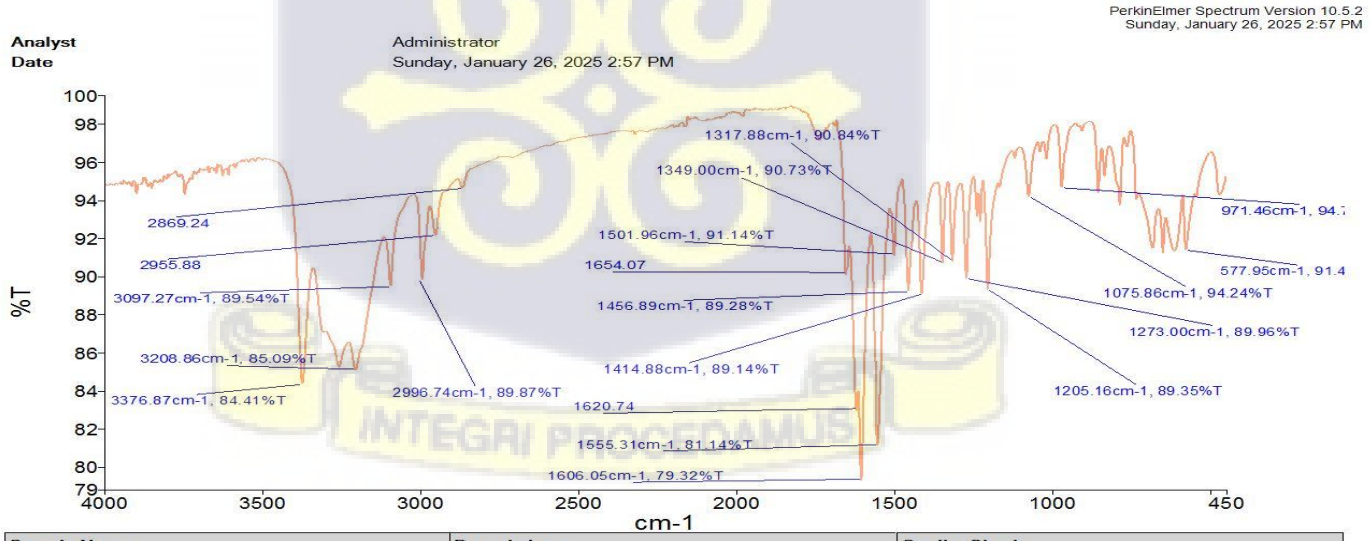
University of Ghana http://ugspace.ug.edu.gh

ADA132



Sample Name	Description	Quality Checks
Administrator 35_1	ADA132	The Quality Checks do not report any warnings for the sample.

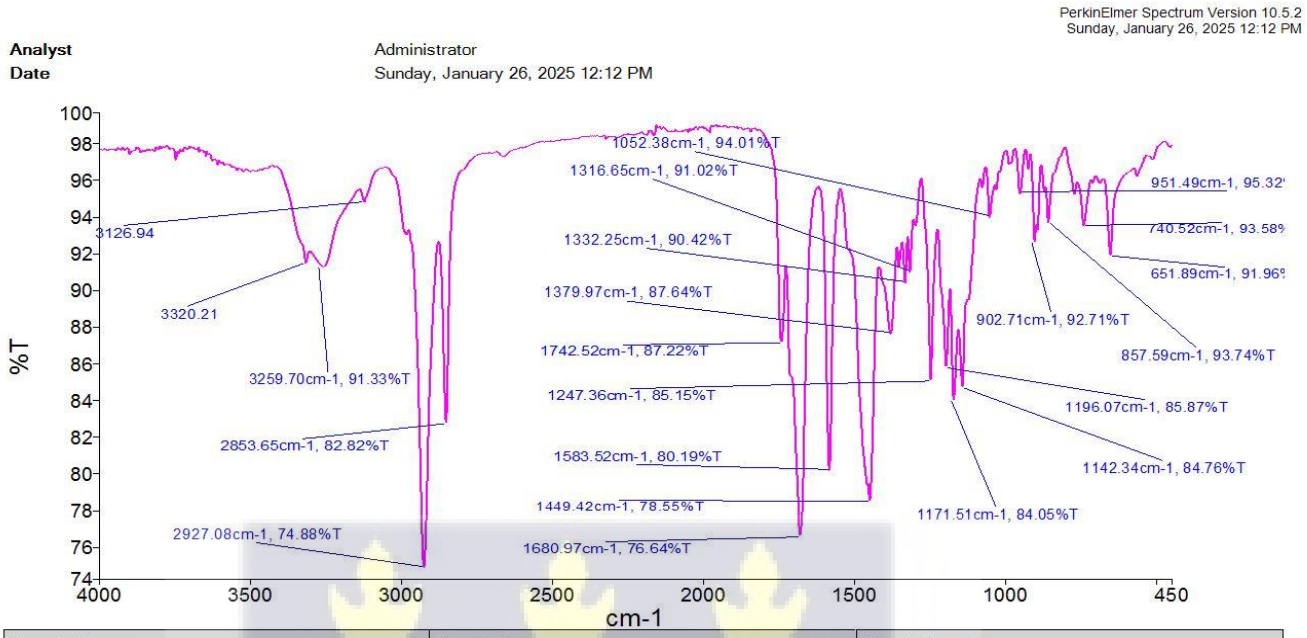
ADA134



Sample Name	Description	Quality Checks
Administrator 45_1	ADA134	The Quality Checks do not report any warnings for the sample.

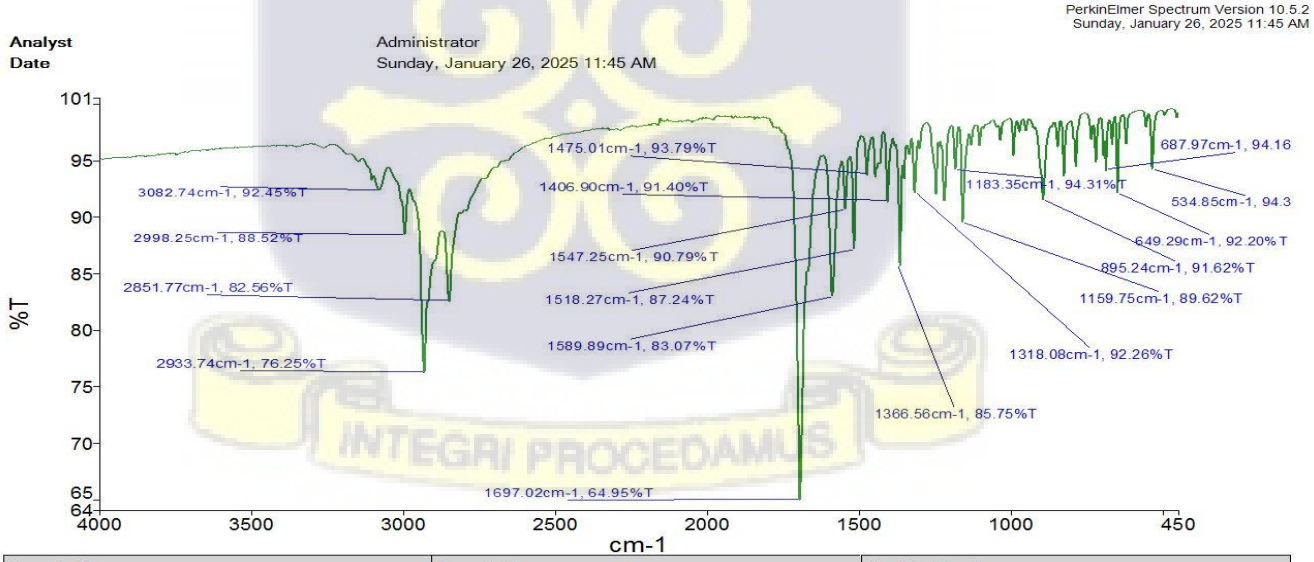
University of Ghana http://ugspace.ug.edu.gh

ADA135



Sample Name	Description	Quality Checks
Administrator 28_1	ADA135	The Quality Checks do not report any warnings for the sample.

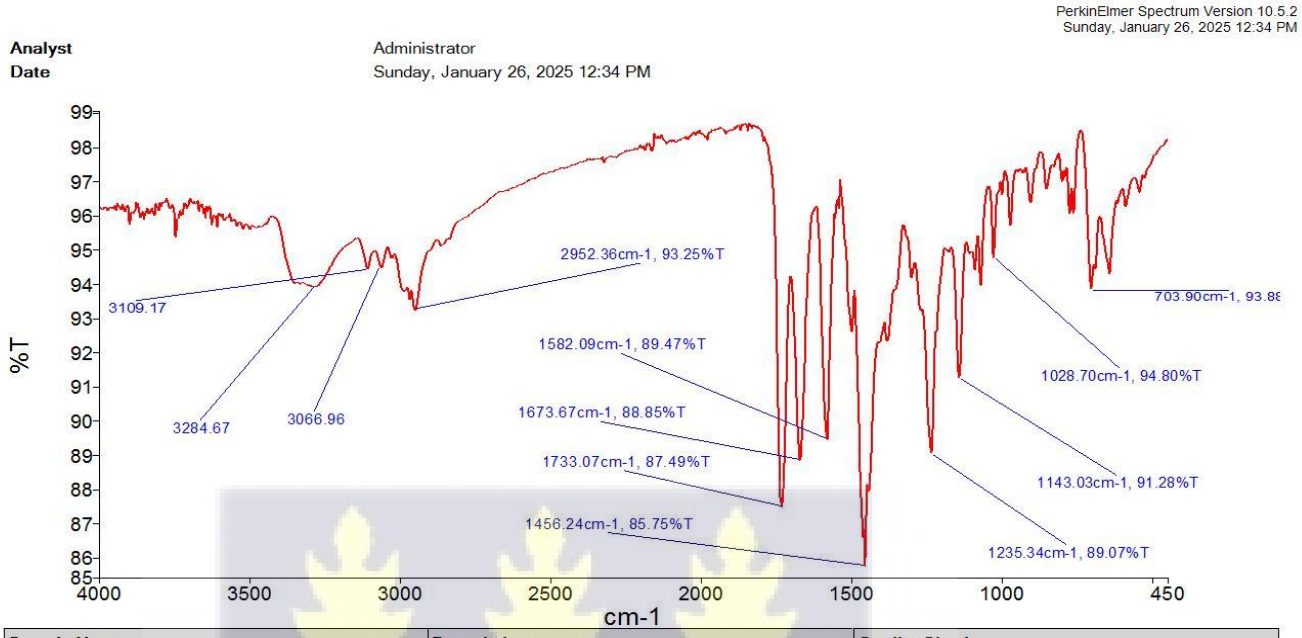
ADA136



Sample Name	Description	Quality Checks
Administrator 23_1	ADA136	The Quality Checks do not report any warnings for the sample.

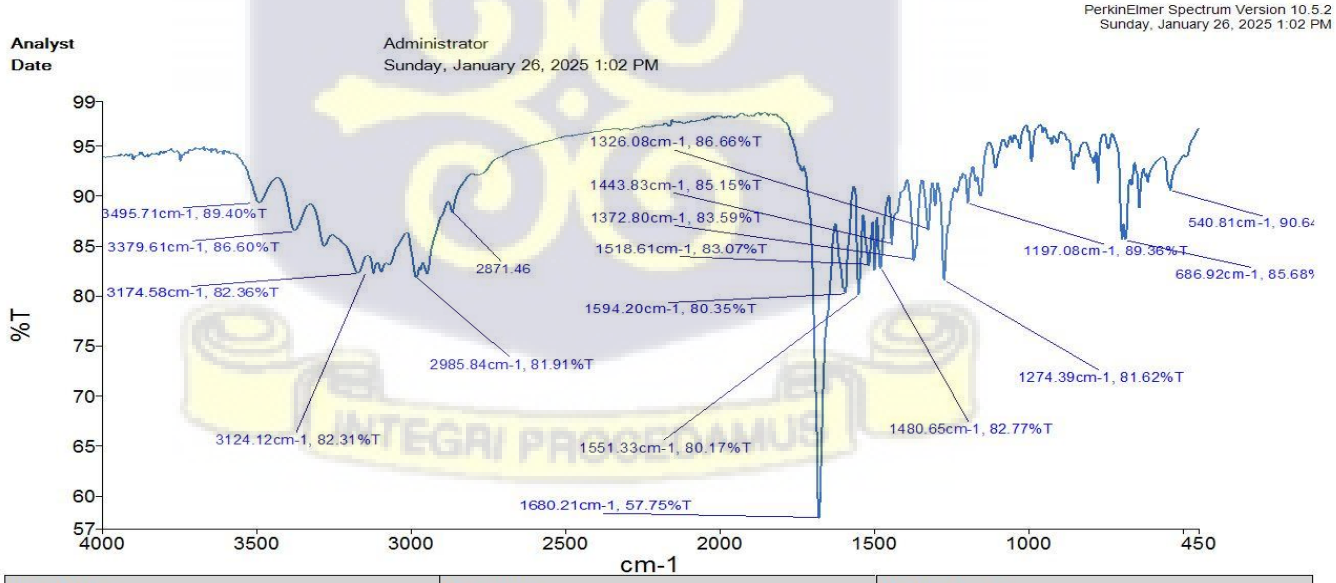
University of Ghana http://ugspace.ug.edu.gh

ADA137



Sample Name	Description	Quality Checks
Administrator 32_1	ADA137	The Quality Checks give rise to a Weak Bands warning for the sample.

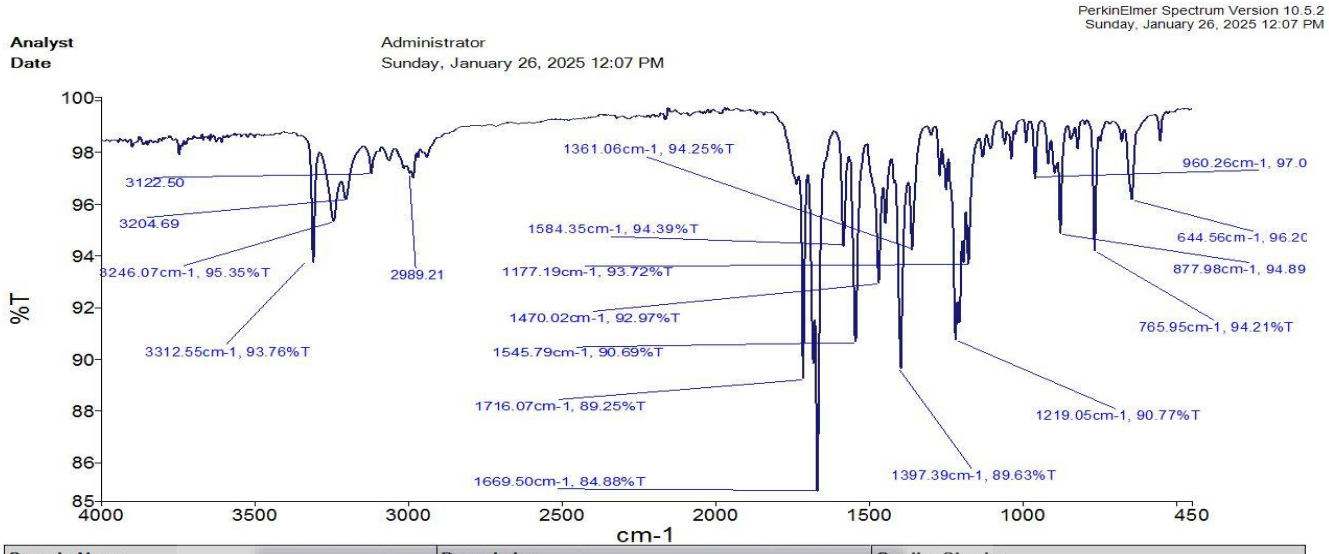
ADA138



Sample Name	Description	Quality Checks
Administrator 37_1	ADA138	The Quality Checks do not report any warnings for the sample.

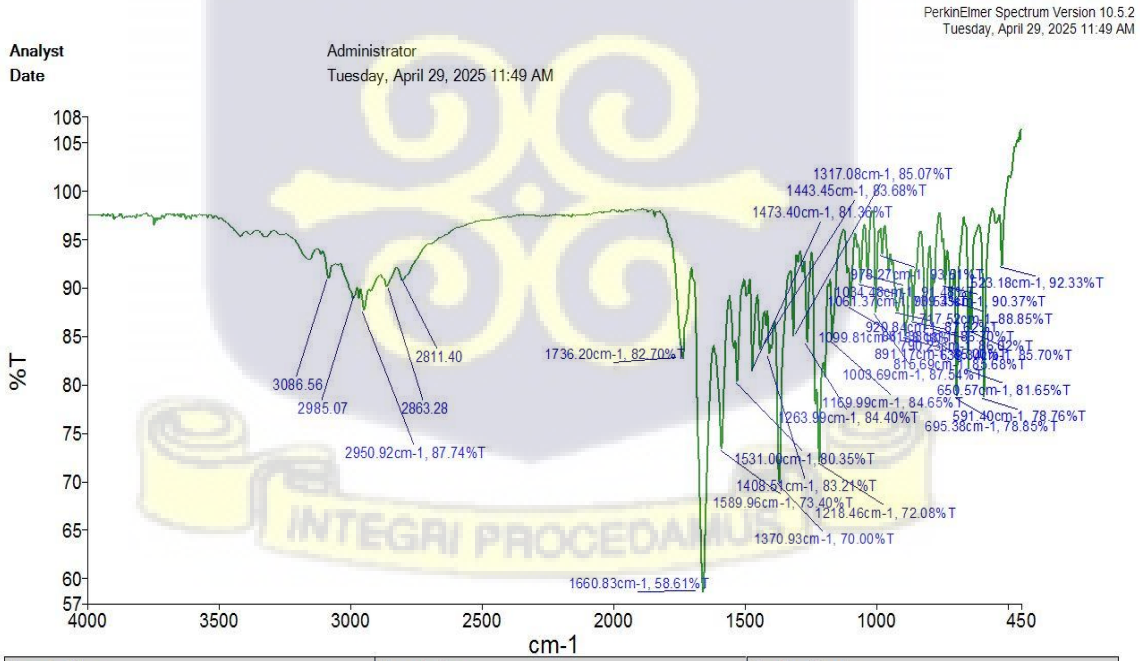
University of Ghana http://ugspace.ug.edu.gh

ADA140



Sample Name	Description	Quality Checks
Administrator 27_1	ADA140	The Quality Checks give rise to a Weak Bands warning for the sample.

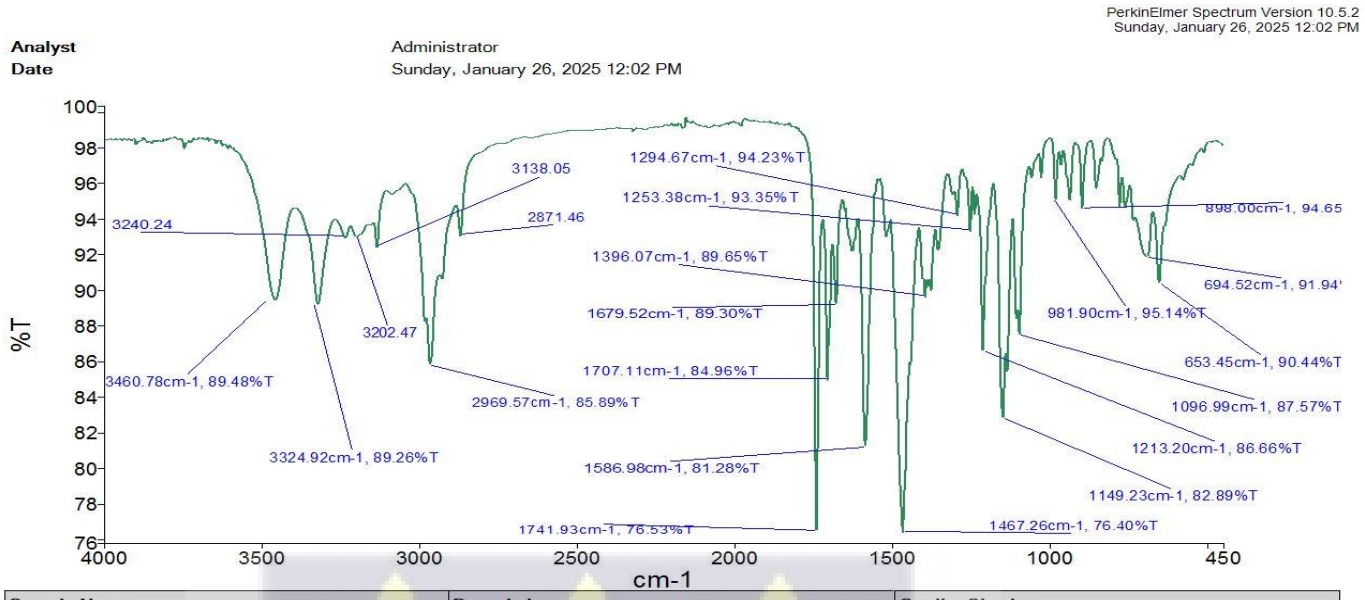
ADA141



Sample Name	Description	Quality Checks
Administrator 101	ADA141	The Quality Checks do not report any warnings for the sample.

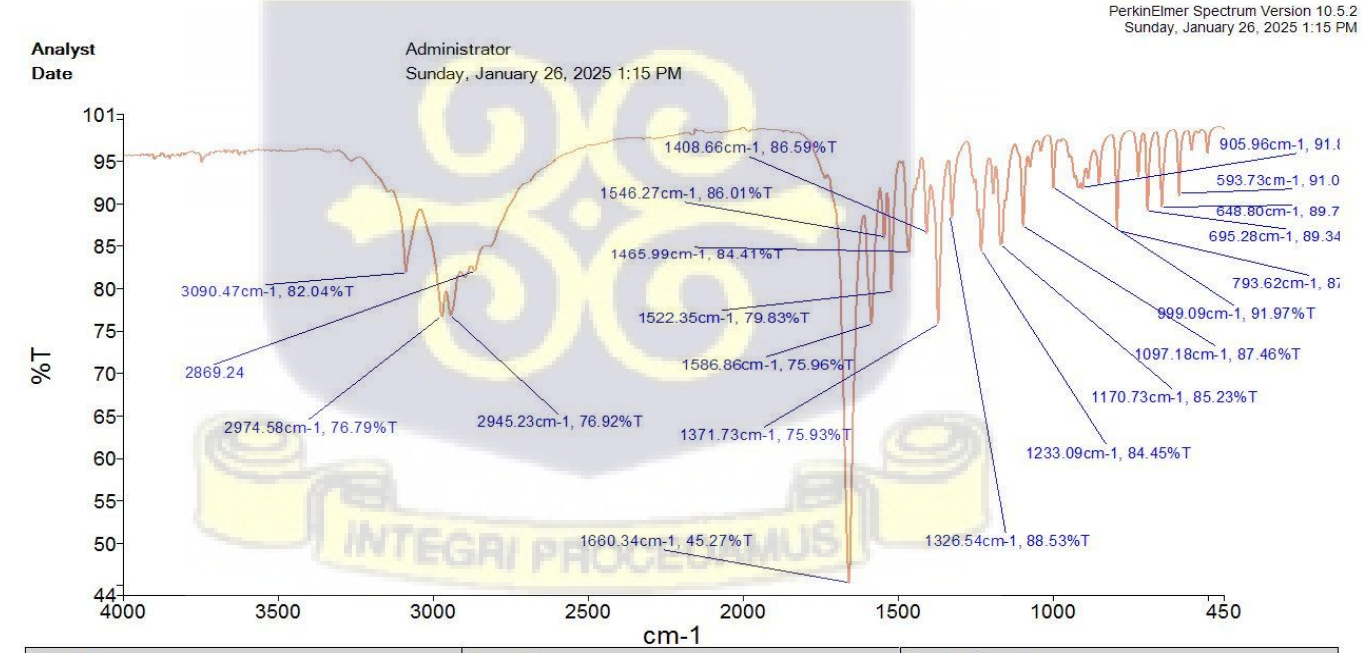
University of Ghana http://ugspace.ug.edu.gh

ADA142



Sample Name	Description	Quality Checks
Administrator 26_1	ADA142	The Quality Checks do not report any warnings for the sample.

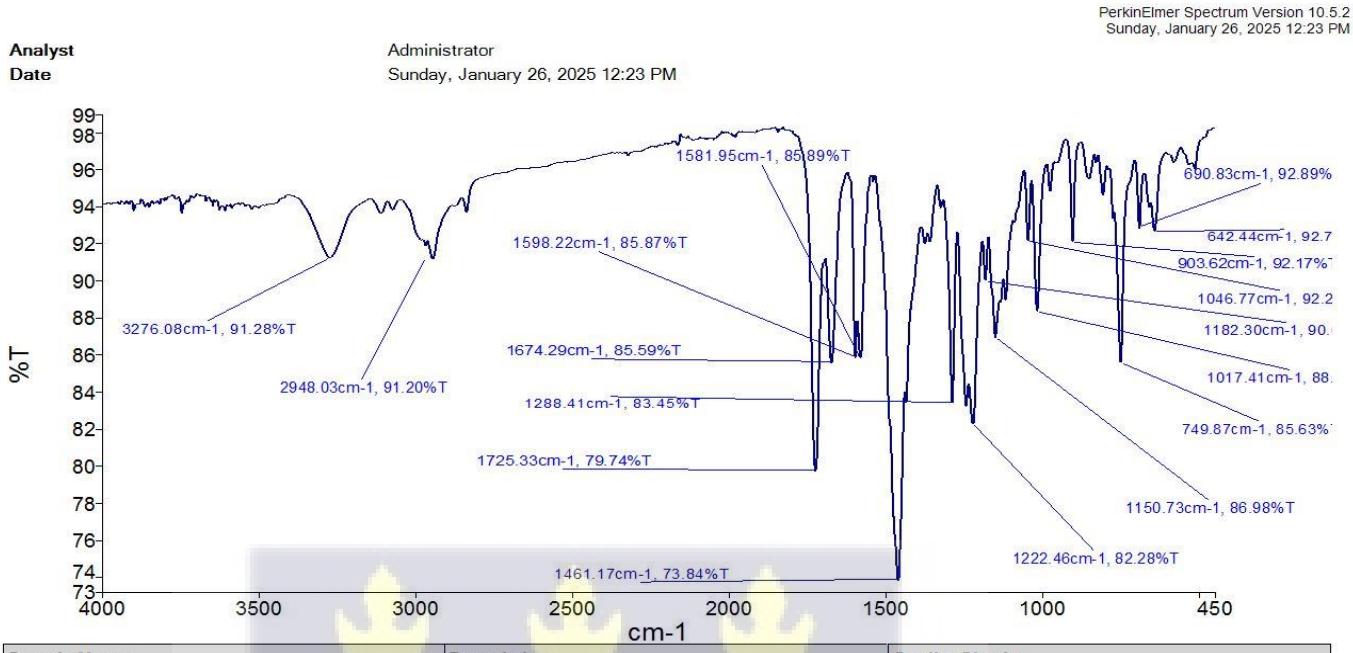
ADA143



Sample Name	Description	Quality Checks
Administrator 38_1	ADA143	The Quality Checks do not report any warnings for the sample.

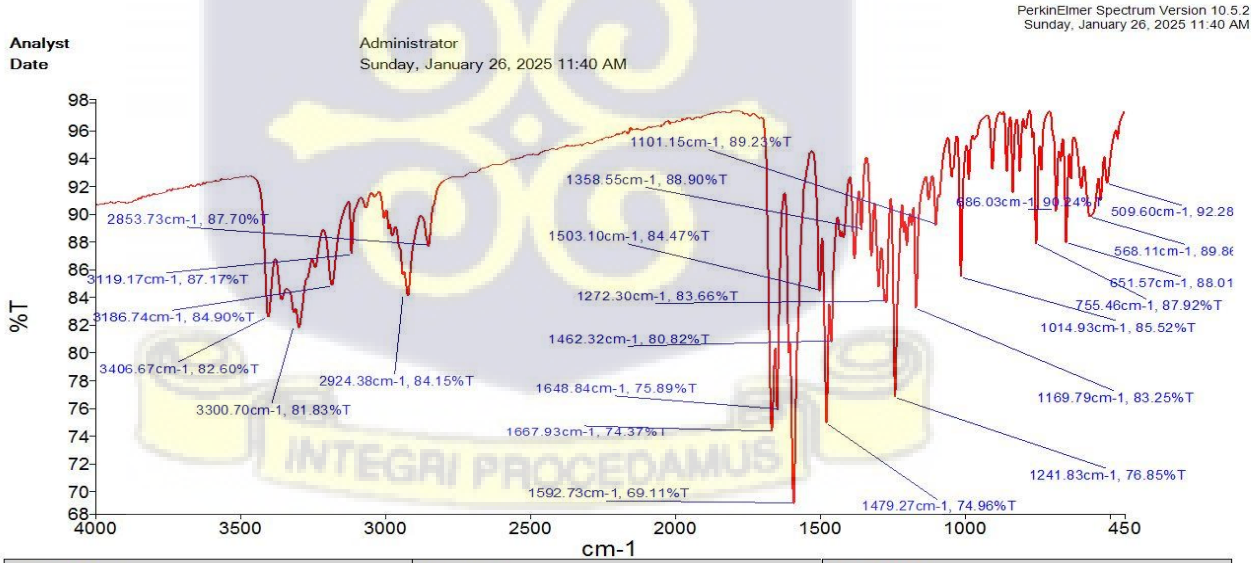
University of Ghana http://ugspace.ug.edu.gh

ADA144



Sample Name	Description	Quality Checks
Administrator 30_1	ADA144	The Quality Checks do not report any warnings for the sample.

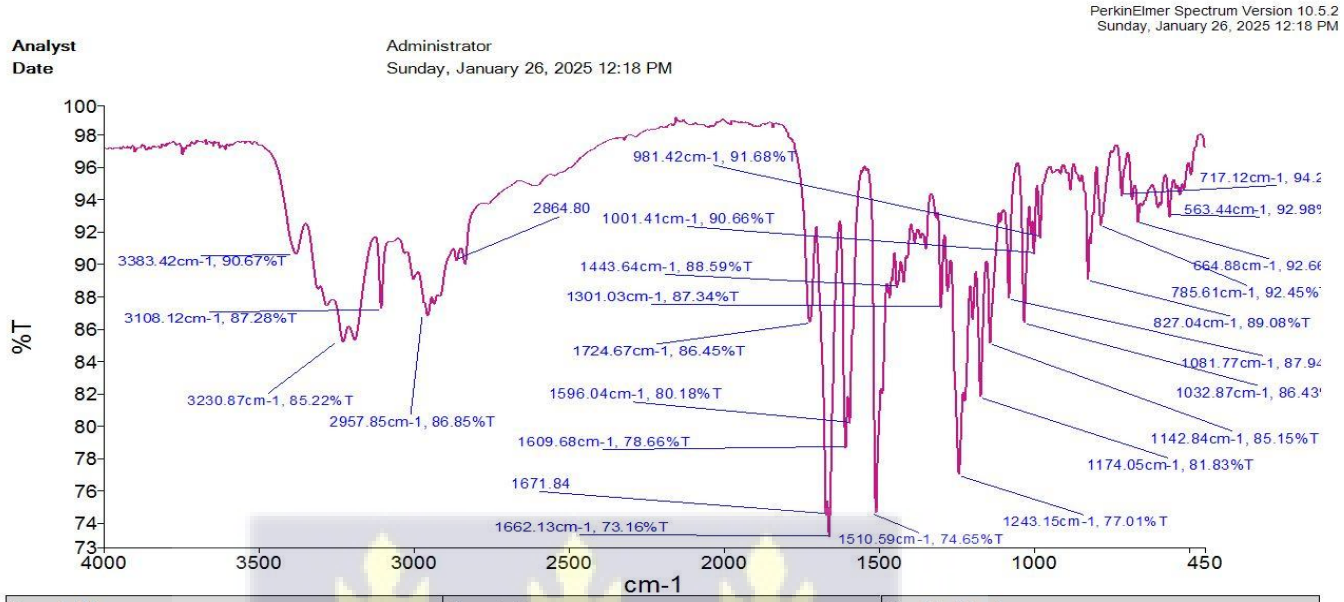
ADA145



Sample Name	Description	Quality Checks
Administrator 22_1	ADA145	The Quality Checks do not report any warnings for the sample.

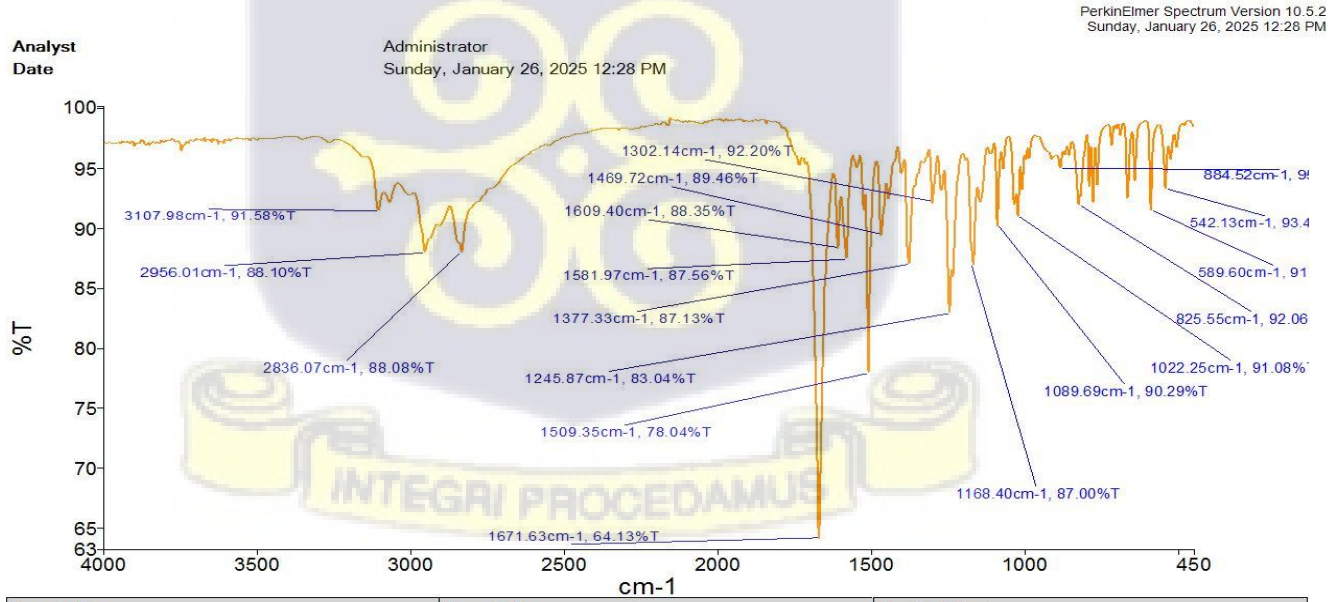
University of Ghana http://ugspace.ug.edu.gh

ADA147



Sample Name	Description	Quality Checks
Administrator 29_1	ADA147	The Quality Checks do not report any warnings for the sample.

ADA148

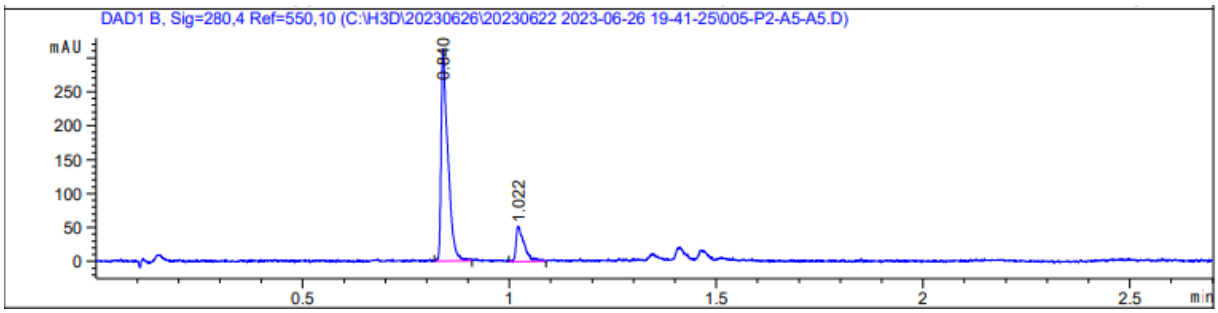


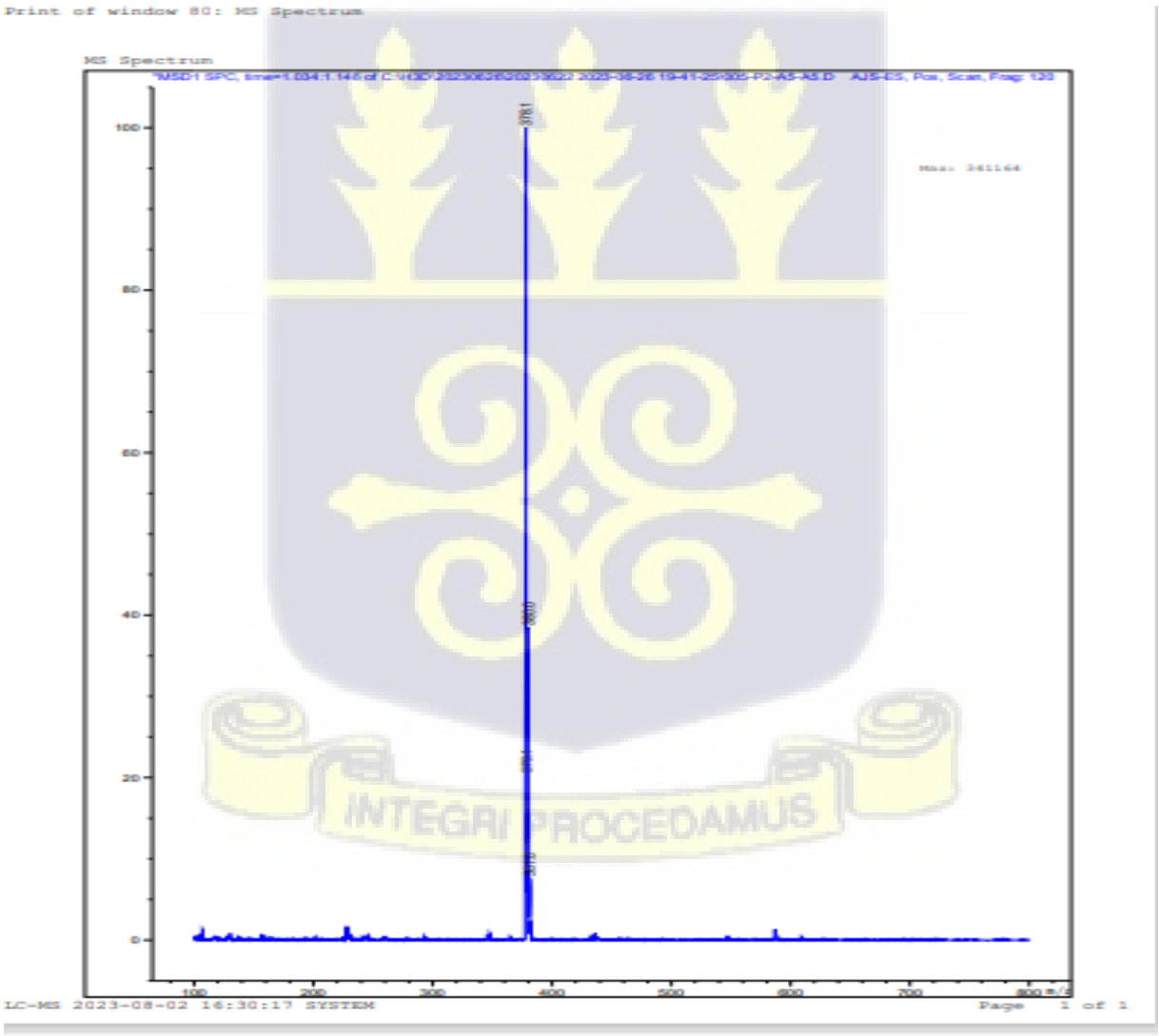
Sample Name	Description	Quality Checks
Administrator 31_1	ADA148	The Quality Checks do not report any warnings for the sample.

University of Ghana http://ugspace.ug.edu.gh

APPENDIX III: LCMS Data

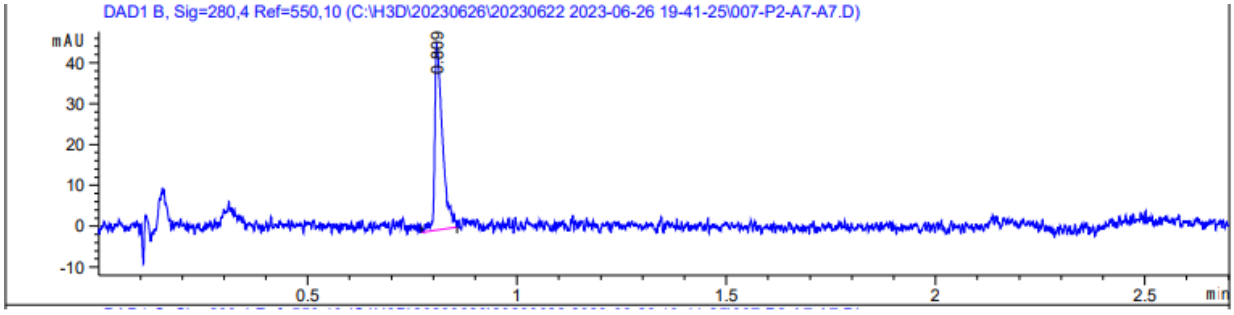
ADA083

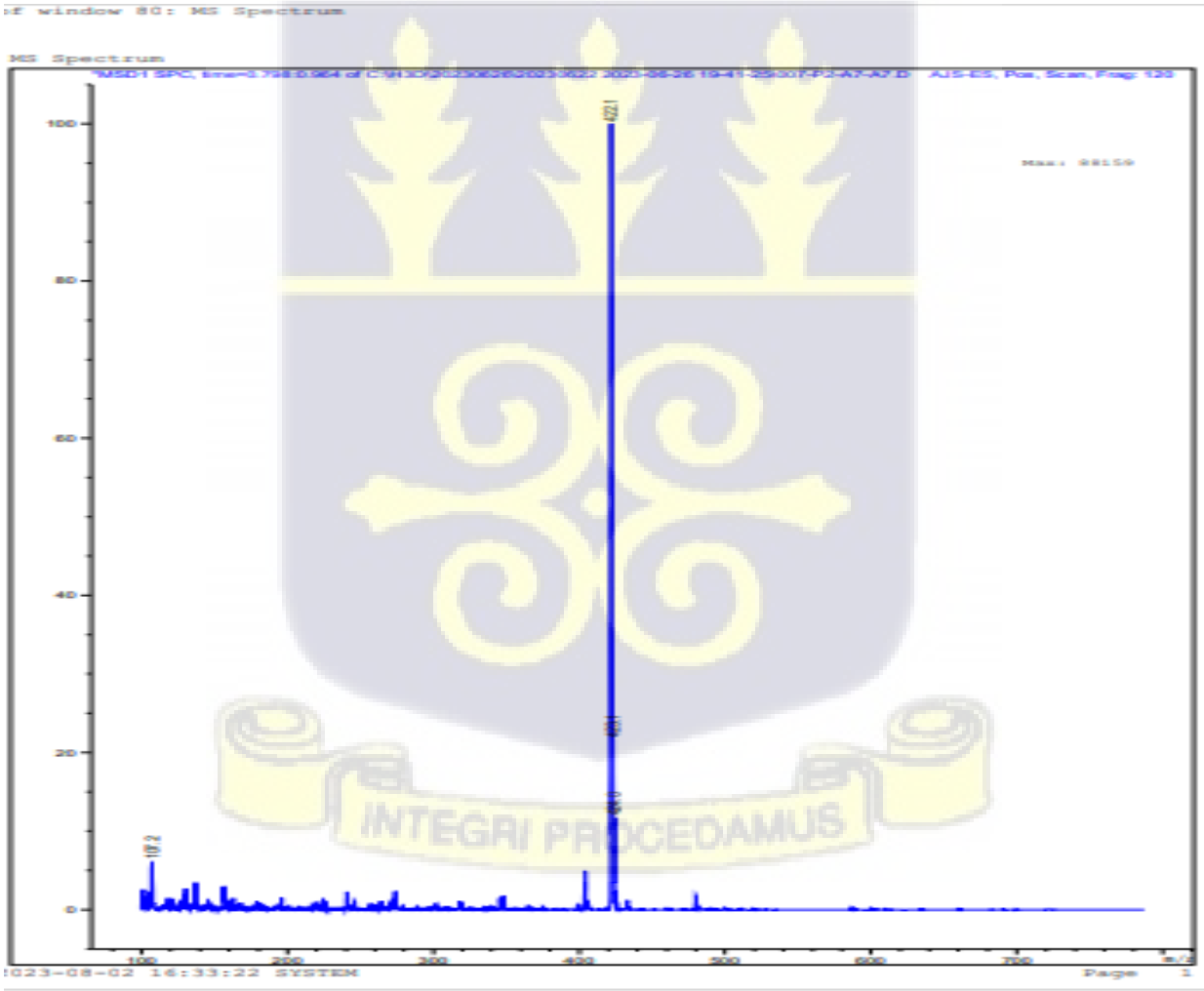




University of Ghana http://ugspace.ug.edu.gh

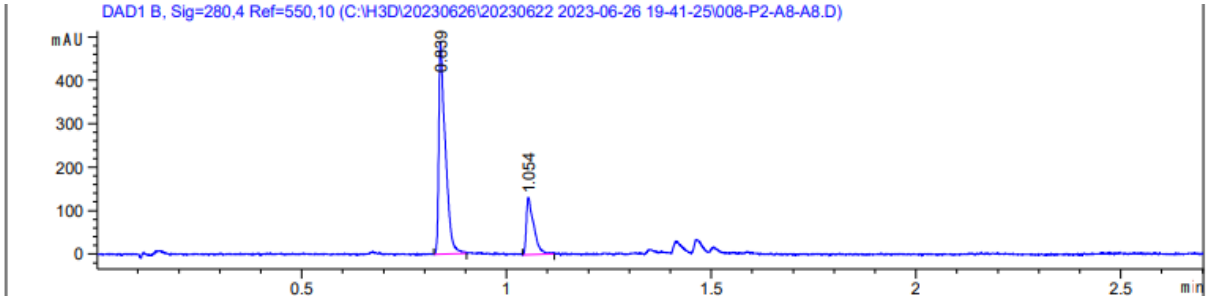
ADA085

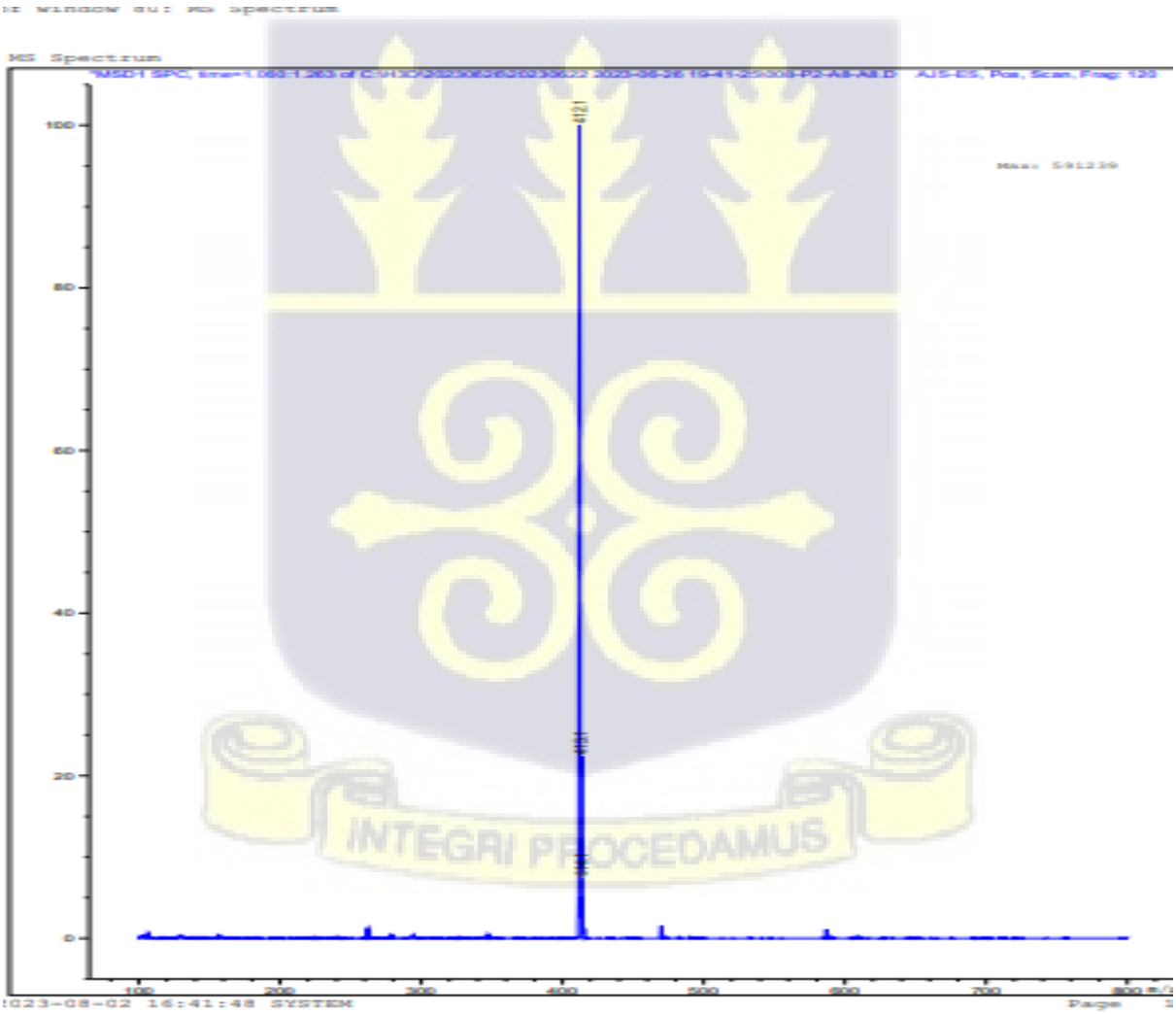




University of Ghana http://ugspace.ug.edu.gh

ADA087

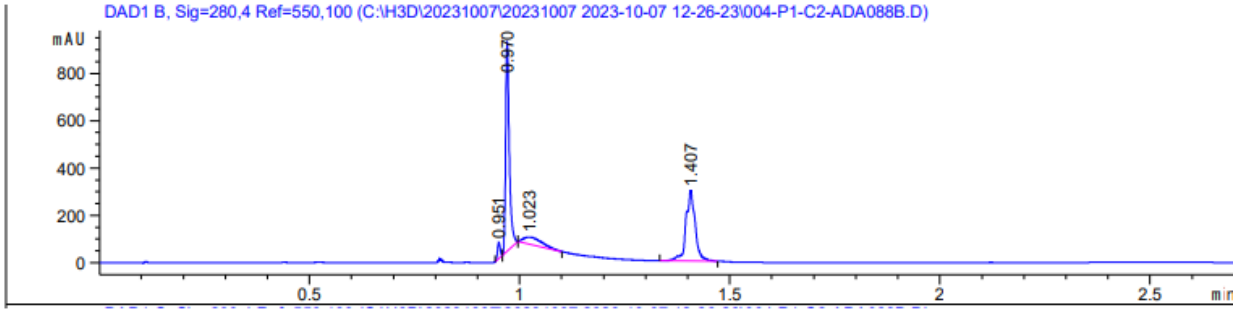


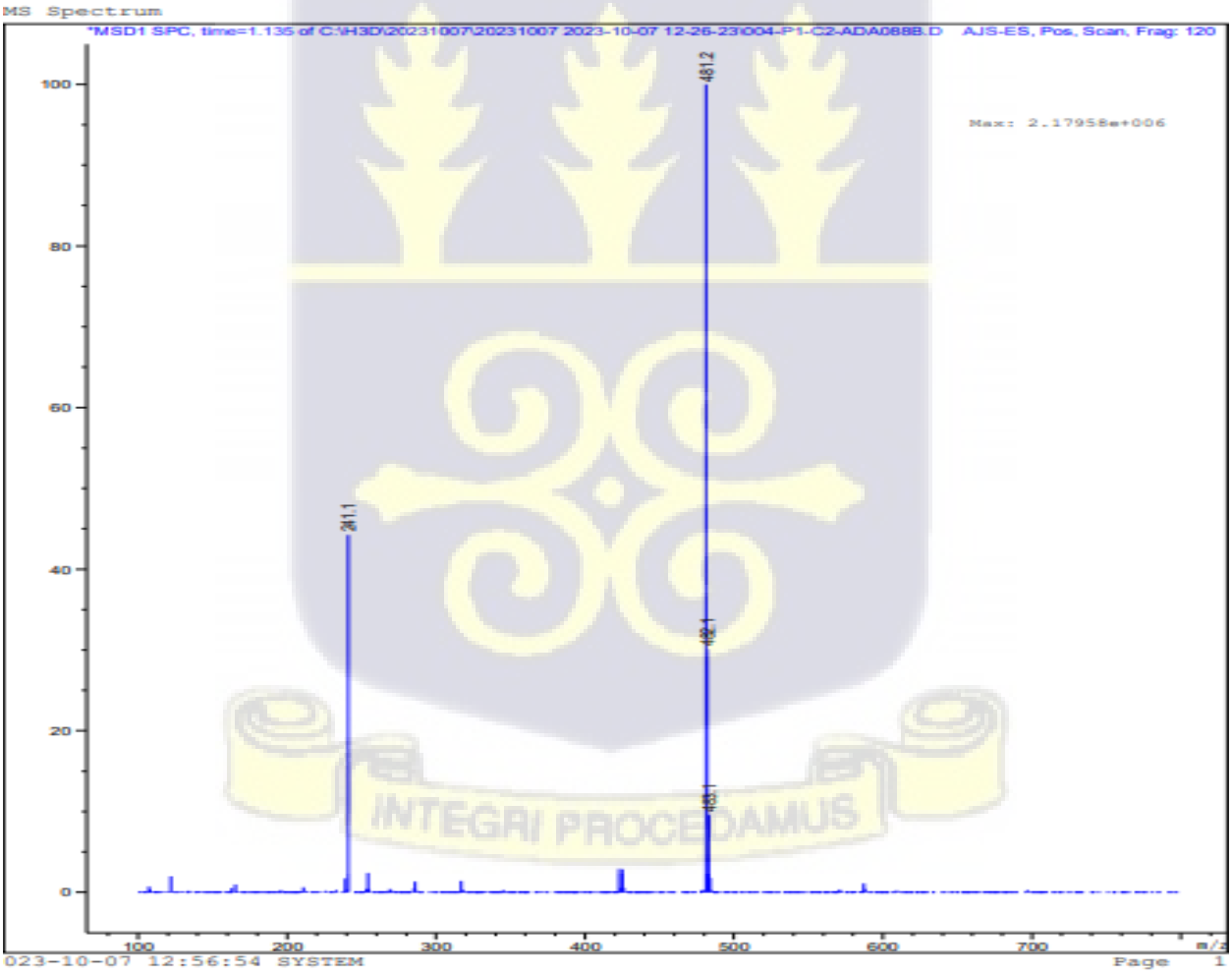


INTEGRI PROCEDAMUS

University of Ghana http://ugspace.ug.edu.gh

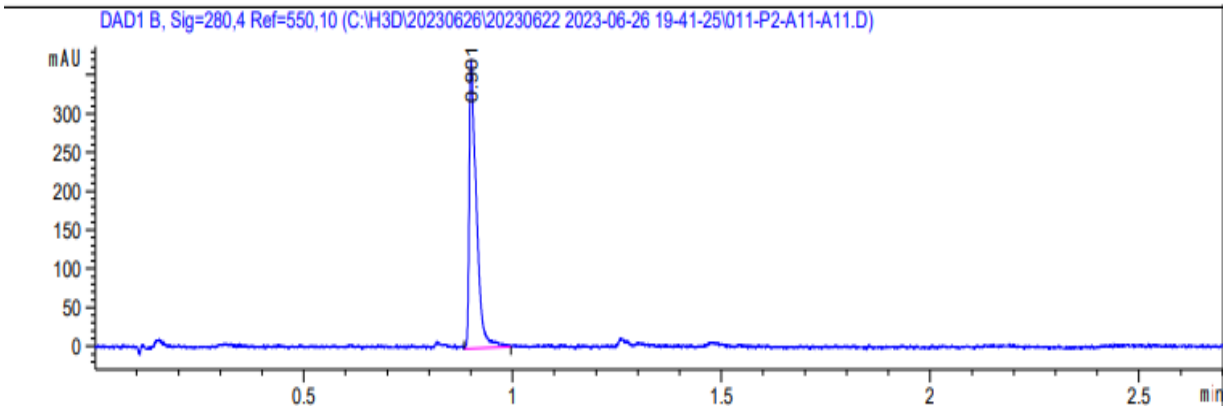
ADA088

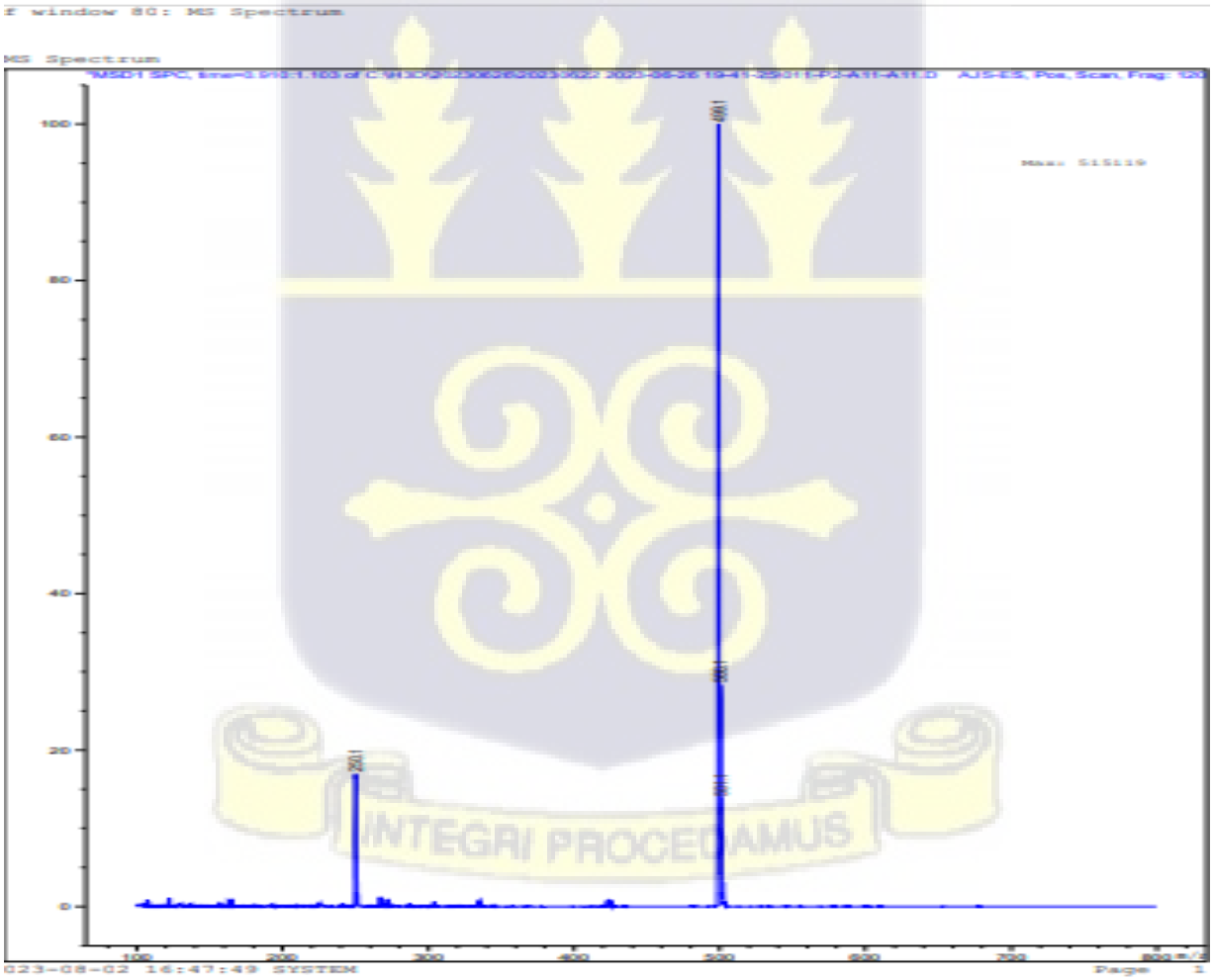




University of Ghana http://ugspace.ug.edu.gh

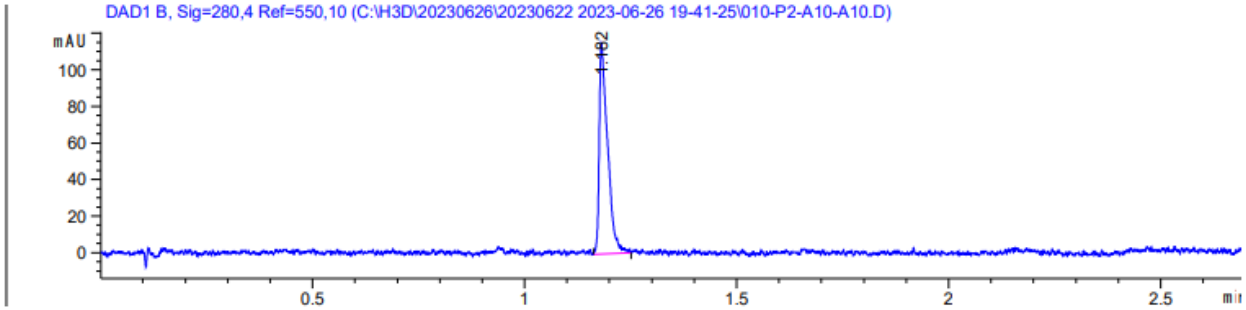
ADA090

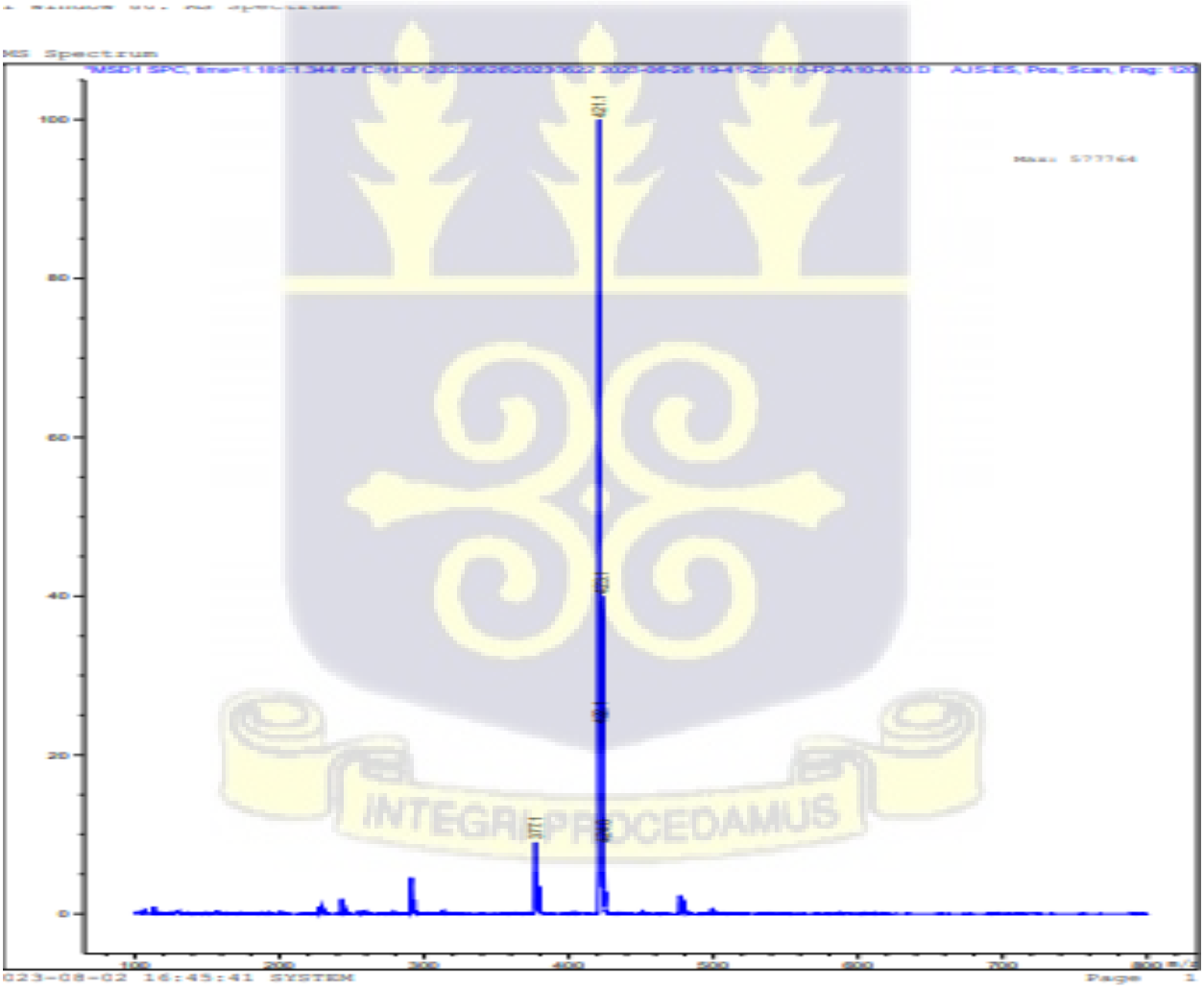




University of Ghana http://ugspace.ug.edu.gh

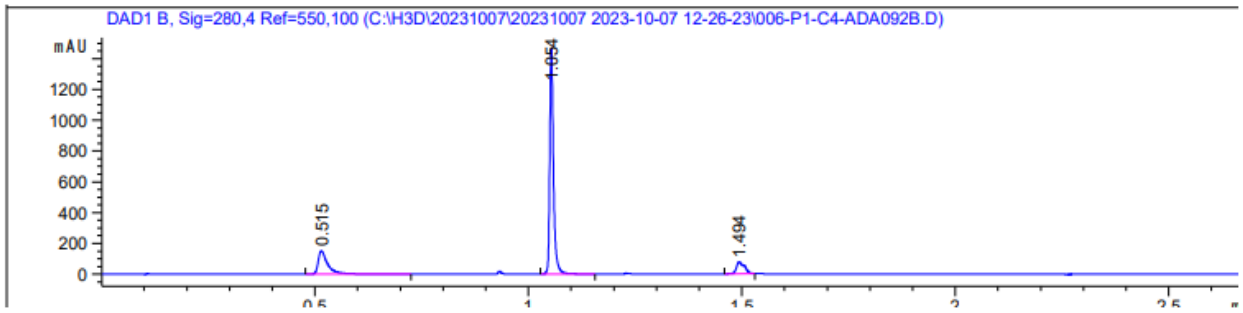
ADA091

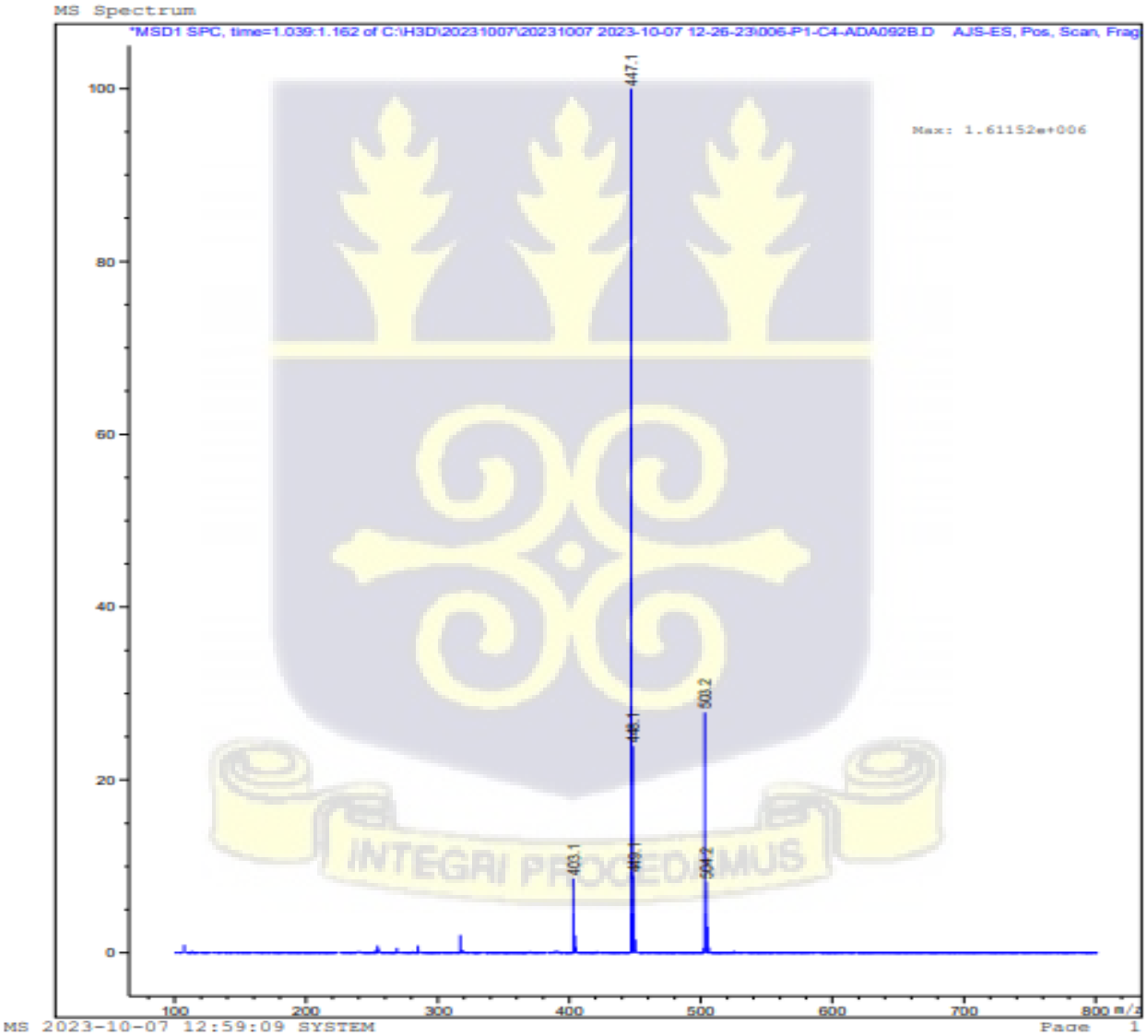




University of Ghana http://ugspace.ug.edu.gh

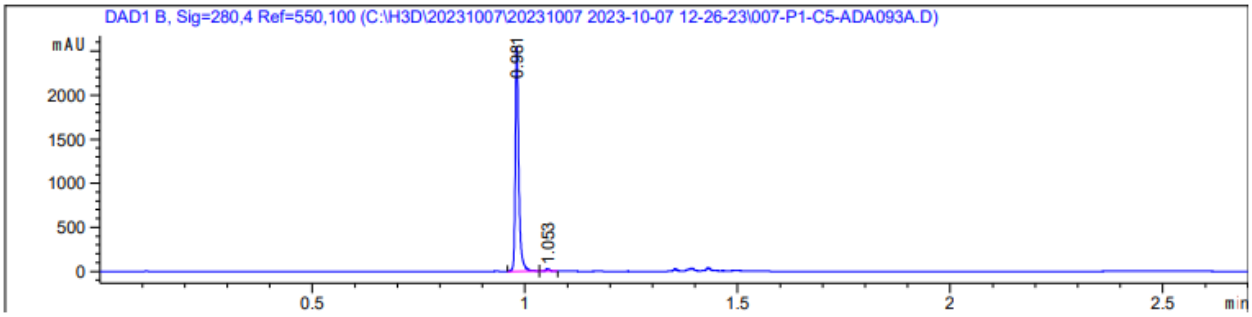
ADA092

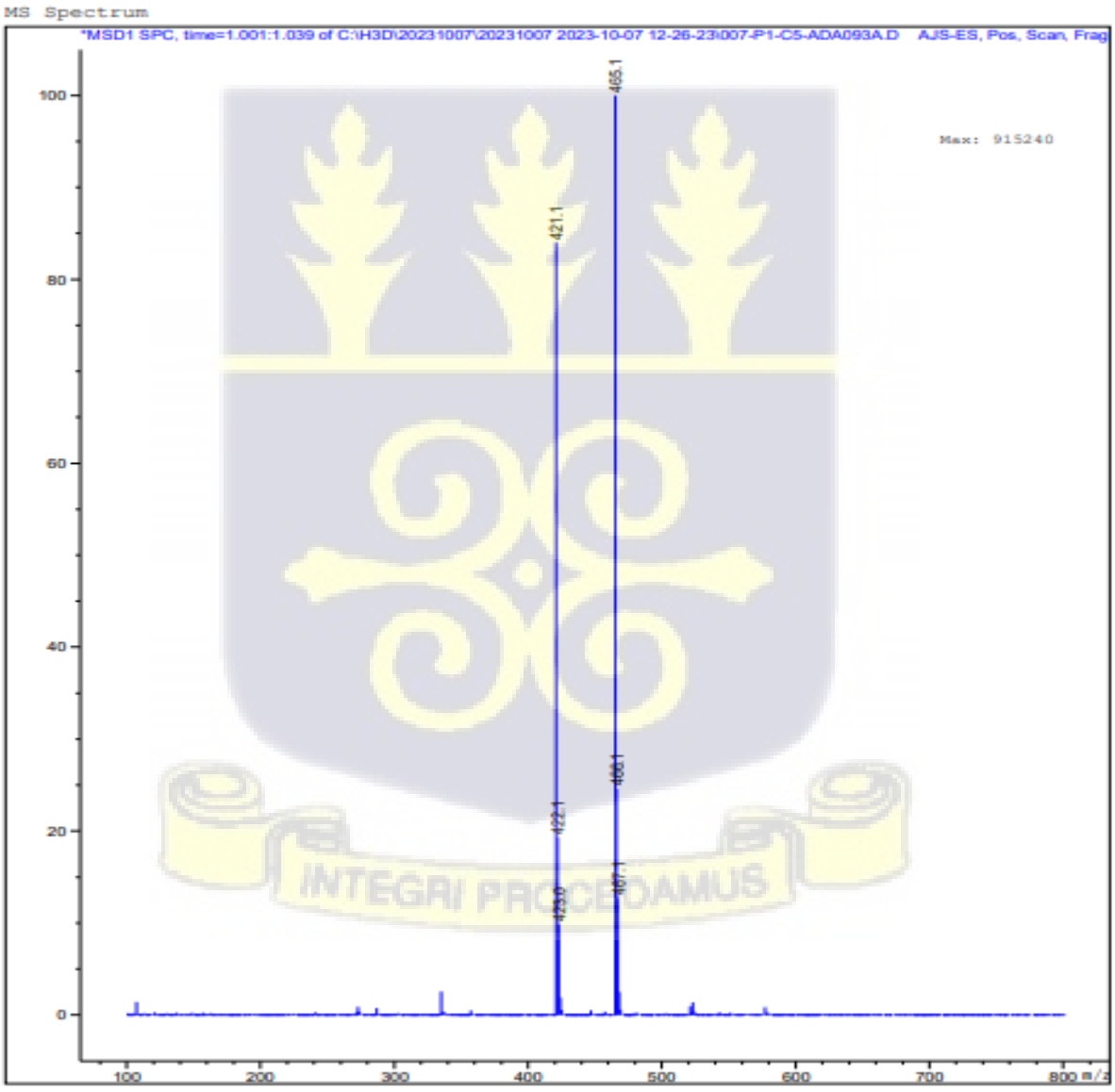




University of Ghana http://ugspace.ug.edu.gh

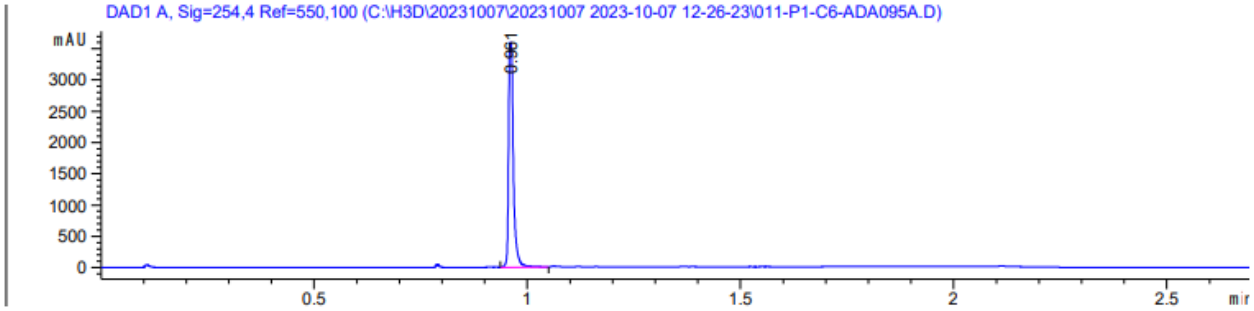
ADA093

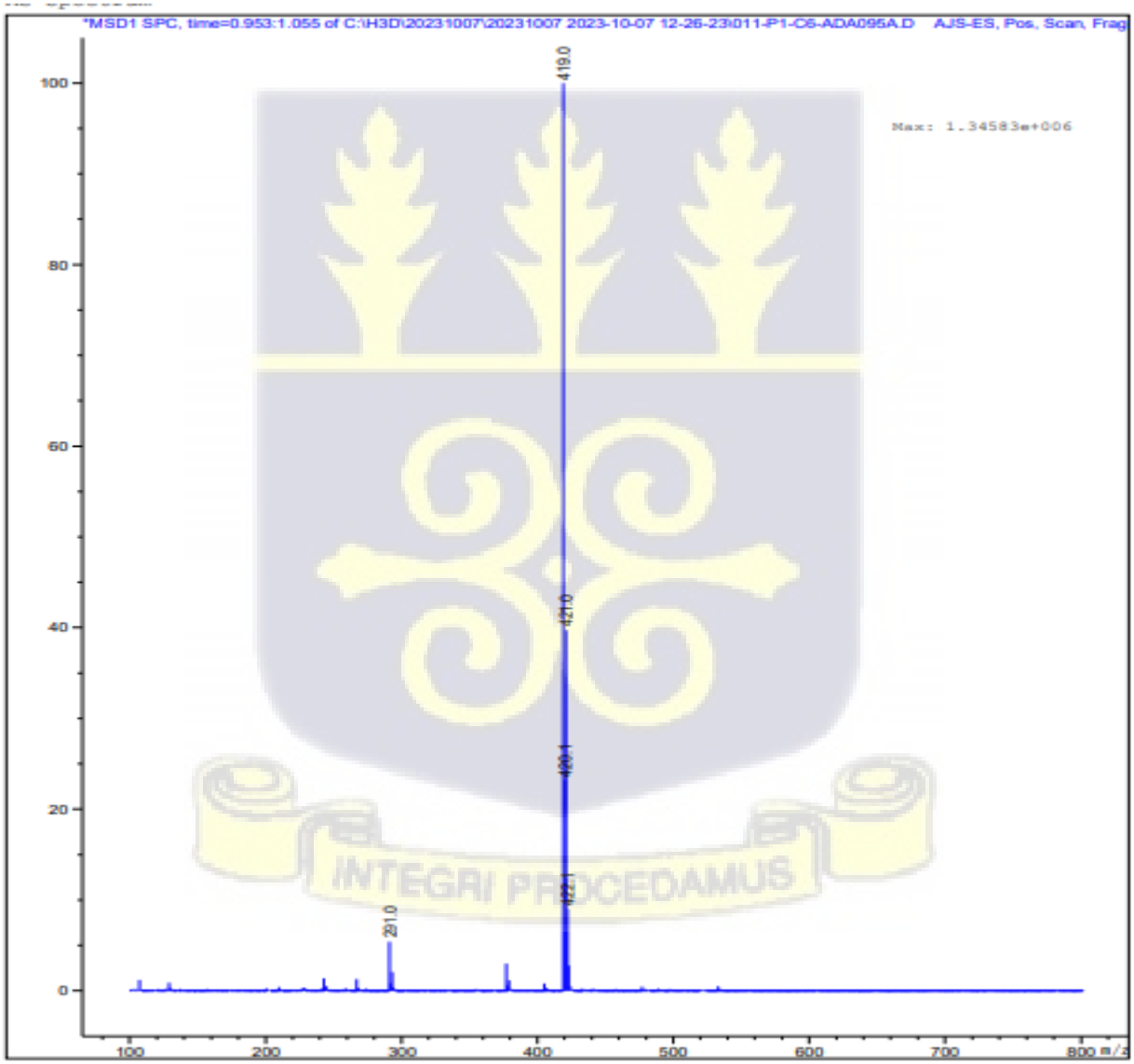




University of Ghana http://ugspace.ug.edu.gh

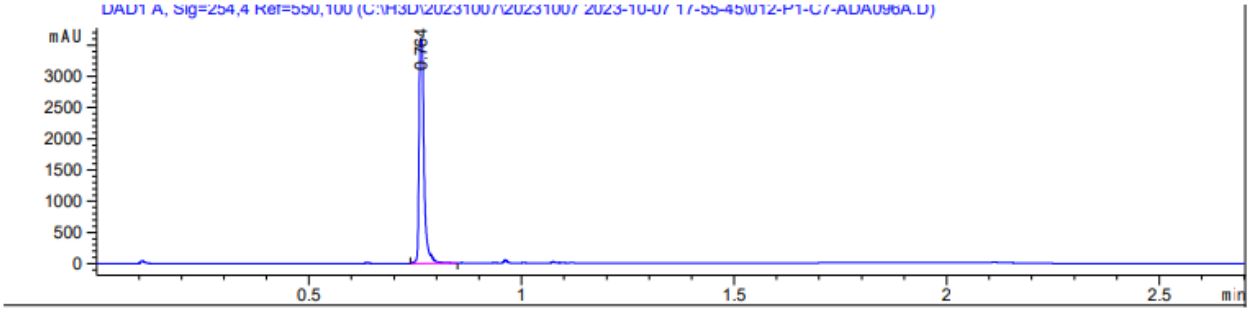
ADA095

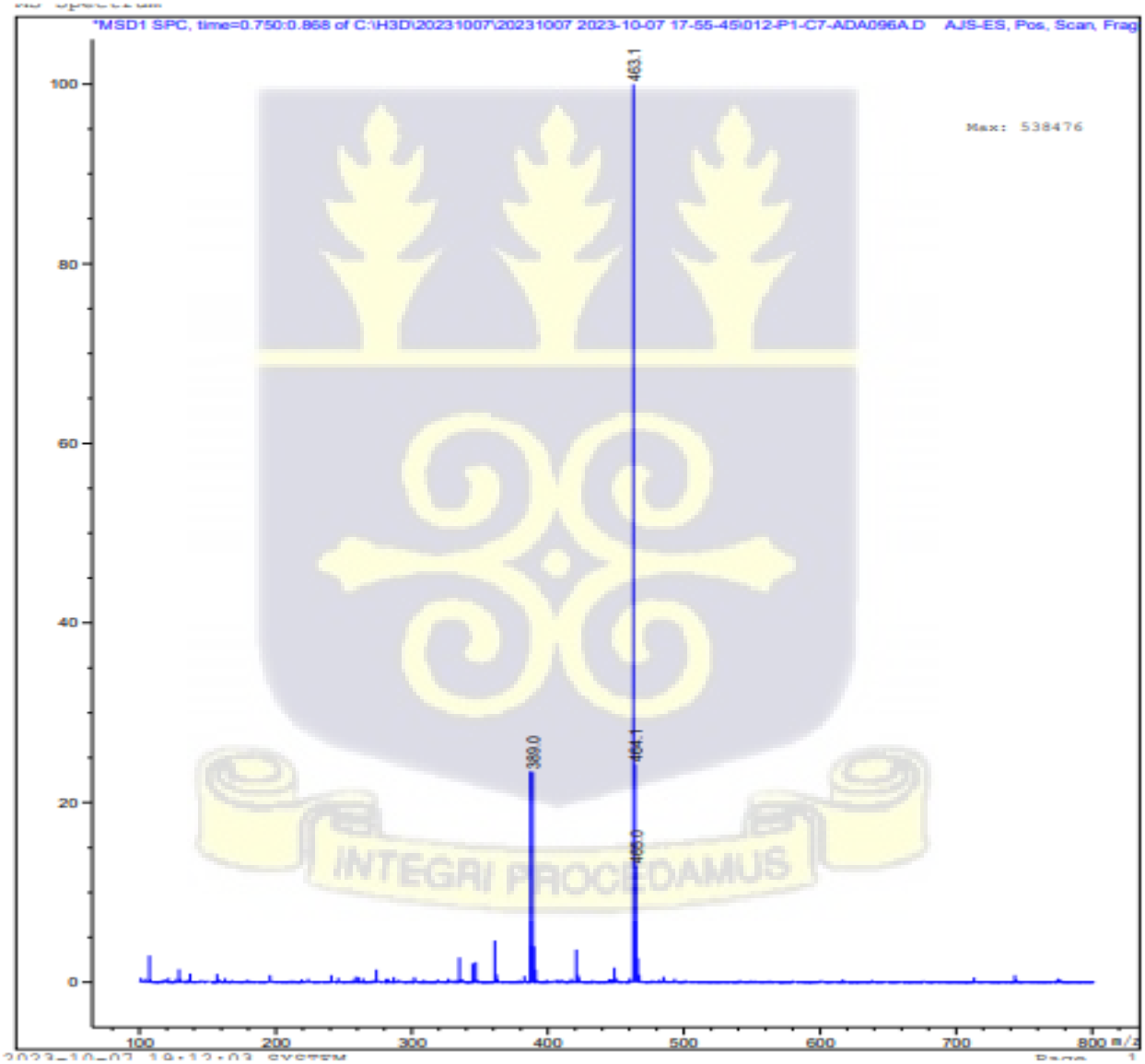




University of Ghana http://ugspace.ug.edu.gh

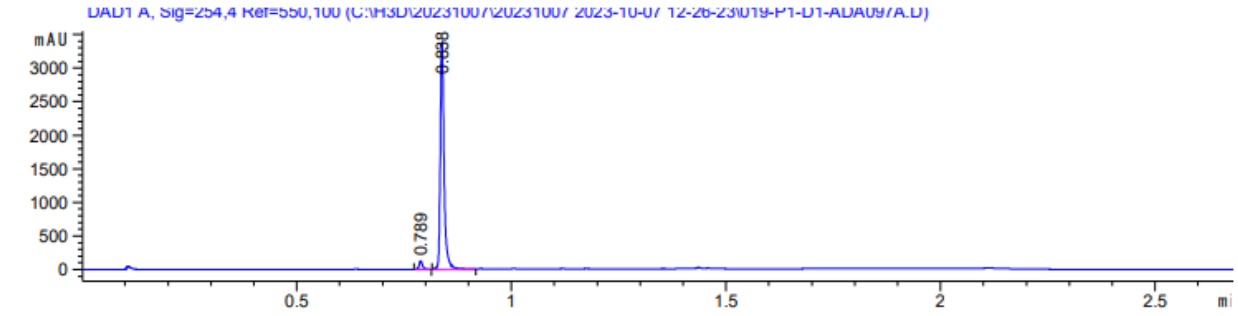
ADA096

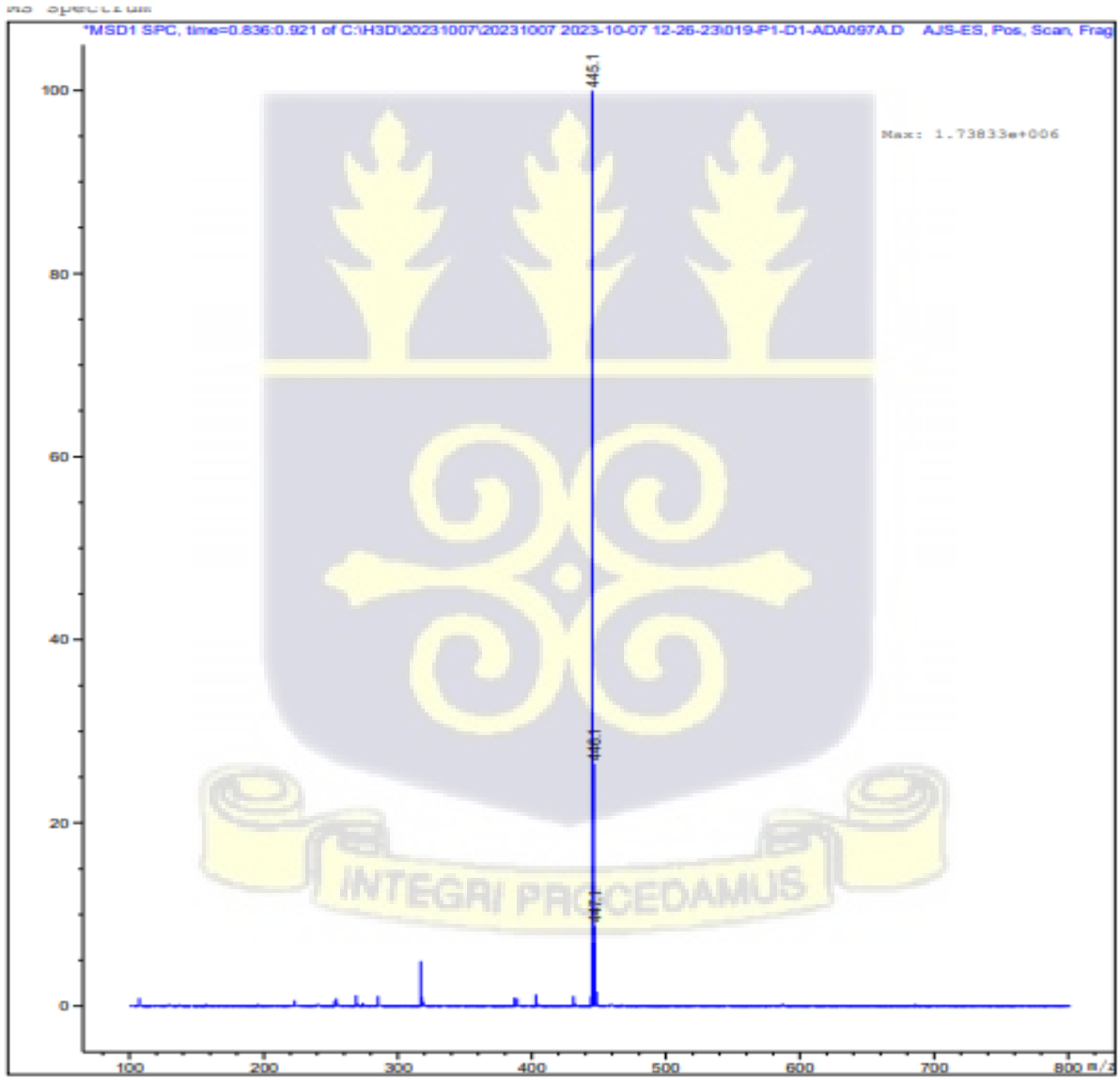




University of Ghana http://ugspace.ug.edu.gh

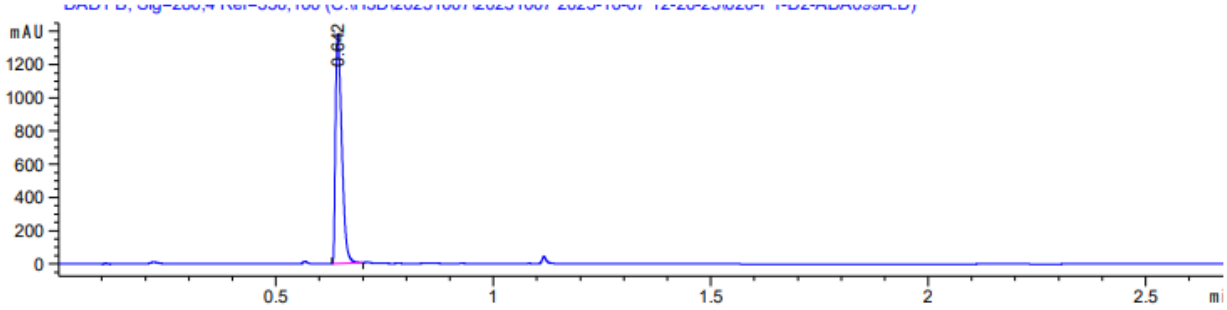
ADA097

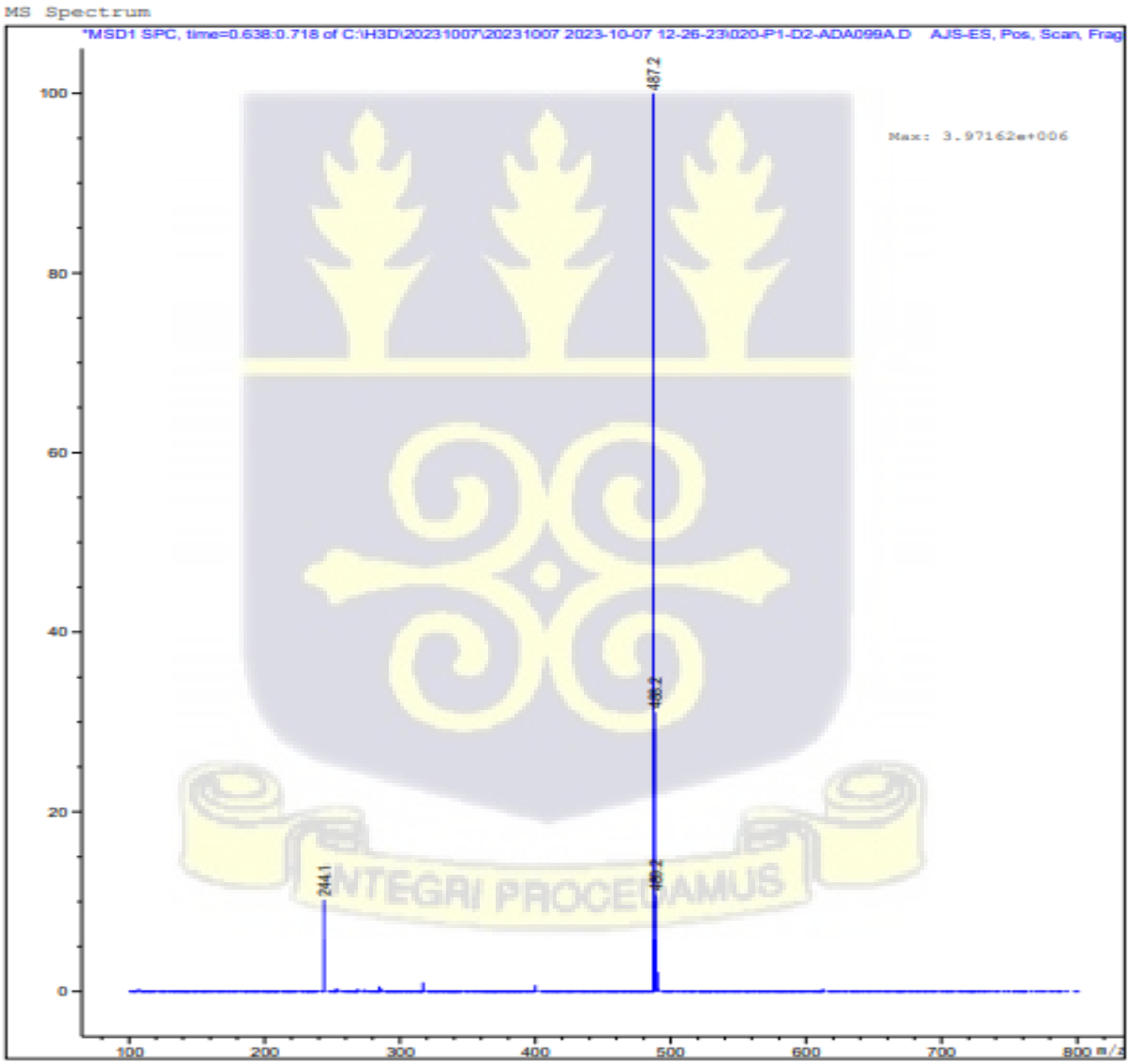




University of Ghana http://ugspace.ug.edu.gh

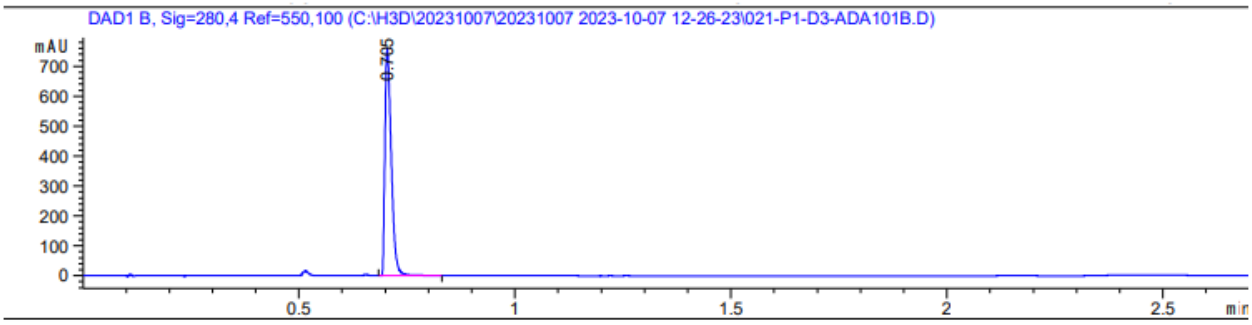
ADA099

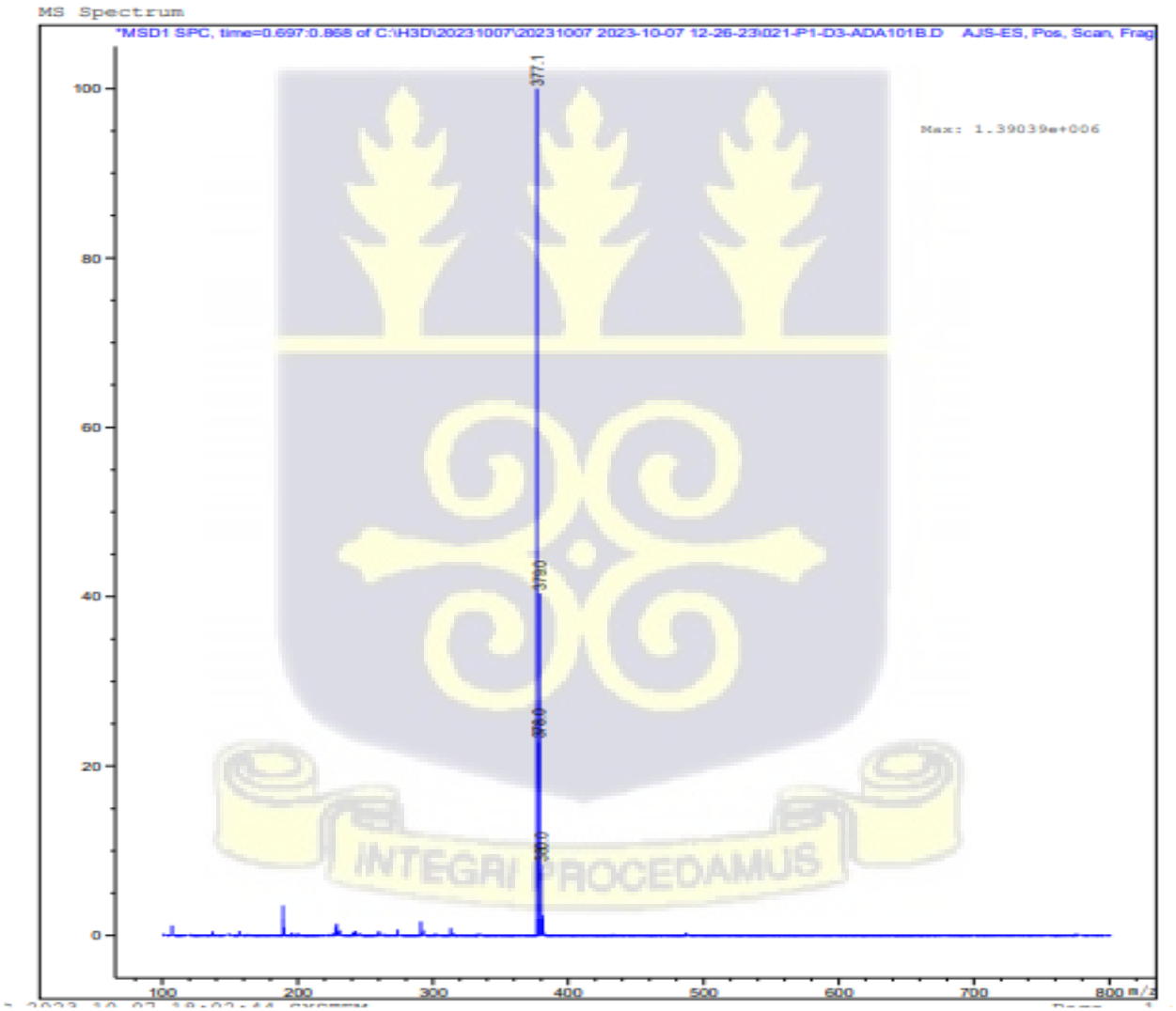




University of Ghana http://ugspace.ug.edu.gh

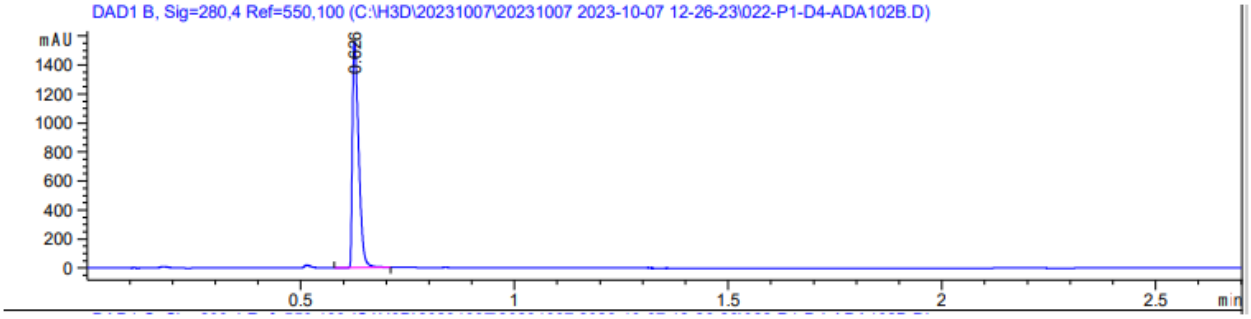
ADA101

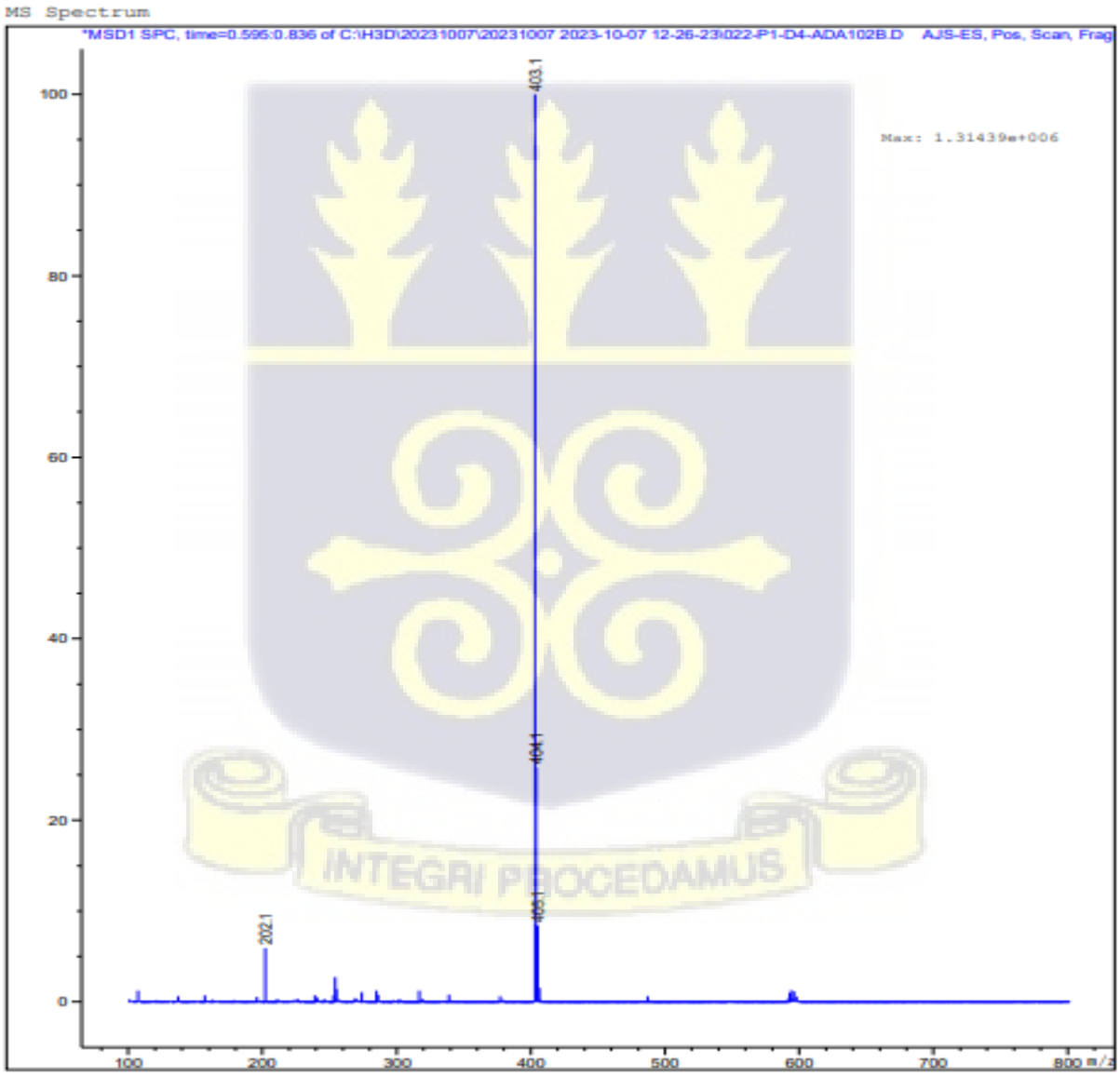




University of Ghana http://ugspace.ug.edu.gh

ADA102





University of Ghana http://ugspace.ug.edu.gh

ADA103

